

**A Neurobehavioral Endophenotype of the CGG KI Mouse Model of the Fragile X
Premutation**

By

Michael Ryan Hunsaker
B.A., University of Utah, 2005

DISSERTATION

Submitted in partial satisfaction of the requirements for the degree of
DOCTOR OF PHILOSOPHY

in

Neuroscience

in the

OFFICE OF GRADUATE STUDIES

Of the

UNIVERSITY OF CALIFORNIA

DAVIS

Approved:

Paul J. Hagerman, M.D., Ph.D. (Chair)

Robert F. Berman, Ph.D.

Kyoungmi Kim, Ph.D.

Isaac N. Pessah, Ph.D.

Susan M. Rivera, Ph.D.

Committee in Charge

2012

UMI Number: 3540517

All rights reserved

INFORMATION TO ALL USERS

The quality of this reproduction is dependent upon the quality of the copy submitted.

In the unlikely event that the author did not send a complete manuscript and there are missing pages, these will be noted. Also, if material had to be removed, a note will indicate the deletion.



UMI 3540517

Published by ProQuest LLC (2012). Copyright in the Dissertation held by the Author.

Microform Edition © ProQuest LLC.

All rights reserved. This work is protected against unauthorized copying under Title 17, United States Code



ProQuest LLC.
789 East Eisenhower Parkway
P.O. Box 1346
Ann Arbor, MI 48106 - 1346

ACKNOWLEDGEMENTS

First and foremost, this dissertation is dedicated to the memory of Patrick Kyle Hunsaker, my late brother, without whom I would never have entered science and none of this would be possible.

I would like to express my appreciation for Naomi Goodrich-Hunsaker, Ph.D., a lifelong co-worker, permanent collaborator, and loving spouse for her stalwart support throughout my graduate career; and for enduring my excitement when experiments worked to my satisfaction and sharing my frustration when they did not.

ABSTRACT

The fragile X premutation is a CGG repeat expansion on the *FMR1* gene between 55 and 200 repeats in length. Carriers of the fragile X premutation show a complex phenotype that includes a number of disparate features, including difficulty with mental arithmetic and visuospatial processing. Despite these reports, there is no agreement concerning which behavioral features are central to the fragile X premutation phenotype. The goal of this dissertation was to develop a series of behavioral tasks that, when looked at as a whole, define a pattern of behavioral phenotypes that scale with the dosage of the *FMR1* CGG repeat lengths (*i.e.*, genetic dosage).

Neuropathological studies were designed to quantify the pathological features in carriers of the fragile X premutation and fragile X syndrome, and subsequently compare those findings with the mouse model. These experiments revealed the CGG KI mouse model of the fragile X premutation recapitulated the pathological features present in aged premutation carriers. These data suggest the CGG KI mouse model is a valid model to study the development and progression of the neuropathological features associated with the premutation.

The present behavioral studies characterized effects of the fragile X premutation on cognitive function by examining the performance of CGG KI mice with CGG repeat expansions ranging between 70-200 repeats using behavioral tasks emphasizing spatiotemporal, visuospatial, and visuomotor function. In all cases CGG KI mice showed deficits that worsened as a function of increasing *Fmr1* CGG repeat lengths. Furthermore, increasing CGG repeat length resulted

in reduced LTP, LTD, and mGluR1/5 LTD during the first 10-20 minutes after conditioning stimuli were applied, but there was no effect for CGG repeat length on plasticity at 40-60 minutes after conditioning stimuli were applied.

These results provide evidence for a complex neurocognitive endophenotype in the CGG KI mouse model. Importantly, the deficits observed for the CGG KI mice on the behavioral tasks and measures of plasticity scale with increasing genetic dosage (i.e., increasing CGG repeat length), supporting reports in human carriers of the fragile X premutation that suggest increasing CGG repeat length modulates cognitive function.

TABLE OF CONTENTS

ACKNOWLEDGEMENTS	ii
ABSTRACT	iii-iv
TABLE OF CONTENTS	v
GENERAL INTRODUCTION	1-6
SECTION 1: NEUROPATHOLOGY	7-8
CHAPTER 1	9-34
CHAPTER 2	35-52
CHAPTER 3	53-89
CHAPTER 4	90-117
CHAPTER 5	118-161
CHAPTER 6	162-192
SECTION 2: BEHAVIORAL PHENOTYPE	193
INTRODUCTION	193-194
CHAPTER 7	195-227
CHAPTER 8	228-251
SECTION 3: BEHAVIORAL ENDOPHENOTYPES	252
CHAPTER 9	253-315
CHAPTER 10	316-362
CHAPTER 11	363-388
INTRODUCTION: NEUROMOTOR FUNCTION	389-390
CHAPTER 12	391-408
CHAPTER 13	409-430
CHAPTER 14	431-458
CONCLUSION	459-463
REFERENCES	464-520

GENERAL INTRODUCTION

Historically, individuals with <200 CGG repeats on the Fragile X Mental Retardation 1 (*FMR1*) gene were thought completely unaffected by the mutation, whereas individuals carrying >200 CGG repeats were known to develop fragile X symptoms (Hagerman & Hagerman, 2004b; Hagerman et al., 2008). As such, carriers of 55-200 CGG repeats were termed *premutation* carriers since the number of CGG repeats showed a tendency toward expansion across generations and premutation carriers gave birth to offspring with the full mutation underlying fragile X syndrome (*i.e.*, >200 CGG repeats).

Molecular findings in premutation carriers with and without FXTAS include 3-8 fold elevations in *FMR1* mRNA in leucocytes and <3 fold in brain tissue, while FMRP levels are only slightly reduced by 10-30% (Hessl et al., 2005). Elevated *FMR1* mRNA has lead to the proposal that FXTAS results from a toxic “RNA gain of function” (Hagerman et al., 2001; Handa et al., 2005; Jin et al., 2003; Jin et al., 2007; Kenneson, Zhang, Hagedorn, & Warren, 2001), where neuropathology thought to result from the sequestration of RNA-binding proteins important for normal cellular functions (*e.g.*, protein trafficking, alternative splicing, microRNA processing) by the elevated *FMR1* mRNA (Willemsen, Levenga, & Oostra, 2011). However, cellular mechanisms responsible for elevated *FMR1* mRNA levels and the pathways that lead to toxicity remain largely unknown (Garcia-Arocena & Hagerman, 2010; Raske & Hagerman, 2009; Todd & Paulson, 2010).

In 2001, however, a late onset neurodegenerative disorder unique to carriers of the fragile X premutation was described, characterized by an intention

tremor and cerebellar gait ataxia (Hagerman et al., 2001). This disorder was termed the Fragile X-Associated Tremor/Ataxia Syndrome, or *FXTAS*. Subsequently, a plethora of neuropsychological and psychiatric manifestations of FXTAS were elucidated and have been well characterized: Psychiatric symptoms are common in FXTAS, especially as movement symptoms become prominent, with anxiety, mood, and cognitive disorders having been reported (Bourgeois et al., 2006; Bourgeois et al., 2007; Bourgeois et al., 2009; Bourgeois et al., 2011). There is higher incidence of autoimmune diseases associated with the premutation in females, including fibromyalgia in 43% and hypothyroidism in 50% of women with FXTAS (Leehey & Hagerman, 2012; Leehey, Legg, Tassone, & Hagerman, 2011). Many individuals with FXTAS also show signs of Parkinsonism, peripheral neuropathy, focal muscle weakness and autonomic problems.

Although FXTAS has been associated with the premutation, only 40% of males and 8-16% of females from known fragile X probands develop FXTAS--and this prevalence increases with age (Hagerman & Hagerman, 2004b; Hagerman & Hagerman, 2008; Hagerman, 2008; Jacquemont et al., 2004a; Jacquemont et al., 2004b; Jacquemont, Leehey, Hagerman, Beckett, & Hagerman, 2006). The cause for this incomplete penetrance is currently unknown, and, unfortunately, at present there are no factors that allow physicians to predict which premutation carriers may or may not develop progressive FXTAS symptoms.

At the radiological level, there have been reports of white matter disease and general brain atrophy in individuals with FXTAS (Brunberg et al., 2002). More specifically, periventricular and pontine white matter disease is common, and white matter disease in the middle cerebellar peduncle has been adopted as a primary diagnostic factor for FXTAS, even though this feature is present in only 58% of males and 13% of women with FXTAS (Jacquemont et al., 2003; Jacquemont et al., 2004b; Jacquemont et al., 2006). Post mortem analyses of FXTAS brain has shown white matter spongiosis throughout the subcortical and cortical white matter, as well as significant white matter disease corresponding the white matter disease observed radiologically in the middle cerebellar peduncle. At an histological level, it has been demonstrated that intranuclear inclusions are present in neurons and astrocytes throughout the brain, spinal cord, and autonomic and enteric nervous system, as well as in some somatic organ systems (Greco et al., 2002; Greco et al., 2006; Greco et al., 2007; Greco et al., 2008; Hunsaker et al., 2011a; Hunsaker et al., 2011b; Tassone et al., 2004a; Tassone, Iwahashi, & Hagerman, 2004b). These inclusions have also been demonstrated in premutation carriers that died at advanced ages without developing clinical signs congruent with a FXTAS diagnosis (Tassone et al., 2012).

Despite these neurological findings in premutation carriers with FXTAS, prior to the onset of FXTAS symptoms it is uncommon to identify gross neurological, or even cognitive, dysfunction using common neuropsychological tests (Brega et al., 2008; Brega et al., 2009; Grigsby et al., 2006a; Grigsby et al.,

2006b; Grigsby et al., 2007; Grigsby et al., 2008). As such, it has been suggested that premutation carriers prior to developing any FXTAS features are cognitively and neurologically unaffected by the mutation (Hunter et al., 2008a; Hunter et al., 2008b; Hunter, Abramowitz, Rusin, & Sherman, 2009; Hunter, Epstein, Tinker, Abramowitz, & Sherman, 2011; Hunter, Sherman, Grigsby, Kogan, & Cornish, 2012). However, more sensitive tests to evaluate cognitive dysfunction in premutation carriers have identified a number of neurocognitive deficits that are associated with the premutation. Research has suggested, furthermore, that there is a dose dependence for the magnitude of deficits in male premutation carriers, mostly involving deficits correlating with increasing *FMR1* mRNA and reducing FMRP protein levels (Hashimoto, Backer, Tassone, Hagerman, & Rivera, 2011; Hessl et al., 2011; Hessl, Rivera, & Reiss, 2004; Koldewyn et al., 2008; Selmeczy et al., 2011). Another line of research has suggested that dorsal visual stream-specific deficits reflect (or cause) impairments for spatial and temporal attention. For example, it has been shown that there are visual processing deficits in premutation carriers selective to the magnocellular but not the parvocellular visual streams, specifically as relating to biological and mechanical motion processing (Keri & Benedek, 2009; Keri & Benedek, 2010; Keri & Benedek, 2011; Keri & Benedek, 2012). In a spatial magnitude comparison task, it has been demonstrated that female premutation carriers show performance for discriminating small differences in spatial magnitude that appears to be modulated by CGG repeat length (*i.e.*, task performance shows a negative association with CGG repeat length), this despite female premutation

carriers showing enhanced reaction times on a simple reaction time task run during the same behavioral session (Goodrich-Hunsaker et al., 2011a; Goodrich-Hunsaker et al., 2011b; Goodrich-Hunsaker et al., 2011c). Similar dosage effects have been demonstrated in an enumeration task that requires sequential shifting of spatial attention (Goodrich-Hunsaker et al., 2011b). In addition to these effects, arithmetic processing deficits have been reported in the female premutation carriers (Lachiewicz, Dawson, Spiridigliozi, & McConkie-Rosell, 2006) that are thought to reflect impaired spatial and temporal attentional processes. Tests evaluating the resolution of spatial processing have also demonstrated spatial deficits in relatively young premutation carriers (Hocking, Kogan, & Cornish, 2012).

To better evaluate the effects of the premutation on brain development and function, a CGG Knock-in (CGG KI) mouse was developed by Rob Willemensen and colleagues using homologous recombination to preserve the endogenous *Fmr1* promotor and gene activity (Bontekoe, de Graaff, Nieuwenhuizen, Willemensen, & Oostra, 1997; Willemensen et al., 2003). This mouse has been shown to recapitulate an array of FXTAS-related features, including intranuclear inclusions in neurons (Berman & Willemensen, 2009; Brouwer et al., 2007; Brouwer et al., 2008a; Brouwer et al., 2008b; Brouwer, Willemensen, & Oostra, 2009; Hunsaker, Arque, Berman, Willemensen, & Hukema, 2012; Willemensen et al., 2003). Unfortunately, to date the CGG KI mouse has not recapitulated any of the cerebellar features associated with FXTAS such as gait ataxia and intention tremors.

The purpose of the research presented in this dissertation has been to use the CGG KI mouse model to model the neurocognitive deficits reported in premutation carriers without FXTAS. Furthermore, the development of neuropathological features in the CGG KI mouse was also studied in order to better understand the development and progression of the neuropathologic features reported in FXTAS.

Section 1 will present the neurohistological findings in the CGG KI mouse as well as human premutation carriers. Section 2 will describe findings from behavioral tasks explicitly modeling the studies evaluating cognitive function in young premutation carriers. Section 3 will extend upon these findings to develop a comprehensive behavioral endophenotype of the CGG KI mouse using a range of behavioral and neurophysiological methods. These fundings are then related back to the specific dosage of the CGG repeat on the *Fmr1* gene (*i.e.*, length of expanded CGG repeat lengths). Together, these results point to a specific set of behavioral strengths and weaknesses that can be used as outcome measures to quantify later disease onset, progression, or as outcome measures for testing potential treatment options in the CGG KI mouse model, and eventually, the fragile X premutation carriers that have developed FXTAS.

Section 1: Neuropathology

As the presence of intranuclear inclusions in neurons and astrocytes in brain has been included as a primary diagnostic criteria in FXTAS (Jacquemont et al., 2003), there has been widespread research into the contents of these inclusions as well as the mechanisms by which they form (Garcia-Arocena & Hagerman, 2010). Systematic analysis of these inclusions shows the presence of more than 20 proteins (Iwahashi et al., 2006). Interestingly, the inclusions contain *FMR1* mRNA, but not FMRP (Iwahashi et al., 2006; Tassone et al., 2004b). There is also Purkinje cell loss in the cerebellum, and evidence of white matter disease in major fiber tracts (white matter hyperintensities in T2 weighted MRI; Brunberg et al., 2002; Greco et al., 2002).

Prior to 2006, the presence of inclusions was accepted as widespread, but there was never any sort of quantitative analysis in human tissues for inclusion distribution and prevalence (*cf.*, Brunberg et al., 2002; Greco et al., 2002; Greco et al., 2006; Greco et al., 2007; Greco et al., 2008; Tassone et al., 2004a; Tassone et al., 2004b; Tassone et al., 2012). In the CGG KI mouse, a rough quantification of intranuclear inclusion presence was carried out by Willemse and colleagues, but inclusions were only identified in neurons, so the role for astroglial pathology was unanswerable using the CGG KI mouse model (Willemse et al., 2003).

The first part of the work presented in this dissertation was to quantify the presence of inclusions in brain in both the premutation carrier with and without

FXTAS as well as in the CGG KI mouse model. Inclusions in neurons and astrocytes were quantified in both FXTAS and CGG KI mice.

Chapter 1 will introduce the CGG KI mouse model being used as a model for FXTAS. Chapter 2 will introduce the neuropathological features present in FXTAS, with an emphasis on pathological features described in male premutation carriers that developed clinical symptomatology associated with FXTAS. Chapter 3 will describe the presence and distribution of intranuclear inclusion in neurons and astroglia of male CGG KI mice. Chapter 4 will provide a quantification of intranuclear inclusions in female premutation carriers with and without FXTAS. Chapter 5 will provide a comprehensive quantification of the presence and distribution of inclusions in female CGG KI mice. Chapter 6 will describe somatic organ pathology as well as autonomic and enteric nervous system pathology in human FXTAS and the CGG KI mouse.

Chapter 1

Mouse Models of the Fragile X Premutation and the Fragile X Associated Tremor/Ataxia Syndrome

Abstract

The use of mutant mouse models of neurodevelopmental and neurodegenerative disease is essential in order to understand the pathogenesis of many genetic diseases such as fragile X syndrome and fragile X-associated tremor/ataxia syndrome (FXTAS). The choice of which animal model is most suitable to mimic a particular disease depends on a range of factors, including anatomical, physiological, and pathological similarities; presence of orthologs of genes of interest; and conservation of basic cell biological and metabolic processes. In this chapter, we will discuss two mouse models of the fragile X premutation which have been generated to study the pathogenesis of FXTAS and the effects of potential therapeutic interventions. Behavioral, molecular, neuropathological, and endocrine features of the mouse models and their relation to human FXTAS are discussed.

This chapter has been published as:

Hunsaker, M. R., Hukema, R. K., Arque, G., Berman, R. F., & Willemsen, R. (2011). *Mouse models of the fragile X premutation and the fragile X associated tremor/ataxia syndrome*. In R. B. Denman (Ed.) *Modeling the Fragile X Syndrome*. Springer-Verlag Press.

Introduction

The *FMR1* gene is polymorphic for the length of a tandem CGG trinucleotide repeat in the 5' untranslated region (UTR). In the general population there are fewer than 55 CGG repeats (mean 30 – Hagerman, 2008). In some individuals there is a repeat expansion wherein the number of CGG repeats expands beyond 200 repeats in length (*i.e.*, full mutation – FM), and this is associated with *FMR1* promoter and CpG island hyper-methylation and subsequent gene silencing – leading to no measurable *FMR1* transcription and no FMRP translation and Fragile X Syndrome (FXS; Hagerman & Hagerman, 2004b). This FM occurs in roughly 1:4,000 males and 1:6,000 females, and virtually all FM males will develop FXS and 60% of FM women will develop FXS. CGG repeat lengths between those found in the general population and the FM are called the Fragile X premutation (55–200 CGGs; PM) zone and occurs in ~1:130–200 females and 1:800 males (Hagerman, 2008). CGG trinucleotide repeat lengths in the PM were historically considered to lack a clinical phenotype, so the PM was used as a descriptor to emphasize the high probability for the PM to maternally expand into the FM across subsequent generations (Hagerman & Hagerman, 2004a; Hagerman & Hagerman, 2004b; Hagerman & Hagerman, 2007; Hagerman et al., 2001; Hagerman, 2008; Jacquemont et al., 2004a; Jacquemont et al., 2004b; Kraff et al., 2007; Leehey et al., 2007a; Leehey et al., 2008; Leehey, Hagerman, & Hagerman, 2007b; Senturk et al., 2009; Tassone et al., 2000c).

In 2001, a late onset neurodegenerative disorder called Fragile-X associated tremor/ataxia (FXTAS) was described in a subset of elderly carriers of PM alleles (Hagerman et al., 2001). FXTAS patients exhibit gait ataxia, intention tremor, and Parkinsonism, as well as presence of eosinophilic, ubiquitin-positive intranuclear inclusions in neurons and astrocytes throughout the brain (Greco et al., 2002; Greco et al., 2006; Greco et al., 2007; Greco et al., 2008; Tassone et al., 2004a). This finding, along with the findings that elevated *FMR1* mRNA levels and concomitant mild reductions in FMRP levels are associated with the PM (Tassone & Hagerman, 2003; Tassone et al., 2000c; Tassone et al., 2000d; Tassone, Hagerman, Chamberlain, & Hagerman, 2000a), has led to the proposal that FXTAS is the result of an RNA gain of function resulting in cellular toxicity, similar to myotonic dystrophy (Garcia-Arocena et al., 2010; Raske & Hagerman, 2009; Sellier et al., 2010; Tassone & Hagerman, 2003). What remains unclear in FXTAS is the cause of incomplete penetrance of FXTAS within PM carriers: in PM carriers from known fragile X probands, only 30% of the males and 10–15% of the females may develop FXTAS, a number that may be lower if samples were ascertained through non-fragile X probands (Jacquemont et al., 2003; Jacquemont et al., 2004b).

Mouse Models of the Fragile X Premutation and FXTAS

The first mouse models were initially developed to model repeat instability and potential expansion to FM across generations. However, these transgenic mouse models, both within and outside the context of the *FMR1* gene, did not show instability in the trinucleotide repeat length (Bontekoe et al., 1997; Bontekoe et al., 2001; Lavedan, Garrett, & Nussbaum, 1997; Lavedan, Grabczyk, Usdin, & Nussbaum, 1998).

The first model to be reported as a putative model for the PM and potentially FXTAS was the CGG Knock-In mouse model (CGG KI), which was generated by a homologous recombination whereby the endogenous mouse CGG repeat (CGG8) was replaced with a PM length CGG repeat of human origin (CGG98) on the endogenous mouse *Fmr1* promoter (Bontekoe et al., 2001; Willemse et al., 2003). These CGG KI mice, with minimal changes to the endogenous mouse *Fmr1* promoter, showed moderate instability upon paternal and maternal transmission, and both expansions and contractions have been observed (Brouwer et al., 2007). Later, another CGG-CCG knock-in mouse (CGG-CCG mouse) was developed wherein CGG-CCG repeats (CGG-CCG124) were serially ligated and expressed in the endogenous mouse CGG repeat on the endogenous promoter (Entezam et al., 2007). This model also shows a trend toward gradual increases in CGG (or CGG-CCG) repeat lengths. Furthermore, the CGG-CCG mice show the same general pattern of repeat instability as that reported in the PM, namely that the paternal mutation shows small repeat expansions, and this expansion occurs preferentially in mice lacking ATM, with a

bias toward greater expansions in males (Entezam & Usdin, 2008; Entezam & Usdin, 2009). Maternally transmitted mutations show larger repeat expansions that occur preferentially in mice lacking ATR. These results support models proposed in the human PM research concerning the differential expansion of male–female PM alleles into FM alleles across generations.

It has recently been reported that there may be environmental contributions to the CGG repeat instability in humans, or at least a contribution of environmental factors in the time course of neurodegeneration (Paul et al., 2010). The CGG-CCG mouse has been used to determine the role of oxidizing agents on CGG-CCG repeat expansion. When a DNA oxidizing agent is introduced to CGG-CCG mice, there appears to be a higher frequency and size of repeat expansions (Entezam, Lokanga, Le, Hoffman, & Usdin, 2010). The authors suggest that such oxidizing agents may play a role in CGG repeat expansion seen in the PM and FXTAS.

Recently, another model of FXTAS has been developed in mice (Hashem et al., 2009). These mice used constructs and promoters either independent of the *Fmr1* gene or used non-*Fmr1* promoters. These mice specifically express CGG90 RNA in Purkinje cells with either *Fmr1* or eGFP. Therefore these models target the implications of CGG90 mRNA overexpression for FXTAS. These models expressing an expanded CGG RNA without the context of the *Fmr1* gene are very promising for the study of the RNA gain of function hypothesis.

There is another transgenic mouse model, into which a 1,057 bp fragment of genomic DNA from *FMR1* including the translation initiation site and a repeat

of 26 CGG repeats was cloned (Baskaran et al., 2002). These mice show intergenerational instability during both male and female transmission. (Baskaran et al., 2002) find methylation in lines lacking repeat expansion and absence of methylation in lines that do show expansion, indicating that methylation and expansion are potentially independent events. This mouse model will not be covered in this chapter, as this mouse serves as a better model for *Fmr1* CGG repeat expansion and gene methylation and thus is a better model for FXS than for FXTAS.

Utility of CGG KI and CGG-CCG Mice for the Study of FXTAS

As FXTAS is a late onset neurodegenerative disorder, it is difficult to determine precisely the factors that may contribute to the cellular dysfunctions thought to underlie the disease progression across the lifespan of any individual. In FXTAS patients we can only study the end-stage of the disease progression in brain tissue. The benefit of evaluating mouse models of neurodegenerative disorders is the relative shortness of the mouse lifespan. If a researcher wished to determine the natural history of the disease process in FXTAS, both the CGG KI and CGG-CCG mouse models will serve to provide invaluable insight (see Table 1).

	FXTAS	CGG KI mouse	CGG-CCG mouse
<i>Molecular Measures</i>			
CGG Repeat	55-200 repeats	70-350 repeats	120 to >200 repeats
FMR1 mRNA	2-8 fold increase	3-5 fold increase	2-6 fold increase
FMRP Level	Slightly reduced	Slightly reduced	Markedly reduced
<i>Neuropathology</i>			
Inclusions	Neurons and astrocytes	Neurons and astrocytes	In cells of brain
Gross Pathology	Purkinje cell dropout	No gross pathology	Purkinje cell dropout
Motor Function	Tremor and ataxia	Motor deficit with age	Normal motor function
<i>Cognition</i>			
Social	Social anxiety	--	Reduced sociability
Anxiety	Anxiety disorders	Elevated anxiety	Reduced anxiety
Memory	Poor memory	Memory impairments	Memory impairments

Table 1. Comparison of FXTAs with CGG KI and CGG-CCG FXTAS mouse models

The CGG KI mouse has been used to evaluate the hypothesis that FXTAS, a late onset neurodegenerative disorder, may be the end stage of earlier, perhaps even neurodevelopmental, effects accumulated across the lifespan (Bourgeois et al., 2011; Cornish et al., 2008b; Cornish et al., 2009; Cornish, Turk, & Hagerman, 2008a; Garcia-Arocena & Hagerman, 2010; Hagerman & Hagerman, 2004b). Recently, it has been shown that the CGG KI mouse shows abnormal cortical neuron differentiation and migration patterns in utero (Cunningham et al., 2011). Furthermore, it has been demonstrated in vitro, using primary neuronal cultures from the CGG KI mice, that immature neuronal morphologies predominate (thinner, filopodial dendrites), and reduce cellular viability (Chen et al., 2010). It has also been shown in vivo that CGG KI mice as young as 12 weeks of age show ubiquitin-positive intranuclear inclusions in neurons and astrocytes in the hippocampus and only later similar pathological features appear to develop in the parietal neocortex (Hunsaker, Wenzel, Willemse, & Berman, 2009). Similarly, intranuclear inclusions are present in the internal granule cell layer in the cerebellum at 12 weeks of age (MR Hunsaker, unpublished observations). These data suggest that there are developmental influences that may contribute to later neurodegenerative processes, or at least that the progressive neuropathology begins to form relatively earlier in life than previously thought.

Modeling Molecular Correlates of FXTAS in CGG KI and CGG-CCG Mice

Both CGG KI and CGG-CCG mice have been used to evaluate the molecular cascades associated with the PM that potentially underlie FXTAS pathophysiology. The brains of the CGG KI mouse show elevated *Fmr1* mRNA levels and reduced Fmrp levels, similar to those observed in the PM and FXTAS (Brouwer et al., 2007; Brouwer et al., 2008a; Brouwer et al., 2008b; D'Hulst et al., 2009; Entezam et al., 2007; Tassone & Hagerman, 2003; Tassone et al., 2000b; Tassone et al., 2000d; Tassone et al., 2004b; Tassone et al., 2007b). An average of twofold elevation in *Fmr1* mRNA levels was detected as early as 1 week of age in CGG KI mice that persisted throughout development (Willemsen et al., 2003). In contrast to what was reported for the linear correlation between *FMR1* mRNA levels and the repeat size in human FXTAS patients (Kenneson et al., 2001), the increase in *Fmr1* mRNA levels was not correlated with the length of the repeat (Brouwer et al., 2008a). However, the data from the human patients were not from brain samples, but from blood samples or lymphoblasts. (Entezam et al., 2007) were able to show a direct relationship between CGG-CCG repeat size and *Fmr1* mRNA levels in the brains of the CGG KI mice, although the number of mice studied for the different repeat sizes was limited. Despite the increase in mRNA levels, both the CGG KI and the CGG-CCG mouse strain show an inverse correlation between CGG repeat length and Fmrp expression in the brain (Brouwer et al., 2008a; Entezam et al., 2007). One explanation is that the CGG repeat hampers the initiation of translation at the ribosome, possibly due to secondary structures formed.

Modeling Cellular Dysfunction Associated with FXTAS in CGG KI and CGG-CCG Mice

The CGG KI mouse has been used (in concert with engineered human cell lines) to demonstrate potential interacting partners of the CGG-expanded *Fmr1* mRNA to directly test a model that suggest the CGG repeat itself acts to sequester proteins from the cell and by that mechanism causes cellular dysfunction (Garcia-Arocena & Hagerman, 2010; Raske & Hagerman, 2009). For example, it was demonstrated that Sam68, a splicing factor, is sequestered by the CGG repeat expansion and thus subsequently titrated out from the rest of the cell. This results in reduced Sam68-dependent splicing events, which may be involved in the events leading up to inclusion formation as increasing Sam68 expression can prevent aggregate formation in mouse and cell lines (Sellier et al., 2010).

The CGG KI mouse has also been used to evaluate more systems level disruptions that may be present in the PM and FXTAS. In addition, the CGG KI mouse has been used to demonstrate altered expression of GABA-B receptors in the cerebellum but not neocortex (D'Hulst et al., 2009), as well as to demonstrate abnormalities along the HPA axis and amygdala similar to those proposed in PM and FXTAS that might explain the molecular mechanisms underlying the psychopathology in PM carriers and FXTAS patients (Brouwer et al., 2008b).

Modeling Pathological Features of FXTAS in CGG KI and CGG-CCG Mice

Pathologic neuroanatomical features have been demonstrated in the CGG KI mice that appear to phenocopy human FXTAS. (Greco et al., 2006) evaluated gray and white matter of brain in a number of cases of FXTAS and found a relatively large percentage (1–5%) of neurons and astrocytes in the brain contained eosinophilic intranuclear inclusions. White matter pallor and apparent thinning of the gray matter were also reported, as well as Purkinje cell dropout and axonal pathology such as torpedo axons in the cerebellum. Both the CGG KI and the CGG-CCG mouse have intranuclear inclusions in neurons throughout the brain (Brouwer et al., 2008a; Entezam et al., 2007; Hunsaker et al., 2009; Wenzel, Hunsaker, Greco, Willemse, & Berman, 2010; Willemse et al., 2003) and the CGG KI mouse has further been shown to have intranuclear inclusions in astrocytes, as well as neurons (Wenzel et al., 2010; Figure 1). In addition to the presence of intranuclear inclusions in neurons inclusion presence or absence in astrocytes has not been reported, the CGG-CCG mouse shows reduced numbers of Purkinje cells and evidence for torpedo axonal morphology similar to that reported in FXTAS (Entezam et al., 2007).

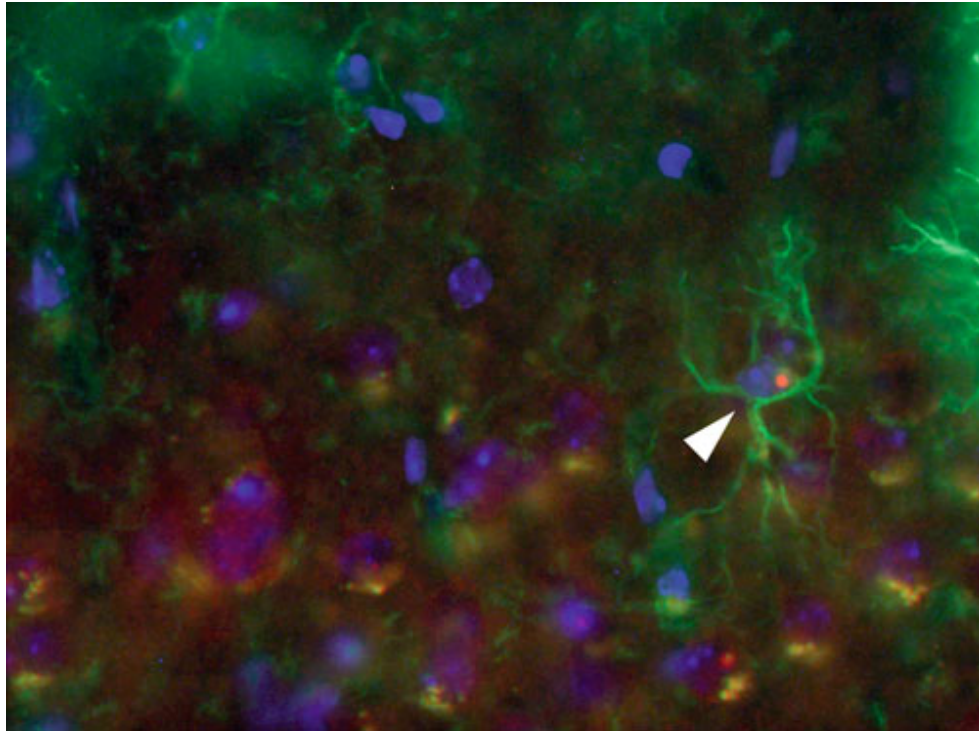


Figure 1. Astroglial cell containing an ubiquitin positive intranuclear inclusion (white arrow head) in the motor cortex of a 70 week old female CGG KI mouse with 9, 128 CGG repeats. Green=GFAP, red=ubiquitin, blue=DAPI.

In the CGG KI mouse, the distribution of intranuclear inclusions has been carried out in mice ranging from 20 to 72 weeks of age (Willemsen et al., 2003). The analysis suggested that CGG KI mouse displays progressive neuropathological features (*i.e.*, inclusions) that are most prominent in the rostral cortices, hypothalamus, olfactory nucleus, parafascicular nucleus of the thalamus, the inferior colliculus, pontine nuclei, vestibular nucleus, superficial dorsal horn of the spinal cord, and 10th cerebellar lobule. A later study further quantified intranuclear inclusion presence in the pituitary gland and amygdala (Brouwer et al., 2008b). Further analysis of CGG KI mice replicated these findings in a limited sample, but saw a much greater quantity of intranuclear inclusions in the hippocampus, particularly in the dentate gyrus (Brouwer et al., 2008a; Wenzel et al., 2010). The CGG-CCG mouse showed similar inclusions, but no regional quantifications were presented (Entezam et al., 2007).

An intriguing pattern can be seen in the distribution of the relatively early presence of intranuclear inclusions in the more primitive cortical structures, and later presence in more evolutionarily recent cortices (*cf.*, Willemsen et al., 2003). A follow-up analysis of the distribution of intranuclear inclusions undertaken by (Wenzel et al., 2010) and to a lesser extent (Hunsaker et al., 2009) demonstrated that granular cells within the olfactory bulb, cerebellum, and dentate gyrus show the highest quantity of intranuclear inclusions (roughly 50% of neurons), followed by subcortical structures including the hypothalamus, thalamus, inferior colliculus, septal nuclei, various brainstem nuclei, and the cerebellum. In the cortex, the paleocortex associated with the amygdala and hippocampus and the

entorhinal cortex (transitional cortex) show the greatest quantity of inclusions, followed by the limbic cortex and finally the rostral (*i.e.*, sensory and motor cortices) and caudal (*i.e.* parietal and visual cortices) neocortex. This pattern suggests the potential for a primarily subcortical and limbic involvement in the neuropathology that spreads to the neocortex later in life.

Although the CGG KI and CGG-CCG mouse models appear to provide very good models for the primary neuropathological features present in FXTAS, there are a number of very important differences between the species that needs to be discussed. In FXTAS, a higher percentage of astrocytes in both the grey and white matter contain intranuclear inclusions compared to the local neuron populations (Greco et al., 2002; Greco et al., 2006; Wenzel et al., 2010). Furthermore, in FXTAS the intranuclear inclusions stain easily for eosin in a hematoxylin and eosin (H&E) stain, whereas the inclusions in mice are more difficult to stain – requiring the use of immunocytochemical techniques to identify the presence of intranuclear inclusions, or at least a careful optimization of H&E staining protocols (*cf.*, Willemse et al., 2003, Figure 2). The reason for these differences is unclear and most likely does not affect the interpretation of the findings in the mouse models; the fundamental differences between species needs to be considered in all studies of comparative neuropathology resultant from the PM. On the other hand, this may be caused by the fact that we study the end stage of the disease in FXTAS patients and the mice we studied might not have reached this stage. These findings highlight the need to study the

development of disease progression in the mice instead of focusing solely on the final stage in patients.

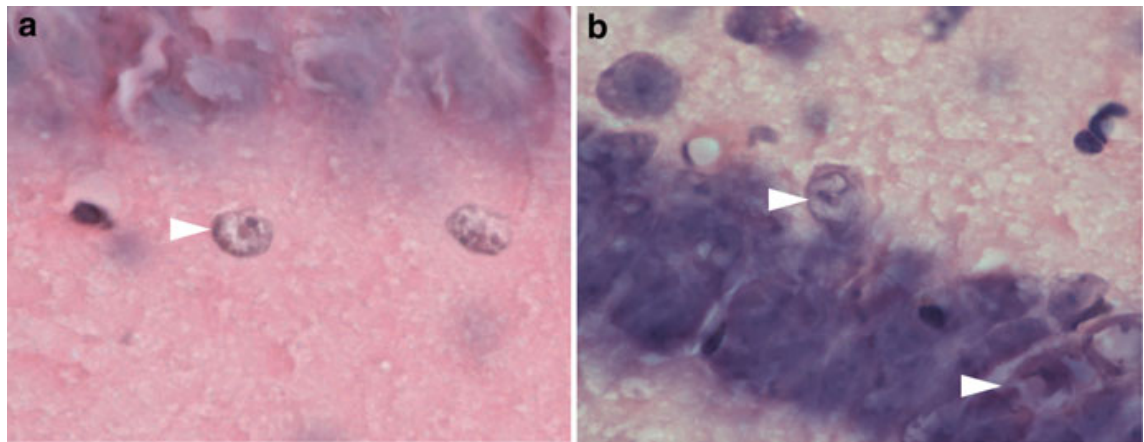


Figure 2. **a.** H&E stained hippocampus demonstrating an interneuron in the stratum radiatum of CA1 with an intranuclear inclusions (arrow head). **b.** H&E stained hippocampus demonstrating CA1 pyramidal cells with intranuclear inclusions (arrow heads). Both images are from a 52 week old female CGG KI mouse with 8, 152 CGG repeats.

What remains unknown about the role of these neuropathological features in the PM and FXTAS is the developmental time course of inclusion formation as well as the role of these inclusions in cellular processing/toxicity. The first of these questions has been preliminarily addressed, for example, using cellular models (Sellier et al., 2010), but no work to date has evaluated CGG KI or CGG-CCG tissue at ages <12 weeks of age. Such work is necessary to determine a potential age where the brain is free from pathological features to evaluate preventative treatment strategies. However, the Purkinje cell specific transgenic mice (Hashem et al., 2009) very nicely show that the formation of inclusions also occurs when expressing expanded CGG RNA independent of *Fmr1* context, suggesting a strong role for tandem CGG repeat containing RNA toxicity in intranuclear inclusion formation.

Modeling Behavioral Sequelae of FXTAS in CGG KI and CGG-CCG Mice

Until recently, the PM was thought to be free of behavioral and molecular sequelae (Cornish et al., 2005; Cornish et al., 2008a; Cornish et al., 2008b; Cornish et al., 2009; Hagerman & Hagerman, 2004b). Once it was determined that there were potential aberrant behavioral and psychiatric phenotypes in the PM prior to FXTAS, the study of the mouse models were expanded to model these phenotypes. Unfortunately, neither the CGG KI nor the CGG-CCG mouse shows classic tremor or ataxia on basic behavioral assays (Qin et al., 2011; Van Dam et al., 2005). This lack of a clear motor phenotype suggests that either the mouse models are lacking, or there are differences between species that prevent potential motor phenotypes from being observed (*i.e.*, methodological differences in tests between species, bipedal gait in humans vs. quadrupedal in mice, etc.).

The CGG-CCG mouse has only been preliminarily evaluated for a behavioral phenotype. The CGG-CCG mouse has been shown to be slightly hyperactive and shows reduced anxiety in the open field and elevated zero mazes. Furthermore, the CGG-CCG mouse shows impaired passive avoidance learning and a slight reduction in social interaction (Qin et al., 2011). They interpret these results to indicate a subtle deficit similar to those reported in the *Fmr1* KO model of FXS.

The CGG KI mouse has been evaluated for the cognitive deficits present in the PM and FXTAS. (Van Dam et al., 2005) demonstrated a clear age-related worsening of motor performance on the accelerating rotarod and memory impairments on the water maze. To further characterize these deficits, (Hunsaker

et al., 2009) evaluated spatial processing in CGG KI mice using tasks designed to more specifically evaluate spatial processing than the water maze. They found that CGG KI mice showed significant deficits in spatial processing compared to littermate control animals as early as 12 weeks of age. On a similar task involving learning the relationship between objects and their location in space, the same mice showed deficits only at 48 weeks of age. Intriguingly, in a separate group of animals, (Hunsaker et al., 2009) evaluated the presence of intranuclear inclusions in the dentate gyrus in the hippocampus (which subserves performance in the first task) and the parietal cortex (which subserves performance in the second task; *cf.*, Goodrich-Hunsaker, Hunsaker, & Kesner, 2005; Goodrich-Hunsaker, Hunsaker, & Kesner, 2008b). They found that there were inclusions (albeit low in number) in the dentate gyrus of the CGG KI mice as early as 12 weeks of age and progressively more with increasing age. Intranuclear inclusions were only detectable in the parietal cortex at 48 weeks of age. These findings suggest that the development of neuropathology follows a similar time course as the emergence of behavioral dysfunction in the CGG KI mouse, implying a potential neuropathological correlate to the spatial processing deficits.

In a subsequent experiment, female CGG KI mice were tested for their ability to learn and remember short sequences of stimuli. In this task, the mice were presented with three pairs of visual objects for 5 min each separated by 5 min intervals. Afterward, the mice were presented with two tests, one for temporal order, wherein the first object and the last object encountered were

presented and the mouse was allowed to preferentially explore. The second test was for novelty, and the first object encountered and a novel, never before seen object was presented. Female CGG KI mice showed a CGG-repeat length-dependent deficit for learning and remembering sequences. Mice with 80–100 CCG trinucleotide repeats performed worse than wild type littermate mice, but performed better than mice with 140–190 CGG repeats. All animals performed the novelty task equally well (Hunsaker, Goodrich-Hunsaker, Willemsen, & Berman, 2010). These data suggest that temporal processing is deficient in CGG KI mice. What makes this finding all the more intriguing is that these data were from female mice, who should be 50% as affected as male mice, and thus should show a more subtle phenotype. As such, male mice should show much more profound deficits on the same task; however, this has yet to be assessed.

To better evaluate the cognitive and behavioral phenotypes in CGG KI mice, there is a need to develop a number of novel tasks to more precisely evaluate specific behaviors proposed to be affected by the PM and FXTAS. As it has been suggested previously that the traditional tasks evaluating motor function often miss subtle pathology, task development is needed in this arena.

In order to identify and potentially quantify more subtle motor deficits, (Hashem et al., 2009) evaluated mice with expanded CGG repeats expressed from the L7/pcp2 promoter in cerebellar Purkinje cells on the rotarod measure of motor function. They found that these mice showed age-related deficits in the rotarod (*i.e.*, the mice fell from the rod at slower speeds and were unable to stay on the rotating drum as long as controls even at slow speeds).

These findings suggest motor deficits in the mouse models of FXTAS, but to date such robust findings using the rotarod have not been found in the other FXTAS mouse models. However, (Van Dam et al., 2005) did find a mild rotarod phenotype in old CGG KI mice. The Purkinje-specific transgenic mice demonstrate that overexpression of the expanded CGG RNA in Purkinje cells is sufficient to cause motor dysfunction.

As the primary tremor present in FXTAS is an intention tremor, it may be worthwhile to evaluate CGG KI and CGG-CCG mice on a skilled forelimb reaching tasks that allow precise quantification of limb use. Such tasks may uncover subtle tremor missed on tests of more gross motor function (Alaverdashvili & Whishaw, 2008; Blume, Cass, & Tseng, 2009; Farr & Whishaw, 2002; Farr, Liu, Colwell, Whishaw, & Metz, 2006; Metz & Whishaw, 2002; Metz & Whishaw, 2009; Ward & Brown, 1997; Whishaw & Metz, 2002; Whishaw et al., 2010). To better model the gait ataxia, skilled walking tasks similar to those used in grid walking paradigms could be applied as they are in models of alcohol intoxication that allow for similarly specific quantification of walking behavior.

Another common cognitive disruption in FXTAS is a sort of dysexecutive syndrome (Brega et al., 2008) involving cognitive control and attentional processing. Although difficult to model in mice, tasks such as the five choice serial reaction time task or biconditional discrimination tasks can be used to model these processes (George, Duffaud, Pothuizen, Haddon, & Killcross, 2010; Haddon, George, & Killcross, 2008; Marquis, Killcross, & Haddon, 2007). Similarly, there are attentional tasks in rats that can be modified for mice that can

get at specific attentional processes affected in FXTAS (Ward & Brown, 1996; Ward & Brown, 1997; Ward, Sharkey, & Brown, 1997; Ward, Sharkey, Marston, & Brown, 1998).

Furthermore, as the parietal lobe appears to be atrophied in FXTAS, tasks specifically evaluating parietal functions need to be performed in mice (similar to the second task mentioned above from Hunsaker et al., 2009). As the time course for the development of neuropathological features has been described in the CGG KI mouse, this mouse provides a unique opportunity to thoroughly evaluate the specific hypotheses concerning the role of molecular factors that may be underlying the neurocognitive deficits present in the PM and FXTAS.

Utility of CGG KI and CGG-CCG Mice for Interventional Studies

To date, no therapeutic studies have been performed on any of the FXTAS mouse models, primarily because there were no clearly defined behavioral outcome measures and no real biomarkers to speak of. The primary difficulty present in evaluating therapies in the FXTAS mouse models is the fact that FXTAS is defined as a late onset neurodegenerative disorder characterized by a motor phenotype. This means that, in theory, animals have to be set aside for the better part of a year prior to treatment and then the outcome measures (*i.e.*, latency to fall on the accelerating rotarod) are not all that clear cut. One potential solution to this problem is to use the mouse models reported by (Hashem et al., 2009) for evaluating treatments of the motor phenotype. In these mice the motor phenotype is specifically exaggerated in those mice at an age earlier than either the CGG KI or CGG-CCG mice; however, these mice are transgenic and express the CGG repeat in Purkinje cells, not all cells, so this model is incomplete from a clinical perspective.

To better dissect the respective roles of different molecular factors for FXTAS disease progression, further/new transgenic mouse models need to be generated to identify the respective roles of different cell types for FXTAS. The development of transgenic mouse models expressing an expanded CGG RNA in different cell populations at higher levels will facilitate the design of experiments evaluating sufficiency, necessity, and timing of disease progression. The generation of inducible mice will facilitate research into treatment options and

outcomes, as well as answer questions concerning the potential reversibility of neuropathology and aid in developing pharmaco- and gene-targeted therapies.

The CGG KI mouse develops subtle behavioral phenotypes that appear to be present from ages as early as 12 weeks or earlier (though the animals have not been tested earlier than 12 weeks of age; Hunsaker et al., 2009; Hunsaker et al., 2010). This mouse model, however, does not show motor deficits in the rotarod until advanced ages (Van Dam et al., 2005). A combined strategy of using the CGG KI and the transgenic mice expressing CGG repeats in Purkinje cells to model different aspects of the FXTAS disease process may provide valuable insights into the nature of behavioral and motor problems in FXTAS.

Finally, an additional outcome measure may be to evaluate effect or stress responses in the CGG KI mouse. As Brouwer et al. (2008b) showed, CGG KI mice exhibit abnormal HPA activity, which correlated with an abnormal stress response in the amygdala. If these findings extend earlier in life similar to the behavioral measures, then reversing a dysfunctional HPA axis/stress response may provide benefit to FXTAS.

Conclusion

The CGG KI and CGG-CCG mouse models for the fragile X PM and FXTAS provide an invaluable resource for the translational scientist to generate and evaluate hypotheses into the molecular correlates of FXTAS disease onset and progression. These mouse models further provide outcome measures and putative biomarkers that may aid in the development and evaluation of therapeutic interventions.

Acknowledgements

This work was made possible by a Roadmap Initiative grant (UL1 DE019583) from the NIDCR in support of the NeuroTherapeutics Research Institute (NTRI) consortium and Grant RL1 NS064211 from NINDS. This work was also supported by a grant (UL1 RR024146) from the National Center for Research Resources, a component of the National Institute of Health, and NIH Roadmap for Medical Research. This work was also supported by a research grant from the National Fragile X Foundation (RKH).

Chapter 2

The Pathology of FXTAS

Abstract

In 2002 a syndrome of tremor, ataxia, cognitive decline, and the presence of unique ubiquitin staining intranuclear inclusions in the brain was discovered in premutation males carrying an expansion of between 55 and 200 CGG trinucleotide repeats on the *FMR1* gene. This clinical syndrome is now known as fragile X-associated tremor/ataxia (FXTAS) and has been found in both male and female carriers of the expanded premutation allele. The goal of this chapter is to summarize what is known about the anatomical pathology associated with the fragile X premutation and particularly in those individuals with FXTAS. Neuropathology in FXTAS was initially found in the central nervous system, but recent evidence has demonstrated pathological features, including intranuclear inclusions, in the peripheral nervous system, the enteric nervous system, and the neuroendocrine system. The precise cellular dysfunctions that underlie these pathologic features are currently under intense investigation with the goal of prevention and treatment of this devastating disorder.

This chapter has been published as:

Greco, C. M., Hunsaker, M. R., & Berman, R. F. (2010). *Pathology of FXTAS*. In F. Tassone & E. Berry-Kravis (Eds.) *The Fragile X-Associated Tremor/Ataxia Syndrome*. Springer Publishing.

Introduction

Fragile X-associated tremor/ataxia syndrome (FXTAS) is a late-onset, progressive neurodegenerative disorder that affects many carriers of an *FMR1* premutation, an expanded trinucleotide repeat sequence (CGG) in the 5' untranslated region (5' UTR) of the *FMR1* gene. The gene is polymorphic, and in unaffected individuals there are roughly 5–45 CGG repeats, while individuals with a premutation carry an allele of 55–200 CGG repeats and show a 2- to 8-fold increase in levels of the *FMR1* mRNA (see Tassone & Hagerman, 2010).

Patients with FXTAS typically show cerebellar ataxia, tremor, cognitive deficits, peripheral neuropathy, autonomic dysfunction, and psychiatric involvement (see Grigsby, Brega, Seritan, & Bourgeois, 2010; Leehey, Berry-Kravis, Goetz, & Hagerman, 2010). The disorder is thought to arise from a toxic RNA gain of function that is caused by over-expression of the expanded CGG *FMR1* mRNA in premutation carriers (Allen, Leehey, Tassone, & Sherman, 2010; Kenneson et al., 2001; Tassone et al., 2000c). Magnetic resonance imaging (MRI) also shows that patients with FXTAS have mild to moderate brain atrophy in both cerebrum and cerebellum and white matter changes in cerebrum and cerebellum. Increased T2 signal intensity in the middle cerebellar peduncles (MCP) is commonly found in subjects affected by FXTAS (Brunberg et al., 2002; Rivera, Stebbins, & Grigsby, 2010). Finally, the neuropathological hallmark of FXTAS is the presence of eosinophilic intranuclear inclusions in both neurons and astrocytes. These inclusions are found throughout the brain and in the autonomic nervous system as well as in non-nervous system tissues (e.g.,

pancreas). In light of these unique findings, the proposed diagnostic criteria for FXTAS have been revised and now include the presence of intranuclear inclusions as a major criterion (Hagerman & Hagerman, 2004a; Jacquemont et al., 2004b).

Intranuclear Inclusions

Intranuclear inclusions are the distinctive pathological finding among premutation carriers affected by FXTAS. They have also been observed in a knock-in mouse model of the *FMR1* premutation (Grigsby et al., 2010; Leehey et al., 2010). Observed initially in human brain tissues (Greco et al., 2002), eosinophilic intranuclear inclusions are widely distributed in both neurons and astrocytes, being found in many different regions throughout the brain, including the frontal cortex, hippocampus, ependymal cells, choroid plexus, brain stem nuclei, and cerebellum (Greco et al., 2002; Greco et al., 2006). Given the significance of clinical symptomatology related to the limbic system, it is important to note that the highest percentage of inclusions in FXTAS cases is in the hippocampus. Immunohistochemically, these inclusions stain positive for ubiquitin, lamin A/C, and a number of heat-shock proteins (Iwahashi et al., 2006). They stain negative for tau isoforms, α -synuclein, and polyglutamine peptides and appear to reflect a new class of nuclear inclusion disorder as compared to other triplet repeat disorders, such as Huntington's disease and some of the spinocerebellar atrophies (SCA). FXTAS is also distinct from neuronal intranuclear inclusion disorder (NIID) (reviewed by Hagerman & Hagerman, 2004a). Furthermore, these inclusions do not contain any single predominant protein species; the most prominent protein accounts for only roughly 7% of the total protein mass (Iwahashi et al., 2006). Also noteworthy is that in patients with FXTAS, and in contrast to patients with CAG repeat degenerative disorders and inclusions, the protein product of the *FMR1* gene, FMRP, is structurally normal.

and present at relatively normal or only slightly reduced expression levels, due to the fact that the expanded CGG repeat occurs in a non-coding portion (5' UTR) of the gene.

A highly efficient, flow-based isolation and purification of inclusions from post-mortem FXTAS brain tissues has allowed for mass spectrometric analysis of the entire protein complement of the isolated inclusions as well as follow-up immunohistochemical analysis to conclusively identify more than 20 inclusion-associated proteins. Several proteins appear to be ubiquinated and/or polyubiquinated in these purified inclusions, but ubiquinated proteins are the minority (Iwahashi et al., 2006). Ubiquitin is present within intracellular aggregates of a wide range of neurological disorders, not just FXTAS (Woulfe, 2008). In the case of FXTAS, ubiquitin, a proteasomal degradation product, is utilized as a marker for isolation or detection of intranuclear inclusions by immunostaining (Greco et al., 2002; Greco et al., 2006; Iwahashi et al., 2006). Among the proteins identified within the inclusions are the RNA-binding protein, hnRNP A2, several intermediate filament (IF) proteins, including lamin A/C, the small heat-shock protein αB-crystallin, α-internexin, and other neurofilament (NF) proteins. The *FMR1* mRNA is present, but only as a minor component within the inclusions (Tassone et al., 2004b), and FMRP has not yet been found to be present in the inclusions. All of the proteins found in the inclusions are potential candidates for involvement in the RNA gain of function that may underlie FXTAS pathology (Hagerman & Hagerman, 2004b; Iwahashi et al., 2006).

The time course of inclusion formation relative to clinical onset of disease is not yet known, nor is it understood whether the intranuclear inclusions are directly causative of FXTAS pathophysiology and symptomatology, or simply a reflection of the progression of the disorder. If the inclusion materials are active or neurotoxic, they may contribute directly to damage to the nervous system. However, it is also possible that the intranuclear inclusions may represent a protective mechanism, serving as a repository for disabled enzymes and their products as has been proposed for Huntington's disease (Bowman, Yoo, Dantuma, & Zoghbi, 2005). Ongoing research is examining these possibilities.

It is unclear whether the *FMR1* premutation predisposes individuals to or accelerates the course of other degenerative diseases of the central nervous system (or vice versa), and this is also a topic of active investigation. A number of FXTAS cases that have come to autopsy showed Lewy body formation in the substantia nigra, whether or not Parkinson's disease (PD) was clinically identified (Greco et al., 2002). Two females carrying the FXTAS premutation who suffered early onset Alzheimer's disease (AD) symptomatology along with tremor and ataxia showed histopathological features of both AD and FXTAS. The superior and middle temporal gyri in these two women showed as high a percentage of intranuclear inclusions as seen in the hippocampus (unpublished data). In a reported case of concurrent FXTAS and multiple sclerosis (MS), the patient showed patchy and diffuse signal intensity alterations in white matter on T2-weighted MRI scans. Histologically, there were numerous regions of demyelination as well as the presence of intranuclear inclusions (Figure 3).

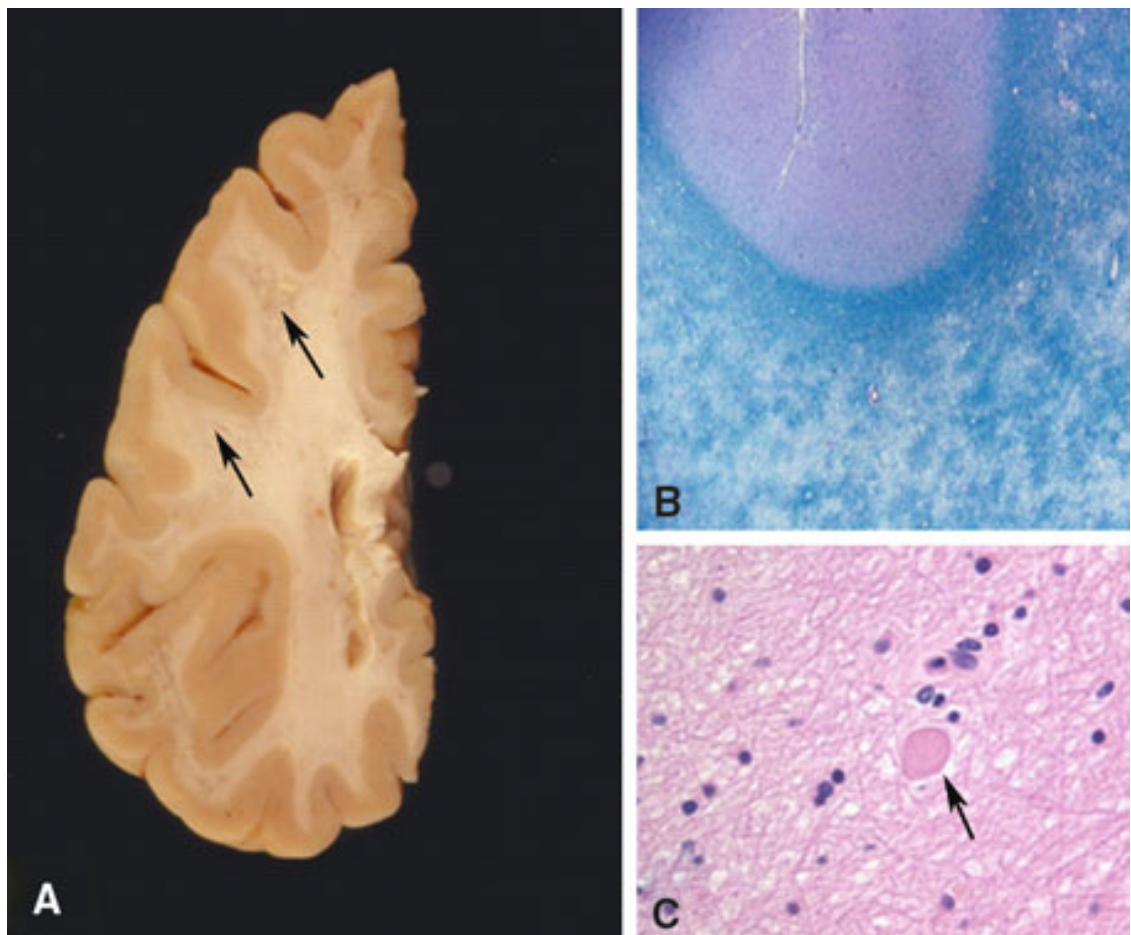


Figure 3. **A.** Severe subcortical white matter degeneration, as seen in some cases of FXTAS autopsy brains; **B.** Corresponding patchy white matter loss, even affecting cortical U-fibers ($\times 40$, LFB-PAS stain); **C.** Occasional swollen axons can be identified in cerebral and cerebellar white matter and middle cerebellar peduncles.

Brain Pathology

Gross Pathology

Gross abnormalities in the brain include varying degrees of cortical atrophy, patchy softening and loss of deep white matter, and brain stem atrophy, especially of the pons. When PD is concurrent, the substantia nigra is pale. There are no notable gross structural changes in the spinal cord. When AD is concurrent, cortical atrophy is often more prominent than that usually seen in FXTAS alone, although only a few cases of this type have been identified.

Microscopic Brain Pathology

At the present time, the intranuclear inclusions of FXTAS lack a distinctive molecular identity. On H&E stains, they are discrete, hyaline-appearing, eosinophilic, round to slightly ovoid bodies (Figure 4). They typically measure 2–5 µm in diameter and are almost unanimously single, and are only very rarely double within a nucleus. They are periodic acid-Schiff (PAS), silver, tau, and neurofilament (NF) negative but stain positively for ubiquitin. Although inclusions have been identified in neurons throughout the brain, they have not been seen in Betz cells of the motor cortex and in only one case have been found in Purkinje cells of the cerebellum. Purkinje cell loss beyond that expected with otherwise normal aging and axonal swellings/torpedoes are commonly seen in FXTAS. Bergmann gliosis accompanies Purkinje cell loss in the cerebellum (Greco et al., 2002; Greco et al., 2006). Inclusions are also present in neurons of the dentate nucleus and astrocytes throughout the cerebellum. When clinical PD has been

diagnosed, cytoplasmic Lewy bodies are seen in pigmented neurons of the substantia nigra, and when FXTAS coexists the intranuclear inclusions can be seen in the pigmented neurons of the substantia nigra, whether or not cytoplasmic Lewy bodies are present. In both symptomatic male and female premutation carriers who also carry a diagnosis of AD (*i.e.*, diagnostic features of AD based on established criteria; 1997; Braak & Braak, 1991), the intranuclear inclusions of FXTAS can be seen in pyramidal neurons of the hippocampus that also contain neurofibrillary tangles.

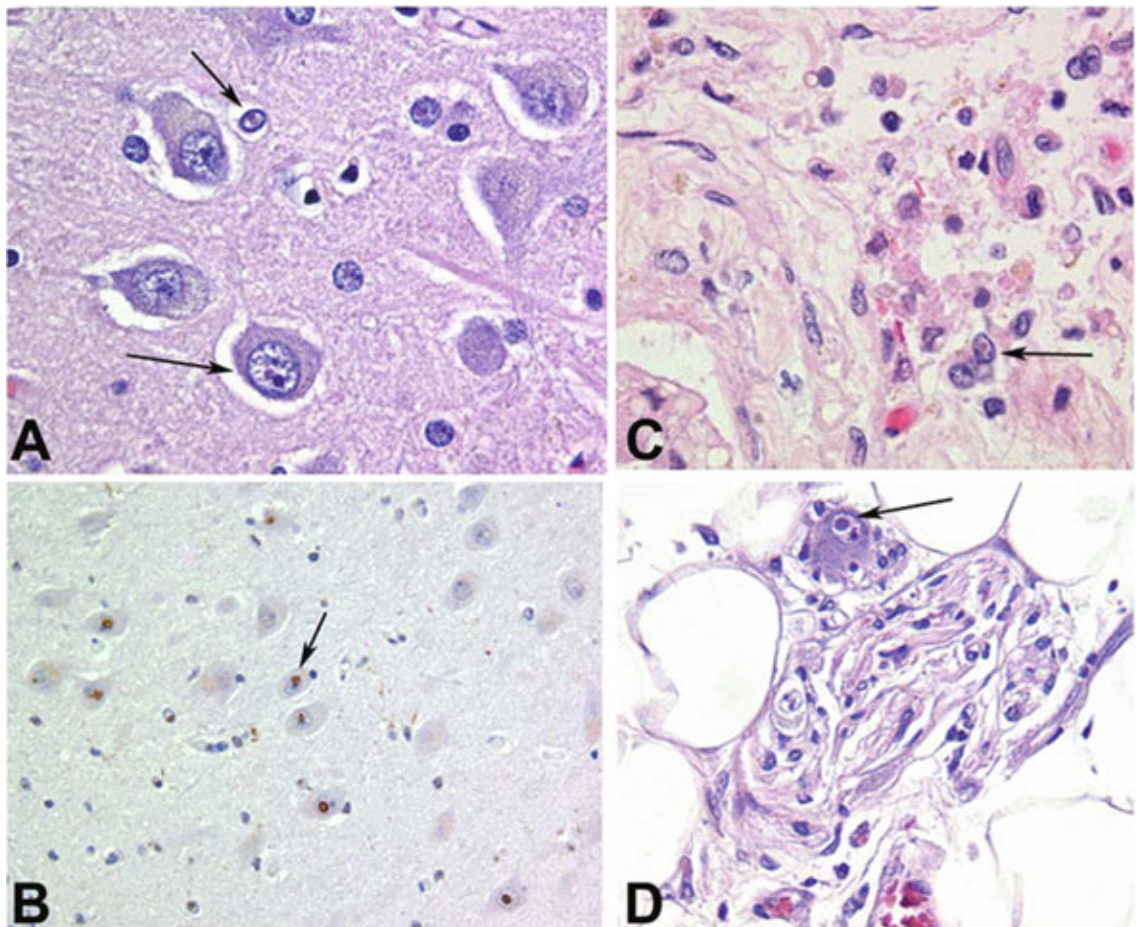


Figure 4. **A.** Neuronal and astrocytic intranuclear inclusions, CA4 ($\times 400$, H&E stain). **B.** Ubiquitin immunoperoxidase stain showing numerous intranuclear inclusions, CA4, of hippocampus ($\times 200$). **C.** Intranuclear inclusions, similar to those seen in the nervous system, are identified in Leydig cells (testosterone producing) of the testicles ($\times 200$, H&E). **D.** Epicardial fat pad autonomic ganglion cell harboring an intranuclear inclusion ($\times 200$, H&E).

In astrocytes, intranuclear inclusions are usually surrounded by a clear halo, although this may be an artifact of tissue preparation. They are present diffusely in both protoplasmic astrocytes of gray matter and fibrillary astrocytes of white matter of the brain and spinal cord. They are also seen in pituicytes, the modified astrocytes of the posterior pituitary gland (Louis, Moskowitz, Friez, Amaya, & Vonsattel, 2006). Inclusions are also present in cells of the choroid plexus and ependyma, both of which have astrocyte lineages. In contrast, they are rarely present in microglia and have not been identified in oligodendrocyte nuclei or endothelial cells of the brain. The appearance of intranuclear inclusions is similar between males and females and between brain and spinal cord. While the spinal cord is otherwise grossly unremarkable, intranuclear inclusions have been identified in astrocytes and autonomic neurons of the intermediolateral column of the spinal cord but not in anterior horn cells (Gokden, Al-Hinti, & Harik, 2009; Greco et al., 2006). Gokden et al. (2009) have also observed intranuclear inclusions in paraspinal sympathetic ganglia.

The appearance of intranuclear inclusions by electron microscopy is similar in neurons and astrocytes and appears as non-membrane-bound collections of granulofilamentous material (Greco et al., 2002). The filaments appear as straight rod-like proteins arranged in a haphazard manner (Gokden et al., 2009; Greco et al., 2002). The ultrastructural appearance of these inclusions is, however, otherwise not particularly informative.

Morphometric Analysis: Neuronal and Inclusion Counts

Percentages of neurons and astrocytes containing intranuclear inclusions have been determined only in one study, for frontal cortex, hippocampus, and the ventral pontine region of 8 male FXTAS patients and 10 normal (no neurological disease), age-matched control subjects. Quantification of inclusions was carried out using a computer-based imaging and cell-counting system (StereoInvestigator, MBI, Inc., Williston, VT) on H&E-stained slides. The number of neurons and astrocytes with intranuclear inclusions (actual counts and percentages) is presented in Table 2 (summary of Tables 3–5 from Greco et al., 2006). No inclusions were seen in control cases.

Brain region	Percentage of neurons with inclusions	Percentage of astrocytes with inclusions
<i>Frontal cortex</i>		
Grey matter	4.4 +/- 1.4	16.7 +/- 3.8
White matter	22.0 +/- 6.4	5.0 +/- 1.9
<i>Hippocampus</i>		
Pyramidal neurons	10.1 +/- 2.8	10.3 +/- 4.2
Granule cells	2.1 +/- 1.0	26.6 +/- 6.1
Hilar neurons	11.0 +/- 3.6	28.3 +/- 6.2
Pontine nuclei	0.2 +/- 0.1	20.8 +/- 3.1

Summary of data contained in Tables 3-5 in (Greco et al., 2006)

Table 2. Percentage of neurons and astrocytes with intranuclear inclusions in FXTAS patients

In general, more intranuclear inclusions were observed in astrocytes than in neurons (the hippocampal CA1 subregion was an exception, but the pyramidal cell layer was counted, which contains relatively few astrocytes compared to neurons relative to the cortex), although there was a great deal of variability across subjects. Statistical correlations (Spearman's rho) were calculated between histological findings and molecular measures. Significant positive correlations were present between the percentages of both neurons and astrocytes with inclusions in several brain regions and the number of CGG repeats. However, correlations between percentage inclusions and peripheral blood leukocyte *FMR1* mRNA or FMRP levels were not statistically significant. This last observation is not surprising in view of the large differences between expression levels in brain and blood and the region-specific differences in *FMR1* mRNA levels in brain (Tassone et al., 2004a). Most striking was the clinical–molecular correlation that showed a significant decrease in age of death with increasing CGG repeat length (*i.e.*, the greater the CGG repeat number, the earlier the age of death; Greco et al., 2006).

White Matter Pathology

White matter changes seen on MRI studies include non-specific, subcortical, patchy regions of increased T2 signal intensity in the cerebrum. In a high percentage of FXTAS cases, increased T2 signal intensity is present in the middle cerebellar peduncles

(Brunberg et al., 2002; Rivera et al., 2010) and can also be seen in the deep cerebellar white matter and brain stem.

When these regions are examined microscopically using histologic and immunochemical stains, abnormal areas of white matter show spongiosis, axonal degeneration, and myelin loss. The same histological features are identified in damaged white matter of the cerebellum (Greco et al., 2002; Greco et al., 2006). In cases with the most severe cerebral white matter changes, scattered fibrillary astrocytes are greatly enlarged by irregular expansion of cytoplasm that contains lysosomal debris. These same cells may also contain intranuclear inclusions. Rare axonal spheroids have been identified in spongiotic middle cerebellar peduncles on H&E and neurofilament stains. The middle cerebellar peduncles may also show myelin pallor on LFB–PAS stain (Greco et al., 2006).

Peripheral Nervous System

While the intranuclear inclusions of FXTAS were first identified in neurons and astrocytes of the brain in 2002 (Greco et al., 2002), systemic locations of the inclusions in the peripheral nervous system and other tissues are rapidly being cataloged and published in the medical literature.

Autonomic System

Inclusions have been observed in paraspinal sympathetic ganglion, ganglion cells of adrenal medulla, ganglion cells of the myenteric plexus of the stomach, and ganglion cells of a subepicardial ganglion. Also, intranuclear

inclusions have been identified in dorsal root ganglion neurons in the spinal cord (autonomic neurons), but not in the ventral root (Gokden et al., 2009). Symptoms corresponding to this autonomic pathology may include mega-esophagus, constipation, bladder spasms, orthostasis, hypertension, and sexual dysfunction (Berry-Kravis, Hall, Leehey, & Hagerman, 2010; Leehey et al., 2010).

Peripheral Nerve

Non-specific features of axonal degeneration have been seen in nerve examined at autopsy. Inclusions have not been observed by light microscopy. Clinically, neuropathic features are seen in male premutation carriers (Berry-Kravis et al., 2007b), and peripheral neuropathy of variable severity is noted in individuals with FXTAS with reduced peripheral nerve conduction velocity (Soontarapornchai et al., 2008). The possible causes of this dysfunction are unknown.

Skeletal Muscle

Light microscopy, including histochemical and enzyme staining, has shown no pathological changes. Ultrastructural examination has yielded no distinctive abnormalities.

Neuroendocrine

In a limited number of cases (one male and one female), intranuclear inclusions within the anterior and posterior pituitary have been identified and may

be associated with dysregulation of neuroendocrine function (Gokden et al., 2009; Greco et al., 2007; Louis et al., 2006). Similar findings have been made for the CGG KI mouse (Willemsen et al., 2010). This observation is of particular interest in view of the elevated cortisol levels found in FXTAS, as well as an increased incidence of anxiety disorders and depression (Bourgeois et al., 2009; Hunter et al., 2008b; Rodriguez-Revenga, Madrigal, Alegret, Santos, & Mila, 2008).

Testicular pathology has been documented in two cases of FXTAS stained with H&E, including tubular fibrosis, decreased numbers of Leydig cells, and decreased spermatogenesis. Sertoli cells were abundant in the tubules along with a scant number of germ cells and spermatozoa that were remnants of germ maturation, but these changes were comparable to those seen in normal age-matched controls. There were also eosinophilic intranuclear inclusions in a small percentage of the Leydig cells in both cases as well as in the myoid cells of the tubular walls. Inclusions within the Leydig cells may be related to decreased levels of testosterone in some younger males with FXTAS who suffer premature erectile dysfunction. The presence of intranuclear inclusions in myoid cells in testicular connective tissue compartments in FXTAS is intriguing. The tunica propria of the testicle is a component of the tunica albuginea and it is the middle of the 3 layers of the fibrous capsule beneath the scrotal skin that protects and supports the testes. Among other cellular components, the tunica albuginea contains myofibroblasts. In the tunica propria smooth muscle cells are involved in contractile and transport functions. Inclusions in these cells suggest that other

cell populations outside of the nervous system may also have inclusions. This finding raises the possibility of identifying easily accessible diagnostic tissue for biopsy, and such tissue samples could be used for diagnostic purposes or for monitoring therapeutic responses to treatment (Greco et al., 2007).

Summary

Since the initial discovery in 2002 that male premutation carriers with a clinical syndrome of tremor, ataxia, and cognitive decline showed a unique intranuclear inclusion disorder in pathological studies, there have been further studies elucidating the histologic, molecular, and biochemical features of the inclusions. The peripheral nervous system, specifically the autonomic system, is clearly involved, as is the neuroendocrine system. Cellular dysfunctions that underlie these pathologic features are currently under intense investigation with the goal of prevention and treatment of this devastating disorder.

Chapter 3

Ubiquitin-Positive Intranuclear Inclusions in Neuronal and Glial Cells in a Mouse Model of the Fragile-X Premutation

Abstract

Fragile X-associated tremor/ataxia syndrome (FXTAS) is an adult-onset neurodegenerative disorder caused by CGG trinucleotide repeat expansions in the fragile X mental retardation 1 (*FMR1*) gene. The neuropathological hallmark of the disease is the presence of ubiquitin-positive intranuclear inclusions in neurons and in astrocytes. Ubiquitin-positive intranuclear inclusions have also been found in the neurons of transgenic mice model carrying an expanded CGG (98) trinucleotide repeat of human origin, but have not previously been described in glial cells. Therefore, we used immunocytochemical methods to determine the pathological features of nuclear and/or cytoplasmic inclusions in astrocytes, Bergmann glia and neurons, as well as relationships between inclusion patterns, age, and repeat length in CGG knock-in (KI) mice in comparison with wild type mice. In CGG KI mice, ubiquitin-positive intranuclear inclusions were found in neurons (e.g., pyramidal cells, GABAergic neurons) throughout the brain in cortical and subcortical brain regions; these inclusions increased in number and size with advanced age. Ubiquitin-positive intranuclear inclusions were also present in protoplasmic astrocytes, including Bergmann glia in the cerebellum. The morphology of intranuclear inclusions in CGG KI mice was compared to that of typical inclusions in human neurons and astrocytes in postmortem FXTAS brain tissue. This new finding of previously unreported pathology in astrocytes of

CGG KI mice now provides an important mouse model to study astrocyte pathology in human FXTAS.

This chapter has been published as:

Wenzel, H. J., Hunsaker, M. R., Greco, C. M., Willemsen, R., & Berman, R. F. (2010). Ubiquitin positive intranuclear inclusions in neuronal and glial cells in a mouse model of the fragile X premutation. Brain Research, 1318, 155-166.

My role in this study was to perform immunoperoxidase and immunofluorescence analysis of mouse tissue in parallel with Dr. Jürgen Wenzel. I also was responsible for analyzing and photographing the human tissue reported in this study.

Introduction

The Fragile X mental retardation gene (*FMR1*) is polymorphic for the length of CGG tandem trinucleotide repeat in the 5'-untranslated region (5'-UTR). Repeat lengths in the general population range from 5–55, while full mutations with repeat lengths above 200 result in hypermethylation of *FMR1*, transcriptional silencing and the clinical syndrome Fragile X mental retardation (FXS). Intermediate length CGG expansions between 55–200, referred to as the fragile X premutation, have now been identified in patient populations and are associated with a unique, progressive, late onset, neurodegenerative disorder called Fragile X-associated tremor/ataxia syndrome (FXTAS). The neurological symptoms of FXTAS include intention tremor and ataxia, peripheral neuropathy, neuropsychological problems (anxiety, depression), and cognitive impairments including dementia at late stages of the disorder (Berry-Kravis et al., 2007b; Hagerman & Hagerman, 2004b; Hagerman et al., 2007). Radiologic changes seen on MRI include patchy T2 signal hyperintensities in cerebral white matter and in the middle cerebellar peduncle (“the MCP sign”), and overall brain atrophy (Brunberg et al., 2002). The neuropathological hallmark of FXTAS is the presence of eosinophilic intranuclear inclusions in neurons and astrocytes throughout the brain that stain positive for ubiquitin (Greco et al., 2002; Greco et al., 2006; Tassone et al., 2004a). In contrast to FXS where gene silencing occurs, FXTAS is associated with increased transcription resulting in 3–8 fold elevations in levels of *FMR1* mRNA in leukocytes. However, translation of the *FMR1* mRNA with expanded CGG repeats in the premutation range is inefficient so that levels

of the gene product, Fragile X mental retardation protein (FMRP) are paradoxically low (Tassone et al., 2000c). The disorder appears to be due to an “RNA toxic gain of function”, although the mechanisms for disease progression, including formation of intranuclear ubiquitin-positive inclusions in neurons and astrocytes are not well understood (Oostra & Willemsen, 2009).

Human carriers with the fragile X premutation underlying FXTAS have intranuclear inclusions in neurons and astrocytes throughout the brain. In humans, it is still unknown at what age inclusions form due to the progressive nature of the disorder and the advanced age at which FXTAS is typically diagnosed, as well as that the tissue diagnosis is made at autopsy. It has been shown that inclusions can form after as few as eight days in vitro after an expanded CGG repeat in the premutation range is introduced into human primary neural progenitor cells and into established cell lines (Arocena et al., 2005). In order to better characterize FXTAS and to study its molecular mechanisms, knock-in (KI) mice bearing expanded CGG trinucleotide repeats in the 5'-UTR have been created. The CGG KI mouse model of the fragile X premutation was generated by replacing the endogenous CGG8 trinucleotide repeat with a CGG98 trinucleotide repeat of human origin via homologous recombination (Bontekoe et al., 1997; Willemsen et al., 2003). Similar to the human cases of FXTAS, neurons of these CGG KI mice show intranuclear inclusions that stain for ubiquitin in neurons in a number of brain regions (Bontekoe et al., 1997; Brouwer et al., 2008a; Willemsen et al., 2003). It is not yet known if the inclusions contribute directly to the neuropathology seen in FXTAS. It has been suggested

that intranuclear inclusions may not be pathological of themselves, but may reflect pathology such as mRNA toxicity due to the increased gene transcription resulting from the premutation or perhaps due to the presence of the mutant *FMR1* mRNA itself (Brouwer et al., 2008a; Oostra & Willemsen, 2009; Willemsen et al., 2003).

Intranuclear inclusions in these CGG KI mice are common in neurons at 50–100 weeks of age, and have been observed as early as 20 weeks of age (Bontekoe et al., 1997; Brouwer et al., 2008a; Willemsen et al., 2003). However, unlike FXTAS, intranuclear inclusions have not been previously reported in astrocytes in the CGG KI mice. The present study replicates the previous findings of intranuclear inclusions in neurons in the CGG KI mouse, and expands upon these findings by describing the presence and distribution of such inclusions in glial cells (*i.e.*, astrocytes).

Results

Nuclear pathology in neurons of CGG KI mice and FXTAS patients

The presence of intranuclear inclusions in neurons and astrocytes is a pathological hallmark of FXTAS. Thus far, similar intranuclear inclusions have not been reported in oligodendrocytes or microglia in human FXTAS or CGG KI mice. Figures 5A, B show typical intranuclear inclusions in neurons and astrocytes in the hippocampus of a patient who was diagnosed with FXTAS at 65 years of age and later died at 78 (case 2 from Greco et al., 2002). These inclusions in a human patient are shown for comparison with intranuclear inclusions found in the brains of CGG KI mice, and both appeared as well-delineated spherical bodies, 2–3 µm diameter, that were intensely eosinophilic with hematoxylin and eosin staining (H&E). Identification of cell types in human tissue were based on methods reported by (Greco et al., 2002; Greco et al., 2006).

Topographical Distribution of Intranuclear Neuronal Inclusions—

Figure 5E shows intranuclear inclusions in neurons in the entorhinal cortex of a CGG KI mouse that immunostained stained for ubiquitin and were similar in appearance to inclusions found in human brain tissue. Immunofluorescent staining of ubiquitin (red) in Figure 5e clearly shows the localization of an intranuclear inclusion within a DAPI-stained nucleus (blue) in a CGG KI mouse brain. Using triple immunofluorescent staining for the potassium channel subunit Kv2.1 (green) to visualize neurons in the motor cortex, and DAPI to label the nucleus (blue), ubiquitin positive intranuclear inclusions (red) are readily

observed in CGG KI mice (Figure 5F), but not in wildtype control mice (Figure 5f, inset). Inclusions in the entorhinal cortex and neocortex of older KI mice (*e.g.*, 52–70 weeks of age) ranged in size from 1.6–2.7 μm diameter. Microscopic examination of both wildtype and male CGG KI mice revealed no additional evidence of gross-anatomical abnormalities and/or neuropathological features (*e.g.*, no obvious neuronal cell loss, astrogliosis) as compared with wildtype mice.

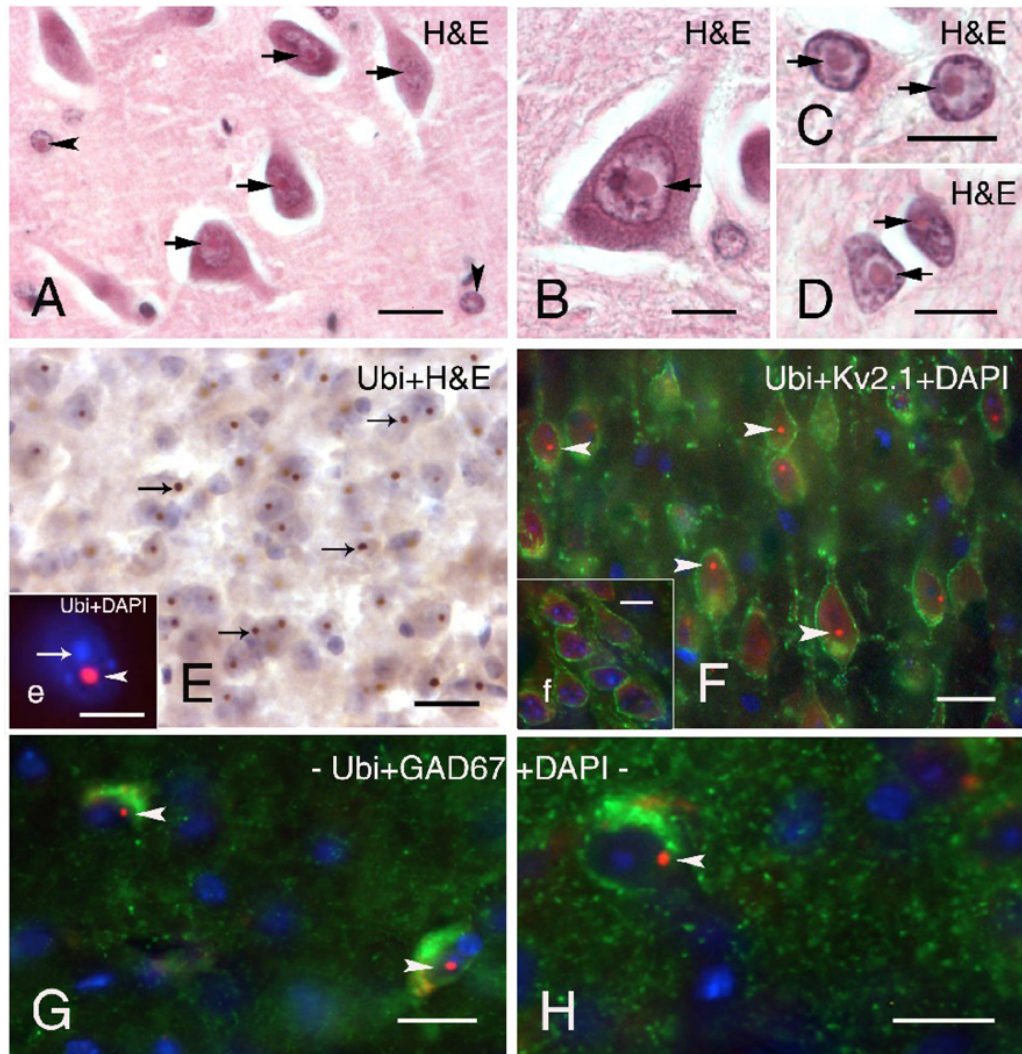


Figure 5. Neuronal intranuclear inclusions in brain tissue from a patient with FXTAS and in CGG KI mice. **A–B.** Typical eosinophilic intranuclear inclusions in neurons (**A, B**; arrows) and astrocyte-like cells (**A**; arrowheads) in the dentate hilus of a FXTAS patient. (H&E; hematoxylin and eosin). **C–D.** Large eosinophilic intranuclear inclusions in protoplasmic astrocytes in gray matter (**C**; arrows) and in fibrous astrocytes (**D**; arrows) located in white matter of the entorhinal cortex of a FXTAS patient. **E.** Intranuclear inclusions (arrows) in neurons in the entorhinal cortex of CGG KI mice stained with DAB (brown reaction product) and counterstained with H&E. **Inset e** shows higher magnification fluorescent image of a DAPI-stained neuronal nucleus (blue, arrow) with a prominent ubiquitin-positive intranuclear inclusion (red, arrowhead). **F.** Pyramidal neurons in motor cortex of CGG KI mice immunolabeled for Kv2.1 potassium channels in the membrane (green), ubiquitin- positive intranuclear inclusions (red, arrowheads), and DAPI staining of the nucleus (blue). **Inset f** shows the absence of intranuclear inclusions in neurons in the cortex of a wildtype mouse. **G–H.** Ubiquitin-positive intranuclear inclusions (red, arrowhead) in GAD67-labeled interneurons (green) in the dentate gyrus molecular layer (**H**) and in the hippocampal CA1 stratum lacunosum moleculare **G**. Scale bars: A, 20 μ m; B–H, 10 μ m.

In CGG KI mice older than 52 weeks of age, ubiquitin-positive intranuclear inclusions were found in neurons in most brain regions, but the frequency and size of individual inclusions differed depending on the brain region under examination and length of the CGG expanded repeats. In the neocortex intranuclear inclusions were observed across all layers, but were most frequent in layers II/III and V, and were more frequently observed in neurons of the rostral neocortex (*i.e.*, sensory and motor areas) and caudal/ventral neocortex (*i.e.*, retrosplenial, visual, and entorhinal cortices), the olfactory bulb and hippocampus (Figures 5E, F). Granule cells within the olfactory bulb and dentate gyrus, and neurons in the hippocampal-amygdala area presented the highest incidence of neuronal intranuclear inclusions, where >50% of neurons exhibited inclusions. Prominent intranuclear inclusions were also present in a high percentage of neurons in hypothalamic nuclei, thalamic subnuclei, inferior colliculus, and specific nuclei of the brain stem (*e.g.*, vestibularis nuclei, and nuclei of the reticular formation). In the cerebellum, neuronal intranuclear inclusions were present in neurons within the cerebellar nuclei, and in the cerebellar cortex inclusions were present in granular cells and interneurons (likely stellate cells, Golgi cells, and/or basket cells based on their location). However, inclusions were rarely observed in Purkinje cells, and were also rarely seen in some brain regions such as the striatum.

Cell Type Distribution of Intranuclear Neuronal Inclusions—To
determine whether GABAergic neurons exhibit ubiquitin-positive intranuclear

inclusions, brain sections of CGG KI mice were immunoreacted for GAD67, one of the two GABA- synthesizing isoenzymes used to identify GABAergic neurons. In neocortex and hippocampus, a high percentage of the GAD67-labeled interneurons showed the presence of intranuclear inclusions identified by their positive immunoreactivity for ubiquitin (Figure 5 G–H).

Age and Gender Dependence of Intranuclear Neuronal Inclusions

Localization —The presence and size of intranuclear inclusions in neurons were clearly age-dependent as previously reported (Hunsaker et al., 2009; Willemse et al., 2003). CGG KI mice at 12–25 weeks of age showed only a small number of neuronal intranuclear inclusions, regardless of brain region, and were more frequent in smaller neurons such as granule cells within the olfactory bulb and dentate gyrus. At this age inclusions were also seen in neurons of rostral neocortical areas, amygdala and hypothalamus, albeit rarely. In addition, intranuclear inclusions at these younger ages appeared to be smaller in size, becoming larger with increasing age (*i.e.*, > than 40 weeks), suggesting a developmental progression in their number and size (data not shown). Wildtype mice ranging from 20–76 weeks of age were examined in parallel with the CGG KI mice, but no ubiquitin-positive inclusions were observed in any of the wildtype mice at any of the ages examined (*e.g.*, Figure 5f, inset).

Additionally, two female CGG KI mice aged 70 and 75 weeks of age that were heterozygous for the CGG repeat expansion were examined for inclusions in the present study. These two female KI mice had CGG repeat expansions of

150 and 152 on one X allele, respectively, with the other allele having the wildtype length of 8–10 CGG trinucleotide repeats. The brains of these female mice showed the presence of ubiquitin- positive intranuclear inclusions that were similar in appearance to male CGG KI mice (data not shown). Female wildtype mice examined in parallel never showed the presence of intranuclear inclusions. It is noteworthy that in both WT and CGG KI mice the majority of large neurons (*e.g.*, pyramidal neurons in the neocortex and neurons in brainstem nuclei) showed diffuse ubiquitin-positive cytoplasmic staining (*e.g.*, Figure 5F). This staining pattern was present in addition to lipofuscin-like accumulations of autofluorescent material within the cytoplasm of neurons in aging animals, but did not obscure the prominent staining pattern of inclusions in CGG KI mice. Control procedures using CuSO₄ to reduce autofluorescence confirmed that the ubiquitin staining of intranuclear inclusions, as well as cytoplasmic staining of ubiquitin, were not due to lipofuscin-like autofluorescence.

Nuclear pathology in astrocytes of CGG KI mice

Previous studies of CGG KI mice did not find intranuclear inclusions in astrocytes of CGG KI mice (Willemse et al., 2003), while such inclusions in astrocytes are consistently observed in the human brain from FXTAS patients (Figures 5C, D; Greco et al., 2002; Greco et al., 2006). Because the CGG KI mouse models much of the other pathology of FXTAS, a major goal of the present study was to determine whether intranuclear inclusions could be demonstrated in the astrocytes of CGG KI mice.

General Topographic Distribution and Localization

Protoplasmic astrocytes, predominantly located in grey matter, and fibrous astrocytes within the white matter were selectively immunolabeled with GFAP and/or S100 β antisera and visualized using immunofluorescence (Figures 6A,D,E) or DAB peroxidase staining (Figures 6B,C). Both labeling techniques revealed the presence of ubiquitin-positive intranuclear inclusions in astrocytes. Inclusions were seen more frequently in protoplasmic astrocytes and only rarely in fibrous astrocytes in the white matter (*e.g.*, fiber tracts). Intranuclear inclusions in astrocytes ranged in size from 1.1 to 2.1 μm diameter and were clearly identified in astrocytic nuclei as ubiquitin-positive spherical bodies (arrowheads; Figures 6A,D,E), that were easily distinguished from surrounding DAPI blue-stained nuclei. Protoplasmic astrocytes with intranuclear inclusions were more diffusely distributed in cortical layer I (large arrows; Figures 6A,D), and clearly distinguished from neuronal intranuclear inclusions as shown in Figures 6A and 6E (neuronal inclusions indicated by small arrows). It is notable that ubiquitin-positive intranuclear inclusions were rarely observed in protoplasmic astrocytes in other brain regions (*e.g.* hypothalamus, caudal brainstem nuclei). Astrocytes bearing ubiquitin-positive intranuclear inclusions were quantitatively assessed in lamina I of the neocortex. Only $10.2 \pm 1.2\%$ of total astrocytes in lamina I of the neocortex exhibited intranuclear inclusions. Quantification of the numbers of astrocytes with inclusions is problematic because of the high degree of variability in the numbers of astrocytes with inclusions found from one brain region to another, and even within a specific brain region. For example, in some lamina I

areas of the neocortex as many as 30–40% of astrocytes show inclusions, while there may few or no astrocytes with inclusions in the immediately adjacent neocortical area. The reason for this pattern of distribution of astrocytes with inclusions is unknown. We are in the process of obtaining more quantitative data on the relationship between age, CGG repeat length, and distribution of neurons and astrocytes with inclusions to be reported as a later date. In the current study there was no evidence for the presence of reactive astrocytes and/or prominent astrogliosis in the brain of CGG KI mice as compared to wildtype mice.

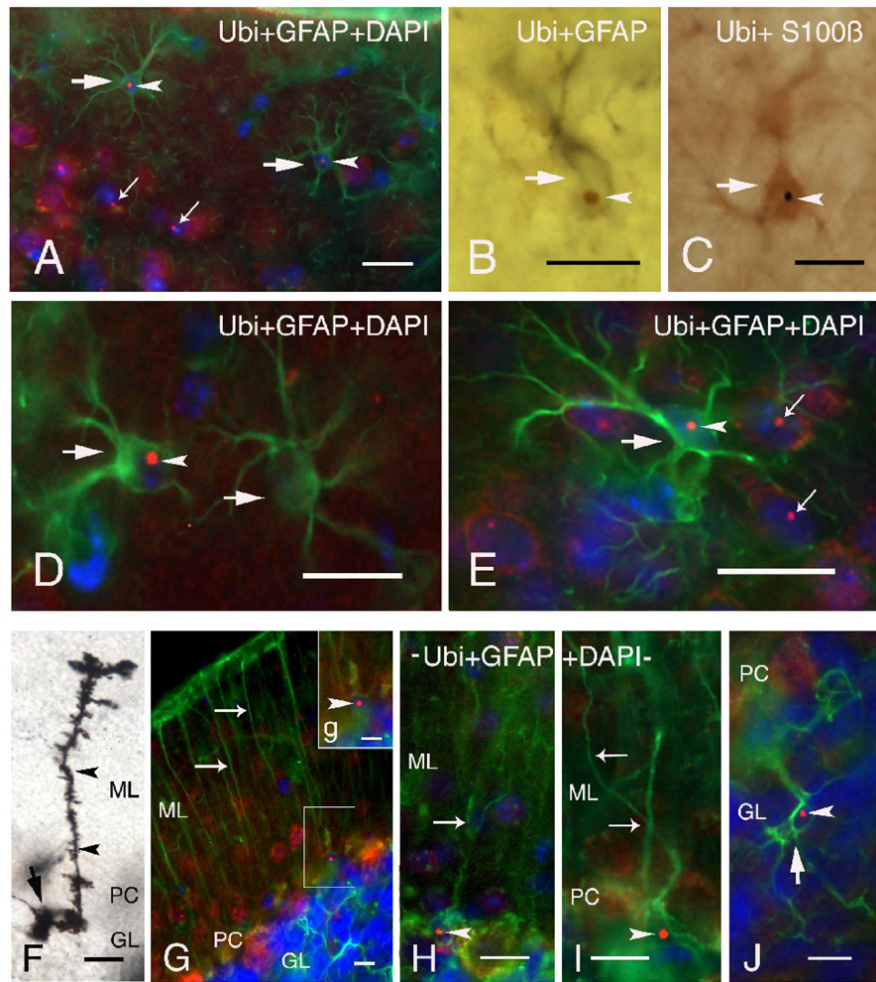


Figure 6. Immunofluorescent labeling of ubiquitin-positive intranuclear inclusions in astrocytes and Bergmann glia of CGG KI mice. **A.** GFAP immunofluorescent labeling (green) of two protoplasmic astrocytes (large arrows) in neocortical lamina I showing ubiquitin-positive intranuclear inclusions (red, arrowheads) within the DAPI stained nucleus (blue). Note the ubiquitin-positive intranuclear inclusions in several neurons (small arrows) located in lamina II/III. **B.** Immunocytochemistry with DAB showing a GFAP-labeled astrocyte (gray, arrow) containing a ubiquitin-positive intranuclear inclusion (brown, arrowhead). **C.** Astrocyte (arrow) with an intranuclear inclusion (black, arrowhead) immunostained with S100 β using a DAB chromogen with a blue-gray reaction product. **D–E.** Higher magnification of protoplasmic astrocytes (arrows) in neocortical lamina I (**D**) and II/III (**E**) labeled for GFAP (green), ubiquitin (red, arrowhead) and with nuclear DAPI staining (blue). Note ubiquitin- positive intranuclear inclusions in several neurons in panel E (small arrows). **F.** Golgi-Cox impregnated Bergmann glia in the cerebellar cortex of a CGG KI mouse with characteristic small cell body (arrow), and radial process (arrowheads) extending through the molecular layer (ML) to the pial membrane. **G.** Fluorescent image of GFAP-positive Bergman glia cells (green) with radial processes (arrows), some of which show ubiquitin-positive intranuclear inclusions (**g** inset, arrowhead). **H–I.** Higher magnification of Bergmann glia with radial processes (arrows) and intranuclear inclusions (arrowheads). **J.** Velate astrocyte (arrow) in the granule layer of the cerebellar cortex labeled with GFAP (green) exhibiting extended processes and a ubiquitin-stained intranuclear inclusions (red, arrowhead) within the DAPI stained nucleus (blue). Abbreviations: GL, granule layer; PC, Purkinje cell layer; ML, molecular layer)

In addition, ubiquitin-positive intranuclear inclusions were also frequently observed in other non-neuronal cells in the brain, including the ependymal/subependymal cells and epithelial cells of the choroid plexus (data not shown) cells that may have the same precursor cell type as astrocytes (*cf.*, Greco et al., 2006).

Localization of Intranuclear Inclusions in Bergmann Glia

In the cerebellum ubiquitin-positive intranuclear inclusions were found diffusely in Bergmann glia and astrocytes, and were widely present in neurons of CGG KI mice. Figure 6F shows an example of a Golgi impregnated Bergmann glia, with its soma located in the Purkinje cell layer (PC) and a long radial process ascending to the pial surface. These radial processes bear irregular, leaf-like appendages that end in bulbous tips or endfeet near the pial surface. Bergmann glia immunostained for GFAP showed a similar morphology, as well as ubiquitin-positive intranuclear inclusions in their soma (Figures 6G–I). These inclusions were always clearly defined, round and localized to the nucleus (Figure 6G, inset g, H and I). In addition to Bergmann glia, protoplasmic astrocytes were commonly seen within the molecular layer, but within the granular layer they represented a morphologically distinct neuroglia cell type, the velate protoplasmic astrocyte. These astrocytes are characterized by veil-like processes ramifying within the granular layer (Palay & Chan-Palay, 1974). A GFAP-labeled velate protoplasmic astrocyte bearing a ubiquitin-positive inclusion is shown in Figure 6J. There was no evidence of reactive astrocytes /or

specifically Bergmann gliosis in the cerebellum of CGG KI mice as shown by GFAP staining and/or Golgi impregnation.

Cytoplasmic inclusions in oligodendrocytes of CGG KI mice

Many oligodendrocytes across cortical and subcortical regions stained positive for myelin basic protein (MBP), but none of these oligodendrocytes showed ubiquitin-positive intranuclear inclusions (Figure 7A, B). However, many oligodendrocytes in both wildtype (Figure 7A) and CGG KI (Figure 7B) mice contained irregular and amorphous inclusions within the cytoplasm which were immunopositive for both MBP and ubiquitin (arrowheads; Figure 7A, B). These inclusions were clearly localized within the cytoplasm, were not in the nucleus (stained blue with DAPI), and measured between 1.1 to 3.3 μ m in diameter.

Cytoplasmic inclusions in microglia of CGG KI mice

Microglia identified by Iba1 staining were distributed throughout the brain, with the majority of cells displaying a ramified morphology and territorial distribution suggesting a “resting microglia phenotype”. However, in the neocortex and brain stem of CGG KI mice some of the microglial cells presented morphological features of activated, but not “phagocytic”, microglia (e.g., bushy morphology, retraction of the processes). Brain macrophages (“phagocytic” microglia) were occasionally observed. The major observation was that none of the microglia subtypes exhibited ubiquitin-positive intranuclear inclusions. However, in both wildtype (Figure 7C) and CGG KI (Figure 7D) mice the majority

of microglial cells had ubiquitin-positive inclusions within the cytoplasm that had an amorphic and/or vacuolar appearance and ranged in size from 3–10 µm in diameter. The majority of those cytoplasmic inclusions also demonstrated autofluorescence in control sections in which the antibodies were omitted. In order to determine if this autofluorescence was due to lipofuscin, sections were treated with CuSO₄ (Schnell, Staines, & Wessendorf, 1999). This procedure did not affect autofluorescence, suggesting that it was not lipofuscin-related. The source of autofluorescence of these cytoplasmic inclusions remains to be determined.

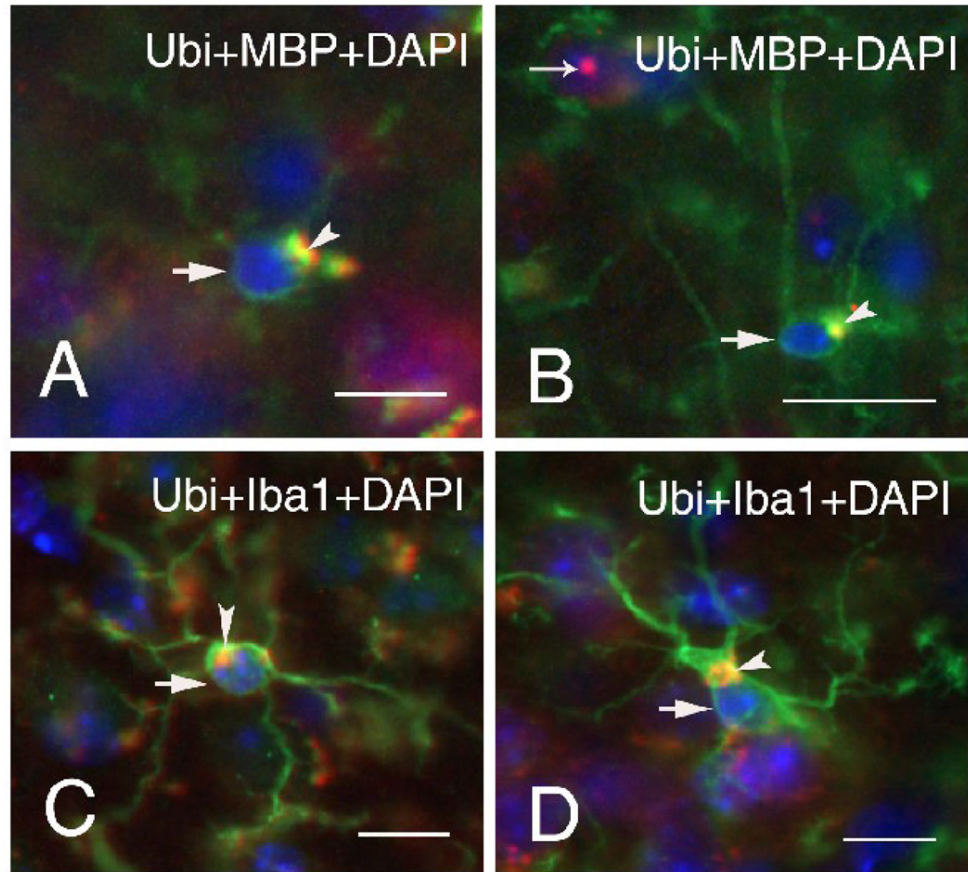


Figure 7. Representative immunofluorescent staining (arrows) of oligodendrocytes of wildtype (**A**) and CGG KI (**B**) mice, and microglia of wildtype (**C**) and CGG KI mice (**D**). Large, irregularly shaped cytoplasmic inclusion bodies were found in oligodendrocytes and microglia of both wildtype and CGG KI mice (arrow heads). Oligodendrocytes were labeled for myelin basic protein (MBP, green) and microglia for Iba1 (green), so that colocalization of ubiquitin in the inclusions with either MBP or Iba1 appears yellow. Nuclei were stained with DAPI (blue). Both wildtype mice were 60 weeks of age (**A**, **C**), and the two CGG KI mice were 70 (**B**) and 59 (**D**) weeks of age. Scale bars are 10 μ m.

Discussion

Intranuclear inclusions in neurons and astrocytes that stain for ubiquitin are the neuropathological hallmark of FXTAS. Similar appearing ubiquitin-positive inclusions are also found in neurons in the brains of CGG KI mice, but previous studies have not demonstrated such inclusions in mouse astrocytes. In this study we extend the description of the cellular and brain regional distribution and appearance of intranuclear inclusions in a CGG KI mouse model of FXTAS to include astrocytes. New evidence is also presented for previously unreported neuropathology in the cytoplasm of oligodendroglia and microglia in both CGG KI as well as wildtype mice that may be related to aging.

Ubiquitin-positive intranuclear inclusions were found in astroglia in neocortex and cerebellum, including Bergmann glia of the cerebellum. Inclusions were preferentially found in protoplasmic astrocytes, and were only rarely observed in fibrous astrocytes. Overall, the occurrence of intranuclear inclusions in glia was markedly less common than in neurons. As expected, intranuclear inclusions were not observed in neurons or glia of wildtype mice. These results are an important extension of previous findings because intranuclear inclusions in astrocytes and Bergmann glia of CGG KI mice were not reported in previous studies (Brouwer et al., 2008b; Entezam et al., 2007; Willemse et al., 2003). This difference may be due to the use of different background strains or to differences in histological methodology (e.g., frozen sections versus paraffin embedding, H&E versus immunofluorescence; difference in section thickness). Since inclusions in astrocytes are a common feature of clinical FXTAS (Greco et

al., 2002; Greco et al., 2006), these findings further validate the mouse model and enhance its value as a model of FXTAS. Although no remarkable histopathologies (e.g., Purkinje cell loss, Bergmann gliosis) were observed in the cerebellum of CGG KI mice in the present study, intranuclear ubiquitin-positive inclusions were found in Bergmann glia and other astroglial cells. These findings suggest involvement of cerebellar glia from CGG mice in the pathogenesis of the disease. The relatively small number of glia showing inclusions may explain, in part, the “milder” motor deficits found in the CGG KI mouse model of FXTAS than that seen in clinically advanced cases of FXTAS (Van Dam et al., 2005). The fact that murine astrocytes appear to be less prone to generate intranuclear inclusions in CGG KI mice when compared to astrocytes in human FXTAS raises important questions concerning differences between murine and human astrocytes in the cellular machinery and molecular mechanisms underlying inclusion formation.

Intranuclear inclusions in neurons of CGG KI mice were found preferentially in cortical/ neocortical areas (e.g., rostral neocortex, olfactory bulb/ nuclei, hippocampus, entorhinal cortex), subcortical regions (e.g., amygdala, hypothalamus, inferior colliculus, brain stem nuclei) and in selected neuronal cell types (e.g., neocortical pyramidal cells, GABAergic neurons/interneurons), similar to previous findings in KI mice (Brouwer et al., 2008b; Entezam et al., 2007; Willemse et al., 2003).

Inclusion formation, CGG repeat length, *Fmr1* mRNA and Fmrp

The precise relationships between CGG repeat number and inclusion formation, neuropathology, and/or clinical involvement are still unclear. In humans, CGG length is highly correlated with the number of intranuclear inclusions in astrocytes and neurons, and appears to be an important predictor of brain pathology (Greco et al., 2006). Similarly, CGG KI mice with larger CGG repeat sizes typically have the greatest numbers and most widespread distributions of intranuclear inclusions in the brain (Brouwer et al., 2008b; Entezam et al., 2007; Willemsen et al., 2003). However, it has also been reported that CGG KI mice with 70 CGG repeats, and CGG KI mice with CGG expansions above 200 show few intranuclear inclusions, suggesting that an upper and lower threshold for CGG repeat length and for inclusion formation may exist (Brouwer et al., 2009).

It is also possible that intranuclear inclusions in FXTAS may not be causally involved in pathology. They may even serve a protective function, possibly sequestering abnormal mRNAs and proteins, thereby protecting cells from pathology as has been suggested for polyglutamine diseases (Saudou, Finkbeiner, Devys, & Greenberg, 1998). Other studies have shown that inhibition of ubiquination of huntingtin fragments and/or reduction of mutant huntingtin results in reduced nuclear inclusion formation which, in turn, significantly decreases the risk of cell death (Arrasate, Mitra, Schweitzer, Segal, & Finkbeiner, 2004). Clarification of the involvement and role of intranuclear inclusions in FXTAS and other neurodegenerative diseases is central to elucidation of disease pathogenesis (Woulfe, 2007).

Similar to FXTAS patients (Hagerman & Hagerman, 2004b), CGG KI mice exhibit elevated *Fmr1* mRNA expression and reduced Fmrp levels (Brouwer et al., 2008a). However, increased *Fmr1* mRNA levels do not appear to correlate in any simple way with the length of the CGG repeat in these mice (Brouwer et al., 2008a; Entezam et al., 2007), and the formation of inclusions may not require elevated *Fmr1* mRNA since inclusions occur in Purkinje cells of mice with ectopic expression of just an expanded CGG trinucleotide repeat (Hashem et al., 2009). These mice also showed a loss of Purkinje cells, other Purkinje cell pathology (swollen axons), and motor deficits on the rotarod test. These reports are in contrast to the positive correlation between *FMR1* mRNA and CGG repeat length reported in human premutation carriers (Brouwer et al., 2007; Brouwer et al., 2008a; Entezam et al., 2007; Greco et al., 2006; Hessl et al., 2005; Kenneson et al., 2001; Primerano et al., 2002).

Intranuclear inclusions and neuropathology

The absence of FXTAS in patients with FXS, where the *FMR1* gene is silent and *FMR1* mRNA is absent, has lead to the proposal that FXTAS may be due to an RNA gain-of-function toxicity resulting from increased *FMR1* mRNA levels (Greco et al., 2002; Hagerman & Hagerman, 2004b; Hagerman et al., 2001; Jacquemont et al., 2003; Tassone et al., 2000d; Tassone et al., 2004a). Toxic RNA gain-of-function mechanisms have been proposed for other neurodegenerative diseases, including myotonic dystrophy and Huntington's disease-like 2 (reviewed in Ranum & Cooper, 2006; Woulfe, 2007). More than 20

inclusion-associated proteins have been identified, including components of the proteasome, HSP27 and 70, $\alpha\beta$ -crystallin, DNA-repair-ubiquitin-associated HR23B, MBP, members of the histone 2A family, and the RNA binding protein hnRNP (Bergink et al., 2006; Iwahashi et al., 2006). The presence of RNA binding proteins suggests that depletion of such proteins when bound to RNA could mediate the proposed toxic RNA gain-of-function mechanism for disease pathogenesis in FXTAS (Hagerman et al., 2001). This is supported by the demonstration that intranuclear inclusions can be formed in both primary neural progenitor cells and established neural cell lines engineered to contain an expanded CGG88 trinucleotide repeat in the *FMR1* 5' untranslated region (UTR) (Arocena et al., 2005). The inclusions were $\alpha\beta$ -crystallin-positive, although not associated with ubiquitin, suggesting that the incorporation of ubiquinated proteins into inclusions may be a later event in inclusion formation. Furthermore, the lamin A/C in the nuclear envelope appeared to become irregular and accumulate in the inclusions as well, demonstrating additional nuclear pathology.

One model for inclusion formation in FXTAS is shown in Figure 8. In this model, transcription of normal *FMR1* results in normal levels of *FMR1* mRNA to which RNA binding proteins bind in the 5' UTR (region shown in red), and no intranuclear inclusions are formed. In contrast, the presence of an expanded CGG repeat in the premutation *FMR1* gene (e.g., carrying an expanded CGG repeat in the range of 55–200) leads to 3–8 fold higher *FMR1* transcription levels, a corresponding increase in binding of RNA binding proteins to the expanded 5' UTR region, and the development of intranuclear inclusions that contain *FMR1*

mRNA and several RNA binding proteins. However, the role of any specific binding protein in FXTAS pathology remains unclear as no single protein found in inclusions has yet to be shown to be dominant among the more than 20 proteins found (Iwahashi et al., 2006).

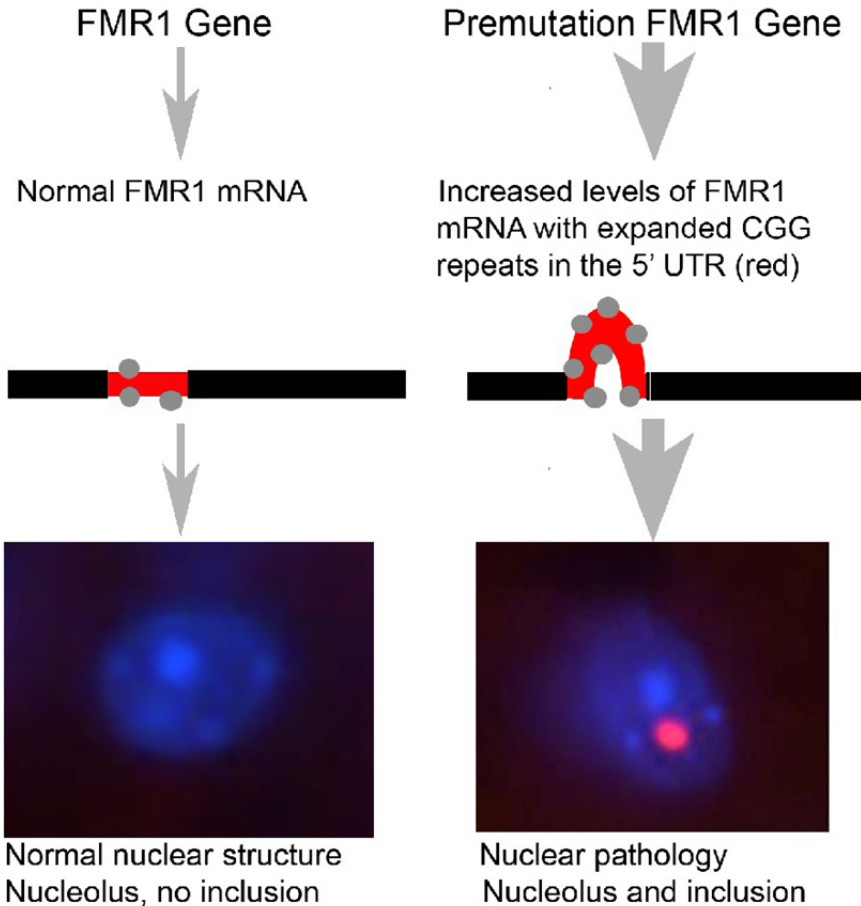


Figure 8. Proposed model of inclusion formation in the fragile X premutation. **Left:** Normal FMR1 gene and transcribed FMR1 mRNA have between 5–40 CGG repeats in the 5' untranslated region (UTR—short red segment on the mRNA). Proteins that bind to RNA, including CGG binding proteins, bind normally to the mRNA (gray dots) and no inclusions are formed (bottom left). **Right:** In the premutation condition FMR1 and mRNA have between 55–200 CGG repeats in the 5'UTR (long red segment on the mRNA). This results in increased levels of mutant FMR1 mRNA as well as excessive binding of RNA binding proteins to the mRNA (gray dots). Although the precise mechanism remains unclear, increased mutant FMR1 mRNA results in intranuclear inclusions that contain CGG binding proteins, ubiquitin, as well as the FMR1 mRNA itself (bottom right—pink inclusion body adjacent to the pale blue nucleolus).

In the current study intranuclear inclusions in neurons far outnumbered inclusions found in GFAP-labeled astrocytes. Currently, there is no clear explanation for this difference in the inclusion numbers between neurons and glial cells. There could be differences between neurons and glia in expression levels of *Fmr1* mRNA, Fmrp, or specific RNA-associated proteins that may explain these differences, but such differences have not been demonstrated. Other neurological disorders, such as Huntington's disease, also include the formation of prominent inclusions in neuronal nuclei that are associated with misfolded proteins. Aggregates of mutant huntingtin protein are found in neurons and in glia, although more prominently in neurons (Tydlacka, Wang, Wang, Li, & Li, 2008). These huntingtin aggregates colocalize with components of the ubiquitin-proteasome system (UPS) which is involved in clearing misfolded proteins (Lehman, 2009). The observation in Huntington's disease that UPS activity is lower in neurons than in astroglial cells, and also lower in the nucleus than the cytoplasm, suggests that lower neuronal UPS activity may be responsible for preferential accumulation of misfolded proteins in neurons, as well as for their selective vulnerability to subsequent cell death. In contrast, higher UPS activity in astroglial cells resulted in less severe glia pathology (*i.e.*, less/or no nuclear inclusions and reduced huntingtin aggregates (Tydlacka et al., 2008)). Based on these findings it is tempting to speculate that there may be a similar relationship between UPS activity and inclusion formation in neurons and glial cells of CGG KI mice resulting in fewer inclusions in glial cells than in neurons. However, further research is needed to establish any relationship

between UPS activity and inclusion formation in neuronal and or glial cells in the CCG KI mouse model of FXTAS.

Conclusions

The CGG KI mouse model exhibits many of the important clinical and neuropathological features of FXTAS in humans (Berman & Willemse, 2009). In particular, the CGG KI mouse model develops ubiquitin-positive intranuclear inclusions in both astrocytes and neurons. The role of intranuclear inclusions in the pathophysiology of FXTAS remains unclear, and continued studies on the CGG KI mouse as a model of FXTAS should contribute to finding answers to these questions. Such studies will not only contribute important information to the study and treatment options for FXTAS and other trinucleotide repeat disorders, but also to other neurodegenerative disorders such as Alzheimer's and Parkinson's disease that are increasingly prevalent in an aging population.

Experimental Procedure

Animals

Genotyping

The generation of an expanded CGG trinucleotide repeat knock-in (CGG KI) mouse model of the fragile X premutation has been described previously in detail (Bontekoe et al., 1997; Willemsen et al., 2003). Briefly, the native CGG8 trinucleotide repeat of human origin in the 5' UTR of the mouse *Fmr1* gene was replaced by a human CGG98 trinucleotide repeat via homologous recombination. Across breedings, the CGG repeats showed mild instability, both expanding and contracting in length within the fragile X premutation range, which is defined as ~55–200 CGG repeats (Brouwer et al., 2008a; Willemsen et al., 2003). The CGG KI mice were originally developed on a mixed FVB/NxC57BL/6J background, and were backcrossed with C57BL/6J mice from Jackson Laboratories (Bar Harbor, ME) until greater than 98% C57BL/6J by microsatellite analysis. Five male wildtype mice between 22–62 weeks old and 8 male CGG KI mice 16–76 weeks of age were used in the current study. The CGG KI mice used in the present study had between 128 and 198 CGG repeats. Brains of two female heterozygous CGG KI mice (70 and 75 weeks old and with 10/150 and 10/162 CGG repeats, respectively) as well as two wildtype female mice were examined for presence of intranuclear inclusions in neurons and astrocytes for comparison with males. Wildtype and CGG KI mice were housed under the same conditions of constant temperature and a 12 / 12 h light-dark cycle, and with food and water ad libitum. All experiments were conducted in compliance with the NIH Guide for

Care and Use of Laboratory Animals, and were approved by the Institutional Animal Care and Use Committee of the University of California at Davis.

DNA was extracted from mouse tails by incubating with 10 mg/ml Proteinase K (Roche Diagnostics) in 300 µl lysis buffer containing 50 mM Tris-HCl, pH 7.5, 10 mM EDTA, 150 mM NaCl, 1% SDS overnight at 55°C. One hundred µl saturated NaCl was then added and the suspension was centrifuged. One volume of 100% ethanol was added, gently mixed, and the DNA was pelleted by centrifugation and the supernatant discarded. The DNA was washed and centrifuged in 500 µl 70% ethanol. The DNA was then dissolved in 100 µl milliQ-H₂O. CGG repeat lengths were determined by PCR using the Expanded High Fidelity Plus PCR System (Roche Diagnostics). Briefly, approximately 500–700 ng of DNA was added to 50 µl of PCR mixture containing 2.0 µM of each primer, 250 µM of each dNTP (Invitrogen), 2% DMSO (Sigma), 2.5 M Betaine (Sigma), 5 U Expand HF buffer with Mg (7.5 µM). The forward primer was 5'-GCTCAGCTCCGTTCGGTTCACTTCCGGT-3' and the reverse primer was 5'-AGCCCCGCAC TTCCACCAC CAGCT CCTCCA-3'. PCR steps were 10 min denaturation at 95°C, followed by 34 cycles of 1 min denaturation at 95°C, annealing for 1 min at 65°C, and elongation for 5 min at 75°C to end each cycle. PCR ends with a final elongation step of 10 min at 75°C. DNA CGG band sizes were determined by running DNA samples on a 2.5% agarose gel and staining DNA with ethidium bromide.

Case Report: Autopsy, Clinical History and Neuropathology

FXTAS neuropathology from a previously described human case is described in this study for comparison with that found in the CGG KI mice (case 2 from Greco et al., 2002). The FXTAS patient was a carrier of an *FMR1* premutation allele of 80 CGG repeats, developed clinical features of FXTAS at 65 years of age, and died at 78 years of age. Description of the clinical history of this case and detailed neuropathology (e.g., standard techniques, including fixation, hematoxylin and eosin (H&E) staining, immunocytochemistry and neurohistological analysis) have been already reported and as described by (Greco et al., 2002; case 2). Brain autopsy of this case was performed in a standard fashion and in accordance with University of California, Davis, IRB-approved protocols.

Tissue Preparation for Light Microscopy/Immunocytochemistry

General tissue preparation—Mice were anesthetized with sodium pentobarbital (100 mg/kg, i.p.), then perfused with isotonic saline with heparin (1000 units/ml saline), followed by a solution of 4% paraformaldehyde (PFA) in 0.1 M sodium phosphate buffer (PB; pH 7.4). The brains were immediately removed from skull and placed in the same fixative for 1 hour at 4°C. After post-fixation, the brains were rinsed in PB, cryoprotected in 10% sucrose in 0.1 M PB for 1 hour, followed by 30% sucrose in 0.1 M PB for 24 hours at 4°C, then rapidly frozen on dry ice. Thirty µm parasagittal serial sections were cut on a sliding microtome equipped with a freezing stage, and collected into series of every fifth section directly into 30% sucrose. Single sets of sections were selected for

further processing which included: cresyl violet and/or H&E staining for general histological evaluation; immunocytochemistry for neuronal and glial cell markers and for ubiquitin to visualize intranuclear inclusions, the hallmark pathology of FXTAS patients that are also features of CGG KI mice (Greco et al., 2002; Greco et al., 2006; Willemse et al., 2003).

Immunocytochemistry

Immunocytochemical and immunofluorescence techniques were used to visualize the occurrence and distribution of intranuclear and cytoplasmic inclusions, with a focus on their presence or absence in glial cells (i.e., astrocytes, including cerebellar Bergmann glia, oligodendrocytes, and microglial cells), as well as in GABA-ergic interneurons neurons of wild-type and CGG KI mice. Subsets of alternate sections were processed for immunocytochemistry using a modification of the avidin-biotin complex (ABC)-peroxidase technique (Hsu, Raine, & Fanger, 1981) as previously described (Wenzel et al., 2004). Briefly, free-floating sections were rinsed in PB (pH 7.4), and pretreated with 0.1% sodium borohydride for antigen retrieval for 15 min followed by treatment with 0.5–2% H₂O₂ in PB for 90 min to inactivate endogenous peroxidases. Sections were then treated with 3% goat, horse, or swine serum (Sigma, St.Louis, MO; DAKO, Inc., Carpinteria, CA) and 0.3% Triton X (TX) in 0.01 M PB, 0.15M NaCl, pH 7.4 (PBS) for 1 hour to reduce nonspecific staining. Sections were rinsed in PBS for 30 minutes and incubated for 48–72 hours at 4° C in the various antibodies and dilutions: mouse monoclonal anti-glutamic acid

decarboxylase (GAD67), (Chemicon, Temecula, CA), 1:1000; mouse monoclonal anti-glial fibrillary acidic protein (GFAP), (DAKO, Inc.), 1:2000 (1:750 for immunofluorescence (IF)); rabbit polyclonal anti-S100 β (Abcam, Inc., Cambridge, MA), 1:1000; mouse monoclonal anti-myelin basic protein (MBP), (Chemicon), 1:500; rabbit polyclonal anti- Iba1 (ionized calcium binding adaptor molecule 1; Wako Chemicals USA, Inc., Richmond, VA), 1:2000 (1:1000 for IF); mouse-monoclonal anti-Kv2.1 (provided by Dr. J.S. Trimmer; UC Davis), 1:500 for IF; and rabbit poly- and mouse monoclonal antibodies against ubiquitin (DAKO, Inc.; Abcam, Inc.) 1:2000 and 1:1000, respectively, (1:1000 for IF) in PBS containing 1% goat, horse or swine serum, 2% BSA and 0.3% TX. Following rinses for 2 hours in PBS, sections were incubated in biotinylated goat or swine anti-rabbit IgG or horse anti-mouse IgG (DAKO, Inc.; Vector Laboratories, Burlingame, CA), diluted 1:500 for 24 hours at 4°C, rinsed 2 hours in PBS and then incubated in ABC (Elite ABC Kit, Vector Laboratories), diluted 1:500 in 1% goat or horse serum, 2% BSA, 0.3% TX and PBS for 24 hours at 4°C. Sections were rinsed thoroughly in PB (pH 7.4), then transferred to Tris-HCl buffers (pH 7.4; 7.6) and then incubated for 15 minutes in 0.025% 3,3'-diaminobenzidine (DAB, Sigma) in TB (pH7.6). After reacting for 5–10 minutes in fresh DAB with 0.003% H₂O₂, sections were rinsed in TB, followed by PB. Iba1-immunostaining was visualized using 0.05% DAB with a blue/grey chromogen (DAB; Vector SG Substrate Kit, Vector Laboratories). Double-immunostaining was performed for GFAP/ubiquitin, as well as for MBP/ubiquitin co-localization using combined incubation of poly- and monoclonal antisera and differently-colored chromogens (Vector SG

Substrate Kits) resulting in a blue staining for GFAP-positive cells and brown reaction product for ubiquitin-positivity of inclusions. Specificity of the immunostaining was evaluated by omitting primary antibodies from the regular staining. Sections were mounted on slides, dehydrated, cleared, and coverslipped with Permount.

Immunofluorescence staining

For single and double-immunofluorescent labeling of ubiquitin colocalized with neuronal/glial cell markers, sections were transferred into 10% sucrose in 0.1 M PB, then rinsed in 0.1 M PB and treated with 0.1% sodium borohydride for 15 min. Thereafter, sections were rinsed again with 0.1 M PB and then permeabilized with 0.5% H₂O₂ in 0.1 M PB for 15 min followed by rinses in 0.1 M PB and 0.01 M PBS. Free- floating sections were treated with 10% goat or horse serum in 0.01M PBS containing 0.3% TX-100 (vehicle) for 1 hr, and then incubated overnight at 4°C in vehicle containing different combinations of mouse monoclonal/rabbit polyclonal antibodies of different IgG isotypes (see above). After rinses in 0.01 M PBS and 10% goat or horse serum (vehicle), sections were incubated in isotype-specific Alexa-conjugated secondary antibodies (1:2000): Alexa 568-labeled goat anti-rabbit IgG and/or Alexa 488-labeled goat anti-mouse IgG (Invitrogen, Carlsbad, CA) for 1–2 hrs as described previously (Wenzel et al., 2007). Following rinses in vehicle, sections were mounted on gelatin-coated slides and coverslipped with mounting medium containing DAPI (4', 6-

diamidino-2-phenyindole di-lactate) for nuclear staining (Vectashield “Hard Set”, Vector Laboratories).

To differentiate between specific immunofluorescent labeling and nonspecific autofluorescence resulting from accumulations of lipofuscin in aging brains, sections were first treated with 10 mM CuSO₄ in 50 mM ammonium acetate buffer (pH 5.0) for 20 min (Schnell et al., 1999). This treatment reduced autofluorescence but did not significantly affect the intensity of specific immunofluorescent labeling; although immunofluorescent staining for ubiquitin within the neuronal cytoplasm was slightly enhanced.

Golgi-Cox staining

The Bergmann glia in the CGG KI mouse cerebellum, including cell bodies and processes, were visualized using a modified Golgi-Cox staining procedure (FD Rapid GolgiStain Kit; FD NeuroTechnologies, Inc. Ellicot City, MD). After initial perfusion with NaCl, the brains were stained following the kit instructions, and sectioned at 120 µm on a vibratome, mounted on slides and stained, then cleared and coverslipped as described above.

Cell Identification and Evaluation of Intranuclear Inclusions

The sections were analyzed using a Nikon ECLIPSE E600 microscope with epifluorescence attachment and digital camera. Images were converted to a file format for processing as an Adobe Photoshop document. Images were analyzed to verify the presence of ubiquitin-positive intranuclear inclusions in

different cell types identified with various neuronal and glial cell markers in brains of CGG KI and wildtype mice. Cresyl violet and/or H&E-stained sets of serial sections from wildtype and CGG KI mouse brains at different ages were used for comparison and evaluation of gross anatomical differences. Identification of different cell types in the brain was carried out based on standard morphological criteria, using Nissl cell staining, and neuronal and glial cell markers (Greco et al., 2002; McKhann, Wenzel, Robbins, Sosunov, & Schwartzkroin, 2003). Neurons were identified by their size, large round nuclei, single or multiple nucleoli, and their abundant cytoplasm, as well as by using specific neuronal markers (*e.g.*, GAD67, Kv2.1 channel protein). Astrocytes were identified by their round/ovoid nuclei with light euchromatin, and absence of nucleoli and cytoplasm. In addition, GFAP- and S100 β - immunocytochemistry and/or immunofluorescence were used to identify subpopulations of astrocytes based on their differing immunoreactivities (*i.e.*, protoplasmic and/or fibrous astrocytes) in different brain regions. To estimate the percentage of astrocytes with intranuclear inclusions, the number of astrocytes and intranuclear inclusions were counted manually in 10 fields on two GFAP- and ubiquitin-immunoreacted sections from 3 CGG KI mice within layer I of the neocortex (including sensory and motor areas) at 400 \times magnification using a microscope and optical imaging system. Oligodendrocytes were identified based on their typically small, round, hyperchromatic nuclei (which did not allow differentiation between nucleus, nucleoli, or cytoplasm), localization in white and grey matter, and confirmed by immunocytochemistry for MBP. Microglia were identified primarily on cellular

morphology obtained from Iba1 immunostaining which displayed small cell bodies with a round nucleus and fine, ramified processes that are characteristic of resting microglia. Microglial cells with retracted and/or hypertrophic processes were defined as activated (but non-phagocytic) microglia which can be transformed into phagocytotic cells (*i.e.*, brain macrophages; Graeber & Moran, 2002). Immunocytochemical staining for ubiquitin was used to specifically label intranuclear inclusions in combination with cell- specific markers to identify the cell type (*i.e.*, neuronal and/or non-neuronal cells). Whenever possible, experiments using immunocytochemistry using DAB and immunofluorescence were carried out in parallel to verify staining patterns as well as to allow for future quantification.

Acknowledgments

We are grateful to Dr. Mareike Wenzel for her excellence in technical support. This research was supported by grants NINDS RL1 NS 062411, NIH Roadmap Consortium NIDCR UL1 DE 19583, and NIA AG032119.

Chapter 4

Neuropathological, Clinical, and Molecular Pathology in Female Fragile X

Premutation Carriers with and without FXTAS.

ABSTRACT

Fragile X-associated tremor/ataxia syndrome (FXTAS) is an adult-onset neurodegenerative disorder associated with premutation alleles of the fragile X mental retardation 1 (*FMR1*) gene. Approximately 40% of older male premutation carriers, and a smaller proportion of females, are affected by FXTAS; due to the lower penetrance the characterization of the disorder in females is much less detailed. Core clinical features of FXTAS include intention tremor, cerebellar gait ataxia, and frequently parkinsonism, autonomic dysfunction, and cognitive deficits progressing to dementia in up to 50% of males.

Here, we report the clinical, molecular, and neuropathological findings of eight female premutation carriers. Significantly, four of these women had dementia; of the four, three had FXTAS plus dementia. Post mortem examination revealed the presence of intranuclear inclusions in all eight cases, which included one asymptomatic premutation carrier who died from cancer. Among the four subjects with dementia, three had sufficient number of cortical amyloid plaques and neurofibrillary tangles to make Alzheimer's disease a highly likely cause of dementia and a fourth case had dementia with cortical Lewy bodies. Dementia appears to be more common than originally reported in females with FXTAS. Although further studies are required, our observation suggests that in a portion

of FXTAS cases and Alzheimer pathologies a synergistic effect on the progression of the disease may occurs.

This chapter has been published as:

Tassone, F., Greco, C. M., Hunsaker, M. R., Berman, R. F., Seritan, A. L., Gane, L. W., et al. (2012). Neuropathological, Clinical, and Molecular Pathology in Female Fragile X Premutation Carriers with and without FXTAS. Genes, Brain, and Behavior. In press

My role in this study was to perform cell counting as well as analyzing and photographing the human tissue reported in this study along with Dr. Claudia Greco.

INTRODUCTION

The FMR1 gene is highly polymorphic for CGG trinucleotide repeats in its 5' untranslated region. CGG expansions in the premutation range (55-200 repeats) give rise to the leading known single-gene cause of primary ovarian insufficiency (Oostra & Willemsen, 2009), and the late-onset neurodegenerative disorder, FXTAS (Hagerman et al., 2001). FXTAS is characterized by intention tremor and gait ataxia, with both age-of-onset and severity being associated with the number of CGG repeats (Tassone & Hagerman, 2010; Tassone et al., 2007a). Cerebral atrophy and white matter disease are prominent imaging findings in individuals with FXTAS (Adams et al., 2007; Adams et al., 2010). White matter MRI hyperintensities in the middle cerebellar peduncles (*i.e.*, “MCP sign”) represent a major diagnostic criterion for FXTAS although observable in only 58% of males and 13% of female carriers (Adams et al., 2007; Brunberg et al., 2002). The pathological hallmark is the presence of intranuclear inclusions in neurons and astrocytes (Greco et al., 2002), in the neuroendocrine system (Louis et al., 2006), in the autonomic nervous system, and myocardial cells (Gokden et al., 2009; Greco et al., 2007; Hunsaker et al., 2011a).

The pathogenesis of premutation-associated disorders, particularly FXTAS, is thought to involve an RNA toxic gain-of-function mechanism, mediated by elevated levels of premutation length *FMR1* mRNA (Allen, He, Yadav-Shah, & Sherman, 2004; Kenneson et al., 2001; Peprah, Allen, Williams, Woodard, & Sherman, 2010b; Tassone et al., 2000c) which has been detected within the intranuclear inclusions present in the brain (Tassone et al., 2004b). Although the

role of these inclusions in the pathogenesis of FXTAS remains unclear, it is likely that they reflect, a much broader process of cellular sequestration of one or more proteins whose functions are thereby compromised (Raske & Hagerman, 2009; Sellier et al., 2010).

FXTAS occurs in approximately 40% of carrier males (Jacquemont et al., 2004b) with an increased likelihood of penetrance with age (Jacquemont et al., 2004a). A reduced FXTAS penetrance (between 8 and 17%) has been observed in female premutation carriers (Chonchaiya et al., 2010a; Coffey et al., 2008; Jacquemont et al., 2004b; Rodriguez-Revenga et al., 2009). This may be primarily due to the protective effect of the normal allele on the second X chromosome (Berry-Kravis, Potanos, Weinberg, Zhou, & Goetz, 2005; Jacquemont et al., 2005). Indeed, female premutation carriers show less frequent clinical and neuropathological features than male premutation carriers, both with and without FXTAS, but in some cases they may have symptoms that are as severe as those of their male counterparts (Adams et al., 2007). FXTAS females have a higher incidence of hypothyroidism, potentially autoimmune thyroid disease and fibromyalgia, than either age-matched controls or males with FXTAS (Coffey et al., 2008; Leehey et al., 2011; Rodriguez-Revenga et al., 2009). They also present hypertension, seizures, and peripheral neuropathy more often than controls (Chonchaiya et al., 2009; Coffey et al., 2008; Hamlin et al., 2011). Co-occurrence of multiple sclerosis (MS) has been described in women carriers (Greco et al., 2008; Zhang et al., 2009). We have studied eight premutation

females and here we report their neuropathological findings, molecular data, and clinical problems.

MATERIALS AND METHODS

Molecular measures

DNA analysis - Genomic DNA was isolated from peripheral blood leucocytes (5 ml of whole blood) obtained prior to death, and from post-mortem sections of approximately 500mg of brain tissue using standard methods (Puregene Kit; Gentra Inc.) and under informed consent according to Institutional Review Board approved protocols. Southern blot analysis, PCR analysis and calculation of the repeat size for both methods were performed as described in (Tassone, Pan, Amiri, Taylor, & Hagerman, 2008). The Activation Ratio (AR), which expresses the percent of cells carrying the normal allele on the active X chromosome, was measured using an Alpha Innotech FluorChem 8800 Image Detection System as previously described (Tassone et al., 1999).

FMR1 mRNA levels - Total RNA was isolated from peripheral blood leukocytes using Tempus tubes (Applied Biosystems, Foster City, CA). Reverse transcriptase reactions and quantifications of *FMR1* mRNA were performed as described in (Tassone et al., 2000c).

Pathology

Formalin-fixed brain tissue for all cases was processed for paraffin sections, and histological and immunohistological staining in standard fashion as previous reported (Greco et al., 2002; Greco et al., 2006). Tissue blocks of frontal cortex and hippocampus were obtained from five age matched control female subjects (age range 60-76 years). Tissues were selected to be the same across

all cases to facilitate comparisons among experimental cases. Control cases were obtained from pathology files at Department of Pathology at University of California, Davis according to UC Davis approved IRB protocol.

Evaluation of AD neuropathology

We evaluated the AD neuropathology, including the Braak and Braak stage and the CERAD plaque score, using the Diagnostic Criteria for the Neuropathological Assessment of Alzheimer's Disease, following the recommendation by the National Institute on Aging and Reagan Institute Working Group (NIA-Reagan criteria; 1997).

Quantitative analysis of intranuclear inclusion number

Percentages of intranuclear inclusions in neurons and astrocytes were determined for frontal cortex, hippocampus, and middle superior temporal gyrus using protocols previously described (Greco et al., 2002; Greco et al., 2006; Greco et al., 2008). Tissue from blocks of frontal cortex and hippocampus were obtained for 8 female cases and middle superior temporal gyrus was obtained for 7 of these cases. Quantifications were compared to previously reported female control cases from (Greco et al., 2006). These control cases matched the age range of the present female cases, and were free of gross neuropathological features or histological artifacts.

Brain tissues were blocked and sectioned in the same orientation to facilitate histological analysis. Tissues were paraffin embedded, sectioned at 10

µm, and stained with hematoxylin and eosin (H&E). Three sections separated by 50 µm were used for unbiased cell counting.

To estimate the number of intranuclear inclusions in females with the fragile X premutation both with and without FXTAS, regions of interest were outlined within the frontal cortex, superior medial temporal gyrus, and hippocampus, using the StereoInvestigator (v 8.0, MBI, Inc.; Williston, TN) software package and a Nikon E600 ECLIPSE microscope at 400x magnification. All parameters explicitly replicated those reported by (Greco et al., 2006) quantifying inclusions presence in male FXTAS cases to facilitate comparison between the results of that study and the present report. To reduce bias in our samples, standard sections were taken from all control cases and premutation cases to allow direct comparisons among cases. Unbiased sampling techniques were used to collect and define a systematic, random sampling of the tissue to ensure an unbiased estimation of inclusion number, but no rigorous stereology was carried out in the present study and we are reporting the actual number of items counted, not estimated values provided by the software. Briefly, these techniques involved tracing the regions of interest at 40X magnification by an experimenter blinded to the identity of each case (*i.e.*, slide blinded). Once the region of interest was traced, the software placed a regular grid of sampling frames across the region of interest using a randomized starting point. The size of the counting frame and spacing of the grids were the same as reported in (Greco et al., 2006). This way, there was a rigorous, systematic sampling of the area contained within the region of interest, but the experimenter did not have

control over precisely which areas of the region of interest were sampled. Counting of cells containing intranuclear inclusions was performed at 400X. Cell identification within the regions of interest was based on standard morphological criteria as previously described (Greco et al., 2002; Greco et al., 2006). The numbers obtained from these cell counts were converted to ratios (# of cell type with inclusions / total # of cell type counted).

RESULTS

Clinical Histories

Key clinical features and molecular characteristics of the eight cases included in this study are presented in Table 3.

	Case	Case 1	Case 2	Case 3	Case 4	Case 5	Case 6	Case 7	Case 8
Clinical Symptoms	Age of death	76	66	85	52	Dementia with memory loss; tremor	65	84	79
	FXTAS	No	Yes	Yes	Yes	Dementia with memory loss; tremor; MS; neuropathy; tremor; ataxia; arrhythmias	DLB ⁽²⁾ ; Breast Cancer; intentional tremor; ataxia; neuropathy; hypertension	Intentional tremor; ataxia, neuropathy	
	CGG repeats	30,70	30,80	29,87	36,75	30,63	Premutation ⁽¹⁾	27,59	30,78
Molecular Activation Ratio	0.80	0.30	0.53	0.44	0.28	-	-	0.63	0.21
	FMR1 mRNA levels	1.31 (0.11)	6.06 (0.16)*	2.31 (0.17)	2.8 (0.12)	na	na	1.83 (0.12)	2.6 (0.04)
Pathology	Intranuclear inclusions (FXTAS)	+	+	+	+	+	+	+	+
	Braak & Braak staging⁽³⁾	0	Braak V-VI	Braak I-II	0	Braak V-VI	Braak V-VI	Braak I-II	Braak V-VI
	CERAD plaque score⁽⁴⁾	0	frequent	sparse	0	frequent	frequent	sparse	moderate
	Addl. significant histopathology	mild arteriolosclerosis	--	--	multiple sclerosis	--	--	Lewy bodies, Lewy bodies, arteriosclerosis	Severe arteriosclerosis

- (1) Fixed tissues only; reported as premutation without allele sizes or AR (Yachnis *et al.*, 2010)
 (2) DLB – Dementia with Lewy body disease
 (3) (Harding *et al.*, 2000)
 (4) (Mirra *et al.*, 1991)

Table 3. Summary of the clinical, molecular, and neuropathological features of the current cases

Case 1:

Case 1 was an asymptomatic premutation carrier who had no neurological, behavioral, or cognitive symptoms by history. She had a 30 CGG repeat normal allele and 70 CGG repeat premutation allele with an activation ratio (AR) = 0.8. Her *FMR1* mRNA levels were 1.31 (+/- 0.11) times normal. At age 40, she experienced an episode of Bell's palsy. She had dry eyes resulting from cataract surgery in her early 70's. At age 73, she developed uterine cancer and had a hysterectomy, followed by radiation treatment and chemotherapy. She died of uterine cancer at age 76, after a downhill course involving weakness and cognitive decline terminally.

Case 2:

Case 2 experienced her first symptoms at the age of 56 years, presenting with expressive and receptive aphasia. The aphasia was not acute and there was no indication of a stroke. The detailed work up ruled out vascular infectious or inflammatory etiology. She had a normal and a premutation allele of 30 and 80 CGG repeats and an AR = 0.3. Her *FMR1* mRNA levels were 6.06 (+/- 0.16) times normal. For this case, transcript levels were measured using frontal cortex as blood samples were not available. She subsequently developed hyperphagia, incontinence, and hallucinations. A positron emission tomography (PET) scan at age 61 showed hypoperfusion in left greater than right temporal lobes, and a brain MRI revealed mild cortical atrophy. Later, she experienced sudden falls and

then swallowing difficulties. She died at 66 years of age after a progressive neurological and cognitive decline, and dementia.

Case 3:

Case 3 had a history of mild FXTAS and was initially reported in (Hagerman et al., 2004). She had a normal and a premutation allele of 29 and 87 CGG repeats, respectively, and an AR = 0.53. Her *FMR1* mRNA level was 2.31 (+/- 0.17) times normal. She was a social worker who had 2 children with FXS. She had a long history of anxiety and she developed depression at age 75, which was treated with fluoxetine. Mild ataxia began at age 79, necessitating use of a cane. She developed an intention tremor and extremity weakness at age 82 years. She required a pacemaker in her 80s for cardiac arrhythmias. She fell and fractured her left hip at age 84. She did not have any significant cognitive deficits except for impaired memory a few months prior to death. She died at age 85 from complications related to gastrointestinal surgery for ileus.

Case 4:

Case 4 was originally reported in 2008 (Greco et al., 2008), emphasizing the co-occurrence diagnosis of FXTAS and multiple sclerosis (MS). The *FMR1* alleles had 36 and 75 CGG repeats in size with an AR = 0.44. Her *FMR1* mRNA levels were 2.80 (+/- 0.12) times normal. She died of MS at age 52, having been found to be a carrier just 2 weeks before her death after her daughter was diagnosed as a carrier by her OB/GYN physician on the basis of ovarian dysfunction. She

developed neurological symptoms at age 32 years, with numbness in her arm and optic neuritis. By age 38 she had developed gait ataxia and loss of dexterity in the right hand. Her MRI demonstrated diffuse atrophy and multiple foci of increased T2 signal intensity in the periventricular and cerebellar white matter including the middle cerebellar peduncles (MCP sign). She was diagnosed with MS and treated with several regimens including methotrexate, but her symptoms gradually progressed. She developed an upper extremity intention tremor, progressive dysarthria, lower extremity numbness, and eventually spastic paraparesis and cognitive decline. She was unable to swallow and she became incontinent and bedridden before her death at age 52.

Case 5:

Case 5 had normal and premutation alleles of 30 and 65 CGG repeats, respectively, and an AR = 0.28. No *FMR1* mRNA levels are available. Her medical history was unremarkable beside AD later in life. Her psychiatric history included anxiety and depression. At 73 years of age she was diagnosed with AD by her neurologist and started taking donepezil. At age 77 years, she was placed in an assisted living setting and a year later she moved to an AD nursing home unit after a fall resulting in a broken ankle. She was unsteady in her walking and had tremor before death. Her downhill course was rapid. She did not have an MRI. She died as a result of AD at age 80 as result of AD.

Case 6:

Case 6 was a premutation carrier; the mother of two sons with FXS, who died of FXTAS at age 65. This case has been previously described by Yachnis et al. (2010). Her *FMR1* mRNA levels and number of CGG repeats are unknown as only fixed tissues were available and results of previous genetic testing were unknown. She had a history of fibromyalgia symptoms starting at age 40 years with pain in her extremities, she also had hypothyroidism, and menopause at age 45. At age 58 she developed handwriting difficulties because of an intention tremor. At age 59 years her tremor worsened and involved hands and arms bilaterally. Her left hand would spasm and would close with increased tone. She also developed bladder incontinence and restless leg syndrome between age 59 and 60. She subsequently became physically weaker, with cognitive decline beginning at age 60 years, leading to a diagnosis of dementia, which was said to be rapidly progressive after age 60. Her cognitive decline was characterized by getting lost, poor judgment and hygiene, eventually she lost the ability to converse. She required a walker at age 61 years due to ataxia, began using a wheelchair regularly at age 62, and by 63 years of age she was bedridden. Her MRI demonstrated white matter disease. She was hospitalized with aspiration pneumonia and died with respiratory failure.

Case 7:

Case 7 died at age 84 years from FXTAS. She had two alleles, of 27 and 59 CGG repeats, and an AR = 0.63. Her *FMR1* mRNA levels were 1.83 (+/- 0.12) times normal. She had two daughters and one son with the premutation, and

three grandchildren with FXS. She was well until age 67 when she developed hypertension. She developed breast cancer in her 70s and was treated with a lumpectomy and radiation. She subsequently developed a hand tremor at age 78 with deteriorating handwriting; she was diagnosed with Parkinson's disease and was treated with carbidopa/levodopa. Ataxia began at age 80 with frequent falling and cognitive decline that necessitated 24-hour care. By age 82 she did not recognize family members and spoke very little. She was diagnosed with dementia with Lewy Bodies (DLB); treatment with donepezil and memantine showed some clinical benefit. She gradually became weaker and was unable to walk independently after age 82 years; she then used a wheelchair consistently. On examination at age 83 she had an intention tremor, global weakness, and severe neuropathy with edema and absent vibration and pin prick sensation in her lower extremities. Her MRI demonstrated severe white matter disease in the pons, caudate, putamen, and thalamus, in addition to global cerebral atrophy. There were ischemic changes in her basal ganglia with iron deposits in her cerebellar dentate nuclei.

Case 8:

Case 8 was originally reported in 2004 as the fifth case of the original case series of women with FXTAS (Hagerman et al., 2004). She had alleles of 30 CGG and 78 CGG repeats, and an AR = 0.21. Her *FMR1* mRNA levels were 2.6 (+/- 0.04) times normal. She developed episodes of lightheadedness, unsteady gait, and frequent falls at age 71 years. She also developed an intention tremor of the

hand that improved first with propranolol and then more markedly with primidone. Subsequently she developed numbness in her lower extremities. At age 74 she had bradykinesia, dystonia of the neck muscles, and upper extremity rigidity in addition to an intention tremor and ataxia. Her symptoms gradually worsened and she died of respiratory failure at the age of 79.

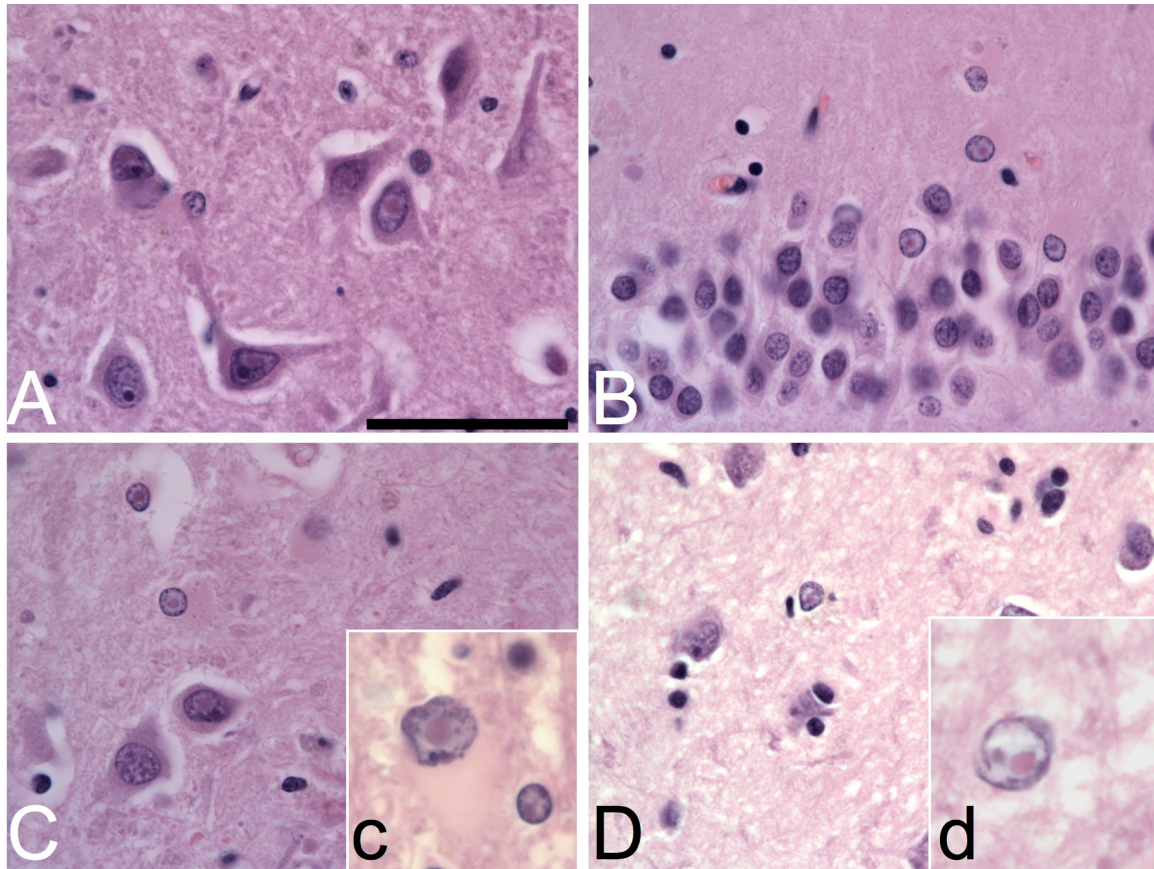


Figure 9. **A.** Intranuclear inclusions in pyramidal cells in CA3b of Case 2. **B.** Intranuclear inclusions in granule cells of the medial blade of the dentate gyrus of Case 2. **C.** Intranuclear infusions in pyramidal cells and neurons in the hilus of case 6. **c.** Inset, intranuclear inclusion in neuron and astrocyte in the white matter adjacent to layer VI of the frontal cortex of Case 6. **D.** Intranuclear inclusion in an astrocyte in layer II if the frontal cortex of Case 1. **d.** Inset, granule cell from layer IV of the frontal cortex in Case 1. All plates are at 1000X magnification. Scale bar = 50 μ m.

Gross and microscopic findings:**Case 1**

Fresh brain weight was 1231 g. Gross examination of the brain showed no pathological changes. Comprehensive microscopic examination of the brain identified intranuclear inclusions in neurons and astrocytes (Figure 9D), and mild vascular hyalinosis of white matter. Neither neurofibrillary tangles (NFTs) changes or plaque formation was seen on the modified Bielschowsky stain (Braak and CERAD stage 0).

Case 2

Total brain weight (fixed) was 1140 g. Gross examination showed global atrophy, and diffuse cerebrovascular atherosclerosis. Microscopic examination of the brain showed intranuclear inclusions as established for the histological diagnosis of FXTAS (Figure 9A,B). Loss of cortical neurons, occasional senile plaques, granulovacuolar degeneration (GVD), and NFTs were identified in frontal and temporal cortices. The hippocampus showed prominent formation of NFTs, GVD, and senile plaques in CA1. Bielschowsky stain showed abundant plaques and NFTs conforming to Braak and Braak Stage V-VI and CERAD plaque assessment as “frequent”.

Case 3

Fresh brain weight was 980 g. Gross examination showed cerebral edema, and small, scattered, atheromatous plaques in the circle of Willis. Neurons and astrocytes demonstrated intranuclear inclusions throughout the central nervous system. There was patchy pallor of subcortical, deep, and periventricular white matter evident on both H&E and myelin stains, and patchy myelin pallor involved arcuate fibers in a patchy distribution. Bielschowsky stain showed few NFTs, plaques and GVD in hippocampus, and only rare plaques in cortical sections, consistent with Braak and Braak Stage I-II and a “sparse” CERAD plaque score.

Case 4

A detailed neuropathological description was presented previously in (Greco et al., 2008). In brief, gross examination showed cortical atrophy and scattered, discrete plaques of demyelination throughout the brain. Histological evaluation identified characteristic features seen with multiple sclerosis, and the intranuclear inclusions in neurons and astrocytes described in FXTAS. Bielschowsky stain showed no NFTs or plaque formation.

Case 5

Brain weight was unavailable. Gross examination of the brain showed moderate frontal lobe atrophy, ventricular enlargement, and cerebrovascular atherosclerosis. Gray matter was thinned to 3 mm in all lobes. Intranuclear inclusions were present in neurons and astrocytes. Histological features seen

corresponded to Braak and Braak Stage V-VI. The CERAD plaque count showed “frequent density” of neuritic and cored plaques.

Case 6

The brain weighed 1040 gm., and showed mild cerebrovascular atherosclerosis. Mild cortical atrophy was present, favoring frontal, insular, and temporal cortices, with severe hippocampal atrophy. Neurons and astrocytes demonstrated intranuclear inclusions throughout the central nervous system (Figure 9C). Marked ventriculomegaly was seen, and some regions of white matter appeared almost translucent. Bielschowsky stain identified AD-like changes that corresponded to Braak and Braak Stage V-VI. According to CERAD criteria, plaques were “frequent” in density.

Case 7

Brain weight was unavailable. There was mild fronto-parietal cortical atrophy without ventriculomegaly, and mild spotty atherosclerosis in the Circle of Willis. Bielschowsky stain showed AD-like pathology that corresponded to Braak and Braak Stage I-II. Lewy bodies were seen in cortical areas and brainstem dopaminergic neurons.

Case 8

Brain weight was 930 gm., and showed moderate ventriculomegaly on cut section. The hippocampus was markedly atrophied. Histologic features as

established for a post-mortem histological diagnosis of FXTAS were present. Bielschowsky stain identified AD-like pathological features corresponding to Braak and Braak Stage V-VI. "Moderate" numbers of plaques were present as per CERAD criteria. Severe arteriosclerosis was prominent in gray and white matter of frontal and temporal cortices.

Quantitative analysis of intranuclear inclusion number

The number of neurons and astrocytes with intranuclear inclusions (actual cell counts and percentages) are presented in Table 4 for frontal cortex, superior middle temporal gyrus, and hippocampus. No inclusions in neurons or astrocytes were observed for any of the similarly aged control subjects counted ($n=6$), and no inclusions were observed in the cytoplasm of neural cells in tissues from control or premutation cases. Intriguingly, the percentages of neurons and astrocytes with intranuclear inclusions were roughly equivalent in the female FXTAS cases, across all three areas evaluated (% \pm SEM) 9.03 \pm 1.62% neurons vs. 8.21 \pm 0.96% of astrocytes), which is in contrast to the findings previously reported in males (Greco et al., 2006). Importantly, there were no differences for number of cells counted among the experimental cases and control tissues counted using the same techniques.

Subject	Frontal Cortex Gray Matter			Frontal Cortex White Matter			Superior Medial Temporal Gyrus					
	Neurons	%	Astrocytes	%	Neurons	%	Astrocytes	%	Neurons	%	Astrocytes	%
Case 1	24/265	9.06	25/680	3.68	3/26	11.54	30/346	8.67	27/384	6.77	54/684	7.89
Case 2	16/190	8.40	2/117	1.80	1/57	1.75	21/615	3.41	--	--	--	--
Case 3	2/231	0.80	5/200	2.50	3/5	60.00	19/333	5.71	25/347	6.94	44/754	5.84
Case 4	0/370	0.00	14/504	2.80	6/19	31.58	12/662	1.81	26/298	8.72	82/730	11.23
Case 5	6/251	0.02	10/403	0.02	1/7	0.14	9/501	0.02	16/316	5.06	44/326	6.06
Case 6	62/456	13.60	240/1729	13.90	6/56	10.70	38/333	11.40	46/234	20.00	146/774	19.00
Case 7	18/221	8.14	21/746	2.82	2/28	7.14	23/552	4.17	20/297	6.73	61/599	10.18
Case 8	17/358	4.75	45/701	6.42	9/77	11.69	23/299	7.69	52/236	22.03	50/722	6.93
Mean	--	5.6	--	4.24	--	16.8	--	5.36	--	11.59	--	9.49
Controls	0/361	0	0/251	0	0/16	0	0/303	0				

Subject	Pyramidal Cell Layer (CA1-CA3)			Granule Cell Layer (DG)			Hilus					
	Neurons	%	Astrocytes	%	Neurons	%	Astrocytes	%	Neurons	%	Astrocytes	%
Case 1	11/361	3.05	38/496	7.66	43/766	5.61	13/90	14.44	6/249	2.41	23/537	4.66
Case 2	1/118	0.90	9/75	12.00	3/260	1.20	1/12	8.30	0/97	0.00	15/109	13.80
Case 3	7/148	4.70	4/127	3.10	6/372	1.70	2/10	20.00	11/100	11.00	17/117	14.50
Case 4	0/538	0.00	0/239	0.00	0/1094	0.00	0/85	0.00	0/251	0.00	0/462	0.00
Case 5	8/289	2.77	17/364	4.67	28/806	3.47	17/199	4.26	3/155	1.94	6/332	1.81
Case 6	79/332	24.00	157/698	22.00	100/899	11.00	12/46	26.00	97/265	37.00	205/831	25.00
Case 7	36/486	7.41	9/123	7.32	27/486	5.56	13/107	12.15	14/160	8.75	14/209	6.70
Case 8	26/263	9.89	72/514	14.01	68/777	8.75	6/82	7.32	54/305	17.70	101/901	11.21
Mean	--	6.59	--	8.84	--	4.66	--	11.56	--	9.85	--	9.71
Controls	0/109	0.00	0/165	0.00	0/483	0.00	0/45	0.00	0/110	0.00	0/280	0.00

Table 4. Quantification of intranuclear inclusions (counts and percent) in neurons and astrocytes

DISCUSSION

The two most significant findings of this study are the presence of intranuclear inclusions in all cases and a high number of them presenting with AD neuropathological changes. Female carriers of the fragile X premutation, both with and without a FXTAS clinical diagnosis, show similar numbers of intranuclear inclusions in neurons in the cortex and hippocampus as do men with FXTAS. The number of intranuclear inclusions in astrocytes, however, was greatly reduced in female carriers relative to the levels observed in male FXTAS cases (Greco et al., 2002; Greco et al., 2006). Additionally, we found evidence of intranuclear inclusions in all cases, even though one woman (Case 1) was asymptomatic. To our knowledge this is the first report of intranuclear inclusions in a fragile X premutation female carrier that showed no clinical symptoms associated with FXTAS. There also appeared to be little to no contribution of comorbid disorders to the number of intranuclear inclusions in any of the female premutation and FXTAS cases. Two other striking findings were the high number of women carriers with dementia (Cases 2, 5, 6, and 7), much higher than expected given previous reports, and the high level of AD-type plaque and tangle pathologies (Cases 2, 5, 6, and 8), with or without corresponding clinical AD signs.

Importantly, we have demonstrated that although the presence of intranuclear inclusions is considered a primary diagnostic criterion for FXTAS (Hagerman & Hagerman, 2004a; Jacquemont et al., 2003), the presence of intranuclear inclusions may be necessary but not sufficient to lead to FXTAS

symptoms. Two of the cases presented here did not have a FXTAS diagnosis at the time of death. Case 1 died of a uterine cancer for which she received radiation and chemotherapy. It is possible that the CNS trauma of the cancer treatment could have precipitated the formation of inclusions and FXTAS as was previously described in (O'Dwyer, Clabby, Crown, Barton, & Hutchinson, 2005) where chemotherapy lead to CNS white matter disease and clinical symptoms of FXTAS. However, the presence of the fragile X premutation appears to be sufficient for the presence of intranuclear inclusions, even when there are relatively normal levels of *FMR1* mRNA, as demonstrated by the findings in Case 1. It is possible that genetic and environmental factors, including the genetic background and a favorable AR, may have played a role in the absence of FXTAS symptoms in Case 1. A high AR (0.8) was in fact measured in Case 1 in both peripheral blood leukocytes and also in brain tissue. Case 5 had a history of anxiety and depression, which are common in carriers (Bourgeois et al., 2009; Bourgeois et al., 2011; Roberts et al., 2009) and then presented with dementia with subsequent decline that included falling. Dementia has occasionally been a presenting sign of FXTAS and in (Sevin et al., 2009)cognitive decline was more common in carriers compared to controls even in those without tremor and ataxia. Our cases demonstrate that the inclusions of FXTAS are more common than previously thought even in female carriers without classical symptoms of FXTAS.

Interestingly, cases 2, 5, 6, and 7 presented with dementia, which has only rarely been described in women with FXTAS. Only five women with FXTAS and

dementia have been reported to date (Al-Hinti, Nagan, & Harik, 2007; Karmon & Gadoth, 2008; Rodriguez-Revenga et al., 2009; Yachnis et al., 2010). Thus, the present case series greatly enriches the existing literature with these additional three cases (cases 2, 6, and 7). In three of the women we described (Cases 2, 5, and 6), there is a high likelihood that dementia was due to AD lesions according to the Diagnostic Criteria for the Neuropathological Assessment of Alzheimer's Disease recommended by the National Institute on Aging and Reagan Institute Working Group (1997). The etiology of dementia in Case 7, who only had low levels of AD lesions, is not clear but the presence of Lewy bodies suggests a diagnosis of DLB (McKeith, 2006) or PD dementia. We have also seen the occurrence of FXTAS inclusions and Lewy bodies in one man with FXTAS (Greco et al., 2002). It is, in fact, possible that individuals with FXTAS who developed cognitive changes may get diagnosed as having AD, PD, or DLB, since dementia in FXTAS has an interesting cortical-subcortical picture which may partially mimic other neurodegenerative dementias (Seritan et al., 2008). Dementia associated with FXTAS has a characteristic profile different than other dementias, even though deficit severity may be of the order of the deficits encountered in AD (Bacalman et al., 2006; Seritan et al., 2008). Patients in more advanced stages of FXTAS (Gane et al., 2010) develop both cortical (apraxia, memory recall, visuospatial skills impairment) and subcortical (memory retrieval, bradyphrenia, latency of speech, mood and personality changes) cognitive deficits, in conjunction with the movement disorders described (ataxia, tremor, bradykinesia, parkinsonian features). Although aphasia may be present, language is typically

spared early in FXTAS (Grigsby et al., 2007). Executive dysfunction is the most prominent deficit (Grigsby et al., 2007; Grigsby et al., 2008), it may occur prior to development of a full dementia and appears to mediate other cognitive deficits (Brega et al., 2008). These women described with FXTAS and neurocognitive changes presented with a variety of clinical features, making a specific dementia diagnosis difficult. It is not clear whether all the cognitively impaired women described here had FXTAS dementia, since one was also diagnosed with AD and another, with DLB. However, co-occurrence of FXTAS with other neurological disorders may exacerbate symptom severity and contribute to a faster decline. Although further studies using a larger series are required, we hypothesize that a previously unrecognized association may exist between the *FMR1* premutation and AD pathology. There may be a synergy of having both disorders because both have mitochondrial dysfunction and both have oxidative stress and these problems could be amplified when they occur together (Karbowski & Neutzner, 2012; Napoli et al., 2011; Ross-Inta et al., 2010; Ye, Tai, & Zhang, 2011). However, this association could be independent of the development of FXTAS, as Case 5 developed AD without FXTAS. Because of the high frequency of female premutation carriers in the general population (1:110-259 females), the contribution of aberrant FMRP (*FMR1* protein) metabolism to the development of AD should be evaluated. FMRP controls amyloid precursor protein (APP) through inhibition (Darnell et al., 2011) and FMRP may be somewhat lower in the brains of carriers (Handa et al., 2005; Qin et al., 2011) and if so APP levels may be

higher in premutation carriers, as reported in (Handa et al., 2005), possibly predisposing them to AD.

In summary, dementia is more common than had been previously observed in female premutation carriers, and the co-occurrence of AD-associated NFTs and plaques and FXTAS neuropathologic changes in this small series is a striking finding. Larger studies will be necessary to further substantiate this finding. The essential role of the premutation (even with normal *FMR1* mRNA levels) in the inclusion formation is a cardinal finding, which will also need to be further explored in subsequent studies.

ACKNOWLEDGEMENTS:

We would like to thank Dr. Anthony T. Yachnis for providing tissue from Case 6. This work was supported by National Institutes of Health grants HD036071; AG032115; UL1DE019583; AG03119; AD02274; National Center for Research Resources UL1RR024116.

This work is dedicated to the memory of Matteo.

Chapter 5

Distribution and Frequency of Intranuclear Inclusions in Female CGG KI Mice Modeling the Fragile X Premutation.

ABSTRACT

The fragile X-associated tremor/ataxia syndrome (FXTAS) is an adult-onset neurodegenerative disorder caused by CGG trinucleotide repeat expansions in the fragile X mental retardation 1 (*FMR1*) gene. The neuropathological hallmark of FXTAS is the presence of ubiquitin-positive intranuclear inclusions in neurons and in astrocytes. Intranuclear inclusions have been reported in the neurons of male CGG KI mice carrying an expanded CGG trinucleotide repeat, but no study has been carried out quantifying these pathology in female CGG KI mice heterozygous for the fragile X premutation. We used histologic and immunocytochemical methods to determine the pathological features of intranuclear inclusions in astrocytes, Bergmann glia and neurons. In female CGG KI mice, ubiquitin-positive intranuclear inclusions were found in neurons and astrocytes throughout the brain in cortical and subcortical brain regions. These inclusions increased in number and size with advanced age and increasing CGG repeat length--supporting hypotheses that these pathologic features are progressive across the lifespan. The number of inclusions in neurons were reduced by 25% compared to male mice, but not so low as the 50% predicted by X inactivation hypotheses. These data suggest closer evaluation of neurocognitive and pathological features in female carriers of the fragile X premutation and FXTAS is necessary.

This chapter has been submitted for publication

Erik W. Schluter, Michael R. Hunsaker, Claudia M. Greco, Rob Willemsen, & Robert F. Berman. (2012). Distribution and Frequency of Intranuclear Inclusions in Female CGG KI Mice Modeling the Fragile X Premutation. Brain Research. Submitted

My role in this study was to perform immunoperoxidase and immunofluorescence staining as well as supervise Erik Schluter, who was performing similar experiments in parallel. I was also responsible for photography and performing cell counting. I was also responsible for analyzing and photographing the human tissue reported in this study along with Dr. Claudia Greco.

1. INTRODUCTION

Fragile X-associated Tremor Ataxia Syndrome (FXTAS) is a neurodegenerative disorder resulting from a 55-200 long CGG trinucleotide repeat expression (fragile X premutation) within the 5' untranslated region of the X-linked *FMR1* gene. Beyond 200 CGG repeat expansions, CpG island methylation of the *FMR1* promoter and the CGG repeat usually occurs (Kenneson et al., 2001; Tassone et al., 2000c; Tassone et al., 2004a; Tassone et al., 2008; Tassone et al., 2012). This silences *FMR1* gene transcription, leading to Fragile X Syndrome (Hagerman & Hagerman, 2004b; Raske & Hagerman, 2009; Tassone & Hagerman, 2010). Approximately 40% of male fragile X premutation carriers over the age of 50 develop motor features associated with FXTAS. These motor features include kinetic, intention, and/or postural tremors, cerebellar gait and limb ataxia, Parkinsonism, as well as peripheral neuropathy and progressive cognitive impairments (Hamlin et al., 2011; Leehey et al., 2011); neurologically, the hallmark pathological feature is ubiquitin-positive intranuclear inclusions throughout the brain and white matter disease on T2 weighted magnetic resonance imaging (MRI) (Brunberg et al., 2002; Greco et al., 2002; Greco et al., 2006; Greco et al., 2008).

Female fragile X premutation carriers also present with symptoms but far less frequently than do male carriers, and with somewhat less profound symptomatology (Berry-Kravis et al., 2005; Karmon & Gadoth, 2008). Approximately 8-16% of female premutation carriers older than 50 years of age present with FXTAS, and a few cases have been described within the literature

(Berry-Kravis et al., 2005; Hagerman et al., 2004; Leehey et al., 2011; Roberts et al., 2009; Tassone et al., 2012; Yachnis et al., 2010). One explanation for the less frequent presentation of FXTAS in female carriers is X-inactivation silences transcription of one of the *FMR1* alleles, one carrying the premutation allele and the other unaffected by the premutation (*i.e.*, CGG repeat length <45 repeats). X-inactivation silences transcription of one of the two copies of the X chromosome, and patterns of X-inactivation are normally thought to be random with no preference for inactivation of paternal or maternal alleles. However, it has also been suggested that in FXTAS skewed (or non-random) X-inactivation may occur in females where a ‘stronger’ allele dominates over a ‘weaker’ allele (*cf.*, Plenge, Stevenson, Lubs, Schwartz, & Willard, 2002; Yonath et al., 2011). Therefore, X-inactivation in females heterozygous for the *FMR1* premutation may favor the unmutated allele, leading to suppression of the FXTAS pathologic phenotype (*cf.*, Tassone et al., 2012). This type of selective action has been described for a number of other X-linked genetic disorders (Plenge, Stevenson, Lubs, Schwartz, & Willard, 2002; Yonath et al., 2011).

It is difficult to correlate human neuropathologies with the dosage of molecular measures such as CGG repeat length due to the lack of available human tissue. Therefore, an *Fmr1* premutation CGG knock-in (KI) mouse model (CGG KI) was developed in Rotterdam and is a useful model of the Fragile X premutation and FXTAS. Willemsen and colleagues (Brouwer et al., 2007; Brouwer et al., 2008a; Willemsen et al., 2003) found that intranuclear inclusions were present in the brain of these CGG KI mice. Wenzel and colleagues reported

astroglia contained inclusions in these same line of CGG KI mice (Wenzel et al., 2010). Previous studies correlating neuropathological features of FXTAS with repeat length have focused primarily on male mice (Brouwer et al., 2007; Brouwer et al., 2008a; Brouwer et al., 2008b); however, there are presently no studies which have examined these features in female CGG KI mice heterozygous for the fragile X premutation. Therefore, this study was carried out to identify the presence and distribution of ubiquitin positive intranuclear inclusions, the hallmark neuropathological feature of FXTAS, throughout the brains of female CGG KI mice heterozygous for the fragile X premutation.

The brains of female CGG KI mice heterozygous for CGG repeat expansions between 71 and 326 were formalin-fixed, sectioned, and examined using histological, immunoperoxidase, and immunofluorescent staining methods. Ubiquitin positive intranuclear inclusions were identified in neurons and astroglia throughout the brain of female CGG KI mice. Further analysis of these findings also suggest that intranuclear inclusion density correlates with increasing dosage of the CGG repeat length, that the number of inclusions increases with age, and that these factors may interact. This study points to the potential for a relationship between ubiquitin positive intranuclear inclusions observed in FXTAS and the pathologic phenotype associated with the fragile X premutation.

2. RESULTS

2.1 General Histological Results

As has been reported previously, there were no gross histological differences among all groups of mice. On H&E, cresyl violet, and thionin stained sections there were no obvious differences in cell distribution, cell packing, cortical thickness, or overall brain morphology (Entezam et al., 2007; Greco et al., 2002; Greco et al., 2006; Greco et al., 2008; Tassone et al., 2012; Wenzel et al., 2010; Willemse et al., 2003). Luxol fast blue stains counterstained with neutral red demonstrated that the CGG KI mice did not show any white matter pallor or reduced integrity of white matter tracts throughout the brain, at least that can be identified at the light microscopic level. More specifically, no differences were observed between wildtype and CGG KI mice for white matter integrity in periventricular regions, brainstem, cerebellar peduncles, internal capsule, or corpus callosum. Subcortical white matter pathways (*e.g.*, fimbria/fornix, anterior commissure) were free of neuropathological features in CGG KI mice.

2.2 Nuclear pathology in neurons of female CGG KI mice and female FXTAS patients

The presence of intranuclear inclusions in neurons and astroglia is a pathological hallmark of FXTAS. Thus far, similar intranuclear inclusions have not been reported in oligodendroglia or microglia in human FXTAS or CGG KI mice. Figure 10 shows typical intranuclear inclusions in the hippocampus of a female premutation carrier without evidence for FXTAS symptomatology at 76 years

of age presented as Case 1 in (Tassone et al., 2012). These inclusions in a female patient are shown for comparison with intranuclear inclusions found in the brains of female CGG KI mice shown in Figure 11 that provides examples of inclusions in the granule cell and inner molecular layer of the hippocampal dentate gyrus and in the posterior nucleus of the amygdala of female CGG KI mice. In both cases inclusions appeared as well-delineated 2-3 μm diameter spherical bodies, were intensely eosinophilic, and hyaline in appearance with H&E staining. Identification of cell types in human tissue was based on methods reported previously (Greco et al., 2002; Greco et al., 2006; Tassone et al., 2012; Wenzel et al., 2010).

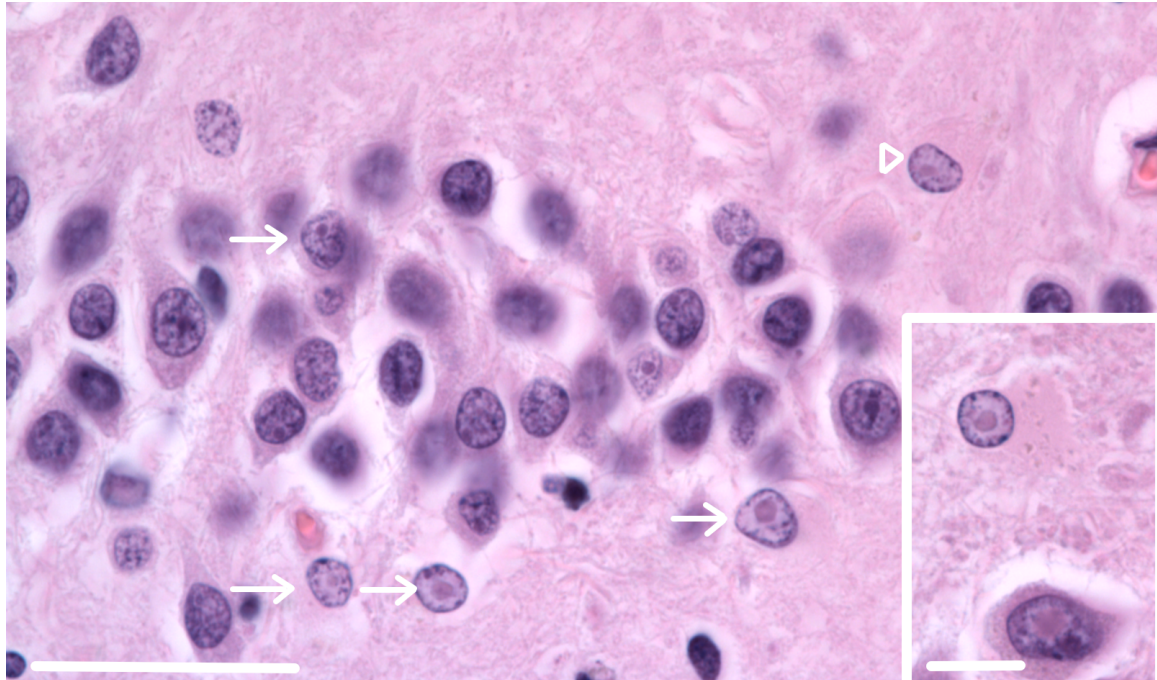


Figure 10. Intranuclear inclusions in the dentate gyrus of a female carrier of the fragile X premutation. Inclusions are present in the granule cell layer (arrow) and an astroglial cell in the hilus (arrowhead). **Inset** Inclusions in a pyramidal neuron and astroglial cell in the hilus. Scale bar = 50 μm .

The results of the semiquantitative analysis for the distribution of intranuclear inclusions are presented in Table 5 (*cf.*, Figure 11 for examples of inclusions the granule cell and inner molecular layer of the dentate gyrus (H&E stain) and in the posterior nucleus of the amygdala (immunoperoxidase stain) of female CGG KI mice). Inspection of the table shows a clear developmental course to the development of the inclusions, such that in nearly all cases mice at 48-52 weeks of age showed a greater number of inclusions than mice aged 24-28 weeks of age. Similarly, a dosage effect for the mutation was identified such that mice with 70-110 CGG repeats showed much fewer inclusions than mice with 140-200 CGG repeats.

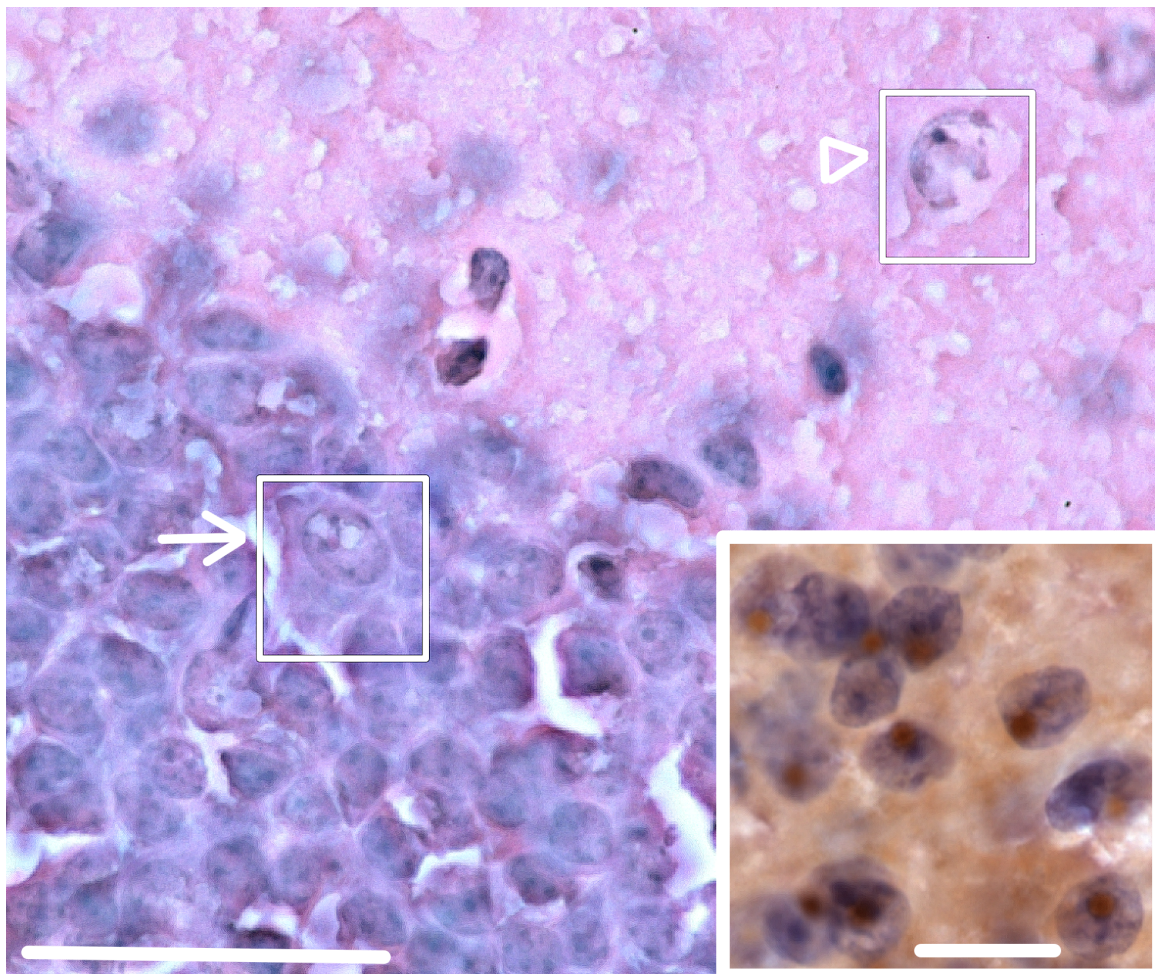


Figure 11. Intranuclear inclusions in dentate gyrus. Hematoxylin and eosin stained section of the dentate gyrus showing inclusions in granule cells (arrow; inset) and putative GABAergic cells in the inner molecular layer (arrowhead). Scale bar = 50 μ m.

	48-52 Weeks of Age		24-28 Weeks of Age	
	70-110 CGG	140-200 CGG	70-110 CGG	140-200 CGG
Prelimbic Cortex [#]	3,8,11,11,14 11/200	11,14,26,27,36 26/200	0,1,1,1, 1/200	5,5,7,9, 7/200
Motor Cortex [#]	0,1,4,4,6 4/200	2,6,9,10,15 9/200	0,0,1,3,3 1/200	0,3,5,6,8 5/200
Posterior Parietal Cortex [#]	4,6,6,9,13 6/200	4,11,13,13,26 13/200	0,0,0,1,3 0/200	2,3,7,11,13 7/200
Visual Cortex [#]	0,1,3,5,5 3/200	1,2,7,8,11 7/200	0,0,0,0,1 0/200	0,3,4,4,6 4/200
Anterior Cingulate Cortex [#]	4,7,8,10,11 8/200	10,19,23,25,26 23/200	0,1,3,3,7 3/200	3,5,14,14,19 14/200
Piriform Cortex ^{\$}	9,13,16,16,22 16/200	25,35,37,39,44 37/200	0,1,2,2,5 2/200	4,11,15,17,23 15/200
Entorhinal Cortex				
Ventromedial Area [#]	15,20,21,24,30 21/200	20,28,35,36,39 35/200	0,0,1,1,3 1/200	4,4,8,9,11 8/200
Dorsolateral Area [#]	4,5,7,7,13 7/200	9,9,11,14,15 11/200	0,0,0,0,1 0/200	1,1,3,5,6 3/200
Hippocampus ^{\$}				
CA1	8,9,13,16,17 13/200	15,22,27,28,31 27/200	2,2,5,5,8 5/200	5,6,9,11,11 9/200
CA3	0,0,2,2,5 2/200	2,3,8,9,12 8/200	0,0,1,1,1 1/200	0,0,1,1,3 1/200

	48-52 Weeks of Age			24-28 Weeks of Age		
	70-110 CGG	140-200 CGG	70-110 CGG	70-110 CGG	140-200 CGG	140-200 CGG
DG	23,31,47,50,61 4/7/200	50,57,76,83,105 76/200		5,10,10,11,11 10/200		15,33,34,37,40 34/200
Subiculum	7,11,13,14,19 13/200	11,20,28,30,39 28/200		0,0,2,2,3 2/200		2,2,6,7,9 6/200
Amygdalar Nuclei						
Central Nucleus†	3,9,9,14,15 9/200	12,15,17,18,22 17/200		1,1,2,2,2 2/200		9,9,11,13,18 11/200
Basolateral Nucleus‡	21,40,41,46,50 41/200	40,44,58,59,65 58/200		2,3,7,7,10 7/200		7,9,15,16,16 15/200
Posterior Nucleus	48,50,51,55,73 51/200	70,94,100,105,117 100/200		9,13,19,22,26 19/200		31,39,43,44,52 43/200
Septal Nuclei						
Lateral Septum¶	4,6,6,8,11 6/200	3,7,8,11,12 8/200		0,0,1,1,2 1/200		2,2,3,3,7 3/200
Medial Septum	2,2,4,4,5 4/200	2,2,5,6,6 5/200		0,0,0,1,1 0/200		1,1,1,3,4 1/200
Lateral Geniculate Nucleus	17,19,22,24,27 22/200	30,46,49,51,55 49/200		0,0,5,9,10 5/200		6,14,20,21,24 20/200
Inferior Colliculus§	11,19,30,37,45 30/200	37,49,61,66,70 61/200		0,1,3,3,4 3/200		2,3,15,18,19 15/200
Superior Colliculus§	0,4,5,6,9 5/200	5,11,16,20,21 16/200		0,0,0,1,1 0/200		0,0,2,2,3 2/200

	48-52 Weeks of Age		24-28 Weeks of Age	
	70-110 CGG	140-200 CGG	70-110 CGG	140-200 CGG
Medial Vestibular Nucleus	7,13,15,15,21 15/200	13,22,24,26,29 24/200	0,1,1,2,2 1/200	5,11,12,14,17 12/200
Cerebellum				
Cerebellar Lobule III&				
PCL	0,0,0,0,0 0/200	0,0,0,1,1 0/200	0,0,0,0,0 0/200	0,0,0,0,0 0/200
GCL	0,0,2,2,5 2/200	5,6,11,11,13 11/200	0,0,0,0,0 0/200	0,0,1,1,2 1/200
Flocculus&				
PCL	0,0,0,0,0 0/200	0,0,0,0,1 0/200	0,0,0,0,0 0/200	0,0,0,0,0 0/200
GCL	6,6,11,12,17 11/200	14,17,19,19,25 19/200	4,5,7,8,12 7/200	8,11,12,16,19 12/200

Table 5. Semiquantitative analysis of the presence and relative distribution of intranuclear inclusions in female CGG KI mouse brains in H&E stained parasagittal sections. n=5 female CGG KI mice were counted for each repeat length and age group. Not included in this table are wildtype littermate mice, which never showed intranuclear inclusions. The numbers of counted intranuclear inclusions across animals is given, along with the median number of inclusions counted per 200 cells. [#] For cortical quantifications, cells were counted in layers II-V of the cortex starting with layer II and moving ventrally into layer V, layers I and VI were not sampled. ^{\$} For hippocampus and piriform cortices, the primary cell layers (pyramidal and granule cell layers) were counted, the plexiform and molecular layers were not sampled. The hippocampus was sampled midway between the septal and temporal poles, sampling the dorsal half of the hippocampus. The piriform cortex was sampled at the most rostral and lateral sections in which it appeared. [†] The posterior part of the basolateral amygdalar nucleus was sampled. [‡] The medial part of the central amygdalar nucleus was sampled. [§]For the Cerebellum, the granule cell layer was counted in the most distal portion of each lobule. The Purkinje cells were sampled along the length of the folia surrounding the GCL regions sampled. The molecular layer was not sampled, and putative Bergmann Glia containing intranuclear inclusion bodies were not counted, although present in low number. [¶]For the colliculi, the dorsal cortex was sampled. ^{||}The rostroventral area of the lateral septal nucleus was sampled. Regions of interest identification were based on the 2009 Allen Mouse Brain Atlas: Sagittal Atlas.

To more fully characterize this pattern, the number of inclusions counted were related to CGG repeat length in both the young and old mice. Table 6 contains the Pearson's correlation coefficients that were calculated for each brain region and associated probability (p) values. In Figure 12 the number of inclusions are shown plotted against CGG repeat length for six brain regions for mice older than 6 months (circles) or younger than 60 month (diamonds) of age, along with the respective correlation coefficients. The most intriguing pattern of results that are apparent in Figure 12 is that the slope of the relationship is similar for young and old mice in a number of regions. The list of regions showing similar correlation slopes across age include: motor cortex, posterior parietal cortex, visual cortex, anterior cingulate cortex, dorsolateral and ventromedial entorhinal cortex, CA1 and the dentate gyrus in the hippocampus, all amygdalar nuclei, septal nuclei, anterior thalamus, vestibular nucleus, and the granule cell layer of the flocculus.

However, in other brain regions, older mice show a steeper slope of the correlation, suggesting age and CGG repeat dosage additively affect the progression of intranuclear inclusions. The few brain regions that showed a greater slope in older relative to young mice include the prelimbic cortex, piriform cortex, CA3 pyramidal cells and the subiculum in the hippocampus, the superior and inferior colliculus, and granule cell layer of lobe II in the cerebellum. Regions that showed near zero inclusions showed no relationship between inclusions number and repeat length, including the Purkinje cell layers of the cerebellum and the flocculus, and no correlations were computed for these regions. These

data suggest that age and CGG repeat length may additively affect the progression of intranuclear inclusions in some, but not all brain regions.

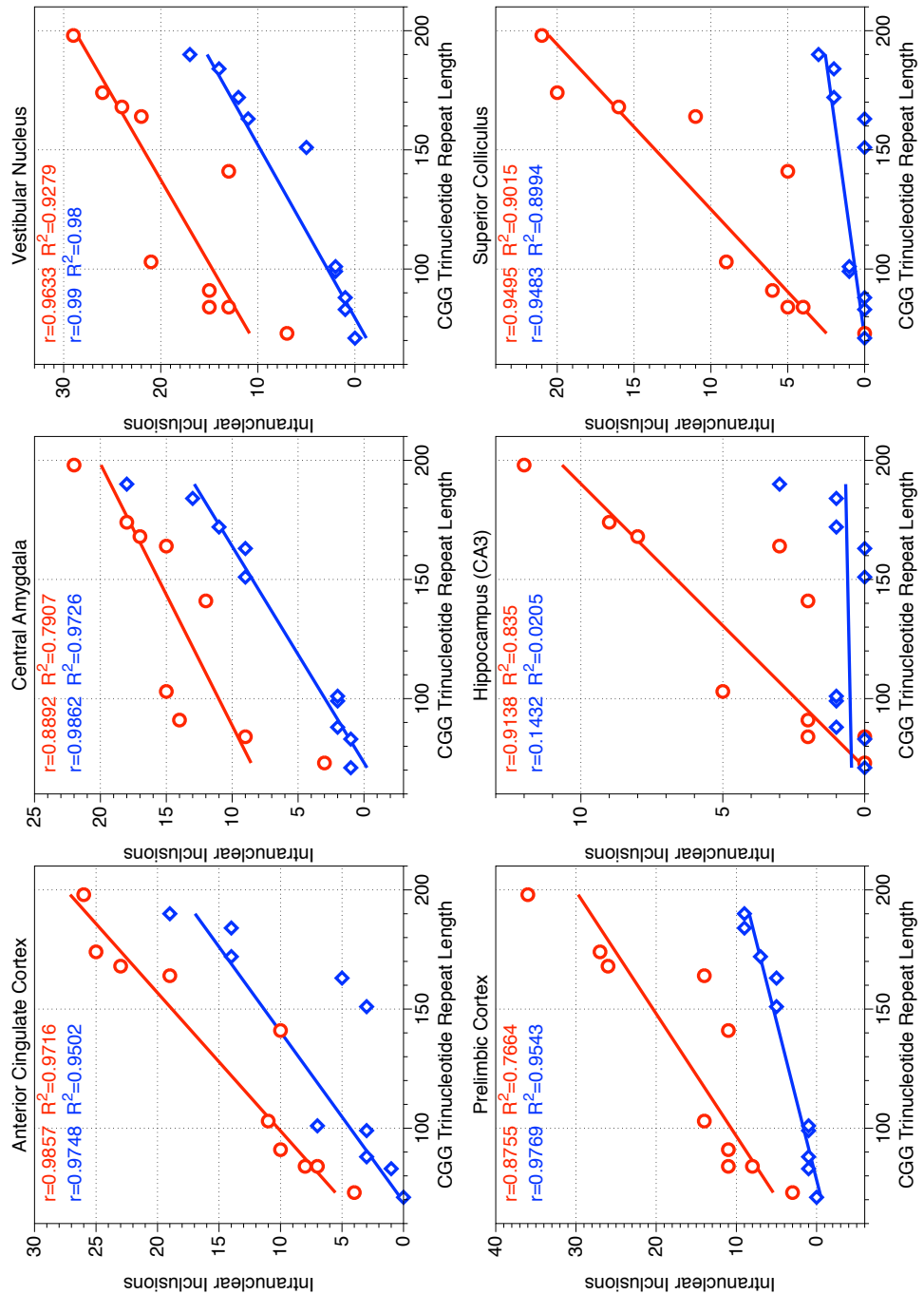


Figure 12 Example correlations between CGG repeat length and intranuclear inclusion number. A. The slope of the correlations are similar between young and old mice, suggesting in these brain regions age may not play a factor in the progression of neuropathologic features. B. The slope of the correlations are dissimilar between young and old mice, suggesting a combination of CGG repeat length and age may accelerate pathological features in these brain regions. Circles = CGG KI mice older than 6 months of age; diamonds = CGG KI mice younger than 6 months of age.

In comparison to previously published results quantifying intranuclear inclusions in male CGG KI mice (Brouwer et al., 2007; Brouwer et al., 2008a; Brouwer et al., 2008b; Wenzel et al., 2010; Willemse et al., 2003), the female CGG KI mice consistently showed 20-35% fewer inclusions, and surprisingly not the 50% fewer predicted by X inactivation. Four female CGG KI mice with 250, 265, 290, and 326 CGG repeats at 50 weeks of age showed a similar pattern of intranuclear inclusion distribution as the CGG KI mice with 70-110 CGG repeats, but 10-15% fewer inclusions in each region (data not shown). These data are consistent with reports of reduced number of intranuclear inclusions in male CGG KI mice when CGG repeat expansions are much greater than 200.

Four female CGG KI mice with 154, 168, 172, and 188 CGG repeats examined at 3 months of age only rarely showed intranuclear inclusions in the granule cell layers in the hippocampus dentate gyrus, olfactory bulb, and cerebellum. This pattern also differed from male CGG KI mice that show a much greater number of intranuclear inclusions in these granule cell populations at 3 months of age (Hunsaker et al., 2009; and unpublished observations).

	48-52 Weeks of Age		24-28 Weeks of Age		
	Pearson's rho	Slope	Pearson's rho	Slope	Difference
Prelimbic Cortex	p=.87; R ² =.77, p<.01	0.194	p=.97; R ² =.95, p<.01	0.07	0.12, p<.05
Motor Cortex	p=.91; R ² =.82, p<.01	0.09	p=.91; R ² =.82, p<.05	0.06	0.03, ns
Posterior Parietal Cortex	p=.80; R ² =.64, p<.01	0.07	p=.97; R ² =.94, p<.01	0.09	0.02, ns
Visual Cortex	p=.92; R ² =.85, p<.05	0.07	p=.96; R ² =.93, p<.05	0.06	0.01, ns
Anterior Cingulate Cortex	p=.98; R ² =.97, p<.01	0.17	p=.97; R ² =.95, p<.05	0.14	0.03, ns
Piriform Cortex	p=.99; R ² =.98, p<.01	0.14	p=.98; R ² =.97, p<.01	0.26	0.12, p<.01
Entorhinal Cortex					
Ventromedial Area	p=.95; R ² =.91, p<.05	0.16	p=.96; R ² =.93, p<.01	0.11	0.05, ns
Dorsolateral Area	p=.93; R ² =.86, p<.01	0.07	p=.96; R ² =.93, p<.01	0.08	0.01, ns
Hippocampus					
CA1	p=.96; R ² =.92, p<.01	0.16	p=.89; R ² =.80, p<.01	0.12	0.04, ns
CA3	p=.91; R ² =.83, p<.05	0.09	p=.14; R ² =.02, p=.17	0.001	0.09, p<.001

	48-52 Weeks of Age			24-28 Weeks of Age		
	Person's rho	Slope	Pearson's rho	Slope	Difference	
DG	p=.91; R ² =.84, p<.01	0.50	p=.99; R ² =.99, p<.001	0.43	0.07, ns	
Subiculum	p=.94; R ² =.88, p<.05	0.20	p=.90; R ² =.81, p<.01	0.06	0.14, p<.01	
Amygdalar Nuclei						
Central Nucleus	p=.88; R ² =.79, p<.01	0.09	p=.98; R ² =.97, p<.001	0.11	0.02, ns	
Basolateral Nucleus	p=.75; R ² =.55, p<.01	0.15	p=.91; R ² =.83, p<.001	0.11	0.04, ns	
Posterior Nucleus	p=.99; R ² =.79, p=.055	0.57	p=.98; R ² =.97, p<.05	0.48	0.09, ns	
Septal Nuclei						
Lateral Septum	p=.82; R ² =.67, p=.061	0.02	p=.90; R ² =.81, p<.05	0.04	0.02, ns	
Medial Septum	p=.67; R ² =.45, p<.05	0.02	p=-.77; R ² =.60, p<.05	0.02	0, ns	
LGN	p=.99; R ² =.99, p<.001	0.31	p=.96; R ² =.92, p<.01	0.17	0.14, p<.01	
Inferior Colliculus	p=.90; R ² =.82, p<.01	0.38	p=.99; R ² =.99, p<.05	0.16	0.22, p<.01	
Superior Colliculus	p=.95; R ² =.90, p<.05	0.14	p=.94; R ² =.89, p=.053	0.02	0.12, p<.05	

	48-52 Weeks of Age		24-28 Weeks of Age		
	Pearson's rho	Slope	Person's rho	Slope	Difference
Medial Vestibular Nucleus	$p=.96; R^2=.93, p<.01$	0.14	$\rho=.99; R^2=.98, p<.01$	0.13	0.01, ns
Cerebellum					
Cerebellar Lobule III					
PCL	N/A	N/A	N/A	N/A	N/A
GCL	$p=.97; R^2=.94, p<.01$	0.10	$\rho=.83; R^2=.70, p<.05$	0.008	0.09, p<.05
Flocculus					
PCL	N/A	N/A	N/A	N/A	N/A
GCL	$p=.95; R^2=.90, p<.01$	0.12	$\rho=.94; R^2=.89, p<.01$	0.10	0.12, ns

Pearson's correlation coefficients were calculated comparing CGG repeat length with intranuclear inclusion number. The differences in slopes of the correlation between young and old mice were compared. All p values have been FDR adjusted to control for false discovery rate.

Table 6. Association between CGG repeat length and intranuclear inclusion number on young and old female CGG KI mice. Pearson's correlation coefficients were calculated comparing CGG repeat length with intranuclear inclusion number. The differences in slopes of the correlation between young and old mice were compared. All p values have been FDR adjusted to control for false discovery rate.

2.3 Nuclear pathology in astroglia of CGG KI mice

Previous studies of male CGG KI mice have identified intranuclear inclusions in astroglia of CGG KI mice (Wenzel et al., 2010). While such inclusions in astroglia are consistently observed in the human brain from FXTAS patients (*cf.*, Greco et al., 2002; Greco et al., 2006; Tassone et al., 2012), fewer inclusions (by percentage) are present in astroglia in female FXTAS cases than in male FXTAS cases (Tassone et al., 2012). Because the CGG KI mouse models other neuropathological features of FXTAS (*e.g.*, elevated *Fmr1* mRNA and slightly reduced *Fmrp* levels), a major goal of the present study was to determine whether intranuclear inclusions could be demonstrated in the astroglia of female CGG KI mice (*cf.*, Figure 13 for examples of astroglia and Bergmann Glia with intranuclear inclusions in the flocculus).

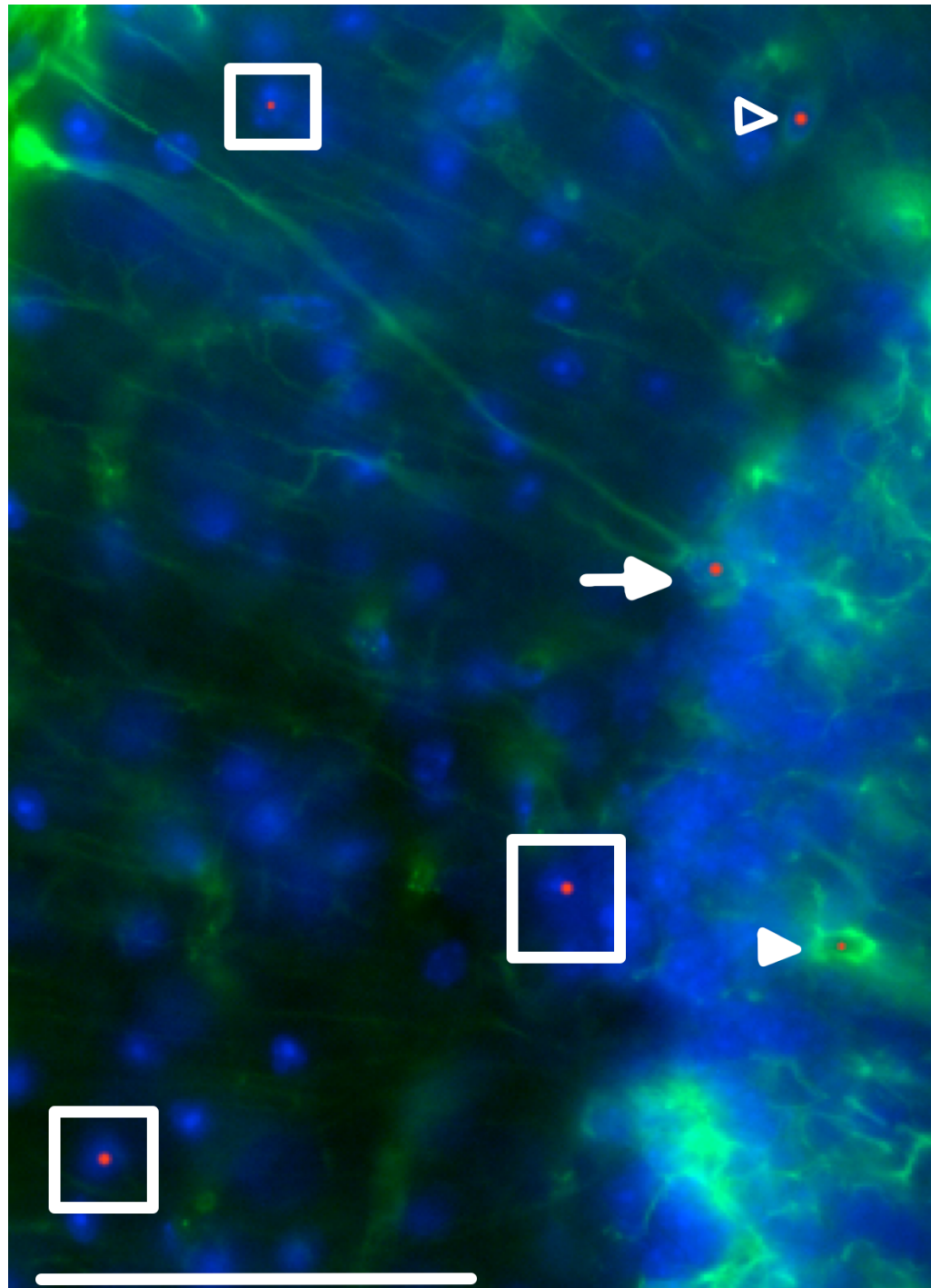


Figure 13. Intranuclear inclusion in astroglia of somatosensory cortex. Protoplasmic astroglial cell (arrowhead) stained for GFAP (green) and ubiquitin (red). Cell nuclei stained with DAPI (blue). Scale bar = 50 μ m.

Using the same methods as reported by (Wenzel et al., 2010), we found that female CGG KI mice show inclusions in 4.9% (+/- 0.83 standard error) of astroglial cells in layer I of the somatosensory and motor cortices in 48-52 week old female CGG KI mice with 140-200 CGG repeats, and 2.1% (+/- .13) in 48-52 week old mice with 70-100 CGG repeats. Similarly, the percentage with inclusions were 3.3% (+/- .09) in 24-28 week old mice with 140-200 CGG repeats, while inclusions were virtually undetectable in 24-28 week old mice with 70-100 CGG repeats. For the oldest female CGG KI mice with 140-200 repeats this quantification corresponds to roughly 50% of the frequency of inclusion in astroglia previously reported in the brains of male CGG KI mice as previously reported. Also, similarly to the male CGG KI mice, the pattern of astroglial intranuclear inclusions was unequally distributed in female CGG KI mice, with some fields of view having a greater density of inclusions than others.

2.4Localization of intranuclear inclusions in Bergmann glia

Ubiquitin-positive intranuclear inclusions were found diffusely in Bergmann glia in the cerebellum of 48-52 week old female CGG KI mice with 140-200 CGG repeat expansions. Compared to male CGG KI mice, these inclusions were relatively rare, being found only about 25% as often in 48-52 week old female CGG KI mice with 140-200 CGG repeats, a 75% reduction compared to the male CGG KI mice. Bergmann glia in all other age and CGG repeat size groups of female CGG KI mice only rarely showed intranuclear inclusions. When identified, these inclusions were always clearly defined, round, and localized to the nucleus.

Similar to what has been reported in male CGG KI mice, there was no evidence for reactive astroglia throughout the brain or Bergmann gliosis in the cerebellum of CGG KI mice as shown by GFAP and S100 β staining in female CGG KI mice.

2.5 Pathologic Features in Microglia and Oligodendroglia

Similar to male CGG KI mice, female CGG KI mice had ubiquitin positive masses with an amorphous or vacuolar appearance in the somal cytoplasm of microglia and oligodendroglia. In the female CGG KI mice these masses were 3-10 μ m in diameter at the widest point. Although similar features were present in wildtype mice, they were only 2-5 μ m in diameter and had a more rounded, less amorphous appearance. Similarly to what was reported by Wenzel et al. (2010), the majority of those cytoplasmic inclusions in female CGG KI mice demonstrated autofluorescence in control sections in which the antibodies were omitted. In order to determine if this autofluorescence was due to lipofuscin, sections were treated with CuSO₄ (Schnell et al., 1999). This procedure did not affect autofluorescence, suggesting that it was not lipofuscin-related. The source of autofluorescence of these cytoplasmic inclusions remains to be determined.

Any role for these pathologic features remains unknown, but it is clear that there is an effect for age in the development of these pathologies, as the brains from CGG KI mice at 24-28 weeks of age only rarely contained these features, whereas the CGG KI mice at 48-52 weeks of age consistently showed these features throughout the brain, regardless of CGG repeat length. It is important to note that female wildtype mice also showed similar features, but only after 60-70

weeks of age. This is similar to what was reported in male wildtype mice by (Wenzel et al., 2010).

3. DISCUSSION

Female CGG KI mice heterozygous for the fragile X premutation develop intranuclear inclusions in neurons and astroglia that are widely distributed throughout the brain. The numbers of inclusions identified in female CGG KI mice were compared to numbers in male CGG KI mice from Brouwer et al. (2008a), Willemsen et al. (2003), and Wenzel et al. (2010). However, although widespread, the numbers of inclusions in neurons in female CGG KI mice were only approximately 25-30% fewer than that seen in male mice of similar age and CGG repeat length. This was somewhat unexpected because a reduction closer to 50% would be expected if random X-inactivation determined the degree of histopathology. That is, random inactivation of one of the two X alleles would predict that on average half of the mutant X alleles in female CGG KI mice would be inactive, and pathology would accordingly be reduced by approximately 50%, including the numbers of intranuclear inclusions. More inclusions than expected in the brains of female CGG KI mice based on X-inactivation is consistent with the observation that intranuclear inclusions in the brains of female carriers of the Fragile X premutation are also more frequent than previously thought (Tassone et al., 2012). These findings are important because female carriers have been assumed to be largely unaffected cognitively and pathologically by the Fragile X premutation. While the numbers of inclusions in neurons in female CGG KI mice were less than expected by X-inactivation, inclusions in astrocytes did approximate the predicted 50% of that seen in astrocytes of male CGG KI mice.

These findings indicate that differences in the factors that influence inclusions formation in neurons versus astrocytes.

These data are important as in humans, female carriers of the premutation have been assumed largely cognitive and pathologically unaffected by the premutation (Hunter et al., 2011; Hunter et al., 2012; Hunter, Rohr, & Sherman, 2010). FXTAS occurs in approximately 40% of male fragile X premutation carriers (Jacquemont et al., 2004b). In contrast, penetrance of FXTAS is reduced (range between 8 and 17%) in female premutation carriers compared to males (Chonchaiya et al., 2010a; Chonchaiya et al., 2010b; Coffey et al., 2008; Jacquemont et al., 2005; Rodriguez-Revenga et al., 2009), and this has been thought to be due primarily to the protective effect of the normal allele on the second X chromosome (Berry-Kravis et al., 2005).

Despite the reduced penetrance of FXTAS in female carriers of the premutation, it remains important to evaluate the pathologic features in both female FXTAS cases as well as female CGG KI mice used as a model of FXTAS. Such studies are necessary to inform research about the development and progression of disorders associated with the premutation leading to the full clinical manifestation of FXTAS. Contrary to the X-inactivation hypothesis, female CGG KI mice showed 75% the neuropathological features as male mice in neurons (25% reduction), but did show the predicted 50% the pathology in astroglia, replicating the finding in human female premutation carriers (Tassone et al., 2012).

Examination of H&E and luxol fast blue stained brain tissue section showed no gross pathological features and no evidence for white matter pathology in brain compared to wildtype mice, including no evidence for white matter pathology in periventricular regions or in the murine homolog of the middle cerebellar peduncle in female CGG KI mice (*cf.*, Brunberg et al., 2002; Hagerman et al., 2004; Jacquemont et al., 2004a; Jacquemont et al., 2004b; Jacquemont et al., 2005).

Although females are thought to have milder symptoms of FXTAS than males, those who do develop FXTAS may have neurological and psychiatric symptoms that are at least as severe as those of their male counterparts (Adams et al., 2007; Karmon & Gadoth, 2008). Moreover, and somewhat paradoxically, female premutation carriers with and without FXTAS symptomatology show a higher incidence of immunological disorders, such as thyroid disease and fibromyalgia, than male premutation carriers with FXTAS (Coffey et al., 2008; Hunsaker et al., 2011a; Leehey et al., 2011; Rodriguez-Revenga et al., 2009), as well as elevated prevalence of depression and anxiety (Hamlin et al., 2011; Roberts et al., 2009). Hypertension, seizures, and peripheral neuropathy also have higher prevalence in female premutation carriers with FXTAS compared to non premutation carriers (Chonchaiya et al., 2010b), as has the co-occurrence of multiple sclerosis and Alzheimer's disease (*cf.*, Tassone et al., 2012). To date, these features have not been compared between genders, but preliminarily it appears these features are more prevalent in female over male FXTAS. Additionally, in a previous report evaluating pathological features in the

autonomic nervous system and somatic organ systems of human FXTAS and CGG KI mice, female CGG KI mice and a female premutation carrier with FXTAS showed comparable cardiac pathology. Female CGG KI mice also show pathologic features in both the pineal and pituitary glands (Hunsaker et al., 2011a).

An important feature of female CGG KI mice heterozygous for the fragile X premutation is that they model a number of cognitive and behavioral features reported in human female premutation carriers (Al-Hinti et al., 2007; Goodrich-Hunsaker et al., 2011a; Goodrich-Hunsaker et al., 2011b; Goodrich-Hunsaker et al., 2011c; Hunsaker et al., 2010; Hunsaker et al., 2011c). What remains unclear is if there are any relationships between performance on cognitive tasks and the increase in neuropathological features present in the female CGG KI mice similar to that suggested in male CGG KI mice (e.g., increase in the number intranuclear inclusions associated with worsening of spatial processing; cf., Hunsaker et al., 2009).

In the context of FXTAS, there are at least two consequences of inclusion formation. First, inclusions may be directly pathological and contribute to the cognitive deficits observed in the fragile X premutation and FXTAS. Alternatively, inclusions may not contribute to symptomatology and may be more simply formed as a reaction to the expanded CGG repeats on the *FMR1* mRNA and serve to sequester expanded CGG repeat-containing RNA and associated RNA binding proteins. The latter possibility suggests a neuroprotective effect of inclusions similar to that proposed in Huntington's disease (cf., Wenzel et al.,

2010). In CGG KI female mice (Diep et al., 2012; Hunsaker et al., 2011a; Hunsaker et al., 2011c) and in male CGG KI mice there have been reports suggesting inclusion presence may correlate with cognitive deficits, but no causative relationship was elucidated (Hunsaker et al., 2009). More work must be done to establish the connection between inclusion formation and cognitive deficits.

In male CGG KI mice, the presence of intranuclear inclusions in granule cell populations was commonly observed from 3 months of age, whereas these pathological features were only rarely seen in female CGG KI mice at this age. These data support hypotheses that higher expression of the *Fmr1* mRNA with expanded CGG repeats in male premutation carriers relative to female premutation carriers (due to X inactivation) results in more profound neurocognitive deficits and more numerous pathological features in males than females (Berry-Kravis et al., 2005; Jacquemont et al., 2005; Tassone et al., 2012). However, previous studies have found that X-inactivation patterns in patients with other X-linked mental retardation disorders preferentially inactivate the X-chromosome carrying the mutated or diseased allele (Plenge et al., 2002; Zhang et al., 2009).

It remains surprising that we observed less than 50% of the numbers of intranuclear inclusions formed in female CGG KI mice compared to male CGG KI mice. If X-inactivation patterns were completely random then we would expect to see a 50% reduction to the number of the inclusions in female mice compared to what is seen in male CGG KI mice. Alternatively, if X-inactivation patterns were

skewed towards inactivation of the premutation *Fmr1* gene then we would expect to see <50% inclusion formation. Instead, the present data suggest that X-inactivation may be skewed toward inactivation of the wildtype allele. A study in two human sisters with FXTAS showed that X-inactivation could favor either X-chromosome, leading to the expression of disparate pathologic phenotypes (Berry-Kravis et al., 2005). Our results provide potential evidence that X-inactivation may favor the X-chromosome carrying the premutation, at least in the CGG KI mouse model of the fragile X premutation. Evaluating both male and female CGG KI mice across a wide range of CGG repeat lengths and ages may serve to elucidate the effects of genetic dosage for expression of the premutation allele on the premutation phenotype.

In summary, this report provides new information on the prevalence and distribution of intranuclear inclusions in female CGG KI mice, as well as the relationship between frequency of inclusions, age, and CGG repeat length. Female CGG KI mice heterozygous for the fragile X premutation may serve to model a number of features of the fragile X premutation and FXTAS pathology that male CGG KI mice may not model as completely, including potential immunologic and psychiatric disturbances. These studies highlight the need to include female CGG KI mice, and female carriers of the Fragile X premutation in future studies in view of evidence that pathology, but histopathological and neurobehavioral, are more severe than previously predicted.

4.EXPERIMENTAL PROCEDURES

4.1 Mice

Thirty-four female CGG KI mice heterozygous for the fragile X premutation (range 71-326 CGG repeats) at 3-13 months of age and 16 female wildtype mice of the same age range were included in this study. The included wildtype mice were littermates with one of the CGG KI mice described in the study. All female CGG KI mice were bred onto a congenic C57BL/6J background over 9 to >12 generations from founder mice originally on a mixed FVB/N x C57BL/6J background. Sections from the male mice reported by (Hunsaker et al., 2009; Wenzel et al., 2010) were evaluated as well for direct comparison with the female CGG KI mice, as these mice were littermates with the female CGG KI mice evaluated for the present report. Mice were housed in same sex, mixed genotype groups with three or four mice per cage in a temperature and humidity controlled vivarium on a 12 h light-dark cycle. Mice had *ad libitum* access to food and water throughout their lifespan. All experiments conformed to University of California, Davis IACUC approved protocols and all effort was taken to reduce stress in all mice.

4.2 Genotyping

As modest somatic instability of CGG repeats among tissues in the CGG KI mouse has been shown to be negligible (typically under 10 CGG repeats across tissues; *cf.*, Berman & Willemse, 2009; Willemse et al., 2003), genotyping to verify CGG repeat length was carried out upon tail snips. Following

a method kindly provided by Rob Willemsen (Brouwer et al., 2007; Brouwer et al., 2008a; Brouwer et al., 2008b; Willemsen et al., 2003) and modified in collaboration with the laboratories of F Tassone and P Hagerman (Saluto et al., 2005; personal communication), CGG repeat lengths were measured using the FastStart Taq DNA Polymerase, dNTP Pack (Roche Diagnostics; Manheim, Germany) DNA was extracted from mouse tails by incubating with 10 mg/mL Proteinase K (Fermentas, Inc.; Glen Burnie, MD) in 300 μ L lysis buffer containing 50 mM Tris-HCl, pH 7.5, 10 mM EDTA, 150 mM NaCl, 1% SDS overnight at 55°C. One hundred microliters (100 μ L) saturated NaCl was then added, mixed and centrifuged. The supernatant was gently mixed with two volumes of 100% ethanol, and the DNA was pelleted by centrifugation. The DNA was washed and centrifuged in 500 μ L 70% ethanol. The DNA was then dissolved in 100 μ L milliQ-H₂O. CGG repeat lengths were determined by PCR using solutions from the FastStart Taq DNA Polymerase, dNTP Pack (Roche Diagnostics). Briefly, approximately 500-700 ng of DNA was added to 20 μ L of PCR mixture containing 0.5 μ M/L of each primer, 250 μ M/L of each dNTP (Roche Diagnostics). 2.5 M Betaine (Sigma-Aldrich), 1X Buffer 2 and 0.05 U of FastStart Taq DNA Polymerase (Roche Diagnostics) The primers flank the CGG repeat region of *Fmr1* gene, the forward primer was 5'-CGG GCA GTG AAG CAA ACG-3'and the reverse primer was 5'-CCA GCT CCT CCA TCT TCT CG-3 The CGG repeats were amplified using a 3-step PCR with 10 min denaturation at 98 °C, followed by 35 cycles of 35 s denaturation at 98 °C, annealing for 35 s at 55 °C, and at the end each cycle elongation for 2 min at 72 °C . The last step of the PCR

consisted in a 10 minute elongation at 72°C to. The sizes of CGG DNA amplicons were determined by running 20 μ L of PCR reaction per sample and a molecular weight marker (O'GeneRuler 50bp DNA ladder; Fermentas, Inc.) for 2 hrs at 150V on a 2.5% agarose gel with 0.03 μ L/ml ethidium bromide. The number of CGG repeats was calculated from pictures acquired with a GelDoc-It Imaging system (UVP, LLC Upland, CA) and using VisionWorks LS software (UVP, LLC Upland, CA). For female CGG KI mice heterozygous for the fragile X premutation there were two bands present, one corresponding to the wildtype allele (8-12 CGG repeats), and another corresponding to the premutation allele (generally 70-200 CGG repeat length. This method can detect up to 358 CGG repeats from animals in the present mouse colony). For female wildtype mice, only the normal *Fmr1* allele was present. Genotyping was performed twice on each mouse, once using tail snips taken at weaning and again on tail snips and/or brain tissue collected at sacrifice. In all cases the genotypes matched. For CGG repeat lengths >>200 repeats, the genotypes were evaluated a third time, and always matched the previous two genotype results.

4.3 General tissue preparation

CGG KI and wildtype mice were deeply anesthetized with sodium pentobarbital (100 mg/kg, *i.p.*; Euthasol, Virbac AH, Inc., Fort Worth, TX), then intracardially perfused with 12 mL isotonic heparinized saline (1000 U heparin/mL saline) over 1 min, followed by 60 mL of a solution of freshly prepared, slightly chilled 4% paraformaldehyde (PFA) in .1M sodium phosphate buffer (PB; pH 7.4) via gravity feed over 20 min. The brains were immediately removed from the skull and placed in the same fixative for 1 h at 4°C with gentle agitation on a shaker table. After post-fixation, the brains were rinsed twice in .1M PB, cryoprotected in 10% sucrose in .1M PB for 1 h, followed by 30% sucrose in 0.1M PB for 24 h at 4°C, then frozen on dry ice for 1 h. Frozen brains were stored at -80°C to await sectioning. Thirty-micrometer (30 µm) parasagittal serial sections were cut on a sliding microtome equipped with a freezing stage and collected into series of every fifth section directly into 30% sucrose, flash frozen on dry ice for 30 min, and stored at -80°C until further processing.

Single sets of sections were selected for further processing, which included cresyl violet, thionin, and/or H&E staining for general histological evaluation, and luxol fast blue staining with a neutral red counterstain to evaluate white matter integrity. Immunocytochemistry for neuronal and glial cell markers was used to identify cell type as well as for ubiquitin to visualize intranuclear inclusions in different cell classes. Ubiquitin stained intranuclear inclusions are the hallmark pathology of FXTAS patients and are also features of CGG KI mice (Brouwer et al., 2007; Brouwer et al., 2008a; Brouwer et al., 2008b; Entezam et

al., 2007; Greco et al., 2002; Greco et al., 2006; Greco et al., 2007; Greco et al., 2008; Greco, Hunsaker, & Berman, 2010; Hunsaker et al., 2009; Tassone et al., 2012; Wenzel et al., 2010; Willemse et al., 2003).

For the human tissue reported, formalin-fixed brain postmortem tissue was processed for paraffin sections, and histological and immunohistological staining in standard fashion as previously reported (Greco et al., 2002; Greco et al., 2006; Greco et al., 2007; Greco et al., 2008; Hunsaker et al., 2011a; Hunsaker et al., 2011b; Tassone et al., 2004a; Tassone et al., 2012). Tissue blocks of frontal cortex and hippocampus from a patient with FXTAS were sectioned in 7 μm sections. The case reported is Case 1 from Tassone et al. (2012) and all clinical information on this case is provided in that manuscript. This case was obtained in accordance to UC Davis approved IRB protocols.

4.4 Immunocytochemistry

Immunocytochemical and immunofluorescence techniques were used to visualize the occurrence and distribution of intranuclear and cytoplasmic inclusions, with a focus on their presence or absence in glial cells (*i.e.*, astroglia, oligodendroglia, and microglial cells) of female wildtype and CGG KI mice. Subsets of alternate sections were processed for immunocytochemistry using a modification of the avidin–biotin complex (ABC)–peroxidase technique as previously described (Hunsaker et al., 2009; Hunsaker et al., 2011a; Hunsaker et al., 2011b; Wenzel et al., 2010). Briefly, free-floating sections were rinsed in .1M phosphate buffer PB (pH 7.4), and pretreated with .1% sodium borohydride for

15 min followed by treatment with .5–2% H₂O₂ in PB for 90 min to inactivate endogenous peroxidases. Sections were then treated with 3% goat, horse, or swine serum as appropriate (Sigma-Aldrich; DAKO, Inc., Carpinteria, CA) and .3% Triton X-100 (TX-100) in .01 M PB with .15 M NaCl, pH 7.4 (PBS) for 1 h to reduce nonspecific staining. Sections were rinsed in .01M PBS for 30 min and incubated for 48–72 h at 4°C in the various antibodies and dilutions: mouse monoclonal or polyclonal anti-glial fibrillary acidic protein (GFAP; ICN Biomedicals; Irvine, CA; DAKO, Inc.), 1:4000 (1:1000 for immunofluorescence (IF)); rabbit polyclonal anti-S100β (Abcam, Inc., Cambridge, MA), 1:1000; mouse monoclonal anti-myelin basic protein (MBP; ICN Biochemicals), 1:500; rabbit polyclonal anti-Iba1 (ionized calcium binding adaptor molecule 1; Wako Chemicals USA, Inc., Richmond, VA), 1:2000 (1:1000 for IF); and rabbit polyclonal and mouse monoclonal antibodies against ubiquitin (DAKO, Inc.; Abcam, Inc.) 1:2000 and 1:1000, respectively (1:1000 for IF), in PBS containing 1% goat, horse or swine serum, 2% BSA, and 0.3% TX-100. Following rinses for 2 h in PBS, sections were incubated in biotinylated goat or swine anti-rabbit IgG or horse anti-mouse IgG (DAKO, Inc.; Vector Laboratories, Burlingame, CA), diluted 1:500 for 24 h at 4°C, rinsed 2 h in PBS and then incubated in ABC (Elite ABC Kit, Vector Laboratories), diluted 1:500 in 1% goat or horse serum, 2% BSA, 0.3% TX-100, and PBS for 24 h at 4°C. Sections were rinsed thoroughly in PB (pH 7.4), then transferred to Tris–HCl buffers (TB; pH 7.4, 7.6), and then incubated for 15 min in .025% 3,3'-diaminobenzidine (DAB, Sigma) in TB (pH 7.6). After reacting for 5–10 min in fresh DAB with .003% H₂O₂ until staining was

optimized on a positive control section, sections were rinsed in TB, followed by PB, and mounted on gelatinized slides. In some experiments the DAB included .05% nickel ammonium sulfate to enhance the visibility of the DAB reaction product after counterstaining with hematoxylin. For all experiments female CGG KI and wildtype mice were run in parallel.

4.5 Immunofluorescence staining

For single- and double-immunofluorescent labeling of ubiquitin co-localized with neuronal/glial cell markers, sections were transferred into 10% sucrose in 0.1M PB, then rinsed in .1M PB, and treated with .1% sodium borohydride for 15 min. Thereafter, sections were rinsed again with .1M PB and then permeabilized with .5% H₂O₂ in 0.1M PB for 15 min followed by rinses in 0.1M PB and .01M PBS. Free-floating sections were treated with 10% goat or horse serum in .01M PBS containing .3% TX-100 (vehicle) for 1 h and then incubated overnight at 4°C in vehicle containing different combinations of mouse monoclonal/rabbit polyclonal antibodies of different IgG isotypes (see above). After rinses in .01M PBS and 10% goat or horse serum, sections were incubated in isotype-specific Alexa-conjugated secondary antibodies (1:2000): Alexa 568-labeled goat anti-rabbit IgG and/or Alexa 488-labeled goat anti-mouse IgG (Invitrogen, Carlsbad, CA) for 1 h. Following rinses in 10% goat or horse serum followed by .01M PBS, sections were mounted on gelatin-coated slides and coverslipped with mounting medium containing DAPI (4',6-diamidino-2-

phenyindole di-lactate) for nuclear staining (Vectashield “Hard Set”, Vector Laboratories).

To differentiate between specific immunofluorescent labeling and nonspecific autofluorescence resulting from accumulations of lipofuscin in aging brains, sections were first treated with 10mM copper sulfate solution in 50mM ammonium acetate buffer (pH 5.0) for 20 min (Schnell et al., 1999). This treatment reduced autofluorescence but did not significantly affect the intensity of specific immunofluorescent labeling, although immunofluorescent staining for ubiquitin within the neuronal cytoplasm was subtly enhanced, similar to previous reports in male CGG KI mice and human tissues (Hunsaker et al., 2011a; Hunsaker et al., 2011b; Wenzel et al., 2010). For all experiments female CGG KI and wildtype mice were run in parallel.

4.6 Cell identification and evaluation of intranuclear inclusions

Stained tissue sections were analyzed using either a Nikon ECLIPSE E600 microscope with epifluorescence attachment and/or a Zeiss LSM 510 META confocal microscope. In the case of the confocal microscope, single plane confocal images were collected. Images were analyzed to verify the presence of ubiquitin-positive intranuclear inclusions in different cell types identified with various neuronal and glial cell markers in brains of female CGG KI and wild-type mice.

Cresyl violet, thionin, and/or H&E-stained sets of serial sections from wild-type and CGG KI mouse brains at different ages were used for comparison and

evaluation of gross anatomical differences. Identification of different cell types in the brain was carried out based on standard morphological criteria using H&E, cresyl violet, or thionin staining, and immunocytochemistry using specific neuronal and glial cell markers (Wenzel et al., 2010). Neurons were identified by their size, large round nuclei, single or multiple nucleoli or heterochromatin, and their abundant cytoplasm, as well as by using specific neuronal markers. Astroglia were identified by their round/ovoid nuclei with light euchromatin, and absence of nucleoli and cytoplasm. In addition, GFAP and S100 β immunocytochemistry and/or immunofluorescence were used to identify subpopulations of astroglia based on their differing immunoreactivities (*i.e.*, protoplasmic, velate, and/or fibrous astroglia) in different brain regions.

To estimate the percentage of astroglia with intranuclear inclusions, the number of astroglia and intranuclear inclusions was counted manually in 10 high power (*i.e.*, 400X) microscopic fields on two GFAP- and ubiquitin-immunoreacted sections from 20 CGG KI mice within layer I of the neocortex (including sensory and motor areas) using an optical imaging system (StereolInvestigator, MBF Biosciences; Williston, VT). This method precisely replicated the methods used in male CGG KI mice (Wenzel et al., 2010). Wildtype mice were similarly analyzed, though intranuclear inclusions were never observed in wildtype mice. Notably, a similar number of glial cells were counted in wildtype mice as CGG KI mice, suggesting a similar number of astroglia in CGG KI mice and wildtype mice, at least in layer I of the motor and somatosensory neocortex.

Oligodendroglia were identified based on their typically small, round, hyperchromatic nuclei (which did not allow differentiation between nucleus, nucleoli, or cytoplasm), localization in white and grey matter, and confirmed by immunocytochemistry for myelin basic protein (MBP). Microglia were identified primarily from Iba1 immunostaining, which displayed small cell bodies with a round nucleus and fine, ramified processes that are characteristic of resting microglia, as well as on cellular morphology from H&E stained tissues. Microglial cells with retracted and/or hypertrophic processes on Iba1 immunostained sections were defined as activated (but non-phagocytic) microglia, which can be transformed into phagocytotic cells (*i.e.*, brain macrophages; Graeber & Moran, 2002). Immunocytochemical staining for ubiquitin was used to specifically label intranuclear inclusions in combination with cell-specific markers to identify the cell type. Whenever possible, immunocytochemical experiments using immunoperoxidase and immunofluorescence methods were carried out in parallel to verify staining patterns as well as to facilitate quantification.

4.7 Semiquantitative analysis of intranuclear inclusions in neurons

To evaluate the relative number and distribution of inclusions across brain regions, 6 female CGG KI mice 48-52 weeks of age with 70-100 CGG repeats, 6 female CGG KI mice 48-52 weeks of age with 140-200 CGG repeats, 6 female CGG KI mice 24-28 weeks of age with 70-100 CGG repeats, and 6 female CGG KI mice 24-28 weeks of age with 140-200 CGG repeats were processed for H&E staining. Standard histological sections in the parasagittal plane were selected

for quantification. The following regions were evaluated: prelimbic cortex, motor cortex, parietal cortex, visual cortex, anterior cingulate cortex, piriform cortex, ventromedial and dorsolateral entorhinal cortex, the dentate gyrus, CA3, CA1, and subiculum in the hippocampus, the central, basolateral, and posterior nuclei of the amygdala, the medial and lateral septal nuclei, the lateral geniculate nucleus (LGN), the inferior and superior colliculi, medial vestibular nucleus, and lobe III in the inferior lobe of the cerebellum and the flocculus in the cerebellum. The semiquantitative analysis involved counting 200 cells at 1000X magnification in each region of interest across mice at 20X magnification. The 200 counted cells were selected randomly within the region of interest using the optical imaging system. A limited sample of female CGG KI mice with >>200 CGG repeats and CGG KI mice at 3 months of age were evaluated in a similar manner, but the data from these mice were not directly compared to the other groups due to a limited number of mice evaluated. In all cases, adjacent sections were also immunoperoxidase stained for ubiquitin were compared with H&E stained sections to verify inclusion presence, but quantifications were performed using H&E stained tissues.

Differences among age groups were evaluated by computing Pearson's correlation coefficients comparing CGG repeat length and inclusion number within each age group. Data across age groups were not statistically evaluated. Differences between the slope of the correlations the age group were evaluated using the standard error of the different slopes. These analyses were performed using the R 14.1 statistical environment (R Development Core Team, 2012).

Acknowledgements:

The authors would like to acknowledge the contributions of Chou-Yu (James) Fan, Natalie N. Nguyen, Aimee Keyashian, and Kimberley C. D'Antonio for assistance with sectioning tissues used for this study, as well as Binh T. Ta and Dr. Dolores Garcia-Arocena, Ph.D. for assistance with mouse genotyping. The authors would also like to thank Dr. H. Jürgen Wenzel M.D., D.Sc. for helpful discussions concerning histological and immunohistological techniques.

This work was supported by National Institute of Health (NIH) grants, NINDS RL1 NS062411 to RFB and RW. This work was also made possible by a Roadmap Initiative grant (UL1 DE019583) from NIDCR in support of the NeuroTherapeutics Research Institute (NTRI) consortium; by a grant (UL1 RR024146) from the NCRR to MRH; and an NSF Center for Biophotonics Science and Technology Internship to EWS. The contents of this manuscript are solely the responsibility of the authors and do not represent the official view of NCRR, NINDS, NIDCR, or NIH.

Chapter 6

Widespread non-central nervous system organ pathology in fragile X premutation carriers with fragile X-associated tremor/ataxia syndrome and CGG knock-in mice

Abstract

Fragile X-associated tremor/ataxia syndrome (FXTAS) is an adult-onset neurodegenerative disorder generally presenting with intention tremor and gait ataxia, but with a growing list of co-morbid medical conditions including hypothyroidism, hypertension, peripheral neuropathy, and cognitive decline. The pathological hallmark of FXTAS is the presence of intranuclear inclusions in both neurons and astroglia. However, it is unknown to what extent such inclusions are present outside the central nervous system (CNS). To address this issue, we surveyed non-CNS organs in ten human cases with FXTAS and in a CGG repeat knock-in (CGG KI) mouse model known to possess neuronal and astroglial inclusions. We find inclusions in multiple tissues from FXTAS cases and CGG KI mice, including pancreas, thyroid, adrenal gland, gastrointestinal, pituitary gland, pineal gland, heart, and mitral valve, as well as throughout the associated autonomic ganglia. Inclusions were observed in the testes, epididymis, and kidney of FXTAS cases, but were not observed in mice. These observations demonstrate extensive involvement of the peripheral nervous system and systemic organs. The finding of intranuclear inclusions in non-CNS somatic organ systems, throughout the PNS, and in the enteric nervous system of both FXTAS cases as well as CGG KI mice suggests that these tissues may serve as

potential sites to evaluate early intervention strategies or be used as diagnostic factors.

This chapter has been published as:

Hunsaker, M. R., Greco, C. M., Spath, M. A., Smits, A. P. T., Navarro, C. S., Tassone, F., et al. (2011). Widespread non-central nervous system organ pathology in fragile X premutation carriers with fragile X-associated tremor/ataxia syndrome and CGG knock-in mice. *Acta Neuropathologica*. 122(4), 467-479.

My role in this study was to analyze female CGG KI mice for organ pathology as well as to analyze male and female CGG KI mouse pineal gland for pathologic features. I also analyzed female premutation carrier with FXTAS aorta valve biopsy tissue for inclusions, as well as performed photography with Dr. Claudia M. Greco.

Introduction

Fragile X-associated tremor/ataxia syndrome (FXTAS) is a progressive neurodegenerative disorder that is characterized by cerebellar gait ataxia and intention tremor. FXTAS affects carriers of a fragile X mental retardation 1 (*FMR1*) gene containing a CGG trinucleotide repeat expansion in the 5' untranslated region (UTR) within the premutation range (PM; 55–200 CGG repeats). Premutation length CGG trinucleotide repeat expansions are present in as many as 1:251 males and 1:116 females in the population (Allen et al., 2010; Coffey et al., 2008; Nishie et al., 2004). Both male and female PM carriers older than 50 years of age may develop FXTAS, although the incidence of FXTAS in female PM carriers is less than half of males (~40% of male PM carriers vs. 8–16% of female PM carriers develop FXTAS; Berry-Kravis et al., 2005; Coffey et al., 2008; Jacquemont et al., 2004b; Rodriguez-Revenga et al., 2009), primarily thought due to a protective effect of the non-expanded *FMR1* gene on the second X chromosome. Premutation carriers produce elevated levels (2–10 times normal measured in lymphocytes) of PM *FMR1* messenger RNA (mRNA) and normal to moderately reduced levels of *FMR1* protein (FMRP) in leukocytes (Allen et al., 2004; Peprah et al., 2010a; Peprah et al., 2010b; Tassone et al., 2000c), fibroblasts (Garcia-Arocena et al., 2010), and brain tissue (Tassone et al., 2004a). The current hypothesis underlying the pathophysiology of FXTAS focuses on a toxic mRNA gain-of-function mechanism (Jacquemont et al., 2003; Leehey et al., 2007a).

The onset of FXTAS symptomatology begins at a mean age of 60 years, and penetrance is age-dependent (Jacquemont et al., 2003; Leehey et al., 2007a). The core features of FXTAS include progressive intention tremor and cerebellar gait ataxia (Berry-Kravis et al., 2003; Berry-Kravis et al., 2007a; Berry-Kravis et al., 2007b; Hagerman et al., 2001; Jacquemont et al., 2003). Radiologic evaluations using magnetic resonance imaging (MRI) have identified generalized atrophy of the cerebrum, brainstem, and cerebellum in FXTAS (Adams et al., 2007; Adams et al., 2010; Cohen et al., 2006), and a majority of male FXTAS patients show distinctive, bilateral, white matter signal hyperintensities in the middle cerebellar peduncles on T2-weighted or FLAIR MRI scans (Brunberg et al., 2002; Loesch et al., 2005). These radiologic features have been histologically confirmed in multiple post mortem cases (Greco et al., 2002; Greco et al., 2006; Greco et al., 2007; Greco et al., 2008; Tassone et al., 2004a).

Associated clinical features of FXTAS include cognitive decline, Parkinsonism, peripheral neuropathy, and autonomic dysfunction (Cilia et al., 2009; Hagerman et al., 2001; Hagerman et al., 2007; Hall, Pickler, Riley, Tassone, & Hagerman, 2010; Hessl et al., 2005; Jacquemont, Hagerman, Hagerman, & Leehey, 2007; Louis et al., 2006; Munoz, 2002; Reis et al., 2008; Soontarapornchai et al., 2008). The neuropathological hallmark of FXTAS is the presence of eosinophilic, ubiquitin-positive intranuclear inclusions in both neurons and astroglia throughout brain upon post mortem histological analysis (Greco et al., 2002; Greco et al., 2006; Greco et al., 2007; Greco et al., 2008; Tassone et al., 2004a; Yachnis et al., 2010). These inclusions appear as

eosinophilic, hyaline, refractile, 2–5 µm diameter, round to ovoid bodies that show positive reactivity with antibodies against over 20 different proteins including ubiquitin, αB-crystallin, lamin A/C, hnRNP A2, myelin basic protein, DNA repair-ubiquitin-associated HR23B, and Sam68, among others (Bergink et al., 2006; Fernandez-Carvajal et al., 2009; Iwahashi et al., 2006; Ross-Inta et al., 2010). The inclusions are PAS, silver, amyloid, and α-synuclein negative (Greco et al., 2002; Greco et al., 2006). Additionally, the *FMR1* mRNA, but not FMRP, has been found contained within intranuclear inclusions (Iwahashi et al., 2006). Additional neuropathological features present in FXTAS include reduced Purkinje cell number, axonal torpedoes, and prominent cortical and subcortical white matter pathology (Greco et al., 2002; Greco et al., 2006).

The CGG knock-in (CGG KI) mouse model of the PM has proven to be an invaluable tool for the study of the pathophysiology of FXTAS, including neuropathological events that occur with the onset and progression of the disorder (*cf.*, Berman & Willemse, 2009). The CGG KI mouse model was developed by homologous recombination wherein the endogenous mouse (CGG)8 trinucleotide repeat within the mouse *Fmr1* gene was replaced by a (CGG)98 repeat of human origin. As such, expression of the expanded (CGG)98 repeat is on the endogenous mouse *Fmr1* promoter (Willemse et al., 2003). The CGG KI mouse recapitulates many neuropathological features present in FXTAS, including intranuclear inclusions in neurons and astroglia, elevated *Fmr1* mRNA levels, and reduced Fmrp levels (Brouwer et al., 2007; Brouwer et al., 2008a; Brouwer et al., 2008b; Brouwer et al., 2009; Willemse et al., 2003; *cf.*, Entezam

et al., 2007; Qin et al., 2011 for a different knock-in model of the PM demonstrating similar molecular features). In addition, a correlation has been demonstrated between the presence of intranuclear inclusions in brain and phenotypes in CGG KI mice that model the clinical features of FXTAS (Brouwer et al., 2007; Brouwer et al., 2008a; Brouwer et al., 2008b; Hunsaker et al., 2009; Hunsaker et al., 2010; Hunsaker et al., 2011c; Willemse et al., 2003). Furthermore, CGG KI mice show an increase in neurocognitive dysfunction both with increasing age and CGG repeat length across a growing battery of behavioral tests (Hunsaker et al., 2010; Hunsaker et al., 2011a; Hunsaker et al., 2011c; Van Dam et al., 2005).

It has become apparent that the spectrum of clinical involvement in PM carriers with FXTAS extends beyond symptoms and signs that correspond to pathology in the CNS (Berry-Kravis et al., 2007a; Berry-Kravis et al., 2007b; Bourgeois et al., 2006; Bourgeois et al., 2007; Bourgeois et al., 2009; Bourgeois et al., 2011; Coffey et al., 2008; Gokden et al., 2009; Greco et al., 2007; Greco et al., 2008; Soontarapornchai et al., 2008). The increasingly broad clinical spectrum of FXTAS symptomatology seems to encompass a number of medical co-morbidities that include thyroid disease (Coffey et al., 2008; Rodriguez-Revenga et al., 2009), fibromyalgia (Leehey et al., 2011), gastrointestinal symptoms (Berry-Kravis et al., 2010; Hagerman et al., 2008) hypertension (Coffey et al., 2008), migraine (Berry-Kravis et al., 2010), impotence (Greco et al., 2007), autoimmune disease (Coffey et al., 2008; Leehey et al., 2011), peripheral neuropathy (Hagerman et al., 2007; Soontarapornchai et al., 2008),

seizure disorders, and cardiac arrhythmia (Hagerman et al., 2001; Jacquemont et al., 2003). Intriguingly, evidence for this broadened spectrum of immune mediated disorders (Coffey et al., 2008; Leehey et al., 2011) arise primarily in women both with and without FXTAS, but many of the medical co-morbidities are more commonly observed in individuals with FXTAS compared to PM carriers without FXTAS (Coffey et al., 2008; Gokden et al., 2009; Greco et al., 2007; Soontarapornchai et al., 2008). Furthermore, intranuclear inclusions have been identified in non-CNS tissues, but to date have only been evaluated in a limited number of cases (Gokden et al., 2009; Greco et al., 2007; Louis et al., 2006). Here we report the presence of inclusions in autonomic ganglia throughout the peripheral autonomic nervous system, as well as in somatic tissues themselves from ten PM carriers with FXTAS (9 male, 1 female), and compare these findings to homologous pathological features present in the CGG KI mouse model of the fragile X PM.

Materials and methods

FXTAS case autopsies

Clinical history reports for all FXTAS cases included in this report are available in Table 7, along with molecular correlates of the PM. Written informed consent was received for all cases and all experimental protocols conformed to IRB approved protocols. Tissues (pancreas, kidney, brain, thyroid gland, heart, testes, adrenal gland, gastrointestinal, and esophagus) were removed from a subset (*cf.*, Table 7) at autopsy and immersion fixed in 10% formalin, followed by paraffin embedding of representative samples. The brain was also removed from each autopsy case, as was the spinal cord on select cases. In standard fashion, histological sections (5 µm) were stained by hematoxylin and eosin (H&E) for routine histological examination, and immunoperoxidase labeling was performed using rabbit antibodies targeted against ubiquitin (Dako, ZO458, Carpinteria, CA, USA) and counterstained with hematoxylin.

FXTAS Case	CGG mRNA	Tissues sampled	FXTAS Onset	Co-morbid diagnoses	MRI findings	Age at death	Cause of death	FMR1 + relatives
Case 1 80	2.59 ± 0.42	Adrenal Testes Pineal Colon Testes	69	Cognitive decline Neuropathy Choking Seizures COPD History of smoking Type II diabetes Emphysema Depression	Brain atrophy White matter disease White matter disease White matter disease	79 69	Aspiration pneumonia PM daughter	1 grandchild with FXS 4 grandchildren with FXS 3 PM daughters
Case 2 160	Not determined							
Case 3 75	2.02 ± 0.27	Adrenal Colon Testes	69	Dementia, Herpes zoster	Not determined	93	Aspiration pneumonia Pulmonary edema	Grandchildren with FXS 3 PM daughters
Case 4 85	4.25 ± 0.21	Pituitary Adrenal Colon Heart Pituitary Pancreas	67	Hypertension Neuropathy Cognitive decline	Global brain atrophy MCP sign White matter disease	78		
Case 5 72	Not determined	Adrenal Testes Epididymis	80	Neuropathy Dementia Cardiac arrhythmia Hypertension	White matter disease in the pons Angina	87	Stroke with hemiparesis Type II diabetes Irritability	

FXTAS Case	CGG	FMR1 mRNA	Tissues sampled	FXTAS Onset	Co-morbid diagnoses	MRI findings	Age at death	Cause of death	FMR1 + relatives
Case 6 109	Not determined	Heart Kidney Pancreas Thyroid	63	Hypertension COPD Cardiac arrhythmia Cognitive decline Type II diabetes Pacemaker	Global brain atrophy White matter disease	73	Postoperative Carotid endarterectomy	2 grandchildren with FXS	
Case 7 95	3.35 ± 0.27	Esophagus Heart	56	Type II diabetes Cognitive decline Impotence Bladder incontinence	Pituitary cyst Global brain atrophy Diffuse white matter disease	67	Myocardial infarction	Grandchildren with FXS	
Case 8 30, 96 AR = 0.76	2.80± 0.12	Mitral valve biopsy	49	Seizures Neuropathy Hypertension Dementia Hallucination Mood lability PTSD Depression Hypertension	Mild brain atrophy, White matter disease	N/A	N/A	MVP Mitral regurgitation Hypothyroidism Anxiety	

FXTAS Case	CGG	FMR1 mRNA	Tissues sampled	FXTAS Onset	Co-morbid diagnoses	MRI findings	Age at death	Cause of death	FMR1 + relatives
Case 9	80	3.75 ± 0.51	Testes	65	Constipation Neuropathy Impotence Hypertension Type II diabetes Hyperlipidemia Cardiac arrhythmia Pituitary adenoma Adenocarcinoma Impotence Hypertension Stroke Sleep apnea Mood lability Neuropathy Anxiety Prostate cancer Chronic pain Choking Irritability		72	Adenocarcinoma	
Case 10	95	Not determined	Pituitary	61		Global brain atrophy White matter disease	67	Pulmonary edema Congestive heart failure	

FMR1 mRNA levels were not determined for Cases 2, 5, 6, 10 due to the unavailability of unfixed tissues. Activation ratio (AR: ratio of cells with the normal X as the active X) is provided for female Case 8

Table 7. Clinical history and molecular characterizations of all FXTAS cases and tissue samples evaluated from each in the present study

Mitral valve biopsy tissue

A 1 × 1 mm biopsy was taken from the mitral valve of Case 8 during surgery, placed in phosphate-buffered saline for 2 h, postfixed in freshly made 4% phosphate-buffered paraformaldehyde for 2 h, and cryoprotected in 30% sucrose. Microtome sections (30 µm) were taken and stained using iron hematoxylin and eosin for histological analysis as well as a modified Van Gieson's stain (Van Gieson's stain with the addition of Eosin Y) to further characterize specific cell and tissue types. Immunostains were performed using rabbit antibodies targeted against ubiquitin (Dako, ZO458; 1:2,000) and counterstained with hematoxylin.

CGG KI mice

The generation of the expanded CGG mice used in this study has been described previously (Willemsen et al., 2003). For the current study, male mice with repeat sizes between 100 and 150 CGG repeats were used (all experiments), as well as 1 female mouse with 8 and 150 CGG repeats (mitral valve to compare with biopsy material from Case 8). All experiments were carried out in accordance with approved animal use protocols (Erasmus MC; University of California, Davis). CGG repeat lengths were determined as described previously (Brouwer et al., 2008a; Hunsaker et al., 2011c). All mice used in this study were between 48 and 90 weeks of age at time of killing.

Tissues (pancreas, pituitary, heart, kidney, brain, thyroid gland, testis, adrenal gland, and intestine) were dissected immediately following cervical

dislocation and fixed overnight in 4% paraformaldehyde at 4°C. Subsequently, tissues were embedded in paraffin according to standard protocols. Paraffin sections (7 µm) were cut and mounted on gelatin-coated slides. Immunostains were performed with rabbit antibodies against ubiquitin (Dako, ZO458; 1:500) followed by indirect immunoperoxidase labeling with hematoxylin counterstain. For co-localization studies, antibodies targeted against somatostatin and glucagon were combined with ubiquitin labeling using immunofluorescence techniques and counterstained with DAPI to identify cell nuclei.

For experiments evaluating CGG KI heart, mitral valve, and pineal gland, the heart was dissected from a CGG KI mouse immediately following cervical dislocation and immersion fixed in 4% paraformaldehyde for 2 h at 4°C, then transferred overnight into 30% sucrose at 4°C as a cryoprotectant. Concurrently, the brain was trans-aortically perfused with 12 mL of potassium shifted Ringer's solution, followed by 60 mL of 4% paraformaldehyde over 20 min via gravity feed, gently removed from the skull so as not to damage the pineal gland, and transferred into 4% paraformaldehyde at 4°C for 1 h postfixation, followed by 10 and 30% sucrose solutions. The heart and brain, including the pineal gland were sagittally sectioned at 30 µm on a freezing stage microtome and a set of every fifth section was mounted on gelatin-coated slides and stained for H&E. Another section set of heart tissue was stained using a modification of Van Gieson's stain similar to that done for the human aorta tissue. Indirect immunoperoxidase staining was performed on a third set of free floating sections using polyclonal antibodies targeted to ubiquitin (Dako, ZO458; 1:2,000), after which tissues were

mounted on gelatin-coated slides, counterstained with hematoxylin, dehydrated, and coverslipped with Permount resinous mounting media.

Results

Human FXTAS cases

A summary of the organs in which intranuclear inclusions were identified across all cases of FXTAS is presented in Table 8. A brief summary is presented below focusing on the intranuclear inclusions identified in each organ, as well as rough percentages of cell nuclei in which inclusions were present. Novel pathological findings are illustrated in Figure 14.

	Human FXTAS ^a	Cell type(s) with inclusions	CGG KI	Cell type(s) with inclusions
Adrenals	1, 3, 4, 5	Chromaffin secreting cells of medulla Steroid secreting cells of cortex	Yes	Chromaffin secreting cells of medulla
Colon	2, 3, 4	Ganglion cells of myenteric plexus & submucosal plexus	Yes	Steroid secreting cells of cortex
Esophagus	7	Ganglion cells of myenteric plexus	Not analyzed	Ganglion cells of myenteric plexus
Heart	4, 6, 7	Cardiomyocytes	Yes	Cardiomyocytes
Mitral valve	8	Autonomic ganglia Ganglion cells	Yes	Intracardiac autonomic ganglia
Kidney	1, 6	Smooth muscle cells Mesangial cells	None detected	Ganglion cells
Peripheral autonomic ganglia	4	Distal tubular epithelium Ganglion cells	Yes	—
Pituitary gland	3, 10	Acidophilis Basophils	Yes	Ganglion cells
		Chromophobes	Yes	Pars anterior Pars intermedia
		Pituicytes	None detected	—
Testes	1, 2, 3, 5, 9	Leydig cells Myoid cells	Not analyzed	Islets of Langerhans
Epididymis	5	Epithelial cells of distal tubule	Yes	A and D cells
Pancreas	4, 6	Islets of Langerhans	Yes	Parafollicular cells
Thyroid	1, 6	Follicular Cells Parafollicular cells	Yes	—
Pineal gland	1	Ganglion cells Pinealocytes	Yes	Ganglion Cells Pinealocytes
		Astroglia	—	Astroglia

Table 8 Intranuclear inclusions are present in somatic organs and autonomic ganglia in human FXTAS cases and the CGG KI mouse model of the PM, organized by organ system and cell type

^aThe number of organ tissues available for this series varied case by case. Intranuclear inclusions were present in all cases where that tissue was received (e.g., for the adrenals, 4 cases had adrenal tissue available, and intranuclear inclusions were seen in each of the 4 cases). See text for percentages of inclusions in each organ system

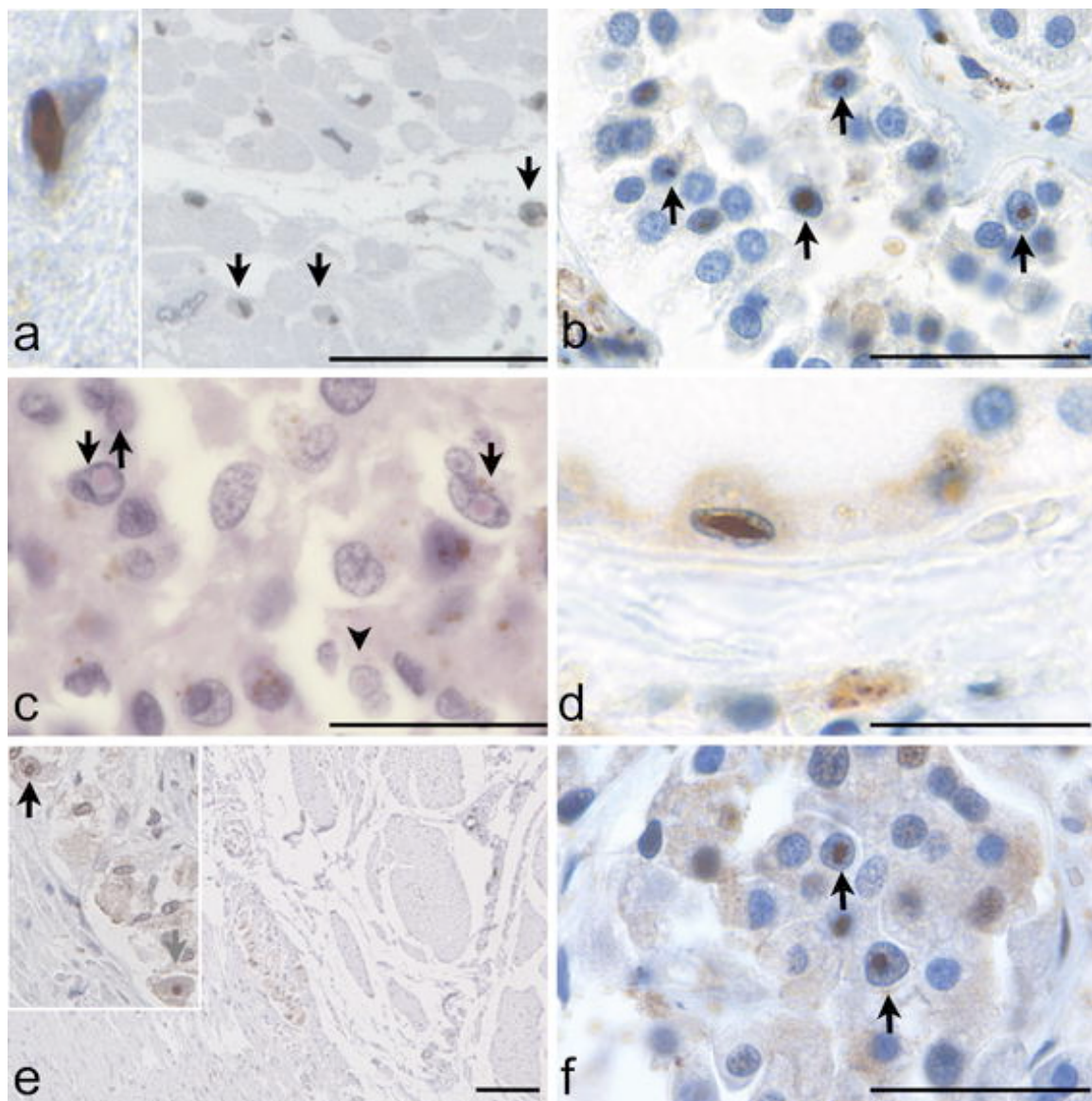


Figure 14 **a.** Intranuclear inclusions in cardiomyocytes in Case 7 ($\times 400$; Immunoperoxidase (IP) stain). **Insert** Extremely large, oval-shaped inclusion in a cardiomyocyte from Case 6 ($\times 1,000$). **b.** Intranuclear inclusions in pinealocytes and astrocytes in pineal gland of Case 1 ($\times 1,000$; H&E stain). **c.** Autonomic ganglion of the myenteric/Auerbach's plexus is seen between longitudinal and circular muscular layers of the rectosigmoid colon ($\times 40$; IP stain) in Case 4. **Insert** Higher magnification identifies intranuclear inclusions in ganglion cells ($\times 400$). **d.** Intranuclear inclusions in cells of the distal tubule of the kidney in Case 6 ($\times 1,000$; IP stain). **e.** Intranuclear inclusions in thyroid of Case 6 ($\times 1,000$; IP stain). **f.** Intranuclear inclusion in pancreas of Case 6 ($\times 1,000$; IP stain). All immunoperoxidase stains counterstained with hematoxylin. All scale bars represent 100 μm

Heart

Intranuclear inclusions were identified in cardiomyocytes in the heart and surrounding autonomic ganglia in Cases 4, 6, and 7 (3–5% of cardiomyocytes), as well as in smooth muscle cells of the mitral valve (~1–2% of cells) and autonomic ganglia in the tunica externa from Case 8 (~5% of cells; Figure 14a).

Pineal

Intranuclear inclusions were identified in pinealocytes and ganglion cells in the pineal gland of Case 1 (1–2% of cells; Figure 14b).

Colon

Intranuclear inclusions were identified in smooth muscle cells, as well as in neurons of the submucosal and myenteric plexi of the rectum (1–2% of cells; Figure 14c), sigmoid colon, and appendix of Cases 2, 3, and 4.

Kidney

Intranuclear inclusions were identified in mesangial cells and epithelial cells of the distal tubules of the kidney in Cases 1 and 6 (3–5% of cells; Figure 14d).

Thyroid

Intranuclear inclusions were identified in the follicular and parafollicular cells in the thyroid glands of Cases 1 and 6 (~1% of cells; Figure 14e).

Pancreas

Intranuclear inclusions were identified in Islets of Langerhans cells in the pancreas of Cases 4 and 6. The precise cell type harboring inclusions was not determined in human cases due to autolytic change (5–10% of cells; Figure 14f).

Adrenal gland

Intranuclear inclusions were identified in the medullary cells of the adrenal gland, as well as in periadrenal ganglia of Cases 1, 3, 4, and 5 (1–2% of cells).

Esophagus

Intranuclear inclusions were identified in neurons of the myenteric plexus of the esophagus of Case 7 (1–2% of cells).

Testes

Intranuclear inclusions were identified in Leydig cells, smooth muscle cells, and nurse cells (1–2% of cells) in the testes of Cases 1, 2, 3, 5, and 9, supporting previous reports of inclusion presence in the testes (Greco et al., 2007).

Epididymis

Intranuclear inclusions were identified in the epithelial cells of the distal tubule of Case 5 (1–2% of cells).

Pituitary

Intranuclear inclusions were identified in basophiles, chromophobes, and acidophiles of the anterior pituitary, and pituicytes of the posterior pituitary of Cases 3 and 10 (1–2% of cells).

CGG KI Mouse

A summary of organ sites of intranuclear inclusions were identified in CGG KI mice compared with the findings in FXTAS is presented in Table 8. A brief summary is provided below organized in a similar manner to the human results (Figure 15).

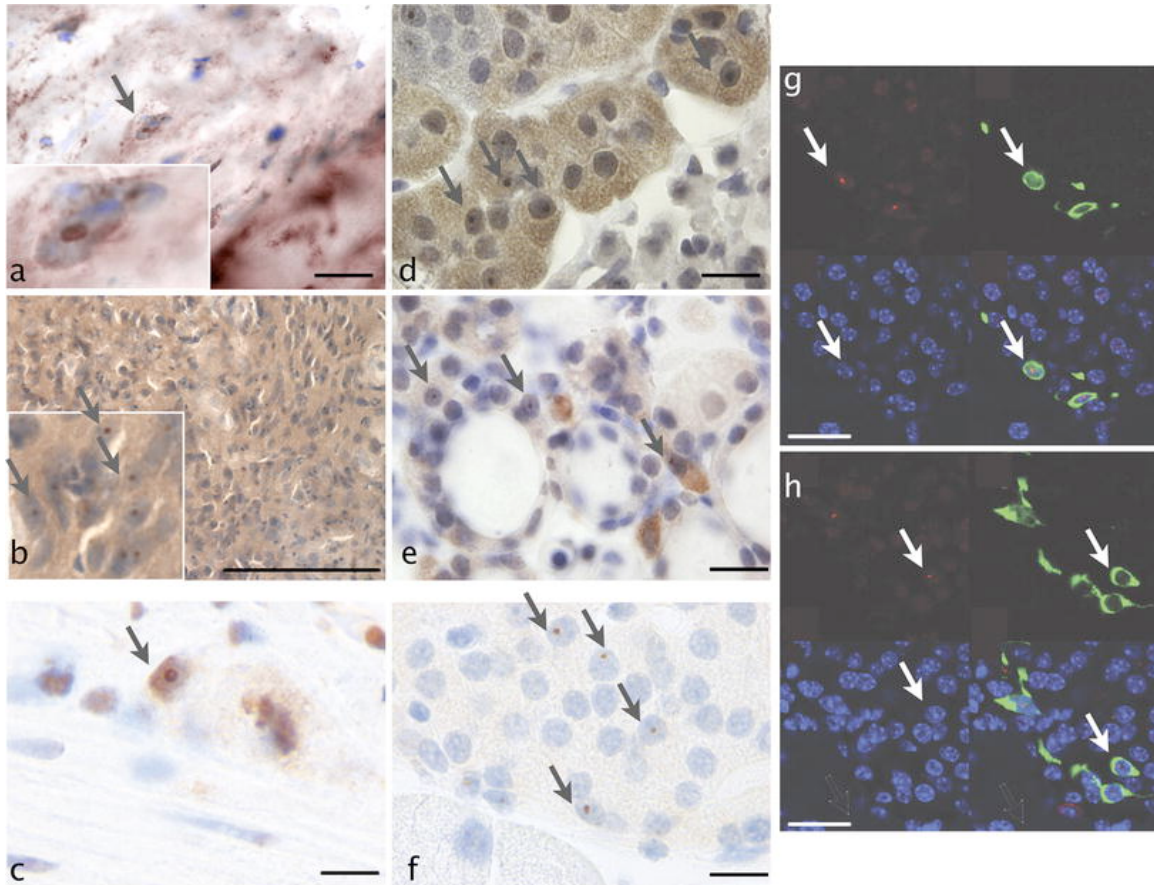


Figure 15 **a.** Intranuclear inclusions in cardiomyocytes of CGG KI mice ($\times 1,000$; IP stain). **b.** Intranuclear inclusions in pinealocytes of CGG KI mouse pineal gland ($\times 1,000$; IP stain). **c.** Intranuclear inclusions in ganglion cells of the myenteric plexus of the colon in CGG KI mice ($\times 1,000$; IP stain). **d.** Intranuclear inclusions in adrenal gland of CGG KI mice ($\times 1,000$; IP stain). **e.** Intranuclear inclusions in thyroid of CGG KI mice ($1,000\times$; IP stain). **f.** Intranuclear inclusions in pancreas of CGG KI mice ($\times 1,000$; IP stain). **g.** Immunofluorescence of intranuclear inclusions (red) and somatostatin (green) in pancreas of CGG KI Mice (nuclei counterstained with DAPI (blue)) ($\times 1,000$; IP stain). **h.** Immunofluorescence of intranuclear inclusions (red) and glucagon (green; IP stain) in pancreas of CGG KI mice (nuclei counterstained with DAPI (blue)) ($\times 1,000$). All scale bars represent 50 μ m.

Heart

A considerable number of cardiac muscle cells contained ubiquitin-positive intranuclear inclusions in 48- to 72-week-old CGG KI mice (~2–3% of cells; Figure 15a) with some being so large as to occupy nearly the entire nucleus of the cell. Intranuclear inclusions were not conclusively identified in the smooth muscle of the mitral valve, but were numerous in the autonomic ganglia in the tunica externa (~5% of cells).

Pineal gland

Intranuclear inclusions were present in pinealocytes, astrocytes, and ganglion cells in the pineal gland (~2–3% of cells; Figure 15b).

Colon

Intranuclear inclusions were identified in myenteric ganglia in the colon (10% of cells; Figure 15c).

Adrenal gland

Ubiquitin-positive intranuclear inclusions were present in chromaffin cells of the adrenal gland (5–10% of cells; Figure 15d).

Thyroid

In thyroid tissue from CGG KI mice, the gland structure was normal in H&E sections. Further examination revealed the presence of ubiquitin-positive

intranuclear inclusions in a significant number of parafollicular cells that secrete calcitonin (3–5% of cells; Figure 15e).

Pancreas

In pancreatic tissue from CGG KI mice, the general histological features on H&E staining were similar to those of normal age-matched controls. However, in sections that were immunostained for ubiquitin we could detect ubiquitin-positive intranuclear inclusions in specific cells of islets of Langerhans (3–5% of cells). To determine which cell types contained intranuclear inclusions (Figure 15f), co-staining for somatostatin and ubiquitin as well as glucagon and ubiquitin were carried out (Figure 15g). Intranuclear inclusions were found in the somatostatin producing D cells of the islets of Langerhans as well as glucagon producing A cells (Figure 15h).

Pituitary

Intranuclear inclusions were identified in the anterior and intermediate pituitary in CGG KI mice with more in the pars intermedia (~58% of cells) than the pars anterior (18% of cells). Few inclusions were detected in the pars posterior (<1% of cells) (Brouwer et al., 2008b). The precise cell types harboring inclusions were not determined.

Testes

No inclusions were detected in the testes of CGG KI mice.

Kidney

No inclusions were detected in the kidney of CGG KI mice.

Discussion

The present results demonstrate pathological features in broad distribution within the peripheral autonomic nervous system as well as neuroendocrine and somatic organs in PM carriers with FXTAS. These findings are consistent with the expanding range of co-morbid medical features reported in FXTAS that include neuroendocrine dysfunction (Coffey et al., 2008; Sullivan et al., 2005), impotence (Greco et al., 2007), gastrointestinal symptoms (Leehey et al., 2010), cardiac arrhythmias (Hagerman et al., 2001; Jacquemont et al., 2004b), peripheral neuropathy (Hagerman et al., 2007; Soontarapornchai et al., 2008), and bladder dysfunction (Berry-Kravis et al., 2010; Coffey et al., 2008; Greco et al., 2007; Hagerman et al., 2008; Jacquemont et al., 2003; Louis et al., 2006; Rodriguez-Revenga et al., 2009; Soontarapornchai et al., 2008). Type II diabetes has not been formally established as an associated clinical feature of FXTAS; however, there is ample anecdotal evidence from case histories that a substantial number of patients develop type II diabetes during their lifetime (*cf.*, Cases 2, 5, 6, 9). Because the incidence of hypothyroidism and other thyroid disorders (*cf.*, Case 8), hypertension (*cf.*, Cases 4, 5, 6, 7, 8, 9, 10), peripheral neuropathy (*cf.*, Cases 1, 4, 5, 6, 7, 8, 9, 10), and fibromyalgia have been reported to be higher in PM carriers with FXTAS as compared to age-matched non-PM carriers, these diseases may well be part of the syndrome of FXTAS, or at least associated medical features (Coffey et al., 2008; Rodriguez-Revenga et al., 2009). In addition, cardiac arrhythmias (*cf.*, Cases 5, 6) and gastrointestinal problems including constipation are commonly encountered in carriers with FXTAS (Berry-

Kravis et al., 2010; Hagerman et al., 2008; *cf.*, Case 9). Previously, Louis et al., (Louis et al., 2006) reported inclusions in pituitary tissue (hypophysis) from one patient with FXTAS, and Gokden et al. (2009) reported inclusions in a number of peripheral tissues including autonomic ganglia of the mesenteric plexus, pericardial tissue, adrenal tissue and paraspinal ganglia. The present report has expanded upon these findings in a larger group of FXTAS cases. Greco et al. (2007) have reported inclusions in the Leydig cells of the testes of men who died of FXTAS and proposed that these inclusions may likely be related to the lowered testosterone levels and impotence seen in these men since the Leydig cells produce testosterone. Impotence is common in PM males (*cf.*, Cases 7, 9), often becoming apparent even before the development of intention tremor or cerebellar gait ataxia related to FXTAS.

Psychiatric problems, particularly anxiety and depression, are CNS-associated disorders that are increased in PM carriers with and without FXTAS compared to controls (Bourgeois et al., 2007; Bourgeois et al., 2011; *cf.*, Cases 2, 5, 6, 8, 10). These disorders may well be elicited by a combination of stress and environmental factors (Bourgeois et al., 2009; Bourgeois et al., 2011), particularly as these factors affect the hypothalamic–pituitary–adrenal (HPA) axis. In addition to the CNS component, widespread peripheral pathology have been observed in the present study, namely the presence of intranuclear inclusions identified throughout the HPA axis, pineal gland, cardiac conduction system, peripheral nerves and autonomic ganglia, thyroid, digestive system, testes, and pancreas. It is quite likely that the medical co-morbidities in systemic organs and

the autonomic nervous system share a common pathogenesis with that observed in the CNS of patients with FXTAS (*i.e.*, mRNA toxicity), and thus may be considered non-CNS-associated features of FXTAS (Bourgeois et al., 2009; Bourgeois et al., 2011; Coffey et al., 2008; Hessl et al., 2005; Roberts et al., 2009; Roberts, Mazzocco, Murphy, & Hoehn-Saric, 2008; Rodriguez-Revenga et al., 2009). The presence of intranuclear inclusions in somatic organs as observed in the present study are not the cause of these conditions co-morbid with FXTAS, but rather signal organ systems affected by the PM *FMR1* mRNA. Specifically, inclusions capture and sequester important proteins necessary for normal function of these cells, including splice factors (Sellier et al., 2010) that may negatively affect organ function.

The broad distribution of intranuclear inclusion formation reported herein further expands the cell types and body systems that may be affected by RNA toxicity and signals new areas for investigation of disease pathology in PM carriers both with and without FXTAS symptomatology. For instance, the prevalence of type II diabetes and hypoglycemic episodes should be investigated in those with the PM and FXTAS compared to the general population, as it appears likely that insulin production may be reduced in FXTAS (*cf.*, Cases 2, 5, 6, 9). The presence of intranuclear inclusions in the Islets of Langerhans may signal disease processes in the pancreas, namely potential RNA toxicity—a potential that warrants further investigation. Such investigations, both in the human and in the CGG KI mouse model, would underscore the value of studying

the basic disease mechanisms in non-CNS tissues that are readily available through surgical and biopsy tissues.

The CGG KI mouse was also evaluated for the presence of inclusions in the same organ systems as the cases with FXTAS, and showed a strikingly similar pattern of inclusion formation in somatic organs and the autonomic nervous system. These results verify that CGG KI mouse models the somatic pathologic anatomical features present in FXTAS, in addition to modeling the neuropathological features of FXTAS (Brouwer et al., 2008b; Brouwer et al., 2009; Hunsaker et al., 2009; Wenzel et al., 2010; Willemsen et al., 2003). This parallel non-CNS pathology underscores the utility of the mouse model for studying the pathogenesis and progression of non-CNS disorders associated with FXTAS.

Our understanding of the molecular mechanisms of RNA toxicity is evolving, and includes dysregulation of a number of proteins such as lamin A/C and heat shock proteins including $\alpha\beta$ crystallin (Chen et al., 2010; Garcia-Arocena & Hagerman, 2010; Raske & Hagerman, 2009); sequestration of Sam68 and the dysregulation of the protein products of mRNAs, whose splicing is modulated by Sam68 (Sellier et al., 2010). Most recently, Ross-Inta et al., (2010) demonstrated mitochondrial abnormalities in fibroblasts and brain tissue in PM carriers both with and without FXTAS. It is not clear what cellular processes underlie inclusion formation; and it is not known whether the inclusions are themselves toxic or simply reflect underlying cellular dysfunction. Nevertheless, intranuclear inclusions clearly provide a cellular marker or signal for the disease

process underlying FXTAS and associated non-CNS disease. Understanding the breadth of pathological involvement in the peripheral tissues in the PM and FXTAS expands our understanding of the spectrum of medical disease associated with FXTAS.

Recent publications (Gokden et al., 2009; Louis et al., 2006) along with our findings place the neurodegenerative condition associated with FXTAS among the neurodegenerative disorders with involvement of the peripheral nervous system (Kaufmann & Biaggioni, 2003; Wakabayashi, Mori, Tanji, Orimo, & Takahashi, 2010), and in some cases, the neuroendocrine system and/or visceral organs. Among these disorders are the Lewy body diseases, including Parkinson's disease and diffuse Lewy body disease (Kovari, Horvath, & Bouras, 2009), multiple system atrophy (Nishie et al., 2004; Takahashi-Fujigasaki, 2003), and neuronal intranuclear inclusion disorder (Kulikova-Schupak et al., 2004). These disorders are marked by the presence of non-CNS inclusions similar in appearance to those found in the brain and spinal cord. Other polyglutamine disorders showing peripheral inclusions are Machado-Joseph disease/spinocerebellar ataxia type 3 (Yamada, Hayashi, Tsuji, & Takahashi, 2001) and spinal and bulbar muscular atrophy (Wakabayashi et al., 2010). The similarity between the presence of inclusions in peripheral and somatic tissues in FXTAS and numerous other inclusion-bearing disorders suggests the inclusions may not cause the medical co-morbidities reported in FXTAS, but rather signal tissues affected by the mRNA toxicity associated with the PM. Furthermore, as the mutation underlying the PM occurs in the 5' untranslated region of the *FMR1*

gene, the *FMR1* protein (FMRP) is structurally normal, despite the expanded CGG repeats present in the *FMR1* mRNA.

Further research is needed to understand the complexity of co-morbid medical problems associated with the PM and how these may be related to RNA toxicity. The finding of intranuclear inclusions in non-CNS somatic organ systems, throughout the PNS, and in the enteric nervous system of both FXTAS cases as well as CGG KI mice suggests that these tissues may serve as potential sites to evaluate early intervention strategies or be used as diagnostic factors. Success in this effort may assist clinicians to confirm a FXTAS diagnosis prior to designing interventions for individuals with the PM, PM-associated diseases, or early FXTAS.

Acknowledgments This work was supported by National Institute of Health (NIH) grants HD036071, HD056031, NS044299, AG024488, HD02274, MH77554, MH078041, RL1 AG032115, RL1NS062411, and RL1 AG032119; the National Fragile X Foundation; the Circle of Service Foundation; and the M.I.N.D. Institute. This work was also made possible by a grant (UL1 DE019583) from the National Institute of Dental and Craniofacial Research (NIDCR) in support of the NeuroTherapeutics Research Institute (NTRI) consortium; and by a grant (UL1 RR024146) from the National Center for Research Resources (NCRR), a component of the National Institutes of Health (NIH), and NIH Roadmap for Medical Research.

Section 2: Behavioral Phenotype

The behavioral phenotype of the CGG KI mouse has only been evaluated in an early experiment from (Van Dam et al., 2005) and a similar model of the premutation, the CGG-CCG mouse has similarly been tested for a behavioral phenotype (Qin et al., 2011). Unfortunately, as is all too common in rodent behavioral research, the phenotypes are inconsistent across the mice, mostly due to inconsistencies in the behavioral protocols, but also due to the relative insensitivity of the behavioral tasks to elucidate subtle deficits.

Van Dam et al. (2005) demonstrated that the CGG KI mouse only showed deficits for spatial memory using a water maze at >1 year of age and only at ~72 weeks of age (or 17 months) was there a somewhat discernible deficit for motor function, but only when the data were creatively analyzed. (Qin et al., 2011) also found barely discernible alterations for sociability and spatial memory, but no alterations for motor behaviors. However, Qin et al. (2011) only evaluated relatively young mice, particularly in comparison with the range of ages tested by Van Dam et al. (2005). When these disparate results are taken in light of the inconsistent (or absent) phenotype in fragile X premutation carriers without FXTAS (*cf.*, Allen et al., 2011; Hunter et al., 2008a; Hunter et al., 2008b; Hunter et al., 2009; Hunter et al., 2010; Hunter et al., 2012), the lack of effects are unsurprising as none of the behavioral tests used tested specific cognitive functions or brain areas (*cf.*, Chapter 1).

To overcome this challenge, the experiment reported in Chapters 7 and 8 were designed specifically to model the experiments being used for study into

premutation carriers; namely spatial and temporal memory function (*cf.*, Goodrich-Hunsaker et al., 2011a; Goodrich-Hunsaker et al., 2011b; Goodrich-Hunsaker et al., 2011c; Hocking et al., 2012). By evaluating cognitive processes proposed to be disrupted by the premutation, these experiments may potentially uncover neurocognitive deficits previously uncovered by the more traditional behavioral paradigms.

Chapter 7

Progressive Spatial Processing Deficits in a Mouse Model of the Fragile X Premutation

Abstract

Fragile X associated tremor/ataxia syndrome (FXTAS) is a neurodegenerative disorder that is the result of a CGG trinucleotide repeat expansion in the range of 55–200 in the 5` UTR of the *FMR1* gene. To better understand the progression of this disorder, a knock-in (CGG KI) mouse was developed by substituting the mouse CGG8 trinucleotide repeat with an expanded CGG98 repeat from human origin. It has been shown that this mouse shows deficits on the water maze at 52 weeks of age. In the present study, this CGG KI mouse model of FXTAS was tested on behavioral tasks that emphasize spatial information processing. The results demonstrate that at 12 and 24 weeks of age, CGG KI mice were unable to detect a change in the distance between two objects (metric task), but showed intact detection of a transposition of the objects (topological task). At 48 weeks of age, CGG KI mice were unable to detect either change in object location. These data indicate that hippocampal-dependent impairments in spatial processing may occur prior to parietal cortex-dependent impairments in FXTAS.

This chapter has been published as:

Hunsaker, M. R., Wenzel, H. J., Willemse, R., & Berman, R. F. (2009). Progressive spatial processing deficits in a mouse model of the fragile X premutation. *Behavioral Neuroscience*. 123 (6), 1315-1324.

My role in this study was experimental design, apparatus set up, performing behavioral experiments, data analysis, and performing immunoperoxidase experiments.

Introduction

Fragile X associated tremor/ataxia (FXTAS) is a progressive neurodegenerative disorder with intention tremor and ataxia (Hagerman & Hagerman, 2004b). Neuropathology includes white matter disease, white matter hyperintensities in the middle cerebellar peduncle on T2 weighted MRI images, subtle brain atrophy, and the presence of intranuclear inclusions in neurons and astrocytes throughout the brain, with a high percentage being located in the hippocampus (Greco et al., 2002; Greco et al., 2006; Tassone et al., 2004a). The cognitive sequelae of the fragile X premutation that underlie FXTAS include deficits for working memory, executive processing, and reduced hippocampal activation during episodic retrieval tasks (Cornish et al., 2008b; Koldewyn et al., 2008; Sevin et al., 2009).

Both fragile X syndrome (FXS) and fragile X-associated tremor/ataxia (FXTAS) are the result of a tandem CGG trinucleotide repeat in the 5' untranslated region (UTR) of the *FMR1* gene. In unaffected individuals, there are between 5 and 40 CGG repeats, in FXTAS there are between 55 and 200 CGG repeats, and in full FXS there are >200 CGG repeats (40–55 is defined as a gray zone between unaffected and premutation status). The mutation affecting individuals with FXS results in gene hyper-methylation, almost complete gene silencing (lack of *FMR1* transcription); and an absence of the *FMR1* gene product, FMRP (fragile X mental retardation protein). In contrast, the CGG repeat expansion underlying FXTAS results in increased *FMR1* transcription, elevated *FMR1* mRNA but, paradoxically, slightly decreased levels of FMRP (Brouwer et

al., 2008a; Brouwer et al., 2009; Hagerman & Hagerman, 2004b; Oostra & Willemsen, 2009). Because the mutation affecting FXTAS carriers was once thought to be without a phenotype, it is commonly referred to as a premutation, in comparison with the *FMR1* full mutation which results in FXS (Brouwer et al., 2009; Hagerman & Hagerman, 2004b).

A knock-in (KI) mouse model of the fragile X premutation has been generated in which the mouse endogenous CGG8 trinucleotide repeat was replaced via homologous recombination with a human CGG98 trinucleotide repeat (Bontekoe et al., 1997; Brouwer et al., 2008a; Brouwer et al., 2008b; Willemsen et al., 2003). Similar to the human cases of FXTAS, the brains of these CGG KI mice show intranuclear inclusions that stain for ubiquitin in a number of brain regions, including the dentate gyrus in the hippocampus (Brouwer et al., 2008a; Willemsen et al., 2003). Further, it has been reported that at 52 weeks of age these CGG KI mice have a deficit on the hidden platform version of the water maze, as well as motor deficits on the rotarod at 70 weeks of age (Van Dam et al., 2005).

Humans with the fragile X premutation underlying FXTAS have intranuclear inclusions in neurons in the hippocampus and neocortex. In humans, it is still unknown at what age inclusions form due to the nature of the disorder and the advanced age at which FXTAS is diagnosed, but it has been shown that inclusions can form after as few as 8 days in vitro after an expanded CGG repeat with an eGFP reporter is introduced into primary neural progenitor cells and established cell lines (Arocena et al., 2005). In CGG KI mice, inclusions are

common at 50–100 weeks of age, but their presence has been reported in the literature as early as 20 weeks of age (Brouwer et al., 2008a; Brouwer et al., 2008b; Willemsen et al., 2003). It is not yet known if the inclusions contribute directly to the neuropathology seen in FXTAS. It has been suggested that intranuclear inclusions may not be pathological of themselves, but may reflect pathology such as mRNA toxicity due to the increased gene transcription resulting from the premutation or perhaps due to the presence of the mutant mRNA itself (Brouwer et al., 2008a; Brouwer et al., 2009; Hagerman & Hagerman, 2004b).

It has recently been proposed for a number of neurodevelopmental disorders that decreased resolution or sensitivity of spatial and temporal processing, referred to as “hypergranularity,” may contribute to cognitive deficits (Simon, 2008). This hypergranularity or poor resolution in the processing of spatial and temporal information leads to inefficient sensory integration and cognitive function. Since individuals with FXTAS show generalized brain atrophy, white matter disease, as well as intranuclear inclusions that may contribute to altered neural function, it follows that hypergranular spatial and temporal information processing may underlie a subset of the cognitive deficits seen in individuals with FXTAS. Furthermore, although FXTAS is currently characterized as a neurodegenerative disorder, the fragile X premutation is already present in utero, so there is reason to believe that there may be some cognitive and/or behavioral deficits early in life, suggesting that one can also view FXTAS, or at least the fragile X premutation, as a neurodevelopmental disorder (Cornish et al.,

2008b; Hagerman & Hagerman, 2004b). There are also recent reports of relatively early cognitive phenotypes in individuals with the fragile X premutation (Farzin et al., 2006; Goodlin-Jones, Tassone, Gane, & Hagerman, 2004; Hagerman, 2006; Hessl et al., 2005).

Additionally, it has been reported that the hippocampus of individuals with the fragile X premutation (without concomitant FXTAS) have slightly reduced hippocampal volumes relative to age- and IQ-matched controls, and that this volume reduction correlates strongly with impaired performance on standardized tests of memory (Jäkälä et al., 1997; Sevin et al., 2009). Koldewyn et al., (2008) further demonstrated that asymptomatic carriers of the fragile X premutation show decreased hippocampal activation during an episodic retrieval task, a task dependent upon hippocampal function. These results suggest that reductions in hippocampal volume in tandem with functional abnormalities in the hippocampus may contribute to the neuropsychiatric symptoms and cognitive decline seen in FXTAS. What remains unknown is whether normal posterior parietal cortex functions are intact in carriers of the fragile X premutation, both with and without FXTAS symptomatology. What is known is that in FXTAS there is cortical atrophy and white matter disease throughout the subcortical white matter (Brunberg et al., 2002; Greco et al., 2006).

The rodent hippocampus has been shown to subserve a process called spatial pattern separation (Adams, Kesner, & Ragozzino, 2001; Gilbert, Kesner, & Lee, 2001; Goodrich-Hunsaker et al., 2005; Goodrich-Hunsaker et al., 2008b; Hunsaker, Rosenberg, & Kesner, 2008b; Kesner, Lee, & Gilbert, 2004; Rolls &

Kesner, 2006). Spatial pattern separation can be described as the ability to discriminate between very small changes in the spatial relationships between stimuli. As such, spatial pattern separation is the mechanism underlying the precision of spatial resolution required to form fine spatial memory. This concept of pattern separation as an important cognitive function has also been formalized into a computational model in rodents and primates by Rolls and Kesner (2006) among many others (*cf.*, Marr, 1971; McNaughton & Morris, 1987).

It has further been proposed that one form of spatial pattern separation called “metric spatial processing” is involved in determining the precise angles and exact distances that separate objects in the environment, without regard to the identity of the objects (Gallistel, 1990a; Goodrich-Hunsaker et al., 2005; Goodrich-Hunsaker et al., 2008b). This form of spatial processing has been localized in rodents to a neural network involving the dentate gyrus. In this sense, objects in a configuration can be transposed and maintain their metric structure, so long as the same spatial locations remain occupied by objects.

In “topological spatial processing,” which is functionally separate from metric processing, it is the overall configuration of the objects and their general relationships to each other that is important, with the precise angles and distances between objects of less importance (Goodrich-Hunsaker et al., 2005; Goodrich-Hunsaker et al., 2008b; Goodrich-Hunsaker, Howard, Hunsaker, & Kesner, 2008a). In this sense, for topological processing the location of each object relative to the others is critical (*i.e.*, in front of, to the left of, between, etc.), but the precision of the relationship is less so (*e.g.*, it does not matter if the

objects are 10 cm apart, 20 cm, or greater, as long as the general relationship between the objects remains the same). This means that all objects in a configuration could be moved further apart or closer together, so long as the configuration of the objects remains otherwise unaltered (*i.e.*, the configuration of objects remain the same, while distances between objects may change). Topological processing has been localized to a neural network involving the parietal cortex (Goodrich-Hunsaker et al., 2005).

Kesner et al. (Goodrich-Hunsaker et al., 2005; Goodrich-Hunsaker et al., 2008b; Hunsaker et al., 2008b) have developed two behavioral tasks to test the contributions of the hippocampus and the parietal cortex for metric and topological spatial information processing, respectively. In the original (Goodrich-Hunsaker et al., 2005) study, rats with lesions restricted to either the dorsal hippocampus or parietal cortex were presented with objects on an open field and allowed to explore. After exploration, the relationships between these objects were changed, either being moved closer together or further apart (metric changes), or by transposing the objects (topological changes). Animals with parietal lesions were unable to detect the transposition, but were capable of noticing and exploring the objects after they had been moved closer together or further apart. Animals with hippocampal ablations were unable to detect the change in the distance between the objects after, but were capable of detecting transposition of the objects. These lesion studies in rats suggest that the hippocampus subserves metric spatial processing and that the parietal cortex subserves topological spatial processing (*i.e.*, a double dissociation was

demonstrated; (Goodrich-Hunsaker et al., 2005)). These findings were further expanded in subsequent lesion studies to implicate the dentate gyrus, and not CA3 or CA1, in metric processing (Goodrich-Hunsaker et al., 2008b). The topological task has also been used to identify alterations to parietal cortex function in transgenic mouse models (cf. (Lee et al., 2009)).

To directly test the whether the CGG KI mice show spatial deficits in the metric or topological tasks, or both, and at what developmental age, CGG KI mice and wild type littermates were evaluated on tests emphasizing either metric or topological spatial processing at one of three ages: 12, 24, or 48 weeks of age. As previous work with this CGG KI mouse has shown deficits during the water maze, it is proposed that tests of metric and topological spatial information processing may provide a sensitive tool to help identify subtle cognitive processing deficits in CGG KI mice that may be missed by other learning and memory tasks (cf., Lee et al., 2009), and may better reflect similar spatial processing deficits in humans with FXTAS.

Materials and Methods

Animals

The generation of an expanded CGG trinucleotide repeat knock-in (CGG KI) mouse model of the fragile X premutation has been described previously (Bontekoe et al., 1997; Willemsen et al., 2003). Briefly, the endogenous CGG8 trinucleotide repeat in the 5' UTR of the mouse *Fmr1* gene was replaced by a human CGG98 trinucleotide repeat via homologous recombination. Across breedings, the CGG repeats was mildly unstable, both expanding and contracting in length within the fragile X premutation range defined as ~55–200 CGG repeat (Brouwer et al., 2008b; Brouwer et al., 2009; Willemsen et al., 2003).

The CGG KI mice were originally on a mixed FVB/N × C57BL/6J background, and were backcrossed with C57BL/6J mice from Jackson Labs (Bar Harbor, ME) until greater than 98% C57BL/6J by microsatellite analysis. Only male mice were used in the present study.

The CGG KI mice used in the present study had between CGG80 and CGG180 repeats. Animals were housed in same sex, mixed genotype groups of up to four littermates per cage with food and water ad libitum, under conditions of constant temperature and a 12/12 h light–dark cycle. Behavioral testing was always conducted during the light portion of the light cycle (between 0900 and 1500 pacific standard time). A previous study (Van Dam et al., 2005) studied spatial memory on the water maze with the CGG KI mice on the mixed FVB/N × C57BL/6J background. To evaluate spatial memory in the present study, CGG KI mice on a congenic C57BL/6J background were used. At 12 weeks of age, 8

male wild type mice, and 8 male CGG KI mice were used for behavioral experimentation. At 24 weeks of age, 8 different male wild type animals and 10 different male CGG KI mice were used for behavioral experimentation. At 48 weeks of age, 10 different male wild type and 8 different male premutation mice were used for behavioral experimentation. All wild type mice were littermates with at least one CGG KI mouse used in the present study. For this initial investigation of metric and topological spatial processing in the CGG KI mouse, mice were not retested on any experiments to avoid any complications with repeated testing. All experimental protocols conformed to University of California, Davis IACUC protocols.

Genotyping

DNA was extracted from mouse tails by incubating with 10 mg/ml Proteinase K (Roche Diagnostics) in 300 µl lysis buffer containing 50 mM Tris-HCl, pH 7.5, 10 mM EDTA, 150 mM NaCl, 1% SDS overnight at 55 °C. One hundred µl saturated NaCl was then added and the suspension was centrifuged. One volume of 100% ethanol was added, gently mixed, and the DNA was pelleted by centrifugation and the supernatant discarded. The DNA was washed and centrifuged in 500 µl 70% ethanol. The DNA was then dissolved in 100 µl milliQ-H₂O. CGG repeat lengths were determined by PCR using the Expanded High Fidelity Plus PCR System (Roche Diagnostics). Briefly, approximately 500–700 ng of DNA was added to 50 µl of PCR mixture containing 2.0 µmol/L of each primer, 250 µmol/L of each dNTP (Invitrogen), 2% dimethyl sulfoxide (Sigma), 2.5

M Betaine (Sigma), 5 U Expand HF buffer with mg (7.5 μ mol/L). The forward primer was 5`-GCTCAGCTCCGTTCGGTTCACTTCCGGT-3` and the reverse primer was 5`-AGCCCCGCACTTCCACCACCAAGCTCCTCCA-3`. PCR steps were 10 min denaturation at 95 °C, followed by 34 cycles of 1 min denaturation at 95 °C, annealing for 1 min at 65 °C, and elongation for 5 min at 75 °C to end each cycle. PCR ends with a final elongation step of 10 min at 75 °C. DNA CGG band sizes were determined by running DNA samples on a 2.5% agarose gel and staining DNA with ethidium bromide.

Behavioral Apparatus

For the metric and topological spatial processing tasks, a circular table measuring 1 m in diameter was covered with a clean, white, plastic cover. Four objects measuring between 2.5–5 cm at the base and between 5 and 15 cm tall were used as stimuli in these tasks (a small bottle filled with green liquid, an overturned coffee mug, a large pipette bulb, and an unused spray paint can). These objects were chosen to be texturally and visually unique and easily distinguishable for the mice. The table was surrounded on two sides by walls (at a distance of ~1 m) with discrete distal cues available at the same level as the table surface affixed to the walls. Between the habituation and test sessions, the mice were placed in a small, opaque holding cup with a single paper towel placed inside. The circular table was wiped down with 70% ethanol after testing of each mouse to remove olfactory cues that could influence object exploration by later tested mice. These spatial processing tasks were developed for use in

rats, but have been modified for use with transgenic mice. The topological spatial processing task has been used in transgenic mice in an earlier study (Lee et al., 2009), but to our knowledge this is the first time the metric task has been used in mice.

Behavioral Methods

Metric spatial processing task

The arrangement of objects for the metric spatial processing tasks is shown in Figure 16 (Goodrich-Hunsaker et al., 2005; Goodrich-Hunsaker et al., 2008b). The mouse was placed on the maze as shown in Figure 16 facing two objects placed 45 cm apart (the animal was placed ~30–40 cm from the objects). The mouse was allowed 15 min to freely explore the tabletop, stimulus objects on the table, and distal environmental cues. Exploration of the objects decreases over the 15 min period as animals habituate. After the 15 min habituation session, the mouse was removed to the small holding cup for 5 min. During this intersession interval the objects were moved 15 cm closer to each other so that the objects were 30 cm apart. The mouse was then again placed on the tabletop as described above and given 5 min to reexplore the objects during this test session.

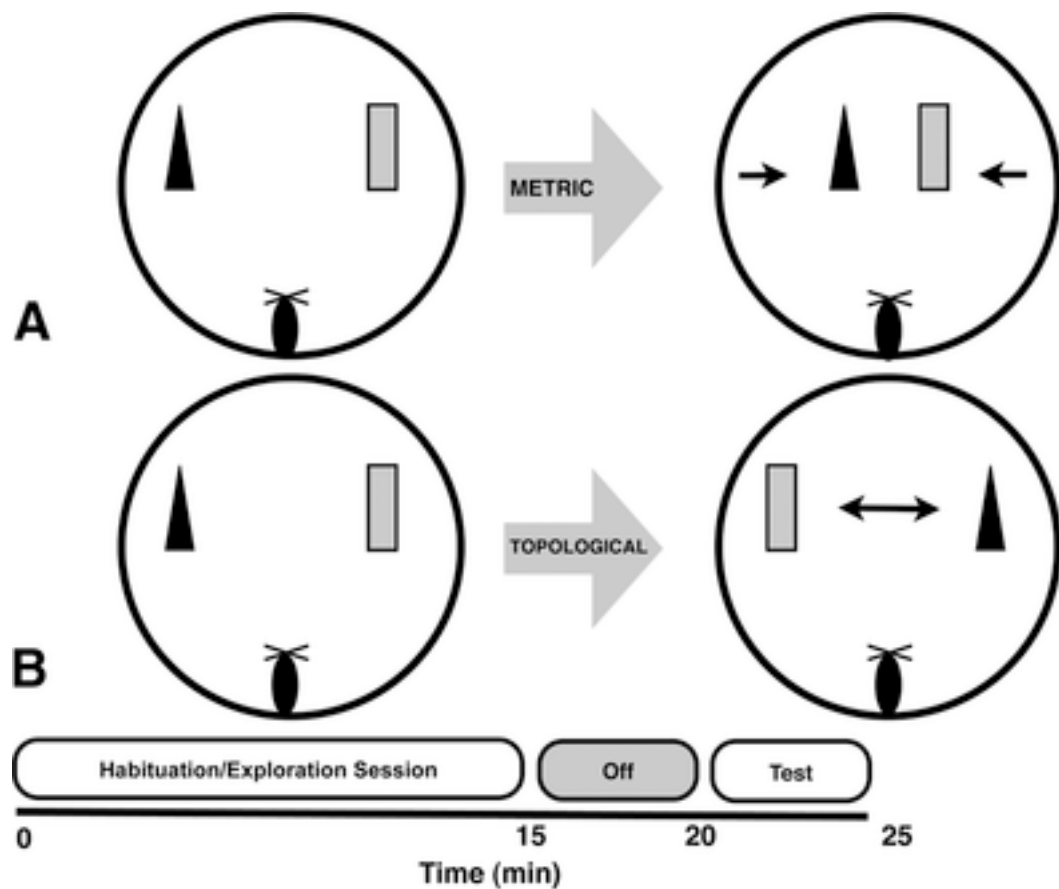


Figure 16. **A.** Diagram and timeline for the metric spatial processing task. **B.** Diagram and timeline for the topological spatial processing task. Notice that the habituation sessions are identical between the tasks, with only the object manipulation differing between the habituation and test sessions.

Topological spatial processing task

For the topological spatial processing task (Figure 16; paradigm slightly modified from Goodrich-Hunsaker et al., 2005; Goodrich-Hunsaker et al., 2008b; Lee et al., 2009), two novel objects, different from those used in the metric task, were used as stimuli. Mice were placed on the table and allowed to habituate to the objects exactly as in the metric task, and then removed from the table for 5 min. During the 5 min between the habituation and test sessions, the objects were transposed, so the left object was now on the right and vice versa. Therefore, objects occupied the same spatial locations as during the habituation session, but their positions were exchanged.

The order of the metric and topological spatial processing tasks was randomized so that half of the wild type and half the CGG KI mice received each task first. The object pairs presented during each task were randomized between mice.

Dependent Measures

For both the metric and topological tasks, the time spent exploring each object was recorded as the dependent variable. This exploratory activity was recorded in 0.5 s increments (*i.e.*, a 0.25 s bout of exploration was recorded as 0.5 s and a 0.75 s bout of exploration was recorded as 1 s). Exploration was defined as the mouse actively sniffing or touching the object with its nose, vibrissa, or forepaws. An animal simply located near the objects without actively interacting with them was not scored as exploration. Object exploration data were

summarized in 5-min epochs during the 15-min habituation period to facilitate comparison with the 5-min test session, as previously described (Goodrich-Hunsaker et al., 2005; Goodrich-Hunsaker et al., 2008b; Hunsaker et al., 2008b). Mice habituate to the objects during the 15-min habituation phase, and show relatively low levels of exploration during the last 5 min. However, during the 5-min test session when mice are put back on the table, mice that remember the object distance (metric) or object position (topological) show increased exploration.

Immunocytochemistry for Intranuclear Inclusions

Immunocytochemistry was carried out on subsets of wild type and CGG KI mice at 12, 24, and 48 weeks of age to document the presence of characteristic intranuclear inclusion in CGG KI mice and absence of such inclusions in wild type mice. Two animals per age per genotype ($n = 2$ wild type, $n = 2$ CGG KI at 12 weeks; $n = 2$ wild type, $n = 2$ CGG KI at 24 weeks; $n = 2$ wild type, $n = 2$ CGG KI at 48 weeks) that were not used in behavioral experiments were deeply anesthetized with sodium pentobarbital and, once unresponsive, intracardially perfused with 10 mL lightly chilled Ringer's solution with heparin followed by 60 mL of lightly chilled, fresh 4% (wt/vol) paraformaldehyde (PFA) in 0.1 M phosphate buffer (PB) at pH 7.4 over 20 min (3 ml/min via gravity flow). The brain was removed and placed into 4% PFA for 1 hr postfixation at 4 °C, rinsed and transferred into 10% (wt/vol) sucrose in 0.1 M PB, pH 7.4 for 1 hr at 4 °C, and

then transferred into 30% (wt/vol) sucrose for 24 hr at 4 °C for cryoprotection. The brains were then frozen on dry ice for 60 min prior to storage at –80 °C.

The left hemisphere was sectioned in the parasagittal plane on a freezing stage microtome at 30 µm and sections were collected into series of every fifth section directly into 30% sucrose (*i.e.*, 5 section sets). One set of sections was immediately mounted onto 1% gelatin coated slides from PB and set aside for hematoxylin and eosin staining for evaluation of overall structural morphology and the presence of intranuclear inclusions, a characteristic feature of CGG KI mice and FXTAS individuals (Greco et al., 2002; Greco et al., 2006; Willemse et al., 2003). The other four sets of sections in sucrose, as well as the right hemisphere were flash frozen on dry ice and stored at –80 °C.

For immunocytochemistry for ubiquitin to visualize intranuclear inclusions, free-floating sections from one of the remaining four sets of frozen sections were rinsed of 30% sucrose with 10% sucrose followed by 0.1 M PB (pH 7.4). After treatment with 0.1% (wt/vol) sodium borohydride (10 min), sections had endogenous peroxidases quenched with hydrogen peroxide (0.5% and 2%). After transfer from 0.1 M PB to a 0.1 M phosphate-buffered saline solution (PBS, pH 7.4), tissue was blocked and permeabilized with a solution of 3% (wt/vol) bovine serum albumin (BSA), 3% (vol/vol) swine serum, and 0.3% (vol/vol) triton-X for 1 hr at room temperature with agitation. Rabbit polyclonal antibodies against ubiquitin (Dako, Inc.; Carpinteria, CA) were diluted 1:2000 in 1% swine serum, 2% BSA, and 0.3% Triton X-100. Sections were placed into the primary antibody solution for 72 hrs on a shaker at 4°C. After primary antibody incubation and

rinsing, a biotinylated swine anti-rabbit immunoglobulin secondary antibody (Dako), diluted 1:500 in the same diluent as the primary antibody was incubated with the tissue for 24 hours on a shaker at 4 °C. After thorough rinsing, the tissue was incubated in an avidin-biotin complex (ABC; Vector Laboratories, Burlingame, CA) for 24 hr. The ubiquitin immunostaining was visualized using 0.05% diaminobenzidine with a blue/gray chromogen (Vector SG) in PBS. After mounting, the tissue was dehydrated, cleared, counterstained with neutral red, and coverslipped with Permount (Fisher Scientific). Presence of intranuclear inclusions was verified at 1000x magnification on a light microscope.

Statistical Analyses

For the 15 min habituation session, total object exploration time (s) was calculated individually for the first, middle and last 5-min epochs to facilitate comparison between the last 5 min of the habituation session and the 5-min test session. A 2 (genotype) × 3 (session) repeated measures analysis of variance (ANOVA) was performed on these exploration data for both metric and topological spatial processing tasks. To facilitate the comparison between the test session and the last 5 min of the habituation session, an exploration ratio was calculated as described by Kesner et al. (Goodrich-Hunsaker et al., 2005). Briefly, the ratio was calculated as: [(exploration time during the 5-min test session)/(exploration time during the 5-min test session + exploration during the last 5 min of the habituation session)]. This constrained all the values between 0 and 1. With this ratio, increased exploration during the 5-min test session

compared to the last 5 min of the habituation session is reflected as a ratio >0.5, while decreased exploration (or continued habituation) is reflected as a ratio <0.5. Prior to comparing CGG KI mice and wild type mice for the ratio scores, it was verified via a one-tailed t test that the ratio score for the wild type mice was >0.5, suggesting heightened exploration of the objects during the test session compared to the final 5 min of the habituation session. To compare ratios between CGG KI mice and wild type mice, one way ANOVA with genotype as the grouping variable were performed for both metric and topological tasks. All statistical analyses were performed with the open source statistical package, "R" (R Development Core Team, 2012), and all data are reported as means and standard errors of the mean. All effects were considered statistically significant at $p < .05$.

Results

Prior to statistical comparison of the ratio scores between CGG KI and wild type mice, it was verified that, as expected, the wild type mice showed heightened exploration of the objects after the metric or topological shifts. To do this, a one-tailed t test was used to assess whether the wild type control group mean ratio scores were >0.5 . In all cases presented below, the wild type animals showed heightened exploration of the metric or topological changes ($p < .05$).

Metric Spatial Processing Task

In the metric spatial processing task the distance between the objects was decreased between the habituation and test periods. Performance in the metric task at 12, 24, and 48 weeks of age is shown in Figure 17A. For the 15-min habituation of object exploration, time spent exploring the object (in s) was analyzed with two-way, repeated measures ANOVA with genotype as the between-group factor and exploration during the three 5-min time blocks as the repeated within-group factor. There was no main effect of group at 12 ($F_{1,44} = 3.70$, $p = .06$), 24 ($F_{1,50} = 1.14$, $p = .2$), or 48 weeks ($F_{1,50} = 2.23$, $p = .15$). As expected, object exploration time decreased significantly over the three time blocks for all groups at each age ($p < .05$) reflecting decreased object exploration (*i.e.*, habituation) over the 15-min habituation period. Although it appears that the 48-week-old animals showed increased exploration during min 6–10, these animals showed reduced exploration during min 11–15 similar to the other ages. The interaction between the two factors was not statistically significant at 12, 24,

or 48 weeks of age. These data indicate that the CGG KI and wild type mice showed similar habituation of object exploration across the three ages during the initial 15-min habituation period. However, during the 5-min test after reposition of the objects, wild type mice, but not CGG KI mice, showed an increase in object exploration.

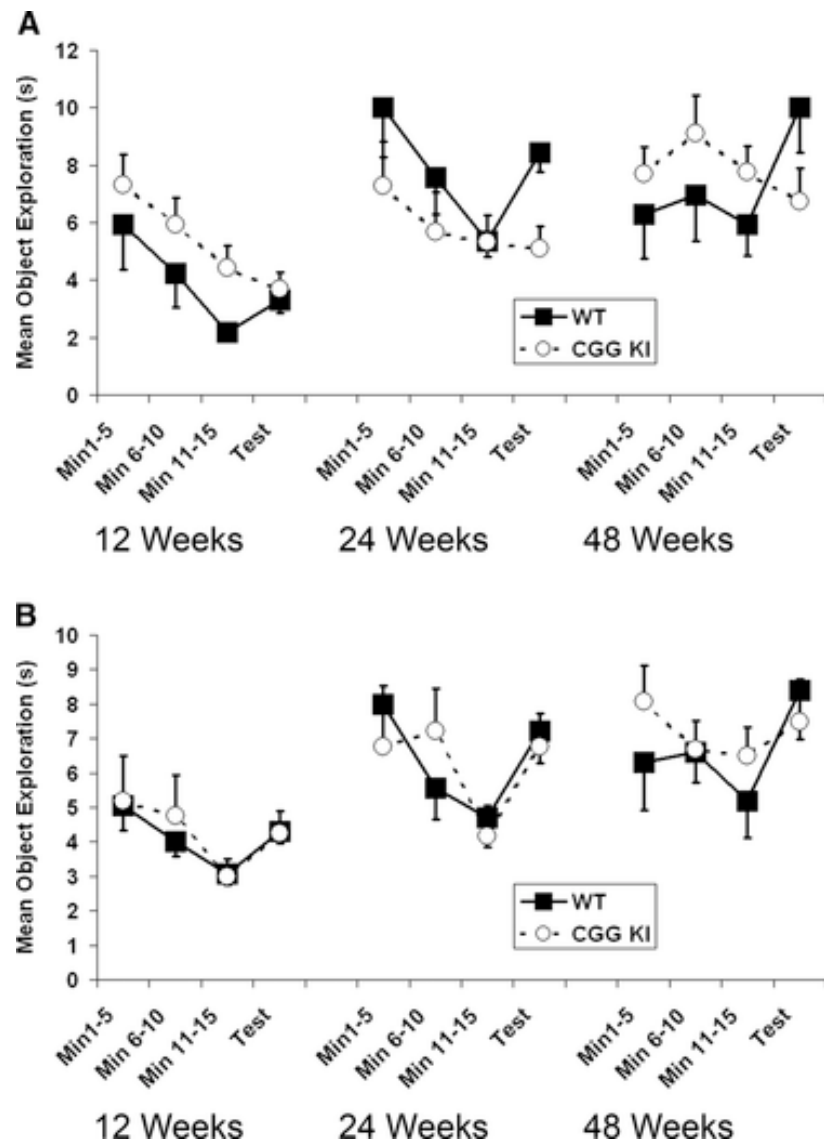


Figure 17. Habituation of object exploration. **A.** Plots showing habituation of object exploration for the metric spatial processing task. At each age the CGG KI group showed a decrease in exploration during the test compared to the last 5 min of the habituation session, whereas the wild type group showed a marked increase in exploration during the test. **B.** Habituation of object exploration for the topological spatial processing task. At 12 weeks and 24 weeks both group showed similar increases in object exploration during the test session. However, at 48 weeks of age the CGG KI group showed similar levels of reexploration during the test session compared to the last 5 min of the habituation session, while the wild type group showed a large increase in exploration. The data for MIN 11–15 and the 5 min TEST sessions were used to generate the mean ratio scores reported in Figures 18A and 18B.

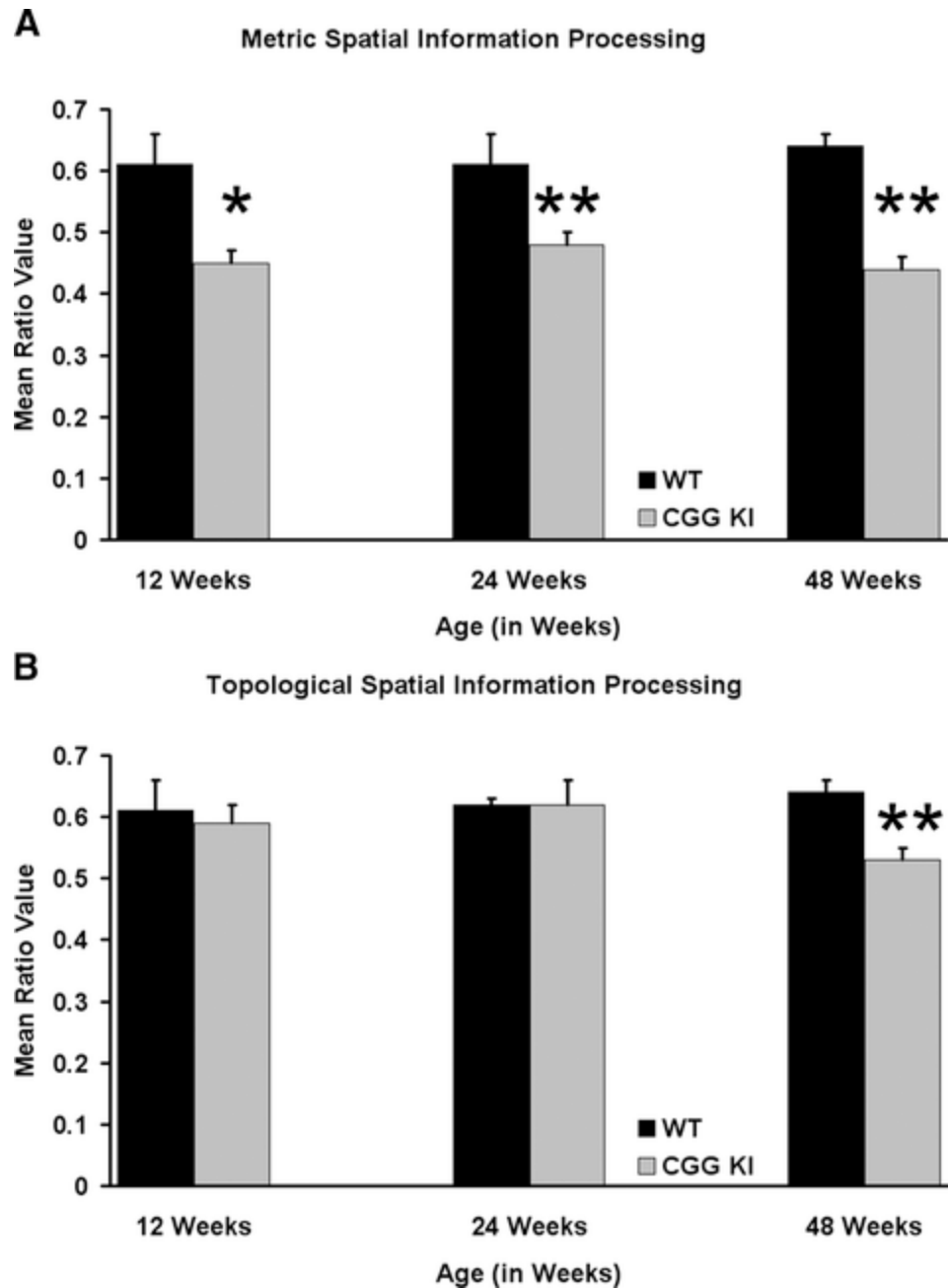


Figure 18: Metric and topological spatial processing. **A.** Mean ratio scores for wild type and CGG KI mice at different ages for the metric task. **B.** Mean ratio scores for the topological task. (12 weeks of age CGG KI $n = 8$, wild type = 8; 24 weeks of age CGG KI $n = 10$, wild type = 8; 48 weeks of age CGG KI $n = 8$, wild type = 10). * $p < 0.05$. ** $p < .01$.

Topological Spatial Processing Task

In the topological spatial processing task the positions of the two novel objects were reversed between the habituation and test periods. Performance in the topological task at 12, 24, and 48 weeks of age is shown in Figure 17B. For the 15-min habituation of object exploration, time spent exploring the object (in s) was analyzed with two-way repeated measures ANOVA with genotype as the between group factor and exploration during the three 5-min time blocks as the repeated within-group factor. There was no main effect of group at 12 weeks ($F_{1,44} = 0.003$, $p = .96$), 24 weeks ($F_{1,50} = 0.04$, $p = .85$), or 48 weeks of age ($F_{1,50} = 0.1.73$, $p = .19$). As expected, object exploration time decreased significantly over the three time blocks for all groups at each age ($p \leq .05$) reflecting habituation to the objects over the 15-min habituation period. As in the metric task, wild type 48 week old mice showed a small increase in exploration during min 6–10, but exploration decreased during the final min 11–15, similar to that seen at the other ages. The interaction between the two factors was not statistically significant at 12, 24, or 48 weeks of age. These data indicate that the CGG KI and wild type mice showed similar habituation of object exploration across the three ages during the initial 15 min habituation period. After exchanging object location during the 5-min test, wild type and CGG KI mice showed increased exploration at 12 and 24 weeks of age. However, at 48 weeks of age the CGG KI mice showed little if any reexploration of the objects, while wild type mice showed marked reexploration compared to the last 5 min of the habituation period.

As was done for the metric task above, changes in object exploration in the topological task were expressed as exploration ratio scores which were then analyzed by one-way ANOVAs with genotype as the grouping factor. As shown in Figure 18B, when the positions of the two objects were reversed in the topological task, the CGG KI group did not differ significantly from wild type mice in exploration of the objects at 12 weeks ($F_{1,14} = 0.09$, $p = .78$; mean ratio 0.61 ± 0.05 CGG KI vs. 0.59 ± 0.02 wild type) or 24 weeks of age ($F_{1,16} = 0.005$, $p = .95$; mean ratio 0.62 ± 0.05 CGG KI vs. 0.62 ± 0.02 wild type). However, the object exploration ratio at 48 weeks of age did differ significantly between CGG KI and wild type mice ($F_{1,16} = 19.40$, $p < .01$; mean ratio 0.53 ± 0.02 CGG KI vs. 0.64 ± 0.02 wild type). These data demonstrate an age-dependent impairment in processing of topological spatial information in CGG KI mice compared to wild type mice, with an impairment observed at 48, but not 12 and 24 weeks of age.

Histology

Intranuclear inclusions in the dentate gyrus of the hippocampus and in the overlying parietal cortex were identified by immunocytochemistry for ubiquitin, with neutral red counterstaining (see Figure 19). The inclusions appear as dark gray/black round/spherical bodies clearly within the nucleus of neurons. These intranuclear inclusions are easily differentiated from the nucleoli, which are only weakly stained by neutral red (nucleoli are more strongly stained by light cresyl violet or hematoxylin counterstaining, but are still easily differentiated from the inclusions—data not shown) and maintains an irregularly shaped appearance in

contrast to the round appearance of inclusions in neurons in CGG KI mice. These inclusions could also be identified by hematoxylin and eosin (H&E) staining as well, but immunocytochemistry was run to verify the presence of inclusions, as inclusions in the CGG KI mouse model have not been previously visualized with H&E staining (*cf.* Brouwer et al., 2008a; Brouwer et al., 2008b; Willemse et al., 2003).

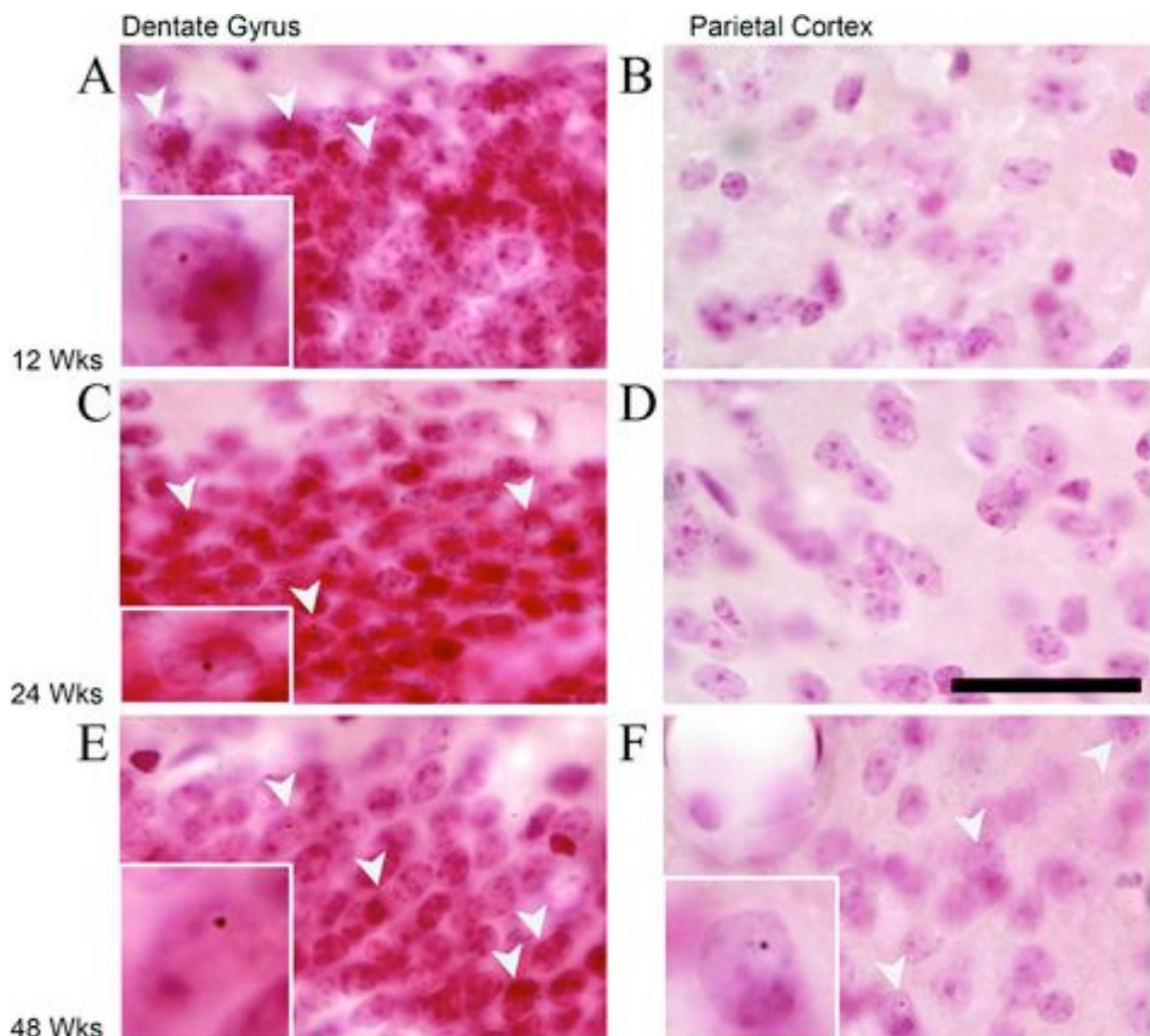


Figure 19: Intranuclear inclusions in 12-, 24-, and 48-week-old animals stained for ubiquitin and counterstained with neutral red. **A.** 12-Week-old animals have inclusions in the dentate gyrus granule cells, but **B.** not in the parietal cortex. **C.** 24-Week-old animals have inclusions in the dentate gyrus granule cells, but **D.** not in the parietal cortex. **E.** 48-week-old animals have inclusions in the granule cells in the dentate gyrus, and **F.** in the parietal cortex. Arrowheads point to neurons with ubiquitin stained intranuclear inclusions. Insets show a representative cell enlarged to show inclusions. Scale bar in (D) is 50 μm and applies to all plates, but not to inserts.

As early as 12 weeks of age, the CGG KI mice showed the presence of intranuclear inclusions in the dentate gyrus granule cells in the hippocampus, as well as some interneurons in the inner molecular layer and hilus. At this age, no inclusions were found in the parietal cortex. At 24 weeks of age, there were a greater number of inclusions in the dentate gyrus, a few in the pyramidal cell layer and stratum radiatum in the hippocampus (esp. CA1), but only rarely in the parietal cortex. At 48 weeks, the CGG KI mice showed the presence of intranuclear inclusions both in the dentate gyrus and pyramidal cell layers of the hippocampus as well as intranuclear inclusions in the parietal cortex. Additionally, these inclusions appeared to be larger in the older mice in the dentate gyrus and the inclusions in the cortex were larger on average than those in the dentate gyrus.

Intranuclear inclusions were also present in the 12 week old CGG KI mice in a very limited number of granule cells in the cerebellum as well as in periglomerular granule cells of the olfactory bulb, as well as rarely present in large neurons in the brainstem (data not shown). The presence of inclusions in these regions was also identified in older mice (24 and 48 week old CGG KI mice). At 24 weeks of age, there were never any inclusions in the neocortex, but the inclusions in the hippocampus were more numerous and slightly larger than those at 12 weeks. In the 48 week old CGG KI mice, inclusions became prevalent in the limbic system, specifically the lateral entorhinal cortex, as well as the retrosplenial/anterior cingulate cortices. Furthermore, at 48 weeks of age intranuclear inclusions appeared in the neocortex, specifically the parietal cortex,

rostral cortex, and occipital cortex. As reported previously, there also were intranuclear inclusions in the amygdala and periamyg达尔 cortices (Brouwer et al., 2008a; Brouwer et al., 2008b; Willemsen et al., 2003). There was also a clear developmental trajectory in the size of inclusions, with intranuclear inclusions being qualitatively larger in each age group (*e.g.*, inclusion size at 12 week old <24 week old <48 week old). In no cases were inclusions ever present in littermate wild type mice run in parallel with CGG KI mice (data not shown).

Discussion

Previous studies have shown that CGG KI mice carrying an expanded CGG trinucleotide repeat in the 5'-untranslated region of the *Fmr1* gene develop several of the neuropathological characteristics of FXTAS in humans (Brouwer et al., 2008a; Brouwer et al., 2008b; Willemse et al., 2003). It has been more difficult, however, to characterize cognitive deficits in this CGG KI mouse. To date, only a single study has attempted to characterize learning and memory performance in these CGG KI mice. In the study by van Dam et al., one year-old CGG KI mice showed relatively subtle spatial learning deficits on the water maze (Van Dam et al., 2005). It should be mentioned that the mice used in the Van Dam et al., (2005) study were on a mixed FVB/N × C57BL/6J background, whereas those used in the present study were on a C57BL/6J background.

The present experiments were conducted in similar mice carrying CGG repeat expansions ranging from CGG80 to CGG180 in order to extend the findings from the water maze to a spatial task that explored metric and topological spatial information processing. Our results reveal that these CGG KI mice show age-related deficits in spatial processing for both the metric and topological tasks. At both 12 and 24 weeks of age, the CGG KI mice showed a marked failure to detect changes in the distance between a pair of objects (e.g., metric changes). However, these same animals were fully capable of detecting a change when the objects were transposed (e.g., topological changes). At 48 weeks of age, the CGG KI mice failed to detect either metric or topological changes in object position. FXTAS has been described as a late developing

neurodegenerative disease that manifests around the 6th decade of life in affected carriers (Hagerman & Hagerman, 2004b). These results in CGG KI mice showing cognitive impairment in the metric task as early as 12 weeks of age suggest that there may also be cognitive impairments in FXTAS at earlier ages than previous thought (*cf.*, Cornish et al., 2008b; Farzin et al., 2006; Hagerman, 2006; Hessl et al., 2005; Jäkälä et al., 1997; Koldewyn et al., 2008; Sevin et al., 2009 for examples of cognitive deficits in young carriers of the fragile X premutation). Further experiments are currently underway to more thoroughly characterize spatial and temporal processing in the CGG KI mouse model of the fragile X premutation using more traditional assays (*e.g.*, water maze, elevated plus maze, associative learning tasks, etc.) to more thoroughly characterize any alterations in memory processes, potential ataxia or tremors in these mice, as well as to more fully characterize any potential anxiety/depressive symptoms that have been reported in carriers of the fragile X premutation (Bourgeois et al., 2009).

These results in mice are consistent with several theories that propose that poor spatial resolution contributes to the overall cognitive deficits that are present in some neurodevelopmental and neurodegenerative diseases (Simon, 2008; *cf.*, Rolls & Kesner, 2006). These theories suggest that a fundamental “hypergranularity” (Simon, 2008), or lack of precision in spatial and/or temporal processing (Rolls & Kesner, 2006) interferes with the formation of memory by reducing the efficiency of how sensory stimuli are processed. Similar models have been proposed for rodents that emphasizes the precise nature of

information processing over performance on learning and memory tasks (Kesner, 1991; Kesner, 2003; Rolls & Kesner, 2006). Under these models, fine spatial resolution (or metric processing) is associated with functions attributed to the hippocampus (esp. dentate gyrus), whereas the processing of topological information is associated with functions attributed to the parietal cortex (Goodrich-Hunsaker et al., 2005; Goodrich-Hunsaker et al., 2008b; Lee et al., 2009).

Considered within these theories focusing on spatial processing, the present data suggest that early deficits (at 12 and 24 weeks) in spatial information processing in CGG KI mice fall within the domain of deficits in metric information processing and may therefore be related to similar studies in rats that associate metric impairments with dysfunction to the dentate gyrus (Goodrich-Hunsaker et al., 2005; Goodrich-Hunsaker et al., 2008b; Hunsaker et al., 2008b). The additional spatial deficits that appear later in development (at 48 weeks) in the CGG KI mice appear to fall within the topological domain and, based on similar studies in rats, suggest dysfunction in the parietal cortex leading to poor processing of topological information (Goodrich-Hunsaker et al., 2005; Goodrich-Hunsaker et al., 2008b; Lee et al., 2009). The present behavioral data showing more complex deficits in spatial processing are also consistent with the progressive neuropathology that has been reported previously in this CGG KI mouse model of FXTAS. Specifically, intranuclear inclusions have been shown to become increasingly prominent in the hippocampus and neocortex, including the parietal cortex, at more advanced ages (Willemse et al., 2003). These

neuropathological findings concerning intranuclear inclusions were essentially replicated in the present study. That is, development of inclusions was progressive, with inclusions present in the brain as early as 12 weeks of age, appearing at earlier ages in the dentate gyrus in the hippocampus and then later in the overlying parietal cortex. Furthermore, if these intranuclear inclusions truly reflect some type of damaging neuronal pathology, then it is reasonable to consider the possibility that poor metric processing in CGG KI mice may be related to abnormalities in dentate gyrus granule cell function. It is important to note that at 12 and 24 weeks of age, the parietal cortex was almost completely devoid of inclusions. At 48 weeks of age, there were inclusions in both the dentate gyrus and pyramidal cell layers of the hippocampus (perhaps deleteriously affecting metric spatial information processing) as well as the parietal cortex, which could potentially contribute to poor topological spatial information processing in the CGG KI mouse at 48 weeks of age but not at earlier ages.

In summary, the present experiment provides evidence for a spatial processing deficits in early adulthood in CGG KI mice used to model clinical FXTAS. These mice at relatively young ages (12 and 24 weeks) showed deficits for processing metric relationships between objects, a process associated with functions of the dentate gyrus in the hippocampus. Later in development (at 48 weeks of age) mice showed deficits for both metric as well as topological spatial processing, the latter of which may be subserved by the parietal cortex. The nature of the cognitive deficits may also relate to the development of the

intranuclear pathology in the hippocampus and parietal cortex during development. Considered together these data demonstrate a progressive development of complex spatial information processing deficits in CGG KI mice that appear to be related to presence of intranuclear inclusions in hippocampus and parietal cortex. The present data also demonstrate the usefulness of behavioral paradigms, such as those used in the present studies, that are designed to assess specific types of spatial processing (e.g., metric and topological). Such tests may provide a valuable tool for identifying early cognitive deficits in mouse models of neurological disorders as well as providing a behavioral outcome measure for potential pharmacological interventions (cf. (Rolls & Kesner, 2006; Simon, 2008)).

Acknowledgements: We thank Drs. Tony J. Simon, Susan M. Rivera, and Paul J. Hagerman for helpful discussions concerning portions of this experiment. This research was supported by Grants NINDS RL1 NS 062411 and National Institutes of Health Roadmap Consortium NIDCR UL1 19583

Chapter 8

Temporal Ordering Deficits in Female CGG KI Mice Heterozygous for the Fragile X Premutation

Abstract.

The fragile X premutation is a tandem CGG trinucleotide repeat expansion on the *FMR1* gene between 55-200 repeats in length. A CGG knock-in (CGG KI) mouse with CGG repeat lengths between 70-350 has been developed and used to characterize the histopathology and cognitive deficits reported in carriers of the fragile X premutation. Previous studies have shown that CGG KI mice show progressive deficits in processing spatial information. To further characterize cognitive deficits in the fragile X premutation, temporal ordering in CGG knock-in (CGG KI) mice was evaluated. Female CGG KI mice were tested for their ability to remember the temporal order in which two objects were presented. The results demonstrate that at 48 weeks of age, female CGG KI mice with CGG repeat expansions between 150-200 CGG repeats performed more poorly on tests of temporal order than wildtype mice, whereas female CGG KI mice with between 80-100 CGG repeats performed similarly to wildtype mice. No mice had any difficulty in detecting the presence of a novel object. These data suggest female CGG KI mice show a CGG repeat length-sensitive deficit for temporal ordering.

This chapter has been published as:

Hunsaker, M. R., Goodrich-Hunsaker, N. J., Willemsen, R., & Berman, R. F. (2010). Temporal ordering deficits in female CGG KI mice heterozygous for the fragile X premutation. *Behavioural Brain Research*, 213(2), 263-268.

My role in this study was experimental design, apparatus design, performing behavioral experiments, and data analysis.

INTRODUCTION

The fragile X premutation is defined as a CGG trinucleotide repeat expansion between ~55-200 repeats in length in the 5' untranslated region (5' UTR) of the fragile X mental retardation 1 (*FMR1*) gene. The fragile X premutation results in a 3-8 fold increase in *FMR1* mRNA levels in leukocytes and, paradoxically, decreased *FMR1* protein (FMRP) levels due to translational inefficiency of the mutant *FMR1* mRNA (Tassone et al., 2000d). Some carriers of the fragile X premutation develop a late onset neurodegenerative disorder: fragile X-associated tremor/ataxia syndrome (FXTAS). This is in contrast to the full mutation in fragile X syndrome (FXS), which results in intellectual disability (Hagerman & Hagerman, 2004b). In FXS the CGG repeat expansion is longer than 200, and *FMR1* mRNA and FMRP levels are too low to be detected due to hypermethylation of the *FMR1* promoter region and subsequent transcriptional silencing (Tassone et al., 2000a; Tassone et al., 2000b).

Until recently, cognitive function in fragile X premutation carriers was presumed to be largely unaffected by the mutation. However, studies into potential cognitive effects of the fragile X premutation are demonstrating neurocognitive impairments related to the length of the CGG repeat expansions, *FMR1* mRNA levels, and FMRP levels (Adams et al., 2007; Koldewyn et al., 2008; Tassone et al., 2000d; Tassone et al., 2007a). Fragile X premutation carriers have reduced hippocampal volumes relative to the general population and this volume reduction correlates with poor performance on memory tests (Jäkälä et al., 1997; Moore et al., 2004b). Using functional magnetic resonance

imaging (fMRI), Koldewyn et al., (2008) reported that fragile X premutation carriers have reduced hippocampal activation during episodic retrieval compared to the general population. These studies suggest that cognitive processing in fragile X premutation carriers is fundamentally altered. These findings, however, are difficult to interpret as there are not always differences in performance between fragile X premutation carriers and the general population for behavioral performance; making comparisons between neural activation as recorded by fMRI and cognitive processing difficult.

To evaluate the nature of neurocognitive deficits in carriers of the fragile X premutation, a CGG knock-in (KI) mouse model has been studied (Berman & Willemse, 2009; Brouwer et al., 2009; Hunsaker et al., 2009; Van Dam et al., 2005; Wenzel et al., 2010; Willemse et al., 2003). This CGG KI mouse has been shown to model much of the neuropathology seen in fragile X premutation carriers with FXTAS, including intranuclear inclusions in neurons and astrocytes, the neuropathological hallmark of FXTAS (Berman & Willemse, 2009; Brouwer et al., 2009; Hunsaker et al., 2009; Van Dam et al., 2005; Wenzel et al., 2010; Willemse et al., 2003).

In a recent review, Simon (2008) showed that many neurogenetic disorders including FXS, Turner syndrome, Williams syndrome, and chromosome 22q11.2 deletion have overlapping cognitive impairments across the spatial and temporal domains. Simon (2007, 2008) proposed that these deficits in spatiotemporal cognition may result from “reduced resolution, or clarity, of mental representations” referred to as ‘spatiotemporal hypergranularity’. In other words,

processing spatial distances or temporal separations between objects becomes increasingly difficult as the spatial or temporal differences become smaller due to cognitive interference. Thus, compared to the general population, individuals with neurodevelopmental disorders may have coarser mental representations, so that identification of one spatial location or time point from another requires a larger between-item difference before they are perceived as distinct. Although the spatiotemporal hypergranularity model was developed and subsequently validated in 22q11.2 deletion syndrome (Simon, 2007; Simon, 2008), it can be extended to include other neurodevelopmental disorders that show spatial and/or temporal processing deficits, which may include FXS (Johnson-Glenberg, 2008; Kemper, Hagerman, & Altshul-Stark, 1988).

Previous research indicates that the hippocampus has a role in processing spatial and temporal relationships between stimuli, and moreover receives inputs from all sensory modalities; suggesting that one function of the hippocampus may be to encode and separate events in time and space by a process called ‘pattern separation’ (Gilbert & Kesner, 2006; Gilbert et al., 2001; Kesner & Hunsaker, 2010; Kesner et al., 2004; Marr, 1971; Myers & Scharfman, 2009; O'Reilly & McClelland, 1994; Pirogovsky et al., 2009; Rolls & Kesner, 2006; Rolls, 1996; Rolls, 2007; Toner, Pirogovsky, Kirwan, & Gilbert, 2009). Pattern separation ensures that incoming sensory information is orthogonalized to minimize interference. One hypothesis is that spatiotemporal hypergranularity may result from impaired spatial and temporal pattern separation processes. Hunsaker et al., (2009) demonstrated that male CGG KI mice have progressive

spatial processing deficits using a task specifically designed to evaluate spatial pattern separation (Goodrich-Hunsaker et al., 2005; Goodrich-Hunsaker et al., 2008b). They further demonstrated that development of spatial processing deficits coincided with the appearance of hippocampal pathology (e.g., intranuclear inclusions).

The spatial processing deficits in CGG KI mice can be interpreted as resulting in or from a hypergranularity in spatial information processing. The present study was designed to evaluate temporal pattern separation in CGG KI mice by evaluating their ability to process temporal relationships between stimuli. This study also serves as an additional test of the spatiotemporal hypergranularity hypothesis in the CGG KI mouse model of the fragile X premutation by directly evaluating temporal pattern separation in CGG KI mice (Kesner & Hunsaker, 2010; Pirogovsky et al., 2009).

In the present study, heterozygous female CGG KI mice at 48 weeks of age were tested on a temporal ordering paradigm used previously in rats (Hannesson, Howland, & Phillips, 2004a; Hannesson, Vacca, Howland, & Phillips, 2004b; Hunsaker, Fieldsted, Rosenberg, & Kesner, 2008a). This paradigm exploits the tendency of rats and mice to explore the earlier item in a sequence of items presented over time if given a choice between two (Mumby, 2001). Performance on this task depends either on temporal sequencing of presented stimuli to guide performance or on judgments of the relative memory strengths among previously presented stimuli (Agster, Fortin, & Eichenbaum, 2002; Fortin, Agster, & Eichenbaum, 2002). An impairment in either of these

memory processes results in similar temporal ordering deficits--namely the lack of preferential exploration of an object presented earlier in a sequence over one presented later (Hunsaker & Kesner, 2008; Hunsaker et al., 2008a; Manns & Eichenbaum, 2005).

Female mice were used in this study as the frequency of the fragile X premutation is higher in females than males (1:250-813 in males and 1:113-259 in females) (Hagerman, 2008), and there are increasing reports of neurocognitive and psychiatric abnormalities in female fragile X premutation carriers (Adams et al., 2007; Brouwer et al., 2009; Cilia et al., 2009; Hagerman & Hagerman, 2004b; Hagerman et al., 2004; Hunter et al., 2009; Kamm & Gasser, 2005; Karmon & Gadoth, 2008; Leehey, 2009; Rodriguez-Revenga et al., 2007; Zuhlke et al., 2004). While most research into FXS and the fragile X premutation has been carried out in males because the mutation is X-linked, it is also important to characterize pathology resulting from X-linked mutations in females (Check Hayden, 2010; Wald & Wu, 2010). The results of the present study suggest that 48 week old female CGG KI mice have difficulty in temporal ordering, but only when the CGG trinucleotide repeat expansion is beyond a certain threshold. These same female CGG KI mice responded normally to a novel visual stimulus. The results of this study suggest that female CGG KI show impaired temporal ordering, supporting the hypothesis that a spatiotemporal hypergranularity may underlie cognitive deficits seen in the fragile X premutation.

MATERIALS AND METHODS

Mice

The generation of a CGG knock-in (CGG KI) mouse model of the fragile X premutation has been described in detail (Bontekoe et al., 1997; Willemsen et al., 2003). The CGG KI mice were developed on a mixed FVB/N x C57BL/6J background, then backcrossed with C57BL/6J mice from Jackson Labs (Bar Harbor, ME) until congenic.

CGG KI mice used in the present study were housed in same sex, mixed genotype groups of up to four littermates per cage with food and water ad libitum, constant temperature, and a 12 h light-dark cycle. Temporal ordering was evaluated in 43 female mice at 48 weeks of age. Fourteen mice were wildtype, with both X alleles having CGG trinucleotide repeats of between 9 and 11 repeats. The remaining 29 mice were heterozygous for the CGG repeat expansion (*i.e.*, one wildtype and one mutant X allele), with 14 carrying a large CGG repeat expansion between 150-190 and 15 carrying a smaller CGG repeat expansion between 80-100 on the mutant X allele. The high and low CGG repeat expansion mouse lines were bred from CGG KI mice with spontaneous expansions or contractions of the trinucleotide repeat and then maintained as separate lines in order to examine the relationship between CGG repeat length and pathological features. All CGG KI mice used in this study were from separate litters and wildtype mice were littermate controls for the CGG KI mice. All experimental procedures and protocols were approved by the University of California, Davis Institutional Animal Care and Use Committee (IACUC).

DNA was extracted from mouse tails and the number of CGG trinucleotide repeats was quantified by PCR following published protocols (Brouwer et al., 2008a; Hunsaker et al., 2009; Wenzel et al., 2010; Willemse et al., 2003). Genotypes were determined twice, once from tail snips taken at weaning and again from tail snips taken at the time of sacrifice to verify genotype. No discrepancies were observed between the two measured genotypes.

Experimental Apparatus

To evaluate temporal ordering in CGG KI mice as a function of CGG trinucleotide repeat length, the three groups of mice (*i.e.*, wildtype, low and high CGG repeats) were tested on a temporal ordering for visual objects task (Hannesson et al., 2004a; Hannesson et al., 2004b; Hunsaker et al., 2008a). The task was run in a transparent Plexiglas box 26 cm long × 20 cm wide × 16 cm tall. Eight objects in triplicate were used as stimuli for this study. These objects ranged in size from 6 cm diameter × 6 cm tall to 4 cm × 2 cm. All objects and the apparatus were wiped down with 70% ethanol between sessions in order to reduce unwanted odor cues. Behavioral data were scored by two experimenters blind to the genotype of the mouse.

Experimental Protocols

Temporal Ordering for Visual Objects—During session 1, two identical copies of a first object (object 1) were placed at the ends of the box 2.5 cm from the end walls and centered between the long walls (Figure 20). The mouse was

placed in the center of the box facing away from both objects. The mouse was given 5 min to freely explore the objects. After 5 min, the mouse was removed to a small holding cup for 5 min. During this time, the first objects were replaced with two duplicates of a second object (object 2). For session 2, the mouse was again placed in the apparatus and allowed to explore. After 5 min, the mouse was removed to the holding cup for 5 min and the objects were replaced with two duplicates of a third object (object 3). For session 3, the mouse was given 5 min to explore. After 5 min, the mouse was removed into a small cup for 5 min and an unused copy of the first and an unused copy of the third object were placed into the box. The mouse was again placed into the box and allowed to explore the two objects (*e.g.*, object 1 and object 3) during a 5 min test session. Mice typically show increased exploration of the first object compared to the third object, and this was used as an index of memory of the temporal order of the object presentation. A lack of preferential exploration of one object over the other indicates temporal ordering impairments (Hunsaker et al., 2008a). An alternative explanation based on relative memory strengths for the visual objects is possible and is considered in the Discussion.

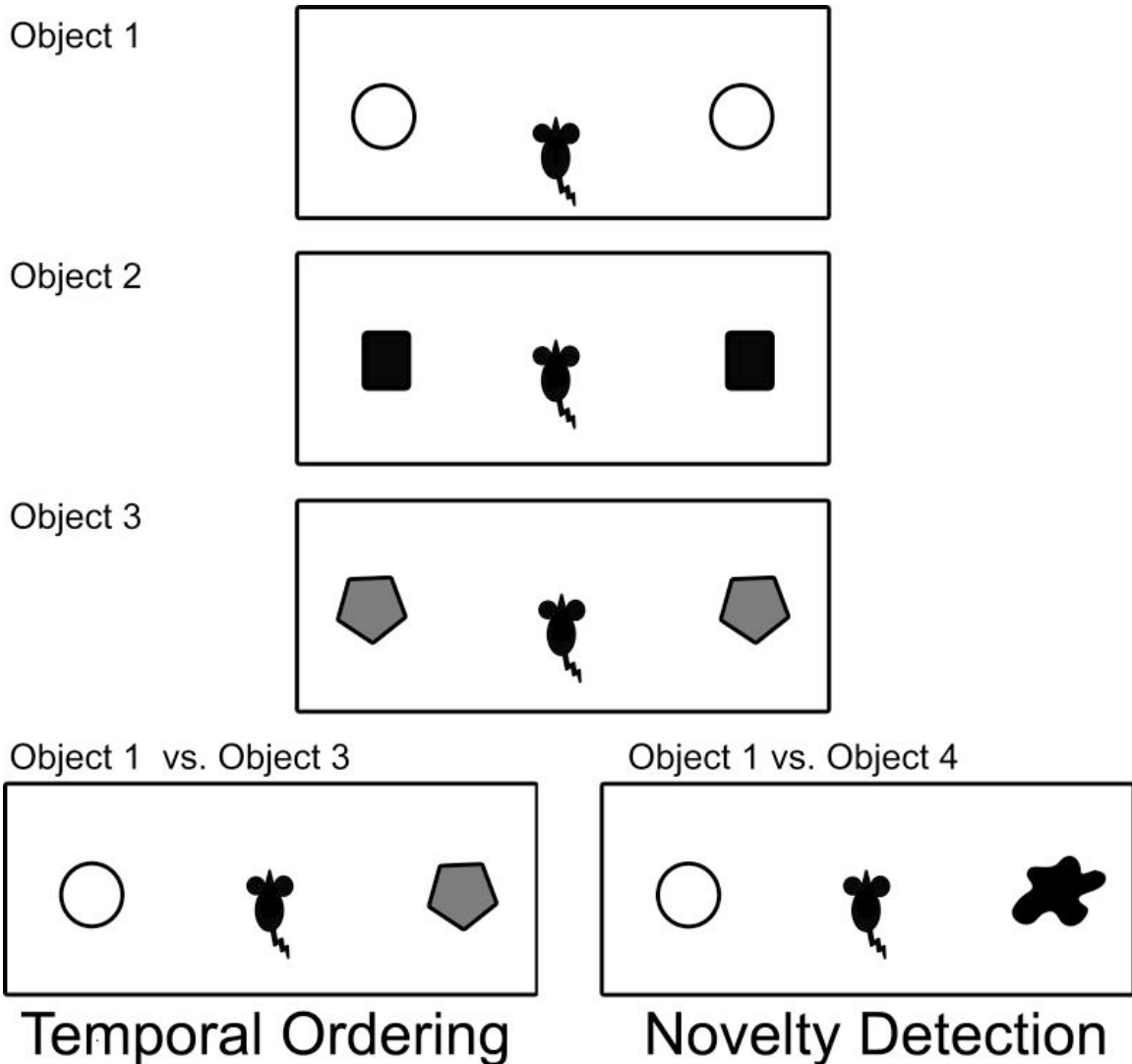


Figure 20. Temporal Ordering for Visual Objects Paradigm. Mice are presented with two copies of object 1 for 5 min followed by a 3 min intersession interval. This is repeated for objects 2 and 3. After the presentation of all three objects, mice are given a preference test wherein object 1 and object 3 are presented to the mouse and they are allowed to explore. Preferential exploration of object 1 over object 3 reflects intact temporal ordering. **Visual Object Novelty Detection Paradigm.** The novelty detection for visual objects paradigm has identical sessions 1-3, but the test session consists of object 1 and a never before seen novel object 4. Preferential exploration of a novel object 4 over object 1 reflects intact memory of object 1 as well as intact novelty detection.

Visual Object Novelty Detection

In addition to reflecting impaired temporal ordering, increased exploration of the first object over the third could also be interpreted as being due to difficulty in remembering the first object prior to the test session. In order to minimize and control for such general memory deficits, a novelty detection of visual objects task was performed. Briefly, on a different day mice received a three sessions during which they were allowed to explore three novel sets of objects (objects 1, 2, 3) similar to the temporal ordering tasks. During the test session, the first object and a novel fourth object (object 4) were presented and the mice were allowed 5 min to explore. Preferential exploration of the novel object 4 over object 1 would indicate that the mouse remembered having previously explored object 1, while equal levels of exploration of the two objects would indicate that forgetting had occurred (Mumby, 2001).

Dependent Measures

For the temporal ordering task, object exploration was defined as active physical contact with the object with the forepaws, whiskers, or nose. With this definition, an mouse standing near an object without interacting with it would not be counted as exploration. Object exploration was recorded in .5 s increments (e.g., >.25s was recorded as .5 s and >.75 s was recorded as 1 s). This conservative definition slightly underestimates the amount of exploration and reduces confounds/experimenter bias if a more liberal criterion for exploration such as if the mouse were within 1 cm of the object was to be employed. These

data were collected during each initial object exploration session as well as during the test session by experimenters blind to the mouse genotype. To control for differences in exploration levels between mice, exploration during the temporal ordering test sessions was converted into a ratio score to constrain the values between -1 and 1. The ratio calculated as follows:

$$\frac{(\text{exploration of object 1} - \text{exploration of object 3})}{(\text{exploration of object 1} + \text{exploration of object 3})}$$

Exploration during the novelty detection test sessions was similarly converted into a ratio score, using exploration of objects 1 and 4 in the calculation.

A ratio value near 1 means that the mouse showed more exploration of the first item presented in the temporal ordering task. A score near -1 suggests the mouse preferentially explored the last object presented. A score near 0 reflects equal exploration of objects indicating a failure to detect the temporal order of visual object presentation. In the novel object test a score near either 1 (*i.e.*, preference for the novel object) or -1 (preference for object 1) would indicate intact memory of object 1, while a score near 0 would suggest that forgetting had occurred. As a measure of general activity levels, locomotor activity was determined by recording the number of times the mouse crossed the midline of the box with all four paws during each session.

Statistical Analysis

Prior to running an analysis of variance (ANOVA), the data were tested for normalcy (Shapiro-Wilk test) and homoscedacity (Browne-Forsythe test).

Locomotor activity was analyzed using a 3 (group; wild-type, low CGG repeat, high CGG repeat) \times 4 (session; session 1, session 2, session 3, test session) repeated measures ANOVA. Any differences in locomotor activity were more fully characterized using Tukey's HSD post hoc paired comparisons test. Object exploration data from each session were analyzed with 3 (group) \times 4 (session) repeated measures ANOVA to verify that mice explored all the objects similarly during the study sessions to verify that unequal exploration would not confound measures of temporal ordering (Mumby, 2001). Furthermore, side preferences during object sessions 1-3 were tested with individual paired t-tests against the null hypothesis of 50% exploration for the object on each side. Exploration data that were converted to ratio values were analyzed by one-way ANOVA. To more fully characterize any differences among groups, Tukey's HSD post hoc paired comparisons test was performed. To verify that locomotor behavior and object exploration during earlier sessions did not contribute to temporal ordering and/or novelty detection measures recorded during the test sessions, analyses of covariance (ANCOVA) were run with both locomotor behavior and object exploration during session 1, both locomotor behavior and object exploration during session 3, as well as locomotor behavior during the test session as covariates. All results were considered significant at $\alpha \leq .05$ and $1-\beta \geq .8$.

RESULTS

Temporal Ordering of Visual Objects

Locomotor Activity

Statistical analysis showed no difference in locomotor activity between groups $F(2,39) = 1.49$, $p = .22$. There was a significant effect of session $F(3,167) = 13.93$, $p < .001$, but the group \times session interaction was not significant, $F(6,167) = .06$, $p = .81$. Individual comparisons between sessions revealed that locomotor activity during session 1 was higher than activity during the other three sessions ($p < .05$), but the other three sessions did not differ (all $p > .1$). The lack of a significant interaction is important, because it suggests that there were no differences in the slope of habituation across groups.

Object Exploration

A two-way repeated measures ANOVA with group (wildtype, low CGG repeat, high CGG repeat) and session (session 1, session 2, session 3, test session) as factors was performed on the object exploration data. The ANOVA showed no difference in exploration between groups, $F(2,39) = 2.64$, $p = .11$, no effect of session, $F(3,167) = 1.51$, $p = .21$, and no interaction, $F(6,167) = 1.86$, $p = .14$. These data suggest that all mice similarly explored objects across sessions 1-3 and did not differ in total object exploration during the test session. Furthermore, no mouse showed side biases during exploration sessions 1-3 (all two-tailed t tests $p > .1$).

Temporal Ordering (Ratio Values)

To determine group differences in temporal ordering, a one-way ANOVA was performed on the ratio values computed from the object exploration during the test session (Figure 21). Since previous research has implicated differences in object exploration during exploration sessions and locomotor activity in exploration measures during preference tests (Mumby, 2001), locomotor activity and object exploration during sessions 1 and 3 were included as covariates in the analysis, as was locomotor activity during the test session. The one way analysis of covariance (ANCOVA) revealed that there were group differences for the ratio score, $F(2,34) = 13.63$, $p < .001$. The locomotor activity or object exploration covariates during sessions 1 or 3 were not statistically significant (all $p > .1$), nor locomotor activity during the test session ($p > .1$). To further characterize the main effect of group, Tukey's HSD post hoc paired comparisons test revealed that the high CGG repeat group showed temporal ordering impairments relative to the wildtype and low CGG repeat groups ($p < .001$, $p < .01$ respectively). The low CGG repeat group showed similar temporal ordering as the wildtype group ($p > .1$).

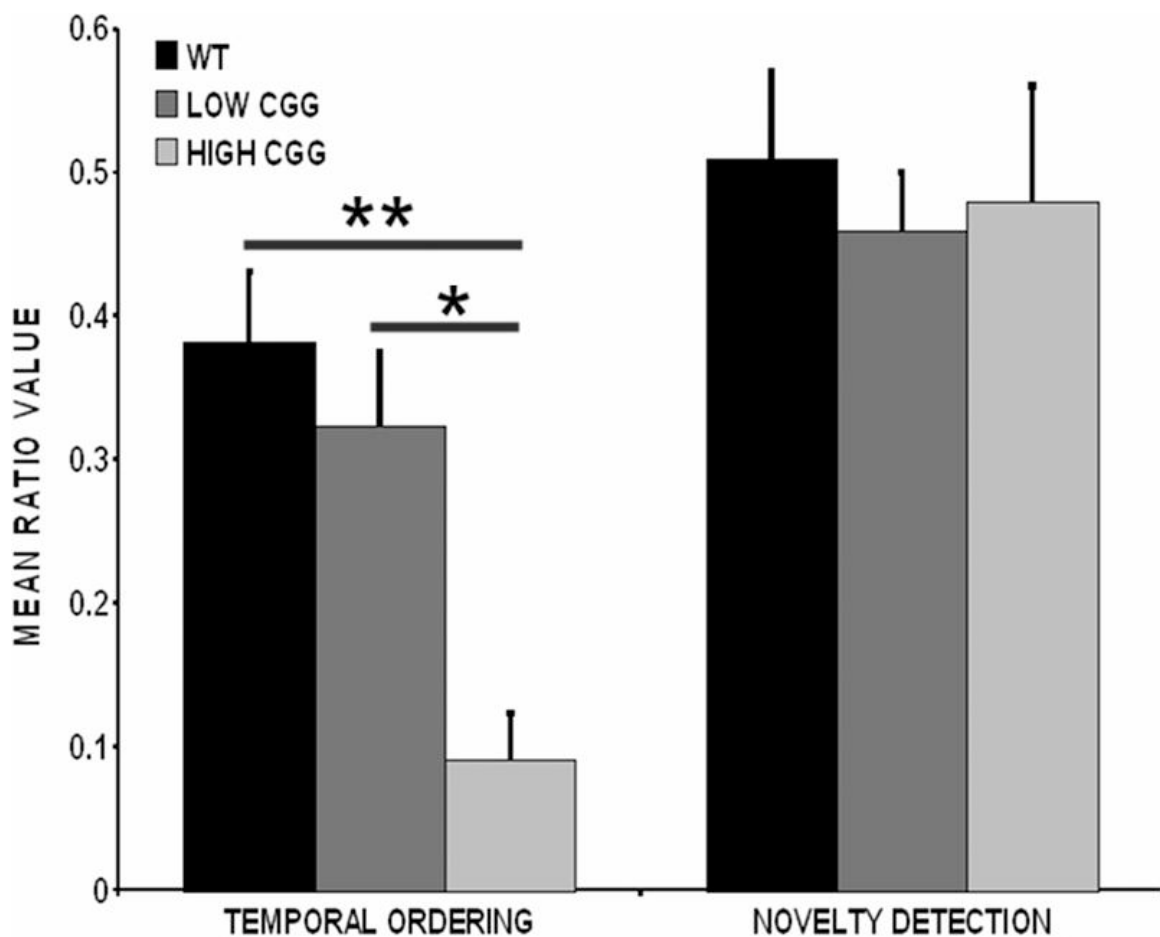


Figure 21. Temporal Ordering and Novelty Detection for Visual Objects in female CGG KI mice. Wildtype mice and CGG KI mice from the low CGG repeat group (70-100 CGG repeats) do not significantly differ, whereas the high CGG repeat group (150-200 CGG repeats) shows a significantly lower ratio value than the other two groups (plotted are means +/- SEM; * p > .01; **p < .001). There were no differences for novel object detection.

Visual Object Novelty Detection

The same analyses performed for the temporal ordering for visual objects were performed for the visual object novelty detection task. The only significant effect was the main effect of session for locomotor behavior, $F(3,167) = 8.56$, $p < .001$. Again, just as in the temporal ordering for visual objects task, locomotor activity during session 1 was higher than the other three sessions ($p < .05$). Session 2, session 3, and the test session did not differ (all $p > .1$). There were no differences in how the different groups reacted to visual object novelty (ANCOVA $p > .2$). These results suggest CGG KI mice reacted similarly to wildtype mice to visual object novelty (Figure 21).

DISCUSSION

The present results show that CGG KI mice with trinucleotide repeat expansions between 150-200 CGG repeats did not preferentially explore the earlier presented object in a sequence of objects, indicating either a deficit in processing sequential relationships among remembered stimuli, or a deficit in judging the relative memory strength among the stimuli (Hopkins, Kesner, & Goldstein, 1995a; Hopkins, Kesner, & Goldstein, 1995b; Kesner, Hopkins, & Fineman, 1994; Manns & Eichenbaum, 2005; Marshuetz, 2005). While the deficit could reflect impaired learning or impaired recall of the order of exposure to the objects, it is not possible to make this distinction based on the present data. This is because the experimental design of the temporal order for visual objects task was not explicitly designed to test for strength of memory for sequences, and thus it is not possible to discriminate between the use of sequential processing per se and judgments of relative memory strengths among stimuli (Agster et al., 2002; Fortin et al., 2002). We assume that the present task could be solved either by explicit sequential processing of the visual object information or by weighting the relative strengths of the memory traces of experienced visual objects (Hunsaker et al., 2008a; Manns & Eichenbaum, 2005). Since the present task was designed to evaluate temporal ordering in CGG KI mice, not to elucidate the component processes underlying the temporal ordering in CGG KI mice, we shall refer to both processes collectively as “temporal ordering” (cf. Hunsaker et al., 2008a; Kesner & Hunsaker, 2010).

Interestingly, CGG KI mice with CGG trinucleotide repeat expansions >150 repeats (High CGG repeat) showed temporal ordering deficits compared to wildtype mice, whereas those with CGG trinucleotide repeat expansions <100 repeats (Low CGG repeat) showed no evidence for temporal ordering deficits and performed similarly to wildtype mice. Both groups of female CGG KI mice were able to identify and selectively explore a novel visual object, suggesting that the temporal ordering deficits reflected impaired temporal processing/judging of relative memory strength and not global memory deficits or altered visual perception (Hauser, Tolentino, Pirogovsky, Weston, & Gilbert, 2009; Mumby, 2001). This is the first report of impaired temporal ordering in the female CGG KI mouse as previous studies have been focused on the spatial domain (Hunsaker et al., 2009; Van Dam et al., 2005).

The temporal ordering or visual objects task presented to CGG KI mice has been described as an episodic-like memory task, as episodic memory relies on the separation of experienced behavioral episodes in time in order to recall specific episodes, either by explicitly recalling time-stamped memories or discriminating the differential strengths of memory traces (Dere, Huston, & De Souza Silva, 2005; Kesner & Hunsaker, 2010; Kesner, Hunsaker, & Ziegler, 2010; Manns & Eichenbaum, 2005). In this way, the temporal ordering deficits in CGG KI mice with >150 CGG trinucleotide repeats supports previous studies that have suggested abnormal hippocampal activity during episodic recall in fragile X premutation carriers (Koldewyn et al., 2008). The present experiment also extends previous work by Van Dam et al. (2005) and Hunsaker et al. (2009) who

were able to demonstrate spatial processing deficits in male CGG KI mice. The Hunsaker et al. (2009) report suggested that male CGG KI mice showed deficits for fine spatial processing that contribute to the memory deficits observed by Van Dam et al. (2005) using the Morris water maze test of spatial learning and memory. A deficit in temporal ordering as revealed in the present study suggests that deficits in the fragile X premutation may involve larger networks of structures that interact in temporal and/or episodic memory (Dobbins, Rice, Wagner, & Schacter, 2003; Hannesson et al., 2004a; Hannesson et al., 2004b; Marshuetz, 2005). Furthermore, the present data in combination with those reported by (Hunsaker et al., 2009) support the hypothesis that a spatiotemporal hypergranularity may underlie some cognitive deficits seen in carriers of the fragile X premutation.

In rat lesion studies, diverse brain regions such as the anterior thalamus (Wolff, Gibb, & Dalrymple-Alford, 2006), rostral infralimbic and prelimbic cortices (referred to as medial prefrontal cortex by Hannesson et al., 2004b; Mitchell & Laiacona, 1998), perirhinal cortex (Hannesson et al., 2004a), and the hippocampus (Hunsaker et al., 2008a; Kesner et al., 2010) have been shown to be involved in temporal ordering. Lesions of any one of these structures lead to qualitatively similar deficits for temporal ordering. In humans, the parietal cortex has further been shown to be involved in processing temporal relationships (Bueti & Walsh, 2009; Marshuetz, 2005). Due to the apparently distributed nature of the processes underlying temporal ordering within the brain (Dobbins et al.,

2003), it is difficult to assign abnormalities within any specific anatomical loci as underlying the observed deficits in temporal ordering in CGG KI mice.

Brain anomalies in fragile X premutation carriers have been reported, and include grey matter volume decreases in the hippocampus (Jäkälä et al., 1997; Moore et al., 2004b), the left thalamus (Moore et al., 2004b; Murphy et al., 1999), the insula, inferior temporal cortex, pre and post central gyrus, and the inferior parietal cortex, as well as white matter abnormalities in the cingulum and frontal-temporal white matter tracts (Moore et al., 2004b; Murphy et al., 1999). All of these areas have been implicated in temporal and/or episodic memory (Dobbins et al., 2003). Unfortunately, studies evaluating similar neuropathological features have not been performed in the CGG KI mouse (Berman & Willemse, 2009; Brouwer et al., 2008a; Brouwer et al., 2008b; Wenzel et al., 2010; Willemse et al., 2003), so it is not yet possible to make comparisons between the human and mouse. Longitudinal studies of large groups of CGG KI mice using noninvasive imaging technologies (*e.g.*, high field MRI) that bypass fixation and histological artifacts are underway to characterize regional volumetric differences in the CGG KI mouse well enough to make a direct comparison between the CGG KI mouse and the fragile X premutation carrier.

Willemse et al. (2003) showed the presence and relative abundance of intranuclear inclusions in male CGG KI mice (on a mixed FVB/N × C57BL/6J background). These inclusions appeared similar to those reported in FXTAS cases. They found that at 48-52 weeks of age, CGG KI mice showed intranuclear inclusions in the thalamus, hypothalamus, cingulate cortex (anterior cingulate),

periamygdaloid cortex, rostral cortex, and in the hippocampus at slightly lower levels—all regions implicated in temporal ordering. Hunsaker et al. (2009) and Wenzel et al. (2010) undertook limited analyses of intranuclear inclusions in male CGG KI mice (on a congenic C57BL/6J background) and found a similar pattern of inclusions, though quantitative analyses were not undertaken. What remains absent from the literature is the distribution and relative abundance of intranuclear inclusions in heterozygous female CGG KI mice. (Wenzel et al., 2010) evaluated a pair of aged female CGG KI mice that would be in the High CGG repeat group in the present study, and found a similar distribution of inclusions as in the male CGG KI mice, but analyses of female mice in the Low CGG repeat group have yet to be undertaken, although these female mice do have intranuclear inclusions (unpublished observations).

Because levels of *Fmr1* mRNA and Fmrp levels have not yet been quantified in female CGG KI mice it is not yet possible to relate these molecular measure to the present temporal order deficits. To date, these measurements have only been carried out in male mice (Brouwer et al., 2008a; Entezam et al., 2007), and unequal X inactivation in females renders any *Fmr1* and Fmrp measurements in males and females impossible to directly compare (*cf.*, Senturk et al., 2009). Studies are currently underway to quantify *Fmr1* and Fmrp levels in female CGG KI mice.

The present data demonstrate impaired temporal ordering in the CGG KI mouse. Furthermore, this study provided insights into potential differences between CGG KI mice with repeat lengths below 100 CGG trinucleotide repeats

and those with repeat lengths above 150 CGG trinucleotide repeats that bear further study using both the murine model as well as with fragile X premutation carriers. These data also suggest some additional parallels in the cognitive deficits seen in fragile X premutation carriers in the CGG KI mouse model of the fragile X premutation, although additional studies will be necessary in order to determine how strong such parallels might be. The present results also point to the need to develop behavioral and neurocognitive tasks for CGG KI mice that more closely model the neurocognitive phenotype of fragile X premutation carriers so that the underlying neural circuitry that is impaired in fragile X premutation carriers (both with and without FXTAS) can be more directly explored. Behavioral tests in CGG KI mice that more closely map onto the neurocognitive deficits reported in fragile X premutation carriers would also make such mice valuable tools for the development and evaluation of treatment for the disorder (Johnson-Glenberg, 2008).

The present data show that female CGG KI mice developed to model the fragile X premutation show deficits in temporal ordering, but only when the repeat expansions approach the upper end of the premutation range. What remains to be studied are the implications of this finding for human fragile X premutation carriers and whether such deficits can be attributed to spatiotemporal hypergranularities as has been suggested (Simon, 2007; Simon, 2008).

Acknowledgments

The authors thank Drs. Tony J. Simon, Ph.D., Susan M. Rivera, Ph.D., and Kyoungmi Kim, Ph.D. for helpful discussions concerning portions of this manuscript, Binh Ta for genotyping, and Andrew Fong for assistance collecting behavioral data. This research was supported by NINDS RL1 NS 062411 and NIDCR UL1 DE19583 and NIH training grant TL1 DA024854.

Section 3: Behavioral Endophenotype

Beyond simply evaluating the behaviors of the CGG KI mouse model of the fragile X premutation, one can take the pattern of behavioral results and correlate performance with the dosage of the genetic mutation, or CGG repeat length in the case of the fragile X premutation. When a collection of behavioral or quantitative traits scale with the dosage of the mutation or another factor, like age, it is referred to as an *endophenotype* (Gottesman & Gould, 2003; Gould & Einat, 2007; Gould & Gottesman, 2006).

Chapter 9 will present the theoretical rationale behind the development of behavioral endophenotypes, with an emphasis on spatiotemporal and proto-numerical processing in the CGG KI mouse model. Also, Chapter 9 will also describe a theory underlying spatial and temporal processing deficits in the premutation and CGG KI mice. Chapter 10 will describe a set of experiments that comprise the first behavioral endophenotype of the CGG KI mouse model of the fragile X premutation by testing spatial and temporal function in turn. Chapter 11 will follow up and extend upon the findings in Chapter 10 by evaluating temporal processing of spatial information. In all cases, the dosage of the mutation will be shown to scale with worsening of performance of the CGG KI mouse on spatial and temporal processing, providing a framework upon which further research hypotheses may be based.

Chapter 9

Comprehensive neurocognitive endophenotyping strategies for mouse models of genetic disorders

Abstract

There is a need for refinement of the current behavioral phenotyping methods for mouse models of genetic disorders. The current approach is to perform a behavioral screen using standardized tasks to define a broad phenotype of the model. This phenotype is then compared to what is known concerning the disorder being modeled. The weakness inherent in this approach is twofold: First, the tasks that make up these standard behavioral screens do not model specific behaviors associated with a given genetic mutation but rather phenotypes affected in various genetic disorders; secondly, these behavioral tasks are insufficiently sensitive to identify subtle phenotypes. An alternate phenotyping strategy is to determine the core behavioral phenotypes of the genetic disorder being studied and develop behavioral tasks to evaluate specific hypotheses concerning the behavioral consequences of the genetic mutation. This approach emphasizes direct comparisons between the mouse and human that facilitate the development of neurobehavioral biomarkers or quantitative outcome measures for studies of genetic disorders across species.

This chapter has been published as:

Hunsaker, M. R. (2012). *Comprehensive Neurocognitive Endophenotyping Strategies for Mouse Models of Genetic Disorders*. *Progress in Neurobiology*. 96, 220-241.

Introduction

With the increasing sophistication of the genetic techniques used to develop mouse models of genetic disorders, it is imperative that the techniques used to elucidate the behavioral phenotype of these models evolve just as rapidly. Although there is a movement toward adopting standardized behavioral phenotyping protocols, to a large part neuroscientists evaluating mouse models of genetic disorders still lack the sensitive behavioral assays that are required to evaluate the core cognitive deficits present in genetic disorders. At present, mouse models, particularly those developed to study neurodevelopmental or other genetic disorders, demonstrate inconsistent phenotypes or lack behavioral phenotypes when tested using the most common behavioral tasks, including the water maze or fear conditioning (Baker et al., 2010; Bohlen, Cameron, Metten, Crabbe, & Wahlsten, 2009; Cannon & Keller, 2006; Kendler & Neale, 2010; Long et al., 2006; Manji, Gottesman, & Gould, 2003; Paylor & Lindsay, 2006; Rustay, Wahlsten, & Crabbe, 2003; Spencer et al., 2011; Weiser, van Os, & Davidson, 2005; Yan, Asafo-Adjei, Arnold, Brown, & Bauchwitz, 2004). Furthermore, it has been shown that minute differences in the protocols used for these common tasks across labs result in altered phenotypes as well (e.g., morris water maze, rotarod, etc.; Crabbe & Wahlsten, 2003; Crabbe, Wahlsten, & Dudek, 1999; Wahlsten et al., 2003; Wahlsten, 1972; Wahlsten, 2001; Wahlsten, Bachmanov, Finn, & Crabbe, 2006; Wahlsten, Metten, & Crabbe, 2003; Wahlsten, Rustay, Metten, & Crabbe, 2003).

Additionally, mouse models often demonstrate phenotypes that are not specifically associated with any genetic disorder in particular, but are more aptly described as shared clinical phenotypes similarly present across a wide array of disorders (e.g., general memory deficits, fear conditioning deficits). The interpretation of such inconclusive findings is often that the mouse model fails to recapitulate the phenotypes observed in patients (*cf.*, Gottesman & Gould, 2003; Gould & Gottesman, 2006; Weiser et al., 2005). I propose that inconsistent behavioral results observed in mouse models do not infer the lack of cognitive impairments, but rather these “null” data reflect the insensitivity of the behavioral tasks commonly employed.

In situations where, based on standardized behavioral tasks, mouse models do not appear to specifically model clinical phenotypes observed in patient populations, one strategy is to evaluate intermediate- or endophenotypes associated specifically with the genetic mutation and subserved by neuroanatomical structures disrupted by the mutation (Figure 22; Karayiorgou, Simon, & Gogos, 2010; Simon, 2008; Simon, 2011). Endophenotypes are collections of quantitative traits hypothesized to represent risk for genetic disorders at more biologically (and empirically) tractable levels than the full clinical phenotype which often contains more profound deficits shared across numerous genetic disorders (Gould & Einat, 2007). This behavioral endophenotyping approach facilitates the identification of behavioral deficits that are specifically associated with both the specific genetic mutation and the pathological features observed in the clinical populations being modeled. When

designed to evaluate specific disease related hypotheses, behavioral endophenotypes model quantitative patterns of behavioral deficits that scale with the size and/or severity of the genetic mutation (Gottesman & Gould, 2003; Gould & Gottesman, 2006; Hasler, Drevets, Gould, Gottesman, & Manji, 2006; Weiser et al., 2005).

The behavioral endophenotyping process deviates from the current method for determining behavioral phenotypes. The present method (using behavioral tasks chosen from collections of common tasks designed without prior consideration of the observed human clinical phenotype) relies on behavioral tasks that are not sufficiently sensitive to characterize gene–brain– behavior interactions (Amann et al., 2010; Gur et al., 2007; Karayiorgou et al., 2010; Simon, 2007; Simon, 2008; Simon, 2011; *cf.*, Figure 22A). In contrast, behavioral endophenotyping emphasizes the use of behavioral paradigms developed to specifically evaluate *a priori* hypotheses concerning the gene–brain–behavior interactions using carefully selected tasks to identify unique phenotypes within each model; and thus are more capable of characterizing the neurocognitive consequences of the specific gene mutations underlying the genetic disorder (Gould & Gottesman, 2006; *cf.*, Figure 22B).

In addition to evaluating behavioral endophenotypes of mouse models, it is critical to evaluate neuroanatomical phenotypes and endophenotypes with equal sophistication. If a genetic mutation disrupts one neural network but spares another, then the identification of analogous neuroanatomical alterations in the

mouse model may guide the selection or development of behavioral tasks to specifically evaluate the function of the affected system.

In this review I will evaluate advances in neurobehavioral endophenotyping, and will propose a clear strategy to efficiently and comprehensively characterize neurobehavioral deficits in mouse models of genetic disorders. This approach uses neurocognitive theory to design and select behavioral tasks that test specific hypotheses concerning the genetic disorder being studied. I propose this novel approach will extend the utility of mouse models by integrating the expertise of clinical neurology and cognitive neuroscience into the mouse behavioral laboratory. Further, I propose that directly emphasizing the reciprocal translation of research between human disease states and the associated mouse models is essential for both groups to mutually inform each other's research to more efficiently generate hypotheses and elucidate treatment strategies.

Behavioral phenotyping strategies

Any discussion concerning the behavioral phenotyping of mouse models of genetic disorders must necessarily begin with a description of what a behavioral phenotype is and what assumptions underly tasks used to evaluate them. In short, behavioral phenotyping quantifies performance of mutant mice across behavioral experiments; and the behavioral performance is related to the clinical population to identify parallels that may exist. The analogy between the phenotype of human genetic disorder and the behavioral phenotype of the mouse model can be expressed as a combination of three factors: face validity, construct (or content) validity, and predictive validity (Crawley, 2004; Guion, 1977).

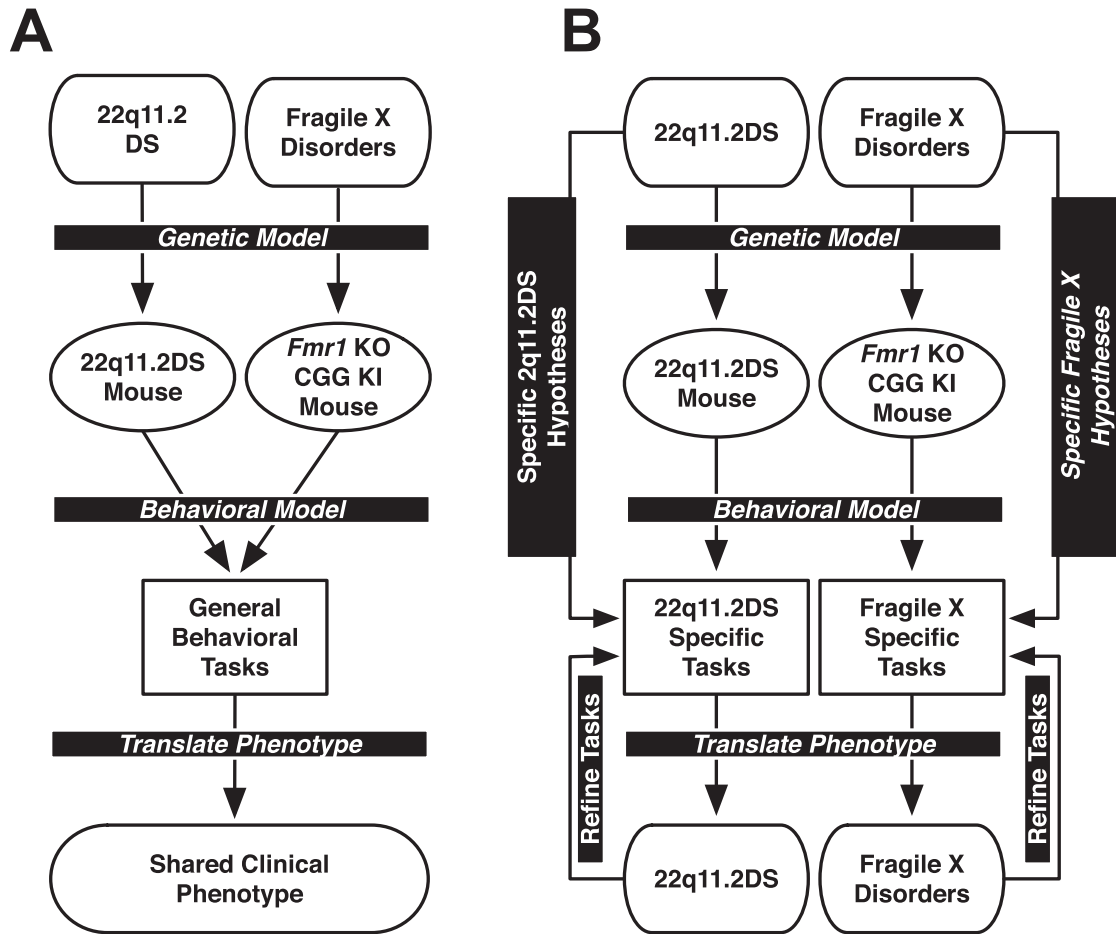


Figure 22. A. Diagram of standard behavioral phenotyping process in which different mouse models are given the same battery of tasks to define a behavioral phenotype. The outcome of the behavioral tasks are compared to the full clinical phenotype of the genetic disorders being modeled. This approach lacks the specificity and selectivity to identify phenotypes unique to a single disorder. **B.** Diagram of behavioral endophenotyping process in which disorder-specific hypotheses are used to develop unique batteries of behavioral tasks that directly translate to the phenotype of the clinical disorder. This approach does not model the general deficits seen across genetic disorders, but rather specifically identifies phenotypes known to be unique to the genetic disorder being modeled. Parallel examples of mice with fragile X-associated disorders and 22q11.2 deletion syndrome are given.

Face validity is the surface similarity between the behavior of the mouse model and the patient on analogous tasks (*i.e.*, does the performance of the mouse and human resemble each other at face value). In other words, if a mouse has to perform a similar response during a task as the patient makes during performance of a similar task, the task shows face validity. Similarly, if the mouse and human behavioral tasks can be intuitively interpreted as being similar, the task shows face validity.

Construct (or content) validity, so far as the development of behavioral experiments is concerned, refers to the similarity between the behavioral or cognitive domains being tested by a given task in the mouse model and human patient. This means that for tests to show construct validity, the tasks must be designed to directly model specific aspects of the genetic disorder and additionally that performance be subserved by similar neural substrates and/or cognitive process across species. More specifically, the tasks need to be developed to explicitly model the human disorder, not solely rely on creative post hoc interpretations of behavioral performance on general behavioral tasks. One necessity of construct validity is that a basic understanding of the disorder being modeled is required, such that the research is into translating a behavioral phenotype across species, not providing the primary elucidation of any phenotype at all in a model.

Predictive validity refers to the utility of a mouse model as a proxy for the patient in studies of disease progression or therapeutic intervention—this can refer to either the endpoints of a behavioral study or the physiology of the model.

Although predictive validity is commonly thought of as a characteristic of phenotyping approaches, it is more accurate to state that predictive validity is the quantified endpoint of an adequately designed behavioral phenotyping experiment—that is, to define some behavior or set of behaviors that serve as valid outcome measures for later studies (Berge, 2011; Greene-Schloesser et al., 2011). In other words, predictive validity is only present when behavioral performance of the model during a given experiment proves useful for inferring or correlating dosage of a given mutation, disease progression, or treatment outcomes in not only the model, but also the clinical population.

Common behavioral approach

Commonly, the selection of behavioral tasks to evaluate a behavioral phenotype emphasizes either a high-throughput battery tasks to determine gross deficits for cognitive function or a limited selection of tasks that roughly assay cognitive processing. There are definite advantages to this approach as it provides a rich array of information from commonly implemented, easily interpreted tasks, but this approach does not explicitly model the behavioral phenotypes of the human disorder being modeled. When a behavioral screening approach becomes essential is for the primary screen for phenotypes in novel mouse disease models. For example, in cases where the mouse model has not been evaluated for gross cognitive function, this process is analogous to initial neuropsychological screens given in the clinic prior to more in depth neurocognitive testing.

Endophenotyping approach

Endophenotypes are collections of quantitative traits hypothesized to represent risk for genetic disorders at more biologically (and empirically) tractable levels than the full clinical phenotype which often contains profound deficits shared across numerous genetic disorders (*e.g.*, memory loss; Gottesman & Gould, 2003; Gould & Einat, 2007; Gould & Gottesman, 2006; Hasler et al., 2006). The overall goal of developing a behavioral test battery to evaluate a behavioral endophenotype is to define a pattern of behavioral strengths and weaknesses in a mouse model comparable with the pattern of deficits observed in clinical populations that can be used as a behavioral biomarker to predict symptom onset or progression, or serve as an outcome measure in studies of intervention or treatment. Optimally, endophenotypes are designed such that observed behavioral deficits will scale with the dosage or severity of the genetic mutation, thus allowing the researcher to more directly evaluate specific roles of the mutation in cognitive deficits associated with the genetic disease (Gould & Gottesman, 2006; Simon, 2007; Simon, 2008; Simon, 2011). Importantly, endophenotypes are made up from a spectrum of tasks covering a broad pattern of deficits and strengths observed in the clinical population, which assists in differentiating similar models.

The weakness in the endophenotyping approach is twofold: when the mouse model has not been previously characterized, and when there may be gross cognitive deficits that overshadow the proposed endophenotype. In both cases, if one would only use the endophenotyping approach, then the true nature

of the underlying phenotype would be overlooked. As a concrete example, if one hopes to study schizophrenia in a mouse model and begins behavioral studies using specific schizophrenia related tasks based on clinical research (e.g., gamma oscillation impairments, working memory impairments, etc.; Carter & Barch, 2007) and fails to find the hypothesized deficits in the mouse model, the mouse line may be prematurely abandoned. However, for such a model a more general screening approach would potentially uncover phenotypes resembling mood disorders that could potentially be investigated further to uncover aspects of known schizophrenia phenotypes. An endophenotyping approach allows researchers to test hypotheses from a number of disorders showing partially overlapping phenotypes to hone in on unique patterns of quantifiable behavioral deficits shared among the clinical population and the mouse model.

In recent years, transgenic mice with targeted deletions or over expression of genes have become important tools for evaluating cognitive processes. These experiments provide behavioral scientists with an invaluable tool to unravel the molecular mechanisms through which genetic and neural networks may affect brain function (Chen & Tonegawa, 1997; Nakazawa et al., 2003; Nakazawa, McHugh, Wilson, & Tonegawa, 2004). In addition to advancing the genetic tools being used to dissect cognitive processes in mice, this research has led to an acceleration in the development of sophisticated behavioral tasks that have been shown to be exquisitely sensitive for evaluating dysfunction to known neural networks and behavioral processes. This means that performance on the behavioral tasks designed for these studies can be used to elucidate relatively

subtle consequences of disruptions to specific anatomical or genetic loci in mouse disease models. For the most part, the tasks developed to evaluate these hypotheses have not been extended to the study of human genetic disorders.

Comparison of the common and endophenotyping approaches

To compare the more common phenotyping approach with the endophenotyping approach, the tasks and underlying hypotheses from each approach will be compared and contrasted based on the cognitive domains being evaluated. In no cases are the tasks described under the common or endophenotyping approaches sections intended to be exhaustive, but rather represent a representative sampling of tasks chosen to demonstrate the level of domain specificity that can be achieved in modeling behavioral endophenotypes. Table 9 contains behavioral tasks organized by the component attribute or process being tested and by phenotyping approach, as well as a collection of references that emphasize the methods for each behavioral protocol.

Memory

Common approach. In the memory domain, the most common behavioral paradigms are the Morris water maze, the water radial arm maze, the Barnes maze, and active/passive avoidance of foot shock. What these tasks have in common is that they are spatial memory tasks subserved by a wide number of different neural networks. Furthermore, it is difficult to identify common memory tasks in humans that are directly modeled by these murine tasks, though some

research has been done using virtual navigation in humans, but rarely in the context of genetic disease (*cf.*, Goodrich-Hunsaker, Livingstone, Skelton, & Hopkins, 2010; MacLeod et al., 2010).

One problematical factor shared among these tasks is the use of negative reinforcement motivating task performance. For the water mazes, the mouse is placed in a pool of cool (usually 24– 28 °C) water and is required to swim to locate a platform to escape the water—something that mice do not do as well as rats (*cf.*, Whishaw & Tomie, 1996). In the Barnes maze, the mouse is placed on a round tabletop with a number of equally-spaced holes along the periphery of the maze and is required to find a hidden goal box placed under one of the holes to escape a bright light and/ or loud noise aversive stimulus (Paylor, Zhao, Libbey, Westphal, & Crawley, 2001). For the active or passive avoidance tasks, the mouse is required to avoid receiving a foot shock by either actively exiting or passively not entering into a predefined area of space (Ellis & Kesner, 1983). This negative reinforcement approach is particularly troublesome for comparison with clinical populations, which do not regularly receive negative reinforcement such as cold or applied electrical stimuli to motivate task performance. Non-aversive versions of a number of the water-based tasks are available, but are not common in mouse behavioral phenotyping screens (*e.g.*, dry land water maze and radial arm maze; Corwin, Fussinger, Meyer, King, & Reep, 1994; Llano Lopez, Hauser, Feldon, Gargiulo, & Yee, 2010).

Endophenotyping approach. For memory processes, an endophenotyping approach tries to get to the core cognitive deficits underlying memory, not just memory itself. As such, memory is separated into a number of component attributes that can be tested individually and more directly evaluate the cognitive processes commonly evaluated in clinical populations. The primary benefit over the more common phenotyping approach is that the tasks presented below were developed to evaluate specific attributes of memory processing and are designed to evaluate the differential roles for cognitive domains in task performance. Furthermore, these tasks were developed to not only evaluate cognitive domains affected in human disease, but also were designed to mimic the behavioral tasks used in human clinical populations as much as possible.

Spatial processing.

Coordinate spatial relationships. For evaluating the spatial attributes of memory, it is important to determine which of the core spatial processes are disrupted by the mutation. One type of spatial processing is coordinate processing, also called metric processing (Gallistel, 1989; Gallistel, 1990a). This type of processing refers to the role of the brain in determining the locations of objects within space with mathematical precision (*i.e.*, precise angles and distances among objects in space, as well as how the individual fits into that “cognitive map”). There are a number of tasks that probe this type of spatial processing, particularly those evaluating spatial pattern separation (Bartko, Vendrell, Saksida, & Bussey, 2011; Hunsaker et al., 2009), a process proposed to

be disrupted in a number of genetic disorders (*cf.*, Hanson & Madison, 2010). These tasks evaluate the ability of mice to specifically determine spatial relationships among stimuli in ways similar to studies in humans (*cf.*, Goodrich-Hunsaker et al., 2011a; Kessels, Rijken, Joosten-Weyn Banningh, Van, & Olde Rikkert, 2010; Kosslyn et al., 1989; Kosslyn, Chabris, Marssolek, & Koenig, 1992).

Categorical spatial relationships. Another type of spatial processing is categorical or topological processing, which evaluates the relationships among stimuli in a somewhat less precise manner (connectedness, enclosure, etc.). This type of processing is best conceptualized as using prepositions to describe the relationships among objects in the environment (*e.g.*, behind, next to, etc.), but lacking the mathematical precision required by coordinate processing. Tasks evaluating these processes are available in the literature, but are not widely utilized in mouse behavioral studies (Goodrich-Hunsaker et al., 2008a; *cf.*, Kessels et al., 2010; Robertson, Triesman, Friedman-Hill, & Groabowecky, 1997).

Attribute tested	Behavioral phenotyping tasks	Behavioral endophenotyping tasks	References
Memory	Water Maze Radial Arm Maze Barnes Maze Active/Passive Avoidance Contextual Fear Conditioning		Babovic et al., 2008; Bainbridge et al., 2008; Corwin et al., 1994; Ellis and Kesner, 1983; Gleason et al., 1999; Holmes et al., 2002; Llano Lopez et al., 2010; Paylor et al., 2001; Sigurdsson et al., 2010; Whishaw and Tomie, 1996
Spatial processing		Categorical (Metric) Processing Coordinate (Topological) Processing Touchscreen Pattern Separation Delay Match to Place with Variable Interference Delay Match to Place with Variable Cues	Bartko et al., 2011; Clelland et al., 2009; Creer et al., 2010; Goodrich-Hunsaker et al., 2005, 2008b; Kesner et al., 2001; Kirwan et al., 2005; McTighe et al., 2009; Talpos et al., 2010
Temporal processing		Trace Fear Conditioning Temporal Ordering of Stimuli Sequence Learning Tasks Sequence Completion Tasks Duration Discrimination	Balci et al., 2008; Balsam and Gallistel, 2009; Chiba et al., 2002; Cordes and Gallistel, 2008; Cordes et al., 2007a,b; Devito and Eichenbaum, 2011; DeVito et al., 2009; Eichenbaum and Fortin, 2009; Fortin et al., 2002; Gallistel et al., 2010; Hunsaker et al., 2010; Kesner and Hunsaker, 2010; Jackson et al., 1998; Bannerman, 2009; Bussey et al., 2011; Gilbert and Kesner, 2003; Kesner et al., 2008; Poirier et al., 2010
Associative memory		Biconditional Discrimination Cued-Recall Task for Trial Unique Associations	
Affect	Classical Fear Conditioning Open Field Elevated Plus Maze Porsolt Test		Cain and LeDoux, 2007; Crawley, 2004, 2007; Debiec et al., 2010; Kopec et al., 2007; Porsolt et al., 1977; Wahlsten et al., 2006
Emotional valence		Reward Contrast with Variable Reward Value	Gilbert and Kesner, 2002; Gilbert et al., 2003
Anhedonia		Anticipatory Contrast Task Species Relevant Sexual Behaviors	Carola et al., 2008; Kesner and Gilbert, 2007; Maasberg et al., 2011; Malkesman et al., 2009
Approach-avoidance		Hyponeophagia Defensive Burial	Bannerman et al., 2002, 2003; Deacon, 2011; Meert and Colpaert, 1986
Fear processing		Defensive Test Battery Classical, Contextual, Trace Fear Conditioning	Blanchard et al., 1993; Ferris et al., 2008; Luisa-Scattoni et al., 2011; Velez et al., 2010
Motor	Rotarod	Skilled Forelimb Reaching Capellini Handling Task Seed Shelling Tasks Parallel Beam or Ladder Walking Tasks	Ryan et al., 2008; Zeyda et al., 2001
Visuomotor			Allred et al., 2008; Ballermann et al., 2000, 2001; Bury and Jones, 2002; Fan et al., 2006; Kamens and Crabbe, 2007; Kamens et al., 2005; Tennant et al., 2010; Tennant and Jones, 2009; Whishaw and Coles, 1996; Whishaw et al., 2008
Motor learning		Acquisition of Skilled Reaching Acquisition of Rotarod (initial training) Working Memory for Motor Movements	Diep et al., 2011; Hunsaker et al., 2011; Kesner and Gilbert, 2006
Sensory	Prepulse Inhibition Acoustic Startle	Prepulse Inhibition Acoustic Startle	Crawley, 2004, 2007; Dulawa and Geyer, 1996; Noble et al., 1964
Social	Hot Plate Analgesia Three Chamber Social Novelty	Psychonomic Threshold Social Dyadic Behavior Resident Intruder Tests Social Transmission of Food Preference Social Dominance	Defensor et al., 2011; Moretti et al., 2005; Nadler et al., 2004; Pearson et al., 2010; Pobbe et al., 2011; Spencer et al., 2008; Uchida et al., 2005; Yang et al., 2011
Executive function	Operant Conditioning Holeboard Exploration Reversal Learning		Crawley, 2007; Spencer et al., 2011; Thomas et al., 2009
Cognitive control		Contextually Cued Biconditional Discrimination Serial Reversal Learning Stop Signal task Probabilistic (80/20) Reversal learning 5 Choice Serial Reaction Time task Covert Attention Tasks	Amodeo et al., 2011; Casten et al., 2011; Endo et al., 2011; Garner et al., 2006; Haddon et al., 2008; Haddon and Killcross, 2005, 2006, 2007; Kesner and Ragazzo, 1998
Attention			Loos et al., 2010; Ward and Brown, 1996, 1997; Ward et al., 1998

Table 9. Summary of behavioral tasks commonly used in behavioral phenotyping strategies organized by general domain. Also summarized are behavioral tasks proposed to be useful for behavioral endophenotyping organized by component attributes. Also included are references for each task that emphasize the methods for each paradigm.

Temporal processing. Another critical aspect of memory is knowledge of the temporal relationships among stimuli. To evaluate this attribute of memory, simple sequence learning tasks can be used (Devito & Eichenbaum, 2011; Kesner & Hunsaker, 2010), tasks evaluating recency judgments (Eichenbaum & Fortin, 2009), or tasks evaluating discrimination of duration information (Chiba, Kesner, & Gibson, 1997; Jackson, Kesner, & Amann, 1998). Processes such as these have been shown to be impaired in a number of genetic disorders but has not been widely applied in research into mouse models of these disorders (Allman, Pelpfrey, & Meck, 2011; Hampstead et al., 2010; Johnson & Kesner, 1997; Pirogovsky et al., 2009; Schwartz, Deutsch, Cohen, Warden, & Deutsch, 1991; Shipley, Deary, Tan, Christie, & Starr, 2002; Vriezen & Moscovitch, 1990).

Associative learning. Associative memory is disrupted in a number of disorders such as Alzheimer's disease and Parkinson's disease (Dierckx et al., 2009; Saka & Elibol, 2009; Vriezen & Moscovitch, 1990), so it is critical to specifically evaluate associative learning in mice. Simple stimulus–stimulus or stimulus–spatial location tasks are commonly used for these types of experiments (Bannerman, 2009; Bussey et al., 2012). Cued recall tasks that serve as useful analogs for list learning tasks used in clinical testing have also been developed for rats, but are not yet prevalent in the mouse literature (Kesner, Hunsaker, & Warthen, 2008).

Affect processing.

Common approach. To evaluate affective or emotional processing in mice, typically variations on conditioned fear are used. Classical fear conditioning pairs an auditory cue and/or a context with a foot shock, and the ability of the mouse to learn or remember this conditioned fear (as measured by freezing behaviors) is used to index emotional learning (Cain & LeDoux, 2007). Again, it is not common in clinical research to perform tasks requiring aversive reactions to physical discomfort similar to these fear conditioning tasks. Furthermore, the response measured in mice (*i.e.*, freezing) appears to be more related to panic states than fearful or phobia-related states and may not be effective measures for emotion-related processing (*cf.*, Gray & McNaughton, 2003).

To evaluate anxiety processes, the elevated plus or elevated zero mazes are typically used, which require the mouse to explore open or enclosed areas, using the tendency of the mouse to explore the environment while preferring enclosed over exposed spaces to serve as a proxy for anxiety (Moy et al., 2007). Alternately, a mouse can be placed in a large box and the relative time the mouse spends near the edges/corners of the box compared to time spent in the center – more exposed – region of the box is used as a proxy measure of anxiety (Crawley, 2004).

To evaluate depression, the most widely used test is the Porsolt test, a test of helplessness behavior seen when mice give up after placed in an unescapable bucket of cool water (Porsolt, Le Pichon, & Jalfre, 1977). What these affect tasks share in common is that they emphasize negative affect by quantifying punishment or the valuation of negative valence, without regard to

positive affect or reward processing. Additionally, the direct comparison between these tasks evaluating affect and measures used in clinical populations are not easily reconcilable (Gray & McNaughton, 2003; McNaughton & Gray, 2000).

Endophenotyping. To evaluate the processing of affect, one has to dissect out different types of affective or emotional processing into attributes, as fear and anxiety are only components of affect, not affect in themselves (*cf.*, Gray & McNaughton, 1996). Furthermore, it is useful to evaluate both positive and negative affect in mouse models, as well as more directly modeling the paradigms used to evaluate anxiety in clinical populations, an approach more in line with studies into phobia, anxiety, and depressive states.

Reward valence. To evaluate the ability of mice to properly process affect information, one relatively simple task that can be used is to measure the conditioned flavor preference for different flavors of liquid containing different concentrations of sucrose reward (Gilbert & Kesner, 2002). One can get at the nature or severity of any impairments by making the sweetness levels of each of the conditioning flavors increasingly similar and looking for differences in discrimination functions among groups (*e.g.*, 16% vs. 2% sucrose is easier to discriminate than 16% sucrose vs. 8% sucrose; *cf.*, Gilbert, Campbell, & Kesner, 2003).

Anhedonia. To evaluate anhedonia or depression-related symptoms, one can use an anticipatory contrast task, which evaluates the tendency of animals to reduce consumption of a given reward if there will be a greater reward in the near future –a direct measure of cognitive processing the differences among rewards (Kesner & Gilbert, 2007). Anhedonia results in mice acting as if both rewards were equivalent, despite being able to discriminate the relative sweetness levels. A simple version of this task is to give mice free access to 2% sucrose for 15 min and then follow that 30 min later with 32% sucrose for 15 min every day for a seven days and determine if the mice consume less and less of the 2% sucrose each subsequent day in anticipation of the 32% sucrose presented later (Maasberg, Shelley, Gracian, & Gilbert, 2011).

The presence or lack of species specific sexual behavior can also be used to quantify anhedonia or anhedonic-like processes (e.g., latency and duration of sniffing female scents for male mice or mating behaviors; Carola, Scalera, Brunamonti, Gross, & D'Amato, 2008; Malkesman et al., 2010).

Approach-avoidance conflict. To better dissect processes underlying anxiety, Gray and McNaughton have conceptualized anxiety as a unique form of approach-avoidance conflict (Gray & McNaughton, 1996; Gray & McNaughton, 2003; McNaughton & Gray, 2000). To evaluate approach-avoidance processes, one can quantify the hesitancy of hungry mice to eat in a novel environment or situation (*i.e.*, hyponeophagia). These protocols have been parameterized in rats to include tests of hyponeophagia in environments across differing levels of

perceived insecurity (Bannerman et al., 2002; Bannerman et al., 2003), and adapted for mice (Deacon, 2011). Various shock probe burial tasks are also classic tests of this model as a test of a mouse's desire to approach the probe to bury it in bedding despite simultaneous fear of the shock (Meert & Colpaert, 1986). The probe burial task has fallen out of favor in recent years, appearing only sporadically in the literature (Chee & Menard, 2011; Saldivar-Gonzalez et al., 2003; Shah & Treit, 2003; Sikiric et al., 2001; Treit & Fundytus, 1988). Conceptually similar approach-avoidance conflict paradigms have been used applied in research of human genetic disease (Drago, Foster, Skidmore, Trifiletti, & Heilman, 2008).

Fear-related processes. To dissect fear more precisely than by using classical conditioning, one can use a collection of tasks evaluating defensive behavior (Blanchard, Griebel, & Blanchard, 2003a; Blanchard, Griebel, & Blanchard, 2003b; Ribeiro-Barbosa, Canteras, Cezario, Blanchard, & Blanchard, 2005; Yang et al., 2004), wherein mice are exposed to different levels of predator stress or aggressive conspecifics and are monitored for their responses using standardized criteria (Blanchard, Sakai, McEwen, Weiss, & Blanchard, 1993). This type of task as a measure of fear is more relevant to human fearful/phobia states; commonly expressed as a heightened vigilance and concern over one's safety and less as a panic state induced by the inescapability present in classical fear conditioning paradigms (Gray & McNaughton, 2003).

Motor function.

Common approach. To evaluate motor function and coordination in mice, the accelerating rotarod is the most common apparatus. In this task mice are placed on a slowly accelerating rod and are required to not fall off. To test motor learning the rotational speed of the rod is increased until the mouse falls (Zeyda, Diehl, Paylor, Brennan, & Hochgeschwender, 2001). For the most part, any data during the acquisition and pretraining are not collected or remain unreported, and as such potential differences among groups of mice may be overcome during this training phase prior to testing. As such, any resulting “lack” of a motor phenotype in mice does not necessarily mean there will not be motor phenotypes uncovered using more sensitive tests or analyses of the acquisition phase.

Endophenotyping. To get at motor function and motor learning, one has to go beyond the rotarod, as it has been shown that mice and rats can develop strategies to perform supranoitionally on the rotarod, which may over shadow motor impairments (*cf.*, Wahlsten et al., 2003). Importantly, a number of cognitive processes underlie potential motor deficits, so it bears dissecting motor function into motor attributes and testing each in turn and not lumping all motor deficits into a single category.

Visuomotor processing. To evaluate the ability of mice to perform voluntary, skilled movements, one can use skilled forelimb reaching or performance tasks. Such tasks include skilled forelimb reaching for pellet tasks, tasks requiring

shelling of seeds, and capellini handling tasks that require skillful limb and digit usage (Allred et al., 2008; Ballermann, Metz, McKenna, Klassen, & Whishaw, 2001; Whishaw & Coles, 1996). Furthermore, skilled walking can be evaluated using horizontal ladder walking tasks adapted to quantify stroke models (Farr et al., 2006) or parallel beam tasks originally designed to evaluate ethanol-induced ataxia (Kamens & Crabbe, 2007; Kamens, Phillips, Holstein, & Crabbe, 2005).

Motor learning. To evaluate motor learning, mice can be tested using modified versions of the tasks mentioned above, but quantifying the learning curve during acquisition or training or by requiring the mouse to learn and perform increasingly skilled movements for reward (Diep et al., 2012; Hunsaker et al., 2011c). Additionally, mice can be tested for memory for motor movements (Kesner & Gilbert, 2006).

Sensory gating.

Common approach. To evaluate sensory gating phenomena in mice, a prepulse inhibition (PPI) protocol is commonly used, a modification of the acoustic startle paradigm (*cf.*, Dulawa & Geyer, 1996). In this task, the natural startle response to a sudden, loud auditory cue is reduced by presenting a slightly softer priming cue. Any attenuated responsively on the part of the animal is taken as a measure of PPI impairment. Intriguingly, sensory gating is a case where the same task used for the common and endophenotyping is the same, PPI.

Endophenotyping. Prior to evaluating sensory gating phenomena in mice, it is important for mice to be evaluated for the ability to discriminate stimuli. To evaluate these sensory and perceptual attributes, mice can be tested using simple psychonomic threshold tasks based on protocols used for discrimination tasks (Noble, Baker, & Jones, 1964). Such measures can be evaluated across all sensory domains. For the endophenotyping approach, the nature of PPI impairment is evaluated and directly compared to the clinical disorder to identify parallels.

Social behavior.

Common approach. To evaluate social behavior or social preferences, the three chamber test is used. In this task, mice are placed in a box with three chambers. In one chamber there is a mouse in a small cage, in a second chamber, there is a small cage without a mouse, and an empty chamber separating the two (Nadler et al., 2004). The preference for a study mouse to spend time in the chamber with the caged mouse is taken as a measure of social behavior. A modification can be used to evaluate social novelty preferences, which involves adding a novel mouse to the previously empty chamber and the preference of the study mouse to explore this novel caged mouse compared to the familiar mouse is used as a dependent measure. The construct validity of this procedure has been recently brought into question as it appears equally likely that mice respond to spatial novelty as much as to social novelty in this task (*i.e.*, a familiar mouse in a previously unoccupied spatial location is just as, if not more, interesting than a

new mouse in a previously occupied location), which is a significant confound that needs to be controlled to clearly interpret the results of this task.

Endophenotyping. To evaluate social behaviors, one can use tasks evaluating social dyadic behavior (Defensor et al., 2011). One can record the behavior of a cage or cages of mice overnight and evaluate the behavior using manual, semiautomated, or automated methods (Pobbe et al., 2011). A modification of this task places two mice in the same box but separated by a grid barrier and quantifies both the time and nature of reciprocal interactions (Moretti, Bouwknecht, Teague, Paylor, & Zoghbi, 2005; Spencer, Graham, Yuva-Paylor, Nelson, & Paylor, 2008). Additionally, to evaluate the role of social hierarchy in behavioral testing, one can place a mouse in a cage or tube and after a set amount of time introduce a second mouse as an intruder and quantify the level of aggressive behaviors associated with social dominance (Uchida et al., 2005). These tasks emphasize the ethological behavior of the mice more so than the three chambered task.

Executive function.

Common approach. Although not completely ignored in the common screening approach to phenotyping mice, executive function is not included in most batteries of behavioral tasks, mostly due to the fairly extensive training (and thus time) required to assay executive function in mice. For the most part, acquisition of simple operant conditioning is used as the measure of executive function in

the screening approach. Although this type of task does assess executive function, simple operant conditioning does not directly test specific aspects of executive function shown to be disrupted in human clinical populations. Recently, creative, but strained, reinterpretations of tasks used in phenotyping screens have come into the literature, including holeboard exploration (Crawley, 2007; Spencer et al., 2011) and marble burying, but these tasks have a number of contradictory interpretations in the literature (Thomas et al., 2009).

Endophenotyping approach. An often ignored aspect of mouse models genetic disorders are the profound effects of genetic mutation on executive function, particularly for cognitive control and attentional deficits (*cf.*, Haddon & Killcross, 2005; Simon, 2007; Simon, 2008; Simon, 2011). This is critical as a number of disorders have executive dysfunction as a core component of the diagnostic tests.

Cognitive control. To evaluate cognitive control in mice, one may use a cued context biconditional discrimination task that has face and construct validity with the Stroop task (Haddon & Killcross, 2005), or else a serial reversal learning task that requires the mouse to explicitly reverse established rules or else to learn to change rules based on changes to presented stimulus sets (Endo et al., 2011). Tasks evaluating intra and extra-dimensional attentional set shifting have also been developed in mice (Casten, Gray, & Burwell, 2011; Garner, Thogerson, Wurbel, Murray, & Mench, 2006). In all cases, preservative behavior can be

explicitly quantified, as well as the ability of mice to learn, apply, and reverse rules (Kesner & Ragazzino, 1998). Additionally, probabilistic reversal learning tasks have been used to model tasks used in humans that rely on an 80/20 reward contingency to guide reversing behavior (Amodeo, Jones, Sweeney, & Ragazzino, 2012). This modification was critical as it has been demonstrated that individuals with genetic disorders have a greater difficulty reversing learned rules under 80/20 reward contingencies than 100% reward contingencies. Stop signal tasks can also be used to evaluate the ability of mice to inhibit either prepotent or highly trained responses in a manner both methodologically and cognitively similar to procedures used in clinical populations to evaluate cognitive control (Eagle, Tufft, Goodchild, & Robbins, 2007).

Attentional processes. In mice, it has been difficult to explicitly assess attention as mice do not stay “on task” as well as human subjects and are notoriously slow to learn reward contingency rules, but a number of sufficiently simple paradigms have emerged. The 3 or 5 choice serial reaction time tasks and simple reaction time tasks can be used to evaluate sustained attentional processes in mice (Loos et al., 2010). Furthermore, exogenous and endogenous cueing tasks have been developed for mice that probe covert attentional processes in mice (Ward & Brown, 1996) in a manner similar to the spatial cueing task introduced by Posner (Posner, Walker, Friedrich, & Rafal, 1987) that is an invaluable tool used to evaluate attentional deficits across wide arrays of clinical disorders.

Evaluating neuropathological features

Neuroanatomical phenotypes

It is critical to identify and characterize any pathologic neuroanatomical features that result from the genetic mutation as precisely as possible. In clinical populations, such neuropathology are principally characterized through magnetic resonance imaging (MRI); optimally followed by thorough post mortem histopathological analysis. In mouse models, such neuroanatomic sequelae are characterized primarily through gross histological studies.

Unfortunately, subtle pathological anatomical features are often very easily overshadowed by histological artifacts and differences in techniques that render comparisons among (and within) labs difficult (*cf.*, Simmons & Swanson, 2009; Swanson & Orr, 2007 for a consideration of these challenges; *cf.*, Wenzel et al., 2010; Willemse et al., 2003 for a specific example of seemingly contradictory findings in the same mouse model explained by subtle methodological differences). Recently, *in vivo* MRI analyses of brain in mouse models of genetic disorders have been developed with variable levels of success (Ellegood, Pacey, Hampson, Lerch, & Henkelman, 2010; Kooy et al., 1999; Kovacevic et al., 2005). Increasingly sophisticated analysis techniques and imaging technologies are necessary to allow true cross-species comparison of neuropathological features *in vivo*.

Neuroanatomical endophenotypes

Neurological phenotypes that appear at more of a functional, rather than grossly anatomic, level have emerged in clinical research. Much of this work has been advanced by improvements in diffusion weighted imaging quantifying white matter in the brain as well as functional MRI (fMRI) that can evaluate regional brain activity in response to cognitive or behavioral tasks (Adamczak, Farr, Seehafer, Kalthoff, & Hoehn, 2010; Rivera, Menon, White, Glaser, & Reiss, 2002). Abnormal patterns of brain activation during a task (*i.e.*, reduced or enhanced task-related signal relative a comparison group) may also inform further investigations into microscopic anatomical changes or altered connectivity that remain undetected using traditional MRI analyses focusing on gross brain structure.

Patterns of brain responses triggered by stimuli called event related potentials (ERPs) can be measured on the scalp electroencephalogram in both humans and mice and serve as a neurophysiological outcome measure for abnormal information processing (Choi, Koch, Poppendieck, Lee, & Shin, 2010; He, Lian, Spencer, Dien, & Donchin, 2001; Olichney et al., 2010). Direct *in vivo* neurophysiological recording has become more readily accessible in mice to evaluate the firing patterns of cells across brain regions during task performance (*cf.*, Sigurdsson, Stark, Karayiorgou, Gogos, & Gordon, 2010). Also, evaluating task related gene transcription of so called immediate early genes (IEGs) has also proven a useful tool for evaluating the role of different brain regions for cognitive processing during behavioral tasks in mouse models of genetic disorders (Drew et al., 2011b; Krueger, Osterweil, Chen, Tye, & Bear, 2011).

Proposed comprehensive behavioral phenotyping approaches

Currently implemented behavioral screens have the benefit of clear face validity as the implications of behavioral deficits on a task or collection of tasks are intuitively applicable in the context of the clinical phenotype, but often these tasks lack construct validity (cf., Chadman, Yang, & Crawley, 2009; Crawley, 1985; Humby, Wilkinson, & Dawson, 2005; McFarlane et al., 2008; Moy et al., 2008a; Moy et al., 2008b; Nadler et al., 2006; Ricceri, Moles, & Crawley, 2007; Ryan, Young, Crawley, Bodfish, & Moy, 2010; Silverman et al., 2010; Silverman, Yang, Lord, & Crawley, 2010; Yang, Silverman, & Crawley, 2011). The behavioral endophenotyping process I am proposing emphasizes clearly defined construct validity across paradigms designed to test specific disease or mutation-related hypotheses.

An optimal, comprehensive behavioral phenotyping strategy integrates common behavioral tasks as well as endophenotyping approaches performed across the lifespan. Such an approach is important because a number of genetic disorders show distinct early and late manifestations of disease that bear independent scrutiny. Often times, carriers of genetic mutations show few or at most subtle characteristics of later clinical disease early in life, but with increasing age these symptomatology emerge and the individuals receive a clinical diagnosis (Chonchaiya et al., 2009; Chonchaiya, Schneider, & Hagerman, 2009; Pirogovsky et al., 2009; Rupp et al., 2010). This does not infer, however, that early in life these individuals are unaffected by the mutation; more likely the

consequences of the mutation are present early in life, but require more sophisticated analyses to identify patterns of behavioral abnormalities (*cf.*, Goodrich-Hunsaker et al., 2011a; Goodrich-Hunsaker et al., 2011b; Goodrich-Hunsaker et al., 2011c).

In cases of genetic disorders, it is useful to evaluate the cognitive domains that underly later clinical phenotypes early in life to determine if there are markers that can quantify or predict disease progression (Devanand et al., 2000; Pirogovsky et al., 2009; Salomonczyk et al., 2010; Yong-Kee, Salomonczyk, & Nash, 2011). Research into a number of neurodegenerative disorders have been able to characterize subclinical endophenotypes early in the disease process that seem to predict the severity of disease progression (Gilbert & Murphy, 2004a; Gilbert & Murphy, 2004b; Karayiorgou et al., 2010; Salomonczyk et al., 2010; Xu, Hsu, Karayiorgou, & Gogos, 2012; Yong-Kee et al., 2011).

Similar strategies in neuroimaging can dissect alterations to the trajectories of brain growth and development across the lifespan and how these neuroanatomical factors relate to cognitive development (Carrion et al., 2009; Gothelf et al., 2011; Hall, Howard, Hagerman, & Leehey, 2009; Hoeft et al., 2010; Reiss, 2009; Walter, Mazaika, & Reiss, 2009). These approaches will illuminate not only the genetic contributions to behavioral phenotypes, but also the neurocognitive substrates underlying the observed behavioral phenotypes.

Specific examples

In the evaluation of mouse models of neurodevelopmental disorders, there is not yet an organized movement toward synthesizing the traditional behavioral phenotyping with emerging endophenotyping approaches. The examples below are provided to illustrate the advances in determining the clinical phenotypes and endophenotypes of patient populations and the need for rapid advancement in techniques used for behavioral analysis in mouse models.

The specific examples covered in this review will include disorders among the spectrum of fragile X-associated disorders caused by a polymorphic expansion of CGG trinucleotide repeats in the FMR1 gene: 55-200 CGG repeats is the fragile X premutation, and >200 CGG repeats is the fragile X full mutation that results in fragile X syndrome (FXS; Hagerman & Hagerman, 2004b). An analysis of the behavioral phenotypes and endophenotypes associated with fragile X-associated disorders allows researchers to elucidate the role of the dosage of a single-gene mutation in brain function (*i.e.*, expanded CGG repeat length parametrically modulates behavioral phenotypes).

Also evaluated in this review will be the 22q11.2 deletion syndrome (22q11.2DS; historically referred to as DiGeorge Syndrome or velo-cardio-facial syndrome (VCFS)) which is the result of a spontaneous deletion of a variable number of genes on the 22q11.2 locus. These mutations range in size from deletions of virtually the complete 22q11.2 locus (~60% of cases) to various single or multiple gene deletions within the 22q11.2 locus (remaining ~40%; (Karayiorgou & Gogos, 2004; Karayiorgou et al., 1996; Kiehl, Chow, Mikulis,

George, & Bassett, 2009; Long et al., 2006; Meechan et al., 2006; Mukai et al., 2004; Paylor et al., 2006; Sporn et al., 2004; Walter et al., 2009; Yamagishi & Srivastava, 2003) —thus providing a metric by which to evaluate neurobehavioral disruptions, the dosage of 22q11.2 deletion per individual or mouse model. Importantly, upwards of 50% of individuals with 22q11.2DS develop schizophrenia, so the need for identifying a risk prodrome is critical to identify at risk populations prior to the onset of schizophrenic symptomatology (Karayiorgou et al., 2010).

The present analysis of the neurobehavioral endophenotypes of fragile X-associated disorders and 22q11.2DS will focus on a theory suggesting that a number of neurodevelopmental disorders, including 22q11.2DS and fragile X-associated disorders, show nonverbal learning impairments: particularly reduced resolution of spatial and temporal attention (Johnson-Glenberg, 2008; Simon, 2007; Simon, 2008; Simon, 2011). By no means is this theory all inclusive to the potential deficits present in these populations, but this spatiotemporal processing theory provides a useful scaffold upon which to design and evaluate behavioral research into one of many potential endophenotypes.

Fragile X-associated disorders—fragile X premutation and CGG KI mouse

The fragile X premutation underlying results in a different phenotype than the full mutation, that of increased (2–8 fold) *FMR1* mRNA and concomitant slight reductions to *FMR1* protein (FMRP) levels (*i.e.*, 10–25% reductions; Garcia-Arocena & Hagerman, 2010; Raske & Hagerman, 2009; Tassone & Hagerman,

2003; Tassone et al., 2000c; Tassone et al., 2007a; Tassone et al., 2007b). The CGG KI mouse model of the fragile X premutation was developed by selectively inserting a human premutation CGG repeat (99 CGG repeats) into the mouse *Fmr1* gene by homologous recombination (Willemse et al., 2003) and models the molecular phenotypes of the human premutation (*e.g.*, elevated *Fmr1* mRNA and reduced Fmrp levels; Brouwer et al., 2007; Brouwer et al., 2008a; Brouwer et al., 2008b). A second mouse, a CGG-CCG KI mouse has also been evaluated by (Entezam et al., 2007) and shows similar, albeit more profound, molecular phenotypes (>70% reduction in Fmrp levels; Qin et al., 2011).

Human fragile X premutation neurobehavioral phenotype

Fragile X premutation carriers have been long considered largely cognitively unaffected by the premutation in carriers under the age of 50 (Hunter et al., 2008a; Hunter et al., 2009), after which premutation carriers are prone to a neurodegenerative course that results in late onset neurodegenerative states characterized by cerebellar gait ataxia and intention tremor (Hagerman & Hagerman, 2004b; Yachnis et al., 2010). Once the carriers demonstrate neurodegeneration, the premutation is associated with profound memory deficits, visuomotor performance, and deficient executive function (Berry-Kravis et al., 2007a; Bourgeois et al., 2006; Bourgeois et al., 2007; Grigsby et al., 2006a; Grigsby et al., 2006b; Grigsby et al., 2008).

The neuropathological hallmarks seen in premutation carriers presenting with late onset neurodegeneration are cortical atrophy, white matter disease

(particularly in subcortical and pontocerebellar white matter tracts) as well as the presence of intranuclear inclusions in neurons and astrocytes in brain (Greco et al., 2006). There have been reports of altered neuroanatomical volumes in carriers of the premutation prior to the onset of neurodegeneration, but these reports appear incomplete and contradictory, suggesting more rigorous studies are needed to characterize any true brain phenotype of young premutation carriers (*cf.*, Moore et al., 2004a; Moore et al., 2004b; Murphy et al., 1999).

CGG KI mouse neurobehavioral phenotype

Only two studies to date have evaluated the behavioral phenotype of the CGG KI and CGG-CCG mouse using a targeted screening process. Van Dam et al. (2005) reported age related worsening of memory using the water maze and declining motor function using the accelerating rotarod in CGG KI mice with age (though the studies were carried out using separate groups of mice so no causative relationship of age could be elucidated). A study evaluating CGG-CCG mice demonstrated very subtle abnormalities for social behavior using the three chambered apparatus, reductions in levels of anxiety in the open field, and a subtle memory deficit evaluated by performance on a passive avoidance paradigm (Qin et al., 2011). Importantly, no cerebellar ataxia or tremor-like phenotypes have been described in either mouse model.

To date, the presence of intranuclear inclusions in neurons and astrocytes have been identified in CGG KI mice (Brouwer et al., 2008a; Brouwer et al., 2008b; Hunsaker et al., 2009; Wenzel et al., 2010; Willemse et al., 2003), and

inclusions in brain cells in addition to Purkinje cell pathology (axonal torpedos) have been identified in the CGG-CCG mouse (Entezam et al., 2007). No gross histopathological features have been reported in either mouse model.

Human fragile X premutation neurobehavioral endophenotype

It has been shown that there are visual processing deficits in premutation carriers selective to the magnocellular but not the parvocellular visual streams, specifically as relating to biological and mechanical motion processing (Keri & Benedek, 2009; Keri & Benedek, 2010). It has been suggested that this dorsal visual stream-specific deficit reflects (or causes) impairments for spatial and temporal attention. In a spatial magnitude comparison task, it has been demonstrated that female premutation carriers show performance for discriminating small differences in magnitude that appears to be modulated by both CGG repeat length and age (*i.e.*, task performance shows a negative association with CGG repeat length), this despite female premutation carriers showing enhanced reaction times on a simple reaction time task run during the same behavioral session (Goodrich-Hunsaker et al., 2011a; Goodrich-Hunsaker et al., 2011c). Similar dosage effects have been demonstrated in an enumeration task that requires sequential shifting of spatial attention (Goodrich-Hunsaker et al., 2011b). In addition to these effects, arithmetic processing deficits have been reported in the female premutation carriers (Lachiewicz et al., 2006), a further indication that a fundamental spatiotemporal attention deficit is present in the fragile X premutation (*cf.*, Simon, 1999).

In studies using fMRI, it has been demonstrated that both the amygdala and hippocampus in premutation carriers show less task related neural activity than control participants (Hessl et al., 2007; Hessl et al., 2011; Koldewyn et al., 2008), and ERP studies have revealed abnormal cortical function during a semantic oddball detection paradigm (Olichney et al., 2010). Furthermore, there are evidence for reduced task-related activation of the dorsal and ventral inferior frontal cortex during working memory tasks (Hashimoto et al., 2011). It has also been reported that there is reduced white matter integrity in ponto-cerebellar white matter tracts, the fornix, and the stria terminalis in premutation carriers (Hashimoto, Javan, Tassone, Hagerman, & Rivera, 2011; Hashimoto, Srivastava, Tassone, Hagerman, & Rivera, 2011).

CGG KI mouse neurobehavioral endophenotype

In evaluating the endophenotype of the CGG KI mouse model of the premutation, the focus has been on directly evaluating spatiotemporal processing and visuomotor function. (Hunsaker et al., 2009) using a coordinate spatial processing task, demonstrated that CGG KI mice showed a CGG repeat length dependent impairment for processing the distance between objects, a task analogous to the spatial magnitude comparison tasks reported in female premutation carriers (Goodrich-Hunsaker et al., 2011a). Furthermore, CGG KI mice also demonstrated a CGG repeat dependent deficit for temporal processing in a simple sequence learning task for visual objects (Hunsaker et al., 2010). It has also been demonstrated that CGG KI mice show impaired visuomotor

function, even at ages as young as 2 months of age on a skilled walking task (Hunsaker et al., 2011c). This visuomotor deficit is interpreted as a selective impairment to spatiotemporal coordination as relating to motor control. Similar effects were seen in a skilled forelimb reaching task (Diep et al., 2012). What is unique about this overall pattern of deficits in the CGG KI mouse is that there is a clear negative association between task performance and the dosage of the gene mutation (e.g., increasing CGG repeat length on the *Fmr1* gene), such that performance deteriorates as CGG repeat length increases across spatiotemporal and visuomotor domains. Furthermore, these deficits arise relatively early in life (2–3 months of age), and thus may provide behavioral biomarkers prior to the onset of any neurodegenerative features associated with the premutation.

The CGG-CCG mouse model of the premutation has altered dendritic morphology throughout the brain, suggesting altered brain function. The CGG KI mouse has recently been evaluated for the presence of these same neuropathological features, and reduced dendritic complexity in basal, but not apical dendrites in visual cortex layer 3 pyramidal neurons was observed, but no alteration in the pattern of dendritic spine morphology was detected (unpublished observations). There also appears to be reduced protein synthesis in the cortex of the CGG-CCG mouse (Qin et al., 2011). To date, protein synthesis levels have not been evaluated in CGG KI mouse brain.

Fragile X-associated disorders—fragile X full mutation and *Fmr1* KO mouse

The full mutation underlying fragile X syndrome results in a molecular null phenotype for *FMR1* mRNA and *FMR1* protein (FMRP) levels. The *Fmr1* KO mouse was developed by selectively knocking out function of the *Fmr1* gene (Bakker & Oostra, 2003; 1994). Although the *Fmr1* KO mouse does not directly model the genetics of the fragile X full mutation, it does model the molecular consequences of the full mutation, that of virtual absence of *Fmr1* mRNA and Fmrp, and is thus comparable with the full mutation molecular phenotype (Tassone et al., 1999); but cf., Yan et al., 2004).

Human fragile X full mutation neurobehavioral phenotype

The cognitive or behavioral deficits identified in carriers of the fragile X full mutation underlying Fragile X Syndrome (FXS) include heightened anxiety levels, reduced Full Scale IQ (FSIQ), poor sensorimotor gating, and poor visuomotor function (Kemper et al., 1988; Kemper, Hagerman, Ahmad, & Mariner, 1986). Heightened anxiety reported in FXS includes social and nonsocial anxiety, with particular elevations in anxiety to novelty in either situations or objects (*i.e.*, neophobia). It has been reported that the FSIQ of male FXS patients is typically below 50, with pronounced verbal IQ (VIQ) and nonverbal IQ (performance—PIQ) deficits and mild to severe memory problems. FXS patients also often demonstrate an attenuated prepulse inhibition (PPI) response, meaning the natural startle response to a loud auditory stimulus is not reduced when a quieter priming stimulus is presented 50–200 ms beforehand. Attenuated PPI responses are cited as evidence for sensorimotor gating abnormalities in FXS, though there

are also reports of abnormal sensorimotor integration, similar to that reported in autism (Hessl et al., 2008; Hessl et al., 2009; McConkie-Rosell et al., 2007; Utari et al., 2010; Yuhas et al., 2011). Poor visuomotor function has also been reported in FXS, as has general clumsiness and awkward movements (Bennetto, Pennington, Porter, Taylor, & Hagerman, 2001; Mazzocco, Pennington, & Hagerman, 1993).

Based on structural MRI and limited post mortem histological analyses of FXS brain, a consistent pattern has emerged pointing to specific neuropathological features in FXS. It has been reported that the cerebellar vermis, specifically the superior lobe, is reduced in volume, and the caudate is larger than normal—even when corrected for brain volume, as are the hippocampus and several thalamic nuclei (Hagerman et al., 2004; Hessl et al., 2008; Mostofsky et al., 1998; Reiss, Aylward, Freund, Joshi, & Bryan, 1991; Reiss, Freund, Tseng, & Joshi, 1991; Reiss, Patel, Kumar, & Freund, 1988). Interestingly, the superior temporal sulcus, an area hypothesized to be critical for social cognition is reduced in volume in FXS (Gothelf et al., 2008). Post mortem analyses have confirmed a number of these radiological findings and further identified histopathological features in both the cerebellar vermis and hippocampal formation (Greco et al., 2011). It has further been demonstrated that the neuronal architecture in FXS is disrupted, with dendritic spines appearing more thin and immature in FXS brain than in non FXS brain throughout the hippocampus and neocortex (Irwin et al., 2001; Rudelli et al., 1985).

***Fmr1* KO mouse neurobehavioral phenotype**

In evaluating the mouse model(s) for FXS, primarily the *Fmr1* knockout (KO) mouse has been studied (and will be the focus of discussion here as the other FXS models demonstrate a very similar phenotypes; cf., I304N point mutation model; Zang et al., 2009). There has been a wide discrepancy in the behavioral findings that appear to be related to background strain of the specific mice in the lab, as well as with different lab procedures. There have been reports of *Fmr1* KO mice having alternately elevated or reduced anxiety levels measured in the open field and elevated plus maze tests of anxiety (Eadie et al., 2009; Yan et al., 2004; Zang et al., 2009), and abnormal marble burying phenotypes that are suggested to measure general activity, repetitive behaviors, and anxiety levels (Spencer, Alekseyenko, Serysheva, Yuva-Paylor, & Paylor, 2005; Thomas et al., 2009); however, these phenotypes are highly background strain dependent (Baker et al., 2010; Moy et al., 2007; Moy et al., 2008b). There have been tests of working memory and general memory using the Morris water maze, Barnes maze, and water radial arm mazes that demonstrate marginal effects at times, but these effects have been difficult to consistently replicate among labs, with even reports of *Fmr1* KO mice performing better than wildtype mice during different aspects of task performance relatively prevalent in the literature (Baker et al., 2010; Hayashi et al., 2007; Larson, Kim, Patel, & Floreani, 2008; Mineur & Crusio, 2002; Mineur, Huynh, & Crusio, 2006; Mineur, Sluyter, de Wit, Oostra, & Crusio, 2002; Yan et al., 2004). Attenuated PPI responses in *Fmr1* KO mice also

vary among strains and among labs, as does a susceptibility to audiogenic seizures (Spencer et al., 2005; Zang et al., 2009).

Recently, to mitigate complications arising from intra-strain differences, it has been proposed that an albino C57BL/6J Tyrc-Brd background strain be used for behavioral and pharmacological evaluation of FXS in *Fmr1* KO mice as both male and female *Fmr1* KO mice bred onto this background strain show profound behavioral deficits (Baker et al., 2010). It has also been proposed that F1 hybrid between C57BL/6J *Fmr1* KO mice and DBA/2J wildtype mice are a preferable model for FXS, as the resulting F1 hybrid mice show a greater number of autism-like phenotypes that other strains lack (Spencer et al., 2011). Though efficacious for modeling various aspects of disease pathogenesis, the initial choice of a background strain based solely upon a desire that the mouse model fulfill or demonstrate a particular phenotype is not in itself a valid rationale to develop or choose a mouse disease model; however, breeding a model onto a different background strain with the intent to further characterize or understand deficits across strains could serve to provide useful information to better understand a given phenotype.

Structural MRI analyses of *Fmr1* KO mouse brains report that there are no major volumetric or morphological differences between wildtype mice and *Fmr1* KO mice for any of the neuroanatomical structures identified in human studies as being abnormal, but those negative findings likely result from insufficiently sensitive MRI techniques rather than provide evidence for a definitive lack of a neuroanatomical phenotype (*cf.*, Kooy et al., 1999). More recently, volumetric

reductions in the deep cerebellar nuclei have been identified by MRI in *Fmr1* KO mice, which may prove to be somewhat analogous to the cerebellar pathology identified in FXS cases (Ellegood et al., 2010). At an histological level, dendritic abnormalities identified in human FXS have been confirmed in *Fmr1* KO mice using both Golgi-Cox/Golgi-Kopsch staining techniques and more advanced genetic techniques that allow in vivo analysis of neuronal architecture (Grossman, Elisseou, McKinney, & Greenough, 2006; Kao, Aldridge, Weiler, & Greenough, 2010; Pan, Aldridge, Greenough, & Gan, 2010).

Human fragile X full mutation neurobehavioral endophenotype

Work identifying endophenotypes in FXS has demonstrated behavioral deficits across the domains of spatiotemporal processing, numerical or arithmetic processing, to some extent executive function, and specific visual biological motion processing abnormalities (Bregman, Dykens, Watson, Ort, & Leckman, 1987; Curfs, Borghgraef, Wiegers, Schreppers-Tijdink, & Fryns, 1989; Curfs, Schreppers-Tijdink, Wiegers, Borghgraef, & Fryns, 1989; Curfs, Schreppers-Tijdink, Wiegers, van Velzen, & Fryns, 1989; Dykens, Hodapp, & Leckman, 1987; Mazzocco et al., 1993; Van der Molen et al., 2010). In the spatiotemporal domain, there have been reports of specific deficits in spatial and temporal memory performance in FXS, even in cases where FSIQ is controlled as a covariate and verbal performance is equal to or surpasses that of controls (*cf.*, (Farzin & Rivera, 2010; Farzin, Whitney, Hagerman, & Rivera, 2008; Johnson-Glenberg, 2008; Kemper et al., 1986; Kemper et al., 1988; Mazzocco et al.,

1993; Mazzocco, Hagerman, & Pennington, 1992; Simon, 2007). Executive function as defined as poor performance on the Stroop task as well as other tests of attentional and executive function is impaired in FXS (Cornish et al., 2004b; Cornish et al., 2004c; Cornish et al., 2008b; Cornish et al., 2009; Cornish, Munir, & Cross, 1998; Cornish, Munir, & Cross, 1999; Cornish, Pilgram, & Shaw, 1997; Cornish, Sudhalter, & Turk, 2004a; Loesch et al., 2003; Schneider et al., 2008; Schneider, Hagerman, & Hessl, 2009; Tamm, Menon, Johnston, Hessl, & Reiss, 2002). Even in cases of females with FXS that have normal FSIQ, there appear to be robust behavioral deficits when visuospatial attention is required for task performance (Steyaert, Borghgraef, & Fryns, 1994; Steyaert, Borghgraef, Gaulthier, Fryns, & Van den Berghe, 1992).

Furthermore, there have been numerous reports in behavioral and functional MRI studies demonstrating arithmetic/numerical processing deficits in both males and females with FXS (Bennetto et al., 2001; Mazzocco et al., 1992; Mazzocco et al., 1993; Mazzocco et al., 2006; Mazzocco, 2000; Mazzocco, 2001; Mazzocco, 2009; Mazzocco, Baumgardner, Freund, & Reiss, 1998; Mazzocco, Hagerman, Cronister-Silverman, & Pennington, 1992; Mazzocco, Pennington, & Hagerman, 1994; Murphy & Mazzocco, 2008; Murphy, Mazzocco, Hanich, & Early, 2007; Rivera et al., 2002). It has also been shown that a specific visual motion processing deficit is present in both male and female FXS that reflects visual motion processing deficits in FXS and spatiotemporal processing abnormalities that implicate the dorsal visual stream and parietal lobe function (Bertone, Hanck, Kogan, Chaudhuri, & Cornish, 2010; Keri & Benedek, 2009;

Keri & Benedek, 2010; Kogan et al., 2004a; Kogan et al., 2004b; Kogan et al., 2009; Kogan, Turk, Hagerman, & Cornish, 2008; MacLeod et al., 2010). Intriguingly, this visual deficit is similar, but more profound than, similar deficits reported in the fragile X premutation using identical tasks (Keri & Benedek, 2009; Keri & Benedek, 2010), suggesting a potential role for the dosage of the CGG repeat on the *FMR1* gene for visual processing in fragile X-associated disorders. Recent work bears out this hypothesis in control subjects, demonstrating a positive association between peripheral (e.g., leukocyte) FMRP levels and performance for this task (*i.e.*, higher FMRP levels are associated with better performance; Keri & Benedek, 2011).

Advanced measures of functional activation during cognitive tasks as well as diffusion weighted imaging have revealed a clear pattern of abnormalities in FXS. It has been shown that while performing simple arithmetic tasks individuals with FXS do not show typical increases in neural activity in the intraparietal sulcus that scale with task difficulty, suggesting abnormal cortical function in FXS (Rivera et al., 2002). There are also reduced levels of task-related hippocampus and basal forebrain activation during memory tasks (Greicius et al., 2003; Greicius, 2008; Greicius, Boyett-Anderson, Menon, & Reiss, 2004), and reduced amygdala activation to emotionally salient stimuli (Watson, Hoeft, Garrett, Hall, & Reiss, 2008). There have also been reports of abnormal fronto-striatal white matter pathways that may participate in cognitive control processes as well as abnormal white matter pathways in the parietal-sensory-motor tracts (Barnea-Goraly et al., 2003; Haas et al., 2009). Additionally, brain region-specific altered

neurodevelopmental trajectories have been identified in 1–3 year old FXS children, providing an invaluable insight into the development of neuroanatomical abnormalities reported in FXS adults (Hoeft et al., 2008; Hoeft et al., 2010). These altered fiber pathways and reduced functional activation are candidate neuroanatomical loci that are specifically affected by the *FMR1* mutation and underlie the neurocognitive deficits present in FXS.

Mouse FXS neurobehavioral endophenotype

There has not been a systematic effort to model the behavioral endophenotypes described in human FXS in the *Fmr1* KO mouse. The current focus is to optimize behavioral tasks to better caputulate the behavioral phenotypes of clinical FXS for use in interventional studies and drug testing. Tasks measuring social deficits and attenuated PPI responses have been proposed to serve as primary screens for therapeutic studies (Crawley & Paylor, 1997; Crawley et al., 1997; Paylor & Crawley, 1997; Spencer et al., 2005; Spencer et al., 2011; Zang et al., 2009). The paradigms evaluating categorical and coordinate spatial processing and temporal attention used in the CGG KI mouse have not yet been applied to *Fmr1* KO mice (Hunsaker et al., 2009; Hunsaker et al., 2010).

One study evaluating a behavioral parallel between the *Fmr1* KO mouse and FXS using analogous behavioral tasks suggests that both FXS and *Fmr1* KO mice are impaired on a spatial reasoning task, the modified Hebb Williams maze for mice and a computerized Hebb Williams Maze for humans (MacLeod et al.,

2010). Though cross-species comparisons are difficult to interpret for this particular behavioral paradigm emphasizing spatial navigation, the data provide compelling rationale to pursue cross species studies using tasks with both face and construct validity.

22q11.2 deletion syndrome in humans and mice

The 22q11.2DS results from a number of spontaneous mutations along the 22q11.2 locus, ranging from deletion of the whole locus to single or multiple gene mutations along the 22q11.2 locus. A number of different mutations encompassing the 22q11.2DS have been modeled in a number of mouse models. For the present review, the following models are included and collectively referred to as 22q11.2DS mouse models: *Lgdel*, *Del(Dgcr2-Hira)1Ra*, *DF(16)A*, *Del(Dgcr2-Hira)2Aam*, *Df1*, *Del(16Es2d-Ufd1l)2I7Bld*, *Smdel*, *Tbx1*, *Dgcr8*, and *Del(16Zpf520-Slc25a1)1Awb*. All 22q11.2DS mouse models were generated via targeted deletions of the analogous portions of mouse chromosome 16 covering the same complement of genes deleted across the different 22q11.2 deletions characterized in human 22q11.2DS (Arguello, Markx, Gogos, & Karayiorgou, 2010; Babovic et al., 2007; Gogos & Gerber, 2006; Gogos & Karayiorgou, 2001; Gogos, 2007; Kaenmaki et al., 2010; Karayiorgou & Gogos, 2004; Karayiorgou et al., 1996; Karayiorgou et al., 2010; Long et al., 2006; Mukai et al., 2004; Mukai et al., 2008; Paylor & Lindsay, 2006; Stark, Burt, Gogos, & Karayiorgou, 2009).

Human 22q11.2DS neurobehavioral phenotype

22q11.2DS patients demonstrate behavioral phenotypes ranging from learning disabilities to mild–moderate intellectual disability, but severe intellectual disability is present only in rare instances (Karayiorgou et al., 2010). Full Scale IQ (FSIQ) is usually around 75, but discrepancies between a typically average to high VIQ and typically low PIQ have led to the hypothesis that individuals with the 22q11.2DS have a nonverbal learning disability (similar to that reported in fragile X-associated disorders). Behavioral and psychiatric disorders are common in children with 22q11.2DS and include emotional instability, social withdrawal, attention-deficit/hyperactivity disorder, anxiety disorders, and depression (Bearden et al., 2004a; Bearden et al., 2005; Bearden, Wang, & Simon, 2002; Bish, Chiodo, Mattei, & Simon, 2007; Bish, Ferrante, McDonald-McGinn, Zackai, & Simon, 2005; Gothelf, Steinberg, Golan, & Apter, 2010; Karayiorgou et al., 2010; Kiehl et al., 2009; Simon et al., 2005b; Simon et al., 2008a; Simon et al., 2008b; Simon, 2008; Simon, Bearden, Mc-Ginn, & Zackai, 2005a; Stoddard, Niendam, Hendren, Carter, & Simon, 2010; Takarae, Schmidt, Tassone, & Simon, 2009; Xu, Karayiorgou, & Gogos, 2010; Yamagishi & Srivastava, 2003).

In the 22q11.2DS, there have been a number of neuroanatomical phenotypes identified that appear to result from altered developmental trajectories as the phenotypic pattern in adults and children differs. There is the occasional presence of a large cavum septum pellucidum reflecting incomplete subcortical midline development (Beaton et al., 2010), polymicrogyria has been reported (Gerkes et al., 2010; Kiehl et al., 2009; Sztriha et al., 2004), and white

matter hyperintensities are often reported throughout the brain (Bearden et al., 2004b; Kiehl et al., 2009). In children, there is increased ventricular volume, reduced parietal lobe volume (but with normal frontal and temporal lobe volumes), reduced cortical thickness, developmental anomalies along the subcortical midline, and reduced cerebellar volumes (Beaton et al., 2010; Bish et al., 2006; Bish, Nguyen, Ding, Ferrante, & Simon, 2004; Campbell et al., 2006; Gerkes et al., 2010; Karayiorgou et al., 2010; Machado et al., 2007; Schaer et al., 2006; Simon et al., 2005c; Simon, 2008; Sporn et al., 2004). Interestingly, this pattern of anatomical sequelae suggest that in the 22q11.2DS there is a specific reduction or delayed development of posterior neocortical structures, whereas anterior structures appear normal, at least in children.

In adults with 22q11.2DS, there is a general reduction in brain volume, reduced frontal and temporal lobe volumes (the opposite pattern to that observed in children), increased ventricular volume, reduced cerebellar volume, and diffuse white matter abnormalities seen on diffusion weighted imaging in parietal-parietal and frontal-frontal white matter projections as well as frontal-temporal white matter tracts (Bearden et al., 2004b; Chow et al., 1999; Connor, Crawford, & Akbarian, 2011; Drew et al., 2011a; Gothelf et al., 2010; Karayiorgou et al., 2010; Kiehl et al., 2009; Machado et al., 2007; Madan et al., 2010; Schaer et al., 2006; Schaer et al., 2009; Simon et al., 2005c; Sundram et al., 2010). The altered developmental trajectories underlying distinct patterns of neuropathology in children and adults are presently under investigation.

Mouse 22q11.2DS neurobehavioral phenotype

In different mouse models of the 22q11.2DS there are distinct patterns of behavioral phenotypes (Drew et al., 2011b; Karayiorgou et al., 2010; Long et al., 2006; Paylor & Lindsay, 2006; Paylor et al., 2006; Sigurdsson et al., 2010; Stark et al., 2008; Stark et al., 2009). Behaviorally, poor working memory has been reported in a 22q11.2DS mouse model, but the task used in those studies was actually a test of short-term spatial memory (Lee & Kesner, 2003; Sigurdsson et al., 2010; Stark et al., 2008) rather than working memory as evaluated in human populations. There have been reports of impaired sensorimotor gating, reduced grip strength, reduced nociception, and impaired movement initiation in 22q11.2DS mice; but phenotypes depend upon the specific mouse model and background strain used in the studies (Drew et al., 2011b; Long et al., 2006; Paylor & Lindsay, 2006; Paylor et al., 2006). A robust behavioral measure identified in a number of studies has demonstrated impaired classical fear conditioning in 22q11.2DS mouse models, but the relative contributions of the hippocampus, rostral cortex, and the amygdala have yet to be elucidated (Drew et al., 2011b; Karayiorgou et al., 2010; Sigurdsson et al., 2010; Stark et al., 2008; Stark et al., 2009).

It has been demonstrated that haploinsufficiency of a number of different genes deleted in the human 22q11.2DS leads to abnormal cortical development in a 22q11.2DS mouse model (Meechan, Tucker, Maynard, & LaMantia, 2009). The 22q11.2DS mouse model has immature dendritic structures that appear similar to what is observed in FXS and the *Fmr1* KO mouse model; to date,

whether such neuropathology is present in the human 22q11.2DS remains unknown (Drew et al., 2011a; Drew et al., 2011b; Karayiorgou et al., 2010; Mukai et al., 2008).

Human 22q11.2DS neurobehavioral endophenotype

It has been demonstrated that a number of neurodevelopmental disorders, such as fragile X-associated disorders and 22q11.2DS, share common nonverbal learning impairments. These impairments involve reduced resolution of spatial and temporal attention, as well as poor executive function. Collectively, these impairments result in, among other measures, an impairment in arithmetic processing (Sathian et al., 1999; Simon, 2008). Recent work has quantified nonverbal learning impairments in the 22q11.2DS by evaluating the behavioral endophenotypes predicted by the spatial and temporal attention model (Bearden et al., 2002; Bearden et al., 2004a; Bearden et al., 2005; Bish et al., 2005; Bish et al., 2007; Deboer, Wu, Lee, & Simon, 2007; Karayiorgou et al., 2010; Kiehl et al., 2009; Simon et al., 2005a; Simon et al., 2005b; Simon, 2008; Stoddard et al., 2010; Takarae et al., 2009; Xu et al., 2012; Yamagishi & Srivastava, 2003). Individuals with the 22q11.2DS show impaired spatiotemporal processing, impaired executive function, and profound impairments in numerical and arithmetic processing. These findings have been placed into the context of a reduced resolution of spatial and temporal attention such that greater differences in space and time are needed to allow the individual to normally process stimuli,

a process proposed to underly the nonverbal learning impairments characterized in the 22q11.2DS (Simon, 2008).

Counterintuitively, it has been shown the individuals with the 22q11.2DS show increased parietal cortex activation, but reduced frontal cortex activation, compared to a control population when confronted with a go/no-go response inhibition task that has been shown to depend upon the frontal, but not parietal, cortex. Since the task performance did not differ between the two groups, it is suggested that adults with the 22q11.2DS recruit posterior cingulate and parietal cortices to assist a hypofunctional frontal cortex to perform attentionally demanding tasks. Reduced frontal cortex activity in 22q11.2DS was also reported by Kates et al. (2007a, 2007b) who reported reduced task-related dorsolateral prefrontal cortex activity in 22q11.2DS compared to both sibling and non-sibling controls—without apparent behavioral differences on the working memory task presented. Together, these findings suggest that there are alterations to the fronto- parietal attentional network that fundamentally change the way individuals with the 22q11.2DS process information. Altered white matter pathways have been identified in diffusion weighted imaging studies of the 22q11.2DS that demonstrate abnormal connectivity patterns throughout the 22q11.2DS brain, including abnormal corpus callosum location, shape, and diffusivity, as well as abnormal long and short distance white matter projections throughout the neocortex (Aneja et al., 2007; Karayiorgou et al., 2010; Kiehl et al., 2009; Machado et al., 2007; Simon et al., 2005c; Simon et al., 2008b).

Mouse 22q11.2DS neurobehavioral endophenotype

At present, the phenotype that receives the most attention for the mouse models of 22q11.2DS is an attenuated PPI response, similar to the *Fmr1* KO mouse model (Long et al., 2006; Paylor & Lindsay, 2006; Stark et al., 2009). Potential behavioral endophenotypes are not widely studied in 22q11.2DS mouse models as the focus has been on modeling the aspects of the 22q11.2DS phenotype associated with schizophrenia and not on elucidating the underlying cognitive deficits in the 22q11.2DS population (cf., Karayiorgou et al., 2010; Paylor & Lindsay, 2006). One study has evaluated a few endophenotypes in the mouse models of 22q11.2DS, which was the report from (Sigurdsson et al., 2010; Stark et al., 2008) demonstrating altered fear processing, attenuated PPI response, and poor spatial memory retrieval in the 22q11.2DS mouse model. To the author's knowledge, current research into the 22q11.2DS mouse models have not evaluated any of the hypotheses from the spatiotemporal attention model tested in humans. This may be because these mouse models have been used to model schizophrenic symptomatology more than the 22q11.2DS disorder associated with the genetic mutation (Drew et al., 2011b; Karayiorgou et al., 2010).

At present, the genetics of the 22q11.2DS mouse models and the downstream consequences of the genetic dysregulation have been elucidated (e.g., micro-RNA disruption), and those findings have been correlated with behavioral outcomes (Stark et al., 2008). One study has evaluated abnormal temporoammonic connectivity in 22q11.2DS mice evaluated as an abnormal lack

of synchrony between hippocampal and rostral cortical neural activity during performance of a behavioral task shown to involve the interaction between these structures (Sigurdsson et al., 2010). This finding supports the reports of abnormal temporal–frontal lobe connectivity as well as hypoactivation in the prefrontal cortex during frontal-dependent tasks reported in 22q11.2DS individuals (Gothelf et al., 2010; Gothelf et al., 2011; Gothelf, Frisch, Michaelovsky, Weizman, & Shprintzen, 2009). Another task suggests impaired hippocampal area CA3 function using immediate early gene transcription in response to novelty as a measure (Drew et al., 2011b).

Comprehensive behavioral phenotyping strategy

As demonstrated above, the research into mouse models of fragile X-associated disorders and the 22q11.2DS show promise for the general behavioral phenotypes associated with the full clinical manifestation of the disorders, but the results are often mixed and difficult to interpret (Karayiorgou et al., 2010; Van Dam et al., 2000; Van Dam et al., 2005). Additionally, the research into behavioral endophenotypes have been largely absent. To overcome these challenges, it is necessary to evaluate the general health and well being of a mouse model with a strategy similar to using behavioral phenotyping screens and common behavioral tasks while, in parallel, evaluating how well the mouse models the cognitive deficits associated with specific genetic disorder in humans by applying what is known about the disorder from clinical neurology and cognitive neuroscience to develop specific hypotheses concerning the core deficits underlying the disorders. These hypotheses can then be used to selectively choose tasks to model the disorder in such a way as to maximize the application of the behavioral phenotype.

Behavioral screening—evaluating gross-level disruptions

Although the direction of this review has been an emphasis on the need for behavioral endophenotyping techniques in the study of mouse models of neurodevelopmental disorders, it does not mitigate the necessity for a thorough analysis of the gross behavioral phenotype of the model using a standardized behavioral task battery (Crawley, 2004; Wahlsten, 1974; Wahlsten, 2001).

Optimally, a wide reaching behavioral assessment should be performed, ranging from an analysis of basic sensory function to tasks evaluating general memory—a process analogous to neurological/neuropsychological testing in patient populations (e.g., SHIRPA Hatcher et al., 2001; Rogers et al., 1997; Rogers et al., 1999; Rogers et al., 2001; other protocols Deo, Costa, DeLisi, DeSalle, & Haghghi, 2010; Kendler & Neale, 2010; Kuang, Mei, Cui, Lin, & Tsien, 2010; Matsuo et al., 2010; Ryan et al., 2010; Ryan, Young, Moy, & Crawley, 2008; Takao et al., 2010; Taylor, Greene, & Miller, 2010; Tennant & Jones, 2009; Wang, Simpson, & Dulawa, 2009; Zang et al., 2009). With such a battery, any confounding factors related to strain background may be identified and controlled for by comparison of the model with littermate or strain-related controls, as it is important to determine whether any major behavioral phenotypes are present in the mouse model at the outset of experimentation.

As neuroimaging techniques are being developed and applied to mouse models of genetic disorders, behavioral neuroscientists need to apply careful histological techniques to the study of neurodevelopmental and neurodegenerative disease. As a concrete example, in a number of disorders altered hippocampal volume has been reported (FXS patients show enlarged hippocampal volumes; Gothelf et al., 2008; Hallahan et al., 2011; Hessl et al., 2004; fragile X premutation carriers and individuals with 22q11.2DS show reductions in hippocampal volumes; Adams et al., 2010; Deboer et al., 2007; Jäkälä et al., 1997). It is important to evaluate whether analogous neuroanatomical features are present in the mouse model. One way to

specifically evaluate these types of anatomical changes is to perform unbiased stereological estimates of not only regional volumes, but also of cellular number in regions of interest (*cf.*, West, Slomianka, & Gundersen, 1991). Stereological techniques involve relatively automated processes that require a trained technician, but do not require advanced technologies beyond those available at most research institutions. The benefit of stereological methods over gross histological analysis is the ability to quantify anatomical features using a process that minimizes experimental bias and is significantly less time intensive as exhaustive counting procedures (Gatome, Slomianka, Lipp, & Amrein, 2010; Simmons & Swanson, 2009; Swanson, 1995; West et al., 1991). Similar techniques can be used not only using classic histological stains, but also can be used to quantify immunohistochemical staining or tissue processed for *in situ* hybridization (Jinno, 2011).

Endophenotypes—uncovering subtle, disease specific effects

Once a behavioral phenotype (or lack of behavioral phenotype) is defined using common tasks, it is worthwhile to evaluate not only the disease being modeled by the mouse, but also the cognitive paradigms commonly administered to the population and the tasks used in the behavioral phenotyping strategy defined above. One concrete example within the fragile X-associated disorders and the 22q11.2DS, nonverbal learning impairments often manifest in clinical populations as difficulty in numerical or mathematical/arithmetic processing (Johnson-Glenberg, 2008; Simon, 2007; Simon, 2011). Reports such as these

are problematic for the mouse researcher as no tasks clearly evaluating arithmetic or numerical processing have been undertaken in mice, and very little work has been undertaken evaluating spatial magnitude estimation. There have been limited studies into processes conceptualized as counting or enumeration in rats (Suzuki & Kobayashi, 2000), but nothing truly arithmetic (and the interpretation of rodent “counting” tasks remains controversial; *cf.*, Gallistel & Gelman, 1992; Gallistel & Gelman, 2000; Rayburn-Reeves, Miller, & Zentall, 2010; Simon, 1999). In contrast, if one approaches arithmetic deficits as the end behavioral outcome of a number of fundamental cognitive processes involving spatial and temporal attention, a potential experimental battery becomes apparent (Gallistel, 1989; Gallistel, 1990a; Simon, 1999; Simon, 2008).

Numerical processing is a high level cognitive process encompassing spatial and temporal attentional components that underlie judgment of temporal magnitude or duration (Cordes, King, & Gallistel, 2007; Gallistel, 1989; Gallistel, 1990a; Gallistel, 1990b; Hunsaker et al., 2009; Hunsaker et al., 2010; Johnson-Glenberg, 2008; Leslie, Gelman, & Gallistel, 2008). For example, one can evaluate mouse models for the ability to discriminate the temporal duration of tones to evaluate the ability of mice to judge temporal magnitude or evaluate the ability of mice to learn simple temporal sequences of stimuli (Balci et al., 2008; Balsam & Gallistel, 2009; Chiba et al., 1997; Cordes et al., 2007; Cordes, Gelman, Gallistel, & Whalen, 2001; Gallistel et al., 2010; Hunsaker et al., 2010; Jackson et al., 1998). One can further use tests evaluating the relative size of objects or absolute distance between objects compared to some standard to

evaluate the ability of the mouse model to judge spatial magnitude (Clelland et al., 2009; Hunsaker et al., 2009; cf., Goodrich-Hunsaker et al., 2011a). None of these tasks evaluate numerical processing in themselves, but the processes being evaluated are the same as those shown to underly numerical cognition in humans (Gallistel, 1990b; Simon, 1999). The 22q11.2DS and FXS populations show deficits for spatial and temporal magnitude processing (Simon, 2007, 2008, 2011), and there are reports of the same in the fragile X premutation (Goodrich-Hunsaker et al., 2011a; Goodrich-Hunsaker et al., 2011b), so if the corresponding mouse models show deficits for processing spatial or temporal magnitude (cf., Hunsaker et al., 2009; Hunsaker et al., 2010), then inferences can be made concerning analogous processes underlying numerical processing in the mouse model and human disorder.

As functional imaging in rodents is in its infancy and used primarily in paralyzed preparations that do not allow for concurrent behavioral analysis (cf., Adamczak et al., 2010), it becomes important to use molecular tools to provide a functional snapshot of brain activity during task performance in mouse models of disease. Recently, in the learning and memory literature, early immediate genes such as *Homer1a*, *Arc/Arg3.1*, *zif268*, and *c-Fos* have been used as markers of neural activity and correlated with learning (Drew et al., 2011b; Guzowski & Worley, 2001; Guzowski et al., 2005; Shepherd & Bear, 2011). Although such a technique (*in situ* hybridization) only allows for a snapshot of neural activity in response to very limited stimuli conditions, the technique can potentially be extended to include evaluation of regional differences in protein expression that

may predict disease onset or severity prior to the emergence of disease-related pathological features (*cf.*, Poirier, Amin, Good, & Aggleton, 2011).

Another functional assay is reported by Sigurdsson et al. (2010) is that of in vivo neurophysiological recording to evaluate differences in either cellular spiking activity or extracellular rhythms that may be altered in disease—a process also being explored in human epilepsy (Jacobs et al., 2010). It has also been shown in mice that electrophysiological correlates of information processing used in humans, specifically event related potentials (ERP) measures on an electroencephalogram. It has further been suggested that the P300 and N400 potentials may show similar patterns in mice as humans when tasks are carefully designed (Choi et al., 2010; Olichney et al., 2010).

Conclusions

In recent years, there has been impetus placed on developing behavioral biomarkers that can be used to predict not only later disease onset or progression, but perhaps disease severity. These collections of intermediate or behavioral endophenotypes serve as outcome measures for pharmacological interventions (Almasy & Blangero, 2001; Amann et al., 2010; Burdick, Goldberg, Harrow, Faull, & Malhotra, 2006; Cannon & Keller, 2006; Castellanos & Tannock, 2002; Einat, 2007; Gottesman & Gould, 2003; Gould & Einat, 2007; Gould & Gottesman, 2006; Gur et al., 2007; Joo, 2008; Kendler & Neale, 2010; Keri & Benedek, 2009; Kuntsi, Andreou, Ma, Borger, & van der Meere, 2005; Saperstein et al., 2006). This search for behavioral biomarkers, however, has not consistently been extended into the mouse models of genetic disorders. To date, the closest research into mouse disease models comes to developing behavioral biomarkers is to thoroughly parameterize a single task (e.g., attenuated PPI response or audiogenic seizures for the *Fmr1* KO mouse model) and apply the biomarker as a screen for various mouse models to choose candidates for drug studies (Long et al., 2006; Spencer et al., 2011; Zang et al., 2009). The strength of the standard approach is the ability to define a canon against which to gauge later models; however, the limitation of this approach is that it lacks the ability to evaluate complimentary models of a given disease to get at the fundamental processes disrupted in the human mutation.

This limitation occurs because a model may fail to model one phenotype, even though the mouse may model any number of other phenotypes that are not

included in the standard behavioral screen. This lack of sensitivity is a major limitation as studies into the therapeutic effects of pharmacological agents will be incomplete in the absence of predefined behavioral biomarkers as outcome measures.

If the recent advances in the cognitive neuroscience of neurodevelopmental disorders are extended to their respective mouse models, perhaps the associated behavioral biomarkers of such disorders may not only be complimented by, but extended through use of mouse models studying the component processes underlying disease states. These well defined behavioral biomarkers can be used as correlates or covariates with molecular studies of underlying disease mechanisms in mice that cannot be directly studied in human patient populations.

Acknowledgements

The author would like to thank Dr. Tony J. Simon for helpful conversations concerning the direction of this manuscript, and Drs. Raymond P. Kesner, Ph.D. and Naomi J. Goodrich-Hunsaker, Ph.D. for critical reading and discussions of preliminary versions of this manuscript.

Funding

MRH was supported by NINDS RL1 NS062411 awarded to Robert F. Berman. This work was also made possible by a Roadmap Initiative grant (UL1 DE019583) from the National Institute of Dental and Craniofacial Research

(NIDCR) in support of the NeuroTherapeutics Research Institute (NTRI) consortium; and MRH was further supported by a training grant (UL1 RR024146) from the National Center for Research Resources (NCRR), a component of the National Institutes of Health (NIH), and NIH Roadmap for Medical Research. The contents of this manuscript are solely the responsibility of the author and do not represent the official view of NCRR, NINDS, NIDCR, or NIH.

Chapter 10

CGG Trinucleotide Repeat Length Modulates Neural Plasticity and Spatiotemporal Processing in a Mouse Model of the Fragile X Premutation

ABSTRACT

The fragile X premutation is a CGG repeat expansion on the *FMR1* gene between 55 and 200 repeats in length. It has been proposed that impaired spatiotemporal function underlies cognitive deficits in genetic disorders, including the fragile X premutation. The present study characterized the role of the premutation for cognitive function by demonstrating CGG KI mice with 70-198 CGG repeats show deficits across tasks requiring spatial and temporal pattern separation. To elucidate mechanisms whereby CGG repeats affect spatiotemporal processing, hippocampal slices were evaluated for LTP, LTD, and mGluR1/5 LTD. Increasing CGG repeat length modulated the induction of LTP, LTD, and mGluR1/5 LTD, as well as behavioral tasks emphasizing spatiotemporal processing. Despite the deficits in the induction of all forms of plasticity, there were no differences in expression of plasticity once evoked. These data provide evidence for a neurocognitive endophenotype in the CGG KI mouse model of the premutation in which CGG repeat length negatively modulates plasticity and spatiotemporal attention.

This chapter has been published as:

Michael R. Hunsaker, Kyoungmi Kim, Rob Willemsen, Robert F. Berman (2012). CGG Trinucleotide Repeat Length Modulates Neural Plasticity and Spatiotemporal Processing in a Mouse Model of the Fragile X Premutation. Hippocampus. In press.

My role in this study was experimental design, apparatus set up, performing behavioral and neurophysiological experiments, and data analysis.

INTRODUCTION

The fragile X premutation is a CGG trinucleotide repeat expansion between 55 and 200 repeats in length on the fragile X mental retardation 1 (*FMR1*) gene. The premutation results in a 2-8 fold increase in *FMR1* mRNA levels in leukocytes and reduced *FMR1* protein (FMRP) levels (Tassone et al., 2000c; Tassone et al., 2000d; Tassone et al., 2008). In fragile X syndrome (FXS) there are >200 CGG repeats, resulting in virtually undetectable *FMR1* mRNA and FMRP levels due to transcriptional silencing (Hunsaker et al., 2011b; Tassone et al., 2008).

Until recently, premutation carriers have been largely presumed to be cognitively unaffected by the mutation (Hunter et al., 2009; Hunter et al., 2010). However, potential neurocognitive effects of the premutation have been reported (Cornish et al., 2009; Goodrich-Hunsaker et al., 2011a; Goodrich-Hunsaker et al., 2011b; Goodrich-Hunsaker et al., 2011c; Hessl et al., 2011; Keri & Benedek, 2009; Keri & Benedek, 2010; Koldewyn et al., 2008). These studies suggest cognitive function in premutation carriers are modulated by the dosage of the *FMR1* mutation (*i.e.*, increasing CGG repeat length), such that performance deteriorates as the CGG repeat length increases.

(Simon, 2008; Simon, 2011) proposed that neurogenetic disorders including fragile X-associated disorders, Turner syndrome, Williams syndrome, and 22q11.2 deletion syndrome have overlapping cognitive impairments involving spatiotemporal attention that result from reductions in the resolution, or clarity, of mental representations, referred to as a *spatiotemporal hypergranularity*. As

such, discriminating spatial distances or temporal separations among stimuli becomes increasingly difficult as the spatial or temporal differences become smaller due to increasing interference (*cf.*, Hunsaker et al., 2012; Hunsaker, 2012b). Thus, many individuals with neurogenetic disorders have relatively coarse mental representations, so identification of one spatial location or time point from another requires a larger between-item difference before the two can be perceived as distinct (*cf.*, Hanson & Madison, 2010).

It has been demonstrated that the hippocampus is critical for processing spatial and temporal relationships between stimuli in such a way that incoming sensory information is orthogonalized to minimize interference across both time and space via a process called *pattern separation* (Kesner et al., 2004; Kesner, 2007; Rolls & Kesner, 2006). It is likely that impaired hippocampus-dependent spatial and temporal pattern separation contributes to the spatiotemporal hypergranularity observed in genetic disorders, including the fragile X premutation (Hanson & Madison, 2010).

To characterize the molecular effects disrupted by the fragile X premutation, (Willemse et al., 2003) generated a CGG KI mouse model of the premutation via homologous recombination in which the mouse 5' untranslated region containing 8-12 CGG repeats on the *Fmr1* gene was replaced with a 5' untranslated region containing 98 CGG repeats of human origin. Importantly, the CGG KI mouse recapitulates the molecular phenotypes observed in the human premutation: CGG KI mice show 2-5 times elevated levels of *Fmr1* mRNA and 20-30% reductions in Fmrp levels that scale with CGG repeat length (Brouwer et

al., 2008a). Another model of the premutation was generated by (Entezam et al., 2007) by serial ligation of CGG-CCG repeats in the 5' untranslated region in the mouse *Fmr1* gene. This mouse shows similar elevations in *Fmr1* mRNA levels, but profound reductions in Fmrp expression that are not present in the human fragile X premutation. Both mouse models have been tested using behavioral screens evaluating spatial memory, motor function, anxiety, and social behavior (Qin et al., 2011; Van Dam et al., 2005); but the results of these tasks failed to recapitulate altered neurocognition as reported carriers of the fragile X premutation. As such, the present experiment used the CGG KI mice as subjects to be more directly comparable with the cognitive research into carriers of the fragile X premutation (*cf.*, Goodrich-Hunsaker et al., 2011a; Goodrich-Hunsaker et al., 2011b; Goodrich-Hunsaker et al., 2011c).

The present study was designed to firmly establish the effects of increasing CGG repeat length for spatiotemporal attention by testing CGG KI mice with 70-198 CGG repeats in length on behavioral tasks requiring spatial and temporal pattern separation. To elucidate mechanisms whereby increasing CGG repeats may affect spatiotemporal processing, mice were evaluated for induction and expression of NMDA receptor dependent long term potentiation (LTP) and long term depression (LTD) and mGluR1/5 dependent LTD at the Schaffer collateral synapse in acute hippocampal slices. The data provide the first demonstration that CGG KI mice have a spatiotemporal hypergranularity as well as reduced hippocampal plasticity induction, both of which are modulated by the dosage of increasing CGG trinucleotide repeat lengths. Together these data

provide evidence for a behavioral endophenotype, and provides a candidate mechanism whereby increasing CGG repeat lengths may negatively impact cognitive function.

MATERIALS AND METHODS

Animals

Forty-eight male CGG KI mice and 24 wildtype (Wildtype) littermate mice were used as subjects for this task. CGG KI mice were mice with 70-116 CGG repeats (Low CGG n=24) and mice with 132-198 CGG repeats (High CGG n=24). These groups emerged during breeding and are grouped in this manner because of the 166 CGG repeat gap between the groups, not to model any known difference between these repeat length groups in human premutation carriers. CGG KI mice were on a congenic C57BL/6J background. All mice were 9 months of age (+/- 0.32 SEM) at the beginning of experimentation to model the effects of the premutation during mid to late adulthood in human premutation carriers. Mice were housed in same sex, mixed genotype groups with one to four mice per cage on a 12 h light-dark cycle. Mice were maintained at 90-95% of their free feeding weight and had ad libitum access to water during experimentation. All experiments conformed to UC Davis IACUC approved protocols and all effort was taken to reduce stress in all mice during experimentation.

Genotyping

As somatic instability of CGG repeats on the *Fmr1* gene among tissues in the CGG KI mouse has been shown to be negligible (typically under 10 CGG repeats across tissues; Willemsen et al., 2003), genotyping to verify CGG repeat length was carried out upon tail snips. Following a method kindly provided by

Rob Willemsen (Brouwer et al., 2008a) and modified in collaboration with the laboratories of F Tassone and PJ Hagerman (Saluto et al., 2005; personal communication), CGG repeat lengths were measured using the FastStart Taq DNA Polymerase, dNTP Pack(Roche Diagnostics; Manheim, Germany) DNA was extracted from mouse tails by incubating with 10 mg/mL Proteinase K (Fermentas, Inc.; Glen Burnie, MD) in 300 μ L lysis buffer containing 50 mM Tris-HCl, pH 7.5, 10 mM EDTA, 150 mM NaCl, 1% SDS overnight at 55°C. One hundred microliters (100 μ L) saturated NaCl was then added, mixed and centrifuged. The supernatant was gently mixed with two volumes of 100% ethanol, and the DNA was pelleted by centrifugation. The DNA was washed and centrifuged in 500 μ L 70% ethanol. The DNA was then dissolved in 100 μ L milliQ-H₂O. CGG repeat lengths were determined by PCR using solutions from the FastStart Taq DNA Polymerase, dNTP Pack (Roche Diagnostics). Briefly, approximately 500-700 ng of DNA was added to 20 μ L of PCR mixture containing 0.5 μ M/L of each primer, 250 μ M/L of each dNTP (Roche Diagnostics). 2.5 M Betaine (Sigma-Aldrich), 1X Buffer 2 and 0.05 U of FastStart Taq DNA Polymerase (Roche Diagnostics) The primers flank the CGG repeat region of Fmr1 gene, the forward primer was 5'-CGG GCA GTG AAG CAA ACG-3'and the reverse primer was 5'-CCA GCT CCT CCA TCT TCT CG-3 The CGG repeats were amplified using a 3-step PCR with 10 min denaturation at 98 °C, followed by 35 cycles of 35 s denaturation at 98 °C, annealing for 35 s at 55 °C, and at the end each cycle elongation for 2 min at 72 °C . The last step of the PCR consisted in a 10 minute elongation at 72°C to. The sizes of CGG DNA amplicons

were determined by running 20 μ L of PCR reaction per sample and a molecular weight marker (O'GeneRuler 50bp DNA ladder; Fermentas, Inc.) for 2 hrs at 150V on a 2.5% agarose gel with 0.03 μ L/ml ethidium bromide. The number of CGG repeats was calculated from pictures acquired with a GelDoc-It Imaging system (UVP, LLC Upland, CA) and using VisionWorks LS software (UVP, LLC Upland, CA). This method can detect up to 358 CGG repeats from animals in the present mouse colony). Genotyping was performed twice on each mouse, once using tail snips taken at weaning and again on tail snips and/or brain tissue collected at sacrifice. In all cases the genotypes matched.

Experimental Design

The order in which the four behavioral tasks were presented to each mouse was randomized in the Wildtype group, and 7 d separated each task; furthermore, the order during each testing session during which a given mouse was tested was randomized. Once behavior was finished, all mice were prepared for physiology. For physiology, the order of experiments was randomized across slices within each mouse. From each mouse, three sequential hippocampal slices were evaluated from the dorsal-intermediate hippocampus (sections taken between 1-3.5 mm caudal to the septal pole of the hippocampus). The order in which slices were used, as well as which form of plasticity was evaluated on which slice were randomized and order was included as a covariate in all statistical analyses. For both behavior and physiology, each Wildtype mouse was paired with an individual CGG KI mouse with 70-116 CGG repeats as well as an

individual CGG KI mouse with 132-198 CGG repeats as an explicit control for potential effects of experimental order in task performance across CGG repeat groups. Experimental order was included as a covariate in all statistical analyses.

Behavioral testing took place between 9-10 months of age for all mice and physiology took place between 10-13 months of age for all mice. Importantly, all mice used for behavior were also used for physiological studies. To control for potential effects of mouse age during physiology, mouse age was used as a covariate in all physiological data analyses.

Coordinate and Categorical Spatial Processing Tasks

Behavioral Apparatus

For the coordinate and categorical spatial processing tasks (Hunsaker et al., 2009; called “metric” and “topological” in that study) a circular table measuring 1 m in diameter was covered with a white, plastic sheet (*i.e.*, shower curtain). Four objects measuring between 2.5–5 cm in diameter at the base and between 5-15 cm tall were used as stimuli. The table was enclosed by four white curtains 1 m away from the table edge with visually complex distal cues placed at the same level as the table surface affixed to the curtains.

Between the habituation and test sessions, the mice were placed in an opaque holding cup. The circular table was wiped down with 70% ethanol after each mouse to reduce and mask olfactory cues. All trials were digitally recorded by a camera located above the tabletop that was connected to a computer

running ANY-maze behavioral tracking software (v4.3; Stoelting Co.; Wood Dale, IL).

Behavioral Methods

Coordinate spatial processing task

Each mouse was placed on the edge of the table facing two objects placed 45 cm apart. The mouse was allowed 15 min to freely explore the tabletop, objects, and distal environment. Exploration of the objects decreased over the 15 min period as animals habituated. After the 15 min habituation session, the mouse was removed to the small holding cup for 5 min. During this intersession interval, the objects were shifted 15 cm closer to each other so that the objects were now spaced 30 cm apart. After the objects were shifted closer together, the mouse was placed on the table and given 5 min to explore the objects during the test session.

Categorical spatial processing task

For the categorical spatial processing task, two novel objects, different from those used for the coordinate task, were used as stimuli. Mice were placed on the table and allowed to habituate to the objects exactly as in the coordinate task, and then removed from the table for 5 min. During the 5 min between the habituation and test sessions, the objects were transposed, such that the left object was now on the right side and vice versa, but the spatial locations occupied by objects were held constant.

Dependent Measures

For both the coordinate and categorical tasks, the time spent exploring each object was recorded as the dependent variable. Exploration was defined as the mouse actively sniffing or touching the object with its nose, vibrissa, mouth, or forepaws. An animal simply located near or standing on top of the objects without actively interacting with them was not scored as exploration. Object exploration data were summarized in 5-min epochs during the 15-min habituation period to facilitate comparison with the 5-min test session, as previously described (Hunsaker et al., 2009). Mice habituated to the objects during the 15-min habituation phase, and show relatively low levels of exploration during the last 5 min compared to the first 5 min. However, during the 5-min test session when mice are returned to the table, mice that remember the object distance (coordinate or metric) or object position (categorical or topological) show increased exploration of the objects. Locomotor activity was collected by the ANY-maze system.

Statistical Methods

Locomotor activity was analyzed using a 3 (binned CGG repeat group) \times 4 (session; three 5-min bins during habituation, test session) repeated measures analysis of covariance (ANCOVA). Experiment order was included as a covariate in the analysis. Total object exploration time during the 15 min habituation session was calculated for the first, second, and last 5-min epochs to facilitate

comparison between the last 5 min of the habituation session and the 5-min test session. A 3 (CGG repeat group) x 3 (session) repeated measures ANCOVA was performed on these exploration data for both coordinate and categorical spatial processing tasks, with experiment order as a covariate in the analysis.

To facilitate the comparison between the test session and the last 5 min of the habituation session, an exploration ratio was calculated as: [(exploration time during the 5-min test session)/(exploration time during the 5-min test session + exploration during the last 5 min of the habituation session)]. This constrained all values between 0 and 1. With this ratio, increased exploration during the 5 min test session compared to the last 5 min of the habituation session is reflected as a ratio $>.5$, and decreased exploration (or continued habituation) is reflected as a ratio $<.5$. Prior to comparing CGG KI mice and Wildtype mice for the ratio scores, it was verified that the ratio score for the Wildtype mice was $\neq .5$ via a one-tailed t-test against the null hypothesis of a ratio score $=.5$, suggesting heightened exploration of the objects during the test session compared to the final 5 min of the habituation session.

To compare ratios between CGG KI mice and Wildtype mice, one way ANCOVA with CGG repeat group as the grouping variable were performed for both coordinate and categorical tasks, with experiment order as a covariate. To more directly elucidate a role for CGG repeat length modulation of any effects within the CGG KI mice, two-tailed Pearson's correlation coefficients were calculated to assess the relationship of the ratio values with CGG repeat length in only the CGG KI mice.

Temporal Ordering for Visual Objects Task

Behavioral Apparatus

To evaluate temporal ordering in CGG KI mice as a function of CGG trinucleotide repeat length, mice were tested on a temporal ordering for visual objects task (Hunsaker et al., 2010). The task was run in a transparent Plexiglas box 26 cm long × 20 cm wide × 16 cm tall. Eight objects in triplicate were used as stimuli for this study. These objects ranged in size from 6 cm diameter × 6 cm tall to 4 cm × 2 cm. All objects and the apparatus were wiped down with 70% ethanol between sessions in order to reduce odor cues.

Behavioral methods

Temporal ordering for visual objects task

During session 1, two identical copies of a first object (object 1) were placed at the ends of the box 2.5 cm from the end walls and centered between the long walls. The mouse was placed in the center of the box facing away from both objects. The mouse was given 5 min to freely explore the objects. After 5 min, the mouse was removed to a small holding cup for 5 min. During this time, the first objects were replaced with two duplicates of a second object (object 2). For session 2, the mouse was again placed in the apparatus and allowed to explore. After 5 min, the mouse was removed to the holding cup for 5 min and the objects were replaced with two duplicates of a third object (object 3). For session 3, the mouse was given 5 min to explore. After 5 min, the mouse was removed into a small cup for 5 min and an unused copy of the first and an

unused copy of the third object were placed into the box. The mouse was again placed into the box and allowed to explore the two objects (*i.e.*, object 1 and object 3) during a 5 min test session. All trials were recorded by a camera located directly above the tabletop that was connected to a PC laptop computer running ANY-maze behavioral tracking software.

Mice typically show increased exploration of the first object compared to the third object, and this was used as an index of memory of the temporal order of the object presentation. A lack of preferential exploration of one object over the other indicates temporal ordering impairments.

Visual object novelty detection task

In addition to reflecting impaired temporal ordering, increased exploration of the first object over the third could also be interpreted as being due to difficulty in remembering the first object prior to the test session. In order to minimize and control for such general memory deficits, a novelty detection of visual objects task was performed. Briefly, on a different day mice received three sessions during which they were allowed to explore three novel sets of objects (objects 4, 5, 6) similarly to the temporal ordering tasks. During the test session, the first object and a novel fourth object (object 7) were presented and the mice were allowed 5 min to explore. Preferential exploration of the novel object 7 over object 4 would indicate that the mouse remembered having previously explored object 4, whereas equal levels of exploration of the two objects would indicate that forgetting had occurred.

Dependent measures

For the temporal ordering task, object exploration was defined as active physical contact with the object with the forepaws, whiskers, or nose. With this definition, an mouse standing near an object without interacting with it would not be counted as exploration. To control for differences in exploration levels between mice, exploration during the temporal ordering test sessions was converted into a ratio score to constrain the values between –1 and 1. The ratio calculated as follows: $(\text{exploration of object 1} - \text{exploration of object 3}) / (\text{exploration of object 1} + \text{exploration of object 3})$. Exploration during the novelty detection test sessions was similarly converted into a ratio score, using exploration of objects 4 and 7 in the calculation: $(\text{exploration of novel object 7} - \text{exploration of object 4}) / (\text{exploration of object 4} + \text{exploration of novel object 7})$.

A ratio value near 1 means that the mouse showed more exploration of the first item presented in the temporal ordering task. A score near –1 suggests the mouse preferentially explored the last object presented. A score near 0 reflects equal exploration of objects indicating a failure to detect the temporal order of visual object presentation.

In the novel object test a score approaching either 1 (*i.e.*, preference for the novel object) or –1 (preference for object 1) would indicate intact memory of object 4, while a score near 0 would suggest that forgetting had occurred. As a measure of general activity levels, locomotor activity was determined by

recording the number of times the mouse crossed the midline of the box with all four paws during each session.

Statistical methods

Locomotor activity was analyzed using a 3 (binned CGG repeat group) \times 4 (session) repeated measures ANCOVA. Experiment order was included as a covariate in the analysis. Any differences in locomotor activity were more fully characterized using Tukey's HSD post hoc pairwise comparisons test when the overall group comparison was significant. Object exploration data from each session were analyzed with 3 (CGG repeat group) \times 4 (session) repeated measures ANCOVA with experiment order as a covariate to verify that mice explored all the objects similarly during the study sessions to verify that unequal exploration would not confound measures of temporal ordering. Furthermore, side preferences during object sessions 1–3 were tested with individual paired t-tests against the null hypothesis of 50% exploration for the object on each side. Prior to comparing CGG KI mice and Wildtype mice for the ratio scores, it was verified that the ratio score for the Wildtype mice was $\neq .0$ via a one-tailed t-test against the null hypothesis of a ratio score $= .0$ to verify preferential exploration of the first object during the temporal order test and novel object during the novelty test.

Exploration data that were converted to ratio values were analyzed by one-way ANCOVA with experiment order as a covariate. To more fully characterize any differences among groups, Tukey's HSD post hoc pairwise

comparisons test was performed when the overall group comparison was significant. To verify that locomotor behavior and object exploration during earlier sessions did not contribute to temporal ordering and/or novelty detection measures recorded during the test sessions, ANCOVA were performed with both locomotor behavior and object exploration during session 1, both locomotor behavior and object exploration during session 3, as well as locomotor behavior during the test session as covariates, as well as experiment order. To elucidate a role for CGG repeat length modulation of any effects within the CGG KI mice, Pearson's correlation coefficients were calculated to assess the relationship of the ratio values with CGG repeat length in only the CGG KI mice.

Neurophysiology

Slice preparation

Mice were anesthetized with isoflurane, decapitated, and the brains were rapidly transferred to cold, oxygenated artificial CSF (aCSF) containing (in mM) 124 NaCl, 3 KCl, 1.25 NaH₂PO₄, 2 MgSO₄, 26 NaCO₃, 2 CaCl₂, and 10 dextrose. Brains were then blocked in the coronal plane to contain the hippocampus; a Vibratome (Vibratome Company; St. Louis, MO) was used to cut 400 µm-thick slices transverse to the longitudinal axis of the hippocampus into a bath of oxygenated aCSF at 1°C. Individual slices, from the dorsal/intermediate third of the hippocampus, were placed in a holding chamber at 30°C with oxygenated aCSF and allowed to equilibrate for at least 60 min before transfer to a slice interface recording chamber (Fine Science Tools; Foster City, CA) for

electrophysiological experiments. Slices rested on a nylon mesh over a well perfused with warmed (32–35°C), oxygenated aCSF (2 mL/min perfusion rate); the slice surface was exposed to a warmed, humidified 95% O₂ / 5% CO₂ environment. Slices were exposed to this environment for 30 min prior to the placement of any electrodes, and an additional 10 min after electrode placement prior to delivery of any stimuli.

Neurophysiological Methods

Field evoked post synaptic potentials (fEPSPs) were recorded with extracellular electrodes made from borosilicate glass pulled on a horizontal puller (Sutter Instruments; Novato, CA) and filled with 0.1M NaCl (~5 MΩ resistance) and placed in the middle of the stratum radiatum in distal CA1. Synaptic responses were evoked by a 200-μs current pulse to Schaffer collateral axons in proximal CA1 near the CA2/CA3 border with a concentric bipolar tungsten stimulating electrode connected to a stimulus isolation unit (World Precision Instruments, Inc.; Sarasota, FL). Stable baseline responses were collected every 30 s after adjusting stimulus intensity (10-30μA) to achieve 50% of the maximal fEPSP slope in the absence of population spikes. Only slices in which fEPSPs in which maximal amplitudes >1.5 mV could be maintained for 15 min were used (in total, 15% of slices were discarded for failure to meet this threshold).

Plasticity induction methods

NMDA receptor dependent long-term potentiation (LTP) of fEPSPs was induced using a conditioning stimulus consisting of four trains of 50 pulses at 100 Hz, 30 s apart (high-frequency stimulation; HFS). NMDA receptor dependent long-term depression (LTD) of fEPSPs was induced using conditioning stimulus of 900 pulses delivered at 1 Hz delivered over 15 min (low-frequency stimulation; LFS). Metabotropic GluR1/5 (mGluR1/5) receptor dependent LTD was induced by applying 3,5-dihydroxyphenylglycine (DHPG) into the perfusing medium (50 μ M final concentration perfused across the tissue at 2 mL/min) and continuing with baseline stimulation for 15 min followed by immediate washout.

R,S-DHPG was purchased from Tocris (St. Louis, MO). All other chemicals were purchased from Sigma. DHPG was prepared as a 100 times stock in H₂O, aliquoted and stored at -20°C. Fresh stocks were made once a week and diluted in aCSF to achieve their final concentrations for perfusion application.

Histology

After performing neurophysiological analyses, the hippocampal slices were placed in 4% buffered paraformaldehyde for 24 h at room temperature on a shaker table before being cyroprotected in 10% and 30% sucrose and flash frozen. Thirty μ m sections from a random subset of hippocampal slices that were recorded from were stained for hematoxylin and eosin and evaluated for viability and structural abnormalities that may contribute to any differences among mice for physiological measures.

Dependent Measures

All electrophysiological data were recorded using an Axoclamp 2A amplifier (Axon Instruments; Foster City, CA), high pass filtered at 3 Hz, low-pass filtered at 10kHz, digitized (20 kHz) using an Axon Digidata 1200 digital acquisition system (Axon Instruments), and stored on a personal computer system. Data were quantified with Axoscope software (Clampfit 10.0; Axon Instruments) to evaluate the slope of the fEPSP from 10-90% of the rising phase of the potential. All data were plotted using Datagraph 3 (Visual Data Tools, Inc.; Chapel Hill, NC), and are reported as % (+/- SEM) of the baseline (preconditioning) values. For analysis, data collected over 60 min post induction of plasticity were collected and the mean of the 2 responses evoked during each 1 min bin were used as the unit of analysis. Furthermore, mean fEPSP slope from each mouse averaged over 10-20 min post conditioning were used for any correlation analyses, as was mean fEPSP slope averaged over 40-50 min post conditioning.

Statistical Methods

To determine differences among groups for plasticity, a 3 (binned CGG repeat group) x 60 (min) repeated measures ANCOVA was performed for each of NMDA receptor dependent LTP and LTD, as well as mGluR1/5 dependent LTD. Experiment order and mouse age were included as covariates.

To further evaluate any differences in physiological measurements among CGG repeat groups, the mean level of LTP or LTD (fEPSP slope relative to

baseline) between 10-20 min post conditioning stimulus or DHPG application was evaluated by comparing CGG groups by ANCOVA with experiment order and mouse age as covariates, as was mean fEPSP slope 40-50 min post conditioning.

To elucidate a specific role for CGG repeat length modulation of any effects within the CGG KI mice, Pearson's correlation analyses were performed to determine the relationship of the mean fEPSP slope between min 10-20 and min 40-50 post induction with CGG repeat length in only the CGG KI mice.

Omnibus Statistical Methods

Hypothesis testing

Prior to statistical analyses, the data were tested for normalcy (Shapiro–Wilk test) and homoscedacity (Browne–Forsythe test). To account for any potential effects of order or multiple comparisons arising from performing ANCOVA and correlation analyses on four separate behavioral datasets as well as three plasticity datasets all collected from the same animals, a 3 (group) x 4 (task) multivariate analysis of covariance (MANCOVA) was performed with experiment order and mouse age as covariates. Main effects of the MANCOVA were characterized by individual ANCOVA. All results were considered significant at $\alpha \leq .05$ and $1 - \beta \geq .8$, and analyses were performed to determine observed power and effect size of all main effects. Statistical analyses were performed in R 2.13.1 language and environment (R Development Core Team, 2012) and statistical power was calculated using both R and the statistical program G*Power 3 (Faul,

Erdfelder, Buchner, & Lang, 2009; Faul, Erdfelder, Lang, & Buchner, 2007). All reported p values were adjusted for False Discovery Rate (FDR; Benjamini, Drai, Elmer, Kafkafi, & Golani, 2001) using a custom script written in R 2.13.1.

Unsupervised cluster analysis

Initial characterization and clustering of the data were performed using unsupervised hierachal clustering in R 2.13.1. Hierachal cluster analysis was performed to organize subjects into clusters such that subjects within a cluster are more “similar” to each other than they are to subjects in the other clusters based on a measure of their similarity/dissimilarity in behavioral and neurophysiological measurements and to show how the different clusters are related to each other. The process starts with each subject in a separate cluster and then combines the clusters sequentially, reducing the number of clusters at each step. At each stage, distances between clusters were computed by Ward’s linkage algorithm (*i.e.*, to minimize the increase in the mean error sum of squares; Ward, 1963). The dendograms were examined for separation or clusters relating to the three groups of CGG repeat length, Wildtype, Low CGG repeat, and High CGG repeat groups.

Support vector machines classification and validation

Further, support vector machines (SVM), a supervised machine learning technique, were performed to determine whether patterns in the behavioral and neurophysiological data can be interpreted as indications of the expansion of

CGG repeat length. SVM are linear classifiers that seek to find the optimal (*i.e.*, provides maximum margin) hyperplane separating groups using patterns of all measurements. The margin is defined as the distance between the hyperplane and the samples of the two classes (CGG KI vs. Wildtype) that are closest to the hyperplane among those being correctly classified. To assess the performance of the SVM classifier, iterative K-fold cross validation (10-fold, 5-fold, 3-fold, and leave-one-out cross validation) methods were used to estimate the accuracy of the classifier that predicts the group classification of a test sample. For k-fold cross validation (CV), the data set is randomly split into a training set for model construction and a test set for assessing predictive performance- this procedure is repeated, leaving out each test set at a time until all samples in the test set have been classified and then averaging the prediction error rates over all the possible test sets. For subsequent analyses the Wildtype mice were removed from the dataset and the analyses were repeated to verify that CGG KI mice could be correctly classified by CGG repeat length (*i.e.*, Low CGG repeat vs. High CGG repeat).

RESULTS

Multivariate analysis of covariance.

Prior to performance of any statistical analyses, it was determined that all individual data sets met the assumptions for the usage of parametric statistics; that is the data were normally distributed and homoscedastic. An omnibus MANCOVA demonstrated that there were no significant effects of experiment order for performance on behavioral tasks or measure of neural plasticity ($p_{(adj)}=.26$), nor were there effects for mouse age ($p_{(adj)}=.43$). There was a significant effect of CGG repeat group for experimental performance ($F(14,116)=47.57$, $p_{(adj)}<2e^{-16}$, $1-\beta=.98$). The main effect of group was characterized by individually evaluating each experiment and we are reporting p values corrected for multiple comparisons across all analyses using the false discovery rate procedure (Benjamini et al., 2001). Furthermore, there were no differences in structural integrity or cellular viability among hippocampal slices across groups that would have contributed to group differences in physiological measures. Table 10 provides a summary of statistical analyses.

Experiment	Wildtype	Low CGG (CGG 70-116)	High CGG (CGG 132-198)	P _(adj) value	Correlation with CGG repeat
Behavior:					
Coordinate	.65+/- .01	.56+/- .01	.48+/- .02	p _(adj) =3.9e-13	$\rho = -.71; R^2_{(adj)} = .51$
Categorical	.64+/- .01	.57+/- .01	.50+/- .02	p _(adj) =4.9e-9	$\rho = -.57; R^2_{(adj)} = .34$
Temporal	.65+/- .03	.56+/- .01	.11+/- .01	p _(adj) =1.2e-14	$\rho = -.77; R^2_{(adj)} = .60$
Novelty	.38+/- .03	.38+/- .03	.36+/- .02	p _(adj) =.96	$\rho = -.09; R^2_{(adj)} = .02$
Physiology:					
NMDAR LTD					
min 10-20	273.24+/-3.7%	248.22+/-6.4%	240.30+/-4.5%	p _(adj) =2.4e-15	$\rho = -.59; R^2_{(adj)} = .62$
min 40-50	189.31+/-18.9%	181.01+/-6.8%	169.79+/-14.3%	p _(adj) =.15	$\rho = -.10; R^2_{(adj)} = .09$
NMDAR LTD					
min 10-20	57.35+/-3.5%	76.23+/-3.7%	84.92+/-4.2%	p _(adj) =2.4e-15	$\rho = .74; R^2_{(adj)} = .46$
min 40-50	73.75+/-6.5%	78.01+/-5.6%	82.00+/-6.7%	p _(adj) =.45	$\rho = .02; R^2_{(adj)} = .01$
mGluR1/5 LTD					
min 10-20	48.65+/-4.0%	60.90+/-3.9%	74.28+/-3.2%	p _(adj) =2.4e-15	$\rho = .64; R^2_{(adj)} = .59$
min 40-50	85.75+/-6.6%	92.20+/-8.1%	85.01+/-10.24	p _(adj) =.54	$\rho = .05; R^2_{(adj)} = .03$

Table 10: Summary of Experimental Results. Mean (+/- Standard error of the mean) ratio values for behavioral experiments and mean (+/- SEM) % change in fEPSP slope relative to baseline for minutes 10-20 and minutes 40-50 post conditioning for Wildtype and CGG KI mice. Correlations between experimental performance and CGG repeat length within the CGG KI mice are also presented. All p values were adjusted for false discovery rate as were all R² values. See text for ratio value calculations.

Coordinate spatial processing

For the coordinate task, there was a significant main effect of CGG repeat group ($F(2,65)=51.56$, $p_{(adj)}=3.9e^{-13}$, $1-\beta=.98$), and no effect of task order among groups for this task ($F(4,65)=1.73$, $p_{(adj)}=.71$). Furthermore, there were no significant differences among groups for either locomotor behavior or object exploration during the 15 min habituation session (all $p_{(adj)}>.20$). Tukey's HSD post hoc pairwise comparisons demonstrated that the High CGG repeat group performed significantly worse than the Low CGG repeat group and Wildtype group (both $p_{(adj)}<.001$), and the Low CGG group performed worse than the Wildtype group ($p_{(adj)}<.01$).

To characterize any possible relationship between CGG repeat length and coordinate spatial processing in CGG animals with expanded CGG trinucleotide repeats, a correlation coefficient was calculated. A negative association was observed between the CGG trinucleotide repeat length and the ratio value during performance of the coordinate task (Fig 23A; corr $\rho=-.71$; $p_{(adj)}=1.7e^{-15}$, $R^2_{(adj)}=.51$), suggesting that the coordinate spatial processing is inversely related with the CGG repeat length.

Categorical spatial processing

For the categorical task, there was a significant main effect of CGG repeat group ($F(2,65)=30.17$, $p_{(adj)}=4.9e^{-9}$, $1-\beta=.97$), and no significant effect of task order among groups for this task ($F(4,65)=1.29$, $p_{(adj)}=.36$). Furthermore, there

were no significant differences among groups for either locomotor behavior or object exploration during the 15 min habituation session (all $p_{(adj)} > .30$). Tukey's HSD post hoc pairwise comparisons demonstrated that the High CGG repeat group performed significantly worse than the Low CGG repeat group and Wildtype group (both $p_{(adj)} < .001$), and the Low CGG group performed worse than the Wildtype group ($p_{(adj)} < .01$).

To characterize any possible relationship between CGG repeat length and categorical spatial processing in CGG animals with expanded CGG trinucleotide repeats, a correlation coefficient was calculated. A negative association was observed between the CGG trinucleotide repeat length and the ratio value during performance of the categorical task (Fig 23B; corr $p = -.57$; $p_{(adj)} = 5.79e^{-12}$, $R^2_{(adj)} = .34$).

Temporal ordering for visual objects

For the temporal ordering for visual objects task, there was a significant main effect of CGG repeat group ($F(2,65) = 61.33$, $p_{(adj)} = 1.2e^{-14}$, $1-\beta = .99$), and no effect of task order among groups for this task ($F(4,65) = 1.78$, $p_{(adj)} = .70$). Furthermore, there were no significant differences among groups for either locomotor behavior or object exploration during the three, 5 min object presentation sessions (all $p_{(adj)} > .25$). Tukey's HSD post hoc pairwise comparisons demonstrated that the High CGG repeat group performed significantly worse than the Low CGG repeat group and Wildtype group (both p

(adj)<.001), and the Low CGG group performed worse than the Wildtype group (p (adj)<.01).

To characterize any possible relationship between CGG repeat length and temporal ordering for visual object information in CGG animals with expanded CGG trinucleotide repeats, a correlation coefficient was calculated. A negative association was observed between the CGG trinucleotide repeat length and the ratio value during performance of the temporal ordering task (Fig 23C; corr $\rho = -.77$; $p_{(adj)}=3.2e^{-16}$, $R^2_{(adj)}=.60$).

Novelty detection for visual objects

For the visual object novelty detection task, there were no significant effect for CGG repeat group ($F(2,65)=.24$, $p_{(adj)}=.96$, $1-\beta=.99$), and no effect of task order among groups for this task ($F(4,65)=.16$, $p_{(adj)}=.93$). Furthermore, there were no significant differences among groups for either locomotor behavior or object exploration during the three, 5 min object presentation sessions (all $p_{(adj)}>.25$).

To verify there was no significant relationship between CGG repeat length and visual object novelty detection information in CGG animals with expanded CGG trinucleotide repeats, a correlation coefficient was calculated. No association was observed between the CGG trinucleotide repeat length and the ratio value during performance of the visual object novelty detection (Fig 23D; corr $\rho=-.09$; $p_{(adj)}=.5$, $R^2_{(adj)}=.02$).

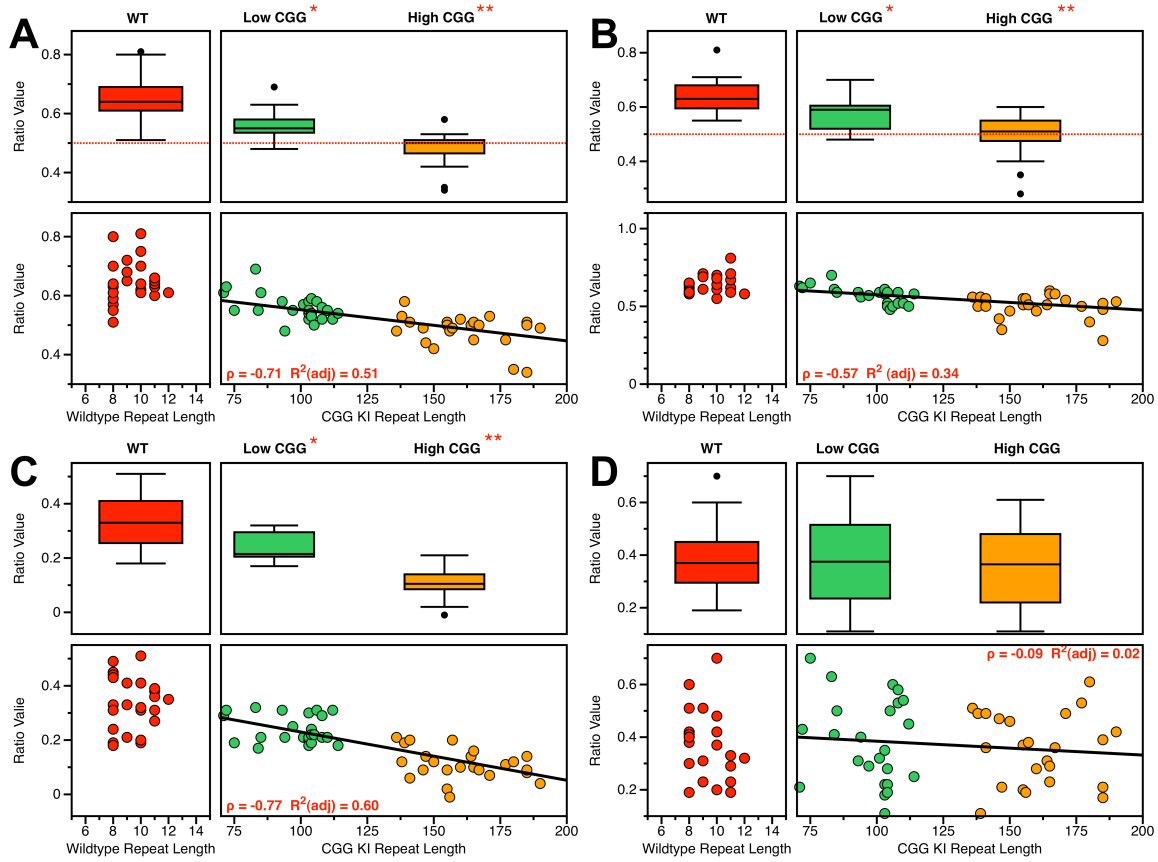


Figure 23. CGG repeats modulate behavior in CGG KI Mice. **A. Performance during the coordinate spatial information processing task.** All CGG KI mice performed more poorly than WT mice for this task, with High CGG repeat mice showing no re-exploration of moved objects. There is a strong negative relationship between CGG repeat length and behavioral performance, suggesting CGG repeat length modulates coordinate spatial processing. **B. Performance during the categorical spatial information processing task.** All CGG KI mice performed more poorly than WT mice for this task, with High CGG repeat mice showing no re-exploration of transposed objects. There is a strong negative relationship between CGG repeat length and behavioral performance, suggesting CGG repeat length modulates categorical spatial processing. **C. Performance during the temporal order for visual objects task.** All CGG KI mice performed more poorly than WT mice for this task. There is a strong negative relationship between CGG repeat length and behavioral performance, suggesting CGG repeat length modulates temporal processing. **D. Performance during the novelty detection for visual objects task.** All mice performed similarly on this task and there is no relationship between CGG repeat length and behavioral performance. * $p < 0.01$, ** $p < 0.001$. Red = WT, Green = Low CGG, Orange = High CGG.

NMDA receptor dependent Long Term Potentiation

For the NMDA receptor dependent LTP measures, there was a significant effect of both CGG repeat group ($F(2,4243)=197.14$, $p_{(adj)}=2e^{-16}$, $1-\beta=.96$), and 1 min time bin ($F(59,4243)=172.15$, $p_{(adj)}=2e^{-16}$, $1-\beta=.97$), as well as a significant group x bin interaction ($F(59,4243)=1.09$ $p_{(adj)}=.29$, $1-\beta=.98$) (Fig 24A). Further ANCOVA were performed to characterize these effects.

For the NMDA receptor dependent LTP, during min 10-20 there was a significant effect for CGG repeat group ($F(2,67)=297.53$, $p_{(adj)}=2.4e^{-15}$, $1-\beta=.99$), and no effect of task order among groups ($F(3,67)=.01$, $p_{(adj)}=.96$), mouse age ($F(3,67)=.13$, $p_{(adj)}=.85$), nor order in which each hippocampal slice was used ($F(2,67)=.06$, $p_{(adj)}=.91$). Tukey's HSD post hoc pairwise comparisons demonstrated that the High CGG repeat group has significantly less LTP than the Low CGG repeat group and Wildtype group (both $p_{(adj)}<.001$), and the Low CGG group had less LTP than the Wildtype group ($p_{(adj)}<.01$). However, during 40-50 min post conditioning there were no differences among the groups (all $p_{(adj)}>.15$).

To characterize the relationship between CGG repeat length and NDMA receptor dependent LTP in CGG animals with expanded CGG trinucleotide repeats, a correlation coefficient was calculated. A negative association was observed between the CGG trinucleotide repeat length and fEPSP slope during min 10-20, suggesting increasingly poor LTP as a function of CGG repeat length (Fig 24B; corr $\rho=-.59$; $p_{(adj)}<2.2e^{-16}$, $R^2_{(adj)}=.62$). No association was observed between the CGG trinucleotide repeat lengths and fEPSP slope during min

40-50, suggesting no effect of CGG repeat length on this later phase of plasticity (Fig 24C; corr $\rho=-.1$; $p_{(adj)}=.24$, $R^2_{(adj)}=.09$).

NMDA receptor dependent Long Term Depression

For the NMDA receptor dependent LTD, there was a significant effect of both CGG repeat group ($F(2,4243)=210.04$, $p_{(adj)}=2e^{-16}$, $1-\beta=.98$), and 1 min time bin ($F(59,4243)=104.82$, $p_{(adj)}=2e^{-16}$, $1-\beta=.99$), as well as a significant group x bin interaction ($F(59,4243)=150.01$ $p_{(adj)}=5.7e^{-9}$, $1-\beta=.98$) (Fig 24D). Further ANCOVA were performed to characterize these effects.

For the NMDA receptor dependent LTD, during min 10-20 there was a significant effect for CGG repeat group ($F(2,67)=184.59$, $p_{(adj)}=2.4e^{-15}$, $1-\beta=.97$), and no effect of task order among groups ($F(3,67)=1.72$, $p_{(adj)}=.86$), mouse age ($F(3,67)=.08$, $p_{(adj)}=.94$), nor order in which each hippocampal slice was used ($F(2,67)=1.10$, $p_{(adj)}=.83$). Tukey's HSD post hoc pairwise comparisons demonstrated that the High CGG repeat group has significantly greater LTD than the Low CGG repeat group and Wildtype group (both $p_{(adj)}<.001$), and the Low CGG group had greater LTD than the Wildtype group ($p_{(adj)}<.01$). However, during min 40-50 there were no main effects (all $p_{(adj)}>.45$).

To characterize the relationship between CGG repeat length and NMDA receptor dependent LTD in CGG animals with expanded CGG trinucleotide repeats, a correlation coefficient was calculated. A positive association was observed between the CGG trinucleotide repeat length and fEPSP slope during min 10-20, indicating increasing LTD as a function of CGG repeat length (Fig

24E; corr $p=.74$; $p_{(adj)}<2.2e^{-16}$, $R^2_{(adj)}=.46$). No association was observed between the CGG trinucleotide repeat lengths and fEPSP slope during min 40-50, suggesting no effect of CGG repeat length on this later phase of plasticity (Fig 24F; corr $p=.02$; $p_{(adj)}=.45$, $R^2_{(adj)}=.01$).

mGluR1/5 receptor dependent Long Term Depression

For the mGluR1/5 receptor dependent LTD measures, there was a significant effect of both CGG repeat group ($F(2,4243)=195.4$, $p_{(adj)}=2e^{-16}$, $1-\beta=.98$), and 1 min time bin ($F(59,4243)=301.57$, $p_{(adj)}=2e^{-16}$, $1-\beta=.99$), as well as a significant group x bin interaction ($F(59,4243)=160.88$, $p_{(adj)}=5.9e^{-9}$, $1-\beta=.95$) (Fig 24G). Further ANCOVA were performed to characterize these effects.

For the mGluR1/5 receptor dependent LTD, during min 10-20 there was a significant effect for CGG repeat group ($F(2,67)=203.21$, $p_{(adj)}=2.4e^{-15}$, $1-\beta=.97$), and no effect of task order among groups ($F(3,67)=.47$, $p_{(adj)}=.98$), mouse age ($F(3,67)=.55$, $p_{(adj)}=.91$), nor order in which each hippocampal slice was used ($F(2,67)=1.85$, $p_{(adj)}=.79$). Tukey's HSD post hoc pairwise comparisons demonstrated that the High CGG repeat group has significantly greater LTD than the Low CGG repeat group and Wildtype groups (both $p_{(adj)}<.001$), and the Low CGG group had greater LTD than the Wildtype group ($p_{(adj)}<.01$). However, during min 40-50 there were no main effects (all $p_{(adj)}>.54$).

To characterize the relationship between CGG repeat length and mGluR1/5 receptor dependent LTD in CGG animals with expanded CGG trinucleotide repeats, a correlation coefficient was calculated. A positive

association was observed between the CGG trinucleotide repeat length and fEPSP slope during min 10-20, indicating increasing mGluR1/5 receptor dependent LTD as a function of CGG repeat length (Fig 24H; corr $p=.64$; $p_{(adj)}<2.2e^{-16}$, $R^2_{(adj)}=.59$). No association was observed between the CGG trinucleotide repeat lengths and fEPSP slope during min 40-50, suggesting no effect of CGG repeat length on this later phase of plasticity (Fig 24I; corr $p=.05$; $p_{(adj)}=.39$, $R^2_{(adj)}=.03$).

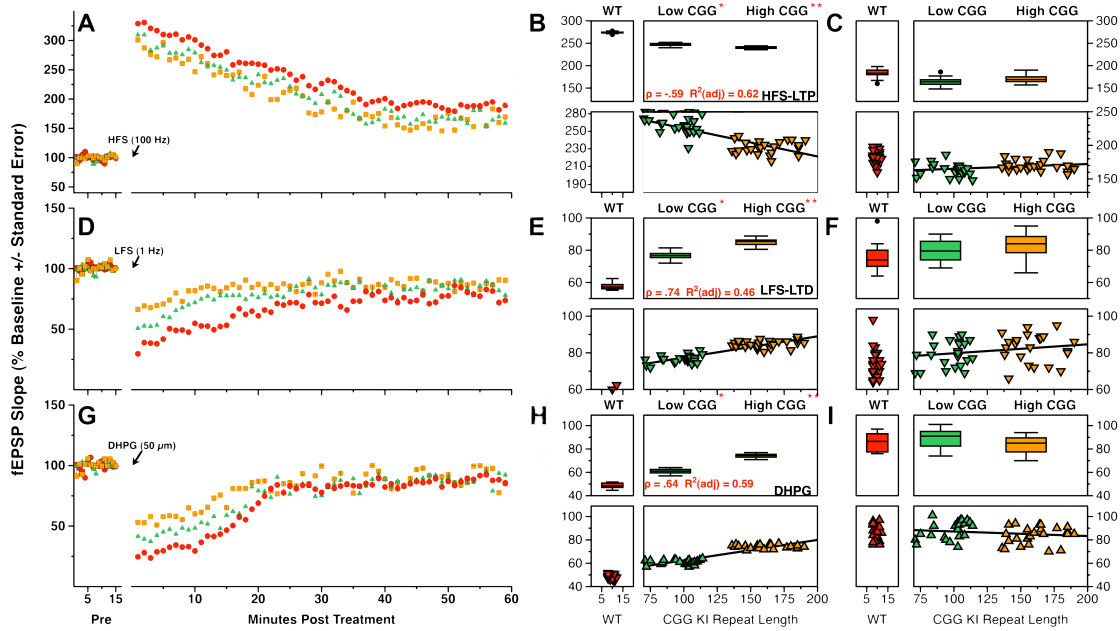


Figure 24. CGG repeats modulate neurophysiological responses in CGG KI Mice. **A.** fEPSP slope (% baseline) pre and post NMDA receptor dependent LTP induction. All CGG KI mice show reduced LTP induction than WT mice. **B.** fEPSP slope during min 10-20. There is a strong negative relationship between CGG repeat length and fEPSP slope, suggesting CGG repeat length negatively affects induction of NMDA receptor dependent LTP. **C.** fEPSP slope during min 40-50. There is no relationship between CGG repeat length and fEPSP slope, suggesting CGG repeat length does not affect expression of NMDA receptor dependent LTP once evoked. **D.** fEPSP slope (% baseline) pre and post NMDA receptor dependent LTD. All CGG KI mice show reduced induction of LTD than WT mice. **E.** fEPSP slope during min 10-20. There is a strong positive relationship between CGG repeat length and fEPSP slope, suggesting CGG repeat length negatively affects induction of NMDA receptor dependent LTD. **F.** fEPSP slope during min 40-50. There is no relationship between CGG repeat length and fEPSP slope, suggesting CGG repeat length does not affect expression of NMDA receptor dependent LTD once evoked. **G.** fEPSP slope (% baseline) pre and post mGluR1/5 receptor dependent LTD. All CGG KI mice show less LTD than WT mice. Insets are scaled traces demonstrating these differences. **H.** fEPSP slope during min 10-20. There is a strong positive relationship between CGG repeat length and fEPSP slope, suggesting CGG repeat length negatively affects induction of mGluR1/5 receptor dependent LTP. **I.** fEPSP slope during min 40-50. There is no relationship between CGG repeat length and fEPSP slope, suggesting CGG repeat length does not affect expression of mGluR1/5 receptor dependent LTD once evoked.* $p < 0.01$, ** $p < 0.001$. Red = WT, Green = Low CGG, Orange = High CGG.

Classification of mice by CGG repeat length using cluster analysis

Unsupervised hierachal cluster analysis was first performed to investigate whether CGG KI mice separated according to CGG repeat length. The dendograms based on the performance on behavioral and neurophysiological experiments showed clear separation between Wildtype and CGG KI mice into two distinct clusters (Fig 25A,B). Furthermore, within the CGG KI mouse cluster the Low CGG KI mice, defined as mice with 70-116 CGG repeats were perfectly separated into a unique cluster from the High CGG mice defined as mice having 132-198 CGG repeats. Furthermore, CGG KI mice were correctly grouped into similar CGG repeat length sub-clusters in the Low CGG repeat group and nearly correctly in the High CGG repeat group.

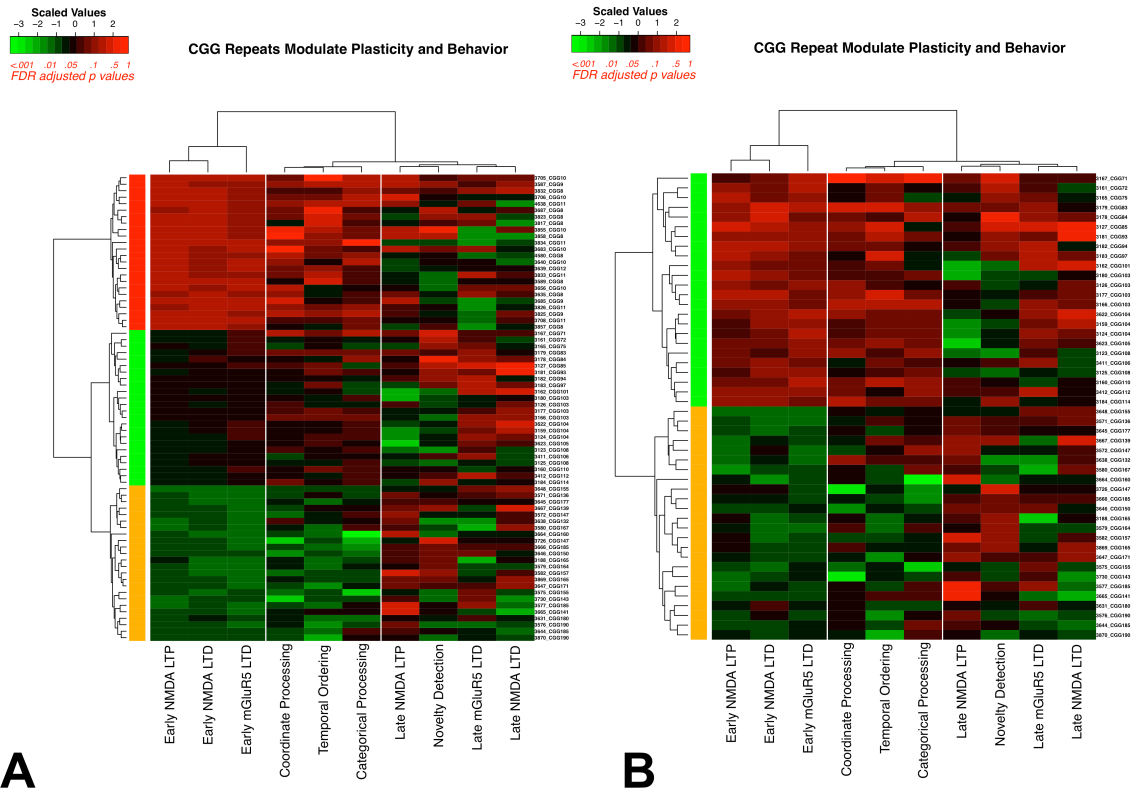


Figure 25. CGG repeat length directly modulates physiology and spatiotemporal performance. A. Predictive validity of classifier. Behavioral performance and physiological measures discriminate WT mice from CGG KI mice, and further discriminate CGG KI mice with 70-116 CGG repeats from CGG KI mice with 132-200 CGG repeats. The colored bars along the left correspond to animal group as arbitrarily defined by the unsupervised clustering algorithm and match the colors used for the plotted data in Figure 1. The dendrogram along the top demonstrates the relationships among experiments performed with these CGG KI mice. White bars were placed on the heatmap separating columns that belong to different clusters. **B. Predictive validity of classifier within CGG KI mice.** Early LTP/LTD refers to min 10-20 post induction. Late LTP/LTD refers to min 40-50 post induction. Bars along the right side of the heatmap correspond to group identity: Red = WT, Green = Low CGG, Orange = High CGG.

Identifying the groups of like experiments using cluster analysis

Similarly unsupervised hierachal cluster analysis was performed to identify patterns and clusters among the different experiments and express the data in such a way to highlight similarities and differences. The novelty detection task, appeared to have no correlation with the CGG repeat length, and was separated from the other behavioral tasks. From there, the coordinate spatial processing and temporal ordering for visual objects task placed in the same cluster and together segregated animals well according to the CGG repeat length grouping. The categorical spatial processing task was less correlated with not only the coordinate and temporal tasks, but also CGG repeat length. When WT mice were excluded from the analysis and only CGG KI mice were included, the same groupings emerged within the CGG KI mice as well as the task groupings. This observation suggests that there was distinct separation of the Low CGG repeat group cluster from the High CGG repeat cluster.

For the physiological data, NMDA receptor dependent LTP and LTD induction at min 10-20 were grouped into the same cluster, and showed similarities between them. mGluR1/5 dependent LTD induction at min 10-20 was more related to NMDA receptor dependent plasticity and the CGG repeat category than behavior, but their similarities to NMDA receptor dependent LTP and LTD induction was less profound. As mentioned above, all plasticity measures at 40-50 min post induction were non-predictive and were placed in the same cluster as the novelty detection behavioral task. These findings were

consistent when only the CGG KI mice were analyzed. Importantly, all measures of plasticity at min 10-20 were in a single larger cluster that was independent of all behavioral tasks and plasticity at min 40-50, which were placed in separate clusters by the analysis.

Prediction of sample classification of CGG KI mice by repeat length

The cluster analysis results showed differences between the CGG repeat groups and similarities of phenotypic profiles within a CGG repeat group (Figure 25B). Thus we investigated whether phenotypic values of experiments could make inference about CGG repeat length of CGG KI mice. SVM (Support Vector Machines) was carried out to derive a linear classifier comprised of task performance scores that can classify the CGG KI mice by repeat length (*i.e.*, Low CGG repeat vs. High CGG repeat) using a training set. The predictive performance of the linear classifier was validated using test samples.

When the classifier was developed based on scores for the coordinate spatial processing and temporal ordering, the classifier performed well with 92% accuracy based on iterative 5 fold CV (94% based on 10 fold CV; Figure 26B). When the categorical spatial task was added to the model, a poor classification was attained as expected due to the lack of separation between the coordinate spatial processing and temporal ordering task and categorical spatial task as shown in clustering, only classifying 69% of the CGG KI mice correctly based on iterative 5-fold CV (71% based on 10 fold CV; Figure 26A). With inclusion of the WT mice, the model improved the classification of the CGG KI mice using the

coordinate and temporal order experiments to 98% accuracy, but adding the categorical task into the model still reduced the predictive power of the model to 75% accuracy based on 5 fold CV (78% based on 10 fold CV). Addition of the novelty detection task resulted in a large decrease in predictive value of the model, resulting in correct classification of only 44% of the mice based on 5 fold CV (48% based on 10 fold CV; data not shown).

In the case where the coordinate and temporal order tasks were used to correctly classify the CGG KI mice by repeat group 92% of the time, the four misclassified mice into the Low CGG repeat group were the four mice with the lowest number of CGG repeats (132, 136, 138, and 141 CGG repeats) in the High CGG repeat group. In no cases were mice from the Low CGG repeat group misclassified as High CGG repeat mice. In cases where 5 fold and 10 fold CV provide different results for the classification, the mouse with 141 repeats was correctly classified into the High CGG repeat group by iterative 10 fold CV, while 5 fold CV misclassified this mouse into the Low CGG repeat group. Iterative three-fold CV and leave one out CV all gave the same classifications as 5 fold CV for all classifications.

When the classifier was developed based on scores for the NMDA receptor dependent LTP and LTD induction measures at min 10-20 and 40-50, the classifier performed with 100% accuracy based on iterative 5 fold CV (100% based on 10 fold CV; Figure 26C). When the mGluR1/5 dependent LTD was added to the model, the classifications did not change, still classifying mice into

CGG repeat groups with 100% accuracy based on iterative 5-fold CV (100% based on 10 fold CV; Figure 26D).

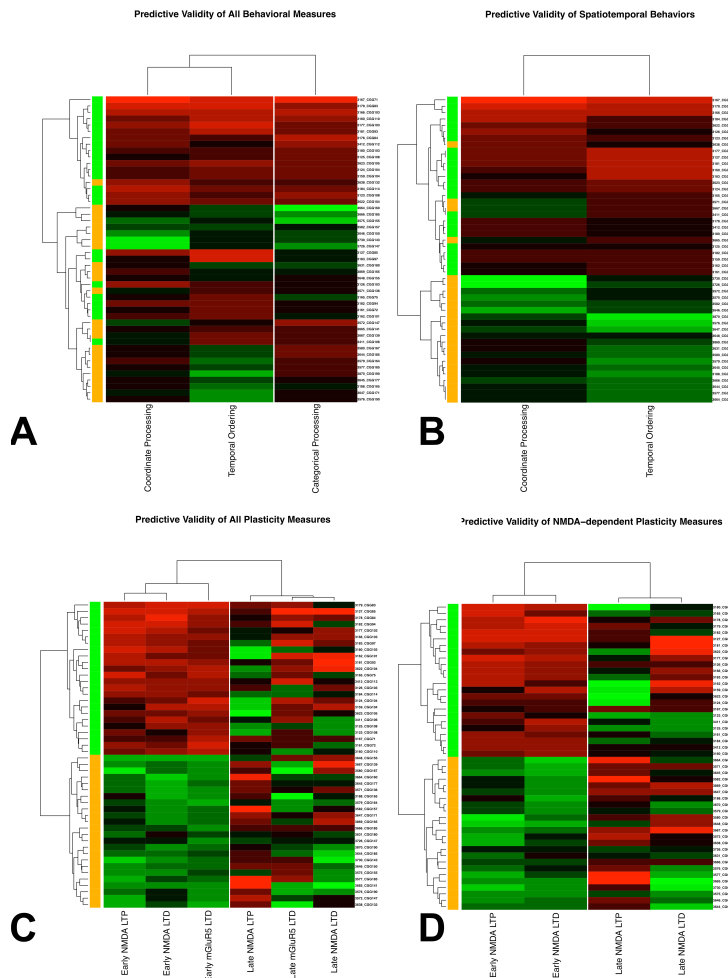


Figure 26. Physiology and spatiotemporal behavioral performance can be used to predict CGG repeat length. **A.** Behavioral measures including the temporal ordering, coordinate and categorical processing task was only able to classify the CGG repeat groups with 69% accuracy, however **B.** the cluster containing coordinate spatial processing and temporal ordering tasks alone, excluding the categorical task, improved the performance of the classifier to 92% accuracy. **C.** All plasticity measures were able to correctly classify mice by CGG repeat length, and **D.** even just the NMDA receptor dependent physiological measures were sufficient to correctly classify CGG KI mice. All classification based on 5 fold cross validation. Early LTP/LTD refers to min 10-20 post induction. Late LTP/LTD refers to min 40-50 post induction. Bars along the right side of the heatmap correspond to group identity: Green = Low CGG, Orange = High CGG.

DISCUSSION

Previous analyses of CGG KI mouse cognitive function have been unable to conclusively determine any direct relationships between CGG repeat length and cognitive function due to insufficient sample size and incomplete coverage of the premutation range (*i.e.*, 70-200 repeats; Diep et al., 2012; Hunsaker et al., 2009; Hunsaker et al., 2010; Hunsaker et al., 2011c). The behavioral results previously reported in the CGG KI and CGG-CCG mice, unfortunately, did not directly model the reports in carriers of the premutation (Qin et al., 2011; Van Dam et al., 2005).

In fact, only few reports in the human premutation have been able to demonstrate similar relationships between genetic dosage and neurocognitive function, but were limited by a confined CGG repeat ranges and a wide range of ages in their studies (CGG range 67-143 repeats, age range 21-42 years of age; Goodrich-Hunsaker et al., 2011a; Goodrich-Hunsaker et al., 2011b; Goodrich-Hunsaker et al., 2011c). The present report overcomes this challenge and provides clear evidence for a linear inverse relationship between cognitive function and CGG repeat length in CGG KI mice at a single time point (9 mo of age). Specifically, the CGG KI mice showed CGG repeat length modulated deficits for spatial and temporal processing, but spared novel object detection (Fig 23). These data argue for specific impairments in spatiotemporal processing with intact sensory/perceptual function, suggesting impaired spatial and temporal pattern separation underlie some cognitive dysfunction in the premutation (*cf.*, Johnson-Glenberg, 2008; Simon, 2011).

Furthermore, the CGG KI mice had CGG repeat length modulated reductions in NMDA receptor dependent LTP and LTD induction, as well as mGluR1/5 dependent LTD induction at the Schaffer collateral synapse (*i.e.*, by generally reducing induction, but not expression, of neuronal plasticity in the hippocampus; Fig 24). Importantly, as induction, but not expression, of both NMDA and mGluR1/5 dependent plasticity appear to be similarly disrupted by increasing CGG repeat lengths, it appears likely that the observed reductions in plasticity induction resulted from a general disruption of neuronal function, as opposed to effects selectively acting upon one receptor system over another, as has been described in FXS (*e.g.*, mGluR1/5 LTD enhancement; Bear, Huber, & Warren, 2004). Furthermore, it has recently been demonstrated that the CGG KI mouse shown a small but significant reduction in dendritic complexity as well as spine density in pyramidal neurons of visual cortex (Berman, Murray, Arque, Hunsaker, & Wenzel, 2012), and a similar trend appears in CA1 pyramidal neurons (unpublished observations). These dendritic abnormalities may underlie the reduced plasticity observed in CGG KI mice relative to wildtype littermate animals. These data support models that propose elevations in *Fmr1* mRNA underlie premutation neuropathology as *Fmr1* mRNA expression scales linearly with CGG repeat length across the premutation range, whereas Fmrp levels show significant reductions only as the CGG repeat lengths approach 200 (Brouwer et al., 2008a; Hoem et al., 2011; Jin et al., 2003; Raske & Hagerman, 2009; Tassone et al., 2008). Alternate possibilities are that the effects of mitochondrial dysfunction in the premutation (Napoli et al., 2011; Ross-Inta et al.,

2010) or some unknown metabolic or physiological abnormality in neurons reduces neuronal viability *in vitro* (Chen et al., 2010).

To better characterize the utility of the behavioral tasks and measures of plasticity to separate CGG KI mice into groups corresponding to CGG repeat length, a hierachal cluster analysis was performed using only the physiological and behavioral data and shown in Fig 25. The CGG KI mice were separated into two groups corresponding to mice with 70-116 CGG repeats in one group (Low CGG; green in all figures) and mice with 132-198 CGG repeats in the second group (High CGG; orange in all figures). Again it must be mentioned that these CGG repeat groupings emerged in the mouse colony through breeding, and do not reflect different states among human fragile X premutation carriers so far as has been reported. Furthermore, when all experiments were included in the clustering, the CGG KI mice were correctly grouped according to CGG repeat length within the Low CGG repeat group, but less so in the High CGG repeat group.

The classification analysis suggest that a mouse's performance on these spatiotemporal processing tasks and measures of plasticity are sufficient to classify CGG KI mice by CGG repeat length within the premutation length to 92% accuracy based on 5 fold cross validation (CV; Fig 25B). In other words, these experiments serve as a behavioral endophenotype that can be used to determine the severity of the PM, at least in the CGG KI mouse model. Intriguingly, the two behavioral tasks demonstrating the highest predictive validity (coordinate and temporal ordering tasks) were also the tasks demonstrated previously to require

fine-scale spatial or temporal attention/pattern separation processes shown to require hippocampal integrity (Goodrich-Hunsaker et al., 2005; Goodrich-Hunsaker et al., 2008b; Kesner et al., 2004; Rolls & Kesner, 2006). The categorical task has been shown to depend primarily upon the neocortex and utilizes a more coarse level of spatial processing (Goodrich-Hunsaker et al., 2005; Hunsaker et al., 2009), and the novelty detection task (which proved non-predictive) depends upon a distributed network involving rostral and rhinal cortices (Cowell, Bussey, & Saksida, 2010; McTighe, Mar, Romberg, Bussey, & Saksida, 2009).

Together these findings suggest the feasibility of developing a behavioral endophenotype that can be used to predict cognitive dysfunction in CGG KI mice. More to the point, it appears that a focus on tasks evaluating spatial and temporal pattern separation can be used to classify the CGG KI mice by repeat lengths with 92% certainty. Inclusion of performance measures from tasks that do not emphasize spatial or temporal attention/pattern separation (*i.e.*, categorical spatial processing and novelty detection) do not contribute to the classification. This hypothesis is supported by the classification analyses, which demonstrate clearly that spatiotemporal processing and measures of synaptic plasticity are sufficient to predict dosage of the premutation in the CGG KI mice. Evidence for a direct effect of the dosage or size of the premutation on behavioral and neurophysiological measures is the definition of an endophenotype (Gottesman & Gould, 2003; Hunsaker et al., 2012; Hunsaker, 2012b).

It is important to state the categorical task was useful to clearly separate CGG KI mice from Wildtype mice, but proved to be unsuitable to classify CGG KI mice by CGG repeat lengths. What these data suggest is that the coordinate spatial processing and temporal ordering tasks were not only predictive to classify Wildtype mice from CGG KI mice, but critically, the performance on these tasks was directly modulated by the length of the CGG trinucleotide repeat. These data support the spatiotemporal hypergranularity model (Hunsaker et al., 2012; Hunsaker, 2012b; Simon, 2008; Simon, 2011), that posits specific impairments to spatial and temporal attention. As such, an emphasis on behavioral tasks evaluating fine-scale spatial and temporal attention (or pattern separation; Aimone, Deng, & Gage, 2011; Hunsaker et al., 2012; Hunsaker, 2012b; Yassa & Stark, 2011), may be perfectly suited to quantifying the fundamental cognitive disruptions observed in the CGG KI mouse model of the premutation.

Although beyond the scope of the present study, the addition of tasks involving a high demand for attention or executive function may improve the behavioral endophenotype reported here (Johnson-Glenberg, 2008; Simon, 2011). Furthermore, these results serve only to provide preliminary support for a behavioral endophenotype in the CGG KI mouse model of the fragile X premutation. Besides executive function, affect, response, social behaviors, and anxiety domains remain untested in the CGG KI mice. Such data would provide more information toward a pattern of not only weaknesses, but also neurocognitive strengths that are modulated by CGG repeat lengths.

Furthermore, the present study was unable to elucidate the mechanisms underlying the impaired induction of synaptic plasticity with concomitantly spared expression of evoked plasticity. Further research is necessary to provide answer these questions and uncover the mechanisms by which increasing CGG repeats affect plasticity and cognitive function.

The present experiment provides the first clear demonstration of a CGG repeat length dependent decline in cognitive function in the premutation across virtually the full extent of premutation CGG repeat lengths. Measures of synaptic plasticity and behavioral tasks requiring spatial and temporal attention were sufficient to classify CGG KI mice by CGG repeat length, even correctly predicting actual CGG repeat length. These data provide a physiological and behavioral biomarker in CGG KI mice that may be used as an outcome measure for studies into treatment options for the premutation or else to predict disease severity or eventual progression toward a neurodegenerative trajectory.

Chapter 11

Spatiotemporal Processing Deficits in Female CGG KI Mice Modeling the Fragile X Premutation.

ABSTRACT

The fragile X premutation is a tandem CGG trinucleotide repeat expansion in the fragile X mental retardation 1 (*FMR1*) gene between 55 and 200 repeats in length. A CGG knock-in (CGG KI) mouse has been developed that models the neuropathology and cognitive deficits reported in fragile X premutation carriers. It has been suggested that carriers of the premutation demonstrate a spatiotemporal hypergranularity, or reduced resolution of spatial and temporal processing. A temporal ordering of spatial locations task was used to evaluate the ability of CGG KI mice to process temporal and spatial information with either high or low levels of spatial interference. The results indicate that CGG KI mice showed difficulty performing the novelty detection task when there were high levels of spatial interference, but were able to perform the novelty detection task when there was low spatial interference. These data suggest that CGG KI mice show spatial and temporal pattern separation deficits that are modulated by the dosage of the *Fmr1* gene mutation, such that when behavioral tasks require mice to overcome high spatial or temporal interference, the CGG KI mice perform increasingly poorly as the CGG repeat length increases.

This chapter has been published as:

Rachel M. Borthwell, Michael R. Hunsaker, Rob Willemsen, Robert F. Berman. (2012). Spatiotemporal Processing Deficits in Female CGG KI Mice Modeling the Fragile X Premutation. Behavioural Brain Research. In press.

My role in this study was study design, development of the apparatus, piloting experiments, supervising Rachel Borthwell in performing the actual experiments, and data analysis.

INTRODUCTION

Fragile-X Associated Tremor/Ataxia Syndrome (FXTAS) is a late onset neurodegenerative disease resulting from a tandem CGG trinucleotide repeat expansion between 55 and 200 in the 5' untranslated region of the fragile X mental retardation 1 gene (*FMR1*) called the fragile X premutation (Leehey & Hagerman, 2012). Though not all carriers of the fragile X premutation develop FXTAS, it is estimated that 40% of male and 16% of female premutation carriers develop FXTAS (Leehey et al., 2007b). Clinical manifestations of FXTAS include intention tremor, gait ataxia, and Parkinsonism, along with post-mortem presence of eosinophilic, ubiquitin positive intranuclear inclusions in neurons and astrocytes throughout the brain (Leehey & Hagerman, 2012; Leehey et al., 2007b).

Where it was previously thought that fragile X premutation carriers were cognitively unaffected by the mutation, a growing body of evidence now demonstrates a spectrum of neurocognitive impairment (Grigsby et al., 2008; Hessl et al., 2007; Hessl et al., 2011; Keri & Benedek, 2009; Keri & Benedek, 2010; Keri & Benedek, 2011; Keri & Benedek, 2012; Lachiewicz et al., 2006). Despite this debate, studies into cognitive effects of the fragile X premutation reveal an association between the length of CGG repeat expansion with genetic dosage or CGG repeat length. Goodrich-Hunsaker et al. (2011a, 2011b, 2011c) reports genetically modulated cognitive performance on spatial and numerical magnitude comparison tasks using asymptomatic female fragile X premutation carriers between 21-42 years of age. Similarly, results from an attentionally

based enumeration task also demonstrated some slight, but significant impairments in numerical cognition related to genetic dosage (Goodrich-Hunsaker et al., 2011b). These studies along with previous results in male fragile X premutation carriers implicate cognitive deficits across several domains: including working memory, executive function memory, and arithmetic processing (cf., Bourgeois et al., 2009; Goodrich-Hunsaker et al., 2011a; Goodrich-Hunsaker et al., 2011b; Grigsby et al., 2008; Hashimoto et al., 2011; Hessl et al., 2007; Hessl et al., 2011). In order to better understand the extent and nature of neurocognitive impairments in the fragile X premutation, the behavior of a CGG knock-in (CGG KI) mouse model of the fragile X premutation has been evaluated. In accordance with human carriers of the fragile X premutation, the CGG KI mice develop intranuclear inclusions throughout the brain (Wenzel et al., 2010; Willemse et al., 2003). Recent studies report both temporal ordering deficits and visuomotor impairments in female CGG KI mice modeling the fragile X premutation, with the latter displaying a correlation with CGG repeat length (Diep et al., 2012; Hunsaker et al., 2009; Hunsaker et al., 2010). These results are consistent with reports of genetic dosage modulating neurocognition among premutation carriers (Goodrich-Hunsaker et al., 2011a; Goodrich-Hunsaker et al., 2011b; Goodrich-Hunsaker et al., 2011c; Koldewyn et al., 2008).

In a review of neurocognitive impairments in space, time, and number processing in children with neurodevelopmental disorders such as fragile X-associated disorders (*i.e.*, fragile X syndrome and the fragile X premutation) and the 22q11.2 deletion syndrome, (Simon, 2007, 2008, 2011) proposed a

spatiotemporal hypergranularity underlies deficits present across the spatial and temporal domains. Recently, Hunsaker (Hunsaker, 2012a, 2012b) has extended this theory into research into mouse models of neurodevelopmental genetic disease and showed it was consistent with the spatial processing and temporal ordering deficits observed in male and female CGG KI mice.

More specifically, the spatiotemporal hypergranularity proposed to underlie spatiotemporal dysfunction in CGG KI mice stems from abnormal development of neural networks that underlie spatial and temporal attention; namely the hippocampus, parietal cortex, and rostral cortices. As the premutation is present at development, these mice have abnormal neural circuitry that process spatial and temporal relationships among stimuli in a suboptimal manner. What this theory proposes is that for a CGG KI mouse to discriminate among spatial stimuli they need to be separated in space more than a wildtype mice needs to make the same discrimination. Similarly, temporal relationships among stimuli need to have a greater separation than wildtype mice require to make the temporal judgment. This can be conceptualized as a reduction of resolution in spatial and temporal processing capabilities. These spatial and temporal judgments have been proposed to be similar in nature to the spatial and temporal pattern separation processes that act to minimize spatial and temporal interference to allow for efficient encoding of stimuli (Rolls & Kesner, 2006; Simon, 2008, 2011).

In order to specifically evaluate spatiotemporal processing deficits in CGG KI Mice, female CGG KI mice heterozygous for the fragile X premutation were tested for their ability to process the temporal order in which objects occupying

specific spatial locations were presented (Hunsaker & Kesner, 2008; Hunsaker et al., 2008a; Hunsaker et al., 2009; Hunsaker et al., 2010). The paradigm chosen has been shown to evaluate the temporal processing of spatial information--which has been shown to be subserved by different neural networks than temporal processing of simple object information (Hunsaker & Kesner, 2008; Hunsaker et al., 2008a). We hypothesize that a spatial hypergranularity resulting from suboptimal spatial pattern separation accounts for any inability to perform a spatial novelty detection tasks when very high levels of spatial interference must be overcome; and a temporal hypergranularity resulting from suboptimal temporal pattern separation accounts for impaired temporal ordering for spatial locations in cases of very low spatial interference. Taken together, these deficits compound to result in a spatiotemporal hypergranularity, impairing the ability of the CGG KI mice to efficiently process a temporal order for spatial locations. We further hypothesize that CGG KI mice will be able to perform spatial novelty detection tasks when the levels of spatial interference are minimal, suggesting intact spatial memory function.

The results for the present study support our initial hypotheses: female CGG KI mice heterozygous for the fragile X premutation showed hypergranular spatial and temporal processing (*i.e.*, reduced memory resolution) that resulted in inefficient encoding or retrieval of spatiotemporal relationships required for task performance, but showed intact spatial memory.

MATERIALS AND METHODS

Mice

Sixteen female CGG KI mice heterozygous for the fragile X premutation at 6 months of age (n=8 Low CGG repeat (CGG 77-110); n=8 High CGG repeat (CGG 145-194)) and eight female wildtype mice (CGG 8-12) of the same age were used as subjects for this task. All wildtype mice were littermates with CGG KI mice included in the study. All CGG KI mice were bred onto a congenic C57BL/6J background over >12 generations from founder mice on a mixed FVB/N x C57BL/6J background (Willemse et al., 2003). Mice were housed in same sex, mixed genotype groups with three to four mice per cage in a temperature and humidity controlled vivarium on a 12 h light-dark cycle. Mice had ad libitum access to food and water throughout experimentation. Mouse weights did not differ among genotypes throughout experimentation. All experiments were conducted during the light phase of the diurnal cycle. The experiment were conducted under University of California, Davis approved IACUC protocols.

Genotyping

Genotyping was carried out upon tail snips. DNA was extracted from mouse tails by incubating overnight at 55°C with 10 mg/mL Proteinase K (Roche Diagnostics; Mannheim, Germany) in 300 µL lysis buffer containing 50 mM Tris-HCl, pH 7.5, 10 mM EDTA, 150 mM NaCl, 1% SDS. One hundred µL saturated NaCl was then added and the suspension was centrifuged. One volume of 100% ethanol was added, gently mixed, and the DNA was pelleted by centrifugation

and the supernatant discarded. The DNA was washed and centrifuged in 500 μ L 70% ethanol. The DNA was then dissolved in 100 μ L milliQ-H₂O. CGG repeat lengths were determined by PCR using the Expanded High Fidelity Plus PCR System (Roche Diagnostics). Briefly, approximately 500–700 ng of DNA was added to 50 μ L of PCR mixture containing 2.0 μ M/L of each primer, 250 μ M/L of each dNTP (Invitrogen; Tigard, OR), 2% dimethyl sulfoxide (Sigma-Aldrich; St. Louis, MO), 2.5 M Betaine (Sigma-Aldrich), 5 U Expand HF buffer with mg (7.5 μ M/L). The forward primer was 5'-GCT CAG CTC CGT TTC GGT ACT TCC GGT-3' and the reverse primer was 5'-AGC CCC GCA CTT CCA CCA CCA GCT CCT CCA-3'. PCR steps were 10 min denaturation at 95°C, followed by 34 cycles of 1 min denaturation at 95°C, annealing for 1 min at 65°C, and elongation for 5 min at 75°C to end each cycle. PCR ends with a final elongation step of 10 min at 75 °C. DNA CGG repeat band sizes were determined by running DNA samples on a 2.5% agarose gel and staining DNA with ethidium bromide [7,10]. For female CGG KI mice heterozygous for the fragile X premutation there were two bands present, one corresponding to the wildtype allele (CGG repeat length 8-12), and another corresponding to the expanded premutation allele (CGG repeat length 70-200). For wildtype mice, only the wildtype allele was present. Genotyping was performed twice on each mouse, once using tail snips taken at weaning and again on tail snips collected at sacrifice. In all cases the genotypes matched.

Behavioral Apparatus

For this experiment, a white square Plexiglas box was used measuring 70 cm on all sides, and 40 cm in height. A digital camera was positioned over the box capturing an overhead view of the experimental set-up. Different, distinctive geometric shapes were placed on the walls as spatial cues to help spatially orient the mice. These cues were placed slightly off center on each of the walls. Two identical cylindrical or conical objects measuring 4-7 cm in diameter and 11-15 cm in height were chosen and set in distinct spatial locations during experimentation for each task. Different pairs of identical objects were used for each task. Objects placed in different spatial locations were placed approximately 5 cm from each wall or corner of the box. This distinct placement of the object allowed for complete circumnavigation of the object by the mouse. The apparatus and experimental parameters were modified from a task developed for use in rats (Hunsaker & Kesner, 2008; Hunsaker et al., 2008a). At the start of each experiment, the box was thoroughly wiped down using 70% ethanol to dilute and spread out any unwanted odors.

Experimental Methods

The order of experiments was pseudorandomized for all mice to control for any effects of task order influencing behavioral performance. Two experimenters independently scored the data blinded to mouse genotype from the digital recordings. A computerized tracking system (ANY-Maze v4.3; Stoelting Co.; Wood Dale, IL) collected locomotor activity from the videos.

Temporal Order for Spatial Locations (Figure 27A).

For this experiment a mouse was then placed in the lower left hand corner of the box, as viewed from above, and allowed to explore a cylindrical or conical object placed in the first spatial location (location 1). At the end of 5 min, a blue plastic rectangular container measuring 7.5 cm in length, 7.5 cm in height, and 7.5 cm in width was used to cover the mouse and slowly moved until positioned in the original starting point. This method was used rather than removing the mouse between each session to reduce stress and/or anxiety responses in the mouse that may mask behavioral performance. A 5 min intersession period followed. The blue container was then removed and the mouse was allowed to explore the same object in the second spatial location (location 2) for another 5 min. The mouse was covered once more and moved to the original starting point for a 5 min intersession interval before being allowed to explore the object in the last spatial location for 5 min (location 3). Once the mouse had explored the object in all three spatial locations, the mouse was covered with the blue plastic rectangular container for 10 min. For the test phase, the mouse was presented with two identical objects, one placed in the first spatial location (location 1) and the other in the third spatial location (location 3) along opposite walls of the apparatus for 5 min. The distance between the objects measured 80 cm. The start location of each mouse was determined such that the starting location for each mouse was equidistant from the first and third locations during the test session. Mouse performance was video recorded and was later assessed using the videos acquired during each trial. For each mouse, time

spent in active exploration (*i.e.*, sniffing, touching) with the object was recorded, and total locomotor activity was collected. It was determined that when mice climbed, stood, or sat upon an object was not considered exploratory activity.

Novelty Detection for Spatial Location with High Spatial Interference (Figure 27B).

The three locations were presented the same way as in the temporal ordering for spatial locations task, but with a different object pair that the mice had never previously encountered. However, during this high interference novelty test, the familiar spatial location (location 1) and the novel spatial location (location 4) were located very near each other (along adjacent walls of the apparatus). The distance between the objects measured 35 cm, less than half the distance apart as the temporal ordering test. Conceptually, this testing procedure results in increased spatial interference between the two spatial locations occupied by the identical objects. For this task, the start location for each mouse was adjusted so the start location for all mice during the last session was equidistant from the familiar and novel spatial location.

Novelty Detection for Spatial Location with Low Spatial Interference (Figure 27C).

The location presentations were presented similarly to the temporal ordering for spatial locations task, but using a different object pair the mice had never previously encountered with the following modification: The locations were

chosen so that the familiar and novel spatial locations used during the test session were along opposite walls of the apparatus. This larger spatial separation was the same separation as the temporal ordering test, and a greater separation than the high spatial interference test (*cf.*, Figure 27B). This modification was used to reduce spatial interference among the locations. The distance between the objects measured 80 cm, and was the same as during the temporal ordering for spatial locations test. The start location of each mouse was determined such that the starting location for each mouse was equidistant from the familiar and novel spatial locations during the test session.

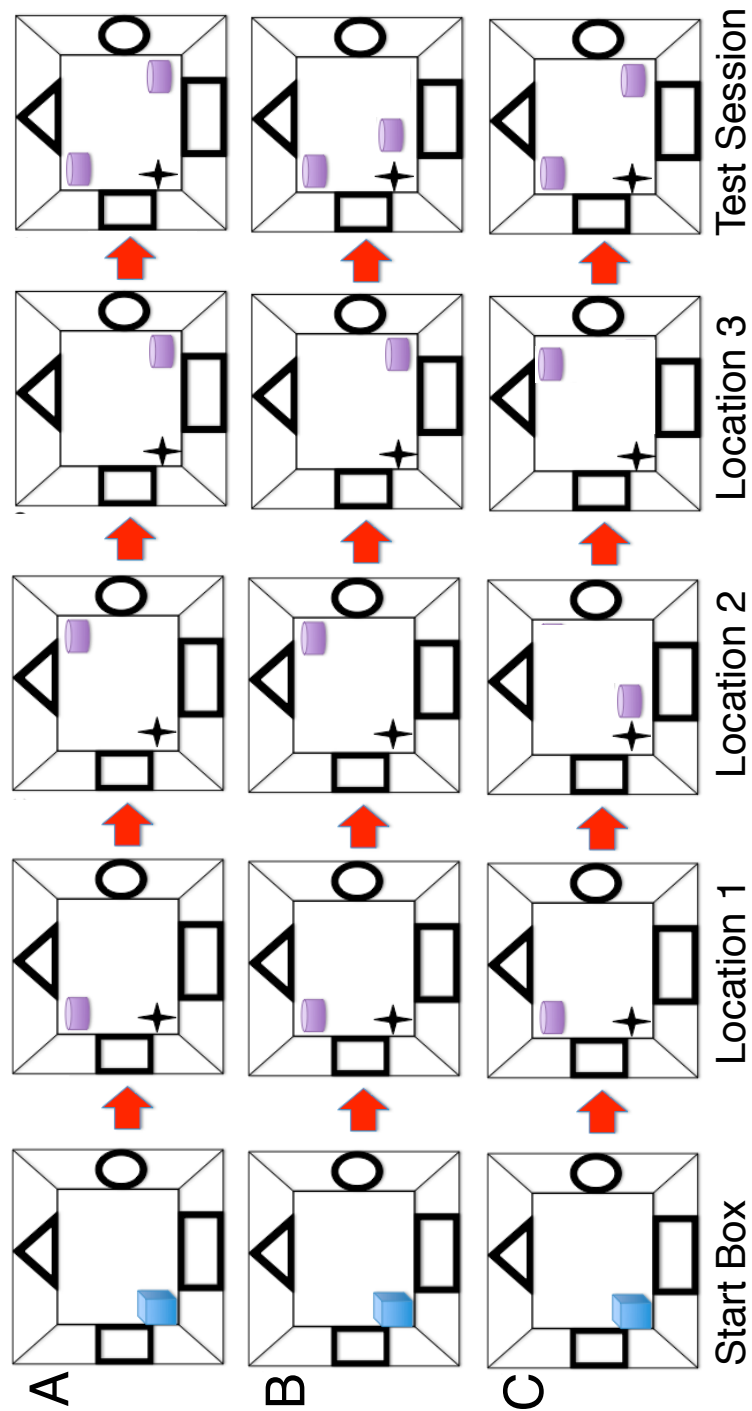


Figure 27. Experimental Apparatus and Task Design. **A.** Temporal Ordering for Spatial Locations **B.** Novelty Detection for Spatial Locations with High Spatial Interference. **C.** Novelty Detection for Spatial Locations with Low Spatial Interference.

Dependent measures

For the temporal ordering and novelty detection for spatial locations tasks, spatial location exploration was defined as active physical contact with the object in the spatial location using the forepaws, whiskers or nose. With this definition, standing near an object without interacting with it would not be counted as exploration, nor would standing or sitting upon an object. To control for differences in exploration levels between mice, exploration during the temporal ordering test sessions was converted into a ratio score to constrain the values between -1 and 1. The ratio was calculated as follows: (exploration in location 1 – exploration in location 3)/(exploration in location 1 + exploration in location 3). Exploration during the novelty detection test sessions was similarly converted into a ratio score, using exploration of the object in location 1 and an object in the novel location 4 in the calculation: (exploration in novel location 4 – exploration in location 1)/(exploration in location 1 + exploration in novel location 4).

A ratio value near 1 means that the mouse showed more exploration of the first location presented in the temporal ordering task. A score near -1 suggests the mouse preferentially explored the last location presented. A score near 0 reflects equal exploration of spatial locations indicating a failure to detect or retrieve the temporal order of spatial locations.

In the novel location tests, a score approaching 1 would indicate a preferential exploration for the novel location, and therefore intact spatial novelty detection, a score approaching -1 indicated preferential exploration for the object

in location 1, also indicating memory for the first spatial location. A score near 0 would indicate equal exploration for the familiar and novel locations, suggesting that either an excess of interference at retrieval or forgetting had occurred as reflected in a failure to discriminate between the locations (Hunsaker & Kesner, 2008). As a measure of general activity levels, locomotor activity was collected by an overhead tracking system and confirmed by experimenters recording the number of crossings of a 3×3 grid overlaid on the video (*cf.*, Hunsaker & Kesner, 2008; Hunsaker et al., 2008a).

Statistical methods

Locomotor activity was analyzed using a 3 (binned CGG repeat group: wildtype, Low CGG repeat (CGG 77-110), High CGG repeat (CGG 145-194)) \times 4 (session) repeated measures ANOVA. Object/Location exploration data from each session were analyzed with 3 (CGG repeat group) \times 3 (session) repeated measures ANOVA to verify that mice explored all the locations similarly during the study sessions to verify that unequal exploration would not confound measures of temporal ordering. Prior to comparing CGG KI mice and wildtype mice for the ratio scores, it was verified that the ratio score for the wildtype mice was $\neq 0$ via a one-tailed t-test against the null hypothesis of a ratio score = 0 to verify preferential exploration of the first location during the temporal order test and novel location during the novelty tests.

Exploration data that were converted to ratio values were analyzed by one-way ANOVA with experiment order as a covariate. To more fully characterize

any differences among groups, Tukey's HSD post hoc pairwise comparisons test was performed when the overall group comparison was significant. To verify that locomotor behavior and location exploration during earlier sessions did not contribute to temporal ordering and/or novelty detection measures recorded during the test sessions, ANOVA were performed with both locomotor behavior and location exploration during all sessions as well as experimental order as covariates. To elucidate a role for CGG repeat length modulation of any effects within the CGG KI mice, Pearson's correlation coefficients were calculated to assess the relationship of the ratio values with CGG repeat length in only the CGG KI mice as the range of CGG repeat values were too limited in wildtype mice to perform such analyses (range 8-12 in wildtype compared with 77-194 in CGG KI mice). Furthermore, it was determined that, owing to the large gap in CGG repeat values between the wildtype and any CGG KI mice (gap in the CGG repeat lengths = 55), including wildtype mice in any correlation was inappropriate given the structure of the dataset. All p values were adjusted to control for false discovery rate (FDR) and were considered significant at $p_{(adj)} < 0.05$ when power was maintained at $1-\beta > .80$.

For plotted data, Low CGG and High CGG mice were plotted separately as boxplots to demonstrate group differences. These groups were treated separately for ANOVA as there is a 35 CGG repeat between the groups, suggesting the potential for two separate groups. Below the boxplots are scatterplots of the combined CGG KI mouse data with the correlation analyses that were performed. As the y axis of these plots have been adjusted to best

visualize the relationship between performance and CGG repeat in the CGG KI mice, the wildtype mouse data were not included in these plots. This decision was made to better characterize the association between increasing CGG repeat lengths and neurocognitive function in the CGG KI mice, and not to directly characterize differences between CGG KI mouse groups and wildtype mice (*cf.*, similar presentation and statistical analyses presented in Diep et al., 2012; Hunsaker et al., 2011c).

RESULTS

Temporal ordering for spatial locations

For the temporal ordering for spatial locations task, there was a significant main effect of CGG repeat group ($F(2,21)=121.52$, $p_{(adj)}<.0001$). Tukey's HSD post hoc pairwise comparisons demonstrated that the High CGG repeat group performed significantly more poorly than the Low CGG repeat group and wildtype group (both $p_{(adj)}<.0001$), and the Low CGG group performed more poorly than the wildtype group ($p_{(adj)}<.001$). There were no significant differences among groups for either locomotor behavior or spatial location exploration during the three, 5 min location presentation sessions (all $p_{(adj)}>.30$), and experimental order did not contribute to task performance ($p_{(adj)}=.71$).

To characterize any possible relationship between CGG repeat length and temporal ordering for spatial locations in CGG KI mice with expanded CGG trinucleotide repeats, a Pearson's correlation coefficient was calculated across Low CGG and High CGG groups of CGG KI mice. A negative association was observed between the CGG trinucleotide repeat length and the ratio value during performance of the temporal ordering for spatial locations task (Figure 28A; corr $\rho = -.85$; $p_{(adj)}<.0001$, $R^2_{(adj)}=.73$).

Novelty detection for spatial locations with high spatial interference

Similar to the temporal ordering for spatial locations task, there was a significant main effect of CGG repeat group for the spatial locations with high spatial interference task ($F(2,21)= 89.92$, $p_{(adj)}<.0001$). Tukey's HSD post hoc

pairwise comparisons demonstrated that the High CGG repeat group performed significantly worse than the Low CGG repeat group and wildtype group (both $p_{(adj)}<.0001$), and the Low CGG group performed worse than the wildtype group ($p_{(adj)}<.001$). There were no significant differences among groups for either locomotor behavior or spatial location exploration during the three, 5 min location presentation sessions (all $p_{(adj)}>.40$), and experimental order did not contribute to task performance ($p_{(adj)}=.71$).

To characterize any possible relationship between CGG repeat length and spatial location novelty detection with high interference in CGG mice with expanded CGG trinucleotide repeats, a Pearson's correlation coefficient was calculated across Low CGG and High CGG groups of CGG KI mice. A negative association was observed between the CGG trinucleotide repeat length and the ratio value during performance of the spatial location novelty detection with high spatial interference task (Figure 28B; corr $\rho =-.88$; $p_{(adj)}<.0001$, $R^2_{(adj)}=.77$).

Novelty detection for spatial locations with low spatial interference

For the novelty detection for spatial locations with low spatial interference task there was no significant effect for CGG repeat group ($F(2,21)=.12$, $p_{(adj)}=.88$), nor were there significant differences among groups for either locomotor behavior or spatial location exploration during the three, 5 min object presentation sessions (all $p_{(adj)}>.20$), and experimental order did not contribute to task performance ($p_{(adj)}=.71$). Furthermore, no association was observed between the CGG trinucleotide repeat length and the ratio value during

performance of the spatial location novelty detection with low spatial interference
(Figure 28C; corr $\rho = -.03$; $p_{(adj)} = .92$, $R^2_{(adj)} = .0007$).

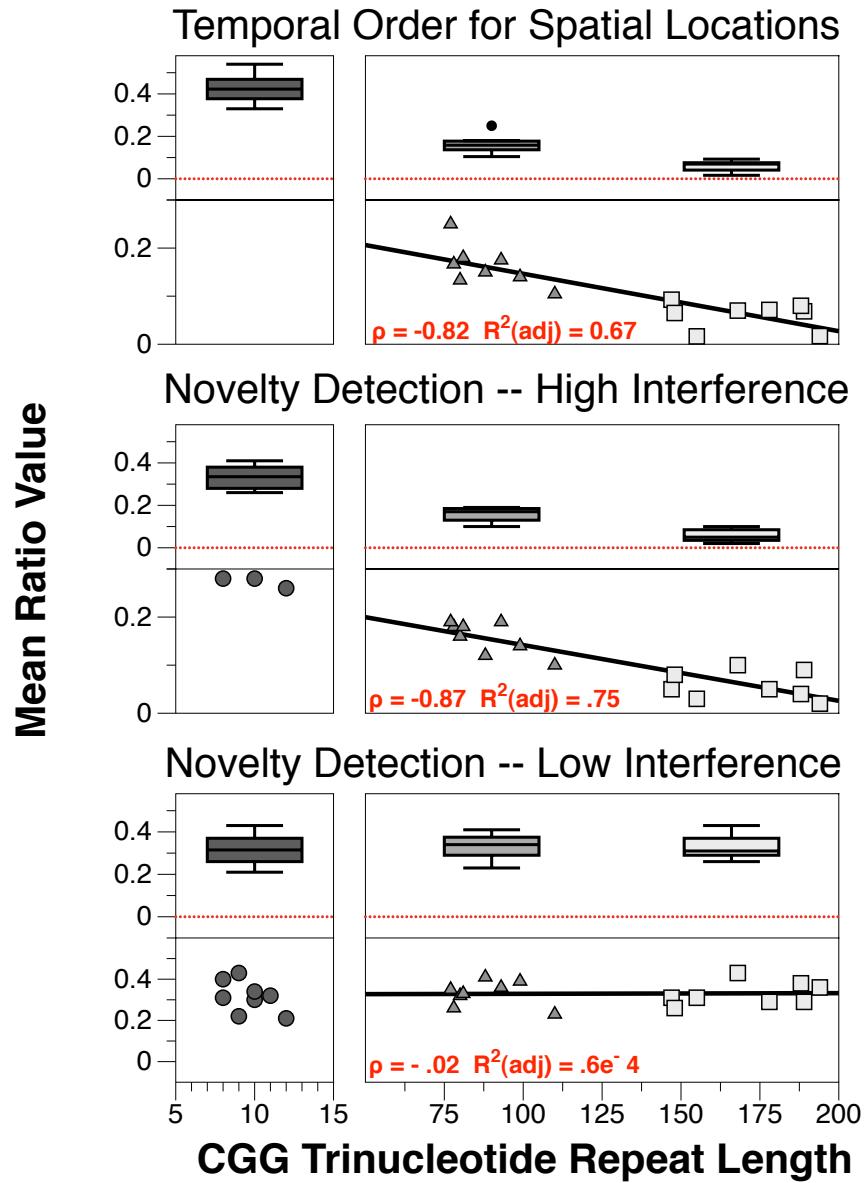


Figure 28. Experimental Data. **A.** Temporal Ordering for Spatial Locations. **B.** Novelty Detection for Spatial Locations with High Spatial Interference. **C.** Novelty Detection for Spatial Locations with Low Spatial Interference.

DISCUSSION

Female CGG KI mice heterozygous for the fragile X premutation were impaired on a temporal order for spatial locations task, a task shown previously to require intact spatial and temporal processing (*cf.*, Hunsaker & Kesner, 2008; Hunsaker et al., 2008a). These mice also showed impairments for a novelty detection for spatial locations task requiring the mice to overcome high levels of spatial interference to make the discrimination between the novel and familiar spatial location. However these mice were unimpaired on a novelty detection for spatial locations task wherein the spatial interference was minimized, suggesting these mice showed intact spatial memory.

In a review of neurocognitive impairments in children with genetic disorders, Simon proposed the theory of a spatiotemporal hypergranularity to describe deficits spanning the spatial and temporal domains (Hunsaker, 2012a, 2012b; Simon, 2008, 2011). He proposed a coarser or "grainier" resolution of mental representations with respect to space and time accounts for deficits observed in these disorders. In the present study, whereas wildtype mice are able to recall and separate events in time and space, with increasing CGG repeat length, both spatial and temporal processing become more coarse or grainier, resulting in impaired discrimination of spatial and temporal relationships among stimuli (Simon, 2007, 2008, 2011; *cf.*, Hunsaker, 2012a; Rolls & Kesner, 2006).

The present temporal ordering for spatial locations data can be interpreted as a deficit in spatiotemporal processing because the CGG KI mice were unable to determine which spatial location presented during a test came earlier in a

sequence. These impairments cannot be attributed to global deficits for spatial processing because the same CGG KI mice selectively explored a novel spatial location, suggesting the mice showed intact spatial memory. Based on the spatiotemporal hypergranularity model, it is likely the resolution of temporal processing in CGG KI mice is coarser than that of wildtype mice--such that larger temporal distances are required for the CGG KI mice to correctly process the temporal order for spatial locations.

To explore the resolution of spatial processing in CGG KI mice, mice were tested on a spatial location novelty task with high levels of spatial interference among the familiar and novel spatial location. The CGG KI mice were unable to discriminate these spatial locations as well as wildtype mice, evidenced by reduced preferential exploration of the novel spatial location over the familiar location. Based on the spatiotemporal hypergranularity model, it is likely the resolution of spatial processing in CGG KI mice is coarser than that of wildtype mice, as has been previously reported (Hunsaker et al., 2009).

Critical to the interpretation of the spatial novelty with high interference task as being related to reduced resolution of spatial processing is the finding that CGG KI mice were able to perform a spatial novelty detection task when the spatial interference was minimal (*i.e.*, 80 cm separation of locations). As mentioned above, the same CGG KI mice were overcome by the levels of spatial interference in the high interference condition (*i.e.*, 35 cm separation). In other words, a larger spatial separation is necessary for CGG KI mice to discriminate

the familiar and novel spatial location than wildtype mice require to make a similar discrimination.

An nontrivial point in this analysis is the fact that wildtype mice performed similarly well for both spatial novelty irrespective the level of spatial interference. One potential hypothesis would be that the high levels of spatial novelty would result in impaired discrimination in the wildtype mice. If the levels of spatial interference were increased sufficiently, this would surely be the case. In the present experiment, the high spatial interference condition was defined as the two spatial locations to be discriminated being located within 35 cm of each other, whereas the low spatial interference condition was defined as a separation of the two spatial locations of approximately 80 cm. We propose the lack of impairment on the part of the wildtype mice was due to the degree of interference being too low to result in behavioral deficits. This idea is supported by previous work with male CGG KI mice that showed intact spatial processing at distances as low as 30 cm (Hunsaker et al., 2009) and rats have been shown to have intact spatial discrimination as low as 15 cm (Gilbert et al., 2001). Also, in the original version of the present task used in rats, there was no statistical difference for the high and low interference conditions in control, CA3, or CA1 lesioned rats--only the dentate gyrus lesioned rats (Gilbert & Kesner, 2006). Despite the fact that we did not see an effect of spatial interference in the wildtype mice, it remains a clear possibility that increasing spatial interference sufficiently would indeed impair spatial discrimination in wildtype mice.

Critically, the effects of this spatiotemporal hypergranularity on task performance scaled with the dosage or the fragile X premutation. In other words, the performance of the female CGG KI mice worsened as the number of CGG repeats on the *Fmr1* gene increased for both the temporal ordering and spatial novelty task with high interference. These data support the assertion that increasing CGG repeats are associated with increasingly coarse spatial and temporal mental representations as posited by (Simon, 2007, 2008, 2011). This negative association between genetic dosage and behavioral performance supports previous findings in the CGG KI mice, namely that visuomotor function as measured by skillful walking and skilled reaching tasks similarly deteriorates as a function of increasing CGG repeat length (Diep et al., 2012; Hunsaker et al., 2011c). This provides evidence for impaired spatiotemporal processing as a potential neurocognitive endophenotype for the fragile X premutation, as the degree of impairment scales with dosage of the genetic mutation (Hunsaker, 2012a, 2012b; Simon, 2008, 2011).

As has been described previously, CGG KI mice show neuropathological features, including intranuclear inclusion bodies, throughout neural networks known to subserve spatial and temporal processing including: the hippocampus and limbic cortices (*i.e.*, anterior cingulate), the parietal lobe, and the murine analog of the medial prefrontal cortex (*i.e.*, infralimbic/prelimbic cortices) (Hunsaker et al., 2009; Hunsaker et al., 2010; Wenzel et al., 2010). There are also evidence for reduced Fmrp levels and concomitant elevation in *Fmr1* mRNA levels in these networks, which may negatively affect spatiotemporal processing

in CGG KI mice. We propose that molecular and anatomic pathology in neural networks involving these structures underly the present results. Furthermore, these are the same networks proposed by (Simon, 1999, 2007, 2008, 2011) to subserve the attentional processes that underly the spatiotemporal hypergranularity observed in many neurodevelopmental disorders.

What the present experiment was unable to address was the exact nature of the spatiotemporal hypergranularity observed in CGG KI mice. (Simon, 1999, 2007, 2008, 2011) postulation for the spatiotemporal hypergranularity was that it results from an alteration or abnormal development of the neural circuits underlying spatial and temporal attention, not directly from impairments to the temporal and spatial pattern separation processes commonly tested in rodent lesion models (*cf.*, Aimone et al., 2011; Burke et al., 2011; Burke, Wallace, Nematollahi, Uprety, & Barnes, 2010; Gilbert et al., 2001; Kesner et al., 2004; Rolls, Stringer, & Elliot, 2006; Sahay, Wilson, & Hen, 2011; Wilson, 2009). More recently, however, it has been suggested that pattern separation occurs not only at the most basic level of information processing, but also at a mnemonic level analogous to the attentionally-modulated description of the spatiotemporal hypergranularity (*i.e.*, pattern separation among memory representations rather than among stimuli; *cf.*, Aimone et al., 2011). We propose these impairments in attentional or mnemonic pattern separation processes are analogous to the spatiotemporal hypergranularity and thus underlie the reduced or coarse temporal spatial resolution observed in CGG KI mice.

In summary, female CGG KI mice heterozygous for the fragile X premutation showed impaired spatiotemporal processing that are consistent with a spatiotemporal hypergranularity. These data demonstrate the fragile X premutation alters the manner by which CGG KI mice process spatial and temporal relationships among stimuli in the environment in a dose-dependent manner. These data support models postulating abnormal development negatively influences spatiotemporal processing in neurodevelopmental disorders (Hunsaker, 2012a, 2012b; Simon, 2008, 2011), and suggests spatiotemporal processing serves as a valid outcome measure that can be used in studies evaluating neurocognitive sequelae in these disorders--particularly in studies evaluating potential treatment options.

Funding:

This work was supported by National Institute of Health (NIH) grants, NINDS RL1 NS062411. This work was also made possible by a Roadmap Initiative grant (UL1 DE019583) from NIDCR in support of the NeuroTherapeutics Research Institute (NTRI) consortium; and by a grant (UL1 RR024146) from the NCRR.

Section 3: Neuromotor Function

Although not characterized, there are numerous anecdotal reports of a subclinical apraxia and general clumsiness among premutation carriers (e.g., tripping over own feet). To date, these motor dysfunctions have not been rigorously evaluated and characterized. One possibility is that these subclinical motor dysfunctions have a basis in impaired spatiotemporal processing for visual information. In other words, it is quite possible that. Any coordinated sequence of body movements requires coupled visual perception and action (Bertenthal & Von Hofsten, 1998; Bertenthal, Rose, & Bai, 1997; Warren, 2006). Active muscle forces are modulated by visual information to ensure a functionally organized and goal-directed response (Benson & Haith, 2009; Jeannerod, 1997). Also, the tight integration of spatial and motor functioning has long been recognized since accurate spatial representations are critical for representing, computing, executing and monitoring motor actions (Ladavas & Serino, 2008; Marshall & Fink, 2001; Weiss et al., 2000). The temporal characteristics of these representations are also critical since moving through space necessarily involves moving through time; thus real world attentional, spatial and coordinated motor actions are implicitly spatiotemporal in nature (Aghdaee & Cavanagh, 2007; Alvarez & Franconeri, 2007; Casasanto & Boroditsky, 2008; Chaston & Kingstone, 2004; Verstraten, Cavanagh, & Labianca, 2000; Yeshurun & Levy, 2003).

Chapters 12 and 13 report test for this potential motor endophenotype. Chapter 12 will report the results of a skilled walking experiment with analogy to

gait anomalies reported in FXATS, and Chapter 13 will report the results from a skilled forelimb reaching task with some level of analogy to tasks resulting in intention tremoring behavior in FXTAS. The results of these tasks will be related to the dosage of the premutation to elucidate a motor endophenotype. Chapter 14 will further characterize potential effects for skilled forelimb reaching by comparing performance not only with the dosage of the mutation, but also with markers of *Fmr1* related protein expression in brain.

Chapter 12

Motor deficits on a ladder rung task in male and female adolescent and adult CGG knock-in mice

Abstract

The fragile X premutation is a tandem CGG trinucleotide repeat expansion on the *FMR1* gene between 55 and 200 repeats in length. A CGG knock-in (CGG KI) mouse with CGG trinucleotide repeat lengths between 70 and 350 has been developed and used to model the histopathology and cognitive deficits reported in carriers of the fragile X premutation. Previous studies have shown that CGG KI mice show progressive deficits in processing spatial and temporal information. To characterize the motor deficits associated with the fragile X premutation, male and female CGG KI mice ranging from 2 to 16 months of age with trinucleotide repeats ranging from 72 to 240 CGG in length were tested for their ability to perform a skilled ladder rung walking test. The results demonstrate that both male and female CGG KI mice showed a greater number of foot slips as a function of increased CGG repeat length, independent of the age of the animal or general activity level.

This chapter has been published as:

Hunsaker, M. R., von Leden, R. E., Ta, B. T, Goodrich-Hunsaker, N. J., Arque, G., Kim, K. M., et al. (2011). Motor Deficits on a Ladder Rung Task in Male and Female Adolescent CGG Knock-in Mice. *Behavioural Brain Research*, 222, 117-121.

My role in this study was experimental design, building the apparatus, performing the research, and analyzing the data.

Introduction

The *FMR1* gene is polymorphic for the length of a CGG trinucleotide repeat in the 5' untranslated region. In the general population there are <45 CGG repeats on the *FMR1* gene, while in the full mutation underlying fragile X syndrome (FXS) there are >200 CGG repeats and the *FMR1* gene is transcriptionally silenced. In the fragile X premutation there are between 55 and 200 CGG repeats and increased transcription of *FMR1* mRNA (Hagerman & Hagerman, 2004b). Additionally, the fragile X premutation has now been associated with a number of neurocognitive sequelae, such as working memory deficits and impaired spatial information processing (Adams et al., 2007; Aziz et al., 2003; Bourgeois et al., 2009; Cellini et al., 2006; Chonchaiya et al., 2009; Goodrich-Hunsaker et al., 2011a; Greco et al., 2008; Keri & Benedek, 2009; Keri & Benedek, 2010; Kogan & Cornish, 2010; Kogan et al., 2008). The fragile X premutation can also result in the late onset neurodegenerative disorder called fragile X-associated tremor/ataxia (FXTAS), which occurs in upwards of 40% in males and 8–16% of female carriers of the fragile X premutation identified from known fragile X probands (Brunberg et al., 2002; Jacquemont et al., 2004b; Leehey et al., 2007a; Ortigas et al., 2010). FXTAS sequelae include cerebellar gait ataxia and intention tremor that may be targetable symptoms for pharmacological intervention (Grigsby, Kemper, & Hagerman, 1992; Ortigas et al., 2010).

To further investigate the consequences of the fragile X premutation, a CGG knock-in (KI) mouse has been developed (Berman & Willemsen, 2009;

Brouwer et al., 2008a; Brouwer et al., 2008b; Brouwer et al., 2009; Willemse et al., 2003). Behavioral characterizations of these mice have demonstrated subtle motor deficits on an accelerating rotarod as well as impaired spatial memory in the water maze, but only when mice were tested at greater than 12 months of age (Qin et al., 2011; Van Dam et al., 2005). Subsequent studies have identified abnormal embryonic development as well as spatial memory deficits evident as early as 12 weeks of age in CGG KI mice (Chen et al., 2010; Cunningham et al., 2011; Hunsaker et al., 2009; Hunsaker et al., 2010). Whether there are early motor deficits in CGG KI mice has yet to be determined.

To determine whether the CGG KI mouse model shows specific motor performance deficits at earlier ages than 12 months of age, more sensitive motor tasks are needed. Therefore, in the present study male and female mice ranging from 2 to 16 months of age were tested on a ladder rung task adapted from procedures reported by Soblosky et al., (1997a, 1997b) and refined by Whishaw and co-workers (Farr & Whishaw, 2002; Farr et al., 2006; Metz & Whishaw, 2002; Metz & Whishaw, 2009), among others (Cummings, Engesser-Cesar, Cadena, & Anderson, 2007; Schmidt, Zuckerman, Martin, & Wolfe, 1971; Shriner, Drever, & Metz, 2009). This task was chosen because it has been shown to be sensitive to subtle sensorimotor deficits in both mice and rats (Farr & Whishaw, 2002; Soblosky et al., 1997a, 1997b). In the ladder rung task, mice were allowed to walk along a narrow walkway on a floor made of parallel thin rounded rods at a constant separation. Successful performance in this task requires the animal to precisely determine where to place a paw on a narrow rung, followed by a skillful

limb advance and paw placement. In this task, foot slips, defined as the number of times the mouse's paw fell through the rung floor, were used as an index of skilled motor performance during walking. We found that both male and female CGG KI mice show a greater number of foot slips in this test than wildtype littermates. Furthermore, a CGG dosage effect was evident because within the CGG KI mice with expanded CGG trinucleotide repeats on the *Fmr1* gene, the number of foot slips showed a positive association with CGG repeat length, such that mice with long CGG repeat lengths had a greater number of foot slips than mice with more intermediate length CGG repeats.

Methods and materials

Animals

Forty-two male and 30 female CGG KI mice from 2 to 16 months of age as well as 41 male and 20 female wildtype mice of the same ages were used as subjects for this task. All wildtype mice were littermates with CGG KI mice included in the study. All CGG KI mice were bred onto a congenic C57BL/6J background as verified by microsatellite analysis from founder mice on a mixed FVB/N × C57BL/6J background

(Hunsaker et al., 2009; Wenzel et al., 2010; Willemse et al., 2003). Mice were housed in same sex, mixed genotype groups with between one and four mice per cage in a temperature and humidity controlled vivarium. A 12 h light–dark cycle was used with ad libitum access to water and food. All experiments were conducted during the light phase of the cycle and conformed to UC Davis IACUC approved protocols.

Genotyping

DNA was extracted from mouse tails by incubating with 10 mg/mL Proteinase K (Roche Diagnostics; Mannheim, Germany) in 300 µL lysis buffer containing 50 mM Tris–HCl, pH 7.5, 10 mM EDTA, 150 mM NaCl, 1% SDS overnight at 55 °C. One hundred micro litre saturated NaCl was then added and the suspension was centrifuged. One volume of 100% ethanol was added, gently mixed, and the DNA was pelleted by centrifugation and the supernatant discarded. The DNA was washed and centrifuged in 500 µL 70% ethanol. The

DNA was then dissolved in 100 µL milliQ-H₂O. CGG repeat lengths were determined by PCR using the Expanded High Fidelity Plus PCR System (Roche Diagnostics). Briefly, approximately 500–700 ng of DNA was added to 50 µL of PCR mixture containing 2.0 µM/L of each primer, 250 µM/L of each dNTP (Invitrogen; Tigard, OR), 2% dimethyl sulfoxide (Sigma–Aldrich; St. Louis, MO), 2.5 M Betaine (Sigma–Aldrich), 5 U Expand HF buffer with mg (7.5 µM/L). The forward primer was 5'-GCTCAGCTCCGTTCGGTTCACTTCCGGT-3' and the reverse primer was 5'-AGCCCCGCAC TTCCACCAGCTCCTCCA-3'. PCR steps were 10 min denaturation at 95 °C, followed by 34 cycles of 1 min denaturation at 95 °C, annealing for 1 min at 65 °C, and elongation for 5 min at 75 °C to end each cycle. PCR ends with a final elongation step of 10 min at 75 °C. DNA CGG band sizes were determined by running DNA samples on a 2.5% agarose gel and staining DNA with ethidium bromide (Brouwer et al., 2008b; Hunsaker et al., 2010; Wenzel et al., 2010; Willemse et al., 2003). Genotyping was performed twice on each animal, once using tail snips taken at weaning and again on tail snips collected at sacrifice. In all cases the genotypes matched.

Apparatus

The ladder rung apparatus was modeled on previously described ladder rung walk apparatus (Cummings et al., 2007; Farr & Whishaw, 2002; Farr et al., 2006; Metz & Whishaw, 2002; Metz & Whishaw, 2009; Schmidt et al., 1971; Shriner et al., 2009; Soblosky et al., 1997a; Soblosky et al., 1997b). The

apparatus consisted of two, 28 cm tall × 65 cm long black walls separated by 10 cm. The floor was elevated 10 cm from the bottom of the walls and was made from 43 parallel 1 mm diameter bars separated by 1.5 cm.

Ladder rung testing

All performance on the ladder rung test was recorded with a digital video camera (Sony Handycam; Sony, Inc., Tokyo, Japan) connected by a firewire connector to a PC laptop. The video camera was positioned at one end of the apparatus to record the full length of the beam floor. This allowed the experimenter to score whether the mouse's limbs extended below the beam floor as well as allowed the experimenter to observe the general posture of the mouse above the beam floor.

For testing, mice were gently placed in the apparatus and allowed to freely explore the apparatus and walk back and forth along the apparatus for 2 min. Mice typically explored the apparatus by walking the length of the apparatus, looking over the edge, and returning to the start position. During testing, the experimenter recorded how many times the mouse moved between the two ends of the apparatus as a general activity measure. All experiments were performed by the same experimenter. The digital recordings were later independently scored from the recordings by two experimenters blinded to the genotype of the animals (intraclass correlation coefficient = 0.94, $p < 0.001$).

Dependent measures and statistical analysis

Along with recording the number of times each mouse traversed the apparatus, the number of times the animals' fore or hind paws slipped below the ladder rungs was recorded as the dependent variable. A foot slip was recorded whenever the limb of the mouse passed below a rung sufficiently to clearly see the wrist of the animal. In this way, slipping was defined as the mouse completely missing or falling off a rung while walking across the apparatus.

To determine whether parametric analyses of variance (ANOVA) were appropriate for the data, tests of normality and homoscedasticity were performed. Once it was determined that parametric statistics were appropriate for the data, the data were plotted and placed into CGG repeat length groups as follows: the mice in the wildtype group all had between 8 and 12 CGG repeats (mean 10 ± 0.25 SEM; $n = 61$), mice included in the Low CGG repeat group ranged between 72 and 116 CGG repeats (mean 86 ± 3.1 ; $n = 20$), and the mice included in the High CGG repeat group ranged between 140 and 240 CGG repeats (mean 170 ± 9.2 ; $n = 52$). These groupings were used to categorize group by CGG repeat length because it was determined that the 24 CGG gap in the data between the Low (*e.g.*, 116) and the High (*e.g.*, 140) CGG repeat groups as well as the large gap between Wildtype (8–12 CGG repeats) and Low (*e.g.*, 72) CGG repeat groups invalidated any using CGG repeat length as a continuous variable for statistical analysis. Similar groupings were also used in previous studies of the CGG KI mice (Hunsaker et al., 2010). To determine if age significantly contributed to ladder rung test performance, mice were further separated into two groups based upon a median split of age, with one group ≤ 6

months of age (mean 4.5 ± 0.99 months; range 2–6 months) and the other ≥ 7 months of age (mean 10.75 ± 2.1 months; range 7–16 months). The data were analyzed as follows. A 3 (Group) \times 2 (Sex) \times 2 (Age) analysis of covariance (ANCOVA) with locomotor activity as a potential covariate was used to determine which factors contribute to task performance. Subsequent analyses were performed to further characterize all main effects. All analyses were considered significant at $p < 0.05$. Statistical analyses were performed in R 2.11.1 language and environment (R Development Core Team, 2012) and statistical power was calculated using both R and the statistical program G*Power 3 (Faul et al., 2007; Faul et al., 2009).

Results

For all mice, data were grouped by CGG repeat length (wildtype, Low CGG, High CGG), Sex (male, female), and Age (≤ 6 months, ≥ 7 months) and analyzed using three way ANCOVA with number of foot slips as the dependent variable and locomotor activity as a covariate. There was a main effect of CGG repeat length group ($F(2,120) = 5.4373$, $p = .005$), but no main effect of Age ($F(1,120) = 0.54$, $p = 0.47$) or Sex ($F(1,120) = 0.06$, $p = 0.94$), nor were there any significant interactions among variables (lowest p value $p = 0.45$). There was also no significant contribution of locomotor behavior for performance on the ladder rung task ($F(1,120) = 0.23$, $p = 0.63$). These results suggest that Age, Sex, and activity level did not contribute to task performance and only the CGG repeat length group factor significantly contributed to ladder rung task performance (Figure 29A).

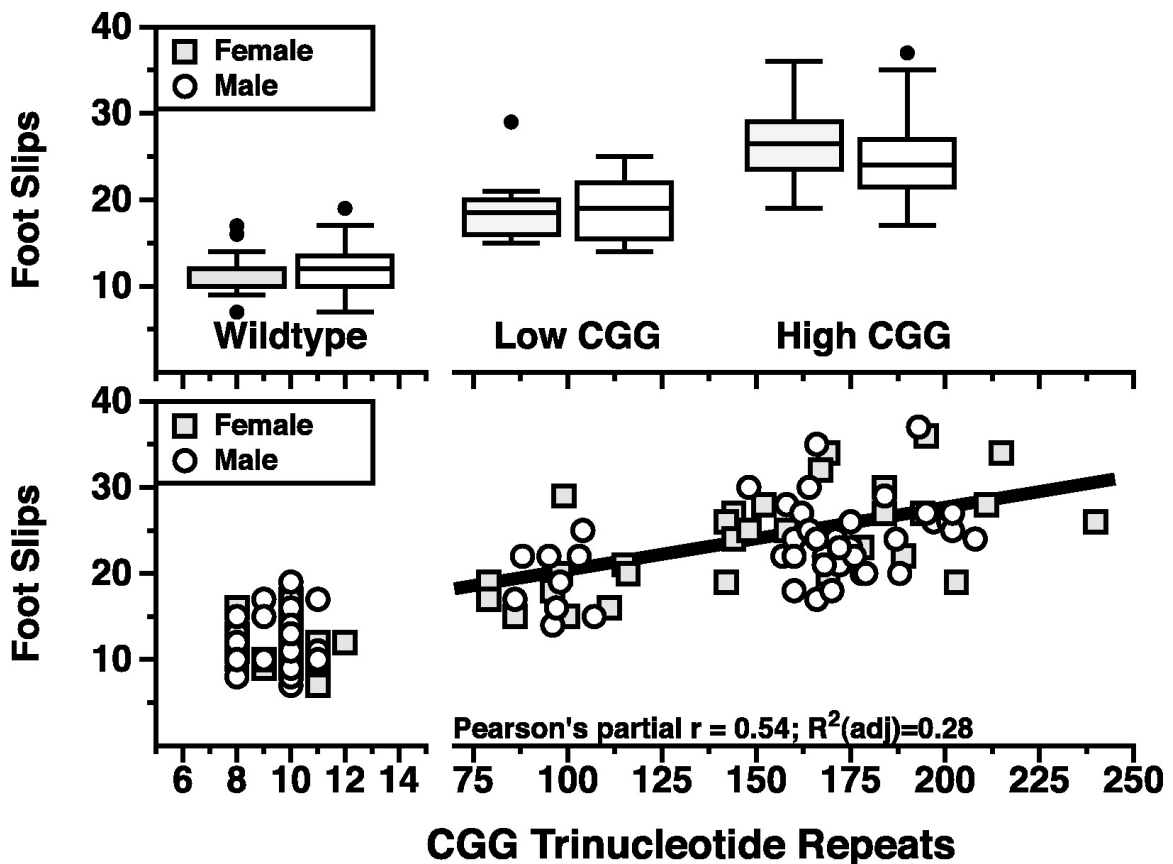


Figure 29. CGG repeat length modulates ladder rung task performance. **A.** Boxplots stratified by Sex and CGG repeat length group. Note that the High CGG repeat group showed a greater number of foot slips than mice in the Low CGG repeat group ($p < 0.005$). Both the High and Low CGG repeat groups had a greater number of foot slips than wildtype mice ($p < 0.0001$, $p < 0.005$ respectively). Wildtype male $n = 41$, female $n = 20$; Low CGG male $n = 10$, female $n = 10$; High CGG male $n = 32$, female $n = 20$. **B.** Scatterplot of CGG repeat length and the number of foot slips for each animal included the present study. A partial correlation performed comparing the number of foot slips to CGG repeat length (adjusted for influence of Sex) within CGG KI mice with expanded CGG trinucleotide repeats demonstrated a positive association between CGG repeats and the number of foot slips (Pearson's partial $r = 0.54$; $R^2(\text{adj})=.28$).

To further characterize the significant main effect of CGG repeat length group, a Tukey-Kramer post hoc pairwise comparisons test demonstrated that the wildtype mice showed significantly fewer foot slips (mean 12.8 ± 0.55) than the Low (mean 19.1 ± 0.88) or High (mean 25.3 ± 0.65) CGG repeat groups ($p < 0.005$, $p < 0.0001$ respectively), and that the Low CGG repeat groups had significantly fewer foot slips than the High CGG repeat group ($p < 0.005$) (Figure 29A).

To characterize any possible relationship between CGG repeat length and performance on the ladder rung task in CGG animals with expanded CGG trinucleotide repeats, a partial correlation coefficient adjusted for Sex was calculated. A positive association was observed between the CGG trinucleotide repeat length and the number of foot slips during ladder rung task performance (Figure 29B; Pearson's partial $r = 0.54$; $R^2_{(adj)}=.28$).

Discussion

The current experimental results reveal that both male and female CGG KI mice are impaired in performance of a skilled ladder rung walking task compared to wildtype littermates. Specifically, CGG KI mice showed a greater number of foot slips with increasing CGG repeat length (Figure 29B). These findings suggest that the length of an expanded CGG trinucleotide repeat on the *Fmr1* gene is related to impaired locomotor performance in CGG KI mice as observed in the ladder rung task. The present data also provide the first demonstration of motor deficits in CGG KI mice under 12 months of age. Interestingly, mice as young as 2 months of age appeared to show motor deficits similar to the mice over 12 months of age. Contrary to our initial hypotheses, age did not contribute to task performance, nor were there differences between sexes for skilled ladder rung performance. Male and female mice showed similar decrements in performance with increasing CGG repeat length (Figure 29A and 29B). These data suggest that the ladder rung task is likely revealing an early motor deficit as opposed to directly modeling the late onset cerebellar gait ataxia reported in human cases of FXTAS.

The early appearance of motor deficits was not entirely unexpected, considering recent reports that embryonic cortical development is abnormal in CGG KI mice (Cunningham et al., 2011) and that dendritic complexity is reduced and synaptic structure is altered in cultured hippocampal neurons (Chen et al., 2010). Furthermore, it has been found that CGG repeat length and age modulate

performance on a spatial processing task in 23–43 year old human female fragile X premutation carriers (Goodrich-Hunsaker et al., 2011a).

The lack of differential performance between sexes was unexpected as it has been reported that fragile X syndrome and FXTAS are more prevalent in males than females, presumably due to a protective influence of a second non mutated *FMR1* gene on the second X chromosome (Berry-Kravis et al., 2005; Jacquemont et al., 2004b). Despite the reduced prevalence of FXTAS in female carriers of the fragile X premutation relative to males, females with FXTAS do not show reduced FXTAS symptoms once diagnosed (Berry-Kravis et al., 2005; Hagerman et al., 2004). Furthermore, it is possible that the ladder rung task is sensitive enough to probe the underlying motor networks that may be similarly disrupted in male and female CGG KI mice.

Although not quantified, CGG KI mice also showed a hunched posture all ages and a discernible shaking while walking along the ladder rung apparatus. Similar behaviors were not observed in wildtype mice. This tremoring during the performance of a motor task is of interest because no gross motor abnormalities or tremoring are apparent when CGG KI mice are observed in an open field. These results suggest that motor abnormalities in CGG KI mice may not be apparent until the mice are challenged by a difficult motor task, such as the ladder rung task, which may unmask a previously unidentified motor tremor. These postural tremor-like behaviors need to be further investigated and carefully described in CGG KI mice.

These results also indicate that the ladder rung task is a sensitive and robust assay that allows for a high throughput analysis of motor function in CGG KI mice. As each mouse was only exposed to the apparatus for approximately 2 min in the present experiment and there was no adaptation period preceding data collection, performance of the task served as a rapid assay of motor function without the potential confounds of motor learning that may mask between group effects, as suggested in earlier studies (Farr et al., 2006; Soblosky et al., 1997b). This point is important as the rotarod task used to test motor function in mice requires the mouse be placed on a rotating drum and the time to fall is typically used as the outcome measure. For the rotarod, there are often early training trials given to mice on the rotarod apparatus that may potentially mask any differences that are present in baseline motor function as mice are trained to set performance criteria before administration of accelerating rotarod testing (Soblosky et al., 1997a, 1997b).

The present experiment did not explicitly employ the subtle gait measurements described by Whishaw and co-workers (Blume et al., 2009; Farr et al., 2006; Metz & Whishaw, 2009). This is because the sides of the apparatus used in this study were opaque and prevented the requisite recording the mouse's foot placement from the side for more precise analysis of limb movements. Such measurements could provide additional evidence for subtle motor deficits, as well as the precise nature of the observed missteps. For example, more sophisticated analyses of gait would reveal whether animals make predictable errors such as consistently under or overestimating the location

of subsequent beams. Such errors could indicate a possible dysfunction in frontal-parietal network-dependent vector calculations underlying action in peripersonal space (Drew, Andujar, Lajoie, & Yakovenko, 2008; Redish & Touretzky, 1994; Ward & Brown, 1996). Alternately, if animals showed a trend toward a general clumsiness or lack of precision in motor performance that could indicate a more purely motor deficit (Beloozerova & Sirota, 1993a, 2003). The first possibility is intriguing in for the CGG KI mice as frontal-parietal network dysfunction is hypothesized to underlie spatiotemporal, arithmetic, and attentional deficits in FXS as well as the fragile X permutation (Aziz et al., 2003; Bregman et al., 1987; Cornish et al., 2004a; Cornish et al., 2004b; Cornish et al., 2004c; Franke et al., 1998; Goodrich-Hunsaker et al., 2011a; Goodrich-Hunsaker et al., 2011b; Goodrich-Hunsaker et al., 2011c; Hodapp, Dykens, Ort, Zelinsky, & Leckman, 1991; Kaufmann, Abrams, Chen, & Reiss, 1999; Kemper et al., 1986; Kogan et al., 2004b; Loat, Craig, Plomin, & Craig, 2006; Miezejeski et al., 1986; Rivera et al., 2002; Steyaert et al., 1994; Tassone et al., 2000d), as well as being involved in skilled walking behaviors (Andujar, Lajoie, & Drew, 2010; Beloozerova & Sirota, 1993a; Beloozerova & Sirota, 1993b, 1998, 2003; Drew et al., 2008; Lajoie, Andujar, Pearson, & Drew, 2010). The latter possibility, based more directly on motor function is also important for the extension of the CGG KI mouse as a murine model of motor deficits present in FXTAS (Van Dam et al., 2005). Such follow-up studies are currently underway to explore these possibilities in CGG KI mice as well as to correlate any performance deficits to neuropathological features, which are present throughout the neocortex and

cerebellum of CGG KI mice (Hunsaker et al., 2009; Van Dam et al., 2005; Wenzel et al., 2010).

The primary benefit of this modification of the ladder rung task is that extensive pre-training is not required and that testing times and trials are significantly shortened compared to the versions of the task reported previously (Farr et al., 2006; Metz, 2008). Furthermore, spontaneous exploration is encouraged, and the effect of this behavior on potential error production can be considered. This results in a high throughput screen that is sufficiently sensitive to detect subtle motor impairments in transgenic mouse models.

In summary, the present experiment identified age-independent motor deficits in CGG KI mice. The detection of motor deficits in young CGG KI mice is important as performance on the ladder rung task may be used as outcome measures for behavioral or pharmacological therapeutic intervention in this mouse model as it pertains to FXTAS as well as other late onset neurodegenerative disorders. This modification might make the test more attractive to other groups. Because mice as young as 2 months of age show deficits, the need to limit testing to mice greater than 12 months of age to identify potential endpoints and outcome measures is mitigated.

Funding

This work was supported by National Institute of Health (NIH) grants, NINDSRL1 NS062411 and TL1 DA024854. This work was also made possible by a Roadmap Initiative grant (UL1 DE019583) from the National Institute of Dental

and Craniofacial Research (NIDCR) in support of the NeuroTherapeutics Research Institute (NTRI) consortium; and by a grant (UL1 RR024146) from the National Center for Research Resources (NCRR), a component of the National Institutes of Health (NIH), and NIH Roadmap for Medical Research.

Chapter 13

Female CGG Knock-In Mice Modeling the Fragile X Premutation are Impaired on a Skilled Forelimb Reaching Task

Abstract

The fragile X premutation is a tandem CGG trinucleotide repeat expansion in the Fragile X Mental Retardation 1 (*FMR1*) gene between 55 and 200 repeats in length. A CGG knock-in (CGG KI) mouse has been developed that models the neuropathology and cognitive deficits reported in fragile X premutation carriers. Previous studies have demonstrated that CGG KI mice have spatiotemporal information processing deficits and impaired visuomotor function that worsen with increasing CGG repeat length. Since skilled forelimb reaching requires integration of information from the visual and motor systems, skilled reaching performance could identify potential visuomotor dysfunction in CGG KI mice. To characterize motor deficits associated with the fragile X premutation, 6 month old female CGG KI mice heterozygous for trinucleotide repeats ranging from 70- 200 CGG in length were tested for their ability to learn a skilled forelimb reaching task. The results demonstrate that female CGG KI mice show deficits for learning a skilled forelimb reaching task compared to wildtype littermates, and that these deficits worsen with increasing CGG repeat lengths.

This chapter has been published as:

Diep, A. A., Hunsaker, M. R., Kwock, R., Kim, K. M., Willemse, R., & Berman, R. F. (2012). Female CGG Knock-In Mice Modeling the Fragile X Premutation are Impaired on a Skilled Forelimb Reaching Task. Neurobiology of Learning and Memory. 97, 229-234.

My role in this study was experimental design, building the apparatus, piloting the experimental protocol, supervising Amanda Diep as she performed the research, and analyzing the data.

Introduction

The Fragile X Mental retardation 1 (*FMR1*) gene is polymorphic for the length of a CGG trinucleotide repeat in the 5' untranslated region (UTR). In the general population there are fewer than 45 CGG repeats in the *FMR1* gene, while in the full mutation underlying fragile X syndrome (FXS) there are greater than 200 CGG repeats and the *FMR1* gene is transcriptionally silenced. In the fragile X premutation there are between 55-200 CGG repeats and increased transcription of *FMR1* mRNA (Garcia-Arocena & Hagerman, 2010).

To investigate the pathological and behavioral consequences of the fragile X premutation, a transgenic CGG knock-in (KI) mouse was developed in which the 5' UTR containing 8 CGG repeats in the endogenous murine *Fmr1* gene was replaced, via homologous recombination, with a human NheI-Xhol fragment containing 98 CGG repeats

(Willemsen et al., 2003). Behavioral analyses of these mice have demonstrated spatiotemporal processing deficits (Hunsaker et al., 2009; Hunsaker et al., 2010) and an early motor phenotype evaluated by a skilled ladder walking task that was interpreted as impaired visuomotor processing (Hunsaker et al., 2011c).

To further characterize the nature of the motor performance deficits in CGG KI mice, female CGG KI mice heterozygous for the fragile X premutation were trained on a skilled reaching task based on work by Whishaw et al. (Farr & Whishaw, 2002), among others (Buitrago, Ringer, Schulz, Dichgans, & Luft, 2004; Hermer-Vazquez, Hermer-Vazquez, & Chapin, 2007; Tennant & Jones, 2009). Female mice heterozygous for the fragile X premutation were chosen for

this study over male mice because the frequency of fragile X premutation is higher in females than males (1:113 females vs 1:250 in males; *cf.*, Hagerman, 2008). Additionally, there have also been emerging reports of neurocognitive abnormalities in human females carrying the fragile X premutation and heterozygous female CGG KI mice (Goodrich-Hunsaker et al., 2011a; Goodrich-Hunsaker et al., 2011b; Goodrich-Hunsaker et al., 2011c; Hunsaker et al., 2010; Hunsaker et al., 2011c; Lachiewicz et al., 2006). The importance of studying female premutation carriers and CGG KI mice is that the identification of subtle phenotypes in these less affected populations may inform research into the underlying mechanisms subserving the more profound phenotypes observed in males. A skilled forelimb reaching task was chosen as it has been shown that reaching in peripersonal space (*i.e.*, space within reach of a limb) depends upon integration of visuospatial and motor information across widespread neural circuitry involving the basal ganglia, motor and posterior parietal cortices (Beloozerova & Sirota, 2003; Beurze, Toni, Pisella, & Medendorp, 2010; Kolb, Teskey, & Gibb, 2010; Redish & Touretzky, 1994; Simon, 2008), superior colliculus, and cerebellum (MacKinnon, Gross, & Bender, 1976). Each of these structures are affected to some degree in the carriers of the fragile X premutation and the CGG KI mouse (Adams et al., 2007; Hunsaker et al., 2009; Hunsaker et al., 2010; Hunsaker et al., 2011c; Keri & Benedek, 2009; Keri & Benedek, 2010; Lachiewicz et al., 2006; Van Dam et al., 2005; Wenzel et al., 2010; Willemse et al., 2003). Furthermore, previous studies with rats using single pellet reaching tasks demonstrate a relationship between impaired motor control and onset/

severity of neurological disease, particularly focusing on the deleterious effects of dopamine depletion on skilled reaching performance (*cf.*, Vergara-Aragon, Gonzalez, & Whishaw, 2003).

In the present study, CGG KI mice were trained to extend their forelimb through an opening to grasp and retrieve a sucrose pellet. We demonstrated that heterozygous female CGG KI mice took between 1 and 2 days longer to reach asymptotic performance on the skilled forelimb reaching task and that the CGG KI mice failed to reach the same asymptotic level of performance as wildtype littermates (*i.e.*, never reached with the same level of success). Furthermore, a CGG repeat length dosage effect was evident within the CGG KI mice: such that mice with longer CGG repeat lengths (136-200) had a lower percentage of successful reaches than CGG KI mice with more intermediate length CGG repeats (70-116), and took longer to acquire the task. Furthermore, within the CGG KI mice there was a negative association between increasing CGG repeats and performance on the skilled reaching task.

Methods and Materials

Animals

Twelve female CGG KI mice heterozygous for the fragile X premutation at 6 months of age and 6 female wildtype mice of the same age were used as subjects for this task. All wildtype mice were littermates with CGG KI mice included in the study. All CGG KI mice were bred onto a congenic C57BL/6J background over greater than 12 generations from founder mice on a mixed FVB/N x C57BL/6J background (Willemsen et al., 2003). Mice were housed in same sex, mixed genotype groups with three or four mice per cage in a temperature and humidity controlled vivarium on A 12 h light-dark cycle. Mice had ad libitum access to water and were maintained at 90-95% their free feeding weight throughout experimentation. Mouse weights did not differ among genotypes during experimentation. All experiments were conducted during the light phase of the diurnal cycle and conformed to University of California, Davis IACUC approved protocols.

Genotyping

As somatic instability of CGG repeats among tissues in the CGG KI mouse has been shown to be negligible (under 10 CGG repeats across tissues; (Berman & Willemsen, 2009; Willemsen et al., 2003)), genotyping was carried out upon tail snips. DNA was extracted from mouse tails by incubating with 10 mg/mL Proteinase K (Roche Diagnostics; Mannheim, Germany) in 300 μ L lysis buffer containing 50 mM Tris-HCl, pH 7.5, 10 mM EDTA, 150 mM NaCl, 1% SDS

overnight at 55°C. One hundred μ L saturated NaCl was then added and the suspension was centrifuged. One volume of 100% ethanol was added, gently mixed, and the DNA was pelleted by centrifugation and the supernatant discarded. The DNA was washed and centrifuged in 500 μ L 70% ethanol. The DNA was then dissolved in 100 μ L milliQ-H₂O. CGG repeat lengths were determined by PCR using the Expanded High Fidelity Plus PCR System (Roche Diagnostics). Briefly, approximately 500–700 ng of DNA was added to 50 μ L of PCR mixture containing 2.0 μ M/L of each primer, 250 μ M/L of each dNTP (Invitrogen; Tigard, OR), 2% dimethyl sulfoxide (Sigma-Aldrich; St. Louis, MO), 2.5 M Betaine (Sigma-Aldrich), 5 U Expand HF buffer with mg (7.5 μ M/L). The forward primer was 5'-GCT CAG CTC CGT TTC GGT TTC ACT TCC GGT-3' and the reverse primer was 5'-AGC CCC GCA CTT CCA CCA CCA GCT CCT CCA-3'. PCR steps were 10 min denaturation at 95°C, followed by 34 cycles of 1 min denaturation at 95°C, annealing for 1 min at 65°C, and elongation for 5 min at 75°C to end each cycle. PCR ends with a final elongation step of 10 min at 75°C. DNA CGG repeat band sizes were determined by running DNA samples on a 2.5% agarose gel and staining DNA with ethidium bromide (Brouwer et al., 2008a; Hunsaker et al., 2011c). For female CGG KI mice heterozygous for the fragile X premutation there were two bands present, one corresponding to the wildtype allele (CGG repeat length 8-12), and another corresponding to the premutation allele (CGG repeat length 70-200). For wildtype mice, only the wildtype allele was present. Genotyping was performed twice on each animal,

once using tail snips taken at weaning and again on tail snips collected at sacrifice. In all cases the genotypes matched.

Skilled Forelimb Reaching Apparatus

The apparatus for the skilled forelimb reaching task was a transparent Plexiglas box 19.5 cm long, 8 cm wide, and 20 cm tall. A 1-cm wide vertical window ran up the front of the box centered along the front wall. A .2-cm thick plastic shelf (8.3 cm long and 3.8 cm wide) was mounted 1.1 cm from the floor on the front of the box. Twenty mg banana-flavored sucrose pellets (Bioserve Inc.; Frenchtown, NJ) could be placed in indentations spaced 1 cm away from the window and centered on its edges such that the mouse could only reach each indentation with one paw and could not reach the pellets with their tongue (*cf.*, Farr & Whishaw, 2002).

Experimental Methods

Skilled Forelimb Reaching Task

Pretraining

Mice were food deprived to 90-95% free feeding weight and given access to 20 mg banana flavored sucrose pellets in their home cage to habituate to the food reward for 2 days. Throughout experimentation mice were provided sufficient food to maintain 95% free feeding weight 30 min after experimentation each day.

Training

On days 3-5, mice were placed in the apparatus with sucrose pellets on the floor and in the open window within reach of the mouse's tongue for 30 min and allowed to consume sucrose pellets. On days 6-10, mice were placed in the apparatus with sucrose pellets available straight ahead immediately outside the open window for 15 min, allowing the mouse to use their tongue to obtain the reward pellet. When mice freely ate rewards, they moved on to task acquisition.

Acquisition

Prior to the first day of acquisition, mice were placed in the apparatus with the indentations on both sides outside the window containing sucrose pellets. The mice were allowed to reach and obtain as many rewards as possible for 15 min. The paw preference of each mouse was determined as the paw used during

the majority of individual reaches. Starting the next day, all mice were trained against their paw preference.

Mice were placed in the apparatus for 15 min with one sucrose pellet placed on the side of the open window such that the mouse could only obtain it with the non-preferred paw. Each time the mouse reached, an experimenter blinded to mouse genotype recorded whether the reach was successful or whether or not errors occurred and immediately replaced the reward pellet when displaced. A successful reach was defined as the mouse obtaining and consuming the food pellet. If the mouse knocked the pellet away or dropped it prior to eating it an error was recorded. This acquisition was continued for 15 days.

Dependent Measures and Statistical Analysis

Because the fragile X premutation is present developmentally and has been shown to alter neurodevelopmental trajectories (Cunningham et al., 2011), data were collected during acquisition of the skilled reaching task rather than during post-acquisition performance tests as per the more common approach in brain lesion studies (*cf.*, Farr & Whishaw, 2002).

The number of times that the mouse successfully reached and obtained a sucrose pellet reward was collected as the dependent variable. If the mouse reached and missed/displaced the pellet during a reach or dropped the pellet before consuming it, an error was recorded and the pellet was immediately replaced. Qualitative observations concerning the behavior/strategy of each

mouse was also recorded by the observer. For analysis, the percentage of reaches that were successful was calculated for each day: (% successful reaches = [number of successful reaches / total number of reaches] * 100).

To determine whether parametric analyses of variance (ANOVA) were appropriate for the data, tests of normality, homoscedasticity, and sphericity were performed. Once it was determined that parametric statistics were appropriate for the data, the data were plotted and placed into CGG repeat length groups as follows: the mice in the wildtype group all had between 8-12 CGG repeats (mean 10 +/- .2 SEM; n=6), mice included in the Low CGG repeat group ranged between 70-116 CGG repeats (mean 86 +/- 7; n=6), and the mice included in the High CGG repeat group ranged between 136-200 CGG repeats (mean 168 +/- 12; n=6). Similar groupings were also used in previous studies of male and female CGG KI mice (Hunsaker et al., 2010; Hunsaker et al., 2011c). A 3 (CGG repeat group) x 15 (Day) repeated measures analysis of covariance (ANCOVA) was used to determine differences among the groups for acquisition of the skilled reaching task with total number of times each mouse reached during each session as a covariate. Similar ANOVA were used to confirm that the total number of reaches did not differ among genotypes.

To specifically determine differences in the day the mice learned the task to asymptotic performance levels, the data for each animal was evaluated for the point at which the learning curve changed from being linear to curvilinear and confirmed using the change point algorithm reported by Gallistel et al. (2004; translated into R from the original MATLAB code). The first change point in the

returned change point array corresponded to the first point at which the learning curve statistically significantly changed (discrimination threshold was set at logit = 3: odds against = 1,000:1 or $p < 0.001$) was chosen as the index of learning for each mouse. This change point for each animal was then used to compare the learning index across groups using a one way ANOVA.

Subsequent analyses were performed to further characterize all main effects, and Tukey-HSD post hoc pairwise comparisons tests were used to characterize all significant main effects and interactions among factors. To characterize any possible relationship of performance on the skilled forelimb reaching task as a function of CGG repeat length in CGG KI animals with expanded (70-200) CGG trinucleotide repeats, a Pearson's correlation coefficient was calculated comparing asymptotic performance (performance averaged across days 12-15) and CGG repeat length. To control for the false discovery rate (FDR) given the number of analyses performed on the data, p values were FDR adjusted as outlined by (Benjamini et al., 2001). All analyses were considered significant at $p(\text{adj}) < .05$. Statistical analyses were performed in R 2.13.1 language and environment (R Development Core Team, 2012).

Results

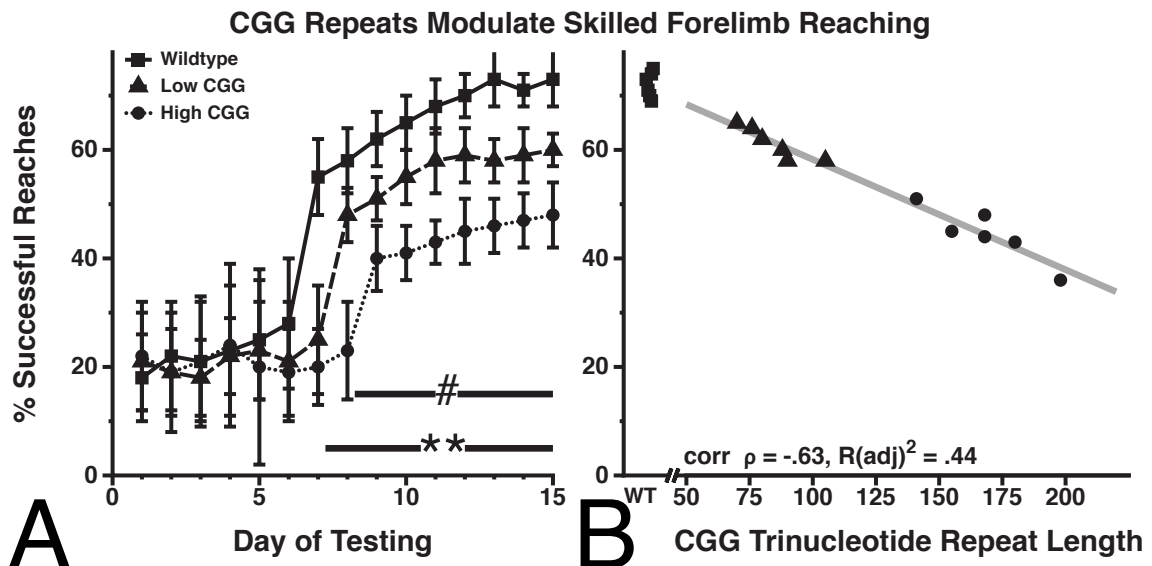


Figure 30: CGG repeat length modulates skilled reaching task performance. **A.** During the first 6 days of learning, all mice performed similarly. After day 7, CGG KI mice show deficits for skilled forelimb reaching compared to wildtype littermate controls (**). Beginning on day 8, the CGG KI mice with 136-200 CGG repeats (High CGG) are impaired relative to CGG KI mice with 70-116 CGG repeats (Low CGG) (#). ** $p < .001$, # $p < .01$. **B.** A Pearson's correlation coefficient was calculated within CGG KI mice performance during days 12-15 demonstrating an inverse linear association between increasing CGG repeat length and asymptotic performance levels of the skilled reaching task (wildtype mice were excluded from the analysis to focus on mice with expanded CGG repeat lengths; corr $\rho = -.63$, $p_{(adj)} = .03$; $R^2_{(adj)} = .44$).

For all mice, data were grouped by CGG repeat length (wildtype, Low CGG, High CGG) and analyzed across days of training using repeated measures ANCOVA with percent successful reaches as the dependent variable, CGG repeat group as the grouping factor, and day of training as a repeated within-subjects factor with total number of attempted reaches during each session as a covariate. All p values have been FDR adjusted per Benjamini et al. (2001). There was a main effect of CGG repeat length group ($F(2,211)= 54.75$, $p_{(adj)}<.001$), an effect for training day ($F(14,211)=26.38$, $p_{(adj)}<.001$), and there was a significant interaction between group and day ($F(28,211)=1.69$, $p_{(adj)}=.02$), suggesting that the longitudinal performance trajectory differed among CGG repeat groups. Total number of reaches per session did not significantly contribute to skilled forelimb reaching task acquisition ($F(14, 211)=1.08$, $p_{(adj)}=.30$), and did not differ among CGG repeat groups ($F(28,211)=.94$, $p_{(adj)}=.56$; wildtype mean $46 +/- 12$ (SEM) reaches per session; Low CGG repeat group $53 +/- 19$ reaches per session; High CGG repeat group $51 +/- 9$ reaches per session).

To further characterize the significant interaction, a Tukey-HSD post hoc pairwise comparisons test demonstrated that no groups differed during days 1-6 of training (all $p_{(adj)}>.15$), on day 7-15 the wildtype group showed a greater percentage of successful reaches than the CGG KI mouse groups (all $p_{(adj)}<.001$). On day 8-15 the Low CGG group with 70-116 CGG repeats showed a greater percentage of successful reaches than the High CGG repeat group with 136-200 CGG repeats (all $p_{(adj)}<.01$).

Based on the results of the paired comparisons, it appears that the three groups show differential time-courses for reaching asymptotic performance on the skilled forelimb reaching task (Figure 30A). To evaluate differential learning rates, the day of training at which the learning curve changed from linear to curvilinear was determined for each group, and used to define the day of acquisition during which significant improvement in performance had occurred. All groups showed a clear linear trend for days 1-6 of training (all $p_{(adj)} < .01$). Beginning on day 7 the learning curve for the wildtype group became curvilinear (i.e., significant quadratic trend emerged; $F(1,5)=12.04$, $p_{(adj)}=.01$), reflecting the marked increase in successful reaches beginning day 7. The Low CGG group did not show a curvilinear trend until day 8 ($F(1,5)=8.25$, $p_{(adj)}=.03$), and the High CGG group did not show a curvilinear trend until day 9 ($F(1,5)=7.13$, $p_{(adj)}=.04$). A one way ANOVA comparing the days when the trend became curvilinear across CGG groups revealed a main effect of CGG repeat grouping ($F(2,16)=39.39$, $p_{(adj)}<.001$). A Tukey-HSD post hoc pairwise comparisons test revealed the wildtype group showed a curvilinear trend earlier than the high CGG repeat group ($p_{(adj)}<.001$) and low CGG repeat group ($p_{(adj)}<.01$). The low CGG repeat group showed a curvilinear trend earlier than the high CGG repeat group ($p_{(adj)}<.01$).

A confirmatory analysis of differences in the learning curve among CGG groups was performed using a change point algorithm described by Gallistel et al. (2004). The first change point in the data (corresponding to the first alteration to the learning curve at a $p<0.001$ threshold) returned by the algorithm was

selected for each mouse and compared across groups: the wildtype mice showed a significant change in the slope of the learning curve on day 7 (group mean 6.9 +/- .25 SEM), the Low CGG repeat group showed a change in slope on day 8 (group mean 8.1 +/- .33), and the High CGG repeat group showed a change in slope on day 9 (group mean 9.25 +/- .35), confirming the analysis using the curvilinear trend as the measure of learning rate.

To characterize any possible relationship between CGG repeat length and performance on the skilled forelimb reaching task in CGG KI animals with expanded CGG trinucleotide repeats, a Pearson's correlation coefficient was calculated between CGG repeat length and averaged performance for days 12-15 for CGG KI mice (Figure 30B). A negative association was observed between the CGG trinucleotide repeat length and the asymptotic level of skilled reaching performance in the CGG KI mice (wildtype mice were excluded from the analysis to focus on expanded CGG repeat lengths unique to CGG KI mice; corr $\rho = -.63$, $p_{(adj)}=.03$; $R_{(adj)}^2=.44$).

Qualitative observations collected during the reaching task suggest the CGG KI mice's reaching patterns differed from the wildtype mice. The wildtype mice reached with a linear trajectory toward the reward pellet, grasped the pellet, and returned the pellet to the mouth for consumption. The CGG KI mice, however, generally reached with a less precise, nonlinear trajectory, specifically using a more sweeping or arcing motion to reach for the reward pellets. Additionally, on the attempts when the CGG KI mice reached with a linear trajectory, they appeared to close the hand either too soon or too late, generally

displacing the sucrose pellet. Both of these differences resulted in skilled reaching errors. Once the reward was grasped by a CGG KI mouse; however, the CGG KI mice did not show any tendency to drop the reward prior to consumption.

Discussion

The current experimental results provide evidence for impaired reaching abilities in CGG KI mice that are modulated by CGG repeat length in female CGG KI mice modeling the fragile X premutation. These data model subclinical motor features present in female carriers of the fragile X premutation as young as 36 years of age that show no features of FXTAS (Narcisa et al., 2011). These female premutation carriers demonstrated impaired finger tapping used as a measure of manual coordination in both the dominant and non dominant hands, as well as slower reaction time with the non-dominant hand. Importantly, in the same study no gross motor disturbances were identified. As such, the skilled reaching deficits observed in CGG KI mice may serve as a valid behavioral biomarker for studies into progression of motor symptoms in CGG KI mice across age or to evaluate treatment options.

The present deficits for skilled reaching in CGG KI mice suggest CGG KI mice have an impairment along neural circuits involving the basal ganglia, motor and parietal neocortices, cerebellum, and superior colliculus that are critical for integrating visuospatial information with motor efferent copy to guide successful performance of a skillful reaching task (*i.e.*, a basal ganglia-cortical-collicular-cerebellar circuit; cf., Redish & Touretzky, 1994). This hypothesis is supported by observations pertaining to the CGG KI mice's reaching patterns. Wildtype mice reached with a consistent linear trajectory toward the reward pellet, grasped the pellet, and returned the pellet to the mouth for consumption. The CGG KI mice, however, reached with a less precise, nonlinear trajectory, specifically using a

more sweeping or arcing motion to reach for the reward pellets. Additionally, at times the CGG KI mice reached with a linear trajectory, but appeared to close the hand either too soon or too late, resulting in displacing the sucrose pellet. Both of these differences resulted in skilled reaching errors. Once the reward was grasped, however, the CGG KI mice, similar to the wildtype mice, did not show any tendency to drop the reward prior to consumption, suggesting intact motor function sufficient to manipulate foodstuffs. These data are congruent with impaired visuomotor integration leading to an inability to generate, modify, or alter initial reaching trajectories to effectively obtain the reward pellets more reliably than ataxic or cerebellar symptoms--implicating not only functional impairments within the basal ganglia and cerebellum, but also impairments within the parietal lobe and superior colliculus.

Previous research has implicated the superior colliculus as a critical structure underlying much of this visuomotor integration via reciprocal connections with the intraparietal lobule in the parietal cortex, which has been implicated in visuospatial processing necessary to guide skilled reaching and walking behaviors (Beloozerova & Sirota, 2003; Hikosaka, Nakamura, Sakai, & Nakahara, 2002; Mutha, Sainburg, & Haaland, 2010), as well as reciprocal connectivity with the cerebellum. Furthermore, communication between the cortex and cerebellum (via cortico-cerebellar projections) is required for skilled motor behavior (Bays, Singh-Curry, Gorgoraptis, Driver, & Husain, 2010). Anatomically, the superior colliculus is located in an optimal location to bridge communication between incoming sensory input, visuospatial information, and

motor output (Clower, Dum, & Strick, 2005; Meredith & Stein, 1986). Specifically, the superior colliculus receives projections from the parietal cortex carrying visuospatial and somatosensory information as well as motor efferent copy via projections from the cerebellum (Goodale, Foreman, & Milner, 1978; Sprague & Meikle, 1965). It has further been proposed reciprocal connections within the intraparietal lobule that may be sufficient to subserve the reciprocal transfer of visuospatial and motor information necessary to guide skilled reaching. These inputs are integrated in the superior colliculus and feedback projections are sent back to the parietal lobes, frontal lobes (primarily the primary motor and premotor cortices), and cerebellum to guide fine on-line corrections to ongoing skilled motor movements (Bernier & Grafton, 2010).

It is also likely that an interaction between the basal ganglia and the rostral/parietal cortices contribute to the observed deficits. It has been demonstrated that disruptions to the dopaminergic system in the basal ganglia is sufficient to result in impaired skilled reaching (Barneoud, Descombris, Aubin, & Abrous, 2000; Faraji & Metz, 2007; Galvan, Floran, Erlij, & Aceves, 2001; Jeyasingham, Baird, Meldrum, & Dunnett, 2001; Melvin et al., 2005; Whishaw, Zeeb, Erickson, & McDonald, 2007). This is important since both full mutation and premutation length CGG repeat expansions in the *FMR1* gene disrupt dopaminergic signaling (Ceravolo et al., 2005; Hall et al., 2006; Scaglione et al., 2008), particularly post-synaptic signaling (Wang, Kim, & Zhuo, 2010). These data suggest that the basal ganglia-cortical interactions provide motor and visuospatial information necessary for effective visually guided reaching.

(Hikosaka et al., 2002; Redish & Touretzky, 1994). In fact, basal ganglia and cerebellum projections terminate in adjacent portions of the parietal cortex to inputs from the superior colliculus projections (*i.e.*, intraparietal lobule; Clower et al., 2005; Clower, West, Lynch, & Strick, 2001).

There are ample evidence for neuropathological features (*e.g.*, intranuclear inclusion bodies in neuronal and astroglial nuclei) in CGG KI mice along the basal ganglia-cortical-collicular-cerebellar circuit described above (Hunsaker et al., 2009; Wenzel et al., 2010; Willemse et al., 2003). Intranuclear inclusions are present in the cerebellum, specifically in the granule cell layers and Bergmann Glia, inclusions are present in neurons in the superior colliculus at ages as young as 6 months in male and female CGG KI mice, and there are inclusions present in neurons and astrocytes of the rostral and parietal neocortices beginning around 6 months of age in male and female CGG KI mice. Only rarely were inclusions found in the caudate, putamen, or globus pallidus in CGG KI mice. (Hunsaker et al., 2009; Wenzel et al., 2010; Willemse et al., 2003; MR Hunsaker unpublished observations). Although intranuclear inclusion bodies are less prevalent in the brains of CGG KI mice at 6 months of age compared to 12-17 months of age, it is not correct to assume that the cell populations are unaffected by the premutation prior to the emergence of pathological features, as behavioral deficits have been identified in the CGG KI mouse model as early as 2 months of age (Hunsaker et al., 2011c). Despite these pathologic anatomical features being present, in depth functional analyses of the role for these areas in cognitive function have not been undertaken in CGG

KI mice. The present experiment provides experimental rationale toward undertaking such studies using more functional assays more fully characterize the neurocognitive dysfunction reported in carriers of the fragile X premutation (*cf.*, Goodrich-Hunsaker et al., 2011a; Goodrich-Hunsaker et al., 2011b; Goodrich-Hunsaker et al., 2011c; Lachiewicz et al., 2006).

Due to the nature of the present skilled reaching task as an acquisition, rather than performance, task the present experiment did not quantify the specific outcome measures used by Whishaw and colleagues (Farr & Whishaw, 2002) such as the sequences of arm and hand movements that may be able to better dissect out the relative contributions of purely motor and cognitive contributions to task performance in CGG KI mice. More specifically, such more sophisticated analyses would reveal whether the mice were demonstrating symptoms congruent with motor dysmetria or else symptoms more reliably associated with general clumsiness or ataxia. Such data would allow for more sophisticated analyses of function in the CGG KI mouse brain, and provide a greater analogy to the measures used to quantify motor symptoms in the human fragile X premutation, such as the CATSYS system (Narcisa et al., 2011).

In summary, these data provide further evidence that the female heterozygous CGG KI mouse model of the fragile X premutation shows visuomotor processing deficits that appear to derive from neurocognitive impairments, rather than purely motor performance impairments. These data further suggest behavioral tasks emphasizing visuomotor integration may be required to observe mild, prodromal motor phenotypes in carriers of the fragile X

premutation prior to the onset of any neurodegenerative processes. As such, the skilled forelimb reaching task can be used as a translational endpoint or biomarker for future therapeutic intervention studies.

Acknowledgements

The authors wish to thank Lara E. Cardy, Gian G. Greenberg, Lindsey C. Curley, and Ramona E. von Leden for assistance with preliminary versions of this experiment, and Binh T. Ta for assistance with mouse genotyping.

Funding

This work was supported by National Institute of Health (NIH) grants, NINDS RL1 NS062411 and TL1 DA024854. This work was also made possible by a Roadmap Initiative grant (UL1 DE019583) from the National Institute of Dental and Craniofacial Research (NIDCR) in support of the NeuroTherapeutics Research Institute (NTRI) consortium; and by a grant (UL1 RR024146) from the National Center for Research Resources (NCRR), a component of the National Institutes of Health (NIH), and NIH Roadmap for Medical Research.

Chapter 14

Reduced Activity-Dependent Protein Translation in a Mouse Model of the Fragile X Premutation

ABSTRACT

It has been reported that environmental enrichment results in increased levels of Fmrp in brain and increased dendritic complexity after training on a skilled reaching task. The present experiment evaluated activity-dependent increases in Fmrp levels in the motor cortex in response to training on a skilled forelimb reaching task in the CGG KI mouse model of the fragile X premutation. Mice trained to reach for sucrose pellets with a non-preferred paw had Fmrp, Arc, and c-Fos quantified by Western blot in the contralateral motor cortex and compared to levels in the ipsilateral motor cortex. After training, all mice showed increases in Fmrp, Arc, and c-Fos protein levels in the contralateral compared to the ipsilateral hemisphere; however, the increase in CGG KI mice was less than wildtypes. Increased Fmrp and Arc proteins scaled with learning, whereas no such relationship was observed with the c-Fos levels in all mice. These data suggest the possibility that reduced levels of activity-dependent proteins associated with synaptic plasticity such as Fmrp and Arc may contribute to the neurocognitive phenotype reported in the CGG KI mice and the fragile X premutation.

My role in this study was experimental design, building the apparatus, performing the behavioral research, supervising the Western Blotting, and analyzing the data.

INTRODUCTION

The fragile X mental retardation gene (*FMR1*), a gene that codes for fragile X mental retardation protein (FMRP), is polymorphic for the length of a CGG trinucleotide repeat in the 5' untranslated region. Individuals in the general population have 6-45 CGG repeats in the *FMR1* gene. Carriers of the full mutation underlying fragile X syndrome (FXS) carry greater than 200 CGG repeats, which transcriptionally silences the *FMR1* gene and FMRP translation (Hagerman & Hagerman, 2004b). In the fragile X premutation there are between 55 and 200 CGG repeats in the *FMR1* gene leading to increased transcription of *FMR1* mRNA (Garcia-Arocena & Hagerman, 2010) and decreased FMRP levels (Tassone & Hagerman, 2003; Tassone et al., 2000c; Tassone et al., 2000d). The premutation is associated with a late onset neurodegenerative disorder known as Fragile-X associated tremor/ataxia syndrome, (FXTAS), which results in cognitive and behavioral deficits characterized by motor ataxia and intention tremor (Hagerman et al., 2001).

To investigate the consequences of the fragile X premutation, a transgenic CGG knock-in (KI) mouse was developed by homologous recombination of the endogenous mouse CGG repeat, containing 8-12 CGG repeats, with a fragment of human origin containing 98 CGG repeats on the endogenous *Fmr1* promoter (Willemsen et al., 2003). Behavioral analysis of these CGG KI mice have shown deficits in spatiotemporal processing (Hunsaker et al., 2009; Hunsaker et al., 2010) and impaired visuomotor processing (Hunsaker et al., 2011c). Furthermore, female CGG KI mice trained on a skilled reaching task showed impaired reaching

abilities, suggesting visuomotor processing deficits derived from neurocognitive impairments (Diep et al., 2012). Many of the molecular processes underlying these impairments are unknown, but they are thought to be related to the mutated *FMR1* gene.

It is known that Fmrp associates with translating polyribosomes and mRNA and is therefore believed to act as a regulator of protein synthesis (Huber, Gallagher, Warren, & Bear, 2002). Fmrp is translated in vitro in response to neurotransmitter activation. Weiler et al. (1997) and Irwin et al., (2000, 2005) reported an increase in the Fmrp/Actin ratio in Western blot analysis of the hippocampus and visual cortex of rats after exposure to a complex environment, suggesting that levels of FMRP can be altered by increased neuronal activity and activity-dependent plasticity (Irwin et al., 2000; Irwin et al., 2005). As it has been shown that there is an increase in dendritic complexity in the motor cortex of mice after training on a skilled forelimb reaching task (Greenough, Larson, & Withers, 1985), it is possible that elevations in Fmrp levels to activity result in, or are the result of increased synaptic density in the cortex.

The present experiment was designed to evaluate Fmrp levels in response to training on a skilled forelimb reaching task, based on work by Whishaw and colleagues (Farr & Whishaw, 2002) to determine whether there is an activity-dependent increase in Fmrp levels in the motor cortex of mice. As skilled reaching is the product of several discrete movements, neuronal plasticity may link area responsible for learning the fluid motion necessary for successful reaching (Whishaw, Alaverdashvili, & Kolb, 2008). We also used the task to

evaluate levels of activity-dependent translation of Arc (also called Arg3.1) and c-Fos, two additional proteins associated with brain activity and correlated with learning (Bramham, Worley, Moore, & Guzowski, 2008; Chawla et al., 2004; Park et al., 2008; Vazdarjanova & Guzowski, 2004; Vazdarjanova et al., 2006; Vazdarjanova, McNaughton, Barnes, Worley, & Guzowski, 2002). *Arc* mRNA has been shown to associate with Fmrp at the polyribosome and is translated when Fmrp is phosphorylated after group I mGluR (mGluR1/5) activation (Pfeiffer & Huber, 2006; cf., Chowdhury et al., 2006). This is important as *Arc* mRNA has been shown to be elevated after learning and memory tasks (Vazdarjanova & Guzowski, 2004; Vazdarjanova et al., 2002; Vazdarjanova et al., 2006), whereas *c-Fos* mRNA have not been shown to be related to learning, but rather to cellular activation (Dragunow & Faull, 1989).

CGG KI were trained to reach for a sucrose pellet with a non-preferred paw. Levels of Fmrp, Arc, and c-Fos proteins in the contralateral motor cortex (in relation to the trained hand) were quantified by Western blot and compared to levels in the ipsilateral motor cortex, as well as Actin and Gapdh as loading controls. The difference in Fmrp levels between the two hemispheres was used as a measure of activity-dependent increase in protein levels.

After training in the task, both CGG KI and wildtype littermate mice showed activity-dependent increases in Fmrp, Arc, and c-Fos protein levels in the contralateral motor cortex as compared to the ipsilateral motor cortex. However, the increase in all three proteins in the CGG KI mice was less than that seen in wildtype mice. These results, showing reduced protein synthesis, suggests that

the reduced levels of activity-dependent proteins associated with synaptic plasticity may contribute to the neurocognitive deficits seen in CGG KI mice with the fragile X premutation.

MATERIALS AND METHODS

Mice

Nine male CGG KI mice heterozygous for the fragile X premutation at 6 months of age and 9 male wildtype mice of the same age were used as subjects for this task. All wildtype mice were littermates with CGG KI mice included in the study. All CGG KI mice were bred onto a congenic C57BL/6J background over greater than 12 generations from founder mice on a mixed FVB/N x C57BL/6J background (Willemse et al., 2003). Mice were housed in same sex, mixed genotype groups with three or four mice per cage in a temperature and humidity controlled vivarium on a 12 h light-dark cycle. Mice had ad libitum access to water and were maintained at 90-95% their free feeding weight throughout experimentation. Mouse weights did not differ among genotypes during experimentation. All experiments were conducted during the light phase of the diurnal cycle and conformed to University of California, Davis IACUC approved protocols.

Genotyping

As somatic instability of CGG repeats on the *Fmr1* gene among tissues in the CGG KI mouse has been shown to be negligible (typically under 10 CGG repeats across tissues; Willemse et al., 2003), genotyping to verify CGG repeat length was carried out upon tail snips. Following a method kindly provided by Rob Willemse (Brouwer et al., 2007; Brouwer et al., 2008a) and modified in collaboration with the laboratories of F Tassone and PJ Hagerman (Saluto et al.,

2005; personal communication), CGG repeat lengths were measured using the FastStart Taq DNA Polymerase, dNTP Pack(Roche Diagnostics; Manheim, Germany) DNA was extracted from mouse tails by incubating with 10 mg/mL Proteinase K (Fermentas, Inc.; Glen Burnie, MD) in 300 μ L lysis buffer containing 50 mM Tris-HCl, pH 7.5, 10 mM EDTA, 150 mM NaCl, 1% SDS overnight at 55°C. One hundred microliters (100 μ L) saturated NaCl was then added, mixed and centrifuged. The supernatant was gently mixed with two volumes of 100% ethanol, and the DNA was pelleted by centrifugation. The DNA was washed and centrifuged in 500 μ L 70% ethanol. The DNA was then dissolved in 100 μ L milliQ-H₂O. CGG repeat lengths were determined by PCR using solutions from the FastStart Taq DNA Polymerase, dNTP Pack (Roche Diagnostics). Briefly, approximately 500-700 ng of DNA was added to 20 μ L of PCR mixture containing 0.5 μ M/L of each primer, 250 μ M/L of each dNTP (Roche Diagnostics). 2.5 M Betaine (Sigma-Aldrich), 1X Buffer 2 and 0.05 U of FastStart Taq DNA Polymerase (Roche Diagnostics) The primers flank the CGG repeat region of Fmr1 gene, the forward primer was 5'-CGG GCA GTG AAG CAA ACG-3'and the reverse primer was 5'-CCA GCT CCT CCA TCT TCT CG-3 The CGG repeats were amplified using a 3-step PCR with 10 min denaturation at 98 °C, followed by 35 cycles of 35 s denaturation at 98 °C, annealing for 35 s at 55 °C, and at the end each cycle elongation for 2 min at 72 °C . The last step of the PCR consisted in a 10 minute elongation at 72°C to. The sizes of CGG DNA amplicons were determined by running 20 μ L of PCR reaction per sample and a molecular weight marker (O'GeneRuler 50bp DNA ladder; Fermentas, Inc.) for 2 hrs at

150V on a 2.5% agarose gel with 0.03 μ L/ml ethidium bromide. The number of CGG repeats was calculated from pictures acquired with a GelDoc-It Imaging system (UVP, LLC Upland, CA) and using VisionWorks LS software (UVP, LLC Upland, CA). This method can detect up to 358 CGG repeats from animals in the present mouse colony. Genotyping was performed twice on each mouse, once using tail snips taken at weaning and again on tail snips and/or brain tissue collected at sacrifice. In all cases the genotypes matched.

Skilled Forelimb Reaching Apparatus

The apparatus for the skilled forelimb reaching task was a transparent Plexiglas box 19.5 cm long, 8 cm wide, and 20 cm tall. A 1-cm wide vertical window ran up the front of the box centered along the front wall. A .2-cm thick plastic shelf (8.3 cm long and 3.8 cm wide) was mounted 1.1 cm from the floor on the front of the box. Twenty mg banana-flavored sucrose pellets (Bioserve Inc.; Frenchtown, NJ) could be placed in indentations spaced 1 cm away from the window and centered on its edges such that the mouse could only reach each indentation with one paw and could not reach the pellets with their tongue (*cf.*, Diep et al., 2012; Farr & Whishaw, 2002).

Experimental Methods

Skilled Forelimb Reaching Task

Pretraining

Mice were food deprived to 90-95% free feeding weight and given access to 20 mg banana flavored sucrose pellets in their home cage to habituate to the food reward for 2 days. Throughout experimentation mice were provided sufficient food to maintain 95% free feeding weight 30 min after experimentation each day. All training was carried out following the protocols described in (Diep et al., 2012).

Six additional wildtype and 6 CGG KI mice were randomly chosen to receive skilled reaching task training and 3 CGG KI and 3 wildtype mice were chosen to simply receive daily exposures to the testing apparatus but not receive skilled reaching training.

Training

On days 3-5, mice were placed in the apparatus with sucrose pellets on the floor and in the open window within reach of the mouse's tongue for 30 min and allowed to consume sucrose pellets. On days 6-10, mice were placed in the apparatus with sucrose pellets available straight ahead immediately outside the open window for 15 min, allowing the mouse to use their tongue to obtain the reward pellet. When mice freely ate rewards, they moved on to task acquisition.

Acquisition

Prior to the first day of acquisition, mice were placed in the apparatus with the indentations on both sides outside the window containing sucrose pellets. The mice were allowed to reach and obtain as many rewards as possible for 15

min. The paw preference of each mouse was determined as the paw used during the majority of individual reaches. Starting the next day, all mice were trained against their paw preference.

Mice were placed in the apparatus for 15 min with one sucrose pellet placed on the side of the open window such that the mouse could only obtain it with the non-preferred paw. Each time the mouse reached, an experimenter blinded to mouse genotype recorded whether the reach was successful or whether or not errors occurred and immediately replaced the reward pellet when displaced. A successful reach was defined as the mouse obtaining and consuming the food pellet. If the mouse knocked the pellet away or dropped it prior to eating it an error was recorded. This acquisition was continued for 11 days.

The untrained group of mice ($n=6$; 3 wildtype and 3 CGG KI Mice) were placed in the apparatus daily with access to sucrose reward pellets but were never trained to reach. This served as a control for any nonspecific effects on brain protein levels associated with exposure to the reaching task apparatus or sucrose reward.

Western Blotting

On Day 11, mice were given one final session in the reaching task and then returned to their home cage for 60 min. After 60 min, the mice were sacrificed by cervical dislocation and the somatosensory/motor cortices were dissected and flash frozen on liquid nitrogen by experimenters blinded to the

mouse genotype and stored at -80°C until further processing. The rest of the brain was separated into hippocampus, brainstem, cortex, midbrain, and subcortical forebrain (*i.e.*, Basal Ganglia, Thalamus, Septal Nuclei), similarly frozen, and stored at -80°C.

The somatosensory/motor cortex tissue was homogenized (1000 µl buffer x 0.01 g of tissue) in HEPES buffer (10 mM HEPES, 300 mM KCl, 3 mM MgCl₂, 100 µM CaCl₂, 0.45% Triton X-100, and 0.05% Tween 20, pH 7.6) with protease inhibitor cocktail (Roche Diagnostics) in a sterilized vial, and centrifuged for 30 min at 12,000 rpm at 4°C. The supernatant was collected and assayed for total protein concentration using a Bradford assay (Bradford, 1976).

Sixty micrograms (µm) of protein was diluted with Laemmli sample buffer (BioRad, Hercules, CA) and were heat denatured for 5 mins at 98°C. Denatured samples were loaded onto an acrylamide gel (4% stacking gel and 8% separating gel). Gels were evaluated for total protein using coomassie blue staining prior to transfer to a nitrocellulose filter paper at 4°C. Efficient protein transfer was confirmed using ponceau red staining. The blot was placed in a blocking solution for 120 minutes in a rotating 50 mL conical vial in Odyssey blocking buffer (BioRad). After blocking, the tissue was incubated in primary antibodies in blocking buffer with 0.1% Tween-20 overnight at 4°C with gentle agitation. Primary antibodies included an antibody targeting the C terminus of Fmrp raised in chicken (1:15,000; Hunsaker et al., 2011b; Iwahashi et al., 2009), the 1C3 clone monoclonal antibody targeting the N terminus of Fmrp (1:250; Millipore, Inc, Billerica, MA), a rabbit polyclonal antibody targeting Arc protein

(1:500; Santa Cruz Biotechnology, Santa Cruz, CA), a polyclonal antibody targeting c-Fos (1:1000; Cell Signaling Technology, Danvers, MA), a monoclonal antibody targeting β-Actin (Abcam, Inc., 1:10,000), and a monoclonal antibody targeted to Gapdh (Abcam, Inc; 1:5,000). After incubation in the appropriate primary antibodies, the blots were incubated in secondary antibodies (1:10,000) designed to work with the Odyssey imaging system (Li-Cor, Lincoln, NE) for 60 min at room temperature and rinsed. Levels of Fmrp, Arc, and c-Fos were quantified using the Odyssey system and normalized to either β-Actin or Gapdh as loading controls. Data normalized to Gapdh are reported, but values using Actin as a loading control gave the same pattern of results.

Dependent Measures and Statistical Analysis

Behavior

The number of times that the mouse successfully reached and obtained a sucrose pellet reward was collected as the dependent variable. If the mouse reached and missed/displaced the pellet during a reach or dropped the pellet before consuming it, an error was recorded and the pellet was immediately replaced. Qualitative observations concerning the behavior/strategy of each mouse was also recorded by the observer. For analysis, the percentage of reaches that were successful was calculated for each day:

(% successful reaches = [number of successful reaches / total number of reaches] * 100).

To determine whether parametric analyses of variance (ANOVA) were appropriate for the data, tests of normality, homoscedasticity, and sphericity were performed. Once it was determined that parametric statistics were appropriate for the data, the data were plotted and placed into groups as follows: the mice in the wildtype group all had between 8-12 CGG repeats (mean 10 +/- .2 SEM; n=6), and the mice included in the CGG KI group ranged between 138-185 CGG repeats (mean 168 +/- 19; n=6). A 3 (CGG repeat group) x 11 (Day) repeated measures analysis of covariance (ANCOVA) was used to determine differences among the groups for acquisition of the skilled reaching task with total number of times each mouse reached during each session as a covariate. ANOVA were used to confirm that the total number of reaches did not differ among genotypes.

To specifically determine differences in the day the mice learned the task to asymptotic performance levels, the data for each mouse was evaluated for the point at which the learning curve changed from being linear to curvilinear and confirmed using the change point algorithm reported by Gallistel et al. (2004; translated into R from the original MATLAB code; cf., Diep et al., 2012). The first change point in the returned change point array corresponded to the first point at which the learning curve statistically significantly changed (discrimination threshold was set at logit=3: odds against=1,000:1 or p<.001) was chosen as the index of learning for each mouse. This change point for each mouse was then used to compare the learning index across groups using a one way ANOVA.

Subsequent analyses were performed to further characterize all main effects, and Tukey-HSD post hoc pairwise comparisons tests were used to characterize all significant main effects and interactions among factors. All analyses were considered significant at $p_{(adj)} < .05$. Statistical analyses were performed in R 2.14 language and environment (R Development Core Team, 2012).

Western Blotting

Western blotting data for Fmrp, Arc, and c-Fos were first normalized to Gapdh as a loading control. The values for the brain hemisphere contralateral to the trained hand were then normalized to the protein values in the hemisphere ipsilateral to the trained hand. This normalized value was used as the unit of statistical analysis. In all cases each Western Blot was stripped and re-probed with antibodies for each protein by a second experimenter blinded to the results of the first experiment. Reported data are from the first probe of each blot.

Once it was determined that parametric statistics were appropriate for the data, the data were plotted and placed into the same groups as for behavior, with the addition of a group of mice that were exposed to reward and the reaching task apparatus, but were never trained to reach ($n=3$ wildtype mice, $n=3$ CGG KI mice with CGG repeats between 145-180 repeats; mean 165 \pm 12). A 1 way (CGG repeat group) ANOVA was used to determine differences among the groups for the amount of activity-dependent increases in of Fmrp, Arc, and c-Fos

levels. Similar ANOVA were used to confirm that the total number of reaches did not differ among genotypes.

To characterize any possible relationship of performance on the skilled forelimb reaching task and increasing protein levels a Pearson's correlation coefficient was calculated comparing performance averaged across days 10-11 and Fmrp, Arc, and c-Fos protein levels. To control for the false discovery rate (FDR) given the number of analyses performed on the data, all p values have been FDR adjusted as outlined by (Benjamini et al., 2001).

RESULTS

Behavioral Performance

For all mice, data were grouped by CGG repeat length (Wildtype, CGG KI) and analyzed across days of training using repeated measures ANCOVA with percent successful reaches as the dependent variable, CGG repeat group as the grouping factor, and day of training as a repeated within-subjects factor with total number of attempted reaches during each session as a covariate. There was a main effect of CGG repeat length group ($F(1,64)=21.33$, $p_{(adj)}<.001$), an effect for training day ($F(10,64)=81.92$, $p_{(adj)}<.0001$), and there was a significant interaction between group and day ($F(10,64)=2.92$, $p_{(adj)}<.005$), suggesting that the longitudinal performance trajectory differed among CGG repeat groups (Figure 31). Total number of reaches per session did not significantly contribute to skilled forelimb reaching task acquisition ($F(10,64)=1.33$, $p_{(adj)}=.23$), and did not differ among CGG repeat groups ($F(1,64)=1.96$, $p_{(adj)}=.17$; wildtype mean $68 +/- 11$ (SEM) reaches per session; CGG KI group $57 +/- 9$ reaches per session).

To further characterize the significant interaction, a Tukey-HSD post hoc pairwise comparisons test demonstrated that the groups did not differ in performance during days 1-6 of training (all $p_{(adj)}>.25$), whereas on day 7-11 the wildtype group showed a greater percentage of successful reaches than the CGG KI mouse group (all $p_{(adj)}<.001$).

Based on the results of the paired comparisons, it appears that the two trained groups show differential time-courses for reaching asymptotic performance on the skilled forelimb reaching task (Figure 31). A confirmatory

analysis of differences in the learning curve among CGG groups was performed using a change point algorithm described by Gallistel et al. (2004). The first change point in the data (corresponding to the first alteration to the learning curve at a $p<.001$ threshold) returned by the algorithm was selected for each mouse and compared across groups: There was a significant difference between the wildtype and CGG KI group for this first change point ($F(1,11)=9.3$, $p_{(adj)}=.$ 011). The wildtype mice showed a significant change in the slope of the learning curve on day 7 (group mean $6.7 +/-.45$ SEM), whereas the Low CGG repeat group showed a change in slope on day 9 (group mean $8.8 +/-.23$).

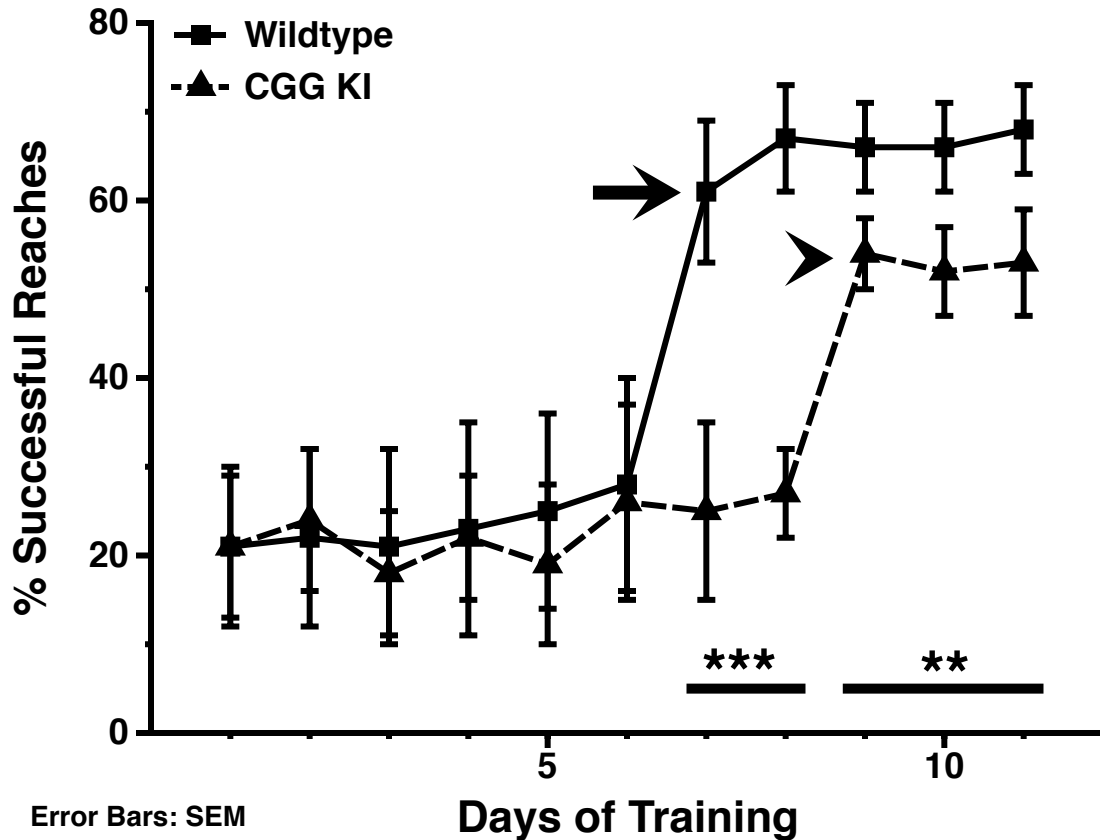


Figure 31: Wildtype perform better at skilled reaching than CGG KI mice. Arrow signals first change point for wildtype mice at day 7. Arrowhead signals the first change point for CGG KI mice at day 9. ** $p < .01$ *** $p < .001$ Day x Group interaction based on Tukey's post hoc paired comparison.

Western Blotting

Overall Protein Levels

For all mice, data were grouped (Wildtype, CGG KI, untrained mice) for analysis. For Fmrp, there was a slight trend toward differences in levels of Fmrp between the wildtype and CGG KI mice in the untrained hemispheres ($F(1,11)=3.30$, $p_{(adj)}=.096$), but no evidence for significant differences in Arc ($F(1,11)=2.13$, $p_{(adj)}=.18$) or c-Fos ($F(1,11)=1.13$, $p_{(adj)}=.31$). Including the untrained CGGKI and wildtype mice into the analysis did not alter these results (Fmrp ($F(1,17)=2.97$, $p_{(adj)}=.11$); Arc ($F(1,17)=1.47$, $p_{(adj)}=.24$); c-Fos ($F(1,17)=.92$, $p_{(adj)}=.35$)).

Activity-Dependent Translation of Fmrp.

There was a significant effect for group ($F(2,15)=37.35$, $p_{(adj)}<.0001$), with CGG KI mice showing reduced activity-dependent protein translation compared to wildtype littermate mice ($p_{(adj)}=.006$; Figure 32). Both wildtype and CGG KI mice showed significantly greater activity-dependent Fmrp translation compared to mice that did not receive skilled reaching training ($p_{(adj)}<.0001$, $p_{(adj)}<0.006$, respectively).

Activity-Dependent Translation of Arc.

There was a significant effect for group ($F(2,15)=37.22$, $p_{(adj)}<.0001$), with CGG KI mice showing reduced activity-dependent protein translation compared

to wildtype littermate mice ($p_{(adj)}<0.002$; Figure 32). Both wildtype and CGG KI mice showed significantly greater activity-dependent Arc translation compared to mice that did not receive skilled reaching training ($p_{(adj)}<.0001$, $p_{(adj)}<.002$, respectively).

Activity-Dependent Translation of c-Fos.

There was a significant effect for group ($F(2,15)=25.70$, $p_{(adj)}<.0001$), with CGG KI mice showing reduced activity-dependent protein translation compared to wildtype littermate mice ($p_{(adj)}=.004$; Figure 32). Both wildtype and CGG KI mice showed significantly greater activity-dependent c-Fos translation compared to mice that did not receive skilled reaching training ($p_{(adj)}<.0001$, $p_{(adj)}=.011$, respectively).

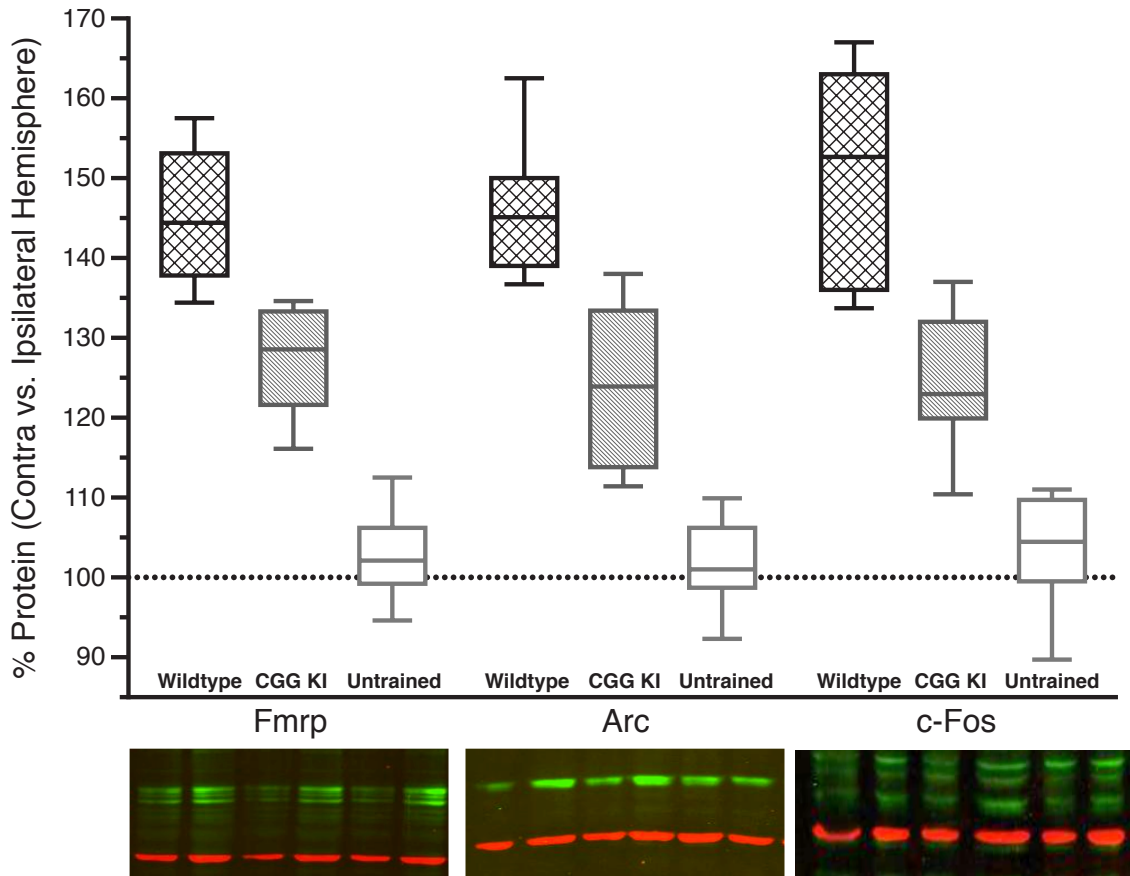


Figure 32: The WT have higher protein levels in the trained hemisphere (contra) vs untrained, ipsilateral hemisphere compared to CGG KI mice. All trained mice have higher activity-dependent protein levels than untrained mice. Below each set of boxplots are example Western blots for Fmrp, Arc, and c-Fos.

Relationship Between Skilled Reaching Performance and Protein Levels

To characterize any possible relationship between performance on the skilled forelimb reaching task and activity-dependent increases in protein levels, Pearson's correlation coefficients were calculated between CGG repeat length and averaged performance across days 10-11 for CGG KI mice (Figure 33). A positive association was observed between the asymptotic level of skilled reaching performance and Fmrp levels in the wildtype and CGG KI mice (wildtype corr $\rho = .79$, $p_{(adj)}=.011$; $R_{(adj)}^2 = .62$; CGG KI corr $\rho = -.72$, $p_{(adj)}=.025$; $R_{(adj)}^2 = .51$). A positive association was also observed between the asymptotic level of skilled reaching performance and Arc levels in the wildtype and CGG KI mice (wildtype corr $\rho = .83$, $p_{(adj)}=.031$; $R_{(adj)}^2 = .69$; CGG KI corr $\rho = .82$, $p_{(adj)}=.028$; $R_{(adj)}^2 = .67$). However, there was no association between the asymptotic level of skilled reaching performance and c-Fos levels in the wildtype and CGG KI mice (wildtype corr $\rho = .25$, $p_{(adj)}=.37$; $R_{(adj)}^2 = .06$; CGG KI corr $\rho = .15$, $p_{(adj)}=.48$; $R_{(adj)}^2 = .02$).

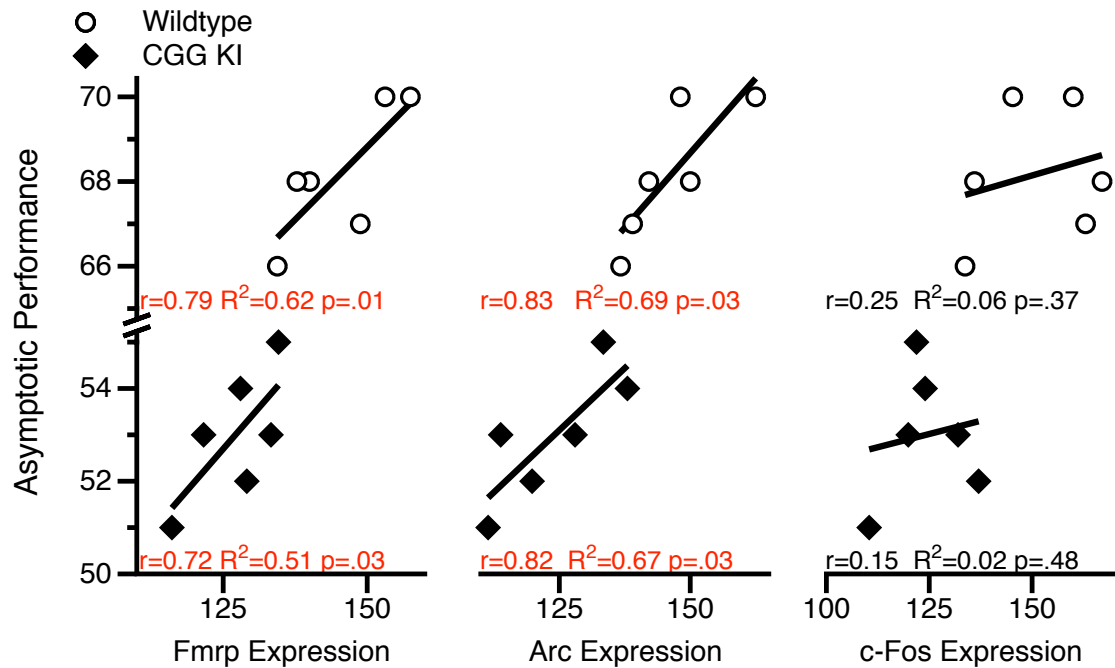


Figure 33: Performance correlated with Protein Expression within WT and CGG KI mice for Arc and Fmrp (both involved with learning/plasticity), but not c-Fos, which reflects cell activity, rather than learning per se.

DISCUSSION

The results of this experiment indicate an activity-dependent increase in protein levels of Fmrp, Arc, and c-Fos as well as a difference in both performance and protein levels between CGG KI and wildtype mice. These findings correlate with previous work that has shown that quantity of Fmrp in the brain is influenced by activity and environmental enrichment (Irwin et al., 2005; Weiler et al., 1997). Additionally, our results indicate a role for Fmrp in learning and memory as shown through the skilled reaching task.

Trained mice displayed higher protein levels than untrained in the trained hemisphere of all examined regions of the brain. This is seen for all three activity markers (Arc, c-Fos, Fmrp) investigated here, indicating a relationship between activity and protein levels. This clearly shows that the skilled task induced stimulation, leading to translational activity and production of proteins. Additionally, although the trained CGG KI mice had reduced magnitude of activity-dependent increases in levels of proteins than the wildtype mice, they had higher levels overall than the untrained mice, further demonstrating the neuronal activity's role on increased protein translation.

Our results show that wildtype mice perform better at the skilled reaching task than CGG KI mice. CGG KI mice required more sessions to learn the task, and never matched the wildtype mice for successful reaches. Although Fmrp levels increased in the contralateral motor cortex in both groups of mice after learning, the effect was less pronounced in CGG KI than wildtype mice. This finding, in light of the observed increased latency to acquire the skilled reaching

task and reduced asymptotic performance levels seen in CGG KI mice supports our hypothesis that Fmrp may play a role in experience dependent plasticity. Our findings correlate with the documented neurocognitive deficits seen in previous studies of CGG KI mice (Diep et al., 2012; Hunsaker et al., 2009; Hunsaker et al., 2010; Hunsaker et al., 2011c).

Knock-out mouse models of fragile X syndrome have been used previously to show that Fmrp is involved in synaptic plasticity (Bear et al., 2004; Huber et al., 2002; Pfeiffer & Huber, 2006; Zang et al., 2009). Protein levels increase in response to stimulation as a part of development as well as in learning and memory (Antar, Dictenberg, Plociniak, Afroz, & Bassell, 2005). Our findings reflect this response through increased levels of Fmrp after training. Additionally, levels were further elevated in mice that had the highest number of successful reaches. Importantly, although we saw the same pattern in CGG KI mice as we did with wildtype mice, the degree of increased Fmrp were reduced in the CGG KI mice.

The Arc protein often used as a marker for activity and plasticity (Chowdhury et al., 2006; Lyford et al., 1995). Due to its translation at activated synaptic sites, it is believed to play a role in learning and memory (McIntyre et al., 2005). We therefore examined Arc protein levels after mice learned the skilled reaching task to verify that activity-dependent changes in the brain had occurred. Accordingly, we observed increased levels of Arc in the contralateral motor cortex of both wildtype and CGG KI mice after training in comparison with untrained mice. Additionally, these activity-dependent increased levels of Arc protein were

markedly higher in wildtype than CGG KI mice, supporting our argument that the mutation in our CGG KI mice causes plasticity to be impeded, leading to lower levels of activity-dependent change after training.

c-Fos is used not as a marker of activity-dependent changes to a cell, but of overall cell activity. c-Fos is expressed at neuronal sites when action potentials are fired, leading to their use as a confirmation of activity in the cell (Dragunow & Faull, 1989). Accordingly, although we saw increased levels of c-Fos in the trained versus untrained hemispheres of brain, we did not find a correlation of overall performance on the task. This shows that c-Fos was activated by the synaptic plasticity involved in learning a new skill, but was not changed by number of successful reaches. Interestingly, levels of c-Fos are still lower in CGG KI mice, correlating nicely with our other markers and further supporting our argument that premutation length CGG repeats on the *Fmr1* gene may lead to decreases in protein translation that are associated with learning.

The similar pattern of activity-dependent increases in protein levels between Fmrp and Arc is likely due to the proposed role of Fmrp as a transcriptional repressor for a number of proteins involved with long term depression, including Arc. It has been proposed that Arc is translated in response to group I mGluR (mGluR1/5) activation and is involved in the internalization of AMPA receptors at the synapse through endocytosis mechanisms (Pfeiffer & Huber, 2006). c-Fos, on the other hand, has not been shown to interact with Fmrp, so there is no reason to assume that Fmrp and c-Fos levels should show

the same relationship with behavior. This hypothesis is supported by the present data seen in Figure 33.

What the present experiment was unable to determine was the mechanism whereby the activity-dependent increase in protein levels were reduced in CGG KI mice relative to their wildtype littermates. Future studies are necessary to determine if these results were mediated by changes to protein turnover, protein synthesis, or reductions in the activity-dependent increases in dendritic complexity seen in wildtype mice, resulting in general increases in protein levels. Additionally, similar motor tasks using more episodic training protocols would be necessary to determine if *Fmr1*, *Arc*, and *c-Fos* mRNA early gene expression show a similar pattern.

In summary, the increased levels of Fmrp and Arc indicate that neuronal activity can be activated by learning and memory tasks like the skilled reaching task. This finding can add to the understanding of Fmrp crucial role in memory formation and learning. Since an increase in Fmrp is seen during learning, it implies that CGG KI mice do not have trouble making synaptic connections and learning new tasks, but rather that it takes longer. Learning can still be achieved given more time for mastering tasks. However, it does appear that even if the task were continued for longer periods of time, Fmrp levels in CGG KI mice will never reach levels as high as the wildtype mice. Thus, though learning itself is not entirely impaired, it does indicate that CGG KI mice may never be able to learn a motor task as quickly as wildtype. However, with this in mind, we may be able to further investigate Fmrp role in neuronal growth and development through

activity tasks, which will add to the understanding of the mouse model. Additionally, we may be able to use our knowledge of activity-dependent translation in using Fmrp as a potential therapeutic target, by developing training tasks that could initiate neuronal growth and induce synaptic plasticity.

Acknowledgements:

The authors wish to thank Dr. Oswald Steward, Ph.D., for helpful discussions about anti-Arc antibodies and Dr. Justin A. Beller and Ali Izadi for assistance with Western Blotting. The authors would like to thank Lara E. Cardy and Norma Cardona for work on a preliminary version of this experiment and Binh T. Ta for genotyping.

This work was supported by National Institute of Health (NIH) grants, NINDS RL1 NS062411, a Roadmap Initiative grant (UL1 DE019583) from NIDCR in support of the NeuroTherapeutics Research Institute (NTRI) consortium, a NIH Neuroscience Training Grant T32 MH 82174, and by a grant (UL1 RR024146) from the NCRR.

CONCLUSIONS

Overall, the data presented in this dissertation point to the CGG KI mouse model of the fragile X premutation as a valid model for not only the neuropathological sequelae, but also the neurocognitive abnormalities associated with increasing dosage of the *FMR1* gene.

The CGG KI mouse model of the fragile X premutation shows neuropathological features in the central nervous system, peripheral autonomic nervous system, and enteric nervous system that are recapitulate features observed in both male and female carriers of the fragile X premutation, both with and without FXTAS. Furthermore, similar pathology are present in the somatic organ systems of both the CGG KI mice as well as human premutation carriers.

Although the behavioral tasks do not directly parallel the behavioral paradigms used for research into human premutation carriers, the behavioral phenotype of the CGG KI mouse appears to recapitulate the premutation neurocognitive phenotype. Both male and female CGG KI mice show impaired spatiotemporal processing as well as neuromotor deficits that are congruent with the proposed premutation phenotype.

More importantly, the behavioral deficits present in the CGG KI mouse model of the fragile X premutation become increasingly profound as the dosage or number of CGG repeats on the *Fmr1* gene increases. This direct relationship between degrading behavioral task performance and increasing CGG repeat lengths appeared relatively constant across spatial and temporal processing tasks, and tasks emphasizing the spatial and temporal coordination of

visuomotor function in both male and female CGG KI mice. These data parallel the effects reported for genetic dosage observed by Goodrich-Hunsaker et al. (2011a, 2011b, 2011c), such that behavioral performance on behavioral tasks emphasizing visuospatial processing worsened as a function of increasing CGG repeat length, even when there is not a group effect with a non-premutation carrier comparison group. This parallel association with genetic dosage among CGG KI mice and premutation carriers suggests the CGG KI mouse may be used as a proxy for premutation carriers, so long as the behavioral tasks are chosen with care and test specific domains, including spatiotemporal processing and visuomotor function.

Because the performance of CGG KI mice on the behavioral paradigms used in this dissertation inversely scaled with repeat length (or dosage of the mutation) and neuropathological features were shown to directly scale with genetic dosage, the data presented in this work comprise a neurocognitive phenotype of the CGG KI mice. This means that the performance on the behavioral tasks can be used to predict factors related to disease states. In the present work, as formally described in Chapter 10, behavioral performance of CGG KI mice on spatiotemporal processing tasks provided sufficient data to classify not only the general mutation status of each mouse (*i.e.*, wildtype, mutant), but more importantly, also classify the general CGG repeat length (*i.e.*, wildtype, 70-116 repeats, 132-198 repeats) of the CGG KI mice with above 90% accuracy. When combined with neurophysiological recordings, these data were able to not only classify mice by general CGG repeat groups, but was also able

to determine for >85% of mice the correct number of CGG repeats and order the mice accordingly using unsupervised classification techniques.

Although not explicitly classified due to an insufficient sample size, performance on a temporal ordering for spatial locations task (Chapter 11), as well as performance on a skilled walking and skilled forelimb reaching task of visuomotor processing (Chapters 12-13) showed direct relationships between decreases in behavioral performance and increasing CGG repeat length--in some cases showing even more highly significant associations than the original spatial and temporal processing tasks described in Chapters 7, 8, and applied in Chapter 11. Additionally, the data from Chapter 14, demonstrating that CGG KI mice show altered synaptic protein dynamics also appear to contribute to a behavioral endophenotype as both behavioral performance as well as activity dependent protein levels inversely scale with genetic dosage similarly to the other behavioral tasks presented in this dissertation.

The CGG KI mouse model of the fragile X premutation has been shown to model the neuropathological and neurocognitive consequences of the premutation as present in human fragile X premutation carriers. The pathological correlates, additionally were able to model features more widely associated with FXTAS, as opposed to the fragile X premutation per se--that is the presence of intranuclear inclusions throughout the central nervous system, peripheral nervous system, enteric nervous system, endocrine system, as well as somatic organ systems. The behavioral phenotypes were initially designed to model research into the fragile X premutation being performed by (Goodrich-Hunsaker

et al., 2011a, 2011b, 2011c), among others (*cf.*, Hocking et al., 2012), and was extended to evaluate cognitive function across domains proposed to be impaired in the premutation (Simon, 2011), but as yet have not been evaluated in premutation carriers. The results of the experiments presented in this dissertation serve to inform the

What remains to be elucidated is whether research into human fragile X premutation carriers shows similar relationships between task performance and dosage of the *FMR1* gene mutation using sensitive behavioral paradigms emphasizing fine spatial, temporal, and visuomotor processing. If similar relationships beyond those reported by (Goodrich-Hunsaker et al., 2011a; Goodrich-Hunsaker et al., 2011b; Goodrich-Hunsaker et al., 2011c) are observed, than the CGG KI mouse will be a useful tool for evaluating disease onset/progression, disease severity, and directly evaluating treatment options prior to introduction in the clinic.

Although the CGG KI mouse has not been shown to develop FXTAS-related symptoms, even with increasing age, it has yet to be determined what factors other than the CGG repeat length contribute to the development of FXTAS. This is an important point as only 40% of male premutation carriers from a highly enriched sample will develop FXTAS with age, so it is highly likely that there are some other co-factor that has yet to be elucidated. Possible options include exposure to reactive oxygen species and impaired zinc transport that result in impaired mitochondrial dysfunction (Napoli et al., 2011; Ross-Inta et al., 2010), some environmental factor or toxin that serves as a sort of trigger

mechanism, allowing the premutation to progress toward FXTAS with age (Paul et al., 2010), direct *FMR1* mRNA toxicity affecting individuals differentially (Galloway & Nelson, 2009; Garcia-Arocena & Hagerman, 2010) and other genetic/epigenetic factors that interact with the *FMR1* mutation (Raske & Hagerman, 2009; Todd & Paulson, 2010). All of these factors can be individually evaluated in CGG KI mice, not only in acute exposure studies, but also in studies of chronic exposure across the lifespan due to the relatively short lifespan of the laboratory mouse. It is possible that one or many of these possibilities may result in overt motor abnormalities, including a gait ataxia and tremoring behavior in the CGG KI mice, but even if they do not, the behavioral paradigms that comprise the neurobehavioral phenotype described in Chapters 10-14 can be applied, and degrading performance on these tasks may be able to be used as a primary outcome measure for studies evaluating interventional strategies.

Together, these results within this dissertation point to a specific set of behavioral strengths and weaknesses that can be used as outcome measures to quantify later disease onset, progression, or as outcome measures for testing potential treatment options in the CGG KI mouse model, and eventually, the fragile X premutation carriers that have developed FXTAS.

REFERENCES

- Adamczak, J., Farr, T., Seehafer, J., Kalthoff, D., & Hoehn, M. (2010). High Field Bold Response to Forepaw Stimulation in the Mouse. *Neuroimage*, 51(2), 704-712. doi:10.1016/j.neuroimage.2010.02.083
- Adams, J., Adams, P., Nguyen, D., Brunberg, J., Tassone, F., Zhang, W., ... Hagerman, R. (2007). Volumetric Brain Changes in Females With Fragile X-Associated Tremor/Ataxia Syndrome (Fxtas). *Neurology*, 69(9), 851-859. doi:10.1212/01.wnl.0000269781.10417.7b
- Adams, P., Adams, J., Nguyen, D., Hessl, D., Brunberg, J., Tassone, F., ... Hagerman, R. (2010). Psychological Symptoms Correlate With Reduced Hippocampal Volume in Fragile X Premutation Carriers. *American Journal of Medical Genetics. Part B, Neuropsychiatric Genetics*, 153B(3), 775-785. doi: 10.1002/ajmg.b.31046
- Adams, S., Kesner, R., & Ragozzino, M. (2001). Role of the Medial and Lateral Caudate-Putamen in Mediating an Auditory Conditional Response Association. *Neurobiology of Learning and Memory*, 76(1), 106-116. doi: 10.1006/nlme.2000.3989
- Aghdsee, S., & Cavanagh, P. (2007). Temporal Limits of Long-Range Phase Discrimination Across the Visual Field. *Vision Research*, 47(16), 2156-2163. doi:10.1016/j.visres.2007.04.016
- Agster, K., Fortin, N., & Eichenbaum, H. (2002). The Hippocampus and Disambiguation of Overlapping Sequences. *Journal of Neuroscience*, 22 (13), 5760-5768. doi:20026559
- Aimone, J., Deng, W., & Gage, F. (2011). Resolving New Memories: A Critical Look At the Dentate Gyrus, Adult Neurogenesis, and Pattern Separation. *Neuron*, 70(4), 589-596. doi:10.1016/j.neuron.2011.05.010
- Al-Hinti, J. T., Nagan, N., & Harik, S. (2007). Fragile X Premutation in a Woman With Cognitive Impairment, Tremor, and History of Premature Ovarian Failure. *Alzheimer Disease and Associated Disorders*, 21(3), 262-264. doi: 10.1097/WAD.0b013e31811ec130
- Alaverdashvili, M., & Whishaw, I. (2008). Motor Cortex Stroke Impairs Individual Digit Movement in Skilled Reaching By the Rat. *European Journal of Neuroscience*, 28(2), 311-322. doi:10.1111/j.1460-9568.2008.06315.x
- Allen, E., Leehey, M. A., Tassone, F., & Sherman, S. (2010). Genotype/Phenotype Relationships in FXTAS. In F. Tassone & E. M. Berry-Kravis (Eds.), *The Fragile X-Associated Tremor/Ataxia Syndrome (FXTAS)* (pp. 95-122). New York: Springer.
- Allen, E., He, W., Yadav-Shah, M., & Sherman, S. (2004). A Study of the Distributional Characteristics of *Fmr1* Transcript Levels in 238 Individuals. *Human Genetics*, 114(5), 439-447. doi:10.1007/s00439-004-1086-x
- Allen, E., Hunter, J., Rusin, M., Juncos, J., Novak, G., Hamilton, D., ... Sherman, S. (2011). Neuropsychological Findings From Older Premutation Carrier Males and Their Noncarrier Siblings From Families With Fragile X Syndrome. *Neuropsychology*, 25(3), 404-411. doi:10.1037/a0021879

- Allman, M., Pelphrey, K., & Meck, W. (2011). Developmental Neuroscience of Time and Number: Implications for Autism and Other Neurodevelopmental Disabilities. *Frontiers in Integrative Neuroscience*, 6, 7. doi:10.3389/fnint.2012.00007
- Allred, R., Adkins, D., Woodlee, M., Husbands, L., Maldonado, M., Kane, J., ... Jones, T. (2008). The Vermicelli Handling Test: A Simple Quantitative Measure of Dexterous Forepaw Function in Rats. *Journal of Neuroscience Methods*, 170(2), 229-244. doi:10.1016/j.jneumeth.2008.01.015
- Almasy, L., & Blangero, J. (2001). Endophenotypes as Quantitative Risk Factors for Psychiatric Disease: Rationale and Study Design. *American Journal of Medical Genetics*, 105(1), 42-44.
- Alvarez, G., & Franconeri, S. (2007). How Many Objects Can You Track? Evidence for a Resource-Limited Attentive Tracking Mechanism. *Journal of Vision*, 7(13), 14.1-1410. doi:10.1167/7.13.14
- Amann, L., Gandal, M., Halene, T., Ehrlichman, R., White, S., McCarren, H., & Siegel, S. (2010). Mouse Behavioral Endophenotypes for Schizophrenia. *Brain Research Bulletin*, 83(3-4), 147-161. doi:10.1016/j.brainresbull.2010.04.008
- Amodeo, D., Jones, J., Sweeney, J., & Ragozzino, M. (2012). Differences in Btbr T+ Tf/J and C57Bl/6j Mice on Probabilistic Reversal Learning and Stereotyped Behaviors. *Behavioural Brain Research*, 227(1), 64-72. doi:10.1016/j.bbr.2011.10.032
- Andujar, J., Lajoie, K., & Drew, T. (2010). A Contribution of Area 5 of the Posterior Parietal Cortex to the Planning of Visually Guided Locomotion: Limb-Specific and Limb-Independent Effects. *Journal of Neurophysiology*, 103(2), 986-1006. doi:10.1152/jn.00912.2009
- Aneja, A., Fremont, W., Antshel, K., Faraone, S., Abdulsabur, N., Higgins, A., ... Kates, W. (2007). Manic Symptoms and Behavioral Dysregulation in Youth With Velocardiofacial Syndrome (22q11.2 Deletion Syndrome). *Journal of Child and Adolescent Psychopharmacology*, 17(1), 105-114. doi:10.1089/cap.2006.0023
- Antar, L., Dictenberg, J., Plociniak, M., Afroz, R., & Bassell, G. (2005). Localization of Fmrp-Associated mRNA Granules and Requirement of Microtubules for Activity-Dependent Trafficking in Hippocampal Neurons. *Genes, Brain, and Behavior*, 4(6), 350-359. doi:10.1111/j.1601-183X.2005.00128.x
- Arguello, P., Markx, S., Gogos, J., & Karayiorgou, M. (2010). Development of Animal Models for Schizophrenia. *Disease Models and Mechanisms*, 3(1-2), 22-26. doi:10.1242/dmm.003996
- Arocena, D., Iwahashi, C., Won, N., Beilina, A., Ludwig, A., Tassone, F., ... Hagerman, P. (2005). Induction of Inclusion Formation and Disruption of Lamin a/C Structure By Premutation CGG-Repeat RNA in Human Cultured Neural Cells. *Human Molecular Genetics*, 14(23), 3661-3671. doi:10.1093/hmg/ddi394

- Arrasate, M., Mitra, S., Schweitzer, E., Segal, M., & Finkbeiner, S. (2004). Inclusion Body Formation Reduces Levels of Mutant Huntingtin and the Risk of Neuronal Death. *Nature*, 431(7010), 805-810. doi:10.1038/nature02998
- Aziz, M., Stathopulu, E., Callias, M., Taylor, C., Turk, J., Oostra, B., ... Patton, M. (2003). Clinical Features of Boys With Fragile X Premutations and Intermediate Alleles. *American Journal of Medical Genetics. Part B, Neuropsychiatric Genetics*, 121B(1), 119-127. doi:10.1002/ajmg.b.20030
- Babovic, D., O'Tuathaigh, C. M., O'Sullivan, G. J., Clifford, J., Tighe, O., Croke, D., ... Waddington, J. (2007). Exploratory and Habituation Phenotype of Heterozygous and Homozygous COMT Knockout Mice. *Behavioural Brain Research*, 183(2), 236-239. doi:10.1016/j.bbr.2007.07.006
- Bacalman, S., Farzin, F., Bourgeois, J., Cogswell, J., Goodlin-Jones, B. L., Gane, L., ... Hagerman, R. (2006). Psychiatric Phenotype of the Fragile X-Associated Tremor/Ataxia Syndrome (Fxtas) in Males: Newly Described Fronto-Subcortical Dementia. *Journal of Clinical Psychiatry*, 67(1), 87-94.
- Baker, K., Wray, S., Ritter, R., Mason, S., Lanthorn, T., & Savelieva, K. (2010). Male and Female Fmr1 Knockout Mice on C57 Albino Background Exhibit Spatial Learning and Memory Impairments. *Genes, Brain, and Behavior*, 9 (6), 562-574. doi:10.1111/j.1601-183X.2010.00585.x
- Bakker, C., & Oostra, B. (2003). Understanding Fragile X Syndrome: Insights From Animal Models. *Cytogenetic and Genome Research*, 100(1-4), 111-123. doi:10.1159/000072845
- Balci, F., Papachristos, E., Gallistel, C., Brunner, D., Gibson, J., & Shumyatsky, G. (2008). Interval Timing in Genetically Modified Mice: A Simple Paradigm. *Genes, Brain, and Behavior*, 7(3), 373-384. doi:10.1111/j.1601-183X.2007.00348.x
- Ballermann, M., Metz, G., Mckenna, J., Klassen, F., & Whishaw, I. (2001). The Pasta Matrix Reaching Task: A Simple Test for Measuring Skilled Reaching Distance, Direction, and Dexterity in Rats. *Journal of Neuroscience Methods*, 106(1), 39-45.
- Balsam, P., & Gallistel, C. (2009). Temporal Maps and Informativeness in Associative Learning. *Trends in Neurosciences*, 32(2), 73-78. doi:10.1016/j.tins.2008.10.004
- Bannerman, D. (2009). Fractionating Spatial Memory With Glutamate Receptor Subunit-Knockout Mice. *Biochemical Society Transactions*, 37(Pt 6), 1323-1327. doi:10.1042/BST0371323
- Bannerman, D., Deacon, R., Offen, S., Friswell, J., Grubb, M., & Rawlins, J. (2002). Double Dissociation of Function Within the Hippocampus: Spatial Memory and Hyponeophagia. *Behavioral Neuroscience*, 116(5), 884-901.
- Bannerman, D., Grubb, M., Deacon, R., Yee, B., Feldon, J., & Rawlins, J. (2003). Ventral Hippocampal Lesions Affect Anxiety But Not Spatial Learning. *Behavioural Brain Research*, 139(1-2), 197-213.
- Barnea-Goraly, N., Eliez, S., Hedeus, M., Menon, V., White, C., Moseley, M., & Reiss, A. (2003). White Matter Tract Alterations in Fragile X Syndrome: Preliminary Evidence From Diffusion Tensor Imaging. *American Journal of*

- Medical Genetics. Part B, Neuropsychiatric Genetics*, 118B(1), 81-88. doi: 10.1002/ajmg.b.10035
- Barneoud, P., Descombris, E., Aubin, N., & Abrous, D. (2000). Evaluation of Simple and Complex Sensorimotor Behaviours in Rats With a Partial Lesion of the Dopaminergic Nigrostriatal System. *European Journal of Neuroscience*, 12(1), 322-336.
- Bartko, S., Vendrell, I., Saksida, L., & Bussey, T. (2011). A Computer-Automated Touchscreen Paired-Associates Learning (Pal) Task for Mice: Impairments Following Administration of Scopolamine or Dicyclomine and Improvements Following Donepezil. *Psychopharmacology*, 214(2), 537-548. doi:10.1007/s00213-010-2050-1
- Baskaran, S., Datta, S., Mandal, A., Gulati, N., Totey, S., Anand, R., & Brahmachari, V. (2002). Instability of Cgg Repeats in Transgenic Mice. *Genomics*, 80(2), 151-157.
- Bays, P., Singh-Curry, V., Gorgoraptis, N., Driver, J., & Husain, M. (2010). Integration of Goal- and Stimulus-Related Visual Signals Revealed By Damage to Human Parietal Cortex. *Journal of Neuroscience*, 30(17), 5968-5978. doi:10.1523/JNEUROSCI.0997-10.2010
- Bear, M., Huber, K., & Warren, S. (2004). The Mglur Theory of Fragile X Mental Retardation. *Trends in Neurosciences*, 27(7), 370-377. doi:10.1016/j.tins.2004.04.009
- Bearden, C., Jawad, A., Lynch, D., Monterosso, J., Sokol, S., McDonald-McGinn, D. M., ... Simon, T. (2005). Effects of Comt Genotype on Behavioral Symptomatology in the 22q11.2 Deletion Syndrome. *Child Neuropsychology*, 11(1), 109-117. doi:10.1080/09297040590911239
- Bearden, C., Jawad, A., Lynch, D., Sokol, S., Kanes, S., McDonald-McGinn, D. M., ... Simon, T. (2004a). Effects of a Functional Comt Polymorphism on Prefrontal Cognitive Function in Patients With 22q11.2 Deletion Syndrome. *American Journal of Psychiatry*, 161(9), 1700-1702. doi:10.1176/appi.ajp.161.9.1700
- Bearden, C., Van Erp, T. G., Monterosso, J., Simon, T., Glahn, D., Saleh, P., ... Cannon, T. (2004b). Regional Brain Abnormalities in 22q11.2 Deletion Syndrome: Association With Cognitive Abilities and Behavioral Symptoms. *Neurocase*, 10(3), 198-206. doi:10.1080/13554790490495519
- Bearden, C., Wang, P., & Simon, T. (2002). Williams Syndrome Cognitive Profile Also Characterizes Velocardiofacial/Digeorge Syndrome. *American Journal of Medical Genetics*, 114(6), 689-692. doi:10.1002/ajmg.10539
- Beaton, E., Qin, Y., Nguyen, V., Johnson, J., Pinter, J., & Simon, T. (2010). Increased Incidence and Size of Cavum Septum Pellucidum in Children With Chromosome 22q11.2 Deletion Syndrome. *Psychiatry Research*, 181 (2), 108-113. doi:10.1016/j.psychresns.2009.10.009
- Beloozerova, I., & Sirota, M. (1993a). The Role of the Motor Cortex in the Control of Accuracy of Locomotor Movements in the Cat. *Journal of Physiology*, 461, 1-25.

- Beloozerova, I., & Sirota, M. (1993b). The Role of the Motor Cortex in the Control of Vigour of Locomotor Movements in the Cat. *Journal of Physiology*, 461, 27-46.
- Beloozerova, I., & Sirota, M. (1998). Cortically Controlled Gait Adjustments in the Cat. *Annals of the New York Academy of Sciences*, 860, 550-553.
- Beloozerova, I., & Sirota, M. (2003). Integration of Motor and Visual Information in the Parietal Area 5 During Locomotion. *Journal of Neurophysiology*, 90 (2), 961-971. doi:10.1152/jn.01147.2002
- Benjamini, Y., Drai, D., Elmer, G., Kafkafi, N., & Golani, I. (2001). Controlling the False Discovery Rate in Behavior Genetics Research. *Behavioural Brain Research*, 125(1-2), 279-284.
- Bennetto, L., Pennington, B., Porter, D., Taylor, A., & Hagerman, R. (2001). Profile of Cognitive Functioning in Women With the Fragile X Mutation. *Neuropsychology*, 15(2), 290-299.
- Benson, J. B., & Haith, M. M. (2009). *Language, Memory, and Cognition in Infancy and Early Childhood*. London: Academic Press.
- Berge, O. (2011). Predictive Validity of Behavioural Animal Models for Chronic Pain. *British Journal of Pharmacology*, 164(4), 1195-1206. doi:10.1111/j.1476-5381.2011.01300.x
- Bergink, S., Severijnen, L., Wijgers, N., Sugashawa, K., Yousaf, H., Kros, J., ... Willemse, R. (2006). The DNA Repair-Ubiquitin-Associated Hr23 Proteins Are Constituents of Neuronal Inclusions in Specific Neurodegenerative Disorders Without Hampering DNA Repair. *Neurobiology of Disease*, 23(3), 708-716. doi:10.1016/j.nbd.2006.06.005
- Berman, R., Murray, K., Arque, G., Hunsaker, M., & Wenzel, H. (2012). Abnormal Dendrite and Spine Morphology in Primary Visual Cortex in the CGG Knock-in Mouse Model of The Fragile X Premutation. *Epilepsia*, 53(Supple 1), 149-159.
- Berman, R., & Willemse, R. (2009). Mouse Models of Fragile X-Associated Tremor Ataxia. *Journal of Investigative Medicine*, 57(8), 837-841. doi: 10.231/JIM.0b013e3181af59d6
- Bernier, P., & Grafton, S. (2010). Human Posterior Parietal Cortex Flexibly Determines Reference Frames for Reaching Based on Sensory Context. *Neuron*, 68(4), 776-788. doi:10.1016/j.neuron.2010.11.002
- Berry-Kravis, E., Abrams, L., Coffey, S., Hall, D., Greco, C., Gane, L., ... Leehey, M. (2007a). Fragile X-Associated Tremor/Ataxia Syndrome: Clinical Features, Genetics, and Testing Guidelines. *Movement Disorders*, 22(14), 2018-30, quiz 2140. doi:10.1002/mds.21493
- Berry-Kravis, E., Goetz, C., Leehey, M., Hagerman, R., Zhang, L., Li, L., ... Hagerman, P. (2007b). Neuropathic Features in Fragile X Premutation Carriers. *American Journal of Medical Genetics. Part A*, 143(1), 19-26. doi: 10.1002/ajmg.a.31559
- Berry-Kravis, E., Lewin, F., Wuu, J., Leehey, M., Hagerman, R., Hagerman, P., & Goetz, C. (2003). Tremor and Ataxia in Fragile X Premutation Carriers: Blinded Videotape Study. *Annals of Neurology*, 53(5), 616-623. doi:10.1002/ana.10522

- Berry-Kravis, E., Potanos, K., Weinberg, D., Zhou, L., & Goetz, C. (2005). Fragile X-Associated Tremor/Ataxia Syndrome in Sisters Related to X-Inactivation. *Annals of Neurology*, 57(1), 144-147. doi:10.1002/ana.20360
- Berry-Kravis, E. M., Hall, D., Leehey, M., & Hagerman, R. J. (2010). Treatment and Management of FXTAS. In F. Tassone & E. M. Berry-Kravis (Eds.), *The fragile X-associated tremor ataxia syndrome (FXTAS)* (pp. 137-154). New York: Springer.
- Bertenthal, B., & Von Hofsten, C. (1998). Eye, Head and Trunk Control: The Foundation for Manual Development. *Neuroscience and Biobehavioral Reviews*, 22(4), 515-520.
- Bertenthal, B., Rose, J., & Bai, D. (1997). Perception-Action Coupling in the Development of Visual Control of Posture. *Journal of Experimental Psychology: Human Perception and Performance*, 23(6), 1631-1643.
- Bertone, A., Hanck, J., Kogan, C., Chaudhuri, A., & Cornish, K. (2010). Associating Neural Alterations and Genotype in Autism and Fragile X Syndrome: Incorporating Perceptual Phenotypes in Causal Modeling. *Journal of Autism and Developmental Disorders*, 40(12), 1541-1548. doi: 10.1007/s10803-010-1110-z
- Beurze, S., Toni, I., Pisella, L., & Medendorp, W. (2010). Reference Frames for Reach Planning in Human Parietofrontal Cortex. *Journal of Neurophysiology*, 104(3), 1736-1745. doi:10.1152/jn.01044.2009
- Bish, J., Chiodo, R., Mattei, V., & Simon, T. (2007). Domain Specific Attentional Impairments in Children With Chromosome 22q11.2 Deletion Syndrome. *Brain and Cognition*, 64(3), 265-273. doi:10.1016/j.bandc.2007.03.007
- Bish, J., Ferrante, S., McDonald-Mcginn, D., Zackai, E., & Simon, T. (2005). Maladaptive Conflict Monitoring as Evidence for Executive Dysfunction in Children With Chromosome 22q11.2 Deletion Syndrome. *Developmental Science*, 8(1), 36-43. doi:10.1111/j.1467-7687.2005.00391.x
- Bish, J., Nguyen, V., Ding, L., Ferrante, S., & Simon, T. (2004). Thalamic Reductions in Children With Chromosome 22q11.2 Deletion Syndrome. *Neuroreport*, 15(9), 1413-1415.
- Bish, J., Pendyal, A., Ding, L., Ferrante, H., Nguyen, V., McDonald-Mcginn, D., ... Simon, T. (2006). Specific Cerebellar Reductions in Children With Chromosome 22q11.2 Deletion Syndrome. *Neuroscience Letters*, 399(3), 245-248. doi:10.1016/j.neulet.2006.02.001
- Blanchard, D., Griebel, G., & Blanchard, R. (2003a). Conditioning and Residual Emotionality Effects of Predator Stimuli: Some Reflections on Stress and Emotion. *Progress in Neuro-Psychopharmacology and Biological Psychiatry*, 27(8), 1177-1185. doi:10.1016/j.pnpbp.2003.09.012
- Blanchard, D., Griebel, G., & Blanchard, R. (2003b). The Mouse Defense Test Battery: Pharmacological and Behavioral Assays for Anxiety and Panic. *European Journal of Pharmacology*, 463(1-3), 97-116.
- Blanchard, D., Sakai, R., McEwen, B., Weiss, S., & Blanchard, R. (1993). Subordination Stress: Behavioral, Brain, and Neuroendocrine Correlates. *Behavioural Brain Research*, 58(1-2), 113-121.

- Blume, S., Cass, D., & Tseng, K. (2009). Stepping Test in Mice: A Reliable Approach in Determining Forelimb Akinesia in Mptp-Induced Parkinsonism. *Experimental Neurology*, 219(1), 208-211. doi:10.1016/j.expneurol. 2009.05.017
- Bohlen, M., Cameron, A., Metten, P., Crabbe, J., & Wahlsten, D. (2009). Calibration of Rotational Acceleration for the Rotarod Test of Rodent Motor Coordination. *Journal of Neuroscience Methods*, 178(1), 10-14. doi:10.1016/j.jneumeth.2008.11.001
- Bontekoe, C., Bakker, C., Nieuwenhuizen, I., Van Der Linde, H., Lans, H., De Lange, D., ... Oostra, B. (2001). Instability of a (Cgg)98 Repeat in the Fmr1 Promoter. *Human Molecular Genetics*, 10(16), 1693-1699.
- Bontekoe, C., De Graaff, E., Nieuwenhuizen, I., Willemsen, R., & Oostra, B. (1997). Fmr1 Premutation Allele (Cgg)81 is Stable in Mice. *European Journal of Human Genetics*, 5(5), 293-298.
- Bourgeois, J., Coffey, S., Rivera, S., Hessl, D., Gane, L., Tassone, F., ... Hagerman, R. (2009). A Review of Fragile X Premutation Disorders: Expanding the Psychiatric Perspective. *Journal of Clinical Psychiatry*, 70(6), 852-862. doi:10.4088/JCP.08m04476
- Bourgeois, J., Cogswell, J., Hessl, D., Zhang, L., Ono, M., Tassone, F., ... Hagerman, R. (2007). Cognitive, Anxiety and Mood Disorders in the Fragile X-Associated Tremor/Ataxia Syndrome. *General Hospital Psychiatry*, 29(4), 349-356. doi:10.1016/j.genhosppsych.2007.03.003
- Bourgeois, J., Farzin, F., Brunberg, J., Tassone, F., Hagerman, P., Zhang, L., ... Hagerman, R. (2006). Dementia With Mood Symptoms in a Fragile X Premutation Carrier With the Fragile X-Associated Tremor/Ataxia Syndrome: Clinical Intervention With Donepezil and Venlafaxine. *Journal of Neuropsychiatry and Clinical Neurosciences*, 18(2), 171-177. doi:10.1176/appi.neuropsych.18.2.171
- Bourgeois, J., Seritan, A., Casillas, E., Hessl, D., Schneider, A., Yang, Y., ... Hagerman, R. (2011). Lifetime Prevalence of Mood and Anxiety Disorders in Fragile X Premutation Carriers. *Journal of Clinical Psychiatry*, 72(2), 175-182. doi:10.4088/JCP.09m05407blu
- Bowman, A., Yoo, S., Dantuma, N., & Zoghbi, H. (2005). Neuronal Dysfunction in a Polyglutamine Disease Model Occurs in the Absence of Ubiquitin-Proteasome System Impairment and Inversely Correlates With the Degree of Nuclear Inclusion Formation. *Human Molecular Genetics*, 14(5), 679-691. doi:10.1093/hmg/ddi064
- Braak, H., & Braak, E. (1991). Neuropathological Stageing of Alzheimer-Related Changes. *Acta Neuropathol*, 82(4), 239-259.
- Bradford, M. (1976). A Rapid and Sensitive Method for the Quantitation of Microgram Quantities of Protein Utilizing the Principle of Protein-Dye Binding. *Analytical Biochemistry*, 72, 248-254.
- Bramham, C., Worley, P., Moore, M., & Guzowski, J. (2008). The Immediate Early Gene Arc/Arg3.1: Regulation, Mechanisms, and Function. *Journal of Neuroscience*, 28(46), 11760-11767. doi:10.1523/JNEUROSCI. 3864-08.2008

- Brega, A., Goodrich, G., Bennett, R., Hessl, D., Engle, K., Leehey, M., ... Grigsby, J. (2008). The Primary Cognitive Deficit Among Males With Fragile X-Associated Tremor/Ataxia Syndrome (Fxtas) is a Dysexecutive Syndrome. *Journal of Clinical and Experimental Neuropsychology*, 30(8), 853-869. doi:10.1080/13803390701819044
- Brega, A., Reynolds, A., Bennett, R., Leehey, M., Bounds, L., Cogswell, J., ... Grigsby, J. (2009). Functional Status of Men With the Fragile X Premutation, With and Without the Tremor/Ataxia Syndrome (Fxtas). *International Journal of Geriatric Psychiatry*, 24(10), 1101-1109. doi:10.1002/gps.2231
- Bregman, J., Dykens, E., Watson, M., Ort, S., & Leckman, J. (1987). Fragile-X Syndrome: Variability of Phenotypic Expression. *Journal of the American Academy of Child and Adolescent Psychiatry*, 26(4), 463-471. doi: 10.1097/00004583-198707000-00001
- Brouwer, J., Huizer, K., Severijnen, L., Hukema, R., Berman, R., Oostra, B., & Willemse, R. (2008a). Cgg-Repeat Length and Neuropathological and Molecular Correlates in a Mouse Model for Fragile X-Associated Tremor/Ataxia Syndrome. *Journal of Neurochemistry*, 107(6), 1671-1682. doi: 10.1111/j.1471-4159.2008.05747.x
- Brouwer, J., Mientjes, E., Bakker, C., Nieuwenhuizen, I., Severijnen, L., Van Der Linde, H. C., ... Willemse, R. (2007). Elevated *Fmr1* mRNA Levels and Reduced Protein Expression in a Mouse Model With an Unmethylated Fragile X Full Mutation. *Experimental Cell Research*, 313(2), 244-253. doi: 10.1016/j.yexcr.2006.10.002
- Brouwer, J., Severijnen, E., De Jong, F. H., Hessl, D., Hagerman, R., Oostra, B., & Willemse, R. (2008b). Altered Hypothalamus-Pituitary-Adrenal Gland Axis Regulation in the Expanded Cgg-Repeat Mouse Model for Fragile X-Associated Tremor/Ataxia Syndrome. *Psychoneuroendocrinology*, 33(6), 863-873. doi:10.1016/j.psyneuen.2008.03.011
- Brouwer, J., Willemse, R., & Oostra, B. (2009). The *Fmr1* Gene and Fragile X-Associated Tremor/Ataxia Syndrome. *American Journal of Medical Genetics. Part B, Neuropsychiatric Genetics*, 150B(6), 782-798. doi: 10.1002/ajmg.b.30910
- Brunberg, J., Jacquemont, S., Hagerman, R., Berry-Kravis, E. M., Grigsby, J., Leehey, M., ... Hagerman, P. (2002). Fragile X Premutation Carriers: Characteristic Mr Imaging Findings of Adult Male Patients With Progressive Cerebellar and Cognitive Dysfunction. *AJNR: American Journal of Neuroradiology*, 23(10), 1757-1766.
- Bueti, D., & Walsh, V. (2009). The Parietal Cortex and the Representation of Time, Space, Number and Other Magnitudes. *Philosophical Transactions of the Royal Society of London. Series B, Biological Sciences*, 364(1525), 1831-1840. doi:10.1098/rstb.2009.0028
- Buitrago, M., Ringer, T., Schulz, J., Dichgans, J., & Luft, A. (2004). Characterization of Motor Skill and Instrumental Learning Time Scales in a Skilled Reaching Task in Rat. *Behavioural Brain Research*, 155(2), 249-256. doi:10.1016/j.bbr.2004.04.025

- Burdick, K., Goldberg, J., Harrow, M., Faull, R., & Malhotra, A. (2006). Neurocognition as a Stable Endophenotype in Bipolar Disorder and Schizophrenia. *Journal of Nervous and Mental Disease*, 194(4), 255-260. doi:10.1097/01.nmd.0000207360.70337.7e
- Burke, S., Wallace, J., Hartzell, A., Nematollahi, S., Plange, K., & Barnes, C. (2011). Age-Associated Deficits in Pattern Separation Functions of the Perirhinal Cortex: A Cross-Species Consensus. *Behavioral Neuroscience*, 125(6), 836-847. doi:10.1037/a0026238
- Burke, S., Wallace, J., Nematollahi, S., Uprety, A., & Barnes, C. (2010). Pattern Separation Deficits May Contribute to Age-Associated Recognition Impairments. *Behavioral Neuroscience*, 124(5), 559-573. doi:10.1037/a0020893
- Bussey, T., Holmes, A., Lyon, L., Mar, A., Mcallister, K., Nithianantharajah, J., ... Saksida, L. (2012). New Translational Assays for Preclinical Modelling of Cognition in Schizophrenia: The Touchscreen Testing Method for Mice and Rats. *Neuropharmacology*, 62(3), 1191-1203. doi:10.1016/j.neuropharm.2011.04.011
- Cain, C., & Ledoux, J. (2007). Escape From Fear: A Detailed Behavioral Analysis of Two Atypical Responses Reinforced By CS Termination. *Journal of Experimental Psychology: Animal Behavior Processes*, 33(4), 451-463. doi:10.1037/0097-7403.33.4.451
- Campbell, L., Daly, E., Toal, F., Stevens, A., Azuma, R., Catani, M., ... Murphy, K. (2006). Brain and Behaviour in Children With 22q11.2 Deletion Syndrome: A Volumetric and Voxel-Based Morphometry MRI Study. *Brain*, 129(Pt 5), 1218-1228. doi:10.1093/brain/awl066
- Cannon, T., & Keller, M. (2006). Endophenotypes in the Genetic Analyses of Mental Disorders. *Annu Rev Clin Psychol*, 2, 267-290. doi:10.1146/annurev.clinpsy.2.022305.095232
- Carola, V., Scalera, E., Brunamonti, E., Gross, C., & D'Amato, F. (2008). Mating-Related Interactions Share Common Features With Anxiety in the Mouse. *Behavioural Brain Research*, 186(2), 185-190. doi:10.1016/j.bbr.2007.08.006
- Carrion, V., Weems, C., Watson, C., Eliez, S., Menon, V., & Reiss, A. (2009). Converging Evidence for Abnormalities of the Prefrontal Cortex and Evaluation of Midsagittal Structures in Pediatric Posttraumatic Stress Disorder: An MRI Study. *Psychiatry Research*, 172(3), 226-234. doi:10.1016/j.psychresns.2008.07.008
- Carter, C., & Barch, D. (2007). Cognitive Neuroscience-Based Approaches to Measuring and Improving Treatment Effects on Cognition in Schizophrenia: The CNTRICS Initiative. *Schizophrenia Bulletin*, 33(5), 1131-1137. doi:10.1093/schbul/sbm081
- Casasanto, D., & Boroditsky, L. (2008). Time in the Mind: Using Space to Think About Time. *Cognition*, 106(2), 579-593. doi:10.1016/j.cognition.2007.03.004

- Castellanos, F., & Tannock, R. (2002). Neuroscience of Attention-Deficit/Hyperactivity Disorder: The Search for Endophenotypes. *Nature Reviews Neuroscience*, 3(8), 617-628. doi:10.1038/nrn896
- Casten, K., Gray, A., & Burwell, R. (2011). Discrimination Learning and Attentional Set Formation in a Mouse Model of Fragile X. *Behavioral Neuroscience*, 125(3), 473-479. doi:10.1037/a0023561
- Cellini, E., Forleo, P., Ginestroni, A., Nacmias, B., Tedde, A., Bagnoli, S., ... Piacentini, S. (2006). Fragile X Premutation With Atypical Symptoms At Onset. *Archives of Neurology*, 63(8), 1135-1138. doi:10.1001/archneur.63.8.1135
- Ceravolo, R., Antonini, A., Volterrani, D., Rossi, C., Goldwurm, S., Di Maria, E., ... Murri, L. (2005). Dopamine Transporter Imaging Study in Parkinsonism Occurring in Fragile X Premutation Carriers. *Neurology*, 65(12), 1971-1973. doi:10.1212/01.wnl.0000188821.51055.52
- Chadman, K., Yang, M., & Crawley, J. (2009). Criteria for Validating Mouse Models of Psychiatric Diseases. *American Journal of Medical Genetics. Part B, Neuropsychiatric Genetics*, 150B(1), 1-11. doi:10.1002/ajmg.b.30777
- Chaston, A., & Kingstone, A. (2004). Time Estimation: The Effect of Cortically Mediated Attention. *Brain and Cognition*, 55(2), 286-289. doi:10.1016/j.bandc.2004.02.013
- Chawla, M., Lin, G., Olson, K., Vazdarjanova, A., Burke, S., Mcnaughton, B., ... Barnes, C. (2004). 3D-Catfish: A System for Automated Quantitative Three-Dimensional Compartmental Analysis of Temporal Gene Transcription Activity Imaged By Fluorescence In Situ Hybridization. *Journal of Neuroscience Methods*, 139(1), 13-24. doi:10.1016/j.jneumeth.2004.04.017
- Check Hayden, E. (2010). Sex Bias Blights Drug Studies. *Nature*, 464(7287), 332-333. doi:10.1038/464332b
- Chee, S., & Menard, J. (2011). Lesions of the Dorsal Lateral Septum Do Not Affect Neophagia in the Novelty Induced Suppression of Feeding Paradigm But Reduce Defensive Behaviours in the Elevated Plus Maze and Shock Probe Burying Tests. *Behavioural Brain Research*, 220(2), 362-366. doi:10.1016/j.bbr.2011.02.027
- Chen, C., & Tonegawa, S. (1997). Molecular Genetic Analysis of Synaptic Plasticity, Activity-Dependent Neural Development, Learning, and Memory in the Mammalian Brain. *Annual Review of Neuroscience*, 20, 157-184. doi:10.1146/annurev.neuro.20.1.157
- Chen, Y., Tassone, F., Berman, R., Hagerman, P., Hagerman, R., Willemsen, R., & Pessah, I. (2010). Murine Hippocampal Neurons Expressing *Fmr1* Gene Mutations Show Early Developmental Deficits and Late Degeneration. *Human Molecular Genetics*, 19(1), 196-208. doi:10.1093/hmg/ddp479
- Chiba, A., Kesner, R., & Gibson, C. (1997). Memory for Temporal Order of New and Familiar Spatial Location Sequences: Role of the Medial Prefrontal Cortex. *Learning and Memory*, 4(4), 311-317.
- Choi, J., Koch, K., Poppendieck, W., Lee, M., & Shin, H. (2010). High Resolution Electroencephalography in Freely Moving Mice. *Journal of Neurophysiology*, 104(3), 1825-1834. doi:10.1152/jn.00188.2010

- Chonchaiya, W., Nguyen, D., Au, J., Campos, L., Berry-Kravis, E. M., Lohse, K., ... Hagerman, R. (2010a). Clinical Involvement in Daughters of Men With Fragile X-Associated Tremor Ataxia Syndrome. *Clinical Genetics*, 78(1), 38-46. doi:10.1111/j.1399-0004.2010.01448.x
- Chonchaiya, W., Schneider, A., & Hagerman, R. (2009). Fragile X: A Family of Disorders. *Advances in Pediatrics*, 56, 165-186. doi:10.1016/j.yapd.2009.08.008
- Chonchaiya, W., Tassone, F., Ashwood, P., Hessl, D., Schneider, A., Campos, L., ... Hagerman, R. (2010b). Autoimmune Disease in Mothers With the *FMR1* Premutation is Associated With Seizures in Their Children With Fragile X Syndrome. *Human Genetics*, 128(5), 539-548. doi:10.1007/s00439-010-0882-8
- Chonchaiya, W., Utari, A., Pereira, G., Tassone, F., Hessl, D., & Hagerman, R. (2009). Broad Clinical Involvement in a Family Affected By the Fragile X Premutation. *Journal of Developmental and Behavioral Pediatrics*, 30(6), 544-551. doi:10.1097/DBP.0b013e3181c35f25
- Chow, E., Mikulis, D., Zipursky, R., Scutt, L., Weksberg, R., & Bassett, A. (1999). Qualitative MRI Findings in Adults With 22q11 Deletion Syndrome and Schizophrenia. *Biological Psychiatry*, 46(10), 1436-1442.
- Chowdhury, S., Shepherd, J., Okuno, H., Lyford, G., Petralia, R., Plath, N., ... Worley, P. (2006). Arc/Arg3.1 Interacts With the Endocytic Machinery to Regulate AMPA Receptor Trafficking. *Neuron*, 52(3), 445-459. doi:10.1016/j.neuron.2006.08.033
- Cilia, R., Kraff, J., Canesi, M., Pezzoli, G., Goldwurm, S., Amiri, K., ... Tassone, F. (2009). Screening for the Presence of *FMR1* Premutation Alleles in Women With Parkinsonism. *Archives of Neurology*, 66(2), 244-249. doi:10.1001/archneurol.2008.548
- Clelland, C., Choi, M., Romberg, C., Clemenson, G. J., Fragniere, A., Tyers, P., ... Bussey, T. (2009). A Functional Role for Adult Hippocampal Neurogenesis in Spatial Pattern Separation. *Science*, 325(5937), 210-213. doi:10.1126/science.1173215
- Clower, D., Dum, R., & Strick, P. (2005). Basal Ganglia and Cerebellar Inputs to 'Aip'. *Cerebral Cortex*, 15(7), 913-920. doi:10.1093/cercor/bhh190
- Clower, D., West, R., Lynch, J., & Strick, P. (2001). The Inferior Parietal Lobule is the Target of Output From the Superior Colliculus, Hippocampus, and Cerebellum. *Journal of Neuroscience*, 21(16), 6283-6291.
- Coffey, S., Cook, K., Tartaglia, N., Tassone, F., Nguyen, D., Pan, R., ... Hagerman, R. (2008). Expanded Clinical Phenotype of Women With the *Fmr1* Premutation. *American Journal of Medical Genetics. Part A*, 146A(8), 1009-1016. doi:10.1002/ajmg.a.32060
- Cohen, S., Masyn, K., Adams, J., Hessl, D., Rivera, S., Tassone, F., ... Hagerman, R. (2006). Molecular and Imaging Correlates of the Fragile X-Associated Tremor/Ataxia Syndrome. *Neurology*, 67(8), 1426-1431. doi:10.1212/01.wnl.0000239837.57475.3a
- Connor, C., Crawford, B., & Akbarian, S. (2011). White Matter Neuron Alterations in Schizophrenia and Related Disorders. *International Journal of*

- Developmental Neuroscience*, 29(3), 325-334. doi:10.1016/j.ijdevneu. 2010.07.236
- (1997). Consensus Recommendations for the Postmortem Diagnosis of Alzheimer's Disease. The National Institute on Aging, and Reagan Institute Working Group on Diagnostic Criteria for the Neuropathological Assessment of Alzheimer's Disease. *Neurobiology of Aging*, 18(4 Suppl), S1-2.
- Cordes, S., Gelman, R., Gallistel, C., & Whalen, J. (2001). Variability Signatures Distinguish Verbal From Nonverbal Counting for Both Large and Small Numbers. *Psychonomic Bulletin and Review*, 8(4), 698-707.
- Cordes, S., King, A., & Gallistel, C. (2007). Time Left in the Mouse. *Behavioural Processes*, 74(2), 142-151. doi:10.1016/j.beproc.2006.10.007
- Cornish, K., Kogan, C., Turk, J., Manly, T., James, N., Mills, A., & Dalton, A. (2005). The Emerging Fragile X Premutation Phenotype: Evidence From the Domain of Social Cognition. *Brain and Cognition*, 57(1), 53-60. doi:10.1016/j.bandc.2004.08.020
- Cornish, K., Sudhalter, V., & Turk, J. (2004a). Attention and Language in Fragile X. *Mental Retardation and Developmental Disabilities Research Reviews*, 10(1), 11-16. doi:10.1002/mrdd.20003
- Cornish, K., Swainson, R., Cunnington, R., Wilding, J., Morris, P., & Jackson, G. (2004b). Do Women With Fragile X Syndrome Have Problems in Switching Attention: Preliminary Findings From Erp and Fmri. *Brain and Cognition*, 54 (3), 235-239. doi:10.1016/j.bandc.2004.02.017
- Cornish, K., Turk, J., & Hagerman, R. (2008a). The Fragile X Continuum: New Advances and Perspectives. *Journal of Intellectual Disability Research*, 52 (Pt 6), 469-482. doi:10.1111/j.1365-2788.2008.01056.x
- Cornish, K., Kogan, C., Li, L., Turk, J., Jacquemont, S., & Hagerman, R. (2009). Lifespan Changes in Working Memory in Fragile X Premutation Males. *Brain and Cognition*, 69(3), 551-558. doi:10.1016/j.bandc.2008.11.006
- Cornish, K., Li, L., Kogan, C., Jacquemont, S., Turk, J., Dalton, A., ... Hagerman, P. (2008b). Age-Dependent Cognitive Changes in Carriers of the Fragile X Syndrome. *Cortex*, 44(6), 628-636. doi:10.1016/j.cortex.2006.11.002
- Cornish, K., Munir, F., & Cross, G. (1998). The Nature of the Spatial Deficit in Young Females With Fragile-X Syndrome: A Neuropsychological and Molecular Perspective. *Neuropsychologia*, 36(11), 1239-1246.
- Cornish, K., Munir, F., & Cross, G. (1999). Spatial Cognition in Males With Fragile-X Syndrome: Evidence for a Neuropsychological Phenotype. *Cortex*, 35(2), 263-271.
- Cornish, K., Pilgram, J., & Shaw, K. (1997). Do Anomalies of Handedness Exist in Children With Fragile-X Syndrome? *Laterality*, 2(2), 91-101. doi: 10.1080/713754261
- Cornish, K., Turk, J., Wilding, J., Sudhalter, V., Munir, F., Kooy, F., & Hagerman, R. (2004c). Annotation: Deconstructing the Attention Deficit in Fragile X Syndrome: A Developmental Neuropsychological Approach. *Journal of Child Psychology and Psychiatry and Allied Disciplines*, 45(6), 1042-1053. doi: 10.1111/j.1469-7610.2004.t01-1-00297.x

- Corwin, J., Fussinger, M., Meyer, R., King, V., & Reep, R. (1994). Bilateral Destruction of the Ventrolateral Orbital Cortex Produces Allocentric But Not Egocentric Spatial Deficits in Rats. *Behavioural Brain Research*, 61(1), 79-86.
- Cowell, R., Bussey, T., & Saksida, L. (2010). Components of Recognition Memory: Dissociable Cognitive Processes or Just Differences in Representational Complexity? *Hippocampus*, 20(11), 1245-1262. doi: 10.1002/hipo.20865
- Crabbe, J., & Wahlsten, D. (2003). Of Mice and Their Environments. *Science*, 299(5611), 1313-1314. doi:10.1126/science.299.5611.1313c
- Crabbe, J., Wahlsten, D., & Dudek, B. (1999). Genetics of Mouse Behavior: Interactions With Laboratory Environment. *Science*, 284(5420), 1670-1672.
- Crawley, J. (1985). Exploratory Behavior Models of Anxiety in Mice. *Neuroscience and Biobehavioral Reviews*, 9(1), 37-44.
- Crawley, J. (2004). Designing Mouse Behavioral Tasks Relevant to Autistic-Like Behaviors. *Mental Retardation and Developmental Disabilities Research Reviews*, 10(4), 248-258. doi:10.1002/mrdd.20039
- Crawley, J. (2007). Mouse Behavioral Assays Relevant to the Symptoms of Autism. *Brain Pathology*, 17(4), 448-459. doi:10.1111/j.1750-3639.2007.00096.x
- Crawley, J., Belknap, J., Collins, A., Crabbe, J., Frankel, W., Henderson, N., ... Paylor, R. (1997). Behavioral Phenotypes of Inbred Mouse Strains: Implications and Recommendations for Molecular Studies. *Psychopharmacology*, 132(2), 107-124.
- Crawley, J., & Paylor, R. (1997). A Proposed Test Battery and Constellations of Specific Behavioral Paradigms to Investigate the Behavioral Phenotypes of Transgenic and Knockout Mice. *Hormones and Behavior*, 31(3), 197-211. doi:10.1006/hbeh.1997.1382
- Cummings, B., Engesser-Cesar, C., Cadena, G., & Anderson, A. (2007). Adaptation of a Ladder Beam Walking Task to Assess Locomotor Recovery in Mice Following Spinal Cord Injury. *Behavioural Brain Research*, 177(2), 232-241. doi:10.1016/j.bbr.2006.11.042
- Cunningham, C., Martinez Cerdeno, V., Navarro Porras, E., Prakash, A., Angelastro, J., Willemse, R., ... Noctor, S. (2011). Premutation Cgg-Repeat Expansion of the *Fmr1* Gene Impairs Mouse Neocortical Development. *Human Molecular Genetics*, 20(1), 64-79. doi:10.1093/hmg/ddq432
- Curfs, L., Borghgraef, M., Wiegers, A., Schreppers-Tijdink, G. A., & Fryns, J. (1989). Strengths and Weaknesses in the Cognitive Profile of Fra(X) Patients. *Clinical Genetics*, 36(6), 405-410.
- Curfs, L., Schreppers-Tijdink, G., Wiegers, A., Borghgraef, M., & Fryns, J. (1989). Intelligence and Cognitive Profile in the Fra(X) Syndrome: A Longitudinal Study in 18 Fra(X) Boys. *Journal of Medical Genetics*, 26(7), 443-446.
- Curfs, P., Schreppers-Tijdink, G. A., Wiegers, A., Van Velzen, W., & Fryns, J. (1989). Adaptive Behavior in the Fra(X) Syndrome: A Longitudinal Study in

- Eight Patients. *American Journal of Medical Genetics*, 34(4), 502-505. doi: 10.1002/ajmg.1320340409
- D'Hulst, C., Heulens, I., Brouwer, J., Willemsen, R., De Geest, N., Reeve, S., ... Kooy, R. (2009). Expression of the Gabaergic System in Animal Models for Fragile X Syndrome and Fragile X Associated Tremor/Ataxia Syndrome (Fxtas). *Brain Research*, 1253, 176-183. doi:10.1016/j.brainres.2008.11.075
- Darnell, J., Van Driesche, S. J., Zhang, C., Hung, K., Mele, A., Fraser, C., ... Darnell, R. (2011). Fmrp Stalls Ribosomal Translocation on mRNAs Linked to Synaptic Function and Autism. *Cell*, 146(2), 247-261. doi:10.1016/j.cell.2011.06.013
- Deacon, R. (2011). Hyponeophagia: A Measure of Anxiety in the Mouse. *Journal of Visualized Experiments*, 51). doi:10.3791/2613
- Deboer, T., Wu, Z., Lee, A., & Simon, T. (2007). Hippocampal Volume Reduction in Children With Chromosome 22q11.2 Deletion Syndrome is Associated With Cognitive Impairment. *Behavioral and Brain Functions*, 3, 54. doi: 10.1186/1744-9081-3-54
- Defensor, E., Pearson, B., Pobbe, R., Bolivar, V., Blanchard, D., & Blanchard, R. (2011). A Novel Social Proximity Test Suggests Patterns of Social Avoidance and Gaze Aversion-Like Behavior in Btbr T+ Tf/J Mice. *Behavioural Brain Research*, 217(2), 302-308. doi:10.1016/j.bbr.2010.10.033
- Deo, A., Costa, R., Delisi, L., Desalle, R., & Haghghi, F. (2010). A Novel Analytical Framework for Dissecting the Genetic Architecture of Behavioral Symptoms in Neuropsychiatric Disorders. *PLoS ONE*, 5(3), e9714. doi: 10.1371/journal.pone.0009714
- Dere, E., Huston, J., & De Souza Silva, M. A. (2005). Integrated Memory for Objects, Places, and Temporal Order: Evidence for Episodic-Like Memory in Mice. *Neurobiology of Learning and Memory*, 84(3), 214-221. doi:10.1016/j.nlm.2005.07.002
- Devanand, D., Michaels-Marston, K. S., Liu, X., Pelton, G., Padilla, M., Marder, K., ... Mayeux, R. (2000). Olfactory Deficits in Patients With Mild Cognitive Impairment Predict Alzheimer's Disease At Follow-Up. *American Journal of Psychiatry*, 157(9), 1399-1405.
- Devito, L., & Eichenbaum, H. (2011). Memory for the Order of Events in Specific Sequences: Contributions of the Hippocampus and Medial Prefrontal Cortex. *Journal of Neuroscience*, 31(9), 3169-3175. doi:10.1523/JNEUROSCI.4202-10.2011
- Diep, A. A., Hunsaker, M. R., Kwock, R., Kim, K., Willemsen, R., & Berman, R. (2012). Female CGG Knock-in Mice Modeling the Fragile X Premutation Are Impaired on a Skilled Forelimb Reaching Task. *Neurobiology of Learning and Memory*, 97(2), 229-234. doi:10.1016/j.nlm.2011.12.006
- Dierckx, E., Engelborghs, S., De Raedt, R., Van Buggenhout, M., De Deyn, P. P., Verte, D., & Ponjaert-Kristoffersen, I. (2009). Verbal Cued Recall as a Predictor of Conversion to Alzheimer's Disease in Mild Cognitive Impairment. *International Journal of Geriatric Psychiatry*, 24(10), 1094-1100. doi:10.1002/gps.2228

- Dobbins, I., Rice, H., Wagner, A., & Schacter, D. (2003). Memory Orientation and Success: Separable Neurocognitive Components Underlying Episodic Recognition. *Neuropsychologia*, 41(3), 318-333.
- Drago, V., Foster, P., Skidmore, F., Trifiletti, D., & Heilman, K. (2008). Spatial Emotional Akinesia in Parkinson Disease. *Cognitive and Behavioral Neurology*, 21(2), 92-97. doi:10.1097/WNN.0b013e31816bdfb2
- Dragunow, M., & Faull, R. (1989). The Use of C-Fos as a Metabolic Marker in Neuronal Pathway Tracing. *Journal of Neuroscience Methods*, 29(3), 261-265.
- Drew, L., Crabtree, G., Markx, S., Stark, K., Chaverneff, F., Xu, B., ... Karayiorgou, M. (2011a). The 22q11.2 Microdeletion: Fifteen Years of Insights Into the Genetic and Neural Complexity of Psychiatric Disorders. *International Journal of Developmental Neuroscience*, 29(3), 259-281. doi: 10.1016/j.ijdevneu.2010.09.007
- Drew, L., Stark, K., Fenelon, K., Karayiorgou, M., Macdermott, A., & Gogos, J. (2011b). Evidence for Altered Hippocampal Function in a Mouse Model of the Human 22q11.2 Microdeletion. *Molecular and Cellular Neurosciences*, 47(4), 293-305. doi:10.1016/j.mcn.2011.05.008
- Drew, T., Andujar, J., Lajoie, K., & Yakovenko, S. (2008). Cortical Mechanisms Involved in Visuomotor Coordination During Precision Walking. *Brain Res Rev*, 57(1), 199-211. doi:10.1016/j.brainresrev.2007.07.017
- Dulawa, S., & Geyer, M. (1996). Psychopharmacology of Prepulse Inhibition in Mice. *Chinese Journal of Physiology*, 39(3), 139-146.
- Dykens, E., Hodapp, R., & Leckman, J. (1987). Strengths and Weaknesses in the Intellectual Functioning of Males With Fragile X Syndrome. *American Journal of Mental Deficiency*, 92(2), 234-236.
- Eadie, B., Zhang, W., Boehme, F., Gil-Mohapel, J., Kainer, L., Simpson, J., & Christie, B. (2009). *Fmr1* Knockout Mice Show Reduced Anxiety and Alterations in Neurogenesis That Are Specific to the Ventral Dentate Gyrus. *Neurobiology of Disease*, 36(2), 361-373. doi:10.1016/j.nbd.2009.08.001
- Eagle, D., Tufft, M., Goodchild, H., & Robbins, T. (2007). Differential Effects of Modafinil and Methylphenidate on Stop-Signal Reaction Time Task Performance in the Rat, and Interactions With the Dopamine Receptor Antagonist Cis-Flupenthixol. *Psychopharmacology*, 192(2), 193-206. doi: 10.1007/s00213-007-0701-7
- Eichenbaum, H., & Fortin, N. (2009). The Neurobiology of Memory Based Predictions. *Philosophical Transactions of the Royal Society of London. Series B, Biological Sciences*, 364(1521), 1183-1191. doi:10.1098/rstb. 2008.0306
- Einat, H. (2007). Establishment of a Battery of Simple Models for Facets of Bipolar Disorder: A Practical Approach to Achieve Increased Validity, Better Screening and Possible Insights Into Endophenotypes of Disease. *Behavior Genetics*, 37(1), 244-255. doi:10.1007/s10519-006-9093-4
- Ellegood, J., Pacey, L., Hampson, D., Lerch, J., & Henkelman, R. (2010). Anatomical Phenotyping in a Mouse Model of Fragile X Syndrome With

- Magnetic Resonance Imaging. *Neuroimage*, 53(3), 1023-1029. doi:10.1016/j.neuroimage.2010.03.038
- Ellis, M., & Kesner, R. (1983). The Noradrenergic System of the Amygdala and Aversive Information Processing. *Behavioral Neuroscience*, 97(3), 399-415.
- Endo, T., Maekawa, F., Voikar, V., Haijima, A., Uemura, Y., Zhang, Y., ... Kakeyama, M. (2011). Automated Test of Behavioral Flexibility in Mice Using a Behavioral Sequencing Task in Intellicage. *Behavioural Brain Research*, 221(1), 172-181. doi:10.1016/j.bbr.2011.02.037
- Entezam, A., Biacsi, R., Orrison, B., Saha, T., Hoffman, G., Grabczyk, E., ... Usdin, K. (2007). Regional Fmrp Deficits and Large Repeat Expansions Into the Full Mutation Range in a New Fragile X Premutation Mouse Model. *Gene*, 395(1-2), 125-134. doi:10.1016/j.gene.2007.02.026
- Entezam, A., Lokanga, A., Le, W., Hoffman, G., & Usdin, K. (2010). Potassium Bromate, a Potent DNA Oxidizing Agent, Exacerbates Germline Repeat Expansion in a Fragile X Premutation Mouse Model. *Human Mutation*, 31(5), 611-616. doi:10.1002/humu.21237
- Entezam, A., & Usdin, K. (2008). Atr Protects the Genome Against CGG.CCG-Repeat Expansion in Fragile X Premutation Mice. *Nucleic Acids Research*, 36(3), 1050-1056. doi:10.1093/nar/gkm1136
- Entezam, A., & Usdin, K. (2009). Atm and Atr Protect the Genome Against Two Different Types of Tandem Repeat Instability in Fragile X Premutation Mice. *Nucleic Acids Research*, 37(19), 6371-6377. doi:10.1093/nar/gkp666
- Faraji, J., & Metz, G. (2007). Sequential Bilateral Striatal Lesions Have Additive Effects on Single Skilled Limb Use in Rats. *Behavioural Brain Research*, 177(2), 195-204. doi:10.1016/j.bbr.2006.11.034
- Farr, T., Liu, L., Colwell, K., Whishaw, I., & Metz, G. (2006). Bilateral Alteration in Stepping Pattern After Unilateral Motor Cortex Injury: A New Test Strategy for Analysis of Skilled Limb Movements in Neurological Mouse Models. *Journal of Neuroscience Methods*, 153(1), 104-113. doi:10.1016/j.jneumeth.2005.10.011
- Farr, T., & Whishaw, I. (2002). Quantitative and Qualitative Impairments in Skilled Reaching in the Mouse (*Mus Musculus*) After a Focal Motor Cortex Stroke. *Stroke*, 33(7), 1869-1875.
- Farzin, F., Perry, H., Hessl, D., Loesch, D., Cohen, J., Bacalman, S., ... Hagerman, R. (2006). Autism Spectrum Disorders and Attention-Deficit/Hyperactivity Disorder in Boys With the Fragile X Premutation. *Journal of Developmental and Behavioral Pediatrics*, 27(2 Suppl), S137-44.
- Farzin, F., & Rivera, S. (2010). Dynamic Object Representations in Infants With and Without Fragile X Syndrome. *Frontiers in Human Neuroscience*, 4, 12. doi:10.3389/neuro.09.012.2010
- Farzin, F., Whitney, D., Hagerman, R., & Rivera, S. (2008). Contrast Detection in Infants With Fragile X Syndrome. *Vision Research*, 48(13), 1471-1478. doi:10.1016/j.visres.2008.03.019
- Faul, F., Erdfelder, E., Buchner, A., & Lang, A. (2009). Statistical Power Analyses Using G*Power 3.1: Tests for Correlation and Regression Analyses. *Behavior Research Methods*, 41(4), 1149-1160. doi:10.3758/BRM.41.4.1149

- Faul, F., Erdfelder, E., Lang, A., & Buchner, A. (2007). G*Power 3: A Flexible Statistical Power Analysis Program for the Social, Behavioral, and Biomedical Sciences. *Behavior Research Methods*, 39(2), 175-191.
- Fernandez-Carvajal, I., Lopez Posadas, B., Pan, R., Raske, C., Hagerman, P., & Tassone, F. (2009). Expansion of an *Fmr1* Grey-Zone Allele to a Full Mutation in Two Generations. *Journal of Molecular Diagnostics*, 11(4), 306-310. doi:10.2353/jmoldx.2009.080174
- (1994). *Fmr1* Knockout Mice: A Model to Study Fragile X Mental Retardation. The Dutch-Belgian Fragile X Consortium. *Cell*, 78(1), 23-33.
- Fortin, N., Agster, K., & Eichenbaum, H. (2002). Critical Role of the Hippocampus in Memory for Sequences of Events. *Nature Neuroscience*, 5(5), 458-462. doi:10.1038/nn834
- Franke, P., Leboyer, M., Gansicke, M., Weiffenbach, O., Biancalana, V., Cornillet-Lefebvre, P., ... Maier, W. (1998). Genotype-Phenotype Relationship in Female Carriers of the Premutation and Full Mutation of *FMR-1*. *Psychiatry Research*, 80(2), 113-127.
- Gallistel, C. (1989). Animal Cognition: The Representation of Space, Time and Number. *Annual Review of Psychology*, 40, 155-189. doi:10.1146/annurev.ps.40.020189.001103
- Gallistel, C. R. (1990a). *The Organization of Learning*. Cambridge, MA: MIT Press.
- Gallistel, C. (1990b). Representations in Animal Cognition: An Introduction. *Cognition*, 37(1-2), 1-22.
- Gallistel, C., Fairhurst, S., & Balsam, P. (2004). The Learning Curve: Implications of a Quantitative Analysis. *Proceedings of the National Academy of Sciences of the United States of America*, 101(36), 13124-13131. doi:10.1073/pnas.0404965101
- Gallistel, C., & Gelman, I. I. (2000). Non-Verbal Numerical Cognition: From Reals to Integers. *Trends Cogn Sci*, 4(2), 59-65.
- Gallistel, C., & Gelman, R. (1992). Preverbal and Verbal Counting and Computation. *Cognition*, 44(1-2), 43-74.
- Gallistel, C., King, A., Daniel, A., Freestone, D., Papachristos, E., Balci, F., ... Kourtev, H. (2010). Screening for Learning and Memory Mutations: A New Approach. *Xin Li Xue Bao*, 42(1), 138-158. doi:10.3724/SP.J.1041.2010.00138
- Galloway, J., & Nelson, D. (2009). Evidence for RNA-Mediated Toxicity in the Fragile X-Associated Tremor/Ataxia Syndrome. *Future Neurol*, 4(6), 785. doi:10.2217/fnl.09.44
- Galvan, A., Floran, B., Erlij, D., & Aceves, J. (2001). Intrapallidal Dopamine Restores Motor Deficits Induced By 6-Hydroxydopamine in the Rat. *Journal of Neural Transmission*, 108(2), 153-166.
- Gane, L., Iosif, A., Flynn-Wilson, L., Venturino, M., Hagerman, R., & Seritan, A. (2010). Assessment of Patient and Caregiver Needs in Fragile X-Associated Tremor/Ataxia Syndrome By Utilizing Q-Sort Methodology. *Aging and Mental Health*, 14(8), 1000-1007. doi:10.1080/13607863.2010.501066

- Garcia-Arocena, D., & Hagerman, P. (2010). Advances in Understanding the Molecular Basis of Fxtas. *Human Molecular Genetics*, 19(R1), R83-9. doi: 10.1093/hmg/ddq166
- Garcia-Arocena, D., Yang, J., Brouwer, J., Tassone, F., Iwahashi, C., Berry-Kravis, E. M., ... Hagerman, P. (2010). Fibroblast Phenotype in Male Carriers of *FMR1* Premutation Alleles. *Human Molecular Genetics*, 19(2), 299-312. doi:10.1093/hmg/ddp497
- Garner, J., Thogerson, C., Wurbel, H., Murray, J., & Mench, J. (2006). Animal Neuropsychology: Validation of the Intra-Dimensional Extra-Dimensional Set Shifting Task for Mice. *Behavioural Brain Research*, 173(1), 53-61. doi: 10.1016/j.bbr.2006.06.002
- Gatome, C., Slomianka, L., Lipp, H., & Amrein, I. (2010). Number Estimates of Neuronal Phenotypes in Layer II of the Medial Entorhinal Cortex of Rat and Mouse. *Neuroscience*, 170(1), 156-165. doi:10.1016/j.neuroscience.2010.06.048
- George, D., Duffaud, A., Pothuizen, H., Haddon, J., & Killcross, S. (2010). Lesions to the Ventral, But Not the Dorsal, Medial Prefrontal Cortex Enhance Latent Inhibition. *European Journal of Neuroscience*, 31(8), 1474-1482. doi:10.1111/j.1460-9568.2010.07178.x
- Gerkes, E., Hordijk, R., Dijkhuizen, T., Sival, D., Meiners, L., Sikkema-Raddatz, B., & Van Ravenswaaij-Arts, C. M. (2010). Bilateral Polymicrogyria as the Indicative Feature in a Child With a 22q11.2 Deletion. *European Journal of Medical Genetics*, 53(5), 344-346. doi:10.1016/j.ejmg.2010.05.003
- Gilbert, P., Campbell, A., & Kesner, R. (2003). The Role of the Amygdala in Conditioned Flavor Preference. *Neurobiology of Learning and Memory*, 79 (1), 118-121.
- Gilbert, P., & Kesner, R. (2002). The Amygdala But Not the Hippocampus is Involved in Pattern Separation Based on Reward Value. *Neurobiology of Learning and Memory*, 77(3), 338-353. doi:10.1006/nlme.2001.4033
- Gilbert, P., & Kesner, R. (2006). The Role of the Dorsal CA3 Hippocampal Subregion in Spatial Working Memory and Pattern Separation. *Behavioural Brain Research*, 169(1), 142-149. doi:10.1016/j.bbr.2006.01.002
- Gilbert, P., Kesner, R., & Lee, I. (2001). Dissociating Hippocampal Subregions: Double Dissociation Between Dentate Gyrus and Ca1. *Hippocampus*, 11(6), 626-636. doi:10.1002/hipo.1077
- Gilbert, P., & Murphy, C. (2004a). Differences Between Recognition Memory and Remote Memory for Olfactory and Visual Stimuli in Nondemented Elderly Individuals Genetically At Risk for Alzheimer's Disease. *Experimental Gerontology*, 39(3), 433-441. doi:10.1016/j.exger.2004.01.001
- Gilbert, P., & Murphy, C. (2004b). The Effect of the ApoE Epsilon4 Allele on Recognition Memory for Olfactory and Visual Stimuli in Patients With Pathologically Confirmed Alzheimer's Disease, Probable Alzheimer's Disease, and Healthy Elderly Controls. *Journal of Clinical and Experimental Neuropsychology*, 26(6), 779-794. doi:10.1080/13803390490509439

- Gogos, J. (2007). Schizophrenia Susceptibility Genes: In Search of a Molecular Logic and Novel Drug Targets for a Devastating Disorder. *International Review of Neurobiology*, 78, 397-422. doi:10.1016/S0074-7742(06)78013-8
- Gogos, J., & Gerber, D. (2006). Schizophrenia Susceptibility Genes: Emergence of Positional Candidates and Future Directions. *Trends in Pharmacological Sciences*, 27(4), 226-233. doi:10.1016/j.tips.2006.02.005
- Gogos, J., & Karayiorgou, M. (2001). "Targeting" Schizophrenia in Mice. *American Journal of Medical Genetics*, 105(1), 50-52.
- Gokden, M., Al-Hinti, J. T., & Harik, S. (2009). Peripheral Nervous System Pathology in Fragile X Tremor/Ataxia Syndrome (Fxtas). *Neuropathology*, 29(3), 280-284. doi:10.1111/j.1440-1789.2008.00948.x
- Goodale, M., Foreman, N., & Milner, A. (1978). Visual Orientation in the Rat: A Dissociation of Deficits Following Cortical and Collicular Lesions. *Experimental Brain Research*, 31(3), 445-457.
- Goodlin-Jones, B. L., Tassone, F., Gane, L., & Hagerman, R. (2004). Autistic Spectrum Disorder and the Fragile X Premutation. *Journal of Developmental and Behavioral Pediatrics*, 25(6), 392-398.
- Goodrich-Hunsaker, N. J., Howard, B., Hunsaker, M., & Kesner, R. (2008a). Human Topological Task Adapted for Rats: Spatial Information Processes of the Parietal Cortex. *Neurobiology of Learning and Memory*, 90(2), 389-394. doi:10.1016/j.nlm.2008.05.002
- Goodrich-Hunsaker, N. J., Hunsaker, M., & Kesner, R. (2005). Dissociating the Role of the Parietal Cortex and Dorsal Hippocampus for Spatial Information Processing. *Behavioral Neuroscience*, 119(5), 1307-1315. doi:10.1037/0735-7044.119.5.1307
- Goodrich-Hunsaker, N. J., Hunsaker, M., & Kesner, R. (2008b). The Interactions and Dissociations of the Dorsal Hippocampus Subregions: How the Dentate Gyrus, CA3, and CA1 Process Spatial Information. *Behavioral Neuroscience*, 122(1), 16-26. doi:10.1037/0735-7044.122.1.16
- Goodrich-Hunsaker, N. J., Livingstone, S., Skelton, R., & Hopkins, R. (2010). Spatial Deficits in a Virtual Water Maze in Amnesic Participants With Hippocampal Damage. *Hippocampus*, 20(4), 481-491. doi:10.1002/hipo.20651
- Goodrich-Hunsaker, N. J., Wong, L., McLennan, Y., Srivastava, S., Tassone, F., Harvey, D., ... Simon, T. (2011a). Young Adult Female Fragile X Premutation Carriers Show Age- and Genetically-Modulated Cognitive Impairments. *Brain and Cognition*, 75(3), 255-260. doi:10.1016/j.bandc.2011.01.001
- Goodrich-Hunsaker, N. J., Wong, L., McLennan, Y., Tassone, F., Harvey, D., Rivera, S., & Simon, T. (2011b). Adult Female Fragile X Premutation Carriers Exhibit Age- and Cgg Repeat Length-Related Impairments on an Attentionally Based Enumeration Task. *Frontiers in Human Neuroscience*, 5, 63. doi:10.3389/fnhum.2011.00063
- Goodrich-Hunsaker, N. J., Wong, L., McLennan, Y., Tassone, F., Harvey, D., Rivera, S., & Simon, T. (2011c). Enhanced Manual and Oral Motor Reaction Time in Young Adult Female Fragile X Premutation Carriers. *Journal of the*

- International Neuropsychological Society*, 1-5. doi:10.1017/S1355617711000634
- Gothelf, D., Frisch, A., Michaelovsky, E., Weizman, A., & Shprintzen, R. (2009). Velo-Cardio-Facial Syndrome. *J Ment Health Res Intellect Disabil*, 2(2), 149-167. doi:10.1080/19315860902756136
- Gothelf, D., Furfaro, J., Hoeft, F., Eckert, M., Hall, S., O'Hara, R., ... Reiss, A. (2008). Neuroanatomy of Fragile X Syndrome is Associated With Aberrant Behavior and the Fragile X Mental Retardation Protein (Fmrp). *Annals of Neurology*, 63(1), 40-51. doi:10.1002/ana.21243
- Gothelf, D., Hoeft, F., Ueno, T., Sugiura, L., Lee, A., Thompson, P., & Reiss, A. (2011). Developmental Changes in Multivariate Neuroanatomical Patterns That Predict Risk for Psychosis in 22q11.2 Deletion Syndrome. *Journal of Psychiatric Research*, 45(3), 322-331. doi:10.1016/j.jpsychires.2010.07.008
- Gothelf, D., Steinberg, T., Golan, O., & Apter, A. (2010). Editorial: Developmental Psychopathology. *Israel Journal of Psychiatry and Related Sciences*, 47(2), 93-94.
- Gottesman, I., & Gould, T. (2003). The Endophenotype Concept in Psychiatry: Etymology and Strategic Intentions. *American Journal of Psychiatry*, 160(4), 636-645.
- Gould, T., & Einat, H. (2007). Animal Models of Bipolar Disorder and Mood Stabilizer Efficacy: A Critical Need for Improvement. *Neuroscience and Biobehavioral Reviews*, 31(6), 825-831. doi:10.1016/j.neubiorev.2007.05.007
- Gould, T., & Gottesman, I. (2006). Psychiatric Endophenotypes and the Development of Valid Animal Models. *Genes, Brain, and Behavior*, 5(2), 113-119. doi:10.1111/j.1601-183X.2005.00186.x
- Graeber, M., & Moran, L. (2002). Mechanisms of Cell Death in Neurodegenerative Diseases: Fiction, Fiction, and Facts. *Brain Pathology*, 12(3), 385-390.
- Gray, J., & McNaughton, N. (1996). The Neuropsychology of Anxiety: Reprise. *Nebraska Symposium on Motivation*, 43, 61-134.
- Gray, J. A., & McNaughton, N. (2003). *The Neuropsychology of Anxiety: An Enquiry into the Functions of the Septo-Hippocampal System* (33).
- Greco, C., Berman, R., Martin, R., Tassone, F., Schwartz, P., Chang, A., ... Hagerman, P. (2006). Neuropathology of Fragile X-Associated Tremor/Ataxia Syndrome (FXTAS). *Brain*, 129(Pt 1), 243-255. doi:10.1093/brain/awh683
- Greco, C., Hagerman, R., Tassone, F., Chudley, A., Del Bigio, M. R., Jacquemont, S., ... Hagerman, P. (2002). Neuronal Intranuclear Inclusions in a New Cerebellar Tremor/Ataxia Syndrome Among Fragile X Carriers. *Brain*, 125(Pt 8), 1760-1771.
- Greco, C. M., Hunsaker, M. R., & Berman, R. F. (2010). The Pathology of FXTAS. In F. Tassone & E. M. Berry-Kravis (Eds.), *The Fragile X-Associated Tremor/Ataxia Syndrome (FXTAS)* (pp. 67-76). New York: Springer.
- Greco, C., Navarro, C., Hunsaker, M., Maezawa, I., Shuler, J., Tassone, F., ... Hagerman, R. (2011). Neuropathologic Features in the Hippocampus and

- Cerebellum of Three Older Men With Fragile X Syndrome. *Molecular Autism*, 2(1), 2. doi:10.1186/2040-2392-2-2
- Greco, C., Soontrapornchai, K., Wirojanan, J., Gould, J., Hagerman, P., & Hagerman, R. (2007). Testicular and Pituitary Inclusion Formation in Fragile X Associated Tremor/Ataxia Syndrome. *Journal of Urology*, 177(4), 1434-1437. doi:10.1016/j.juro.2006.11.097
- Greco, C., Tassone, F., Garcia-Arocena, D., Tartaglia, N., Coffey, S., Vartanian, T., ... Hagerman, R. (2008). Clinical and Neuropathologic Findings in a Woman With the Fmr1 Premutation and Multiple Sclerosis. *Archives of Neurology*, 65(8), 1114-1116. doi:10.1001/archneur.65.8.1114
- Greene-Schloesser, D. M., Van Der Zee, E. A., Sheppard, D., Castillo, M., Gregg, K., Burrow, T., ... Bult-Ito, A. (2011). Predictive Validity of a Non-Induced Mouse Model of Compulsive-Like Behavior. *Behavioural Brain Research*, 221(1), 55-62. doi:10.1016/j.bbr.2011.02.010
- Greenough, W., Larson, J., & Withers, G. (1985). Effects of Unilateral and Bilateral Training in a Reaching Task on Dendritic Branching of Neurons in the Rat Motor-Sensory Forelimb Cortex. *Behavioral and Neural Biology*, 44 (2), 301-314.
- Greicius, M. (2008). Resting-State Functional Connectivity in Neuropsychiatric Disorders. *Current Opinion in Neurology*, 21(4), 424-430. doi:10.1097/WCO.0b013e328306f2c5
- Greicius, M., Boyett-Anderson, J. M., Menon, V., & Reiss, A. (2004). Reduced Basal Forebrain and Hippocampal Activation During Memory Encoding in Girls With Fragile X Syndrome. *Neuroreport*, 15(10), 1579-1583.
- Greicius, M., Krasnow, B., Boyett-Anderson, J. M., Eliez, S., Schatzberg, A., Reiss, A., & Menon, V. (2003). Regional Analysis of Hippocampal Activation During Memory Encoding and Retrieval: FMRI Study. *Hippocampus*, 13(1), 164-174. doi:10.1002/hipo.10064
- Grigsby, J., Brega, A., Engle, K., Leehey, M., Hagerman, R., Tassone, F., ... Reynolds, A. (2008). Cognitive Profile of Fragile X Premutation Carriers With and Without Fragile X-Associated Tremor/Ataxia Syndrome. *Neuropsychology*, 22(1), 48-60. doi:10.1037/0894-4105.22.1.48
- Grigsby, J., Brega, A., Jacquemont, S., Loesch, D., Leehey, M., Goodrich, G., ... Hagerman, P. (2006a). Impairment in the Cognitive Functioning of Men With Fragile X-Associated Tremor/Ataxia Syndrome (FXTAS). *Journal of the Neurological Sciences*, 248(1-2), 227-233. doi:10.1016/j.jns.2006.05.016
- Grigsby, J., Brega, A., Leehey, M., Goodrich, G., Jacquemont, S., Loesch, D., ... Hagerman, R. (2007). Impairment of Executive Cognitive Functioning in Males With Fragile X-Associated Tremor/Ataxia Syndrome. *Movement Disorders*, 22(5), 645-650. doi:10.1002/mds.21359
- Grigsby, J., Brega, A. G., Seritan, A. L., & Bourgeois, J. A. (2010). FXTAS: Neuropsychological/Neuropsychiatric Phenotype. In F. Tassone & E. M. Berry-Kravis (Eds.), *The Fragile X-Associated Tremor/Ataxia Syndrome (FXTAS)* (pp. 31-54). New York: Springer.

- Grigsby, J., Kemper, M., & Hagerman, R. (1992). Verbal Learning and Memory Among Heterozygous Fragile X Females. *American Journal of Medical Genetics*, 43(1-2), 111-115.
- Grigsby, J., Leehey, M., Jacquemont, S., Brunberg, J., Hagerman, R., Wilson, R., ... Hagerman, P. (2006b). Cognitive Impairment in a 65-Year-Old Male With the Fragile X-Associated Tremor-Ataxia Syndrome (Fxtas). *Cognitive and Behavioral Neurology*, 19(3), 165-171. doi:10.1097/01.wnn.0000213906.57148.01
- Grossman, A., Elisseou, N., McKinney, B., & Greenough, W. (2006). Hippocampal Pyramidal Cells in Adult *Fmr1* Knockout Mice Exhibit an Immature-Appearing Profile of Dendritic Spines. *Brain Research*, 1084(1), 158-164. doi:10.1016/j.brainres.2006.02.044
- Guion, R. M. (1977). Content Validity—The Source of My Discontent. *Applied Psychological Measurement*, 1(1), 1-10.
- Gur, R., Calkins, M., Gur, R., Horan, W., Nuechterlein, K., Seidman, L., & Stone, W. (2007). The Consortium on the Genetics of Schizophrenia: Neurocognitive Endophenotypes. *Schizophrenia Bulletin*, 33(1), 49-68. doi: 10.1093/schbul/sbl055
- Guzowski, J., Timlin, J., Roysam, B., McNaughton, B., Worley, P., & Barnes, C. (2005). Mapping Behaviorally Relevant Neural Circuits With Immediate-Early Gene Expression. *Current Opinion in Neurobiology*, 15(5), 599-606. doi:10.1016/j.conb.2005.08.018
- Guzowski, J., & Worley, P. (2001). Cellular Compartment Analysis of Temporal Activity By Fluorescence In Situ Hybridization (CatFISH). *Curr Protoc Neurosci*, Chapter 1, Unit 1.8. doi:10.1002/0471142301.ns0108s15
- Haas, B., Barnea-Goraly, N., Lightbody, A., Patnaik, S., Hoeft, F., Hazlett, H., ... Reiss, A. (2009). Early White-Matter Abnormalities of the Ventral Frontostriatal Pathway in Fragile X Syndrome. *Developmental Medicine and Child Neurology*, 51(8), 593-599. doi:10.1111/j.1469-8749.2009.03295.x
- Haddon, J., George, D., & Killcross, S. (2008). Contextual Control of Biconditional Task Performance: Evidence for Cue and Response Competition in Rats. *Q J Exp Psychol (Hove)*, 61(9), 1307-1320.
- Haddon, J., & Killcross, A. (2005). Medial Prefrontal Cortex Lesions Abolish Contextual Control of Competing Responses. *Journal of the Experimental Analysis of Behavior*, 84(3), 485-504.
- Hagerman, P. (2008). The Fragile X Prevalence Paradox. *Journal of Medical Genetics*, 45(8), 498-499. doi:10.1136/jmg.2008.059055
- Hagerman, P., & Hagerman, R. (2004a). Fragile X-Associated Tremor/Ataxia Syndrome (FXTAS). *Mental Retardation and Developmental Disabilities Research Reviews*, 10(1), 25-30. doi:10.1002/mrdd.20005
- Hagerman, P., & Hagerman, R. (2004b). The Fragile-X Premutation: A Maturing Perspective. *American Journal of Human Genetics*, 74(5), 805-816. doi: 10.1086/386296
- Hagerman, P., & Hagerman, R. (2007). Fragile X-Associated Tremor/Ataxia Syndrome--an Older Face of the Fragile X Gene. *Nature Clinical Practice. Neurology*, 3(2), 107-112. doi:10.1038/ncpneuro0373

- Hagerman, R. (2006). Lessons From Fragile X Regarding Neurobiology, Autism, and Neurodegeneration. *Journal of Developmental and Behavioral Pediatrics*, 27(1), 63-74.
- Hagerman, R., Coffey, S., Maselli, R., Soontarapornchai, K., Brunberg, J., Leehey, M., ... Hagerman, P. (2007). Neuropathy as a Presenting Feature in Fragile X-Associated Tremor/Ataxia Syndrome. *American Journal of Medical Genetics. Part A*, 143A(19), 2256-2260. doi:10.1002/ajmg.a.31920
- Hagerman, R., & Hagerman, P. (2008). Testing for Fragile X Gene Mutations Throughout the Life Span. *JAMA*, 300(20), 2419-2421. doi:10.1001/jama.2008.684
- Hagerman, R., Hall, D., Coffey, S., Leehey, M., Bourgeois, J., Gould, J., ... Hagerman, P. (2008). Treatment of Fragile X-Associated Tremor Ataxia Syndrome (Fxtas) and Related Neurological Problems. *Clinical Interventions in Aging*, 3(2), 251-262.
- Hagerman, R., Leavitt, B., Farzin, F., Jacquemont, S., Greco, C., Brunberg, J., ... Hagerman, P. (2004). Fragile-X-Associated Tremor/Ataxia Syndrome (Fxtas) in Females With the *FMR1* Premutation. *American Journal of Human Genetics*, 74(5), 1051-1056. doi:10.1086/420700
- Hagerman, R., Leehey, M., Heinrichs, W., Tassone, F., Wilson, R., Hills, J., ... Hagerman, P. (2001). Intention Tremor, Parkinsonism, and Generalized Brain Atrophy in Male Carriers of Fragile X. *Neurology*, 57(1), 127-130.
- Hall, D., Pickler, L., Riley, K., Tassone, F., & Hagerman, R. (2010). Parkinsonism and Cognitive Decline in a Fragile X Mosaic Male. *Movement Disorders*, 25(10), 1523-1524. doi:10.1002/mds.23150
- Hall, D., Berry-Kravis, E., Hagerman, R., Hagerman, P., Rice, C., & Leehey, M. (2006). Symptomatic Treatment in the Fragile X-Associated Tremor/Ataxia Syndrome. *Movement Disorders*, 21(10), 1741-1744. doi:10.1002/mds.21001
- Hall, D., Howard, K., Hagerman, R., & Leehey, M. (2009). Parkinsonism in *FMR1* Premutation Carriers May be Indistinguishable From Parkinson Disease. *Parkinsonism & Related Disorders*, 15(2), 156-159. doi:10.1016/j.parkreldis.2008.04.037
- Hallahan, B., Craig, M., Toal, F., Daly, E., Moore, C., Ambikapathy, A., ... Murphy, D. (2011). In Vivo Brain Anatomy of Adult Males With Fragile X Syndrome: An MRI Study. *Neuroimage*, 54(1), 16-24. doi:10.1016/j.neuroimage.2010.08.015
- Hamlin, A., Liu, Y., Nguyen, D., Tassone, F., Zhang, L., & Hagerman, R. (2011). Sleep Apnea in Fragile X Premutation Carriers With and Without FXTAS. *American Journal of Medical Genetics. Part B, Neuropsychiatric Genetics*, 156B(8), 923-928. doi:10.1002/ajmg.b.31237
- Hampstead, B., Libon, D., Moelter, S., Swirsky-Sacchetti, T., Scheffer, L., Platek, S., & Chute, D. (2010). Temporal Order Memory Differences in Alzheimer's Disease and Vascular Dementia. *Journal of Clinical and Experimental Neuropsychology*, 32(6), 645-654. doi:10.1080/13803390903418918
- Handa, V., Goldwater, D., Stiles, D., Cam, M., Poy, G., Kumari, D., & Usdin, K. (2005). Long Cgg-Repeat Tracts Are Toxic to Human Cells: Implications for

- Carriers of Fragile X Premutation Alleles. *FEBS Letters*, 579(12), 2702-2708. doi:10.1016/j.febslet.2005.04.004
- Hannesson, D., Howland, J., & Phillips, A. (2004a). Interaction Between Perirhinal and Medial Prefrontal Cortex is Required for Temporal Order But Not Recognition Memory for Objects in Rats. *Journal of Neuroscience*, 24 (19), 4596-4604. doi:10.1523/JNEUROSCI.5517-03.2004
- Hannesson, D., Vacca, G., Howland, J., & Phillips, A. (2004b). Medial Prefrontal Cortex is Involved in Spatial Temporal Order Memory But Not Spatial Recognition Memory in Tests Relying on Spontaneous Exploration in Rats. *Behavioural Brain Research*, 153(1), 273-285. doi:10.1016/j.bbr.2003.12.004
- Hanson, J., & Madison, D. (2010). Imbalanced Pattern Completion Vs. Separation in Cognitive Disease: Network Simulations of Synaptic Pathologies Predict a Personalized Therapeutics Strategy. *BMC Neuroscience*, 11, 96. doi:10.1186/1471-2202-11-96
- Hashem, V., Galloway, J., Mori, M., Willemsen, R., Oostra, B., Paylor, R., & Nelson, D. (2009). Ectopic Expression of Cgg Containing Mrna is Neurotoxic in Mammals. *Human Molecular Genetics*, 18(13), 2443-2451. doi:10.1093/hmg/ddp182
- Hashimoto, R., Backer, K., Tassone, F., Hagerman, R., & Rivera, S. (2011). An Fmri Study of the Prefrontal Activity During the Performance of a Working Memory Task in Premutation Carriers of the Fragile X Mental Retardation 1 Gene With and Without Fragile X-Associated Tremor/Ataxia Syndrome (Fxtas). *Journal of Psychiatric Research*, 45(1), 36-43. doi:10.1016/j.jpsychires.2010.04.030
- Hashimoto, R., Javan, A., Tassone, F., Hagerman, R., & Rivera, S. (2011). A Voxel-Based Morphometry Study of Grey Matter Loss in Fragile X-Associated Tremor/Ataxia Syndrome. *Brain*, 134(Pt 3), 863-878. doi:10.1093/brain/awq368
- Hashimoto, R., Srivastava, S., Tassone, F., Hagerman, R., & Rivera, S. (2011). Diffusion Tensor Imaging in Male Premutation Carriers of the Fragile X Mental Retardation Gene. *Movement Disorders*, 26(7), 1329-1336. doi:10.1002/mds.23646
- Hasler, G., Drevets, W., Gould, T., Gottesman, I., & Manji, H. (2006). Toward Constructing an Endophenotype Strategy for Bipolar Disorders. *Biological Psychiatry*, 60(2), 93-105. doi:10.1016/j.biopsych.2005.11.006
- Hatcher, J., Jones, D., Rogers, D., Hatcher, P., Reavill, C., Hagan, J., & Hunter, A. (2001). Development of Shirpa to Characterise the Phenotype of Gene-Targeted Mice. *Behavioural Brain Research*, 125(1-2), 43-47.
- Hauser, E., Tolentino, J., Pirogovsky, E., Weston, E., & Gilbert, P. (2009). The Effects of Aging on Memory for Sequentially Presented Objects in Rats. *Behavioral Neuroscience*, 123(6), 1339-1345. doi:10.1037/a0017681
- Hayashi, M., Rao, B., Seo, J., Choi, H., Dolan, B., Choi, S., ... Tonegawa, S. (2007). Inhibition of P21-Activated Kinase Rescues Symptoms of Fragile X Syndrome in Mice. *Proceedings of the National Academy of Sciences of the*

- United States of America, 104(27), 11489-11494. doi:10.1073/pnas.0705003104*
- He, B., Lian, J., Spencer, K., Dien, J., & Donchin, E. (2001). A Cortical Potential Imaging Analysis of the P300 and Novelty P3 Components. *Human Brain Mapping, 12*(2), 120-130.
- Hermer-Vazquez, L., Hermer-Vazquez, R., & Chapin, J. (2007). The Reach-to-Grasp-Food Task for Rats: A Rare Case of Modularity in Animal Behavior? *Behavioural Brain Research, 177*(2), 322-328. doi:10.1016/j.bbr.2006.11.029
- Hessl, D., Nguyen, D., Green, C., Chavez, A., Tassone, F., Hagerman, R., ... Hall, S. (2009). A Solution to Limitations of Cognitive Testing in Children With Intellectual Disabilities: The Case of Fragile X Syndrome. *Journal of Neurodevelopmental Disorders, 1*(1), 33-45. doi:10.1007/s11689-008-9001-8
- Hessl, D., Rivera, S., Koldewyn, K., Cordeiro, L., Adams, J., Tassone, F., ... Hagerman, R. (2007). Amygdala Dysfunction in Men With the Fragile X Premutation. *Brain, 130*(Pt 2), 404-416. doi:10.1093/brain/awl338
- Hessl, D., Rivera, S., & Reiss, A. (2004). The Neuroanatomy and Neuroendocrinology of Fragile X Syndrome. *Mental Retardation and Developmental Disabilities Research Reviews, 10*(1), 17-24. doi:10.1002/mrdd.20004
- Hessl, D., Tassone, F., Cordeiro, L., Koldewyn, K., McCormick, C., Green, C., ... Hagerman, R. (2008). Brief Report: Aggression and Stereotypic Behavior in Males With Fragile X Syndrome--Moderating Secondary Genes in a "Single Gene" Disorder. *Journal of Autism and Developmental Disorders, 38*(1), 184-189. doi:10.1007/s10803-007-0365-5
- Hessl, D., Tassone, F., Loesch, D., Berry-Kravis, E., Leehey, M., Gane, L., ... Hagerman, R. (2005). Abnormal Elevation of *FMR1* mRNA is Associated With Psychological Symptoms in Individuals With the Fragile X Premutation. *American Journal of Medical Genetics. Part B, Neuropsychiatric Genetics, 139B*(1), 115-121. doi:10.1002/ajmg.b.30241
- Hessl, D., Wang, J., Schneider, A., Koldewyn, K., Le, L., Iwahashi, C., ... Rivera, S. (2011). Decreased Fragile X Mental Retardation Protein Expression Underlies Amygdala Dysfunction in Carriers of the Fragile X Premutation. *Biological Psychiatry, 70*(9), 859-865. doi:10.1016/j.biopsych.2011.05.033
- Hikosaka, O., Nakamura, K., Sakai, K., & Nakahara, H. (2002). Central Mechanisms of Motor Skill Learning. *Current Opinion in Neurobiology, 12*(2), 217-222.
- Hocking, D., Kogan, C., & Cornish, K. (2012). Selective Spatial Processing Deficits in an At-Risk Subgroup of the Fragile X Premutation. *Brain and Cognition, 79*(1), 39-44. doi:10.1016/j.bandc.2012.02.005
- Hodapp, R., Dykens, E., Ort, S., Zelinsky, D., & Leckman, J. (1991). Changing Patterns of Intellectual Strengths and Weaknesses in Males With Fragile X Syndrome. *Journal of Autism and Developmental Disorders, 21*(4), 503-516.
- Hoeft, F., Carter, J., Lightbody, A., Cody Hazlett, H., Piven, J., & Reiss, A. (2010). Region-Specific Alterations in Brain Development in One- to Three-Year-Old

- Boys With Fragile X Syndrome. *Proceedings of the National Academy of Sciences of the United States of America*, 107(20), 9335-9339. doi:10.1073/pnas.1002762107
- Hoeft, F., Lightbody, A., Hazlett, H., Patnaik, S., Piven, J., & Reiss, A. (2008). Morphometric Spatial Patterns Differentiating Boys With Fragile X Syndrome, Typically Developing Boys, and Developmentally Delayed Boys Aged 1 to 3 Years. *Archives of General Psychiatry*, 65(9), 1087-1097. doi: 10.1001/archpsyc.65.9.1087
- Hoem, G., Raske, C., Garcia-Arocena, D., Tassone, F., Sanchez, E., Ludwig, A., ... Hagerman, P. (2011). Cgg-Repeat Length Threshold for *FMR1* RNA Pathogenesis in a Cellular Model for FXTAS. *Human Molecular Genetics*, 20(11), 2161-2170. doi:10.1093/hmg/ddr101
- Hopkins, R., Kesner, R., & Goldstein, M. (1995a). Item and Order Recognition Memory in Subjects With Hypoxic Brain Injury. *Brain and Cognition*, 27(2), 180-201. doi:10.1006/brcg.1995.1016
- Hopkins, R., Kesner, R., & Goldstein, M. (1995b). Memory for Novel and Familiar Spatial and Linguistic Temporal Distance Information in Hypoxic Subjects. *Journal of the International Neuropsychological Society*, 1(5), 454-468.
- Hsu, S., Raine, L., & Fanger, H. (1981). Use of Avidin-Biotin-Peroxidase Complex (ABC) in Immunoperoxidase Techniques: A Comparison Between ABC and Unlabeled Antibody (Pap) Procedures. *Journal of Histochemistry and Cytochemistry*, 29(4), 577-580.
- Huber, K., Gallagher, S., Warren, S., & Bear, M. (2002). Altered Synaptic Plasticity in a Mouse Model of Fragile X Mental Retardation. *Proceedings of the National Academy of Sciences of the United States of America*, 99(11), 7746-7750. doi:10.1073/pnas.122205699
- Humby, T., Wilkinson, L., & Dawson, G. (2005). Assaying Aspects of Attention and Impulse Control in Mice Using the 5-Choice Serial Reaction Time Task. *Curr Protoc Neurosci, Chapter 8, Unit 8.5H*. doi: 10.1002/0471142301.ns0805hs31
- Hunsaker, M. (2012a). Comprehensive Neurocognitive Endophenotyping Strategies for Mouse Models of Genetic Disorders. *Progress in Neurobiology*, 96(2), 220-241. doi:10.1016/j.pneurobio.2011.12.001
- Hunsaker, M. (2012b). The Importance of Considering All Attributes of Memory in Behavioral Endophenotyping of Mouse Models of Genetic Disease. *Behavioral Neuroscience*, 126(4). doi:10.1037/a0028453
- Hunsaker, M., Arque, G., Berman, R., Willemsen, R., & Hukema, R. (2012). Mouse Models of the Fragile X Premutation and the Fragile X Associated Tremor/Ataxia Syndrome. *Results and Problems in Cell Differentiation*, 54, 255-269. doi:10.1007/978-3-642-21649-7_14
- Hunsaker, M., Fieldsted, P., Rosenberg, J., & Kesner, R. (2008a). Dissociating the Roles of Dorsal and Ventral CA1 for the Temporal Processing of Spatial Locations, Visual Objects, and Odors. *Behavioral Neuroscience*, 122(3), 643-650. doi:10.1037/0735-7044.122.3.643
- Hunsaker, M., Goodrich-Hunsaker, N. J., Willemsen, R., & Berman, R. (2010). Temporal Ordering Deficits in Female CGG Ki Mice Heterozygous for the

- Fragile X Premutation. *Behavioural Brain Research*, 213(2), 263-268. doi: 10.1016/j.bbr.2010.05.010
- Hunsaker, M., Greco, C., Spath, M., Smits, A., Navarro, C., Tassone, F., ... Hukema, R. (2011a). Widespread Non-Central Nervous System Organ Pathology in Fragile X Premutation Carriers With Fragile X-Associated Tremor/Ataxia Syndrome and Cgg Knock-in Mice. *Acta Neuropathol*, 122(4), 467-479. doi:10.1007/s00401-011-0860-9
- Hunsaker, M., Greco, C., Tassone, F., Berman, R., Willemse, R., Hagerman, R., & Hagerman, P. (2011b). Rare Intranuclear Inclusions in the Brains of 3 Older Adult Males With Fragile X Syndrome: Implications for the Spectrum of Fragile X-Associated Disorders. *Journal of Neuropathology and Experimental Neurology*, 70(6), 462-469. doi:10.1097/NEN.0b013e31821d3194
- Hunsaker, M., & Kesner, R. (2008). Evaluating the Differential Roles of the Dorsal Dentate Gyrus, Dorsal CA3, and Dorsal CA1 During a Temporal Ordering for Spatial Locations Task. *Hippocampus*, 18(9), 955-964. doi:10.1002/hipo.20455
- Hunsaker, M., Rosenberg, J., & Kesner, R. (2008b). The Role of the Dentate Gyrus, CA3a,b, and CA3c for Detecting Spatial and Environmental Novelty. *Hippocampus*, 18(10), 1064-1073. doi:10.1002/hipo.20464
- Hunsaker, M., Tran, G., & Kesner, R. (2009). A Behavioral Analysis of the Role of Ca3 and Ca1 Subcortical Efferents During Classical Fear Conditioning. *Behavioral Neuroscience*, 123(3), 624-630. doi:10.1037/a0015455
- Hunsaker, M., Von Leden, R. E., Ta, B., Goodrich-Hunsaker, N. J., Arque, G., Kim, K., ... Berman, R. (2011c). Motor Deficits on a Ladder Rung Task in Male and Female Adolescent and Adult CGG Knock-in Mice. *Behavioural Brain Research*, 222(1), 117-121. doi:10.1016/j.bbr.2011.03.039
- Hunsaker, M., Wenzel, H., Willemse, R., & Berman, R. (2009). Progressive Spatial Processing Deficits in a Mouse Model of the Fragile X Premutation. *Behavioral Neuroscience*, 123(6), 1315-1324. doi:10.1037/a0017616
- Hunter, J., Abramowitz, A., Rusin, M., & Sherman, S. (2009). Is There Evidence for Neuropsychological and Neurobehavioral Phenotypes Among Adults Without Fxtas Who Carry the Fmr1 Premutation? A Review of Current Literature. *Genetics in Medicine*, 11(2), 79-89. doi:10.1097/GIM.0b013e31818de6ee
- Hunter, J., Allen, E., Abramowitz, A., Rusin, M., Leslie, M., Novak, G., ... Sherman, S. (2008a). No Evidence for a Difference in Neuropsychological Profile Among Carriers and Noncarriers of the *FMR1* Premutation in Adults Under the Age of 50. *American Journal of Human Genetics*, 83(6), 692-702. doi:10.1016/j.ajhg.2008.10.021
- Hunter, J., Allen, E., Abramowitz, A., Rusin, M., Leslie, M., Novak, G., ... Sherman, S. (2008b). Investigation of Phenotypes Associated With Mood and Anxiety Among Male and Female Fragile X Premutation Carriers. *Behavior Genetics*, 38(5), 493-502. doi:10.1007/s10519-008-9214-3
- Hunter, J., Epstein, M., Tinker, S., Abramowitz, A., & Sherman, S. (2011). The Fmr1 Premutation and Attention-Deficit Hyperactivity Disorder (Adhd):

- Evidence for a Complex Inheritance. *Behavior Genetics*,. doi:10.1007/s10519-011-9520-z
- Hunter, J., Rohr, J., & Sherman, S. (2010). Co-Occurring Diagnoses Among Fmr1 Premutation Allele Carriers. *Clinical Genetics*, 77(4), 374-381. doi: 10.1111/j.1399-0004.2009.01317.x
- Hunter, J., Sherman, S., Grigsby, J., Kogan, C., & Cornish, K. (2012). Capturing the Fragile X Premutation Phenotypes: A Collaborative Effort Across Multiple Cohorts. *Neuropsychology*, 26(2), 156-164. doi:10.1037/a0026799
- Irwin, S., Christmon, C., Grossman, A., Galvez, R., Kim, S., Degrush, B., ... Greenough, W. (2005). Fragile X Mental Retardation Protein Levels Increase Following Complex Environment Exposure in Rat Brain Regions Undergoing Active Synaptogenesis. *Neurobiology of Learning and Memory*, 83(3), 180-187. doi:10.1016/j.nlm.2004.11.004
- Irwin, S., Patel, B., Idupulapati, M., Harris, J., Crisostomo, R., Larsen, B., ... Greenough, W. (2001). Abnormal Dendritic Spine Characteristics in the Temporal and Visual Cortices of Patients With Fragile-X Syndrome: A Quantitative Examination. *American Journal of Medical Genetics*, 98(2), 161-167.
- Irwin, S., Swain, R., Christmon, C., Chakravarti, A., Weiler, I., & Greenough, W. (2000). Evidence for Altered Fragile-X Mental Retardation Protein Expression in Response to Behavioral Stimulation. *Neurobiology of Learning and Memory*, 74(1), 87-93.
- Iwahashi, C., Tassone, F., Hagerman, R., Yasui, D., Parrott, G., Nguyen, D., ... Hagerman, P. (2009). A Quantitative Elisa Assay for the Fragile X Mental Retardation 1 Protein. *Journal of Molecular Diagnostics*, 11(4), 281-289. doi: 10.2353/jmoldx.2009.080118
- Iwahashi, C., Yasui, D., An, H., Greco, C., Tassone, F., Nannen, K., ... Hagerman, P. (2006). Protein Composition of the Intranuclear Inclusions of Fxtas. *Brain*, 129(Pt 1), 256-271. doi:10.1093/brain/awh650
- Jackson, P., Kesner, R., & Amann, K. (1998). Memory for Duration: Role of Hippocampus and Medial Prefrontal Cortex. *Neurobiology of Learning and Memory*, 70(3), 328-348. doi:10.1006/nlme.1998.3859
- Jacobs, J., Korolev, I., Caplan, J., Ekstrom, A., Litt, B., Baltuch, G., ... Kahana, M. (2010). Right-Lateralized Brain Oscillations in Human Spatial Navigation. *Journal of Cognitive Neuroscience*, 22(5), 824-836. doi:10.1162/jocn.2009.21240
- Jacquemont, S., Farzin, F., Hall, D., Leehey, M., Tassone, F., Gane, L., ... Hagerman, R. (2004a). Aging in Individuals With the *FMR1* Mutation. *American Journal of Mental Retardation*, 109(2), 154-164. doi: 10.1352/0895-8017(2004)109
- Jacquemont, S., Hagerman, R., Hagerman, P., & Leehey, M. (2007). Fragile-X Syndrome and Fragile X-Associated Tremor/Ataxia Syndrome: Two Faces of Fmr1. *Lancet Neurology*, 6(1), 45-55. doi:10.1016/S1474-4422(06)70676-7
- Jacquemont, S., Hagerman, R., Leehey, M., Grigsby, J., Zhang, L., Brunberg, J., ... Hagerman, P. (2003). Fragile X Premutation Tremor/Ataxia Syndrome:

- Molecular, Clinical, and Neuroimaging Correlates. *American Journal of Human Genetics*, 72(4), 869-878. doi:10.1086/374321
- Jacquemont, S., Hagerman, R., Leehey, M., Hall, D., Levine, R., Brunberg, J., ... Hagerman, P. (2004b). Penetrance of the Fragile X-Associated Tremor/Ataxia Syndrome in a Premutation Carrier Population. *JAMA*, 291(4), 460-469. doi:10.1001/jama.291.4.460
- Jacquemont, S., Leehey, M., Hagerman, R., Beckett, L., & Hagerman, P. (2006). Size Bias of Fragile X Premutation Alleles in Late-Onset Movement Disorders. *Journal of Medical Genetics*, 43(10), 804-809. doi:10.1136/jmg.2006.042374
- Jacquemont, S., Orrico, A., Galli, L., Sahota, P., Brunberg, J., Anichini, C., ... Tassone, F. (2005). Spastic Paraparesis, Cerebellar Ataxia, and Intention Tremor: A Severe Variant of FXTAS? *Journal of Medical Genetics*, 42(2), e14. doi:10.1136/jmg.2004.024190
- Jäkälä, P., Hanninen, T., Ryynanen, M., Laakso, M., Partanen, K., Mannermaa, A., & Soininen, H. (1997). Fragile-X: Neuropsychological Test Performance, Cgg Triplet Repeat Lengths, and Hippocampal Volumes. *Journal of Clinical Investigation*, 100(2), 331-338. doi:10.1172/JCI119538
- Jeannerod, M. (1997). *The cognitive Neuroscience of Action*. Cambridge, MA: Blackwell.
- Jeyasingham, R., Baird, A., Meldrum, A., & Dunnett, S. (2001). Differential Effects of Unilateral Striatal and Nigrostriatal Lesions on Grip Strength, Skilled Paw Reaching and Drug-Induced Rotation in the Rat. *Brain Research Bulletin*, 55 (4), 541-548.
- Jin, P., Duan, R., Qurashi, A., Qin, Y., Tian, D., Rosser, T., ... Warren, S. (2007). Pur Alpha Binds to Rcg repeats and Modulates Repeat-Mediated Neurodegeneration in a Drosophila Model of Fragile X Tremor/Ataxia Syndrome. *Neuron*, 55(4), 556-564. doi:10.1016/j.neuron.2007.07.020
- Jin, P., Zarnescu, D., Zhang, F., Pearson, C., Lucchesi, J., Moses, K., & Warren, S. (2003). RNA-Mediated Neurodegeneration Caused By the Fragile X Premutation Rcg repeats in Drosophila. *Neuron*, 39(5), 739-747.
- Jinno, S. (2011). Topographic Differences in Adult Neurogenesis in the Mouse Hippocampus: A Stereology-Based Study Using Endogenous Markers. *Hippocampus*, 21(5), 467-480. doi:10.1002/hipo.20762
- Johnson-Glenberg, M. C. (2008). Fragile X Syndrome: Neural Network Models of Sequencing and Memory. *Cognitive Systems Research*, 9(4), 274-292. doi: 10.1016/j.cogsys.2008.02.002
- Johnson, D., & Kesner, R. (1997). Comparison of Temporal Order Memory in Early and Middle Stage Alzheimer's Disease. *Journal of Clinical and Experimental Neuropsychology*, 19(1), 83-100. doi: 10.1080/01688639708403839
- Joo, Y. (2008). Neurophysiological and Neurocognitive Endophenotypes for Schizophrenia Genetics Research. *Psychiatry Investig*, 5(4), 199-202. doi: 10.4306/pi.2008.5.4.199
- Kaenmaki, M., Tammimaki, A., Myohanen, T., Pakarinen, K., Amberg, C., Karayiorgou, M., ... Mannisto, P. (2010). Quantitative Role of COMT in

- Dopamine Clearance in the Prefrontal Cortex of Freely Moving Mice. *Journal of Neurochemistry*, 114(6), 1745-1755. doi:10.1111/j.1471-4159.2010.06889.x
- Kamens, H., & Crabbe, J. (2007). The Parallel Rod Floor Test: A Measure of Ataxia in Mice. *Nature Protocols*, 2(2), 277-281. doi:10.1038/nprot.2007.19
- Kamens, H., Phillips, T., Holstein, S., & Crabbe, J. (2005). Characterization of the Parallel Rod Floor Apparatus to Test Motor Incoordination in Mice. *Genes, Brain, and Behavior*, 4(4), 253-266. doi:10.1111/j.1601-183X.2004.00100.x
- Kamm, C., & Gasser, T. (2005). The Variable Phenotype of FXTAS: A Common Cause of "Idiopathic" Disorders. *Neurology*, 65(2), 190-191. doi:10.1212/01.wnl.0000171744.95027.aa
- Kao, D., Aldridge, G., Weiler, I., & Greenough, W. (2010). Altered mRNA Transport, Docking, and Protein Translation in Neurons Lacking Fragile X Mental Retardation Protein. *Proceedings of the National Academy of Sciences of the United States of America*, 107(35), 15601-15606. doi:10.1073/pnas.1010564107
- Karayiorgou, M., & Gogos, J. (2004). The Molecular Genetics of the 22q11-Associated Schizophrenia. *Brain Research. Molecular Brain Research*, 132(2), 95-104. doi:10.1016/j.molbrainres.2004.09.029
- Karayiorgou, M., Gogos, J., Galke, B., Jeffery, J., Nestadt, G., Wolyniec, P., ... Pulver, A. (1996). Genotype and Phenotype Analysis At the 22q11 Schizophrenia Susceptibility Locus. *Cold Spring Harbor Symposia on Quantitative Biology*, 61, 835-843.
- Karayiorgou, M., Simon, T., & Gogos, J. (2010). 22q11.2 Microdeletions: Linking DNA Structural Variation to Brain Dysfunction and Schizophrenia. *Nature Reviews Neuroscience*, 11(6), 402-416. doi:10.1038/nrn2841
- Karbowski, M., & Neutzner, A. (2012). Neurodegeneration as a Consequence of Failed Mitochondrial Maintenance. *Acta Neuropathol*, 123(2), 157-171. doi:10.1007/s00401-011-0921-0
- Karmon, Y., & Gadoth, N. (2008). Fragile X Associated Tremor/Ataxia Syndrome (Fxtas) With Dementia in a Female Harbouring *FMR1* Premutation. *Journal of Neurology, Neurosurgery and Psychiatry*, 79(6), 738-739. doi:10.1136/jnnp.2007.139642
- Kates, W., Antshel, K., Fremont, W., Shprintzen, R., Strunge, L., Burnette, C., & Higgins, A. (2007a). Comparing Phenotypes in Patients With Idiopathic Autism to Patients With Velocardiofacial Syndrome (22q11 Ds) With and Without Autism. *American Journal of Medical Genetics. Part A*, 143A(22), 2642-2650. doi:10.1002/ajmg.a.32012
- Kates, W., Krauss, B., Abdulsabur, N., Colgan, D., Antshel, K., Higgins, A., & Shprintzen, R. (2007b). The Neural Correlates of Non-Spatial Working Memory in Velocardiofacial Syndrome (22q11.2 Deletion Syndrome). *Neuropsychologia*, 45(12), 2863-2873. doi:10.1016/j.neuropsychologia.2007.05.007
- Kaufmann, H., & Biaggioni, I. (2003). Autonomic Failure in Neurodegenerative Disorders. *Seminars in Neurology*, 23(4), 351-363. doi:10.1055/s-2004-817719

- Kaufmann, W., Abrams, M., Chen, W., & Reiss, A. (1999). Genotype, Molecular Phenotype, and Cognitive Phenotype: Correlations in Fragile X Syndrome. *American Journal of Medical Genetics*, 83(4), 286-295.
- Kemper, M., Hagerman, R., Ahmad, R., & Mariner, R. (1986). Cognitive Profiles and the Spectrum of Clinical Manifestations in Heterozygous Fra (X) Females. *American Journal of Medical Genetics*, 23(1-2), 139-156.
- Kemper, M., Hagerman, R., & Altshul-Stark, D. (1988). Cognitive Profiles of Boys With the Fragile X Syndrome. *American Journal of Medical Genetics*, 30 (1-2), 191-200.
- Kandler, K., & Neale, M. (2010). Endophenotype: A Conceptual Analysis. *Molecular Psychiatry*, 15(8), 789-797. doi:10.1038/mp.2010.8
- Kenneson, A., Zhang, F., Hagedorn, C., & Warren, S. (2001). Reduced Fmrp and Increased Fmr1 Transcription is Proportionally Associated With Cgg Repeat Number in Intermediate-Length and Premutation Carriers. *Human Molecular Genetics*, 10(14), 1449-1454.
- Keri, S., & Benedek, G. (2009). Visual Pathway Deficit in Female Fragile X Premutation Carriers: A Potential Endophenotype. *Brain and Cognition*, 69 (2), 291-295. doi:10.1016/j.bandc.2008.08.002
- Keri, S., & Benedek, G. (2010). The Perception of Biological and Mechanical Motion in Female Fragile X Premutation Carriers. *Brain and Cognition*, 72 (2), 197-201. doi:10.1016/j.bandc.2009.08.010
- Keri, S., & Benedek, G. (2011). Fragile X Protein Expression is Linked to Visual Functions in Healthy Male Volunteers. *Neuroscience*, 192, 345-350. doi:10.1016/j.neuroscience.2011.06.074
- Keri, S., & Benedek, G. (2012). Why is Vision Impaired in Fragile X Premutation Carriers? The Role of Fragile X Mental Retardation Protein and Potential Fmr1 Mrna Toxicity. *Neuroscience*, 206, 183-189. doi:10.1016/j.neuroscience.2012.01.005
- Kesner, R. (1991). The Role of the Hippocampus Within an Attribute Model of Memory. *Hippocampus*, 1(3), 279-282. doi:10.1002/hipo.450010316
- Kesner, R. (2003). Functional Specificity of Memory Function Associated With Different Subregions of the Medial Temporal Lobe. *Current Neurology and Neuroscience Reports*, 3(6), 449-451.
- Kesner, R. (2007). A Behavioral Analysis of Dentate Gyrus Function. *Progress in Brain Research*, 163, 567-576. doi:10.1016/S0079-6123(07)63030-1
- Kesner, R., & Gilbert, P. (2006). The Role of the Medial Caudate Nucleus, But Not the Hippocampus, in a Matching-to Sample Task for a Motor Response. *European Journal of Neuroscience*, 23(7), 1888-1894. doi:10.1111/j.1460-9568.2006.04709.x
- Kesner, R., & Gilbert, P. (2007). The Role of the Agranular Insular Cortex in Anticipation of Reward Contrast. *Neurobiology of Learning and Memory*, 88 (1), 82-86. doi:10.1016/j.nlm.2007.02.002
- Kesner, R., Hopkins, R., & Fineman, B. (1994). Item and Order Dissociation in Humans With Prefrontal Cortex Damage. *Neuropsychologia*, 32(8), 881-891.

- Kesner, R., & Hunsaker, M. (2010). The Temporal Attributes of Episodic Memory. *Behavioural Brain Research*, 215(2), 299-309. doi:10.1016/j.bbr.2009.12.029
- Kesner, R., Hunsaker, M., & Warthen, M. (2008). The CA3 Subregion of the Hippocampus is Critical for Episodic Memory Processing By Means of Relational Encoding in Rats. *Behavioral Neuroscience*, 122(6), 1217-1225. doi:10.1037/a0013592
- Kesner, R., Hunsaker, M., & Ziegler, W. (2010). The Role of the Dorsal CA1 and Ventral CA1 in Memory for the Temporal Order of a Sequence of Odors. *Neurobiology of Learning and Memory*, 93(1), 111-116. doi:10.1016/j.nlm.2009.08.010
- Kesner, R., Lee, I., & Gilbert, P. (2004). A Behavioral Assessment of Hippocampal Function Based on a Subregional Analysis. *Reviews in the Neurosciences*, 15(5), 333-351.
- Kesner, R., & Ragozzino, M. (1998). Pharmacological Approaches to Animal Models of Human Working Memory and Shifting Attentional Set. Commentary on Robbins' Homology in Behavioural Pharmacology: An Approach to Animal Models of Human Cognition. *Behavioural Pharmacology*, 9(7), 521-524.
- Kessels, R., Rijken, S., Joosten-Weyn Banningh, L. W., Van, S.-V. E. N., & Olde Rikkert, M. G. (2010). Categorical Spatial Memory in Patients With Mild Cognitive Impairment and Alzheimer Dementia: Positional Versus Object-Location Recall. *Journal of the International Neuropsychological Society*, 16 (1), 200-204. doi:10.1017/S1355617709990944
- Kiehl, T., Chow, E., Mikulis, D., George, S., & Bassett, A. (2009). Neuropathologic Features in Adults With 22q11.2 Deletion Syndrome. *Cerebral Cortex*, 19(1), 153-164. doi:10.1093/cercor/bhn066
- Kogan, C., Bertone, A., Cornish, K., Boutet, I., Der Kaloustian, V. M., Andermann, E., ... Chaudhuri, A. (2004a). Integrative Cortical Dysfunction and Pervasive Motion Perception Deficit in Fragile X Syndrome. *Neurology*, 63(9), 1634-1639.
- Kogan, C., Boutet, I., Cornish, K., Graham, G., Berry-Kravis, E., Drouin, A., & Milgram, N. (2009). A Comparative Neuropsychological Test Battery Differentiates Cognitive Signatures of Fragile X and Down Syndrome. *Journal of Intellectual Disability Research*, 53(2), 125-142. doi:10.1111/j.1365-2788.2008.01135.x
- Kogan, C., Boutet, I., Cornish, K., Zangenehpour, S., Mullen, K., Holden, J., ... Chaudhuri, A. (2004b). Differential Impact of the Fmr1 Gene on Visual Processing in Fragile X Syndrome. *Brain*, 127(Pt 3), 591-601. doi:10.1093/brain/awh069
- Kogan, C., & Cornish, K. (2010). Mapping Self-Reports of Working Memory Deficits to Executive Dysfunction in Fragile X Mental Retardation 1 (*FMR1*) Gene Premutation Carriers Asymptomatic for Fxtas. *Brain and Cognition*, 73 (3), 236-243. doi:10.1016/j.bandc.2010.05.008
- Kogan, C., Turk, J., Hagerman, R., & Cornish, K. (2008). Impact of the Fragile X Mental Retardation 1 (*FMR1*) Gene Premutation on Neuropsychiatric

- Functioning in Adult Males Without Fragile X-Associated Tremor/Ataxia Syndrome: A Controlled Study. *American Journal of Medical Genetics. Part B, Neuropsychiatric Genetics*, 147B(6), 859-872. doi:10.1002/ajmg.b.30685
- Kolb, B., Teskey, G., & Gibb, R. (2010). Factors Influencing Cerebral Plasticity in the Normal and Injured Brain. *Frontiers in Human Neuroscience*, 4, 204. doi:10.3389/fnhum.2010.00204
- Koldewyn, K., Hessl, D., Adams, J., Tassone, F., Hagerman, P., Hagerman, R., & Rivera, S. (2008). Reduced Hippocampal Activation During Recall is Associated With Elevated *FMR1* mRNA and Psychiatric Symptoms in Men With the Fragile X Premutation. *Brain Imaging and Behavior*, 2(2), 105-116. doi:10.1007/s11682-008-9020-9
- Kooy, R., Reyniers, E., Verhoye, M., Sijbers, J., Bakker, C., Oostra, B., ... Van Der Linden, A. (1999). Neuroanatomy of the Fragile X Knockout Mouse Brain Studied Using in Vivo High Resolution Magnetic Resonance Imaging. *European Journal of Human Genetics*, 7(5), 526-532. doi:10.1038/sj.ejhg.5200348
- Kosslyn, S., Chabris, C., Marsolek, C., & Koenig, O. (1992). Categorical Versus Coordinate Spatial Relations: Computational Analyses and Computer Simulations. *Journal of Experimental Psychology: Human Perception and Performance*, 18(2), 562-577.
- Kosslyn, S., Koenig, O., Barrett, A., Cave, C., Tang, J., & Gabrieli, J. (1989). Evidence for Two Types of Spatial Representations: Hemispheric Specialization for Categorical and Coordinate Relations. *Journal of Experimental Psychology: Human Perception and Performance*, 15(4), 723-735.
- Kovacevic, N., Henderson, J., Chan, E., Lifshitz, N., Bishop, J., Evans, A., ... Chen, X. (2005). A Three-Dimensional MRI Atlas of the Mouse Brain With Estimates of the Average and Variability. *Cerebral Cortex*, 15(5), 639-645. doi:10.1093/cercor/bhh165
- Kovari, E., Horvath, J., & Bouras, C. (2009). Neuropathology of Lewy Body Disorders. *Brain Research Bulletin*, 80(4-5), 203-210. doi:10.1016/j.brainresbull.2009.06.018
- Kraff, J., Tang, H., Cilia, R., Canesi, M., Pezzoli, G., Goldwurm, S., ... Tassone, F. (2007). Screen for Excess *FMR1* Premutation Alleles Among Males With Parkinsonism. *Archives of Neurology*, 64(7), 1002-1006. doi:10.1001/archneur.64.7.1002
- Krueger, D., Osterweil, E., Chen, S., Tye, L., & Bear, M. (2011). Cognitive Dysfunction and Prefrontal Synaptic Abnormalities in a Mouse Model of Fragile X Syndrome. *Proceedings of the National Academy of Sciences of the United States of America*, 108(6), 2587-2592. doi:10.1073/pnas.1013855108
- Kuang, H., Mei, B., Cui, Z., Lin, L., & Tsien, J. (2010). A Novel Behavioral Paradigm for Assessing the Concept of Nests in Mice. *Journal of Neuroscience Methods*, 189(2), 169-175. doi:10.1016/j.jneumeth.2010.03.025

- Kulikova-Schupak, R., Knupp, K., Pascual, J., Chin, S., Kairam, R., & Patterson, M. (2004). Rectal Biopsy in the Diagnosis of Neuronal Intranuclear Hyaline Inclusion Disease. *Journal of Child Neurology*, 19(1), 59-62.
- Kuntsi, J., Andreou, P., Ma, J., Borger, N., & Van Der Meere, J. J. (2005). Testing Assumptions for Endophenotype Studies in Adhd: Reliability and Validity of Tasks in a General Population Sample. *BMC Psychiatry*, 5, 40. doi: 10.1186/1471-244X-5-40
- Lachiewicz, A., Dawson, D., Spiridigliozi, G., & Mcconkie-Rosell, A. (2006). Arithmetic Difficulties in Females With the Fragile X Premutation. *American Journal of Medical Genetics. Part A*, 140(7), 665-672. doi:10.1002/ajmg.a.31082
- Ladavas, E., & Serino, A. (2008). Action-Dependent Plasticity in Peripersonal Space Representations. *Cognitive Neuropsychology*, 25(7-8), 1099-1113.
- Lajoie, K., Andujar, J., Pearson, K., & Drew, T. (2010). Neurons in Area 5 of the Posterior Parietal Cortex in the Cat Contribute to Interlimb Coordination During Visually Guided Locomotion: A Role in Working Memory. *Journal of Neurophysiology*, 103(4), 2234-2254. doi:10.1152/jn.01100.2009
- Larson, J., Kim, D., Patel, R., & Floreani, C. (2008). Olfactory Discrimination Learning in Mice Lacking the Fragile X Mental Retardation Protein. *Neurobiology of Learning and Memory*, 90(1), 90-102. doi:10.1016/j.nlm.2008.01.002
- Lavedan, C., Grabczyk, E., Usdin, K., & Nussbaum, R. (1998). Long Uninterrupted Cgg Repeats Within the First Exon of the Human *FMR1* Gene Are Not Intrinsically Unstable in Transgenic Mice. *Genomics*, 50(2), 229-240. doi:10.1006/geno.1998.5299
- Lavedan, C., Garrett, L., & Nussbaum, R. (1997). Trinucleotide Repeats (CGG) 22tGG(CGG)43tGG(CGG)21 From the Fragile X Gene Remain Stable in Transgenic Mice. *Human Genetics*, 100(3-4), 407-414.
- Lee, I., & Kesner, R. (2003). Time-Dependent Relationship Between the Dorsal Hippocampus and the Prefrontal Cortex in Spatial Memory. *Journal of Neuroscience*, 23(4), 1517-1523.
- Lee, J., Huerta, P., Zhang, J., Kowal, C., Bertini, E., Volpe, B., & Diamond, B. (2009). Neurotoxic Autoantibodies Mediate Congenital Cortical Impairment of Offspring in Maternal Lupus. *Nature Medicine*, 15(1), 91-96. doi:10.1038/nm.1892
- Leehey, M., Berry-Kravis, E. M., Goetz, C. G., & Hagerman, R. J. (2010). Clinical neurological phenotype of FXTAS. In F. Tassone & E. M. Berry-Kravis (Eds.), *The fragile X-associated tremor ataxia syndrome (FXTAS)* (pp. 1-16). New York: Springer.
- Leehey, M. (2009). Fragile X-Associated Tremor/Ataxia Syndrome: Clinical Phenotype, Diagnosis, and Treatment. *Journal of Investigative Medicine*, 57 (8), 830-836. doi:10.231/JIM.0b013e3181af59c4
- Leehey, M., Berry-Kravis, E., Goetz, C., Zhang, L., Hall, D., Li, L., ... Hagerman, P. (2008). Fmr1 Cgg Repeat Length Predicts Motor Dysfunction in Premutation Carriers. *Neurology*, 70(16 Pt 2), 1397-1402. doi: 10.1212/01.wnl.0000281692.98200.f5

- Leehey, M., Berry-Kravis, E., Min, S., Hall, D., Rice, C., Zhang, L., ... Hagerman, P. (2007a). Progression of Tremor and Ataxia in Male Carriers of the *FMR1* Premutation. *Movement Disorders*, 22(2), 203-206. doi:10.1002/mds.21252
- Leehey, M., & Hagerman, P. (2012). Fragile X-Associated Tremor/Ataxia Syndrome. *Handb Clin Neurol*, 103, 373-386. doi:10.1016/B978-0-444-51892-7.00023-1
- Leehey, M., Hagerman, R., & Hagerman, P. (2007b). Fragile X Syndrome Vs Fragile X-Associated Tremor/Ataxia Syndrome. *Archives of Neurology*, 64 (2), 289; author reply 289-289; author reply 290. doi:10.1001/archneur.64.2.289-a
- Leehey, M., Legg, W., Tassone, F., & Hagerman, R. (2011). Fibromyalgia in Fragile X Mental Retardation 1 Gene Premutation Carriers. *Rheumatology*, 50(12), 2233-2236. doi:10.1093/rheumatology/ker273
- Lehman, N. (2009). The Ubiquitin Proteasome System in Neuropathology. *Acta Neuropathol*, 118(3), 329-347. doi:10.1007/s00401-009-0560-x
- Leslie, A., Gelman, R., & Gallistel, C. (2008). The Generative Basis of Natural Number Concepts. *Trends Cogn Sci*, 12(6), 213-218. doi:10.1016/j.tics.2008.03.004
- Llano Lopez, L., Hauser, J., Feldon, J., Gargiulo, P., & Yee, B. (2010). Evaluating Spatial Memory Function in Mice: A Within-Subjects Comparison Between the Water Maze Test and Its Adaptation to Dry Land. *Behavioural Brain Research*, 209(1), 85-92. doi:10.1016/j.bbr.2010.01.020
- Loat, C., Craig, G., Plomin, R., & Craig, I. (2006). Investigating the Relationship Between *Fmr1* Allele Length and Cognitive Ability in Children: A Subtle Effect of the Normal Allele Range on the Normal Ability Range? *Annals of Human Genetics*, 70(Pt 5), 555-565. doi:10.1111/j.1469-1809.2006.00269.x
- Loesch, D., Bui, Q., Grigsby, J., Butler, E., Epstein, J., Huggins, R., ... Hagerman, R. (2003). Effect of the Fragile X Status Categories and the Fragile X Mental Retardation Protein Levels on Executive Functioning in Males and Females With Fragile X. *Neuropsychology*, 17(4), 646-657. doi:10.1037/0894-4105.17.4.646
- Loesch, D., Litewka, L., Brotchie, P., Huggins, R., Tassone, F., & Cook, M. (2005). Magnetic Resonance Imaging Study in Older Fragile X Premutation Male Carriers. *Annals of Neurology*, 58(2), 326-330. doi:10.1002/ana.20542
- Long, J., Laporte, P., Merscher, S., Funke, B., Saint-Jore, B., Puech, A., ... Wynshaw-Boris, A. (2006). Behavior of Mice With Mutations in the Conserved Region Deleted in Velocardiofacial/Digeorge Syndrome. *Neurogenetics*, 7(4), 247-257. doi:10.1007/s10048-006-0054-0
- Loos, M., Staal, J., Schoffelmeer, A., Smit, A., Spijker, S., & Pattij, T. (2010). Inhibitory Control and Response Latency Differences Between C57Bl/6j and Dba/2j Mice in a Go/No-Go and 5-Choice Serial Reaction Time Task and Strain-Specific Responsivity to Amphetamine. *Behavioural Brain Research*, 214(2), 216-224. doi:10.1016/j.bbr.2010.05.027
- Louis, E., Moskowitz, C., Friez, M., Amaya, M., & Vonsattel, J. (2006). Parkinsonism, Dysautonomia, and Intracellular Inclusions in a Fragile X

- Carrier: A Clinical-Pathological Study. *Movement Disorders*, 21(3), 420-425. doi:10.1002/mds.20753
- Lyford, G., Yamagata, K., Kaufmann, W., Barnes, C., Sanders, L., Copeland, N., ... Worley, P. (1995). Arc, a Growth Factor and Activity-Regulated Gene, Encodes a Novel Cytoskeleton-Associated Protein That is Enriched in Neuronal Dendrites. *Neuron*, 14(2), 433-445.
- Maasberg, D., Shelley, L., Gracian, E., & Gilbert, P. (2011). Age-Related Differences in the Anticipation of Future Rewards. *Behavioural Brain Research*, 223(2), 371-375. doi:10.1016/j.bbr.2011.05.004
- Machado, A., Simon, T., Nguyen, V., McDonald-McGinn, D. M., Zackai, E., & Gee, J. (2007). Corpus Callosum Morphology and Ventricular Size in Chromosome 22q11.2 Deletion Syndrome. *Brain Research*, 1131(1), 197-210. doi:10.1016/j.brainres.2006.10.082
- Mackinnon, D., Gross, C., & Bender, D. (1976). A Visual Deficit After Superior Colliculus Lesions in Monkeys. *Acta Neurobiol Exp (Wars)*, 36(1-2), 169-180.
- Macleod, L., Kogan, C., Collin, C., Berry-Kravis, E., Messier, C., & Gandhi, R. (2010). A Comparative Study of the Performance of Individuals With Fragile X Syndrome and Fmr1 Knockout Mice on Hebb-Williams Mazes. *Genes, Brain, and Behavior*, 9(1), 53-64. doi:10.1111/j.1601-183X.2009.00534.x
- Madan, S., Madan-Khetarpal, S., Park, S., Surti, U., Bailey, A., McConnell, J., & Tadros, S. (2010). Left Ventricular Non-Compaction on MRI in a Patient With 22q11.2 Distal Deletion. *American Journal of Medical Genetics. Part A*, 152A(5), 1295-1299. doi:10.1002/ajmg.a.33367
- Malkesman, O., Scattoni, M., Paredes, D., Tragon, T., Pearson, B., Shaltiel, G., ... Manji, H. (2010). The Female Urine Sniffing Test: A Novel Approach for Assessing Reward-Seeking Behavior in Rodents. *Biological Psychiatry*, 67 (9), 864-871. doi:10.1016/j.biopsych.2009.10.018
- Manji, H., Gottesman, I., & Gould, T. (2003). Signal Transduction and Genes-to-Behaviors Pathways in Psychiatric Diseases. *Science's STKE*, 2003(207), pe49. doi:10.1126/stke.2003.207.pe49
- Manns, J., & Eichenbaum, H. (2005). Time and Treason to the Trisynaptic Teachings: Theoretical Comment on Kesner et al. (2005). *Behavioral Neuroscience*, 119(4), 1140-1143. doi:10.1037/0735-7044.119.4.1140
- Marquis, J., Killcross, S., & Haddon, J. (2007). Inactivation of the Prelimbic, But Not Infralimbic, Prefrontal Cortex Impairs the Contextual Control of Response Conflict in Rats. *European Journal of Neuroscience*, 25(2), 559-566. doi:10.1111/j.1460-9568.2006.05295.x
- Marr, D. (1971). Simple Memory: A Theory for Archicortex. *Philosophical Transactions of the Royal Society of London. Series B, Biological Sciences*, 262(841), 23-81.
- Marshall, J., & Fink, G. (2001). Spatial Cognition: Where We Were and Where We Are. *Neuroimage*, 14(1 Pt 2), S2-7. doi:10.1006/nimg.2001.0834
- Marshuetz, C. (2005). Order Information in Working Memory: An Integrative Review of Evidence From Brain and Behavior. *Psychological Bulletin*, 131 (3), 323-339. doi:10.1037/0033-2909.131.3.323

- Matsuo, N., Takao, K., Nakanishi, K., Yamasaki, N., Tanda, K., & Miyakawa, T. (2010). Behavioral Profiles of Three C57Bl/6 Substrains. *Frontiers in Behavioral Neuroscience*, 4, 29. doi:10.3389/fnbeh.2010.00029
- Mazzocco, M. (2000). Advances in Research on the Fragile X Syndrome. *Mental Retardation and Developmental Disabilities Research Reviews*, 6(2), 96-106. doi:10.1002/1098-2779(2000)6
- Mazzocco, M. (2001). Math Learning Disability and Math LD Subtypes: Evidence From Studies of Turner Syndrome, Fragile X Syndrome, and Neurofibromatosis Type 1. *Journal of Learning Disabilities*, 34(6), 520-533.
- Mazzocco, M. (2009). Mathematical Learning Disability in Girls With Turner Syndrome: A Challenge to Defining Mild and Its Subtypes. *Developmental Disabilities Research Reviews*, 15(1), 35-44. doi:10.1002/ddrr.50
- Mazzocco, M., Baumgardner, T., Freund, L., & Reiss, A. (1998). Social Functioning Among Girls With Fragile X or Turner Syndrome and Their Sisters. *Journal of Autism and Developmental Disorders*, 28(6), 509-517.
- Mazzocco, M., Hagerman, R., Cronister-Silverman, A., & Pennington, B. (1992). Specific Frontal Lobe Deficits Among Women With the Fragile X Gene. *Journal of the American Academy of Child and Adolescent Psychiatry*, 31(6), 1141-1148. doi:10.1097/00004583-199211000-00025
- Mazzocco, M., Hagerman, R., & Pennington, B. (1992). Problem Solving Limitations Among Cytogenetically Expressing Fragile X Women. *American Journal of Medical Genetics*, 43(1-2), 78-86.
- Mazzocco, M., Pennington, B., & Hagerman, R. (1993). The Neurocognitive Phenotype of Female Carriers of Fragile X: Additional Evidence for Specificity. *Journal of Developmental and Behavioral Pediatrics*, 14(5), 328-335.
- Mazzocco, M., Pennington, B., & Hagerman, R. (1994). Social Cognition Skills Among Females With Fragile X. *Journal of Autism and Developmental Disorders*, 24(4), 473-485.
- Mazzocco, M., Thompson, L., Sudhalter, V., Belser, R., Lesniak-Karpiak, K., & Ross, J. (2006). Language Use in Females With Fragile X or Turner Syndrome During Brief Initial Social Interactions. *Journal of Developmental and Behavioral Pediatrics*, 27(4), 319-328.
- McConkie-Rosell, A., Abrams, L., Finucane, B., Cronister, A., Gane, L., Coffey, S., ... Hagerman, R. (2007). Recommendations From Multi-Disciplinary Focus Groups on Cascade Testing and Genetic Counseling for Fragile X-Associated Disorders. *Journal of Genetic Counseling*, 16(5), 593-606. doi:10.1007/s10897-007-9099-y
- McFarlane, H., Kusek, G., Yang, M., Phoenix, J., Bolivar, V., & Crawley, J. (2008). Autism-Like Behavioral Phenotypes in Btbr T+Tf/J Mice. *Genes, Brain, and Behavior*, 7(2), 152-163. doi:10.1111/j.1601-183X.2007.00330.x
- McIntyre, C., Miyashita, T., Setlow, B., Marjon, K., Steward, O., Guzowski, J., & McGaugh, J. (2005). Memory-Influencing Intra-Basolateral Amygdala Drug Infusions Modulate Expression of Arc Protein in the Hippocampus. *Proceedings of the National Academy of Sciences of the United States of America*, 102(30), 10718-10723. doi:10.1073/pnas.0504436102

- McKeith, I. (2006). Consensus Guidelines for the Clinical and Pathologic Diagnosis of Dementia With Lewy Bodies (Dlb): Report of the Consortium on Dlb International Workshop. *Journal of Alzheimer's Disease*, 9(3 Suppl), 417-423.
- McKhann, G. N., Wenzel, H., Robbins, C., Sosunov, A., & Schwartzkroin, P. (2003). Mouse Strain Differences in Kainic Acid Sensitivity, Seizure Behavior, Mortality, and Hippocampal Pathology. *Neuroscience*, 122(2), 551-561.
- McNaughton, B., & Morris, R. (1987). Hippocampal Synaptic Enhancement and Information Storage Within a Distributed Memory System. *Trends in Neuroscience*, 10, 408-415.
- McNaughton, N., & Gray, J. (2000). Anxiolytic Action on the Behavioural Inhibition System Implies Multiple Types of Arousal Contribute to Anxiety. *Journal of Affective Disorders*, 61(3), 161-176.
- McTighe, S., Mar, A., Romberg, C., Bussey, T., & Saksida, L. (2009). A New Touchscreen Test of Pattern Separation: Effect of Hippocampal Lesions. *Neuroreport*, 20(9), 881-885. doi:10.1097/WNR.0b013e32832c5eb2
- Meechan, D., Maynard, T., Wu, Y., Gopalakrishna, D., Lieberman, J., & Lamantia, A. (2006). Gene Dosage in the Developing and Adult Brain in a Mouse Model of 22q11 Deletion Syndrome. *Molecular and Cellular Neurosciences*, 33(4), 412-428. doi:10.1016/j.mcn.2006.09.001
- Meechan, D., Tucker, E., Maynard, T., & Lamantia, A. (2009). Diminished Dosage of 22q11 Genes Disrupts Neurogenesis and Cortical Development in a Mouse Model of 22q11 Deletion/Digeorge Syndrome. *Proceedings of the National Academy of Sciences of the United States of America*, 106(38), 16434-16445. doi:10.1073/pnas.0905696106
- Meert, T., & Colpaert, F. (1986). The Shock Probe Conflict Procedure. A New Assay Responsive to Benzodiazepines, Barbiturates and Related Compounds. *Psychopharmacology*, 88(4), 445-450.
- Melvin, K., Doan, J., Pellis, S., Brown, L., Whishaw, I., & Suchowersky, O. (2005). Pallidal Deep Brain Stimulation and L-Dopa Do Not Improve Qualitative Aspects of Skilled Reaching in Parkinson's Disease. *Behavioural Brain Research*, 160(1), 188-194. doi:10.1016/j.bbr.2004.12.001
- Meredith, M., & Stein, B. (1986). Visual, Auditory, and Somatosensory Convergence on Cells in Superior Colliculus Results in Multisensory Integration. *Journal of Neurophysiology*, 56(3), 640-662.
- Metz, G. A. (2008). *Skilled Limb Use in Rat Models of Human neurological Disease*. Proceedings from Proceedings of Measuring Behavior, Maastricht, The Nehterlands.
- Metz, G., & Whishaw, I. (2002). Cortical and Subcortical Lesions Impair Skilled Walking in the Ladder Rung Walking Test: A New Task to Evaluate Fore- and Hindlimb Stepping, Placing, and Co-Ordination. *Journal of Neuroscience Methods*, 115(2), 169-179.
- Metz, G., & Whishaw, I. (2009). The Ladder Rung Walking Task: A Scoring System and Its Practical Application. *Journal of Visualized Experiments*, 28). doi:10.3791/1204

- Miezejeski, C., Jenkins, E., Hill, A., Wisniewski, K., French, J., & Brown, W. (1986). A Profile of Cognitive Deficit in Females From Fragile X Families. *Neuropsychologia*, 24(3), 405-409.
- Mineur, Y., & Crusio, W. (2002). Behavioral and Neuroanatomical Characterization of FVB/N Inbred Mice. *Brain Research Bulletin*, 57(1), 41-47.
- Mineur, Y., Huynh, L., & Crusio, W. (2006). Social Behavior Deficits in the *Fmr1* Mutant Mouse. *Behavioural Brain Research*, 168(1), 172-175. doi:10.1016/j.bbr.2005.11.004
- Mineur, Y., Sluyter, F., De Wit, S., Oostra, B., & Crusio, W. (2002). Behavioral and Neuroanatomical Characterization of the *Fmr1* Knockout Mouse. *Hippocampus*, 12(1), 39-46. doi:10.1002/hipo.10005
- Mitchell, J., & Laiacona, J. (1998). The Medial Frontal Cortex and Temporal Memory: Tests Using Spontaneous Exploratory Behaviour in the Rat. *Behavioural Brain Research*, 97(1-2), 107-113.
- Moore, C., Daly, E., Schmitz, N., Tassone, F., Tysoe, C., Hagerman, R., ... Murphy, D. (2004a). A Neuropsychological Investigation of Male Premutation Carriers of Fragile X Syndrome. *Neuropsychologia*, 42(14), 1934-1947. doi:10.1016/j.neuropsychologia.2004.05.002
- Moore, C., Daly, E., Tassone, F., Tysoe, C., Schmitz, N., Ng, V., ... Murphy, D. (2004b). The Effect of Pre-Mutation of X Chromosome Cgg Trinucleotide Repeats on Brain Anatomy. *Brain*, 127(Pt 12), 2672-2681. doi:10.1093/brain/awh256
- Moretti, P., Bouwknecht, J., Teague, R., Paylor, R., & Zoghbi, H. (2005). Abnormalities of Social Interactions and Home-Cage Behavior in a Mouse Model of Rett Syndrome. *Human Molecular Genetics*, 14(2), 205-220. doi:10.1093/hmg/ddi016
- Mostofsky, S., Mazzocco, M., Aakalu, G., Warsofsky, I., Denckla, M., & Reiss, A. (1998). Decreased Cerebellar Posterior Vermis Size in Fragile X Syndrome: Correlation With Neurocognitive Performance. *Neurology*, 50(1), 121-130.
- Moy, S., Nadler, J., Poe, M., Nonneman, R., Young, N., Koller, B., ... Bodfish, J. (2008a). Development of a Mouse Test for Repetitive, Restricted Behaviors: Relevance to Autism. *Behavioural Brain Research*, 188(1), 178-194. doi:10.1016/j.bbr.2007.10.029
- Moy, S., Nadler, J., Young, N., Nonneman, R., Segall, S., Andrade, G., ... Magnuson, T. (2008b). Social Approach and Repetitive Behavior in Eleven Inbred Mouse Strains. *Behavioural Brain Research*, 191(1), 118-129. doi:10.1016/j.bbr.2008.03.015
- Moy, S., Nadler, J., Young, N., Perez, A., Holloway, L., Barbaro, R., ... Crawley, J. (2007). Mouse Behavioral Tasks Relevant to Autism: Phenotypes of 10 Inbred Strains. *Behavioural Brain Research*, 176(1), 4-20. doi:10.1016/j.bbr.2006.07.030
- Mukai, J., Dhilla, A., Drew, L., Stark, K., Cao, L., Macdermott, A., ... Gogos, J. (2008). Palmitoylation-Dependent Neurodevelopmental Deficits in a Mouse Model of 22q11 Microdeletion. *Nature Neuroscience*, 11(11), 1302-1310. doi:10.1038/nn.2204

- Mukai, J., Liu, H., Burt, R., Swor, D., Lai, W., Karayiorgou, M., & Gogos, J. (2004). Evidence That the Gene Encoding Zdhhc8 Contributes to the Risk of Schizophrenia. *Nature Genetics*, 36(7), 725-731. doi:10.1038/ng1375
- Mumby, D. (2001). Perspectives on Object-Recognition Memory Following Hippocampal Damage: Lessons From Studies in Rats. *Behavioural Brain Research*, 127(1-2), 159-181.
- Munoz, D. (2002). Intention Tremor, Parkinsonism, and Generalized Brain Atrophy in Male Carriers of Fragile X. *Neurology*, 58(6), 987; author reply 987-987; author reply 988.
- Murphy, D., Mantis, M., Pietrini, P., Grady, C., Moore, C., Horwitz, B., ... Rapoport, S. (1999). Premutation Female Carriers of Fragile X Syndrome: A Pilot Study on Brain Anatomy and Metabolism. *Journal of the American Academy of Child and Adolescent Psychiatry*, 38(10), 1294-1301. doi: 10.1097/00004583-199910000-00019
- Murphy, M., & Mazzocco, M. (2008). Rote Numeric Skills May Mask Underlying Mathematical Disabilities in Girls With Fragile X Syndrome. *Dev Neuropsychol*, 33(3), 345-364. doi:10.1080/87565640801982429
- Murphy, M., Mazzocco, M., Hanich, L., & Early, M. (2007). Cognitive Characteristics of Children With Mathematics Learning Disability (Mld) Vary as a Function of the Cutoff Criterion Used to Define Mld. *Journal of Learning Disabilities*, 40(5), 458-478.
- Mutha, P., Sainburg, R., & Haaland, K. (2010). Coordination Deficits in Ideomotor Apraxia During Visually Targeted Reaching Reflect Impaired Visuomotor Transformations. *Neuropsychologia*, 48(13), 3855-3867. doi:10.1016/j.neuropsychologia.2010.09.018
- Myers, C., & Scharfman, H. (2009). A Role for Hilar Cells in Pattern Separation in the Dentate Gyrus: A Computational Approach. *Hippocampus*, 19(4), 321-337. doi:10.1002/hipo.20516
- Nadler, J., Moy, S., Dold, G., Trang, D., Simmons, N., Perez, A., ... Crawley, J. (2004). Automated Apparatus for Quantitation of Social Approach Behaviors in Mice. *Genes, Brain, and Behavior*, 3(5), 303-314. doi:10.1111/j.1601-183X.2004.00071.x
- Nadler, J., Zou, F., Huang, H., Moy, S., Lauder, J., Crawley, J., ... Magnuson, T. (2006). Large-Scale Gene Expression Differences Across Brain Regions and Inbred Strains Correlate With a Behavioral Phenotype. *Genetics*, 174 (3), 1229-1236. doi:10.1534/genetics.106.061481
- Nakazawa, K., McHugh, T., Wilson, M., & Tonegawa, S. (2004). Nmda Receptors, Place Cells and Hippocampal Spatial Memory. *Nature Reviews Neuroscience*, 5(5), 361-372. doi:10.1038/nrn1385
- Nakazawa, K., Sun, L., Quirk, M., Rondi-Reig, L., Wilson, M., & Tonegawa, S. (2003). Hippocampal Ca3 Nmda Receptors Are Crucial for Memory Acquisition of One-Time Experience. *Neuron*, 38(2), 305-315.
- Napoli, E., Ross-Inta, C., Wong, S., Omanska-Klusek, A., Barrow, C., Iwahashi, C., ... Giulivi, C. (2011). Altered Zinc Transport Disrupts Mitochondrial Protein Processing/Import in Fragile X-Associated Tremor/Ataxia Syndrome. *Human Molecular Genetics*, 20(15), 3079-3092. doi:10.1093/hmg/ddr211

- Narcisa, V., Aguilar, D., Nguyen, D. V., Campos, L., Brodovsky, J., White, S., ... Hagerman, R. J. (2011). A Quantitative Assessment of Tremor and Ataxia in Female *FMR1* Premutation Carriers Using Catsys. *Current Gerontology and Geriatrics Research, 2011*.
- Nishie, M., Mori, F., Fujiwara, H., Hasegawa, M., Yoshimoto, M., Iwatsubo, T., ... Wakabayashi, K. (2004). Accumulation of Phosphorylated Alpha-Synuclein in the Brain and Peripheral Ganglia of Patients With Multiple System Atrophy. *Acta Neuropathol, 107*(4), 292-298. doi:10.1007/s00401-003-0811-1
- Noble, C., Baker, B., & Jones, T. (1964). Age and Sex Parameters in Psychomotor Learning. *Perceptual and Motor Skills, 19*, 935-945.
- O'Dwyer, J. P., Clabby, C., Crown, J., Barton, D., & Hutchinson, M. (2005). Fragile X-Associated Tremor/Ataxia Syndrome Presenting in a Woman After Chemotherapy. *Neurology, 65*(2), 331-332. doi:10.1212/01.wnl.0000168865.36352.53
- O'Reilly, R. C., & McClelland, J. (1994). Hippocampal Conjunctive Encoding, Storage, and Recall: Avoiding a Trade-Off. *Hippocampus, 4*(6), 661-682. doi:10.1002/hipo.450040605
- Olichney, J., Chan, S., Wong, L., Schneider, A., Seritan, A., Niese, A., ... Hagerman, R. (2010). Abnormal N400 Word Repetition Effects in Fragile X-Associated Tremor/Ataxia Syndrome. *Brain, 133*(Pt 5), 1438-1450. doi:10.1093/brain/awq077
- Oostra, B., & Willemsen, R. (2009). *Fmr1*: A Gene With Three Faces. *Biochimica et Biophysica Acta, 1790*(6), 467-477. doi:10.1016/j.bbagen.2009.02.007
- Ortigas, M., Bourgeois, J., Schneider, A., Olichney, J., Nguyen, D., Cogswell, J., ... Hagerman, R. (2010). Improving Fragile X-Associated Tremor/Ataxia Syndrome Symptoms With Memantine and Venlafaxine. *Journal of Clinical Psychopharmacology, 30*(5), 642-644. doi:10.1097/JCP.0b013e3181f1d10a
- Palay, S. L., & Chan-Palay, V. (1974). *Cerebellar Cortex: Cytology and Organization*. New York: Springer-Verlag.
- Pan, F., Aldridge, G., Greenough, W., & Gan, W. (2010). Dendritic Spine Instability and Insensitivity to Modulation By Sensory Experience in a Mouse Model of Fragile X Syndrome. *Proceedings of the National Academy of Sciences of the United States of America, 107*(41), 17768-17773. doi:10.1073/pnas.1012496107
- Park, S., Park, J., Kim, S., Kim, J., Shepherd, J., Smith-Hicks, C. L., ... Worley, P. (2008). Elongation Factor 2 and Fragile X Mental Retardation Protein Control the Dynamic Translation of Arc/Arg3.1 Essential for Mglur-Ltd. *Neuron, 59*(1), 70-83. doi:10.1016/j.neuron.2008.05.023
- Paul, R., Pessah, I., Gane, L., Ono, M., Hagerman, P., Brunberg, J., ... Hagerman, R. (2010). Early Onset of Neurological Symptoms in Fragile X Premutation Carriers Exposed to Neurotoxins. *Neurotoxicology, 31*(4), 399-402. doi:10.1016/j.neuro.2010.04.002
- Paylor, R., & Crawley, J. (1997). Inbred Strain Differences in Prepulse Inhibition of the Mouse Startle Response. *Psychopharmacology, 132*(2), 169-180.

- Paylor, R., Glaser, B., Mupo, A., Ataliotis, P., Spencer, C., Sobotka, A., ... Lindsay, E. (2006). Tbx1 Haploinsufficiency is Linked to Behavioral Disorders in Mice and Humans: Implications for 22q11 Deletion Syndrome. *Proceedings of the National Academy of Sciences of the United States of America*, 103(20), 7729-7734. doi:10.1073/pnas.0600206103
- Paylor, R., & Lindsay, E. (2006). Mouse Models of 22q11 Deletion Syndrome. *Biological Psychiatry*, 59(12), 1172-1179. doi:10.1016/j.biopsych.2006.01.018
- Paylor, R., Zhao, Y., Libbey, M., Westphal, H., & Crawley, J. (2001). Learning Impairments and Motor Dysfunctions in Adult Lhx5-Deficient Mice Displaying Hippocampal Disorganization. *Physiology and Behavior*, 73(5), 781-792.
- Peprah, E., He, W., Allen, E., Oliver, T., Boyne, A., & Sherman, S. (2010a). Examination of Fmr1 Transcript and Protein Levels Among 74 Premutation Carriers. *Journal of Human Genetics*, 55(1), 66-68. doi:10.1038/jhg.2009.121
- Peprah, E., Allen, E., Williams, S., Woodard, L., & Sherman, S. (2010b). Genetic Diversity of the Fragile X Syndrome Gene (*FMR1*) in a Large Sub-Saharan West African Population. *Annals of Human Genetics*, 74(4), 316-325. doi: 10.1111/j.1469-1809.2010.00582.x
- Pfeiffer, B., & Huber, K. (2006). Current Advances in Local Protein Synthesis and Synaptic Plasticity. *Journal of Neuroscience*, 26(27), 7147-7150. doi: 10.1523/JNEUROSCI.1797-06.2006
- Pirogovsky, E., Goldstein, J., Peavy, G., Jacobson, M., Corey-Bloom, J., & Gilbert, P. (2009). Temporal Order Memory Deficits Prior to Clinical Diagnosis in Huntington's Disease. *Journal of the International Neuropsychological Society*, 15(5), 662-670. doi:10.1017/S1355617709990427
- Plenge, R., Stevenson, R., Lubs, H., Schwartz, C., & Willard, H. (2002). Skewed X-Chromosome Inactivation is a Common Feature of X-Linked Mental Retardation Disorders. *American Journal of Human Genetics*, 71(1), 168-173. doi:10.1086/341123
- Pobbe, R., Defensor, E., Pearson, B., Bolivar, V., Blanchard, D., & Blanchard, R. (2011). General and Social Anxiety in the Btbr T+ Tf/J Mouse Strain. *Behavioural Brain Research*, 216(1), 446-451. doi:10.1016/j.bbr.2010.08.039
- Poirier, G., Amin, E., Good, M., & Aggleton, J. (2011). Early-Onset Dysfunction of Retrosplenial Cortex Precedes Overt Amyloid Plaque Formation in Tg2576 Mice. *Neuroscience*, 174, 71-83. doi:10.1016/j.neuroscience.2010.11.025
- Porsolt, R., Le Pichon, M., & Jalfre, M. (1977). Depression: A New Animal Model Sensitive to Antidepressant Treatments. *Nature*, 266(5604), 730-732.
- Posner, M., Walker, J., Friedrich, F., & Rafal, R. (1987). How Do the Parietal Lobes Direct Covert Attention? *Neuropsychologia*, 25(1A), 135-145.
- Primerano, B., Tassone, F., Hagerman, R., Hagerman, P., Amaldi, F., & Bagni, C. (2002). Reduced Fmr1 Mrna Translation Efficiency in Fragile X Patients With Premutations. *RNA*, 8(12), 1482-1488.

- Qin, M., Entezam, A., Usdin, K., Huang, T., Liu, Z., Hoffman, G., & Smith, C. (2011). A Mouse Model of the Fragile X Premutation: Effects on Behavior, Dendrite Morphology, and Regional Rates of Cerebral Protein Synthesis. *Neurobiology of Disease*, 42(1), 85-98. doi:10.1016/j.nbd.2011.01.008
- Team, R. D. C. (2012). *R: A language and environment for statistical computing*. Vienna, Austria: R Foundation for Statistical Computing.
- Ranum, L., & Cooper, T. (2006). RNA-Mediated Neuromuscular Disorders. *Annual Review of Neuroscience*, 29, 259-277. doi:10.1146/annurev.neuro.29.051605.113014
- Raske, C., & Hagerman, P. (2009). Molecular Pathogenesis of Fragile X-Associated Tremor/Ataxia Syndrome. *Journal of Investigative Medicine*, 57(8), 825-829. doi:10.231/JIM.0b013e3181be329a
- Rayburn-Reeves, R. M., Miller, H., & Zentall, T. (2010). "Counting" By Pigeons: Discrimination of the Number of Biologically Relevant Sequential Events. *Learning and Behavior*, 38(2), 169-176. doi:10.3758/LB.38.2.169
- Redish, A., & Touretzky, D. (1994). The Reaching Task: Evidence for Vector Arithmetic in the Motor System? *Biological Cybernetics*, 71(4), 307-317.
- Reis, A., Ferreira, A., Gomes, K., Aguiar, M., Fonseca, C., Cardoso, F., ... Carvalho, M. (2008). Frequency of Fmr1 Premutation in Individuals With Ataxia and/or Tremor and/or Parkinsonism. *Genetics and Molecular Research*, 7(1), 74-84.
- Reiss, A. (2009). Childhood Developmental Disorders: An Academic and Clinical Convergence Point for Psychiatry, Neurology, Psychology and Pediatrics. *Journal of Child Psychology and Psychiatry and Allied Disciplines*, 50(1-2), 87-98. doi:10.1111/j.1469-7610.2008.02046.x
- Reiss, A., Aylward, E., Freund, L., Joshi, P., & Bryan, R. (1991). Neuroanatomy of Fragile X Syndrome: The Posterior Fossa. *Annals of Neurology*, 29(1), 26-32. doi:10.1002/ana.410290107
- Reiss, A., Freund, L., Tseng, J., & Joshi, P. (1991). Neuroanatomy in Fragile X Females: The Posterior Fossa. *American Journal of Human Genetics*, 49(2), 279-288.
- Reiss, A., Patel, S., Kumar, A., & Freund, L. (1988). Preliminary Communication: Neuroanatomical Variations of the Posterior Fossa in Men With the Fragile X (Martin-Bell) Syndrome. *American Journal of Medical Genetics*, 31(2), 407-414. doi:10.1002/ajmg.1320310220
- Ribeiro-Barbosa, E. R., Canteras, N., Cezario, A., Blanchard, R., & Blanchard, D. (2005). An Alternative Experimental Procedure for Studying Predator-Related Defensive Responses. *Neuroscience and Biobehavioral Reviews*, 29(8), 1255-1263. doi:10.1016/j.neubiorev.2005.04.006
- Ricceri, L., Moles, A., & Crawley, J. (2007). Behavioral Phenotyping of Mouse Models of Neurodevelopmental Disorders: Relevant Social Behavior Patterns Across the Life Span. *Behavioural Brain Research*, 176(1), 40-52. doi:10.1016/j.bbr.2006.08.024
- Rivera, S., Menon, V., White, C., Glaser, B., & Reiss, A. (2002). Functional Brain Activation During Arithmetic Processing in Females With Fragile X

- Syndrome is Related to *FMR1* Protein Expression. *Human Brain Mapping*, 16(4), 206-218. doi:10.1002/hbm.10048
- Rivera, S. M., Stebbins, G. T., & Grigsby, J. (2010). Radiological Findings in FXTAS. In F. Tassone & E. M. Berry-Kravis (Eds.), *The Fragile X-Associated Tremor/Ataxia Syndrome (FXTAS)* (pp. 55-66). New York: Springer.
- Roberts, J., Mazzocco, M., Murphy, M., & Hoehn-Saric, R. (2008). Arousal Modulation in Females With Fragile X or Turner Syndrome. *Journal of Autism and Developmental Disorders*, 38(1), 20-27. doi:10.1007/s10803-007-0356-6
- Roberts, J., Bailey, D. J., Mankowski, J., Ford, A., Sideris, J., Weisenfeld, L., ... Golden, R. (2009). Mood and Anxiety Disorders in Females With the *Fmr1* Premutation. *American Journal of Medical Genetics. Part B, Neuropsychiatric Genetics*, 150B(1), 130-139. doi:10.1002/ajmg.b.30786
- Robertson, L., Triesman, A., Friedman-Hill, S., & Groaboweczyk, M. (1997). The Interaction of Spatial and Object Pathways: Evidence From Balint's Syndrome. *Journal of Cognitive Neuroscience*, 9, 295-317.
- Rodriguez-Revenga, L., Gomez-Anson, B., Munoz, E., Jimenez, D., Santos, M., Tintore, M., ... Mila, M. (2007). Fxtas in Spanish Patients With Ataxia: Support for Female *FMR1* Premutation Screening. *Molecular Neurobiology*, 35(3), 324-328.
- Rodriguez-Revenga, L., Madrigal, I., Alegret, M., Santos, M., & Mila, M. (2008). Evidence of Depressive Symptoms in Fragile-X Syndrome Premutated Females. *Psychiatric Genetics*, 18(4), 153-155. doi:10.1097/YPG.0b013e3282f97e0b
- Rodriguez-Revenga, L., Madrigal, I., Pagonabarraga, J., Xuncla, M., Badenas, C., Kulisevsky, J., ... Mila, M. (2009). Penetrance of *FMR1* Premutation Associated Pathologies in Fragile X Syndrome Families. *European Journal of Human Genetics*, 17(10), 1359-1362. doi:10.1038/ejhg.2009.51
- Rogers, D., Fisher, E., Brown, S., Peters, J., Hunter, A., & Martin, J. (1997). Behavioral and Functional Analysis of Mouse Phenotype: Shirpa, a Proposed Protocol for Comprehensive Phenotype Assessment. *Mammalian Genome*, 8(10), 711-713.
- Rogers, D., Jones, D., Nelson, P., Jones, C., Quilter, C., Robinson, T., & Hagan, J. (1999). Use of Shirpa and Discriminant Analysis to Characterise Marked Differences in the Behavioural Phenotype of Six Inbred Mouse Strains. *Behavioural Brain Research*, 105(2), 207-217.
- Rogers, D., Peters, J., Martin, J., Ball, S., Nicholson, S., Witherden, A., ... Fisher, E. (2001). Shirpa, a Protocol for Behavioral Assessment: Validation for Longitudinal Study of Neurological Dysfunction in Mice. *Neuroscience Letters*, 306(1-2), 89-92.
- Rolls, E. (1996). A Theory of Hippocampal Function in Memory. *Hippocampus*, 6 (6), 601-620. doi:10.1002/(SICI)1098-1063(1996)6:6
- Rolls, E. (2007). An Attractor Network in the Hippocampus: Theory and Neurophysiology. *Learning and Memory*, 14(11), 714-731. doi:10.1101/lm.631207

- Rolls, E., & Kesner, R. (2006). A Computational Theory of Hippocampal Function, and Empirical Tests of the Theory. *Progress in Neurobiology*, 79(1), 1-48. doi:10.1016/j.pneurobio.2006.04.005
- Rolls, E., Stringer, S., & Elliot, T. (2006). Entorhinal Cortex Grid Cells Can Map to Hippocampal Place Cells By Competitive Learning. *Network*, 17(4), 447-465. doi:10.1080/09548980601064846
- Ross-Inta, C., Omanska-Klusek, A., Wong, S., Barrow, C., Garcia-Arocena, D., Iwahashi, C., ... Giulivi, C. (2010). Evidence of Mitochondrial Dysfunction in Fragile X-Associated Tremor/Ataxia Syndrome. *Biochemical Journal*, 429 (3), 545-552. doi:10.1042/BJ20091960
- Rudelli, R., Brown, W., Wisniewski, K., Jenkins, E., Laure-Kamionowska, M., Connell, F., & Wisniewski, H. (1985). Adult Fragile X Syndrome. Clinico-Neuropathologic Findings. *Acta Neuropathol*, 67(3-4), 289-295.
- Rupp, J., Blekher, T., Jackson, J., Beristain, X., Marshall, J., Hui, S., ... Foroud, T. (2010). Progression in Prediagnostic Huntington Disease. *Journal of Neurology, Neurosurgery and Psychiatry*, 81(4), 379-384. doi:10.1136/jnnp.2009.176982
- Rustay, N., Wahlsten, D., & Crabbe, J. (2003). Influence of Task Parameters on Rotarod Performance and Sensitivity to Ethanol in Mice. *Behavioural Brain Research*, 141(2), 237-249.
- Ryan, B., Young, N., Crawley, J., Bodfish, J., & Moy, S. (2010). Social Deficits, Stereotypy and Early Emergence of Repetitive Behavior in the C58/J Inbred Mouse Strain. *Behavioural Brain Research*, 208(1), 178-188. doi:10.1016/j.bbr.2009.11.031
- Ryan, B., Young, N., Moy, S., & Crawley, J. (2008). Olfactory Cues Are Sufficient to Elicit Social Approach Behaviors But Not Social Transmission of Food Preference in C57Bl/6j Mice. *Behavioural Brain Research*, 193(2), 235-242. doi:10.1016/j.bbr.2008.06.002
- Sahay, A., Wilson, D., & Hen, R. (2011). Pattern Separation: A Common Function for New Neurons in Hippocampus and Olfactory Bulb. *Neuron*, 70(4), 582-588. doi:10.1016/j.neuron.2011.05.012
- Saka, E., & Elibol, B. (2009). Enhanced Cued Recall and Clock Drawing Test Performances Differ in Parkinson's and Alzheimer's Disease-Related Cognitive Dysfunction. *Parkinsonism & Related Disorders*, 15(9), 688-691. doi:10.1016/j.parkreldis.2009.04.008
- Saldivar-Gonzalez, J. A., Posadas-Andrews, A., Rodriguez, R., Gomez, C., Hernandez-Manjarrez, M. E., Ortiz-Leon, S., ... Alvarado, R. (2003). Effect of Electrical Stimulation of the Baso-Lateral Amygdala Nucleus on Defensive Burying Shock Probe Test and Elevated Plus Maze in Rats. *Life Sciences*, 72(7), 819-829.
- Salomonczyk, D., Panzera, R., Pirogovosky, E., Goldstein, J., Corey-Bloom, J., Simmons, R., & Gilbert, P. (2010). Impaired Postural Stability as a Marker of Premanifest Huntington's Disease. *Movement Disorders*, 25(14), 2428-2433. doi:10.1002/mds.23309
- Saluto, A., Brussino, A., Tassone, F., Arduino, C., Cagnoli, C., Pappi, P., ... Brusco, A. (2005). An Enhanced Polymerase Chain Reaction Assay to

- Detect Pre- and Full Mutation Alleles of the Fragile X Mental Retardation 1 Gene. *Journal of Molecular Diagnostics*, 7(5), 605-612. doi:10.1016/S1525-1578(10)60594-6
- Saperstein, A., Fuller, R., Avila, M., Adami, H., McMahon, R., Thaker, G., & Gold, J. (2006). Spatial Working Memory as a Cognitive Endophenotype of Schizophrenia: Assessing Risk for Pathophysiological Dysfunction. *Schizophrenia Bulletin*, 32(3), 498-506. doi:10.1093/schbul/sbj072
- Sathian, K., Simon, T., Peterson, S., Patel, G., Hoffman, J., & Grafton, S. (1999). Neural Evidence Linking Visual Object Enumeration and Attention. *Journal of Cognitive Neuroscience*, 11(1), 36-51.
- Saudou, F., Finkbeiner, S., Devys, D., & Greenberg, M. (1998). Huntington Acts in the Nucleus to Induce Apoptosis But Death Does Not Correlate With the Formation of Intranuclear Inclusions. *Cell*, 95(1), 55-66.
- Scaglione, C., Ginestroni, A., Vella, A., Dotti, M., Nave, R., Rizzo, G., ... Mascalchi, M. (2008). MRI and Spect of Midbrain and Striatal Degeneration in Fragile X-Associated Tremor/Ataxia Syndrome. *Journal of Neurology*, 255 (1)(1), 144-146. doi:10.1007/s00415-007-0711-8
- Schaer, M., Debbane, M., Bach Cuadra, M., Ottet, M., Glaser, B., Thiran, J., & Eliez, S. (2009). Deviant Trajectories of Cortical Maturation in 22q11.2 Deletion Syndrome (22q11ds): A Cross-Sectional and Longitudinal Study. *Schizophrenia Research*, 115(2-3), 182-190. doi:10.1016/j.schres.2009.09.016
- Schaer, M., Schmitt, J., Glaser, B., Lazeyras, F., Delavelle, J., & Eliez, S. (2006). Abnormal Patterns of Cortical Gyration in Velo-Cardio-Facial Syndrome (Deletion 22q11.2): An MRI Study. *Psychiatry Research*, 146(1), 1-11. doi:10.1016/j.psychresns.2005.10.002
- Schmidt, R., Zuckerman, J., Martin, H., & Wolfe, K. J. (1971). A Novel Discrete Gross Motor Learning Task: Modifications of the Bachman Ladder. *Research Quarterly*, 42(1), 78-82.
- Schneider, A., Hagerman, R., & Hessl, D. (2009). Fragile X Syndrome -- From Genes to Cognition. *Developmental Disabilities Research Reviews*, 15(4), 333-342. doi:10.1002/ddrr.80
- Schneider, S., Robertson, M., Rizzo, R., Turk, J., Bhatia, K., & Orth, M. (2008). Fragile X Syndrome Associated With Tic Disorders. *Movement Disorders*, 23(8), 1108-1112. doi:10.1002/mds.21995
- Schnell, S., Staines, W., & Wessendorf, M. (1999). Reduction of Lipofuscin-Like Autofluorescence in Fluorescently Labeled Tissue. *Journal of Histochemistry and Cytochemistry*, 47(6), 719-730.
- Schwartz, B., Deutsch, L., Cohen, C., Warden, D., & Deutsch, S. (1991). Memory for Temporal Order in Schizophrenia. *Biological Psychiatry*, 29(4), 329-339.
- Sellier, C., Rau, F., Liu, Y., Tassone, F., Hukema, R., Gattoni, R., ... Charlet-Berguerand, N. (2010). Sam68 Sequestration and Partial Loss of Function Are Associated With Splicing Alterations in FXTAS Patients. *EMBO Journal*, 29(7), 1248-1261. doi:10.1038/emboj.2010.21
- Selmechy, D., Koldewyn, K., Wang, J., Lee, A., Harvey, D., Hessl, D., ... Rivera, S. (2011). Investigation of Amygdala Volume in Men With the Fragile X

- Premutation. *Brain Imaging and Behavior*, 5(4), 285-294. doi:10.1007/s11682-011-9132-5
- Senturk, D., Nguyen, D., Tassone, F., Hagerman, R., Carroll, R., & Hagerman, P. (2009). Covariate Adjusted Correlation Analysis With Application to Fmr1 Premutation Female Carrier Data. *Biometrics*, 65(3), 781-792. doi:10.1111/j.1541-0420.2008.01169.x
- Seritan, A., Nguyen, D., Farias, S., Hinton, L., Grigsby, J., Bourgeois, J., & Hagerman, R. (2008). Dementia in Fragile X-Associated Tremor/Ataxia Syndrome (Fxtas): Comparison With Alzheimer's Disease. *American Journal of Medical Genetics. Part B, Neuropsychiatric Genetics*, 147B(7), 1138-1144. doi:10.1002/ajmg.b.30732
- Sevin, M., Katalik, Z., Bergman, S., Vercelletto, M., Renou, P., Lamy, E., ... Jacquemont, S. (2009). Penetrance of Marked Cognitive Impairment in Older Male Carriers of the Fmr1 Gene Premutation. *Journal of Medical Genetics*, 46(12), 818-824. doi:10.1136/jmg.2008.065953
- Shah, A., & Treit, D. (2003). Excitotoxic Lesions of the Medial Prefrontal Cortex Attenuate Fear Responses in the Elevated-Plus Maze, Social Interaction and Shock Probe Burying Tests. *Brain Research*, 969(1-2), 183-194.
- Shepherd, J., & Bear, M. (2011). New Views of Arc, a Master Regulator of Synaptic Plasticity. *Nature Neuroscience*, 14(3), 279-284. doi:10.1038/nn.2708
- Shipley, B., Deary, I., Tan, J., Christie, G., & Starr, J. (2002). Efficiency of Temporal Order Discrimination as an Indicator of Bradyphrenia in Parkinson's Disease: The Inspection Time Loop Task. *Neuropsychologia*, 40(8), 1488-1493.
- Shriner, A., Drever, F., & Metz, G. (2009). The Development of Skilled Walking in the Rat. *Behavioural Brain Research*, 205(2), 426-435. doi:10.1016/j.bbr.2009.07.029
- Sigurdsson, T., Stark, K., Karayiorgou, M., Gogos, J., & Gordon, J. (2010). Impaired Hippocampal-Prefrontal Synchrony in a Genetic Mouse Model of Schizophrenia. *Nature*, 464(7289), 763-767. doi:10.1038/nature08855
- Sikiric, P., Jelovac, N., Jelovac-Gjeldum, A., Dodig, G., Staresinic, M., Anic, T., ... Ziger, T. (2001). Anxiolytic Effect of Bpc-157, a Gastric Pentadecapeptide: Shock Probe/Burying Test and Light/Dark Test. *Acta Pharmacologica Sinica*, 22(3), 225-230.
- Silverman, J., Yang, M., Lord, C., & Crawley, J. (2010). Behavioural Phenotyping Assays for Mouse Models of Autism. *Nature Reviews. Neuroscience*, 11(7), 490-502. doi:10.1038/nrn2851
- Silverman, J., Yang, M., Turner, S., Katz, A., Bell, D., Koenig, J., & Crawley, J. (2010). Low Stress Reactivity and Neuroendocrine Factors in the Btbr T+Tf/J Mouse Model of Autism. *Neuroscience*, 171(4), 1197-1208. doi:10.1016/j.neuroscience.2010.09.059
- Simmons, D., & Swanson, L. (2009). Comparing Histological Data From Different Brains: Sources of Error and Strategies for Minimizing Them. *Brain Res Rev*, 60(2), 349-367. doi:10.1016/j.brainresrev.2009.02.002

- Simon, T. (1999). The Foundations of Numerical Thinking in a Brain Without Numbers. *Trends Cogn Sci*, 3(10), 363-365.
- Simon, T. (2007). Cognitive Characteristics of Children With Genetic Syndromes. *Child and Adolescent Psychiatric Clinics of North America*, 16(3), 599-616. doi:10.1016/j.chc.2007.03.002
- Simon, T. (2008). A New Account of the Neurocognitive Foundations of Impairments in Space, Time and Number Processing in Children With Chromosome 22q11.2 Deletion Syndrome. *Developmental Disabilities Research Reviews*, 14(1), 52-58.
- Simon, T. (2011). Clues to the Foundations of Numerical Cognitive Impairments: Evidence From Genetic Disorders. *Dev Neuropsychol*, 36(6), 788-805. doi: 10.1080/87565641.2010.549879
- Simon, T., Bearden, C., Mc-Ginn, D. M., & Zackai, E. (2005a). Visuospatial and Numerical Cognitive Deficits in Children With Chromosome 22q11.2 Deletion Syndrome. *Cortex*, 41(2), 145-155.
- Simon, T., Bish, J., Bearden, C., Ding, L., Ferrante, S., Nguyen, V., ... Emanuel, B. (2005b). A Multilevel Analysis of Cognitive Dysfunction and Psychopathology Associated With Chromosome 22q11.2 Deletion Syndrome in Children. *Development and Psychopathology*, 17(3), 753-784. doi:10.1017/S0954579405050364
- Simon, T., Ding, L., Bish, J., McDonald-Mcginn, D. M., Zackai, E., & Gee, J. (2005c). Volumetric, Connective, and Morphologic Changes in the Brains of Children With Chromosome 22q11.2 Deletion Syndrome: An Integrative Study. *Neuroimage*, 25(1), 169-180. doi:10.1016/j.neuroimage.2004.11.018
- Simon, T., Takarae, Y., Deboer, T., McDonald-Mcginn, D. M., Zackai, E., & Ross, J. (2008a). Overlapping Numerical Cognition Impairments in Children With Chromosome 22q11.2 Deletion or Turner Syndromes. *Neuropsychologia*, 46 (1), 82-94. doi:10.1016/j.neuropsychologia.2007.08.016
- Simon, T., Wu, Z., Avants, B., Zhang, H., Gee, J., & Stebbins, G. (2008b). Atypical Cortical Connectivity and Visuospatial Cognitive Impairments Are Related in Children With Chromosome 22q11.2 Deletion Syndrome. *Behavioral and Brain Functions*, 4, 25. doi:10.1186/1744-9081-4-25
- Soblosky, J., Colgin, L., Chorney-Lane, D., Davidson, J., & Carey, M. (1997a). Some Functional Recovery and Behavioral Sparing Occurs Independent of Task-Specific Practice After Injury to the Rat's Sensorimotor Cortex. *Behavioural Brain Research*, 89(1-2), 51-59.
- Soblosky, J., Colgin, L., Chorney-Lane, D., Davidson, J., & Carey, M. (1997b). Ladder Beam and Camera Video Recording System for Evaluating Forelimb and Hindlimb Deficits After Sensorimotor Cortex Injury in Rats. *Journal of Neuroscience Methods*, 78(1-2), 75-83.
- Soontarapornchai, K., Maselli, R., Fenton-Farrell, G., Tassone, F., Hagerman, P., Hessl, D., & Hagerman, R. (2008). Abnormal Nerve Conduction Features in Fragile X Premutation Carriers. *Archives of Neurology*, 65(4), 495-498. doi: 10.1001/archneur.65.4.495
- Spencer, C., Alekseyenko, O., Hamilton, S., Thomas, A., Serysheva, E., Yuval-Paylor, L. A., & Paylor, R. (2011). Modifying Behavioral Phenotypes in

- Fmr1Ko Mice: Genetic Background Differences Reveal Autistic-Like Responses.* *Autism Research*, 4(1), 40-56. doi:10.1002/aur.168
- Spencer, C., Alekseyenko, O., Serysheva, E., Yuva-Paylor, L. A., & Paylor, R. (2005). Altered Anxiety-Related and Social Behaviors in the *Fmr1* Knockout Mouse Model of Fragile X Syndrome. *Genes, Brain, and Behavior*, 4(7), 420-430. doi:10.1111/j.1601-183X.2005.00123.x
- Spencer, C., Graham, D., Yuva-Paylor, L. A., Nelson, D., & Paylor, R. (2008). Social Behavior in *Fmr1* Knockout Mice Carrying a Human *FMR1* Transgene. *Behavioral Neuroscience*, 122(3), 710-715. doi: 10.1037/0735-7044.122.3.710
- Sporn, A., Addington, A., Reiss, A., Dean, M., Gogtay, N., Potocnik, U., ... Rapoport, J. (2004). 22q11 Deletion Syndrome in Childhood Onset Schizophrenia: An Update. *Molecular Psychiatry*, 9(3), 225-226. doi: 10.1038/sj.mp.4001477
- Sprague, J., & Meikle, T. J. (1965). The Role of the Superior Colliculus in Visually Guided Behavior. *Experimental Neurology*, 11, 115-146.
- Stark, K., Burt, R., Gogos, J., & Karayiorgou, M. (2009). Analysis of Prepulse Inhibition in Mouse Lines Overexpressing 22q11.2 Orthologues. *International Journal of Neuropsychopharmacology*, 12(7), 983-989. doi: 10.1017/S1461145709000492
- Stark, K., Xu, B., Bagchi, A., Lai, W., Liu, H., Hsu, R., ... Gogos, J. (2008). Altered Brain MicroRNA Biogenesis Contributes to Phenotypic Deficits in a 22q11-Deletion Mouse Model. *Nature Genetics*, 40(6), 751-760. doi: 10.1038/ng.138
- Steyaert, J., Borghgraef, M., & Fryns, J. (1994). Apparently Enhanced Visual Information Processing in Female Fragile X Carriers: Preliminary Findings. *American Journal of Medical Genetics*, 51(4), 374-377. doi:10.1002/ajmg.1320510415
- Steyaert, J., Borghgraef, M., Gaultier, C., Fryns, J., & Van Den Berghe, H. (1992). Cognitive Profile in Adult, Normal Intelligent Female Fragile X Carriers. *American Journal of Medical Genetics*, 43(1-2), 116-119.
- Stoddard, J., Niendam, T., Hendren, R., Carter, C., & Simon, T. (2010). Attenuated Positive Symptoms of Psychosis in Adolescents With Chromosome 22q11.2 Deletion Syndrome. *Schizophrenia Research*, 118 (1-3), 118-121. doi:10.1016/j.schres.2009.12.011
- Sullivan, A., Marcus, M., Epstein, M., Allen, E., Anido, A., Paquin, J., ... Sherman, S. (2005). Association of *FMR1* Repeat Size With Ovarian Dysfunction. *Human Reproduction*, 20(2), 402-412. doi:10.1093/humrep/deh635
- Sundram, F., Campbell, L., Azuma, R., Daly, E., Bloemen, O., Barker, G., ... Murphy, D. (2010). White Matter Microstructure in 22q11 Deletion Syndrome: A Pilot Diffusion Tensor Imaging and Voxel-Based Morphometry Study of Children and Adolescents. *Journal of Neurodevelopmental Disorders*, 2(2), 77-92. doi:10.1007/s11689-010-9043-6
- Suzuki, K., & Kobayashi, T. (2000). Numerical Competence in Rats (*Rattus Norvegicus*): Davis and Bradford (1986) Extended. *Journal of Comparative Psychology*, 114(1), 73-85.

- Swanson, L. (1995). Mapping the Human Brain: Past, Present, and Future. *Trends in Neurosciences*, 18(11), 471-474.
- Swanson, M., & Orr, H. (2007). Fragile X Tremor/Ataxia Syndrome: Blame the Messenger! *Neuron*, 55(4), 535-537. doi:10.1016/j.neuron.2007.07.032
- Sztriha, L., Guerrini, R., Harding, B., Stewart, F., Chelloug, N., & Johansen, J. (2004). Clinical, Mri, and Pathological Features of Polymicrogyria in Chromosome 22q11 Deletion Syndrome. *American Journal of Medical Genetics. Part A*, 127A(3), 313-317. doi:10.1002/ajmg.a.30014
- Takahashi-Fujigasaki, J. (2003). Neuronal Intranuclear Hyaline Inclusion Disease. *Neuropathology*, 23(4), 351-359.
- Takao, K., Tanda, K., Nakamura, K., Kasahara, J., Nakao, K., Katsuki, M., ... Miyakawa, T. (2010). Comprehensive Behavioral Analysis of Calcium/Calmodulin-Dependent Protein Kinase Iv Knockout Mice. *PLoS ONE*, 5(3), e9460. doi:10.1371/journal.pone.0009460
- Takarae, Y., Schmidt, L., Tassone, F., & Simon, T. (2009). Catechol-O-Methyltransferase Polymorphism Modulates Cognitive Control in Children With Chromosome 22q11.2 Deletion Syndrome. *Cognitive, Affective and Behavioral Neuroscience*, 9(1), 83-90. doi:10.3758/CABN.9.1.83
- Tamm, L., Menon, V., Johnston, C., Hessl, D., & Reiss, A. (2002). FMRI Study of Cognitive Interference Processing in Females With Fragile X Syndrome. *Journal of Cognitive Neuroscience*, 14(2), 160-171. doi:10.1162/089892902317236812
- Tassone, F., Adams, J., Berry-Kravis, E. M., Cohen, S., Brusco, A., Leehey, M., ... Hagerman, P. (2007a). Cgg Repeat Length Correlates With Age of Onset of Motor Signs of the Fragile X-Associated Tremor/Ataxia Syndrome (Fxtas). *American Journal of Medical Genetics. Part B, Neuropsychiatric Genetics*, 144B(4), 566-569. doi:10.1002/ajmg.b.30482
- Tassone, F., Beilina, A., Carosi, C., Albertosi, S., Bagni, C., Li, L., ... Hagerman, P. (2007b). Elevated *FMR1* mRNA in Premutation Carriers is Due to Increased Transcription. *RNA*, 13(4), 555-562. doi:10.1261/rna.280807
- Tassone, F., Greco, C., Hunsaker, M., Berman, R., Seritan, A., Gane, L., ... Rj, H. (2012). Neuropathological, Clinical, and Molecular Pathology in Female Fragile X Premutation Carriers With and Without Fxtas. *Genes, Brain and Behavior*.
- Tassone, F., & Hagerman, P. (2003). Expression of the *FMR1* Gene. *Cytogenetic and Genome Research*, 100(1-4), 124-128. doi:10.1159/000072846
- Tassone, F., & Hagerman, P. J. (2010). The Molecular Biology of FXTAS. In F. Tassone & E. M. Berry-Kravis (Eds.), *The Fragile X-Associated Tremor/Ataxia Syndrome (FXTAS)* (pp. 67-76). New York: Springer.
- Tassone, F., Hagerman, R., Chamberlain, W., & Hagerman, P. (2000a). Transcription of the *FMR1* Gene in Individuals With Fragile X Syndrome. *American Journal of Medical Genetics*, 97(3), 195-203. doi:10.1002/1096-8628(200023)97:3
- Tassone, F., Hagerman, R., Garcia-Arocena, D., Khandjian, E., Greco, C., & Hagerman, P. (2004a). Intranuclear Inclusions in Neural Cells With

- Premutation Alleles in Fragile X Associated Tremor/Ataxia Syndrome. *Journal of Medical Genetics*, 41(4), e43.
- Tassone, F., Hagerman, R., Ikle, D., Dyer, P., Lampe, M., Willemsen, R., ... Taylor, A. (1999). FMRP Expression as a Potential Prognostic Indicator in Fragile X Syndrome. *American Journal of Medical Genetics*, 84(3), 250-261.
- Tassone, F., Hagerman, R., Loesch, D., Lachiewicz, A., Taylor, A., & Hagerman, P. (2000b). Fragile X Males With Unmethylated, Full Mutation Trinucleotide Repeat Expansions Have Elevated Levels of *FMR1* Messenger RNA. *American Journal of Medical Genetics*, 94(3), 232-236.
- Tassone, F., Hagerman, R., Taylor, A., Gane, L., Godfrey, T., & Hagerman, P. (2000c). Elevated Levels of *FMR1* mRNA in Carrier Males: A New Mechanism of Involvement in the Fragile-X Syndrome. *American Journal of Human Genetics*, 66(1), 6-15. doi:10.1086/302720
- Tassone, F., Hagerman, R., Taylor, A., Mills, J., Harris, S., Gane, L., & Hagerman, P. (2000d). Clinical Involvement and Protein Expression in Individuals With the *FMR1* Premutation. *American Journal of Medical Genetics*, 91(2), 144-152.
- Tassone, F., Iwahashi, C., & Hagerman, P. (2004b). *FMR1* RNA Within the Intracellular Inclusions of Fragile X-Associated Tremor/Ataxia Syndrome (FXTAS). *RNA Biology*, 1(2), 103-105.
- Tassone, F., Pan, R., Amiri, K., Taylor, A., & Hagerman, P. (2008). A Rapid Polymerase Chain Reaction-Based Screening Method for Identification of All Expanded Alleles of the Fragile X (*FMR1*) Gene in Newborn and High-Risk Populations. *Journal of Molecular Diagnostics*, 10(1), 43-49. doi:10.2353/jmoldx.2008.070073
- Taylor, T., Greene, J., & Miller, G. (2010). Behavioral Phenotyping of Mouse Models of Parkinson's Disease. *Behavioural Brain Research*, 211(1), 1-10. doi:10.1016/j.bbr.2010.03.004
- Tennant, K., & Jones, T. (2009). Sensorimotor Behavioral Effects of Endothelin-1 Induced Small Cortical Infarcts in C57BL/6 Mice. *Journal of Neuroscience Methods*, 181(1), 18-26. doi:10.1016/j.jneumeth.2009.04.009
- Thomas, A., Burant, A., Bui, N., Graham, D., Yuva-Paylor, L. A., & Paylor, R. (2009). Marble Burying Reflects a Repetitive and Perseverative Behavior More Than Novelty-Induced Anxiety. *Psychopharmacology*, 204(2), 361-373. doi:10.1007/s00213-009-1466-y
- Todd, P., & Paulson, H. (2010). RNA-Mediated Neurodegeneration in Repeat Expansion Disorders. *Annals of Neurology*, 67(3), 291-300. doi:10.1002/ana.21948
- Toner, C., Pirogovsky, E., Kirwan, C., & Gilbert, P. (2009). Visual Object Pattern Separation Deficits in Nondemented Older Adults. *Learning and Memory*, 16(5), 338-342. doi:10.1101/lm.1315109
- Treit, D., & Fundytus, M. (1988). A Comparison of Buspirone and Chlordiazepoxide in the Shock-Probe/Burying Test for Anxiolytics. *Pharmacology, Biochemistry and Behavior*, 30(4), 1071-1075.
- Tydlacka, S., Wang, C., Wang, X., Li, S., & Li, X. (2008). Differential Activities of the Ubiquitin-Proteasome System in Neurons Versus Glia May Account for

- the Preferential Accumulation of Misfolded Proteins in Neurons. *Journal of Neuroscience*, 28(49), 13285-13295. doi:10.1523/JNEUROSCI.4393-08.2008
- Uchida, S., Kitamoto, A., Umeeda, H., Nakagawa, N., Masushige, S., & Kida, S. (2005). Chronic Reduction in Dietary Tryptophan Leads to Changes in the Emotional Response to Stress in Mice. *Journal of Nutritional Science and Vitaminology*, 51(3), 175-181.
- Utari, A., Adams, E., Berry-Kravis, E., Chavez, A., Scaggs, F., Ngotran, L., ... Hagerman, R. (2010). Aging in Fragile X Syndrome. *Journal of Neurodevelopmental Disorders*, 2(2), 70-76. doi:10.1007/s11689-010-9047-2
- Van Dam, D., D'Hooge, R., Hauben, E., Reyniers, E., Gantois, I., Bakker, C., ... De Deyn, P. P. (2000). Spatial Learning, Contextual Fear Conditioning and Conditioned Emotional Response in *Fmr1* Knockout Mice. *Behavioural Brain Research*, 117(1-2), 127-136.
- Van Dam, D., Errijgers, V., Kooy, R., Willemse, R., Mientjes, E., Oostra, B., & De Deyn, P. P. (2005). Cognitive Decline, Neuromotor and Behavioural Disturbances in a Mouse Model for Fragile-X-Associated Tremor/Ataxia Syndrome (Fxtas). *Behavioural Brain Research*, 162(2), 233-239. doi:10.1016/j.bbr.2005.03.007
- Van Der Molen, M. J., Huizinga, M., Huizenga, H., Ridderinkhof, K., Van Der Molen, M. W., Hamel, B., ... Ramakers, G. (2010). Profiling Fragile X Syndrome in Males: Strengths and Weaknesses in Cognitive Abilities. *Research in Developmental Disabilities*, 31(2), 426-439. doi:10.1016/j.ridd.2009.10.013
- Vazdarjanova, A., & Guzowski, J. (2004). Differences in Hippocampal Neuronal Population Responses to Modifications of an Environmental Context: Evidence for Distinct, Yet Complementary, Functions of CA3 and CA1 Ensembles. *Journal of Neuroscience*, 24(29), 6489-6496. doi:10.1523/JNEUROSCI.0350-04.2004
- Vazdarjanova, A., McNaughton, B., Barnes, C., Worley, P., & Guzowski, J. (2002). Experience-Dependent Coincident Expression of the Effector Immediate-Early Genes Arc and Homer 1a in Hippocampal and Neocortical Neuronal Networks. *Journal of Neuroscience*, 22(23), 10067-10071.
- Vazdarjanova, A., Ramirez-Amaya, V., Insel, N., Plummer, T., Rosi, S., Chowdhury, S., ... Barnes, C. (2006). Spatial Exploration Induces Arc, a Plasticity-Related Immediate-Early Gene, Only in Calcium/Calmodulin-Dependent Protein Kinase II-Positive Principal Excitatory and Inhibitory Neurons of the Rat Forebrain. *Journal of Comparative Neurology*, 498(3), 317-329. doi:10.1002/cne.21003
- Vergara-Aragon, P., Gonzalez, C., & Whishaw, I. (2003). A Novel Skilled-Reaching Impairment in Paw Supination on the "Good" Side of the Hemiparkinson Rat Improved With Rehabilitation. *Journal of Neuroscience*, 23(2), 579-586.

- Verstraten, F., Cavanagh, P., & Labianca, A. (2000). Limits of Attentive Tracking Reveal Temporal Properties of Attention. *Vision Research*, 40(26), 3651-3664.
- Vriezen, E., & Moscovitch, M. (1990). Memory for Temporal Order and Conditional Associative-Learning in Patients With Parkinson's Disease. *Neuropsychologia*, 28(12), 1283-1293.
- Wahlsten, D. (1972). Genetic Experiments With Animal Learning: A Critical Review. *Behavioral Biology*, 7(2), 143-182.
- Wahlsten, D. (1974). A Developmental Time Scale for Postnatal Changes in Brain and Behavior of B6D2F2 Mice. *Brain Research*, 72(2), 251-264.
- Wahlsten, D. (2001). Standardizing Tests of Mouse Behavior: Reasons, Recommendations, and Reality. *Physiology and Behavior*, 73(5), 695-704.
- Wahlsten, D., Bachmanov, A., Finn, D., & Crabbe, J. (2006). Stability of Inbred Mouse Strain Differences in Behavior and Brain Size Between Laboratories and Across Decades. *Proceedings of the National Academy of Sciences of the United States of America*, 103(44), 16364-16369. doi:10.1073/pnas.0605342103
- Wahlsten, D., Metten, P., & Crabbe, J. (2003). Survey of 21 Inbred Mouse Strains in Two Laboratories Reveals That Btbr T/+ Tf/Tf Has Severely Reduced Hippocampal Commissure and Absent Corpus Callosum. *Brain Research*, 971(1), 47-54.
- Wahlsten, D., Metten, P., Phillips, T., Boehm, S. N., Burkhart-Kasch, S., Dorow, J., ... Crabbe, J. (2003). Different Data From Different Labs: Lessons From Studies of Gene-Environment Interaction. *Journal of Neurobiology*, 54(1), 283-311. doi:10.1002/neu.10173
- Wahlsten, D., Rustay, N., Metten, P., & Crabbe, J. (2003). In Search of a Better Mouse Test. *Trends in Neurosciences*, 26(3), 132-136.
- Wakabayashi, K., Mori, F., Tanji, K., Orimo, S., & Takahashi, H. (2010). Involvement of the Peripheral Nervous System in Synucleinopathies, Tauopathies and Other Neurodegenerative Proteinopathies of the Brain. *Acta Neuropathol*, 120(1), 1-12. doi:10.1007/s00401-010-0706-x
- Wald, C., & Wu, C. (2010). Biomedical Research. Of Mice and Women: The Bias in Animal Models. *Science*, 327(5973), 1571-1572. doi:10.1126/science.327.5973.1571
- Walter, E., Mazaika, P., & Reiss, A. (2009). Insights Into Brain Development From Neurogenetic Syndromes: Evidence From Fragile X Syndrome, Williams Syndrome, Turner Syndrome and Velocardiofacial Syndrome. *Neuroscience*, 164(1), 257-271. doi:10.1016/j.neuroscience.2009.04.033
- Wang, H., Kim, S., & Zhuo, M. (2010). Roles of Fragile X Mental Retardation Protein in Dopaminergic Stimulation-Induced Synapse-Associated Protein Synthesis and Subsequent Alpha-Amino-3-Hydroxyl-5-Methyl-4-Isoxazole-4-Propionate (Ampa) Receptor Internalization. *Journal of Biological Chemistry*, 285(28), 21888-21901. doi:10.1074/jbc.M110.116293
- Wang, L., Simpson, H., & Dulawa, S. (2009). Assessing the Validity of Current Mouse Genetic Models of Obsessive-Compulsive Disorder. *Behavioural Pharmacology*, 20(2), 119-133. doi:10.1097/FBP.0b013e32832a80ad

- Ward, J. J. (1963). Hierarchical Grouping to Optimize an Objective Function. *Journal of the American Statistical Association*, 58, 236-244.
- Ward, N., & Brown, V. (1996). Covert Orienting of Attention in the Rat and the Role of Striatal Dopamine. *Journal of Neuroscience*, 16(9), 3082-3088.
- Ward, N., & Brown, V. (1997). Deficits in Response Initiation, But Not Attention, Following Excitotoxic Lesions of Posterior Parietal Cortex in the Rat. *Brain Research*, 775(1-2), 81-90.
- Ward, N., Sharkey, J., & Brown, V. (1997). Assessment of Sensorimotor Neglect After Occlusion of the Middle Cerebral Artery in the Rat. *Behavioral Neuroscience*, 111(5), 1133-1145.
- Ward, N., Sharkey, J., Marston, H., & Brown, V. (1998). Simple and Choice Reaction-Time Performance Following Occlusion of the Anterior Cerebral Arteries in the Rat. *Experimental Brain Research*, 123(3), 269-281.
- Warren, W. (2006). The Dynamics of Perception and Action. *Psychological Review*, 113(2), 358-389. doi:10.1037/0033-295X.113.2.358
- Watson, C., Hoeft, F., Garrett, A., Hall, S., & Reiss, A. (2008). Aberrant Brain Activation During Gaze Processing in Boys With Fragile X Syndrome. *Archives of General Psychiatry*, 65(11), 1315-1323. doi:10.1001/archpsyc.65.11.1315
- Weiler, I., Irwin, S., Klintsova, A., Spencer, C., Brazelton, A., Miyashiro, K., ... Greenough, W. (1997). Fragile X Mental Retardation Protein is Translated Near Synapses in Response to Neurotransmitter Activation. *Proceedings of the National Academy of Sciences of the United States of America*, 94(10), 5395-5400.
- Weiser, M., Van Os, J., & Davidson, M. (2005). Time for a Shift in Focus in Schizophrenia: From Narrow Phenotypes to Broad Endophenotypes. *British Journal of Psychiatry*, 187, 203-205. doi:10.1192/bjp.187.3.203
- Weiss, P., Marshall, J., Wunderlich, G., Tellmann, L., Halligan, P., Freund, H., ... Fink, G. (2000). Neural Consequences of Acting in Near Versus Far Space: A Physiological Basis for Clinical Dissociations. *Brain*, 123 Pt 12, 2531-2541.
- Wenzel, H., Hunsaker, M., Greco, C., Willemse, R., & Berman, R. (2010). Ubiquitin-Positive Intranuclear Inclusions in Neuronal and Glial Cells in a Mouse Model of the Fragile X Premutation. *Brain Research*, 1318, 155-166. doi:10.1016/j.brainres.2009.12.077
- Wenzel, H., Patel, L., Robbins, C., Emmi, A., Yeung, R., & Schwartzkroin, P. (2004). Morphology of Cerebral Lesions in the Eker Rat Model of Tuberous Sclerosis. *Acta Neuropathol*, 108(2), 97-108. doi:10.1007/s00401-004-0865-8
- Wenzel, H., Vacher, H., Clark, E., Trimmer, J., Lee, A., Sapolsky, R., ... Schwartzkroin, P. (2007). Structural Consequences of Kcna1 Gene Deletion and Transfer in the Mouse Hippocampus. *Epilepsia*, 48(11), 2023-2046. doi:10.1111/j.1528-1167.2007.01189.x
- West, M., Slomianka, L., & Gundersen, H. (1991). Unbiased Stereological Estimation of the Total Number of Neurons in Thesubdivisions of the Rat

- Hippocampus Using the Optical Fractionator. *Anatomical Record*, 231(4), 482-497. doi:10.1002/ar.1092310411
- Whishaw, I., Alaverdashvili, M., & Kolb, B. (2008). The Problem of Relating Plasticity and Skilled Reaching After Motor Cortex Stroke in the Rat. *Behavioural Brain Research*, 192(1), 124-136. doi:10.1016/j.bbr.2007.12.026
- Whishaw, I., & Coles, B. (1996). Varieties of Paw and Digit Movement During Spontaneous Food Handling in Rats: Postures, Bimanual Coordination, Preferences, and the Effect of Forelimb Cortex Lesions. *Behavioural Brain Research*, 77(1-2), 135-148.
- Whishaw, I., & Metz, G. (2002). Absence of Impairments or Recovery Mediated By the Uncrossed Pyramidal Tract in the Rat Versus Enduring Deficits Produced By the Crossed Pyramidal Tract. *Behavioural Brain Research*, 134(1-2), 323-336.
- Whishaw, I., & Tomie, J. (1996). Of Mice and Mazes: Similarities Between Mice and Rats on Dry Land But Not Water Mazes. *Physiology and Behavior*, 60 (5), 1191-1197.
- Whishaw, I., Travis, S., Koppe, S., Sacrey, L., Gholamrezaei, G., & Gorny, B. (2010). Hand Shaping in the Rat: Conserved Release and Collection Vs. Flexible Manipulation in Overground Walking, Ladder Rung Walking, Cylinder Exploration, and Skilled Reaching. *Behavioural Brain Research*, 206(1), 21-31. doi:10.1016/j.bbr.2009.08.030
- Whishaw, I., Zeeb, F., Erickson, C., & McDonald, R. (2007). Neurotoxic Lesions of the Caudate-Putamen on a Reaching for Food Task in the Rat: Acute Sensorimotor Neglect and Chronic Qualitative Motor Impairment Follow Lateral Lesions and Improved Success Follows Medial Lesions. *Neuroscience*, 146(1), 86-97. doi:10.1016/j.neuroscience.2007.01.034
- Willemsen, R., Hoogeveen-Westerveld, M., Reis, S., Holstege, J., Severijnen, L., Nieuwenhuizen, I., ... Oostra, B. (2003). The *Fmr1* CGG Repeat Mouse Displays Ubiquitin-Positive Intranuclear Neuronal Inclusions; Implications for the Cerebellar Tremor/Ataxia Syndrome. *Human Molecular Genetics*, 12(9), 949-959.
- Willemsen, R., Levenga, J., & Oostra, B. (2011). CGG Repeat in the *Fmr1* Gene: Size Matters. *Clinical Genetics*, 80(3), 214-225. doi:10.1111/j.1399-0004.2011.01723.x
- Willemsen, R., Li, Y., Berman, R. F., Brouwer, J. R., Oostra, B. A., & Jin, P. (2010). Animal Models for FXTAS. In F. Tassone & E. M. Berry-Kravis (Eds.), *The Fragile X-Associated Tremor/Ataxia Syndrome (FXTAS)* (pp. 67-76). New York: Springer.
- Wilson, D. (2009). Pattern Separation and Completion in Olfaction. *Annals of the New York Academy of Sciences*, 1170, 306-312. doi:10.1111/j.1749-6632.2009.04017.x
- Wolff, M., Gibb, S., & Dalrymple-Alford, J. C. (2006). Beyond Spatial Memory: The Anterior Thalamus and Memory for the Temporal Order of a Sequence of Odor Cues. *Journal of Neuroscience*, 26(11), 2907-2913. doi:10.1523/JNEUROSCI.5481-05.2006

- Woulfe, J. (2008). Nuclear Bodies in Neurodegenerative Disease. *Biochimica et Biophysica Acta*, 1783(11), 2195-2206. doi:10.1016/j.bbamcr.2008.05.005
- Woulfe, J. (2007). Abnormalities of the Nucleus and Nuclear Inclusions in Neurodegenerative Disease: A Work in Progress. *Neuropathology and Applied Neurobiology*, 33(1), 2-42. doi:10.1111/j.1365-2990.2006.00819.x
- Xu, B., Hsu, P., Karayiorgou, M., & Gogos, J. (2012). MicroRNA Dysregulation in Neuropsychiatric Disorders and Cognitive Dysfunction. *Neurobiology of Disease*,. doi:10.1016/j.nbd.2012.02.016
- Xu, B., Karayiorgou, M., & Gogos, J. (2010). MicroRNAs in Psychiatric and Neurodevelopmental Disorders. *Brain Research*, 1338, 78-88. doi:10.1016/j.brainres.2010.03.109
- Yachnis, A., Crawley, J., Jensen, R., Mcgrane, M., & Moody, T. (1984). The Antagonism of Bombesin in the Cns By Substance P Analogues. *Life Sciences*, 35(19), 1963-1969.
- Yachnis, A., Roth, H., & Heilman, K. (2010). Fragile X Dementia Parkinsonism Syndrome (Fxdps). *Cognitive and Behavioral Neurology*, 23(1), 39-43. doi: 10.1097/WNN.0b013e3181b6e1b9
- Yamada, M., Hayashi, S., Tsuji, S., & Takahashi, H. (2001). Involvement of the Cerebral Cortex and Autonomic Ganglia in Machado-Joseph Disease. *Acta Neuropathol*, 101(2), 140-144.
- Yamagishi, H., & Srivastava, D. (2003). Unraveling the Genetic and Developmental Mysteries of 22q11 Deletion Syndrome. *Trends in Molecular Medicine*, 9(9), 383-389.
- Yan, Q., Asafo-Adjei, P. K., Arnold, H., Brown, R., & Bauchwitz, R. (2004). A Phenotypic and Molecular Characterization of the *Fmr1-Tm1Cgr* Fragile X Mouse. *Genes, Brain, and Behavior*, 3(6), 337-359. doi:10.1111/j.1601-183X.2004.00087.x
- Yang, M., Augustsson, H., Markham, C., Hubbard, D., Webster, D., Wall, P., ... Blanchard, D. (2004). The Rat Exposure Test: A Model of Mouse Defensive Behaviors. *Physiology and Behavior*, 81(3), 465-473. doi:10.1016/j.physbeh.2004.02.010
- Yang, M., Silverman, J., & Crawley, J. (2011). Automated Three-Chambered Social Approach Task for Mice. *Curr Protoc Neurosci, Chapter 8, Unit 8.26*. doi:10.1002/0471142301.ns0826s56
- Yassa, M., & Stark, C. (2011). Pattern Separation in the Hippocampus. *Trends in Neurosciences*, 34(10), 515-525. doi:10.1016/j.tins.2011.06.006
- Ye, X., Tai, W., & Zhang, D. (2011). The Early Events of Alzheimer's Disease Pathology: From Mitochondrial Dysfunction to BDNF Axonal Transport Deficits. *Neurobiology of Aging*,. doi:10.1016/j.neurobiolaging.2011.11.004
- Yeshurun, Y., & Levy, L. (2003). Transient Spatial Attention Degrades Temporal Resolution. *Psychological Science*, 14(3), 225-231.
- Yonath, H., Marek-Yagel, D., Resnik-Wolf, H., Abu-Horvitz, A., Baris, H., Shohat, M., ... Pras, E. (2011). X Inactivation Testing for Identifying a Non-Syndromic X-Linked Mental Retardation Gene. *J Appl Genet*, 52(4), 437-441. doi:10.1007/s13353-011-0052-2

- Yong-Kee, C. J., Salomonczyk, D., & Nash, J. (2011). Development and Validation of a Screening Assay for the Evaluation of Putative Neuroprotective Agents in the Treatment of Parkinson's Disease. *Neurotoxicity Research, 19*(4), 519-526. doi:10.1007/s12640-010-9174-2
- Yuhas, J., Cordeiro, L., Tassone, F., Ballinger, E., Schneider, A., Long, J., ... Hessl, D. (2011). Brief Report: Sensorimotor Gating in Idiopathic Autism and Autism Associated With Fragile X Syndrome. *Journal of Autism and Developmental Disorders, 41*(2), 248-253. doi:10.1007/s10803-010-1040-9
- Zang, J., Nosyreva, E., Spencer, C., Volk, L., Musunuru, K., Zhong, R., ... Darnell, R. (2009). A Mouse Model of the Human Fragile X Syndrome I304N Mutation. *PLoS Genetics, 5*(12), e1000758. doi:10.1371/journal.pgen.1000758
- Zeyda, T., Diehl, N., Paylor, R., Brennan, M., & Hochgeschwender, U. (2001). Impairment in Motor Learning of Somatostatin Null Mutant Mice. *Brain Research, 906*(1-2), 107-114.
- Zhang, L., Coffey, S., Lua, L., Greco, C., Schafer, J., Brunberg, J., ... Hagerman, R. (2009). Fmr1 Premutation in Females Diagnosed With Multiple Sclerosis. *Journal of Neurology, Neurosurgery and Psychiatry, 80*(7), 812-814. doi:10.1136/jnnp.2008.160960
- Zuhlke, C., Budnik, A., Gehlken, U., Dalski, A., Purmann, S., Naumann, M., ... Schwinger, E. (2004). Fmr1 Premutation as a Rare Cause of Late Onset Ataxia--Evidence for Fxtas in Female Carriers. *Journal of Neurology, 251*(11), 1418-1419. doi:10.1007/s00415-004-0558-1